The development of non-β-lactam inhibitors of bacterial transpeptidases



A thesis submitted to the Department of Chemistry in partial fulfilment of the requirements for the degree of Doctor of Philosophy.

Timothy Francis Suits

Supervisor: Christopher J. Schofield, FRS

St Edmund Hall

Hillary Term 2022

Abstract

Timothy Francis Suits D. Phil
St Edmund Hall Hillary Term 2022

The development of non-β-lactam inhibitors of bacterial transpeptidases

β-Lactams, which inhibit bacterial transpeptidases, are currently the most widely used antibacterials globally. The emergence of bacterial resistance, conferred by β-lactamases in particular, which degrade β-lactam antibiotics, poses a perilous threat to human health. In conjunction with the development of β-lactamase inhibitors (BLIs), new antibiotics are needed that are stable to β-lactamase degradation. As β-lactamases provide bacterial resistance against β-lactam-containing antibiotics, the development of non-β-lactam transpeptidases inhibitors may be a promising strategy.

Chapter 1 provides a review of non-β-lactam analogues synthesised as potential antibacterial inhibitors, from which several promising molecular scaffolds such as the lactivicins and the benzisothiazolinones were identified. Chapter 2 describes the design and synthesis of non-β-lactam analogues using both reported and novel synthetic methodologies. In Chapter 3, synthesised compounds were evaluated for antibacterial and inhibitory activity against transpeptidases produced by *Mycobacterium tuberculosis*. In Chapter 4, synthetic methods for the modification of 2-oxoglutarate (2-OG), originally conceived for the synthesis of γ-lactone-functionalised lactivicin analogues, were repurposed for the synthesis of 2-OG analogues as inhibitors of isocitrate dehydrogenase (IDH) variants. In response to the coronavirus pandemic, Chapter 5 details the development of benzisothiazolinones as inhibitors of SARS-CoV-2 main protease.

The work described in this thesis made substantial progress in developing strategies for the synthesis of non-β-lactam transpeptidase inhibitors, which will be used to combat antimicrobial resistance, and pioneered facile methodology for the synthesis of functionalised 2-OG analogues for biological studies.

Declaration of authorship

The work described in this thesis is entirely my own, except where it has been stated otherwise.

Declaration of experiments conducted by others:

Chapter 2: Variable temperature NMR experiments were performed by Dr. Nader Amin.

Chapter 3: Protein-observed mass spectrometry assays were conducted by Tika R. Malla using proteins produced by Tika R. Malla. Structural refinements were conducted by Tika R. Malla and Dr. Michael A. McDonough. Minimum inhibitory concentration assays were conducted in conjunction with Dr. Karina Calvopiña.

Chapter 4: NADPH absorbance assays were conducted by Raphael Reinbold using IDH variants produced by Raphael Reinbold.

Chapter 5: Protein observed mass spectrometry assays were performed by Tika R. Malla using M^{pro} produced by Eidarus Salah. Inhibition assays were performed by Dr. Anthony Tumber, Tika R. Malla, or Siegfried Thun-Hohenstein. Selected compounds were synthesised by Siegfried Thun-Hohenstein and are included for completeness. Flow cytometry experiments were conducted by Dr. Chris Moon and Dr. Joanna Bacon from Public Health England.

Table of Contents

Abstract ..... **i**

Declaration of authorship ..... **ii**

Table of Contents ..... **iii**

Acknowledgements ..... **ix**

List of Abbreviations ..... **x**

Chapter 1 Introduction **1**

1.1 Bacteria and bacterial infections **1**

1.2 The bacterial cell wall **3**

1.2.1 Structure 3

1.2.2 Bacterial cell wall biosynthesis 4

1.3 β-Lactam antibiotics **8**

1.3.1 Structure-activity relationships for β-lactam antibacterial activity 8

1.3.2 The penicillins 11

1.3.3 The cephalosporins 12

1.3.4 The carbapenems 15

1.3.5 The monobactams 17

1.4 The threat of antimicrobial resistance **20**

1.4.1 Overview of β-lactamases 21

1.4.2 β-Lactamase inhibitors 23

1.5 Non-β-lactam inhibitors of PBPs **25**

1.5.1 Non-covalent *S. aureus* PBP2a inhibitors 25

1.5.2 Cyclopentenones 29

1.5.3 Thioesters 30

1.5.4 Cyclobutanone analogues of β-lactams 31

1.5.5 β-Lactam isosteres 33

1.5.6 Six-membered and larger systems 34

1.5.7 Bridged bicyclic lactam analogues 35

1.5.8 Boronates 38
1.5.9 γ-Lactams 39
1.5.10 Pyrazolidinones 44
1.6 Lactivicins 49
1.6.1 Characterisation of lactivicin 50
1.6.2 Synthesis of lactivicin analogues 53
1.6.3 Selected synthetic lactivicins 55
1.6.4 Lactivicin siderophore conjugates 57
1.6.5 Aminopyrazolidinone lactivicin analogues 59
1.6.6 3-Methoxy lactivicin analogues 59
1.6.7 Homolactivicin analogues 60
1.6.8 Shionogi tricyclic lactivicins 61
1.6.9 Lactivicins and β-lactamases 62
1.6.10 Antibacterial activity of cycloserine analogues 64
1.6.11 Bioisosteres of the lactivicin aminoisoxazolidinone ring 66
1.7 Summary of non-β-lactam-based antibacterials 69
1.8 Project aims 70
Chapter 2 Synthesis of lactivicin analogues 72
2.1 Introduction 72
2.2 Synthesis of reported lactivicin compounds 73
2.2.1 Synthesis of compound 168 73
2.2.2 Synthesis of compound 180 76
2.3 Design and synthesis of substituted cycloserines 79
2.3.1 Design of 3-isoxazolidinone fragment 223 79
2.3.2 Synthesis of bicyclic cycloserine derivatives 81
2.3.3 Synthesis of a "decarboxylactivicin" analogue 87
2.4 Synthesis of *C*-3-modified cycloserines 87
2.4.1 Biosynthesis of acinetobactin 89
2.4.2 Synthesis of acinetobactin analogues 91
2.5 Synthesis of functionalized pyrazolidinones 95
2.5.1 Synthesis of aminopyrazolidinone precursor 265 96
2.5.2 Attempted lactonisation of aminopyrazolidone 264 98

2.5.3 Synthesis of *C*-3-functionalised aminopyrazolidinones 99
2.6 Synthesis of a tricyclic lactivicin analogue 101
2.6.1 Reported synthetic route for tricyclic lactivicins 103
2.6.2 Synthesis of 282 via an *aza*-Michael addition 105
2.6.3 Benzhydryl deprotection and cyclisation of the Michael product 282 108
2.6.4 Optimising the one-pot deprotection/lactonisation reaction 110
2.6.5 N-Boc deprotection and amide coupling 114
2.6.6 Variable-temperature NMR of 'diastereomer B' 116
2.7 Summary of work detailed in Chapter 2 118
Chapter 3 Efficacy of modified lactivicin analogues against *Mycobacterium tuberculosis*. 121
3.1 Introduction 121
3.1.1 Structure and function of L,D-transpeptidases 121
3.2 Protein-observed mass spectrometry studies between Ldts and lactivicin analogues 123
3.2.1 Inhibitor screen for covalent modification of Ldt enzymes. 124
3.2.2 The effect of dithiothreitol on the Ldt_{Mt2}-236b adduct 130
3.2.3 Evaluating the scope of Ldt inhibition 132
3.3 Protein crystallography of Ldt_{mt2} and inhibitors 137
3.4 MIC results 138
3.5 Summary 140
Chapter 4 Methods for the modification of 2-oxoglutarate and their applications 142
4.1 Introduction 142
4.1.1 PBPs can accommodate additional functionality to the lactivicin γ-lactone 144
4.1.2 Crystal structure of compound 179 with paePBP1a 145
4.1.3 Synthesis of the functionalised 2-OG precursor 297. 146
4.1.4 Drawbacks of the Pfizer route to compound 179 147
4.2 Improving the Pfizer route 148
4.2.1 α-Keto-acid synthesis using a cyanosulfur ylide 148

4.3 Sulfide-functionalised lactivicin analogues 149

4.3.1 Functionalisation of Michael acceptor 283. 149

4.3.2 Method exploration 150

4.4 Synthesis of 3-sulfido 2-oxoglutarate analogues 152

4.4.1 2-Oxoglutarate as a co-substrate in enzyme catalysis 153

4.5 Synthesis of a library of 2-oxoglutarate inhibitors of Isocitrate dehydrogenase 155

4.5.1 Introduction to isocitrate dehydrogenase 155

4.5.2 Structure of the $IDH1^{R132H}$ active site 157

4.5.3 Optimisation of the general synthetic route to 3-sulfido-2-OG analogues 159

4.5.4 Synthesis of the initial series of 3-sulfido-2-OG analogues 162

4.5.5 $IDH1^{132H}$ activity screen for the first series of compounds 164

4.5.6 Synthesis of the second series of 3-sulfido-2-oxoglutarate analogues 168

4.5.7 Activity of the second series of 3-sulfido-2-OG analogues 169

4.5.8 Synthesis of a third series of 3-sulfido-2-OG analogues 171

4.5.9 Series 3 activity 175

4.5.10 Determination of IC_{50}s for hit compounds against $IDH1^{R132H}$ 176

4.5.11 Evaluation of modified 2-OG analogues as IDH1 alternative substrates 178

4.5.12 Synthesis of an aliphatic series of 3-sulfido-2-OGs as alternative substrates 179

4.5.13 Activity of the aliphatic series as alternative substrates for IDH1 180

4.5.14 Counter screen of inhibitors as alternative substrates 181

4.5.15 Inhibitory activity of the aliphatic series 182

4.5.16 Counter screen against *wt* IDH1 182

4.5.17 Stability studies on 290f and 290d 184

4.5.18 Development of conditions for C-C couplings 187

4.5.19 Synthesis and validation of the Rh(I) catalyst 187

4.5.20 Reaction optimisation for the 2-OG Michael acceptor 188

4.6 Summary 190

Chapter 5 Synthesis of benzisothiazolinone inhibitors of SARS-CoV-2 Main Protease 193

5.1 Introduction 193

5.1.1 Structure and function of the SARS-CoV-2 main protease 195

5.1.2 Reported inhibitors of the SARS-CoV-2 main protease 196

5.1.3 Mechanistic studies on the inhibition of M^{pro} by compound 203 197
5.1.4 Development of ebsulfur inhibitors against M^{pro} 199
5.2 Synthesis of first generation ebsulfur inhibitors 201
5.2.1 Overview of the synthetic route 201
5.2.2 Determination of IC_{50}s for first generation compounds against M^{pro} 203
5.2.3 Protein-observed mass spectrometry of first-generation compounds with M^{pro} 207
5.2.4 Ebsulfur paper by Sun *et al.* 213
5.3 Second-generation ebsulfur inhibitors 216
5.3.1 Design of second-generation compounds 217
5.3.2 Synthesis of second-generation ebsulfur compounds 218
5.3.3 Inhibitory activity of second-generation ebsulfur compounds against M^{pro} 220
5.3.4 Protein-observed mass spectrometry of second-generation compounds with M^{pro} 222
5.3.5 Future development of ebsulfur M^{pro} inhibitors 228
5.4 Ebsulfur compounds as inhibitors of Ldts 229
5.4.1 Protein Observed Mass Spectrometry experiments with Ldt_{Mt2} 230
5.5 Multi-drug-resistant *M. tuberculosis* cellular assays 237
5.5.1 Introduction 237
5.5.2 Flow Cytometry Assay 237
5.5.3 Results for ebsulfur compounds 238
5.6 Summary 241
Chapter 6 Summary 243
Chapter 7 Experimental 256
7.1 General Information 256
7.2 General Procedures 257
7.2.1 General Procedure A – Sulfa-Michael addition 257
7.2.2 General Procedure B – *tert*-Butyl deprotection 258
7.2.3 General Procedure C – Amide coupling 258
7.2.4 General Procedure D – Oxidative sulfur insertion and ring closure[301] 259
7.3 Compound Synthesis 259
7.3.1 Characterisation Table for compounds synthesised by Siegfried Thun-Hohenstein 353
7.4 Biochemical Assays 354

7.4.1 General information 354
7.4.2 Fluorescence assays 355
7.4.3 Solid-phase extraction coupled to MS assays 356
7.4.4 Protein observed mass spectrometry assays 356
7.4.5 IDH1 expression and purification 357
7.4.6 Absorbance-based spectrophotometric IDH1 activity assay 357
Chapter 8 Bibliography 358
Chapter 9 Appendix ..... a
9.1 IC_{50} curves for compounds 319 against M^{pro} ..... a

Acknowledgements

My foremost thanks go to my supervisor, Professor Christopher J. Schofield, for his immeasurable contributions to my development as a scientist: for the freedom to pursue my own ideas; the encouragement he gave me to explore new areas of science; the opportunity to work in such a scientifically and culturally diverse laboratory; and his unwavering support during the tougher times of being a DPhil student.

My sincerest gratitude goes to the immensely selfless post-docs who always found time to lend me a hand – in particular, Dr. Alistair Farley and Dr. Gonzalo Campillos. I must also thank Dr. Robert Lesniak and Dr. Jurgen Brem, for helping me to find my feet in my project.

The collaborative nature of my work would simply not have been possible without the help of others in the Schofield Group. I must acknowledge the invaluable contributions that Tika Malla has made to my thesis: by running mass spectrometric and fluorescence-based assays for the Ldt and M^{pro} projects; crystal soaking experiments; as well as her patience for my general biological ignorance; and much more. I must thank Raphael Reinbold for his generosity in screening my 2-OG analogues against his IDH variants, and I thank Dr. Karina Calvopiña for teaching me how to run MIC assays, and for tutoring me in the mysterious ways of bacteria. I would also like to thank Dr. Chris Moon and Dr. Joanna Bacon for their collaboration regarding *M. tuberculosis* flow cytometry assays.

I have much gratitude for my LG9 colleagues over the years, with whom working every day was a pleasure. In no particular order, Alen, Daniel, Gayatri, Jimmy, Ziggy, Solange, Tharindi, Alistair, Shifali, Lewis, Rob, Gonzi – you all are the best!

Thank you to Dr. Alen Krajnc, Dr. Alistair Farley, Mark Corbett, Jennifer Carter, Siegfried Thun-Hohenstein, and my parents for their time and energy proof-reading this thesis. I must also thank Tesco PLC and their smorgasbord of Meal Deal combinations for fuelling my write-up.

Thanks to Raphael Reinbold and Klemensas Simelis for fruitful discussions in the lab and vegetable discussions in the allotment, and thanks to Toby John for pushing my triathlon training to the next level.

Thank you to Jenny for brightening every aspect of my life.

Finally, I must thank my parents for their endless support of my education and for making all of this possible.

List of Abbreviations

2-OG	2-oxoglutarate
2-HG	2-hydroxyglutarate
Å	angstrom
ADP	adeonisine diphosphate
Ala	Alanine
AML	acute myeloid leukaemia
AMP	ampicillin
anh.	anhydrous
aq.	aqueous
ATMO	2-amino-4-thiazolyl methoxyimino
ATP	adenosine triphosphine
BIT	benzisothiazolinone
BLI	β-lactamase inhibitor
Boc	*tert*-butyl carbonyl
Boc_2O	di-*tert*-butyl dicarbonate
cf.	*conferatur*
COVID-19	coronavirus disease 2019
CV	calcein violet
DAP	diaminopimelic acid
DAST	diethylaminosulfur trifluoride
DBO	diazabicyclooctane
DBU	1,8-diazabicyclo[5.4.0]undec-7-ene
DCC	dicyclohexylcarbodiimide
Ddl	D-Ala-D-Ala ligase
DIAD	diisopropyl azidodicarboxylate
DIPA	diisopropylamine
DIPEA	diisopropylethylamine
DMA	dimethylacetamide
DMAP	4-dimethylaminopyridine
DMF	dimethylformamide
DMSO	dimethyl sulfoxide
DNA	deoxyribonucleic acid
DTT	dithiothreitol
E	*entgegen*
EDCI	*N*-(3-dimethylaminopropyl)-*N*'-ethylcarbodiimide hydrochloride
ESBL	extended-spectrum β-lactamase
ESI	electrospray ionisation
EtOAc	ethyl acetate
eq.	equivalent
FDA	food and drug administration
Fmoc	fluorenylemthyloxycarbonyl
FRET	Förster resonance energy transfer
g	gram

gem	geminal
gen	generation
GlcNAc	*N*-acetylglucosamine
h	hours
HATU	*N*-[(dimethylamino)-1*H*-1,2,3-triazolo-[4,5-b]pyridin-1-ylmethylene]-*N*-methylmethanaminium hexafluorophosphate *N*-oxide
HIV	human immunodeficiency virus
HMBC	Heteronuclear multiple bond correlation
HNE	human neutrophil elastase
HOBt	hydroxybenzotriazole
HPLC	high-performance liquid chromatography
HRMS	high-resolution mass-spectrometry
HTS	high-throughput screen
IC50	half-maximal inhibitory concentration
ICT	isocitrate
IDH	isocitrate dehydrogenase
IMP	imipenemase
IR	infra-red
JmjC	Jumonji C
KDM	histone demethylase
Ki	inhibitor constant
KOTMS	potassium trimethylsilanoate
L	litre
LC	liquid chromatography
LCMS	liquid-chromatography-mass spectrometry
Ldt	L,D-transpeptidase
LTV	lactivicin
LUMO	lowest unoccupied molecular orbital
Lys	Lysine
M	molar
M/z	mass to charge
MBL	metallo-β-lactamase
MDR-TB	multi-drug resistant tuberculosis
Me	methyl
MeCN	acetonitrile
mg	milligram
MHz	megahertz
MIC	minimum inhibitory concentration
min	minutes
mL	millilitre
mM	millimolar
Mp	melting point
M^{pro}	SARS-CoV-2 main protease
MRSA	methicillin-resistant *Staphalococcus aureus*
MS	mass spectometry
MurA	UDP-*N*-acetylglucosamine enolpyruvyl transferase

MurB	UDP-*N*-acetylenolpyruvoylglucosamine reductase
MurC	UDP-*N*-acetylmuramate-L-alanine ligase
MurD	UDP-*N*-acetylmuramoylalanine-D-glutamate ligase
MurE	UDP-*N*-acetylmuramoyl-L-alanyl-D-glutamate ligase
MurF	UDP-*N*-acetylmuramoyl-tripeptide-D-alanyl-D-alanine ligase
MurNAc	*N*-acetylmuramic acid
NAD	nicotinamide adenine nucleotide
NADP	nicotinamide adenine nucleotide phosphate
NDM	New Delhi MBL
NHS	*N*-hydroxysuccinimide
nM	nanomolar
NMM	*N*-methylmorpholine
NMP	*N*-methyl pyrrolidinone
NMR	nuclear magnetic resonance
NRPS	non-ribosomal peptide synthetase
nt	not tested
PBP	penicillin binding protein
Pd/C	palladium on carbon
PDB	protein data bank
Pl^{pro}	papaein-like protease
PLTV	phenoxylactivicin
POMS	protein-observed mass spectrometry
PyBOP	benzotriazol-1-yloxytripyrrolidinophosphonium hexafluorophosphate
pyr	pyridine
rt	room temperature
R_f	retardation factor
ROS	reactive oxygen species
SAR	structure-activity relationship
SARS-CoV-2	severe acute respiratory syndrome coronavirus 2
sat.	saturated
SBL	Serine β-lactamase
SG	sytox green
SPE-MS	solid-phase extraction mass spectrometry
T3P	propylphosphonic anhydride
TB	tuberculosis
TCA	tricarboxylic acid
TET	ten-eleven translocation oxygenase
TFA	trifluoroacetic acid
THF	tetrahydrofuran
TLC	thin layer chromatography
TOF	time of flight
tol	toluene
TsOH	4-toluenesulfonic acid
UDP	uridine diphosphate
μg	microgram
μL	microlitre

μM	micromolar
UPLC	ultra-high performance liquid chromatography
v/v	volume per volume
VIM	Verona integron-incoded MBL
VRE	vancomycin-resistant *Enterococci*
w/w	weight per weight
WHO	world health organisation
wt	wild-type
Z	*zusammen*

To my parents.

Chapter 1 Introduction

1.1 Bacteria and bacterial infections

Bacteria are a domain of prokaryotic microorganisms that are among the earliest life forms to appear on Earth.[1] Bacteria are typically 0.5-5.0 micrometers in length and generally assume one of three shapes: spherical cocci; rod-shaped bacilli; or spiral-like spirochaetes.[1] While bacteria are apparently unicellular, some species form characteristic multicellular structures and produce protective biofilms.[2] Bacteria inhabit nearly every habitat on Earth and play essential roles in the life cycles of countless other organisms, such as in the decomposition of organic matter and the fixation of molecular nitrogen into bioavailable nitrates.[3-5]

Humans are host to numerous symbiotic bacterial species that assist in the digestion of food, the synthesis of vitamins, and the defense of the host against pathogens (by competitive exclusion).[6, 7] However, pathogenic bacteria are responsible for a myriad of infection-related illnesses ranging from mild infections of the skin and respiratory tract, to debilitating long-term infections like Lyme disease, or life-threatening illnesses such as typhus and meningitis.[8]

Modern approaches to the treatment and prevention of bacterial infections began in the 19th century with Lister's development of aseptic surgical techniques.[9] The implementation of such practices dramatically reduced medical complications associated with post-surgical bacterial infections, though they only served to

prevent bacterial infections rather than treat them. The first modern chemotherapy for the treatment of human bacterial infections was the use of mercuric salts for the treatment of syphilis, however these treatments had poor efficacy and were highly toxic to patients.[10] The discovery of an organoarsenic compound salvarsan (**1**) followed, which displayed lower toxicity and higher efficacy compared to mercurous chloride.[11] In 1936, the diaza compound prontosil (**2**) was discovered as an effective therapy against *Streptococci*.[12]

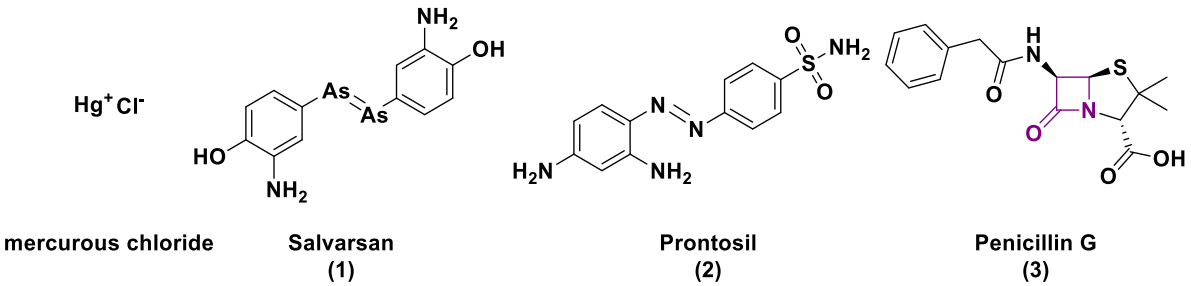

mercurous chloride | Salvarsan (1) | Prontosil (2) | Penicillin G (3)

Figure 1-1 | Structures of early antibacterial agents.

The discovery of the β-lactam-containing penicillin, exemplified by penicillin G (**3**), was arguably one of the most important discoveries in the modern antibiotic era.[13] In the time since the discovery of penicillins, multiple classes of antibiotics with different structures and cellular targets have been discovered.[14] While these other antibiotic classes play integral roles in modern healthcare systems, the β-lactam antibiotics remains the most widely prescribed class of antibiotics worldwide to date. The molecular targets of β-lactam antibiotics are specific proteins (see **Section 1.2.2**) involved in the synthesis of the bacterial cell wall, which are not found in

human cells. The continued success of β-lactams is largely due to their low toxicity as a direct result of their high selectivity for biological targets specific to bacteria.[15]

1.2 The bacterial cell wall

A defining feature of bacterial morphology is the presence of a bacterial cell wall. Cell walls are present in nearly all bacteria and serve many functions.[16] The cell wall provides structural rigidity, resisting the internal osmotic pressure of the cellular contents and thereby protecting the bacterium from external physical forces. The cell wall also acts as a barrier to harmful environmental conditions and toxic chemicals, and it additionally serves as a scaffold for the attachment of various surface proteins and other biomolecules, each with their own importance.

1.2.1 Structure

The bacterial cell wall is primarily constructed from peptidoglycan polymers. Peptidoglycan consists of a carbohydrate backbone made up of *N*-acetylglucosamine (GlcNAc) and *N*-acetylmuramic acid (MurNAc) saccharides that are cross-linked together via polypeptide sidechains. While the exact nature of the cross-links varies between bacterial types and species, the overall effects of such crosslinks are to increase the structural integrity of the bacterial cell wall. [16]

Bacteria are classified as being either Gram-positive or Gram-negative based on a staining methodology developed in the 19th century by Hans Christian Gram, whereby Gram-positive bacteria retain the applied crystal violet stain after being

washed with ethanol, while Gram-negative bacteria do not.[17] This staining pattern is due to the outer cell membrane present in Gram-negative species that prevents the crystal violet stain from permeating their peptidoglycan cell wall. The bacterial cell walls of Gram-negative organisms are also significantly thinner than those of Gram-positive bacteria, and many of the lipopolysaccharides and other biomolecules found on the surface of Gram-positive cell walls are not found on Gram-negative cell walls.[18] Instead the outer membrane performs the functions of these cell wall surface biomolecules, such as acting as a selectively permeable filter for beneficial nutrients. The presence of the outer membrane has a substantial effect on the efficacies of antibiotics (by affecting both their influx and efflux) which will be discussed later in this thesis.

1.2.2 Bacterial cell wall biosynthesis

The synthesis of the typical bacterial cell wall occurs in three distinct stages beginning with the biosynthesis of the peptidoglycan disaccharide subunits (**Figure 1-2**).[19] In *Escherichia coli*, the biosynthesis of peptidoglycan begins in the cytoplasm with the synthesis of UDP-MurNAc from UDP-GlcNAc by the enzymes MurA and MurB. Enzymes MurC, MurD, MurE, and MurF then perform a series of sequential amino acid ligations to construct the pentapeptide sidechain attached to UDP-MurNAc; the final ligation reaction installs the D-Ala-D-Ala dipeptide moiety synthesised by D-Ala-D-Ala ligase (Ddl).

The second stage of bacterial cell wall synthesis involves the synthesis of the peptidoglycan precursor lipid II and its transfer onto the cell surface. The enzyme MraY catalyses the conjugation of the MurNAc-pentapeptide to an undecaprenyl phosphate chain (UP) to create lipid I, which is inserted into the cell membrane. MurG then catalyses the glycosylation of a UDP-GlcNAc onto lipid I to form lipid II. The *trans*-membrane enzyme flippase is proposed to then translocate lipid II to the outer leaflet of the cell membrane for assembly into the peptidoglycan polymer.

The third stage of cell wall biosynthesis involves the installation and cross-linking of lipid II subunits into the existing peptidoglycan polymer. These steps are catalysed by bacterial transpeptidases collectively known as penicillin binding proteins (PBPs).[20] The PBP1, PBP2, and PBP3 subclasses consist of bifunctional proteins with a *C*-terminal transglycosylase domain and an *N*-terminal transpeptidase domain. The glycosylation of the GlcNAc moiety of lipid I to a terminal MurNAc of the existing peptidoglycan polymer is catalysed by the transglycosylase domain of PBP. The transpeptidase domain of PBP then catalyses the cross-linking between the pentapeptide sidechains. PBP transpeptidases catalysis proceeds via reaction of a nucleophilic serine residue within its active site with one peptide substrate (the donor) to form an ester-linked acyl-enzyme complex that then reacts with an amino group (the acceptor) on a second peptide to give a cross-linked amide product.[21]

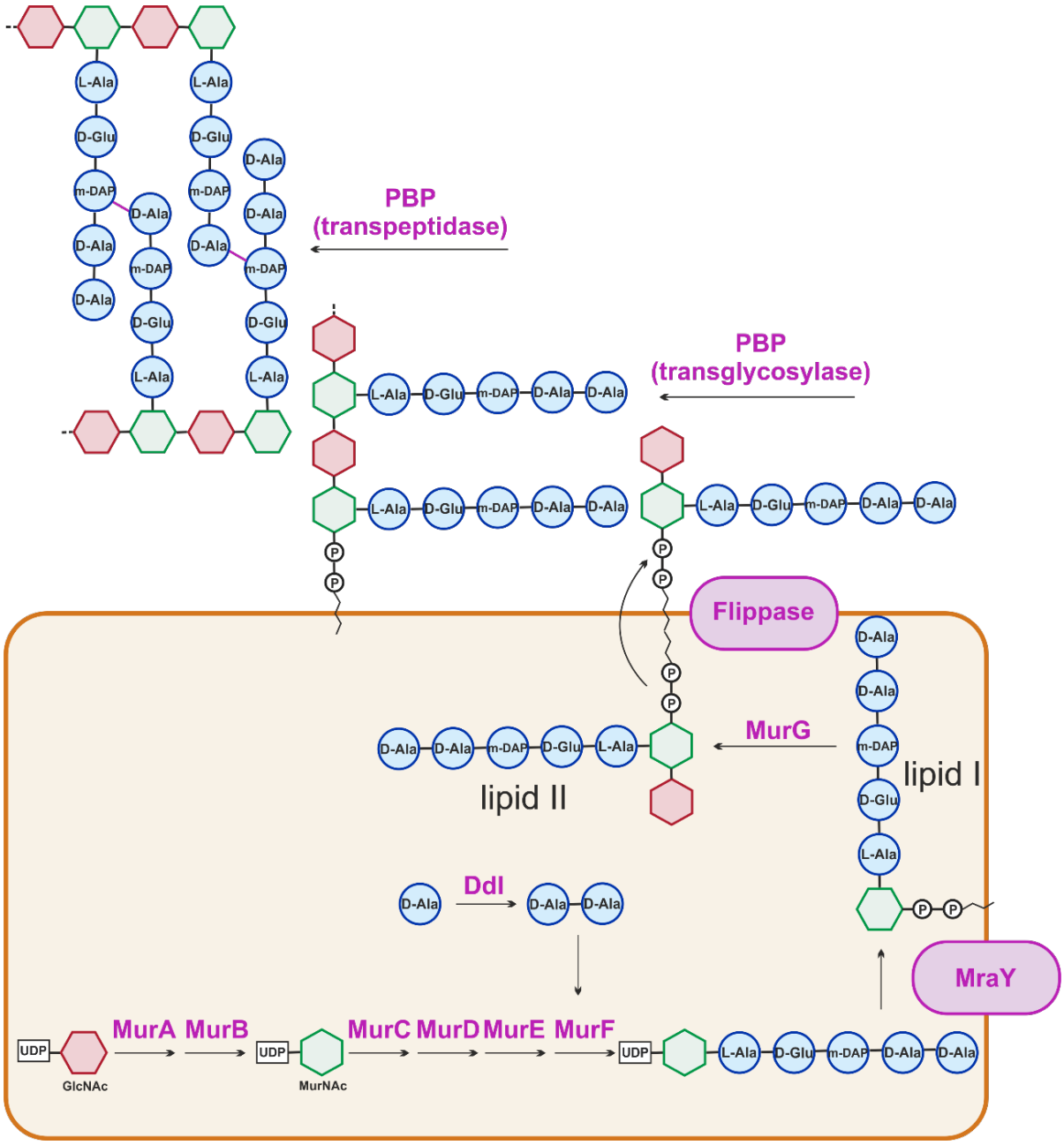

Figure 1-2 | Structure and synthesis of the bacterial peptidoglycan cell wall in *E. coli*. Abbreviations: m-DAP – diaminopimelic acid; UDP – uridine diphosphate. Adapted from Lovering *et al.*[19]

Whilst the bi-functional PBP subclasses (PBP1-3) perform the majority of nascent peptidoglycan synthesis, the subclasses PBP4 and 5 (which lack a transglycosylase domain) are primarily involved in the maintenance and repair of the cell wall.[20] PBP-catalysed 4,3-crosslinking is the dominant form of peptidoglycan crosslinking

in most bacterial species. However, in *Mycobacterium tuberculosis*, PBP-catalysed 4,3-crosslinking is present only in small amounts; the majority of peptidoglycan crosslinking in the *M. tuberculosis* consists of 3,3-crosslinks between *m*-DAP amino acids catalysed by L,D-transpeptidase (Ldt) enzymes.[22] While the transpeptidation reaction catalysed by Ldts is mechanistically analogous to PBPs, Ldts utilise a nucleophilic active-site cysteine rather than a serine residue to catalysed the transpeptidation reaction.[23]

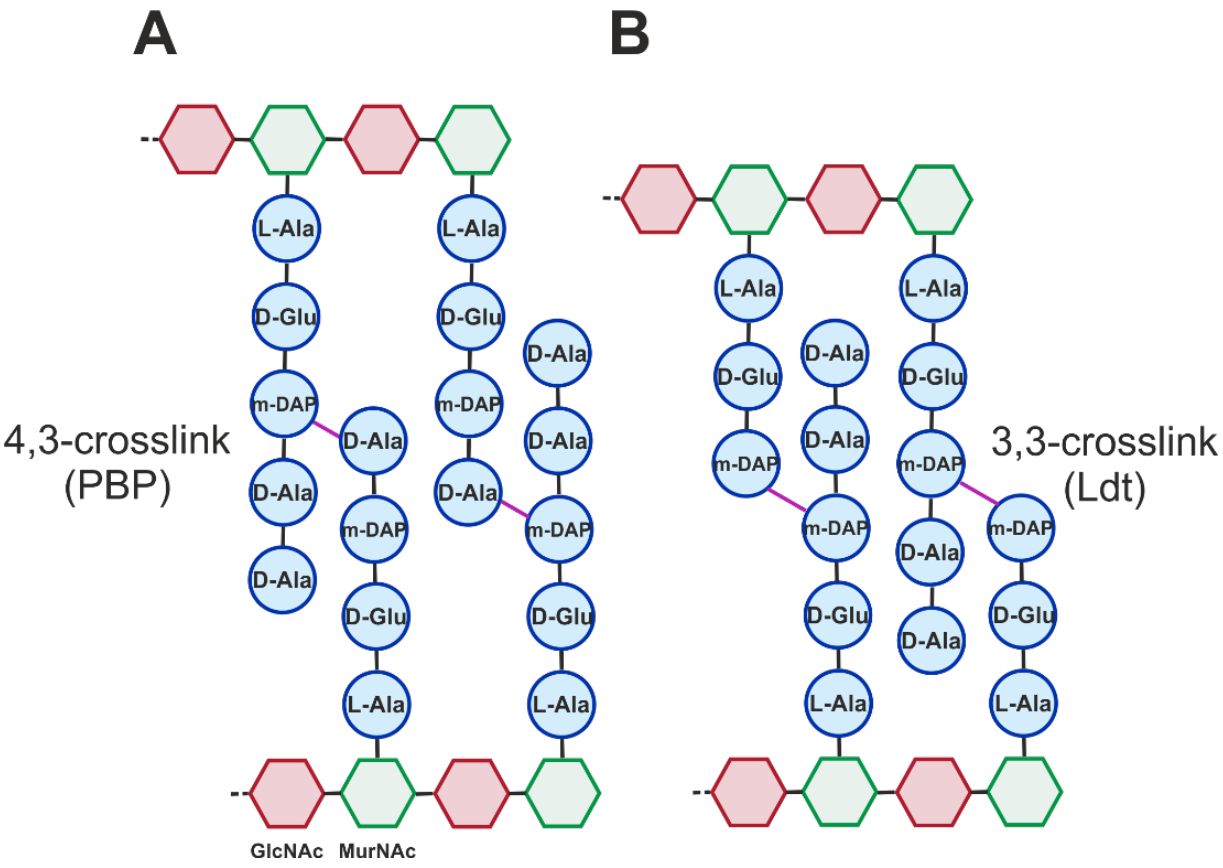

Figure 1-3 | Comparison of peptidoglycan crosslinking. (**A**) 4,3-crosslinking catalysed by PBPs. (**B**) 3,3-crosslinking catalysed by Ldts.

1.3 β-Lactam antibiotics

Since their discovery in the early 20th century,[13] β-lactam antibiotics have been the most widely used antibacterial agents and are regarded as one of the greatest discoveries in modern medicine.[24] The high prevalence of β-lactam antibiotics in contemporary healthcare systems is due to their broad-spectrum antibacterial efficacy, minimal off-target side effects, and the ease of their manufacturing. β-Lactams can be classified into four main groups: penicillins[25], cephalosporins[26], carbapenems[27], and monobactams.[28] The characteristic feature of all classes of β-lactam antibiotics is the β-lactam ring, which is essential for their antibacterial activity (**Figure 1-4**).

1.3.1 Structure-activity relationships for β-lactam antibacterial activity

The established molecular targets of β-lactam antibiotics are PBPs, the inhibition of which leads to the disruption of cell wall biosynthesis and, ultimately, cell death.[24] The structures of clinically useful β-lactam antibiotics consist of three main components: a core β-lactam ring and a carboxylate (or sulfonate); an acylamino sidechain (or hydroxyethyl sidechain for carbapenems); and, in the case of cephalosporins and carbapenems, *C*-3 sidechains. Each of these components contributes to the overall antibacterial activity, and variations of these components can be used to fine-tune the antibacterial properties of the inhibitor to suit specific therapeutic requirements.

The β-lactam antibiotics are structural mimics of the D-Ala-D-Ala moiety of the lipid II pentapeptide subunit (**Figure 1-4**). The ring strain and geometry of the β-lactam ring activate the lactam carbonyl towards an attack by the nucleophilic serine residue in an active site of a PBP. Whilst the mechanism of inhibition is analogous to the activity of the substrate, β-lactams react with PBPs to give an acyl-enzyme complex that is resistant to cleavage by nucleophiles, i.e. the amine of the acceptor substrate or water.[29] The bicyclic β-lactam may mimic a strained conformation of the peptide substrate, thus acting as transition-state analogues of the D-Ala-D-Ala transpeptidation reaction, as originally proposed by Tipper and Strominger.[30] Some classes of β-lactams, such as cephalosporins, which have a leaving group at the *C*-3' position undergo further reaction of the initially formed acyl-enzyme complex in a manner that stabilises the enzyme-inhibitor complex.[31]

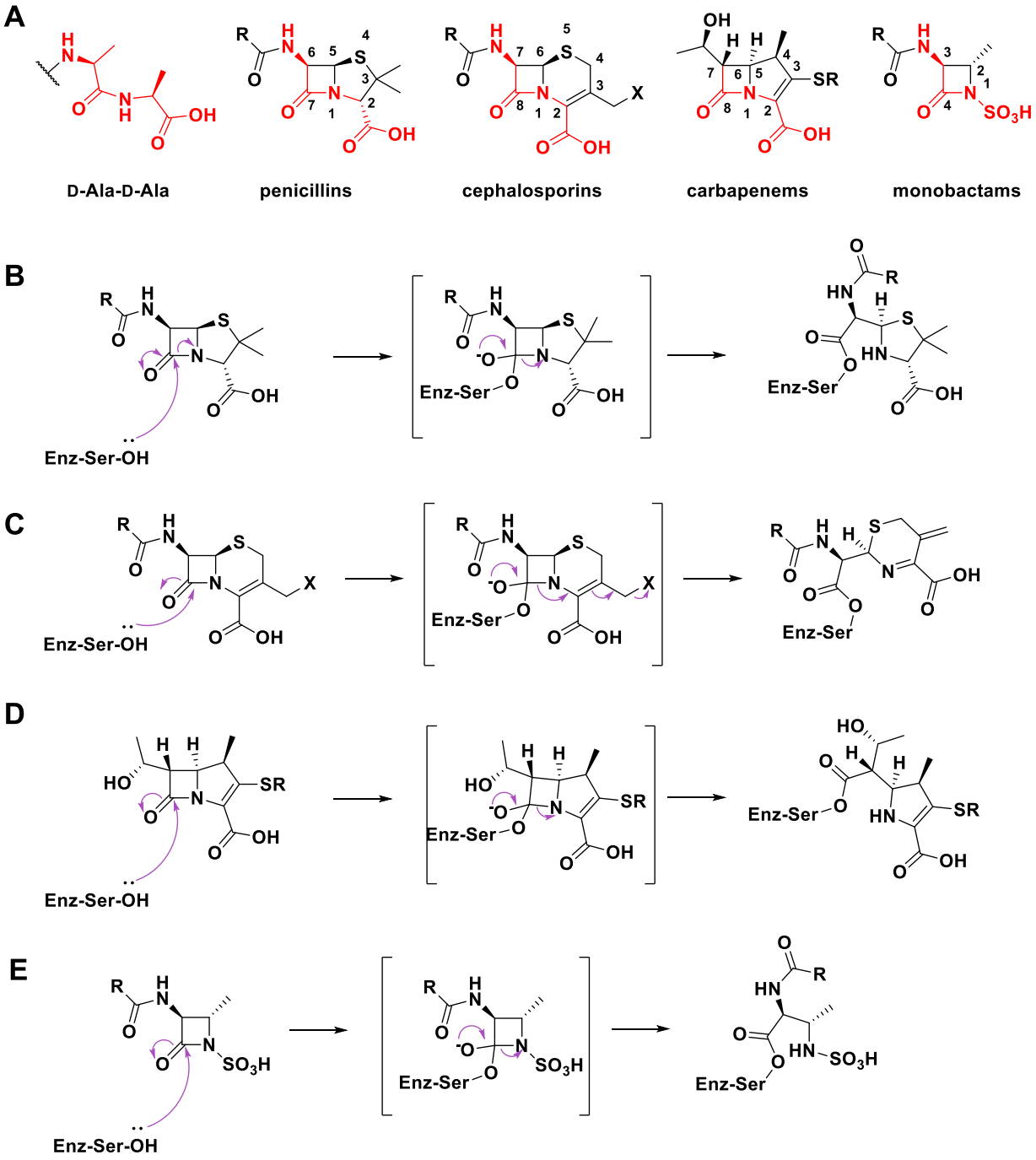

Figure 1-4 | (**A**) Structures of the PBP natural substrate (D-Ala-D-Ala) and β-lactam antibiotics. Reactions of PBPs with (**B**) penicillins, (**C**) cephalosporins, (**D**) carbapenems, and (**E**) monobactams.

1.3.2 The penicillins

The acylamino sidechains of β-lactam antibiotics play a crucial role in potentiating their antibacterial activity, hence the optimisation of the acylamino sidechain has been a key focus in the design of the successive generations of β-lactam antibiotics. (**Figure 1-5**). The natural penicillins, i.e. penicillin G (**4**) and penicillin V (**5**) possessed relatively simple benzyl and phenoxyacetyl sidechains, respectively, and exhibited a relatively narrow spectrum activity limited to susceptible Gram-positive bacteria.[32] Aminopenicillins, e.g. ampicillin (**6**) and amoxicillin (**7**) exhibit broader spectra of inhibitory activity than **3** and **5**, including in Gram-negative organisms such as *Escherichia coli*. However, resistance to these early penicillins quickly emerged via the production of β-lactamases, which can hydrolyse the β-lactam ring (as discussed in more detail in **Section 1.4**), promoting the development of second-generation penicillins with broader spectra of antibacterial activity that are less susceptible to β-lactamases. This generation of penicillins, whose members included methicillin (**8**), oxacillin (**9**), cloxacillin (**10**), and flucloxacillin (**11**) (amongst others), bore sterically bulky sidechains that reduced the binding affinity of the compounds to β-lactamases, which in turn improved their performance against some β-lactamase-producing bacteria.

Further development of the acylamino sidechain resulted in the third generation penicillins, such as carbenicillin (**12**), mezlocillin (**13**), piperacillin (**14**), and ticaricillin (**15**). These penicillins exhibited broader coverage of Gram-negative

strains compared to the earlier analogues, including *Pseudomonas aeruginosa* and, in the case of **15**, *Stenotrophomonas maltophilia*, though their Gram-positive activity was substantially reduced.

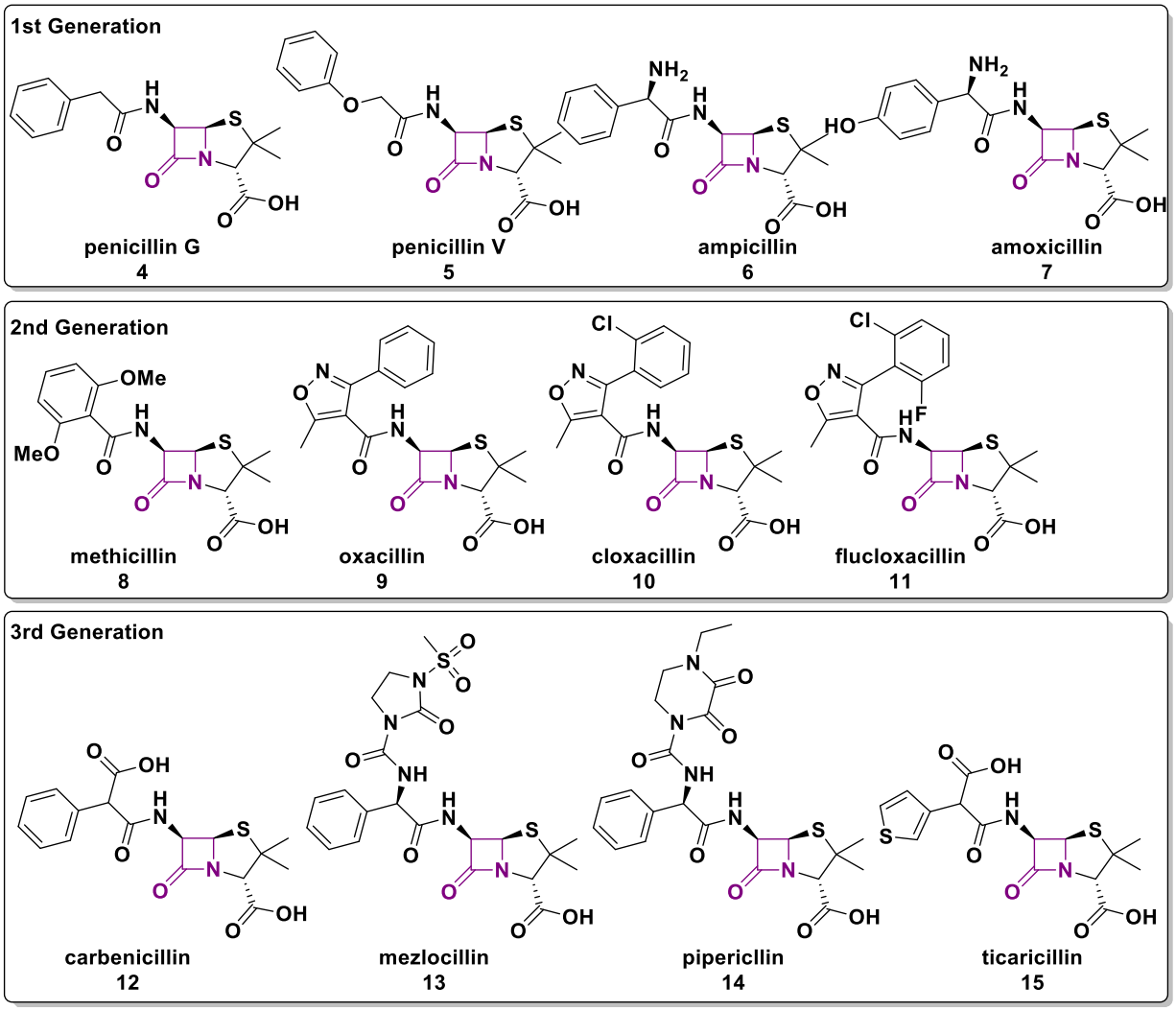

Figure 1-5 | Structures of the three generations of clinically approved penicillins.

1.3.3 The cephalosporins

Like the penicillins, the development of acylamino sidechains for the cephalosporins was an area of substantial research; however, research also focused

on the nature of the *C*-3′ X-group of the cephalosporins (**Figure 1-4**), which influences both the inhibitory activity and the physiochemical properties of the compound.

First-generation cephalosporins such as the representative compound cefalexin (**16**) feature similar acylamino sidechains to first- and second-generation penicillins and typically contain *C*-3 methyl groups. Substantial improvements to the Gram-negative antibacterial activity of second-generation cephalosporins such as cefaclor (**17**) were conferred with the introduction of leaving groups at the *C*-3′ position. While the Gram-negative activity of second generation cephalosporins was improved, the Gram-positive activity again was diminished.[33]

The third-generation cephalosporins continued the trend of increasing Gram-negative activity at the cost of decreasing Gram-positive activity. Like the second-generation cephalosporins, representative third-generation cephalosporins cefotaxime (**18**) and ceftazidime (**19**) had *C*-3′ leaving groups. In the case of **19**, the zwitterionic nature of the cephalosporin due to the pyridinium leaving group and sidechain carboxylate dramatically improved the outer membrane permeability of the compound. The *gem*-dimethyl carboxylate extension to the ATMO sidechain of ceftazidime increased the affinity of the compound for *P. aeruginosa* PBP3, hence ceftazidime shows potent antipseudomonal activity.

As resistance to β-lactams proliferated in anaerobic hospital-acquired bacterial infections, the development of cephalosporins shifted to designing compounds for

the treatment of specific bacterial species. Like **19**, the representative fourth generation cefiderocol (**20**) is an antipseudomonal cephalosporin with a *gem*-dimethyl carboxylate ATMO sidechain. The improvement in activity for **20** over **19** results from the addition of a siderophoric catechol moiety that further improves the uptake into bacteria, especially in low-iron conditions.[34]

The 5th generation cephalosporin ceftobiprole (**21**) also exhibits potent antipseudomonal activity and recent reports suggest that it is less susceptible to bacterial resistance than previous antipseudomonal cephalosporins.[35] Unlike nearly all clinically used cephalosporins, ceftaroline fosamil (**22**) shows potent Gram-positive activity against MRSA as well as strong inhibitory activity against resistant Gram-negative strains.[36]

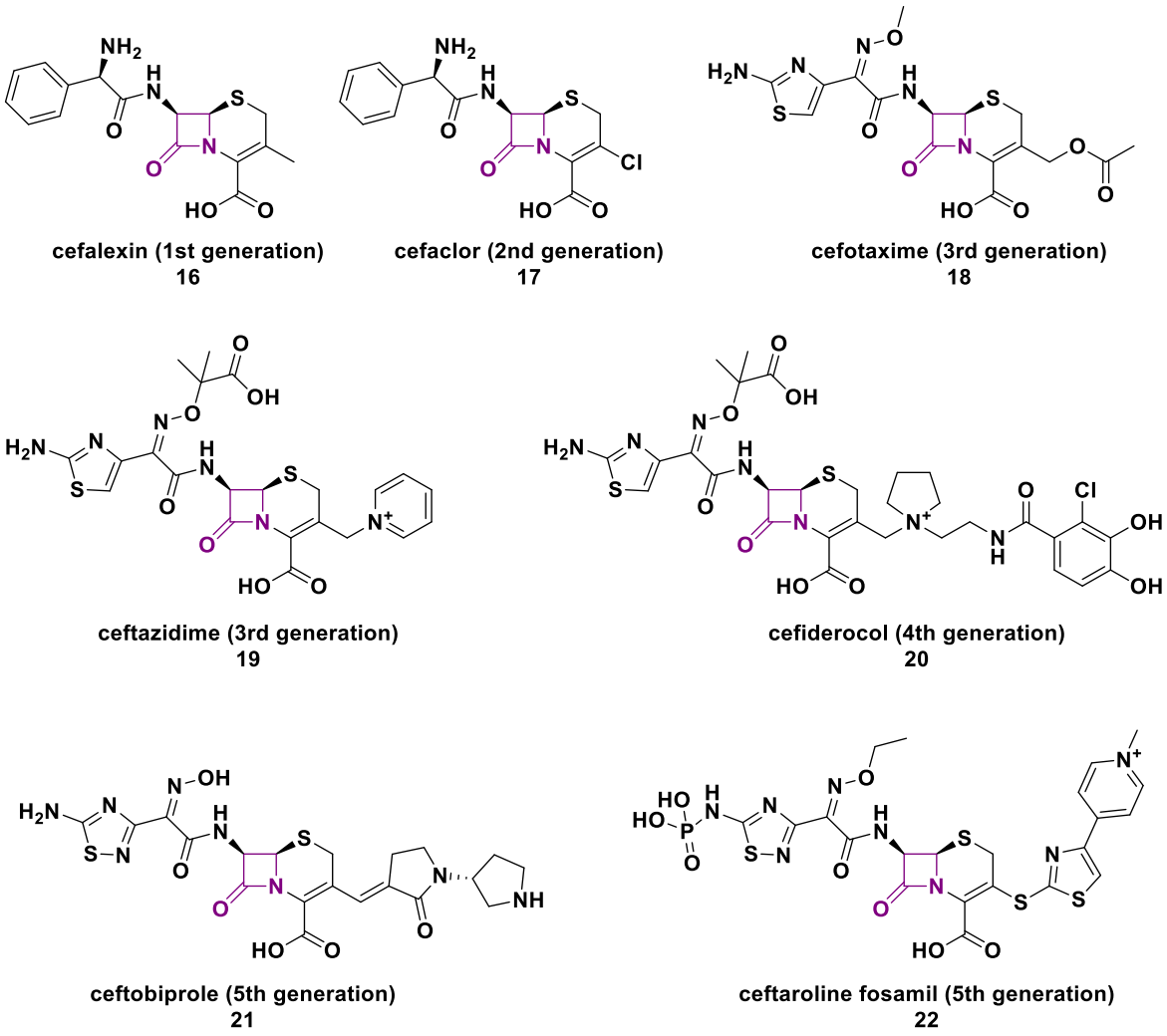

Figure 1-6 | Structures of different generations of clinically relevant cephalosporins.

1.3.4 The carbapenems

Carbapenem antibiotics represent the current state of the art for β-lactams (at least for intravenous administration), with the broadest clinical coverage of resistant bacterial strains. The first identified carbapenem, thienamycin (**23**), was isolated from *Streptomyces cattleya* and exhibited inhibitory activity against *S. aureus* via inhibition of PBP1 and PBP2.[37] Early studies showed that **23** was relatively stable to β-lactamases, prompting the development of synthetic carbapenem analogues.[38]

Imipenem (**24**) was the first clinically approved carbapenem, which was used to treat Gram-negative infections.[39] However, resistance to **24** quickly developed in *P. aeruginosa* and *Stenotrophomonas maltophilia*.[40] **24** is often administered in combination with the dehydropeptidase inhibitor cilastatin to reduce the rate of renal degradation *in vivo*.[41] Meropenem (**25**) exhibits greater potency than **24** against Gram-negative bacteria, but weaker activity against Gram-positive bacteria.[42] Unlike **24**, **25** is not degraded by dehydropeptidase and can be administered without cilastatin.[43] Ertapenem (**26**) is a potent inhibitor of MRSA, however it shows poor efficacy against *Pseudomonas* and *Acinetobacter* infections.[44] Benapenem (**27**) showed comparable activity against vancomycin-resistant *Enterobacteriaceae* (VRE) strains to **26** (MIC_{90} 0.25-4 μg/mL vs 0.5-1 μg/mL).[45] Recently, the sulfapenem sulopenem (**28**) was reported to possess potent antibacterial activity (MIC_{90} < 4 μg/mL) against β-lactamase producing strains of *Clostridium difficile*, *Bacteroides*, and *Prevotella* species – outperforming **24** and piperacillin/tazobactam combinations.[46]

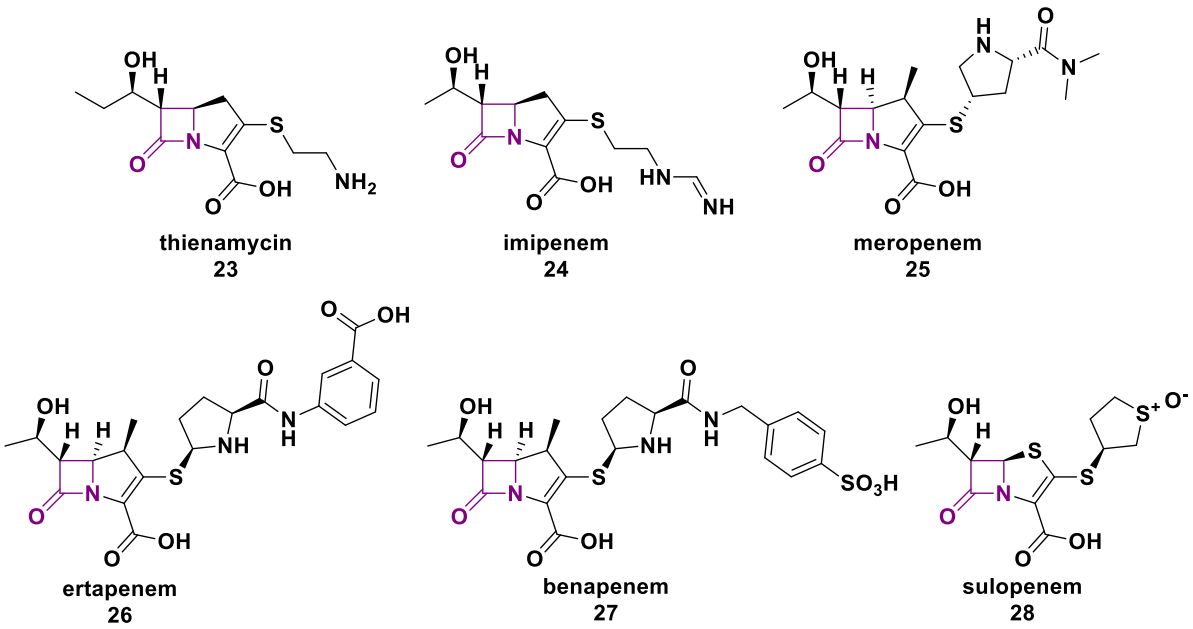

Figure 1-7 | Structures of selected carbapenems.

1.3.5 The monobactams

Monobactam antibiotics were discovered and developed in parallel with cephalosporins during the mid- to late-20th century. Unlike the other classes of β-lactam antibiotics discussed thus far, and as their name suggests, monobactams consist of a monocyclic β-lactam core which does not have the ring strain experienced by bicyclic β-lactams induced by the presence of the second ring. To compensate for this loss of activity, the lactam nitrogen is typically functionalised with a sulfonate group, which acts as a bioisostere of the *C*-2 carboxylate moieties found on bicyclic β-lactam antibiotics. The first monobactams were isolated from *P. acidophila* (compounds **29**, **30**, and **31**) and showed little antibacterial activity.[47] However, the reaction of these monobactams with PBPs encouraged the

development of synthetic analogues with improved antibacterial profiles. Sulfazecin (**32**) isolated from *P. acidophila* – possessed activity against *E. coli* and *P. mirabilis*.[48] The attachment of the ATMO-type sidechains of third- and fourth generation cephalosporins yielded monobactams with potent Gram-negative activity.

Monobactams are typically functionalised with the ATMO sidechains of cephalosporins and have additional ring modifications to improve their stability to β-lactamase hydrolysis. For example, aztreonam (**33**) has an ATMO derivative as an acylamino sidechain as well as a *gem*-dimethyl moiety on the β-lactam ring.[49] Compared to **33**, the monobactam tigemonam (**34**) demonstrated weaker antibacterial activity against *Pseudomonas spp.*, but stronger activity against *Streptococci*.[50] **34** also is substantially more stable than **33** to β-lactamase hydrolysis.[50] Nocardicin (**35**), however, utilizes the electron-withdrawing 2-(4-hydroxyphenyl) acetic acid moiety in place of a sulfonate. The siderophore-functionalised monobactams BAL30072 (**36**) showed high potency against clinically resistant strains of *A. baumannii* and *P. aeruginosa*, including strains expressing MBLs.[51] Similarly, the compound MB-1 (**37**), which featured a siderophore on the *C*-4 position rather than attached to the ATMO sidechain, was proposed to augment cellular uptake via PiuA and PirA siderophore receptors.[52]

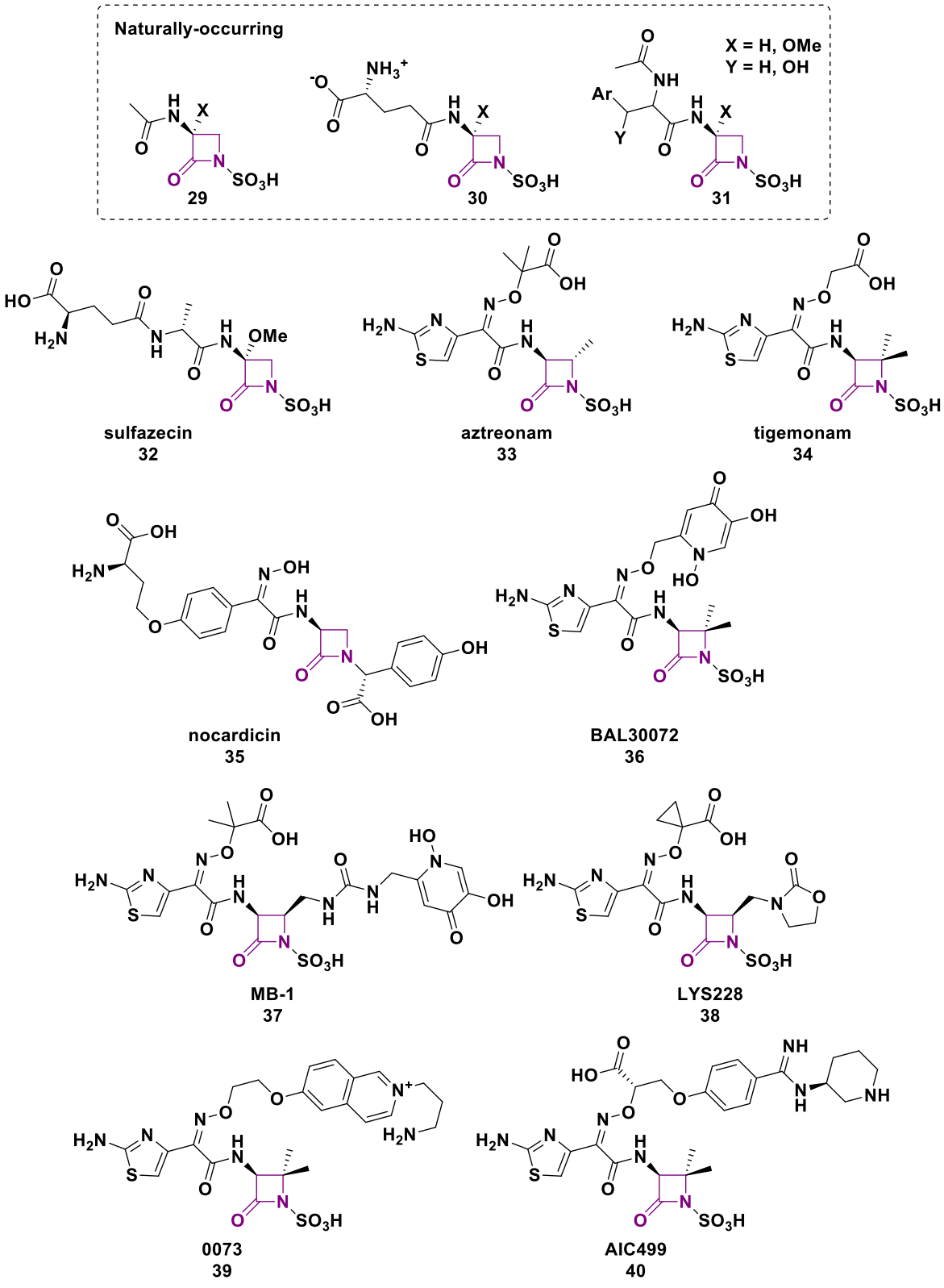

Figure 1-8 | structures of selected monobactams.

Recently, the monobactam LYS228 (**38**) has been reported (**Figure 1-8**), which features the addition of an oxazolidinone ring to the β-lactam via a methylene linker. Like **33**, **38** demonstrates potent inhibition of PBP3. Importantly, **38** shows remarkable resistance to degradation by MBLs, suggesting that the addition of steric bulk to the *C*-4 position of the β-lactam is beneficial to β-lactamase stability.[53] The quinolinium monobactam 0073 (**39**) was reported to exhibit potent antimicrobial activity in both *in vitro* and *in vivo* studies, and was found to inhibit several PBP and SBLs.[54] The zwitterionic nature of **39** might contribute to its improved activity, in a manner like other potent zwitterionic β-lactams.[54] The monobactam AIC499 (**40**) is a potent inhibitor of PBP3 from *E. coli* and *P. aeruginosa*.[55] Crystallographic studies show that the aryl sidechain occupies an aromatic cluster and contributes additional non-covalent binding interactions. It is plausible that a similar phenomenon also occurs for the quinolone moiety of **39**.[55]

1.4 The threat of antimicrobial resistance

Resistance to β-lactam antibiotics was first reported not long after the discovery of penicillin. Since then, bacteria have proven adept at developing resistance mechanisms for each successive generation of β-lactam antibiotics. Bacterial resistance mechanisms include: variations of membrane porins that reduce cell penetration;[56] the overexpression of efflux pumps that expel the antibiotics from the bacterium;[57] upregulation of PBPs; and the expression of β-lactamase inhibitors (amongst others).[58] While all of these resistance mechanisms are of concern, the

bacterial expression of β-lactamases poses the greatest threat to the clinical viability of β-lactam antibiotics.

In recent decades, the frequency and diversity of β-lactamases expressed by bacteria have increased at an alarming rate, caused by multiple factors including: bacterial horizontal gene transfer; improper antibiotic dosing regimens; the prophylactic use of human antibiotics in livestock populations; and many more.[59]

1.4.1 Overview of β-lactamases

There are two main types of β-lactamases: the serine β-lactamases (SBLs), which catalyse the hydrolysis of β-lactam rings using a nucleophilic serine residue; and the metallo-β-lactamases (MBLs), which utilise one or two zinc ions to coordinate a hydroxide ion that then hydrolyses the β-lactam ring. The β-lactamases are classified into four classes (Ambler classes) based on their primary structural homologies.[60] Classes A, C, and D comprise the SBLs while Class B β-lactamases are MBLs. Class A SBLs such as PSE exhibit a relatively narrow spectrum of β-lactam inactivation and are most commonly expressed by Gram-positive cocci.[61] Class A extended spectrum β-lactamases (ESBLs) that are able to hydrolyse cephalosporins in Class A include the TEM and CTX subclasses, as well as the KPC and SHV carbapenemases.[61] An important Class C SBL is the cephalosporinase AmpC, which is expressed primarily by *Enterobacteriacae*.[61] Though AmpC is inhibited by the clinically used SBL inhibitor clavulanic acid (**41**), highly resistant extended spectrum AmpC variants have now been reported.[61] The Class D SBLs are

commonly referred to as the OXA subclass, named after their ability to hydrolyse oxacillin-type penicillins.[61] ESBLs of Class D include the carbapenemases OXA-10, OXA-23, and OXA-48, which are capable of hydrolysing virtually all clinically used carbapenem antibiotics.[61] These enzymes are ubiquitous in resistant hospital-acquired bacterial infections of *A. baumannii* and *P. aeruginosa*, which are of particular concern.[62]

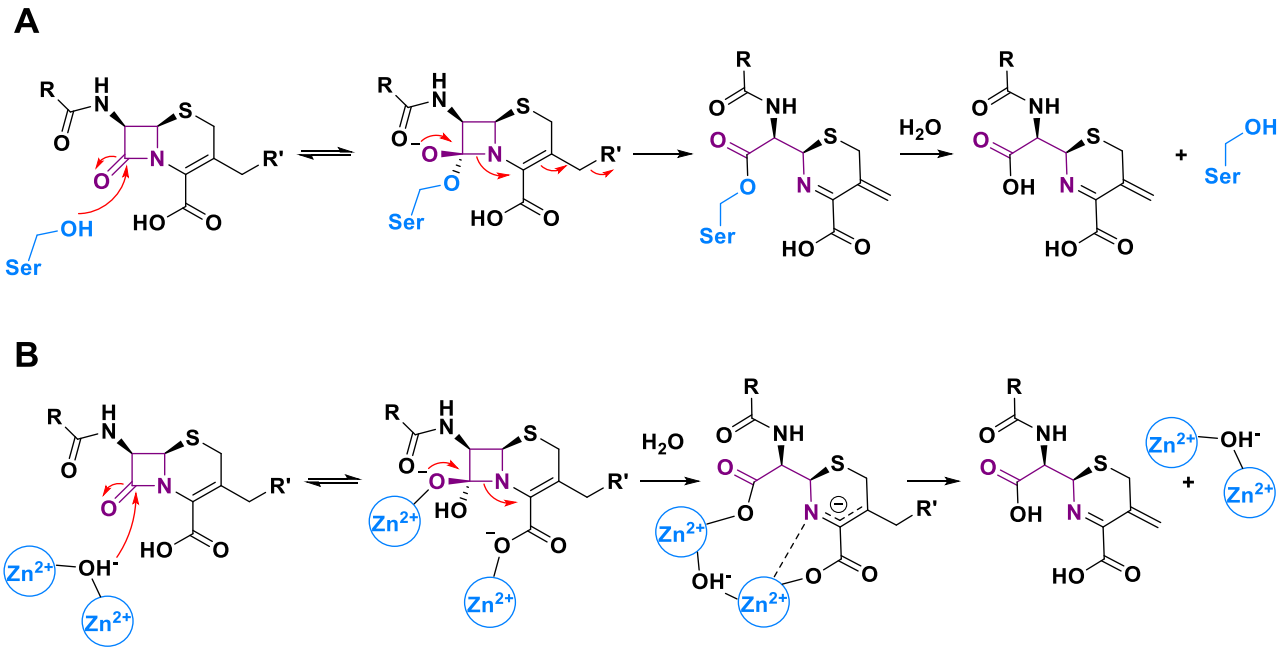

Figure 1-9 | Mechanisms of β-lactam hydrolysis by (**A**) SBLs and (**B**) MBLs. Adapted from Brem *et al.*[63]

Class B MBLs are subdivided into three subclasses (B1, B2, and B3) based on their amino acid sequences.[60] B1 and B3 subclass MBLs utilise two zinc ions in the active site while B2 MBLs use one. B1 MBLs such the imipenemase (IMP), Verona Integron-incoded MBL (VIM), and New Delhi MBL (NDM) families exhibit the

widest spectrum of hydrolytic activity against β-lactams, and therefore impart formidable levels of resistance to the bacteria that express them.[61]

1.4.2 β-Lactamase inhibitors

There are three classes of clinically-approved β-lactamase inhibitors (BLIs): β-lactam-based inhibitors; diazabicyclooctanes (DBOs), and boronic acids (**Figure 1-10**).[64] Clavulanic acid (**41**) is a β-lactam-based BLI with weak inhibitory activity against PBPs.[65] The structure-activity requirements for β-lactam-based BLIs appear to be quite different from β-lactam antibacterials.[66] The primary difference is the absence of an acylamino sidechain on β-lactam-based BLIs, which is not required for substrate binding to SBLs. The absence of this sidechain, however, likely results in the loss of PBP inhibition for these compounds. **41** can react covalently with the nucleophilic serine of SBLs to give a stable acyl-enzyme complex that can further react with other active site residues to give a cross-linked adduct.[67] Like **41**, the sulfone-containing sulbactam (**42**) and tazobactam (**43**) also inhibit SBLs through reaction of the β-lactam with nucleophilic serine residues to give stable covalent adducts that also can undergo further crosslinking.[68, 69]

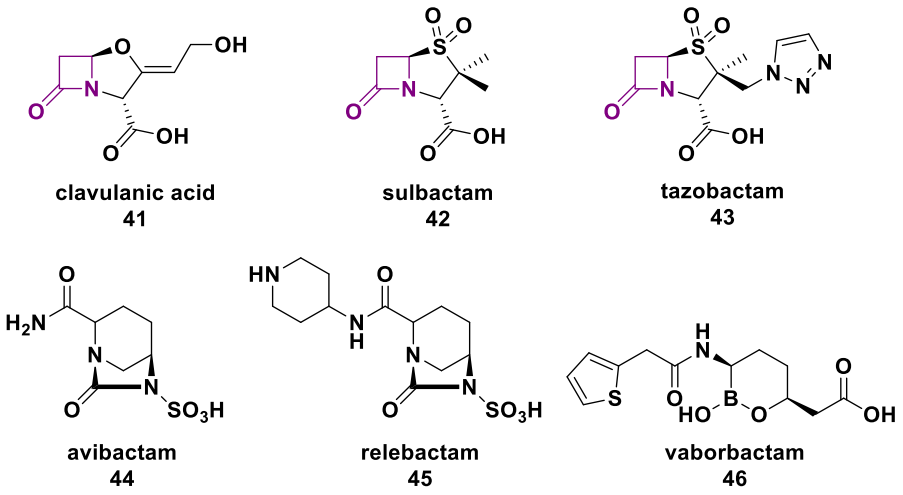

Figure 1-10 | Structures of clinically approved BLIs.

The DBO class of BLIs, which include avibactam (**44**) and relebactam (**45**) (**Figure 1-10**) are potent inhibitors of SBLs, though no clinically-approved DBOs exhibit potency against MBLs.[70] Like β-lactam-based BLIs, DBOs inhibit SBLs via covalent reaction of nucleophilic serine residues with the lactam carbonyl of the inhibitor, however, unlike β-lactam-based inhibitors, DBOs react reversibly.[71]

Boronate-based β-lactamase inhibitors are proposed to act as transition-state analogues of the tetrahedral intermediates arising from SBL/MBL catalysis of the β-lactam substrates.[72] The reaction of the nucleophilic serine with the sp^2-hybridised boronic acid species produces an sp^3-hybridised intermediate that mimics the structure of the tetrahedral intermediate resulting from the attack of a nucleophilic serine onto the carbonyl of a β-lactam antibiotic.[72] As is the case for all other mentioned clinically approved BLIs, the only clinically approved boronate BLI vaborbactam (**46**) shows no inhibitory activity against class B MBLs.[73]

The continued therapeutic use of the existing β-lactam antibacterials will therefore require the development of BLIs capable of inhibiting all classes of β-lactamases. Indeed, many academic and commercial research groups, including in Oxford, are working towards the development of novel BLIs with activity against MBLs.[74] However, the development of novel inhibitors of bacterial transpeptidases that are impervious to degradation by β-lactamases is equally important. The history of the development of non-β-lactam PBP inhibitors will now be described.

1.5 Non-β-lactam inhibitors of PBPs

In addition to the development of effective β-lactamase inhibitors, considerable research has been conducted to develop inhibitors of PBPs that do not contain a β-lactam ring; many of these molecules feature ring systems that aim to mimic the reactivity of the β-lactam ring. This section of the introduction will outline in detail the state of the art for non-β-lactam inhibitors of bacterial transpeptidases.

1.5.1 Non-covalent *S. aureus* PBP2a inhibitors

The 1,2,4-oxadiazole compounds **47a-c** and ND-421 (**48**) were shown to possess antibacterial activity against MRSA strains comparable to linezolid.[75, 76] These compounds were shown to inhibit PBP2a via a macromolecular synthesis assay that monitors the uptake of radiolabelled peptidoglycan precursors.[77] The dichloro-1,2-4 oxadiazole **49** showed moderate activity (MIC 8-32 μg/mL) against both Gram-positive and Gram-negative bacteria.[78] The quinazoline **50** shows bacteriostatic activity against MRSA *in vitro*, but enhances the bactericidal activity of β-lactams.[79]

The mechanism of action of **50** appears to be the allosteric non-competitive binding of **50** to PBP2a, inducing a conformational change such that the active site can accommodate β-lactams that typically do not inhibit *S. aureus* PBP2a such as **14**.[79] Amides **51a-c** and sulfonamide **52** were identified as *S. aureus* PBP2a inhibitors via a high-throughput screen (HTS), however these compounds showed weak antibacterial activity against Gram-positive species.[80] **52** was slightly more potent against *S. aureus* PBP2a than the analogous amides **51** (cf. *S. aureus* PBP2a IC_{50}s: **52** = 97 μM vs **51a** = 210 μM, **51b** = 230 μM, and **51c** = 680 μM), but was inactive against Gram-negative strains (MIC >1024 μg/mL) and showed only moderate activity (MIC 32 μg/mL) against Gram-positive strains while also appearing to have multiple bacterial targets.[80]

Like **50**, the chlorosulfonamide Of1 (**53**) augments the activity of β-lactams against MRSA but does not possess antibacterial activity on its own. Podoll *et al*. reported that **53** can interfere with the expression of β-lactamases in response to β-lactams, suggesting **53** might have use in combination therapies with β-lactam antibitiocs.[81] Aspermerodione (**54**) showed moderate antibacterial activity (32 μg/mL) against MRSA and worked synergistically with β-lactams; docking studies suggest it is a non-covalent inhibitor of PBP2a that binds between the transpeptidases and transglycosylase domains.[82] The thioxanthone compound **55** showed moderate antibacterial activity (16 μg/mL) against *S. aureus* but no activity against Gram-negative bacteria; docking suggested the compound may bind allosterically to

PBP2a.[83] Compounds **56** and **57**, discovered by HTS to inhibit *S. aureus* PBP2a, show potent anti-MRSA activity (4 μg/mL and 6 μg/mL, respectively) and low cytotoxicity against human L-02 cells (IC_{50}s > 20 μM).[84] While these compounds may have shown moderately strong binding to *S. aureus* PBP2a *in silico*, no direct biochemical evidence was presented that confirmed their mode of action was the inhibition of bacterial transpeptidases.

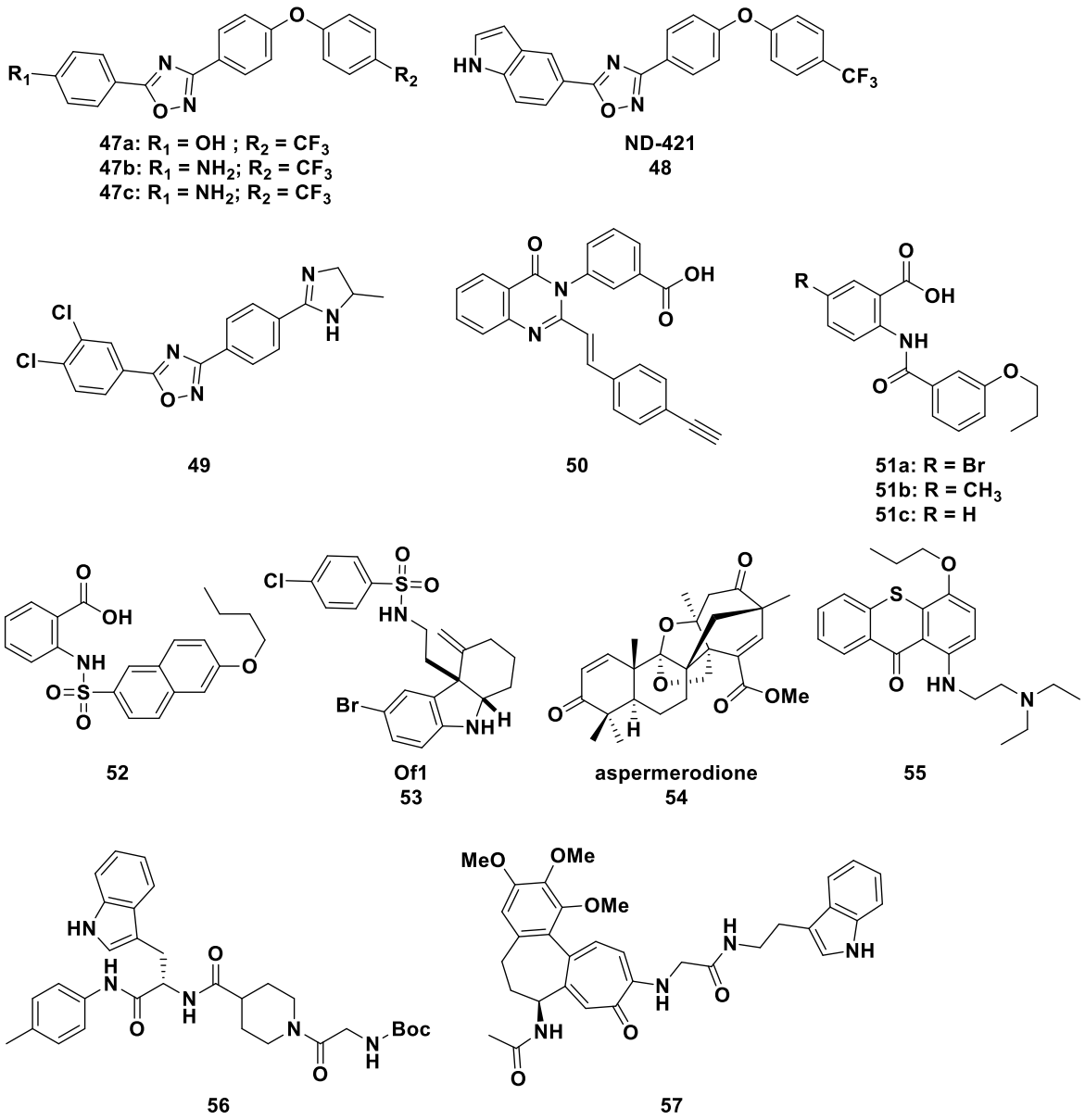

Figure 1-11 | Structures of non-covalent inhibitors of *S. aureus* PBP2a.

The nitroimidazole analogues **58** and **59** were predicted to bind to *S. aureus* PBPs via docking studies; they exhibited potent MICs against *S. aureus* (1 μg/mL and 4 μg/mL, respectively) and showed weak antibacterial activity against Gram-negative bacteria. In addition, co-administration of **58** and/or **59** with the β-lactam antibiotic **10** was found to significantly enhance its inhibitory activity in MRSA.[85, 86] However, their intrinsic antibacterial activity is likely augmented by the presence of the nitroimidazole moiety, which is known to cause DNA disruption to bacterial cells via the generation of nitroso radicals.[87] Quercetin 3-*O*-rutinoside (**60**) possessed weak antibacterial activity and molecular dynamics simulation studies suggested that **60** augmented the activity of β-lactams via allosteric binding to PBP2a.[88, 89] The polyphenol saccharides **61** and **62** augmented the activity of **9** (>128 μg/mL to 1 μg/mL). Similarly to **50**, it was proposed that the binding of compounds **61** and **62** to PBP2a induce conformational changes to the PBP2a active site that in turn allowed for the greater binding affinity of **9**.[90] However, as for the compounds shown in **Figure 1-11**, no empirical measurements of the compounds' inhibitory activity against bacterial transpeptidases was reported, therefore any antibacterial activity exhibited by these compounds cannot be attributed to transpeptidase inhibition at this time.

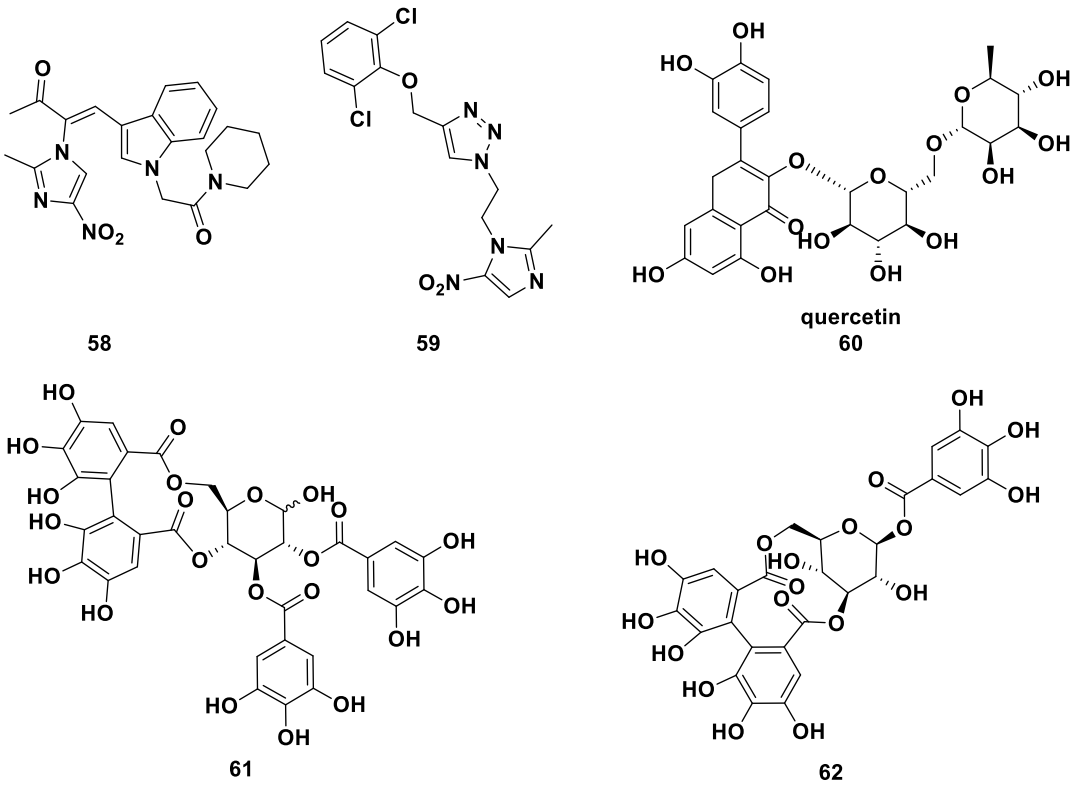

Figure 1-12 | Structures of non-covalent inhibitors of *S. aureus* PBP2a (continued).

1.5.2 Cyclopentenones

The cyclopentanones **63** and **64** were designed as alkylating analogues of β-lactams with acylamino sidechains, an activated carbonyl group, and a carboxylate moiety. However, no antibacterial activity was observed versus Gram-positive or Gram-negative strains, nor there any was inhibition of the *Streptomyces spp.* D,D-carboxypeptidase R39 reported for **63** or **64**.[91]

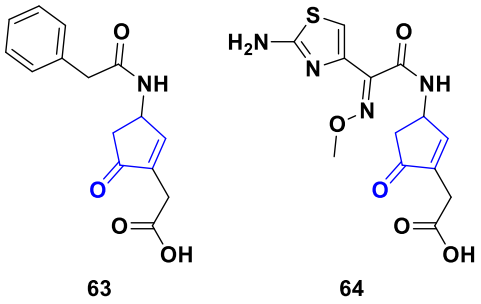

Figure 1-13 | Structures of 2-cyclopenten-1-one derivatives tested for antibacterial activity.

1.5.3 Thioesters

The rhodanine derivatives **65**, **66**, **67**, and **68** showed 10-38 μM inhibition of *S. aureus* PBP2a.[92] Additionally, the antibacterial activity was observed for compounds **65-68** vs MRSA (MIC 2-12 μg/mL), *E. faecalis* (MIC 3-18 μg/mL), *E. faecium* (MIC 4-29 μg/mL), *M. catarrhalis* (MIC 0.6-1 μg/mL), *H. influenzae* (MIC 4 μg/mL), but not for *S. pneumoniae* (MIC >200 μg/mL) or *E. coli* (MIC >200 μg/mL).[92] Compounds **65-68** appeared to be non-competitive inhibitors as the dissociation constants for the inhibitors were unaffected by presence of the natural substrate. **65-68** were shown to interfere with peptidoglycan synthesis via radiolabelled UDP-[^{14}C]GlcNAc uptake assays.[77] However, given the promiscuous nature of rhodanines, their precise mode of action as antibacterial agents should be regarded as uncertain.[93]

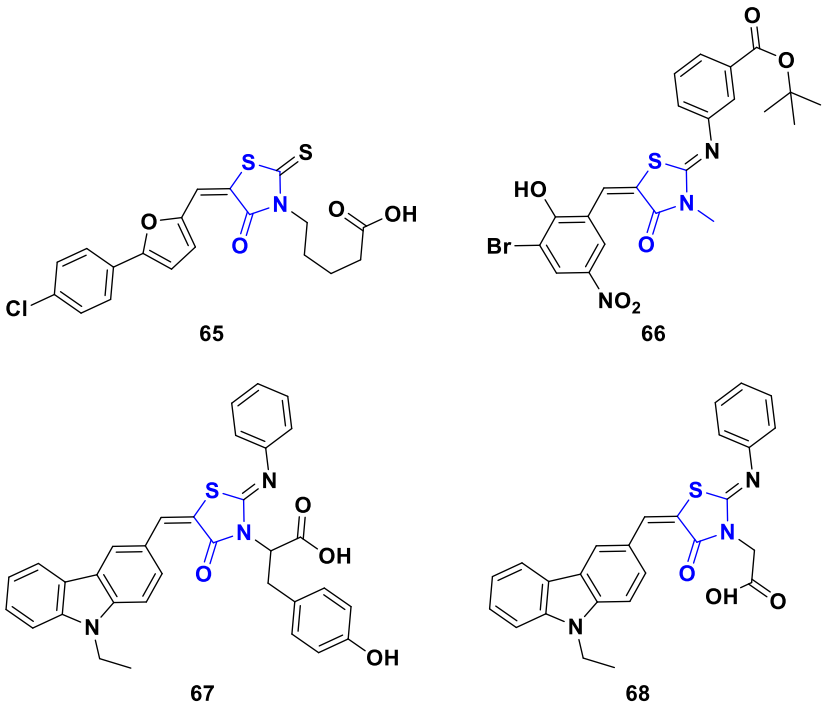

Figure 1-14 | Structures of selected rhodanines and arylaklylidiene iminiothiazolidin-4-one non-covalent PBP inhibitors.

1.5.4 Cyclobutanone analogues of β-lactams

4,5-Bicyclic cyclobutanones were synthesised as analogues of the antibacterial carbapenem **69**.[94] While cyclobutanone analogues with penicillin G-type sidechains **70**, **71** and **72** showed no antibacterial activity, compounds **70** and **71** did show some time-dependent inhibition of TEM and B1 β-lactamases.[94] The chloro- intermediate **73** also demonstrated inhibitory activity against TEM and B1 subclass MBLs.[94] Gordon *et al.* reported the synthesis of bicyclic cyclobutanones **74**, **75**, and **76**, however none exhibited antibacterial activity.[95] The oxime **77** was prepared by Meth-Cohn *et al*. as a potential β-lactamase inhibitor, though no activity data was reported.[96] The dichloro- derivatives **78**, **79**, and **80**, prepared by Johnson *et al.* and

exist as their hydrate forms in aqueous solution, demonstrated modest antibacterial activity and inhibited all tested classes of β-lactamases in the micromolar range.[97] The hydrate form is proposed to act as a transition-state analogue of the tetrahedral β-lactam intermediate formed during β-lactamase hydrolysis.[97] Compound **81** showed no reported antibacterial activity,[98] while sulfoxide **82a** and sulfone **82b** showed moderate activity against *S. aureus* (MIC 25-50 μg/mL) and also augmented the antibacterial function of β-lactams in bacterial strains that produced β-lactamases.[99]

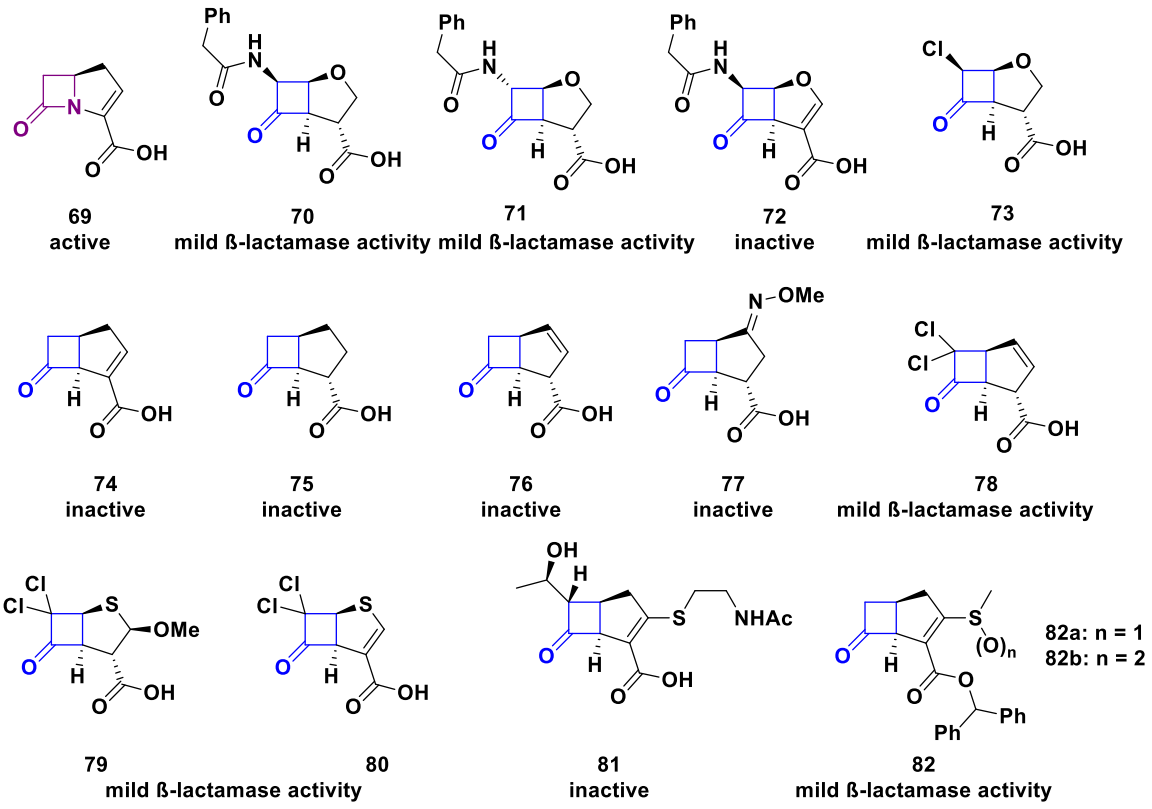

Figure 1-15 | Structures of cyclobutanone analogues of the carbapenem **69**.

1.5.5 β-Lactam isosteres

Compounds featuring bioisosteres of the β-lactam moiety have been investigated by multiple research groups (**Figure 1-16**). Cavagna *et al.* synthesised β-sultam analogues **83** and **84** of penicillanic acid, however these compounds did not exhibit any antibacterial activity.[100] Llinas *et al*. later reported that monocyclic β-sultams **85a-d** inhibit *Strepromyces* D,D-transpeptidase R61.[101] Mechanistic studies revealed that β-sultams are substantially less reactive towards nucleophiles than the analogous β-lactams, and that the amide nitrogen must be made sufficiently electron-deficient by an electron-withdrawing moiety to unlock its reactivity towards biological nucleophiles.[102] The benzoyl analogue **85a**, developed by Beardsell *et al.* showed inhibition of human neutrophil elastase (HNE), spurring the development of β-sultams **86** and **87** as HNE inhibitors.[103, 104] The tosyl-azetidin-2-imine analogues **88** and **89** were reported to show no antibacterial activity, while analogue **90** showed micromolar inhibition of Class A, Class B, and Class D β-lactamases. The β-thiolactam analogue **91** showed a dramatic reduction in activity compared to its penicillin analogue **5**.[105] Obafluorin (**92**) exhibits weak antibacterial activity against Gram-positive and Gram-negative bacteria (MIC > 100 μg/mL) that was shown to react covalently with PBPs.[106, 107] The iron-chelating catechol moiety of **92** acts as a siderophore that is postulated to contribute to the antibacterial activity of **92**.[108] Salinosporamide A (**93**) possesses both a γ-lactam and a β-lactone

ring, and is a proteasome inhibitor being investigated as an anticancer agent; it is not reported to be an antibacterial agent to date.[109]

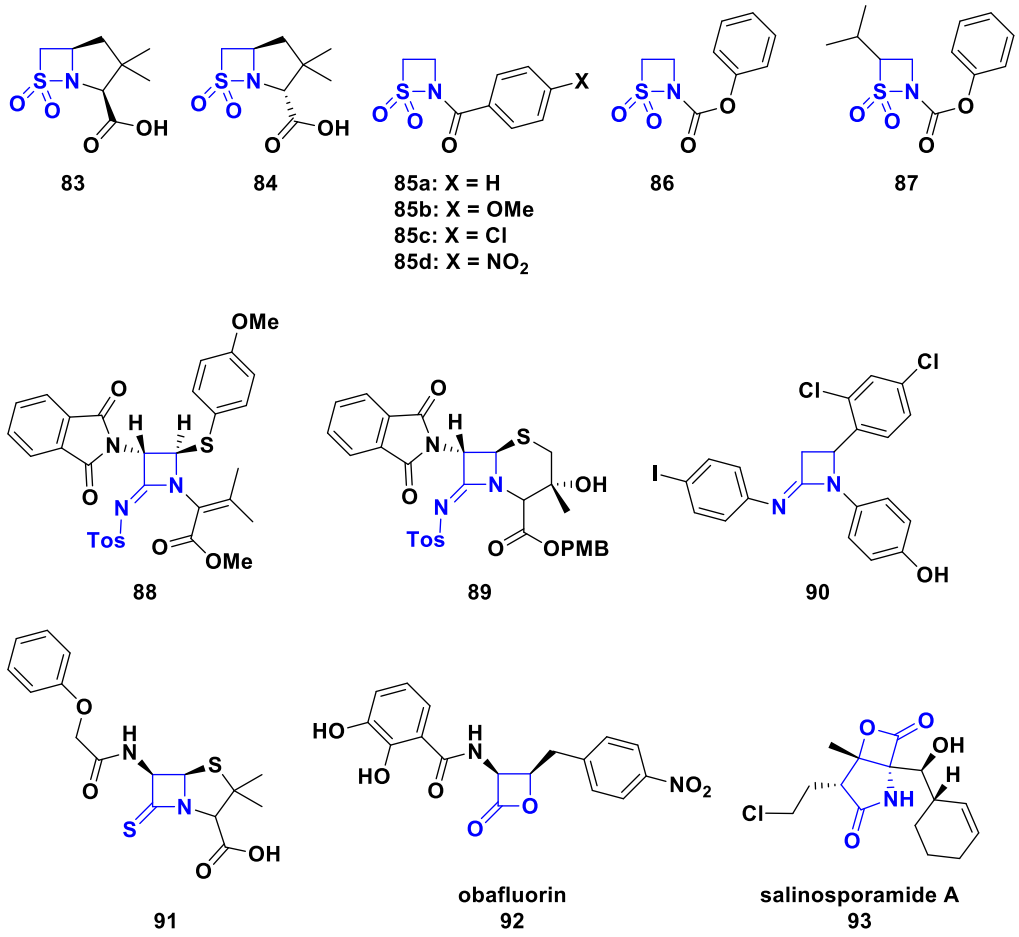

Figure 1-16 | Structures of β-lactam isosteres tested for antibacterial activity.

1.5.6 Six-membered and larger systems

The bicyclic lactams described in this section were synthesised as bioisosteres of β-turn moieties found in oligopeptides.[110, 111] Oligopeptides containing these moieties were shown to exhibit antibacterial activity, however no studies on bacterial transpeptidase inhibition have been reported for these compounds.[112]

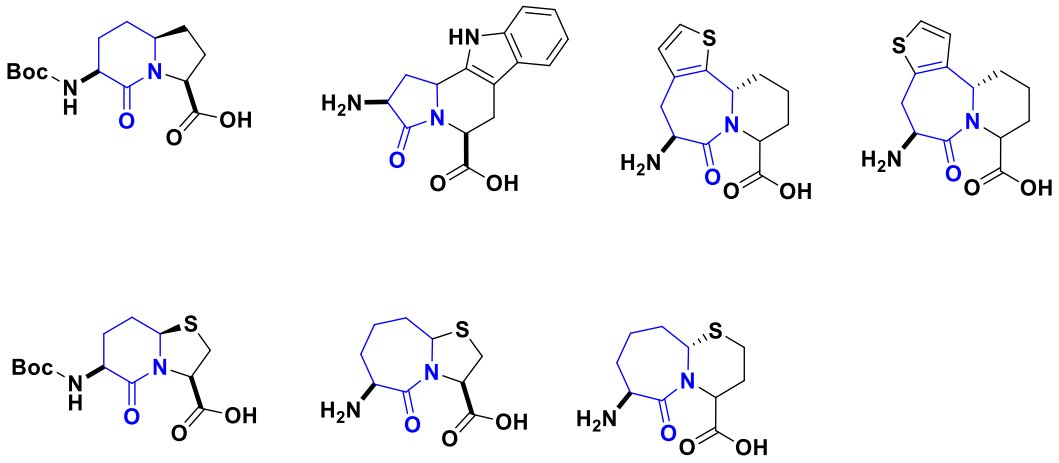

Figure 1-17 | Structures of bicyclic lactams investigated as oligopeptide bioisosteres of β-turns in oligopeptides.

1.5.7 Bridged bicyclic lactam analogues

The bridged bicyclic δ-lactams **94** and **95** showed weak antibacterial activity against *P. aeruginosa*, *S. marcescens*, *E. cloacae*, and *S. aureus* ranging from 40-80 μM.[113] While **95** exhibited micromolar IC_{50}s against *P. aeruginosa* PBPs (PBP1a > 50 μM, PBP1b > 50 μM, PBP2 = 50 μM, PBP3 = 5 μM, PBP4 = 5 μM, and PBP5 > 50 μM), these compounds were still weaker inhibitors compared to imipenem (**24**) (IC_{50}s 0.1 – 2.3 μM).[113] The diazabicyclooctane (DBO) class of β-lactamase inhibitors have also been developed as PBP inhibitors with antibacterial activity. Avibactam (**44**), one of the earliest DBOs, is a potent broad spectrum serine β-lactamase inhibitor with nanomolar IC_{50}s for Class A (TEM-1 = 8 nM), Class C (AmpC = 128 nM) and Class D (OXA-23 = 2.3 μM[114]), but possessed no antibacterial activity despite showing ~0.5 μg/mL inhibition of *E. coli* PBP2.[114, 115]

Nacubactam (**96**) was reported as a potent inhibitor of Class A (IC_{50}s 26.1–869 nM), Class C (IC_{50}s 15.0–845 nM), and Class D (IC_{50}s 3–46 μM) SBLs, but no inhibition of **96** was observed for MBLs.[114] **96** was shown to inhibit *E. coli* PBP2 (IC_{50} 0.12 μg/mL), at a level that is comparable to **14** (IC_{50} 0.44 μg/mL) and cefepime (IC_{50} 0.24 μg/mL), but much weaker than meropenem (IC_{50} < 0.008 μg/mL).[114] An 'enhancer' effect was observed when **96** was co-administered with β-lactams whereby the MICs of *E. coli* PBP3-targeting β-lactams **14**, cefepime, and **33** were reduced up to 32-fold against resistant bacterial strains.[114] Like **96**, zidebactam (**97**) inhibits Class A and class C BLs and potentiates the activity of β-lactams that inhibit PBP3. **97** is an inhibitor of *P. aeruginosa* with MICs ranging from 2-32 μg/mL and is a potent inhibitor of *E. coli* with MICs ranging from 0.06-1 μg/mL, comparable to the carbapenems.[116]

ETX2514 (**98**) is a nanomolar inhibitor of all classes of SBLs, but like other DBOs, it did not appear to inhibit MBLs.[117] **98** was reported to restore inhibitory function to β-lactams against β-lactamase-producing bacteria, including resistant strains of *A. baumannii*, but it possessed very weak inhibition of PBPs and did not possess antibacterial activity if used alone.[117] ETX1317 (**99**) was reported to exhibit potent antibacterial activity against resistant Enterobacteriaceae, with MICs as low as 0.25 μg/mL.[118] In addition, **99** augmented the antibacterial activity of β-lactams and, when given in combination, was shown to act as a broad-spectrum SBL inhibitor that out-performed **44** against Class D carbapenemases (cf. OXA-48 IC_{50} = 77 nM for **99** vs 880 nM for **44**).[118] ETX0282 (**100**) is an orally bioavailable pro-drug of **99**.[119]

While IID572 (**101**) lacks intrinsic antibacterial activity, it is a potent broad-spectrum inhibitor of all classes of SBLs.[120] NXL-105 (**102**) inhibits *E. coli* PBP2 and showed potent antibacterial activity against resistant strains of *P. aeruginosa* (MIC 0.06 μg/mL) and *E. coli* (MIC 0.008 μg/mL); **102** restores β-lactam activity in resistant strains of Gram-negative bacteria.[121] ETX0462 (**103**) is a potent *P. aeruginosa* PBP1 and PBP3 inhibitor (note that no inhibition of PBP2 was observed) and showed potent *in vitro* and *in vivo* antibacterial activity against clinically resistant pathogens.[121]

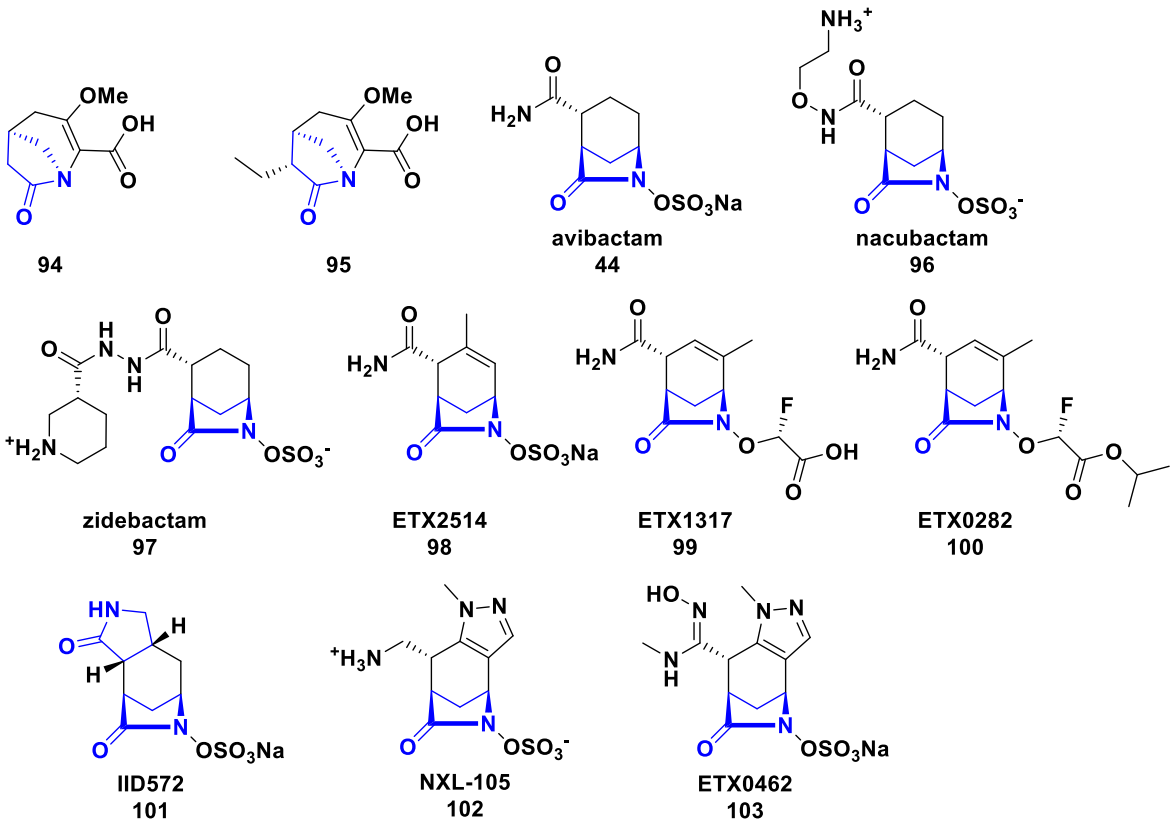

Figure 1-18 | Structures of DBOs with antibacterial and β-lactamase inhibitory activity.

1.5.8 Boronates

As discussed in **Section 1.4.2**, the ability of boronic acids to adopt both sp^2 and sp^3 conformations depending on their coordination number allows boron-based inhibitors to act as transition-state analogues of the tetrahedral intermediates resulting from the attack of a nucleophile onto a carbonyl.[72] Thus, acyclic and cyclic boronates have been investigated extensively as potential inhibitors of both PBPs and β-lactamases (**Figure 1-19**).[63, 122-125] The acyclic boronates **104a-d** were reported to possess micromolar IC_{50}s against *S. pneumoniae* PBP1b as well as moderate antibacterial activity (MICs 31-128 μg/mL) against Gram-positive bacteria.[126] Compounds **105** and **106** exhibited potent inhibition of the transpeptidase R39 from *Actinomadura spp.* (IC_{50} **105** = 1.3 μM, **106** = 0.08 μM), as well as weak inhibition of PBP1 and PBP2.[122] The 'magic methyl'[127] *C*-2 group of **106** helps orient the molecule into the active conformation for inhibition.[128] Vaborbactam (**46**) was reported to be a weak inhibitor of *P. aeruginosa* PBP3 (IC_{50} 262 μM).[124] The 6,6-bicyclic boronate **107** was shown to be a nanomolar *E. coli* PBP5 inhibitor, but no inhibition of *E. coli* PBP3 nor antibacterial activity were reported for **107**.[72] The 6,5-bicyclic boronate compound **108** showed moderate inhibition of *P. aeruginosa* PBP3 (K_i = ~73.9 μM), but no antibacterial activity was reported.[125]

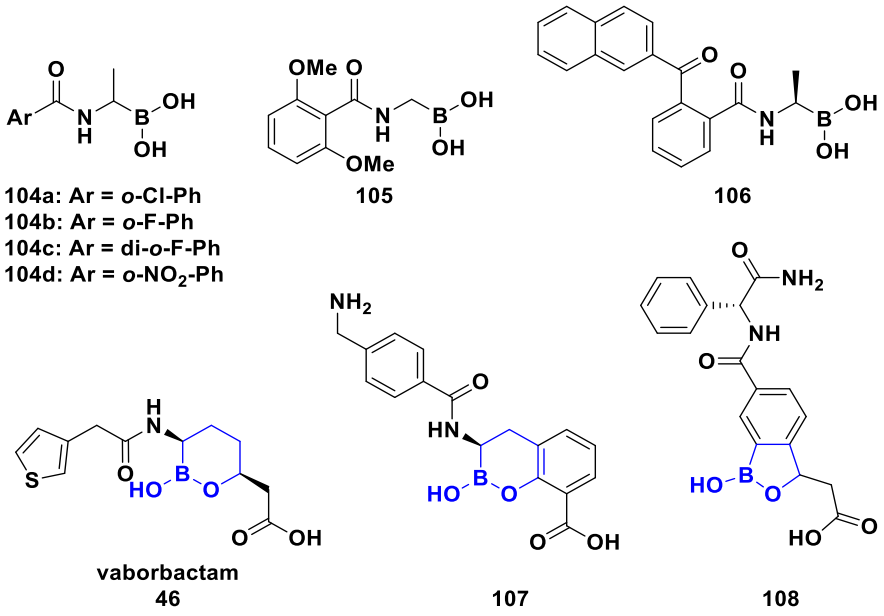

Figure 1-19 | Structures of boron-containing transition-state analogues that inhibit bacterial transpeptidases.

1.5.9 γ-Lactams

Substantial research has been conducted on the development of γ-lactam-based PBP inhibitors. γ-Lactams are significantly more stable to hydrolysis than β-lactams; this is proposed to be due in part to the reduced ring strain of the five-membered ring compared to the 4-membered ring of β-lactams.[110] Hence electron-withdrawing moieties were commonly attached to the lactam nitrogen in order to activate the γ-lactam carbonyl to nucleophilic attack.[129] The monocyclic γ-lactams bearing G and V sidechains **109**, **110**, **111**, and **112** (**Figure 1-20**) reported by Crossley *et al.*[130] showed no antibacterial activity, while moderate antibacterial activities against *E. coli* and *S. aureus* were observed for the thiophene-functionalised compounds **113a-b** and furan-functionalised compounds **114a-b**.[131, 132] The

coumarin derivative **115a** and its methyl ester analogue **115b** showed weak antibacterial activity, possibly suggesting a different mechanism of action to PBP inhibition.[133]

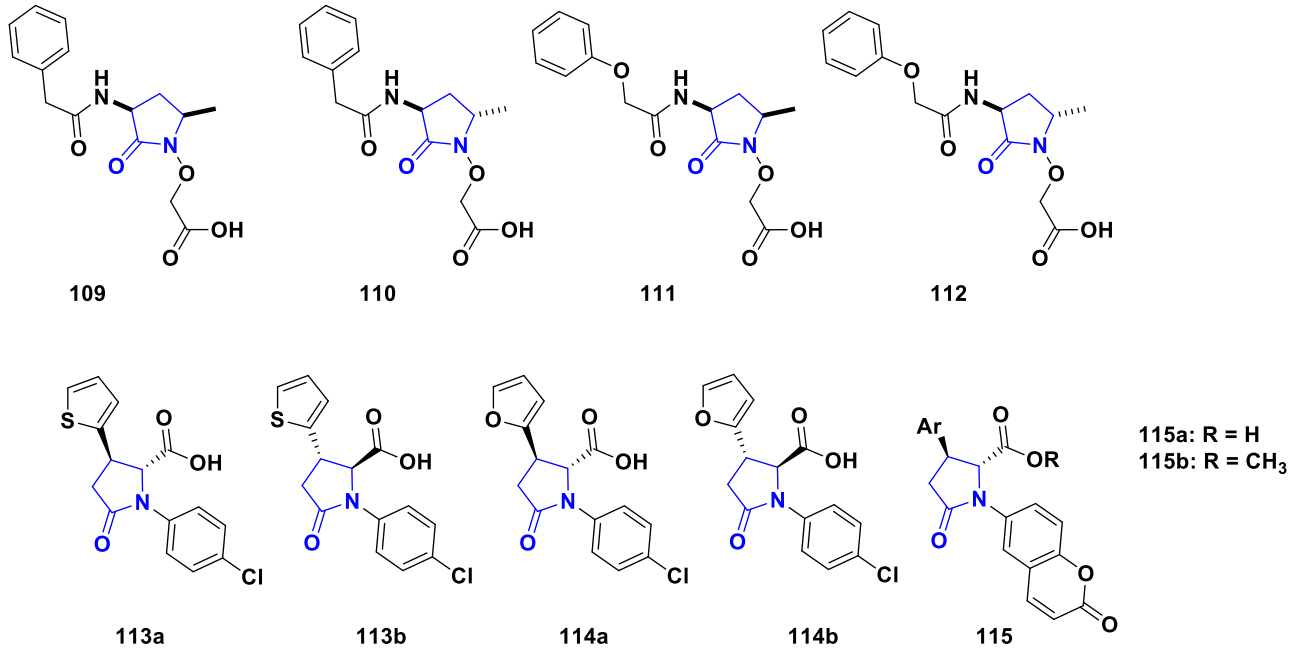

Figure 1-20 | Structures of selected monocyclic γ-lactam analogues tested for antibacterial activity.

Numerous bicyclic γ-lactam configurations were also investigated (**Figure 1-21**). The γ-lactam compounds **116** and **117**, synthesised as analogues of penicillanic acid (**118**), showed no antibacterial activity.[134] 5,4-Bicylic compounds **119**, **120**, and **121** showed no antibacterial activity but the *S*-phenyl compound **122** showed some antibacterial activity.[134-136] The bicyclic thiazoline **123** was the first bicyclic γ-lactam reported to exhibit antibacterial activity.[137] The (*S*)-pyrroline analogue **124** was shown to be weakly active, while the (*R*)-analogue **125** was reported to show moderate antibacterial activity.[138]

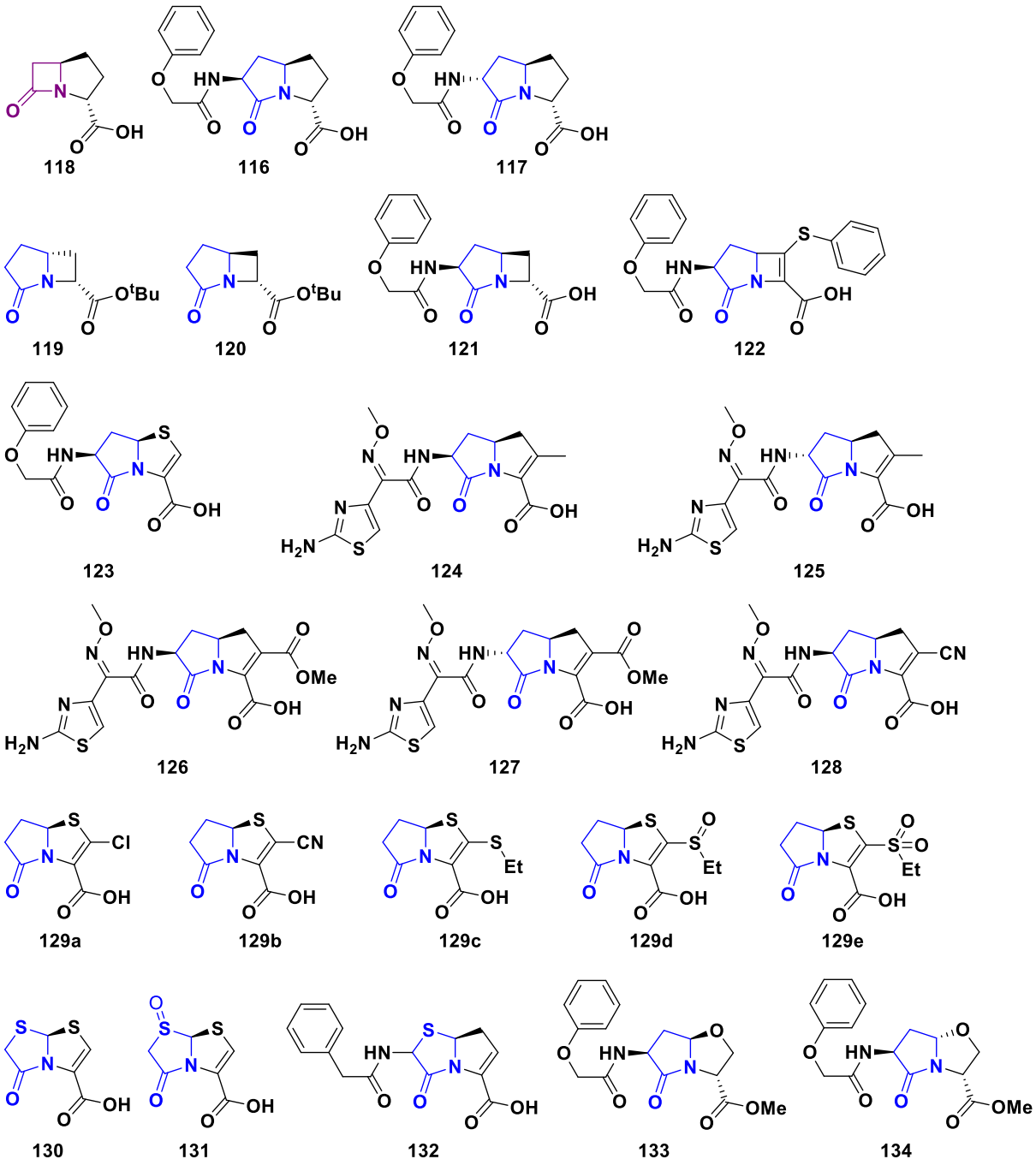

Figure 1-21 | Structures of bicyclic γ-lactams synthesised for testing as antibacterials.

By contrast, the methyl ester-functionalised analogues **126** and **127** exhibited the opposite reactivity trend, with the (*S*)-analogue **126** being reported to show antibacterial while its (*R*)-analogue **127** was reported to be inactive.[139] The nitrile-functionalised compound **128** was not reported to exhibit antibacterial activity.[139] Compounds **129a-c** and **129e** did not exhibit any antibacterial activity, but **129d** showed some activity.[129] Compounds **130**, **131**, and **132** did not exhibit antibacterial activity or β-lactamase inhibition.[140] γ-Lactam analogues **133** and **134**, which are structural analogues of oxapenams, were reported to have no antibacterial activity against *S. aureus*.[141]

The sulfide-functionalised bicyclic γ-lactams **135a-d** (**Table 1-1**) showed variable levels of antibacterial activity, with the sulfone **135d** showing the most potency, possibly due to extra electron-withdrawing effect of the sulfone group on the adjacent alkene.[142] The *trans*-(*S*),(*R*) isomer **136** was reported to be more potent than the *cis* analogue **135a**, contrary to other reports for similar compounds.[129]

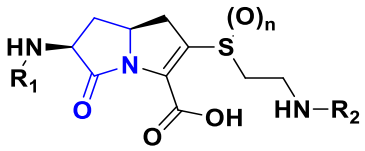

Cpd	R_1	R_2	n	Antibacterial activity[142]
135a	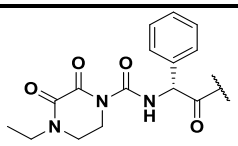	Ac	0	weak
135b	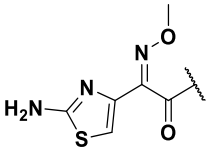	Ac	0	weak
135c	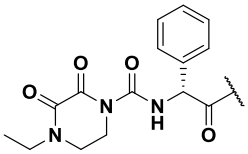	H	0	weak
135d	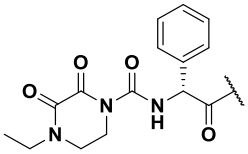	H	2	moderate

Table 1-1 | Structures and activities of amino-5,5-bicyclic gamma lactams reported by Takeda.[142]

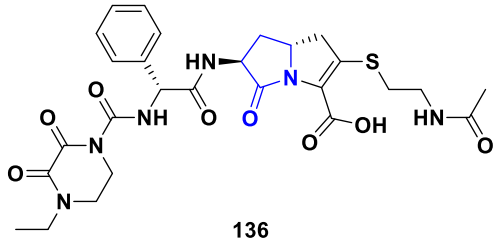

136

Figure 1-22 | Structure of the *trans*-5,5-bicyclic γ-lactam **136**.

The 5,5,3-tricyclic γ-lactams **137a-d** were not reported to show antibacterial activity against resistant Gram-positive or Gram-negative strains, however the activity of **19** in β-lactamase-producing strains was augmented by the presence of compounds

137a-d.[143] The pyrrolodione compounds **138** and **139**, synthesised as analogues of penicillins and cephalosporins, respectively, showed no antibacterial activity against the Gram-negative strains tested.[144] The compound Raja 42 (**140**) showed potent antibacterial activity against resistant *C. difficile*.[145] However, mechanistic studies suggested that the mechanism of action may involve the induction of reactive oxygen species (ROS) near the cell membrane rather than inhibition of PBPs, as was initially proposed.[146]

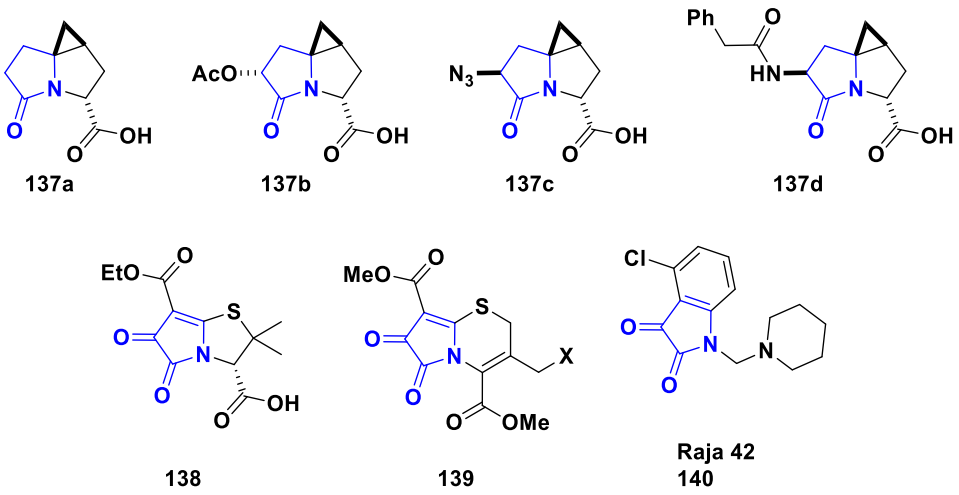

Figure 1-23 | Structures of strained 5,5,3-tricyclic gamma-lactams and pyrrolodiones synthesised as potential PBP inhibitors.

1.5.10 Pyrazolidinones

Another class of compounds that has been heavily researched for antibacterial activity as transpeptidases inhibitors is the pyrazolidinones. The pyrazolidinone ring was proposed to be more electrophilic than analogous lactam rings due to the electron-withdrawing nature of the additional ring nitrogen. Monocyclic

pyrazolidinones (**Figure 1-24**) prepared by Couloigner *et al*. feature β-*N*-methylation and G sidechains, with different functionalisation of the α-nitrogen.[147] Compound **141**, which lacks functionalisation of the α-nitrogen, showed no antibacterial activity, however the compounds **142**, **143**, and **144**, which do have acyl functionalisation of the α-nitrogen, showed weak activity against *S. aureus* (>128 μg/mL).[147] The sulfonate **145** also showed similarly weak activity. The monocyclic pyrazolidinones **146**, **147**, and **148**, functionalised with the generally more potent ATMO sidechains showed no antibacterial activity against tested strains.[148]

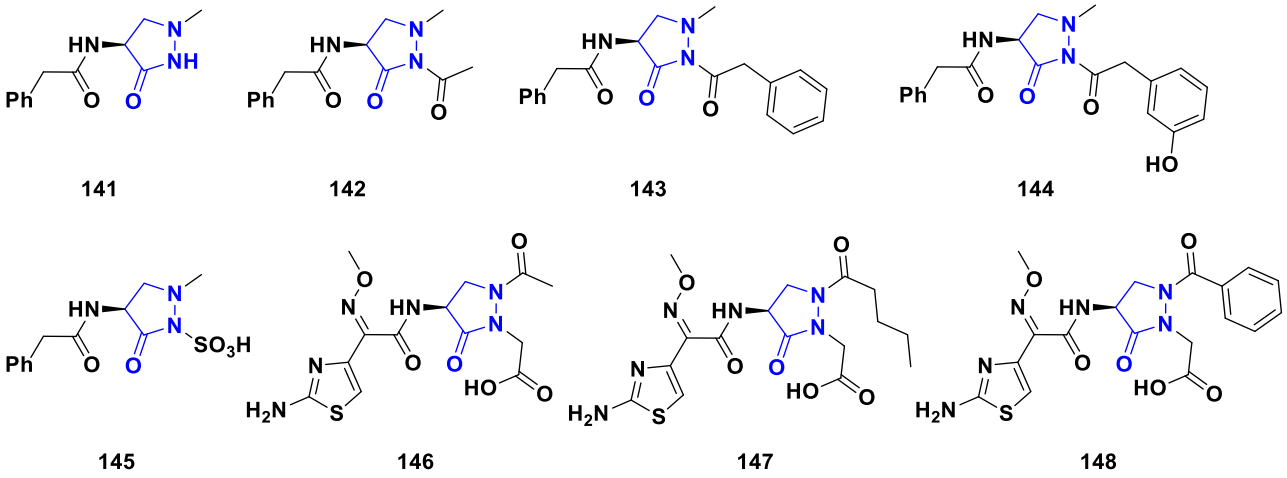

Figure 1-24 | Structures of monocyclic pyrazolidinones tested for antibacterial activity.

In addition to monocyclic pyrazolidinones, bicyclic pyrazolidinones of various ring configurations were also investigated (**Figure 1-25**). Researchers at Eli-Lilly found success with a series of bicyclic pyrazolidinone carboxylates.[149] While compound **149**, which lacks an acylamino sidechain, showed no activity, the ATMO-

functionalised compound **150** showed weak antibacterial activity. Compounds **151a-e** showed potent Gram-negative antibacterial activity, and a strong correlation was observed between the substituent constant σ of *C*-3 substituent and the compound's antibacterial activity, implying that the presence of strong EWGs on the R group is key for their activity.[148, 150] Mechanistic studies later confirmed that their mechanism of inhibition was the disruption of cell-wall biosynthesis.[151] While compounds functionalised with ATMO sidechains (e.g. **151a-e**) generally performed poorly against Gram-positive strains, the dichlorophenyl-functionalised compound **152** exhibited substantial Gram-positive coverage.[152] Contrary to the 5,5-bicyclic pyrazolidinones, the related 5,6-bicyclic pyrazolidinones **153** and **154** showed no antibacterial activity. The *C*-3 sulfur 5,5 bicyclic compounds **155** and **156** were also inactive.

Recently, a siderophore-conjugated bicyclic pyrazolidinone **YU253434** (**157**) has been reported by Goldberg *et al.*[153] This analogue showed potent antibacterial activity against a panel of resistant bacterial strains, including *P. aeruginosa* and *Enterobacteriaceae*, which are both classed as WHO priority 1 pathogens,[154] outperforming both **19** and **25** against a panel of *P. aeruginosa* strains (cf. MIC_{90}: **157** 8 μg/mL; **19** > 16 μg/mL; 25 > 8 μg/mL).[153] The siderophore moiety was shown to be crucial for the activity of these compounds, especially under low-iron conditions.[153] The higher antibacterial activity of the siderophore analogue is likely the result of improved cellular penetration by hijacking bacterial siderophore transporters.[155] A

fluorescence-based competition assay[156] was used to show **157** inhibits *P. aeruginosa* PBP3, with an IC_{50} of 2.5 μM.[153] **157** also demonstrated increased stability to β-lactamase hydrolysis as compared to clinically relevant β-lactams, which was attributed to a difference in the positioning of the aminothiazole sidechain due to the increased ring size of the pyrazolidinone compared to β-lactams.[153]

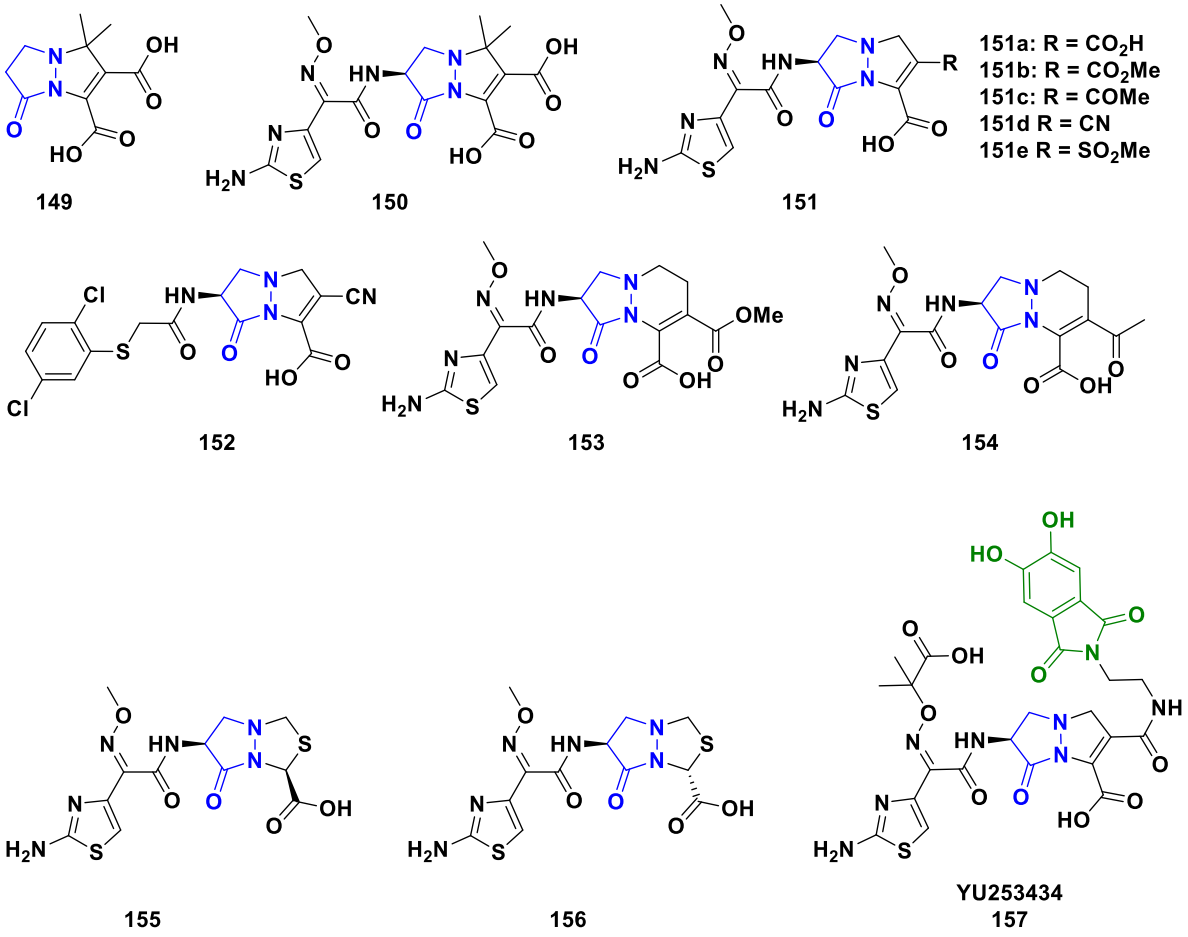

Figure 1-25 | Structures of bicyclic pyrazolidinones tested for antibacterial activity.

Jungheim also reported the synthesis of 5,5-bicyclic pyrazolidinones functionalised with sidechains characteristic of carbapenems (**Figure 1-26**).[157] Ethyl-compounds **158a-b**, (*R*)-hydroxyethyl compounds **159a-b**, and (*S*)-hydroxyethyl compounds

160a-b showed weak antibacterial activity.[157] The nitrile analogue **161** was reported to show greater activity compared to compounds **158-160**, however all compounds from this series were weaker antibacterials compared to the ATMO-functionalised analogue **151**.[157]

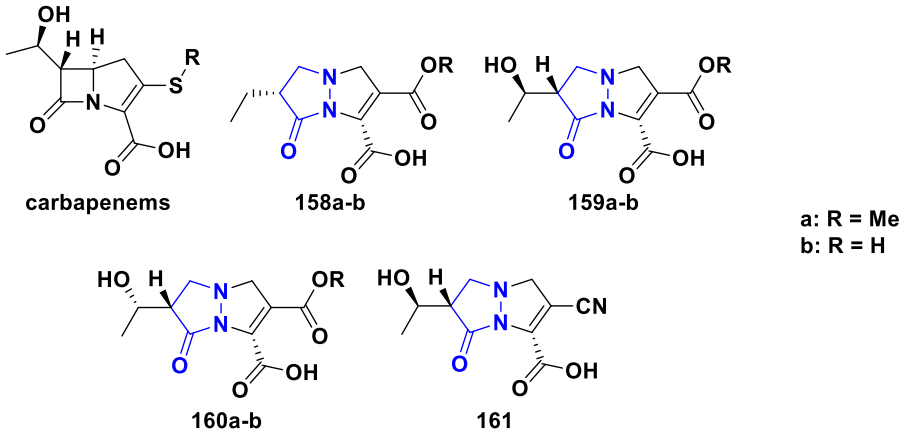

Figure 1-26 | Bicyclic pyrazolidinone analogues of carbapenems.

Panfil *et al.* reported the synthesis and antibacterial activity studies of bicyclic and tricyclic pyrazolidinone lactones as potential antibacterial agents (**Figure 1-27**). Similarly to other pyrazolidinones that did not possess acylamino sidechains, these compounds did not inhibit D,D-carboxypeptidase and subsequently had no reported antibacterial activity, although the authors did not specify which bacterial strains were evaluated.[158]

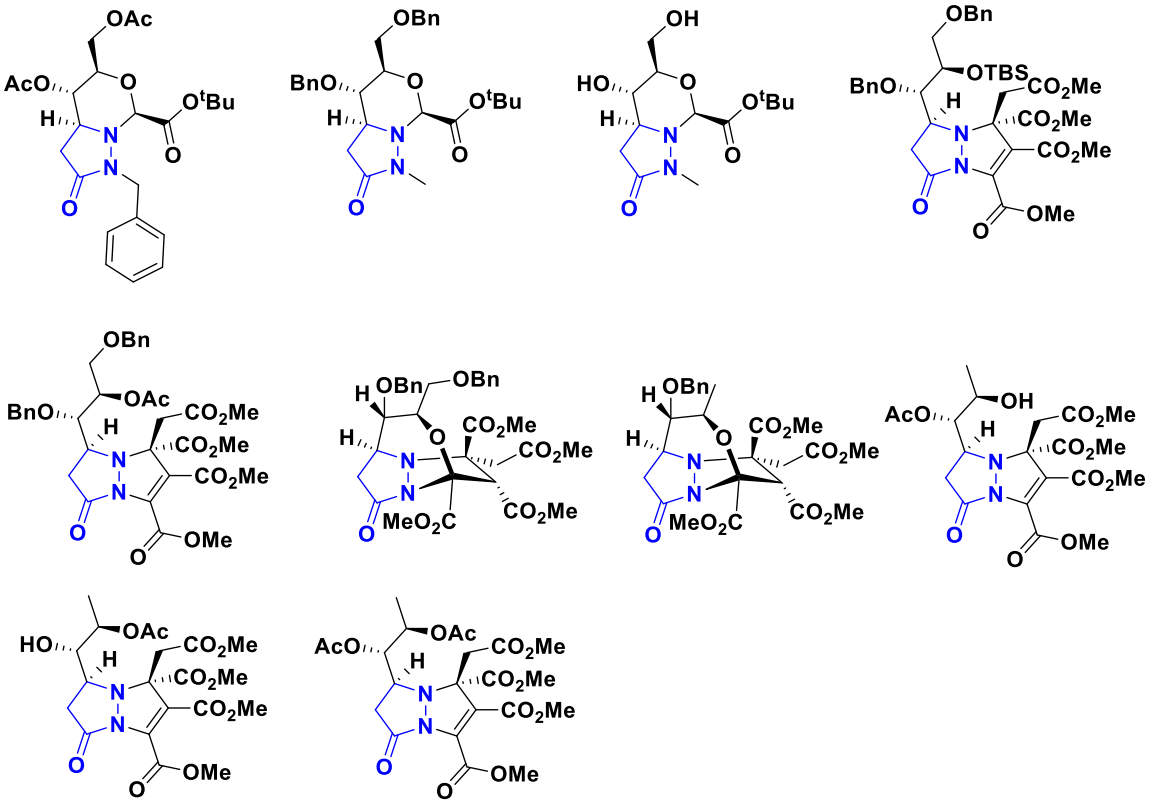

Figure 1-27 | Structures of pyrazolidinones reported by Panfil *et al* that were tested as antibacterials.

1.6 Lactivicins

In the mid-1980s, researchers from Takeda Industries reported the isolation of a new type of transpeptidase inhibitor, dubbed lactivicin (**162**), from two strains of Gram-negative soil bacteria: *Empedobacter lactamgenus* YK-258 and *Lysobacter albus* YK-422.[159] **162**, which has a cycloserine:γ-lactone core structure, was shown to inhibit the same transpeptidase targets as the β-lactam antibiotics. D-Cycloserine (**163**) alone also demonstrated antibacterial activity, although acting by a different molecular mechanism to lactivicin (discussed further in **Section 1.6.10**).[160] Subsequently, structurally related synthetic analogues of the β-lactam antibiotics

with antibacterial activity had been reported near contemporaneously with the initial reports of lactivicin.[129] Since these efforts built on knowledge of known β-lactam antibiotic structures, the discovery of the cycloserine:γ-lactone bicyclic core structure of the naturally occurring antibiotic lactivicin was completely unexpected.

1.6.1 Characterisation of lactivicin

The structure of **162** was determined based on spectroscopic analyses, and with the aid of X-ray crystallography.[159] The studies showed that **162** exists as a 1:1 mixture of *C*-6 epimers in water. The mechanism of equilibration likely involves ring opening of the γ-lactone to give the *N*-acyl iminium ion **164**; there was no evidence for incorporation of ^{18}O from equilibration in $^{18}OH_2$, ruling out a mechanism involving attack by water at the *C*-6 position or hydrolysis of the γ-lactone.[161] The absolute configuration of **162** was assigned by confocal CD analyses and compared with synthetic standards.[159]

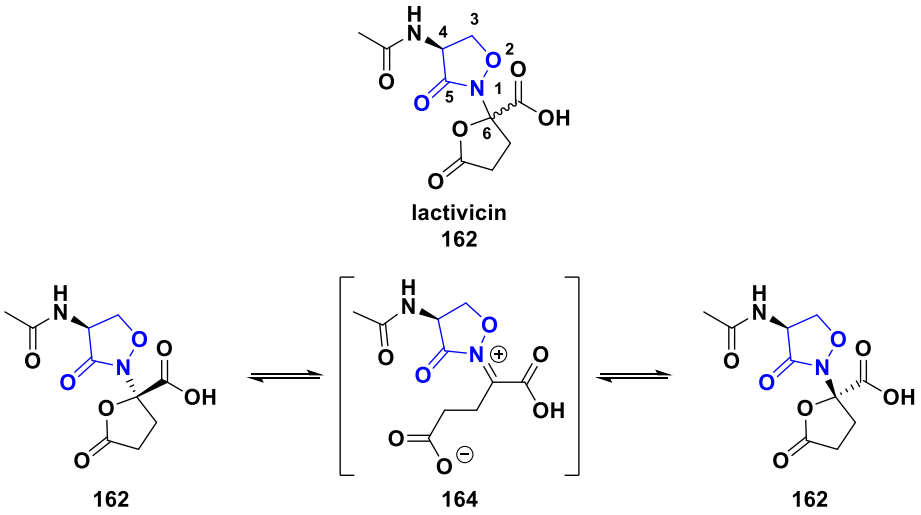

Figure 1-28 | Structure of 162 and the proposed mechanism for its epimerisation.

The products of **162** hydrolysis have been studied. Under basic conditions, fragmentation to give *N*-acetyl cycloserine (**165**) and 2-oxoglurarate (**2-OG**) occurs, presumably via attack of a hydroxide ion onto the γ-lactone ring. Under acidic conditions or in the presence of a β-lactamase, hydrolysis of the cycloserine ring to give the tricarboxylic acid oxime (**166**) has been proposed, which then undergoes further hydrolysis to give **2-OG** and the amino acid hydroxylamine derivative **167**.[161]

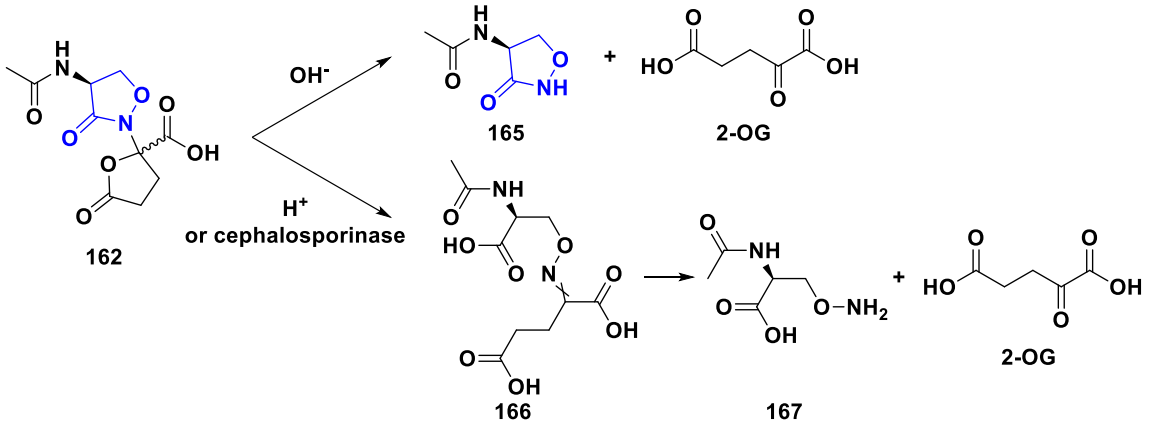

Figure 1-29 | Proposed hydrolysis pathways of **162**.

The cycloserine ring of the lactivicins reacts with both PBPs and some SBLs to give an initial acyl-enzyme complex; a process that, by release of the lactam nitrogen lone pair, triggers ring opening at the γ-lactone ring to give a complex in a manner analogous to that in which a cephalosporin with a *C*-3' leaving group reacts to give a *C*-3 exomethylene product.[162] A crystal structure of the semi-synthetic phenoxylactivicin **168** (**PLTV**) in complex with *S. pneumoniae* PBP1b shows that **168** reacts covalently to the catalytic serine to form a stable ester, opening the

cycloserine and γ-lactone rings in the process. The cycloserine carbonyl inserts into the oxyanion hole and interacts with the amide nitrogen of Ser460 and Thr654, while the carboxylate groups are positioned to bind to Thr652, Thr654, and Tyr498 via non-covalent interactions.[162] The phenoxyacetyl group sterically blocks entry into the catalytic site. Despite the structural differences between the lactivicin and cephalosporin cores, there is a high degree of convergence between the complexes of **162**, **168**, and **18** with *S. pneumoniae* PBP1b.[162] When superimposed, the terminal carboxylates of both molecules overlap and interact with Thr652. The oxime of **18** overlaps with the ring nitrogen of **18**, and both ring-derived carbonyls form hydrogen bonds to Thr654. The sidechains of both point out of the catalytic site in similar ways and serve to sterically hinder the entrance of the catalytic cleft.[162]

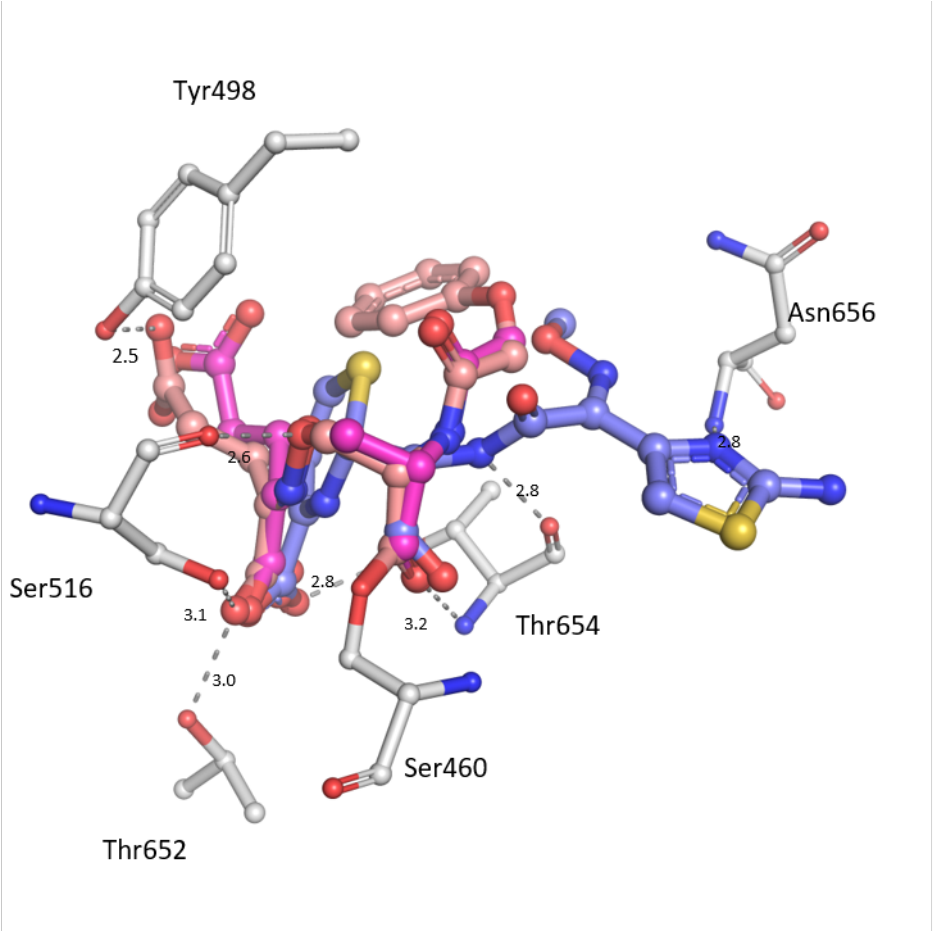

Figure 1-30 | View derived from the overlay of a single diastereomer of **162** (salmon, PDB: 2JE5), **168** (magenta, PDB: 2JCH), and **18** (purple, PDB: 2BG4) with *S. pneumoniae* PBP1b. Despite the structural differences between the backbones of the lactivicins and the cephalosporins, the acyl-enzyme complexes show a high degree of similarity.

1.6.2 Synthesis of lactivicin analogues

The first semi-synthetic analogues of **162** were prepared using bacterially fermented **162** as the starting material (**Figure 1-31A**). The *N*-acetyl group of **162** was cleaved with PCl_5 and pyridine to give the zwitterionic amino carboxylate intermediate **169**, which could then be functionalised by acylation with various acyl chlorides to give the synthetic lactivicins **170**.[163] Later, a fully synthetic route to lactivicins was described (**Figure 1-31B**) that began with the reaction of *N*-Cbz-cycloserine **171** with

the 4-nitrobenzyl 2-OG ester **172** in the presence of a coupling reagent such as dicyclohexylcarbodiimide (DCC), to give an equal mixture of *C*-6 epimers (**173**).

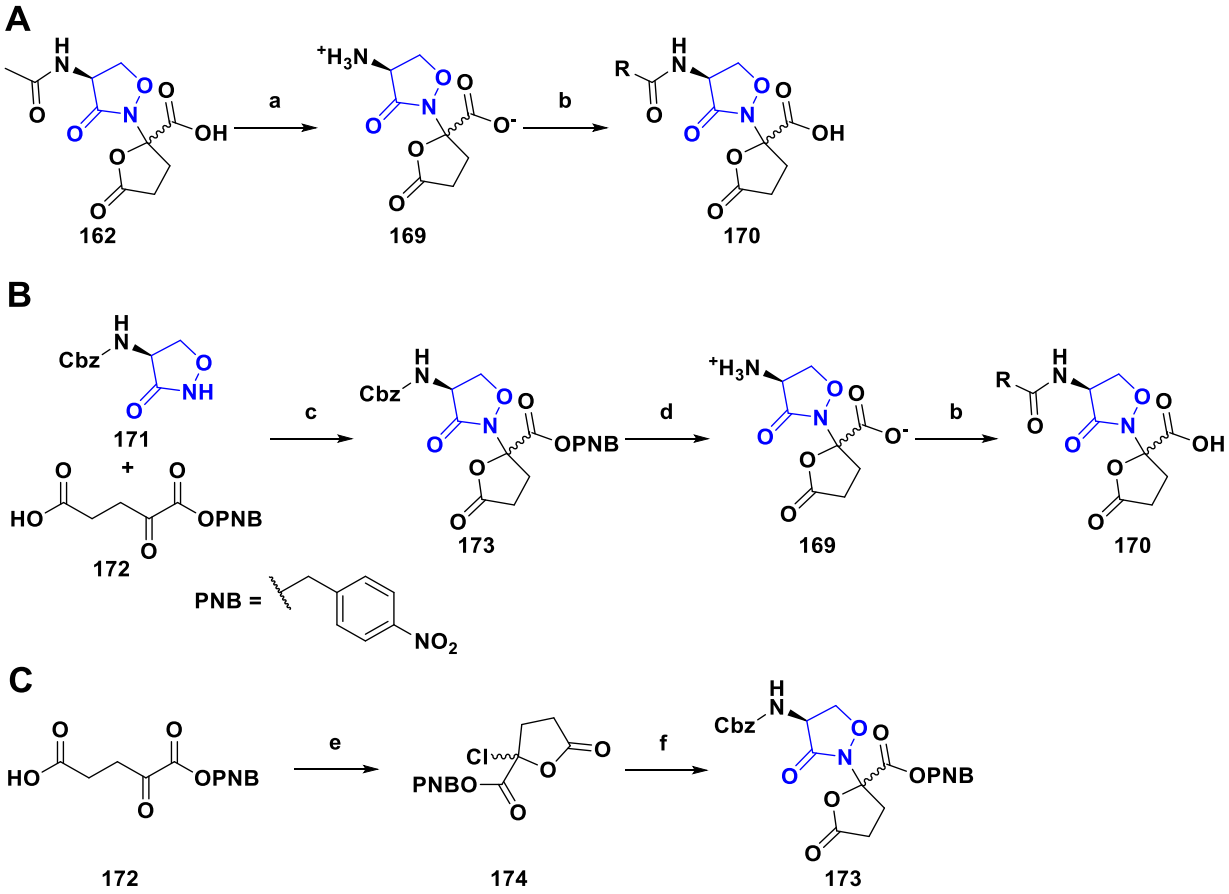

Figure 1-31 | Reported synthetic routes to lactivicin analogues. Reagents and conditions: (**a**) PCl_5, pyridine, rt; (**b**) R-COCl, H_2O, $NaHCO_3$; (**c**) DCC, CH_2Cl_2, rt; (**d**) Pd/C, H_2, THF/H_2O, rt; (**e**) $SOCl_2$, 1,2-dichloroethane, reflux; (**f**) **171**, Et_3N, CH_2Cl_2, rt.

Alternatively, the protected intermediate **173** can be synthesised by the reaction of the γ-chloro-lactone ester (**174**) with **171** in the presence of a non-nucleophilic base (**Figure 1-31C**).[164] **173** can then be deprotected via hydrogenolysis to give **169**.[164] Acylation of **169** with the appropriate acyl chloride then yielded the desired lactivicin products **170**.[164]

1.6.3 Selected synthetic lactivicins

Tamura *et al.* utilised the semi-synthetic route described in **Figure 1-31B** for an in-depth exploration of synthetic lactivicin derivatives (**Table 1-2**).[164] Synthetic lactivicin analogues **175a-h** bearing cephalosporin sidechains generally exhibited potent antibacterial activity against either Gram-positive or Gram-negative bacteria; only one lactivicin analogue exhibited potency against both (**175h**).[164, 165] Compound **175h**, which has a 2-chloropyridyl sidechain, exhibited the greatest Gram-positive potency (*S. aureus* MIC < 0.1 μg/mL).[165] Though the 2-chloropyridyl sidechain does not have a clinically approved cephalosporin analogue, it is closest to the acylamino sidechain of cefapirin, which exhibited potent antibacterial activity against Gram-positive bacteria.[166] Thus, the antibacterial activities of **175a-h** demonstrate that the acylamino SAR for bacterial inhibition by β-lactams generally translates from penicillins and cephalosporins onto the lactivicin core.

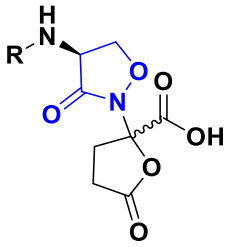

Cpd	R	β-lactam analogue	Active against:
175a	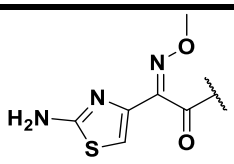	Cefuzonam (2nd gen)	Gram-negative
175b	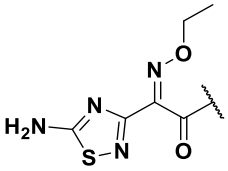	Cefclidine (4th gen)	Gram-negative
175c	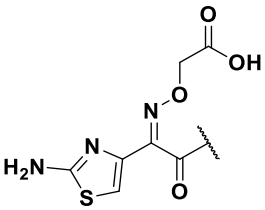	Cefixime (2nd gen)	Gram-negative
175d	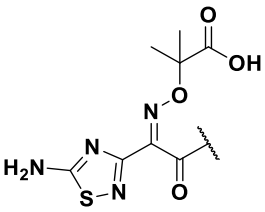	Ceftazidime (3rd gen)	Gram-negative
175e	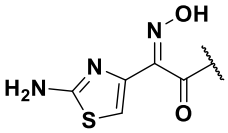	Cefdinir (3rd gen)	Gram-positive and Gram-negative
175f	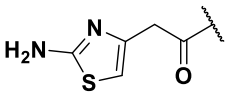	Cefotiam (2nd gen)	Gram-positive
175g	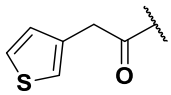	Cefalotin (1st gen)	Gram-positive
175h	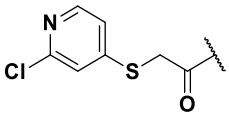	N/A	Gram-positive

Table 1-2 | Structures and activities of lactivicin analogues with cephalosporin sidechains.[165]

Tamura *et al.* also demonstrated that compounds **176** and **177**, which are pivaloxymethyl (POM) ester prodrugs of **175a** and **175g**, respectively, demonstrate increased *in vivo* antibacterial activity against *E. coli* in mice models, suggesting that some of the undesirable physiochemical properties of deprotected lactivicins (namely their instability in aqueous solutions) might be mitigated through protection with prodrug esters that are labile *in vivo*.[165]

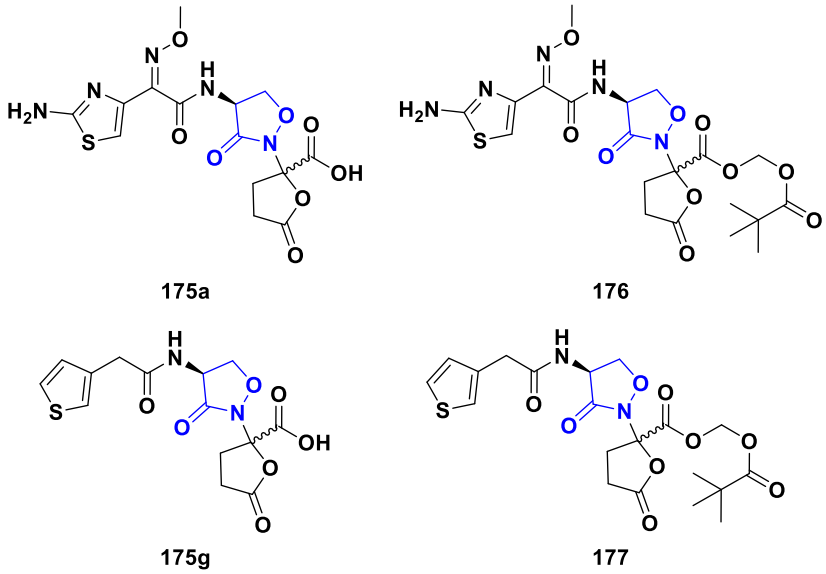

Figure 1-32 | Structures of POM-functionalised lactivicin analogues.

1.6.4 Lactivicin siderophore conjugates

Starr *et al.* combined the lactivicin core with a variety of siderophoric moieties that many Gram-negative bacteria produce during periods of low iron bioavailability.[167] The siderophoric moieties were proposed to improve cellular uptake through bacterial iron-sequestering mechanisms. The analogue LTV-14 (**178**) featured a dihydroxypyridone located on the acylamino sidechain. LTV-17 (**179**) is a

siderophore-functionalised analogue of LTV-13 (**180**) that features a dihydroxyphthalimide attached to the γ-lactone ring. While the dihydroxypyridone-conjugated analogue **178** performed similarly to the aztreonam (**33**) against *P. aeruginosa* strains (MICs 4 μg/mL and 4-8 μg/mL, respectively), the dihydroxyphthalimide **179** exhibited an 8-fold increase in potency (MIC 0.5 μg/mL) against the same *P. aeruginosa* strains. Both **178** and **179** were nanomolar inhibitors of *P. aeruginosa* PBP1a (IC_{50} = 46 nM and 30 nM, respectively) and *P. aeruginosa* PBP3 (IC_{50} = 140 nM and 46 nM, respectively). The siderophore moiety of **179** was shown by Calvopiña *et al*. to improve cell penetration in *S. maltophilia* by facilitating the active transport of **179** across the bacterial outer membrane via the energy transducer TonB, which is proposed to power iron importers displayed on the cell surface.[155, 168]

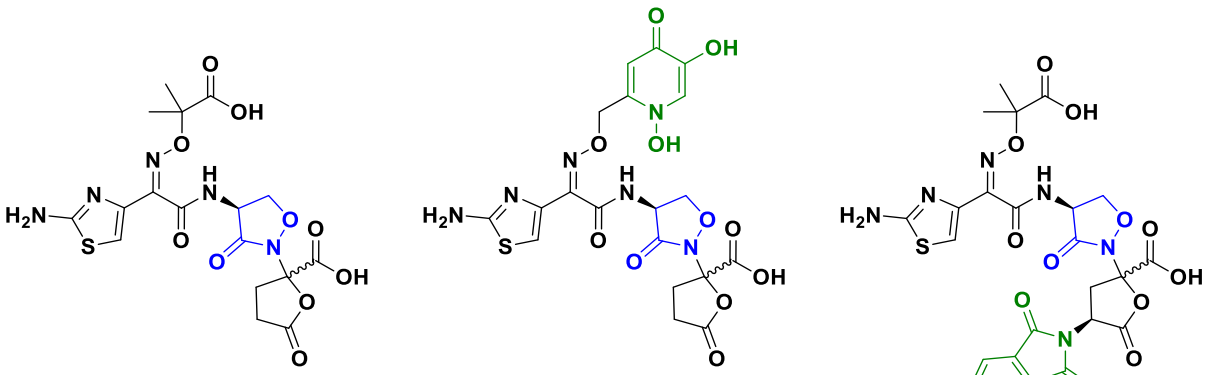

Figure 1-33 | Selected structures of lactivicin analogues reported by Starr *et al.* featuring siderophoric moieties (green).[167]

1.6.5 Aminopyrazolidinone lactivicin analogues

Lactivicin analogues **181**, **182**, and **183** comprising an aminopyrazolidinone ring in place of the cycloserine ring were synthesised by Tamura *et al.* (**Figure 1-34**).[164] The β-ring nitrogen of these aminopyrazolidinone derivatives was alkylated or acylated so in order to prevent the formation of the cyclic hemiaminal intermediate **183** during their chemical synthesis. These compounds, however, showed dramatically reduced antimicrobial activity compared to their lactivicin counterparts (e.g. **168**) against *S. aureus* and *E. coli*.[164]

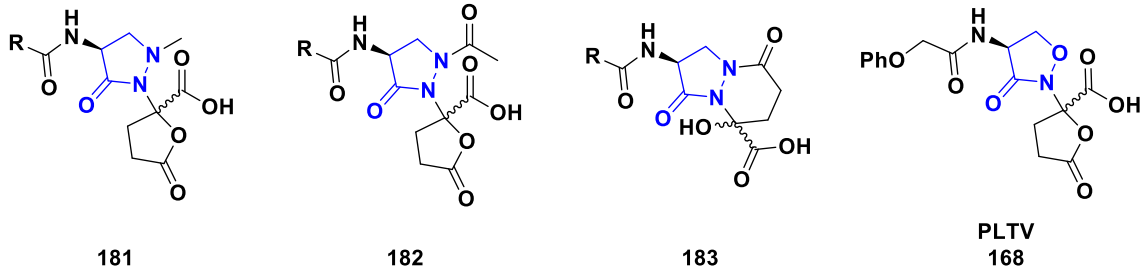

Figure 1-34 | Structures of aminopyrazolidinone analogues of lactivicin.

1.6.6 3-Methoxy lactivicin analogues

The *C*-7 methoxy group found on the β-lactam ring of cephamycin-class antibiotics was shown to dramatically improve the stability of the cephamycins such as cefoxitin (**184**) to β-lactamase hydrolysis, at least in part by preventing the approach of a hydrolytic water molecule during β-lactamase catalysis.[169] As shown in **Section 1.6.1** and **Section 1.6.3**, the SAR for the acylamino sidechains of β-lactams appears to apply also to the lactivicin core. Hence, Tamura *et al.* synthesised the *C*-4-

methoxy lactivicin analogue **185** to investigate whether the methoxy group would confer greater β-lactamase stability to the lactivicin core. However no studies on the analogous *C*-4 methoxy-lactivicin have been reported with respect to antibacterial activity nor β-lactamase stability to date.[165]

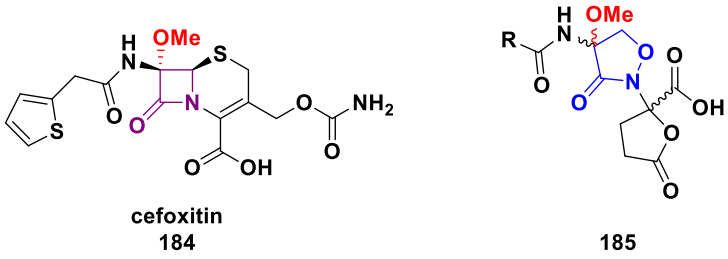

Figure 1-35 | Structures of cefoxitin and an analogous 4-methoxy derivative of lactivicin.

1.6.7 Homolactivicin analogues

Wolfe *et al.* synthesized a series of 6-membered cycloserine analogues (**186**, **187**, and **188**) fused with either a γ-lactone carboxylate group or other electron-withdrawing groups (**Figure 1-34**). These compounds, however, were not screened for antibacterial activity.[170] A subsequent publication reported no antibacterial activity for neither isomer of compound **186** nor compound **187**.[171] The 4-hydroxyisoxazolidinone analogue **188** was disclosed in a patent that claimed

compound **188** had reportedly 'mild' antibacterial activity, however no academic literature exists to support this claim.[172]

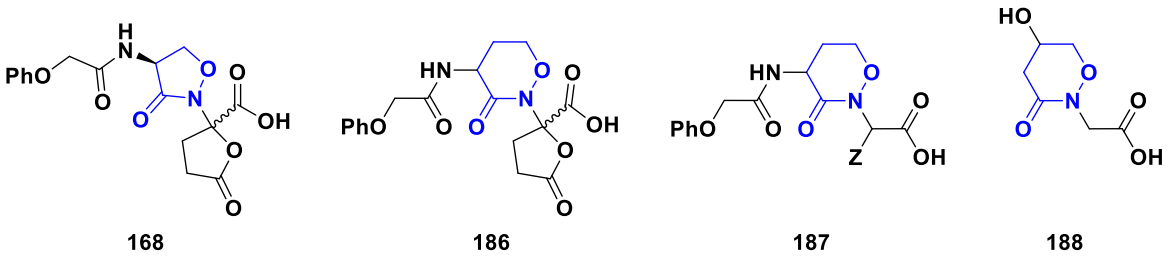

Figure 1-36 | Structures of homolactivicin analogues synthesised by Wolfe *et al.*[170]

1.6.8 Shionogi tricyclic lactivicins

Shionogi Inc. recently disclosed structures of the tricyclic lactivicin analogues **189a-e** in a 2016 patent (**Figure 2-23**).[173] While these tricyclic lactivicin analogues share the bicyclic pyrazolidinone core of the bicyclic pyrazolidinones developed by Eli-Lilly, a cis-fused γ-lactone replaces the enone moiety otherwise found on the Eli-Lilly pyrazolidinones. The molecular replacement of the enone for a γ-lactone changes the hybridization of the *C*-7 and *C*-8 carbons from sp^2 to sp^3, resulting in the breaking of the electronic conjugation that extends from the γ-lactam to the *C*-7 ketone of the bicyclic pyrazolidinones. However, the γ-lactone moiety still provides an electron sink for the nitrogen anion formed following the nucleophilic attack onto the γ-lactam, which should sufficiently activate the pyrazolidinone carbonyl towards an attack by nucleophilic serine residues in the active sites of PBPs.

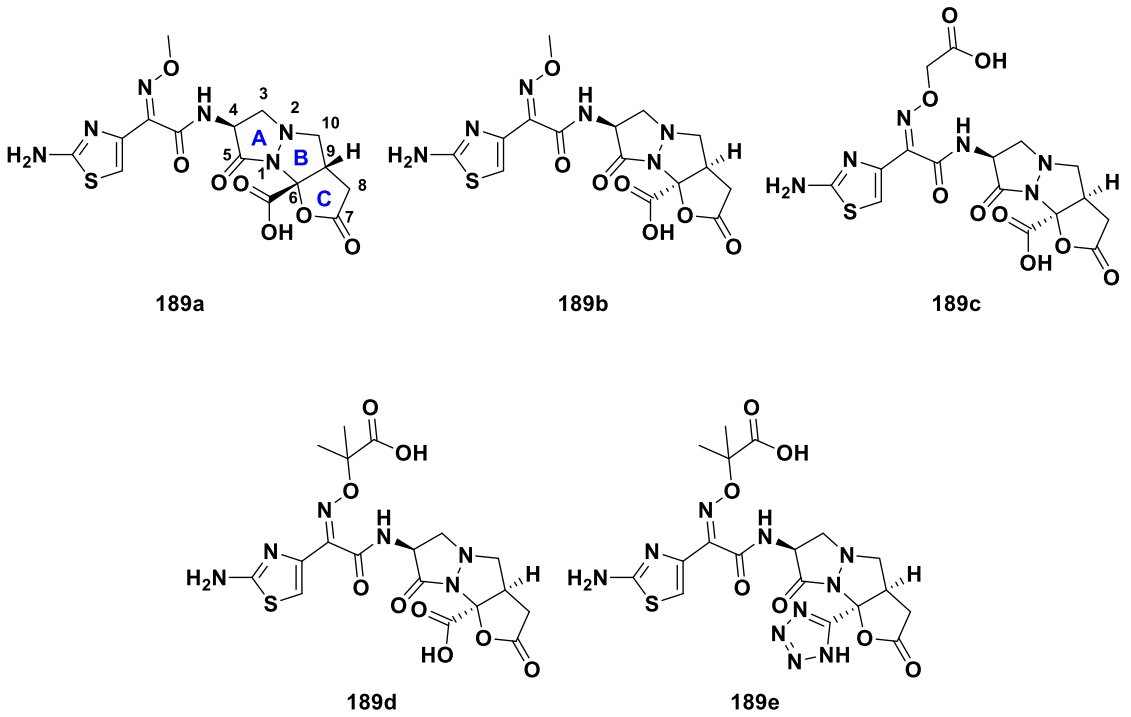

Figure 1-37 | Structures of Shionogi tricyclic lactivicin analogues.[173]

1.6.9 Lactivicins and β-lactamases

As discussed in **Section 1.4.1**, important mechanisms of resistance to β-lactam antibiotics include the modification of their transpeptidase targets and their hydrolytic inactivation by β-lactamases. Compared to **3**, lactivicins **162** and **168** demonstrated superior inhibition of *Pneumonoccoci* that express PBP variants resistant to β-lactam inhibition.[162] Against highly β-lactam-resistant pneumonococcal strains with modified PBPs that evade inhibition by β-lactams, **3** showed a 150- to 600-fold increase in minimum inhibitory concentration (MIC) compared to susceptible strains. By contrast, **162** and **168** showed only 5- to 10-fold increases, respectively, in MIC for resistant strains, suggesting that the

modifications to PBPs that reduced their susceptibility to β-lactams did not provide protection against lactivicins.[162]

One of the main hopes of replacing the β-lactam ring of β-lactam antibiotics has been to decrease the susceptibility to β-lactamase-catalysed inactivation. Indeed, while **162** and **168** were shown to be hydrolysed at comparable rates to β-lactams, synthetic analogues **180** and **179** showed up to 64-fold decreases in hydrolysis rates, demonstrating lower susceptibility to SBL-catalysed hydrolysis.[167, 174] Analogues **180** and **179** were readily hydrolysed by MBLs, however, showing no improvement over β-lactams.[167] The reactions of **162** and **168** were studied by electrospray ionisation mass spectrometry (ESI-MS), and it was observed that **168** and the Class A SBL BS3 formed a semi-stable acyl-enzyme complex with a lifetime of ~10 minutes.[174] This was a significant result considering the high catalytic efficiency of Class A SBLs for β-lactam antibiotics.

Crystal structures of the BS3-**162** complex were solved to 2.1 Å and revealed similarities to the acyl-enzyme complex of **162** with *P. aeruginosa* PBP1b. Notably, in both cases, the nucleophilic serine had reacted with the γ-lactam and the γ-lactone ring was opened. Six of seven hydrogen bonds between **162** and the active site of PBP1b were also conserved in the BS3 complex and **162** forms three additional hydrogen bonds in the BS3 complex. The crystal structures further revealed that the acyl-enzyme intermediate of **168** occupies the 'oxy-anion hole'

through which water could have otherwise approached and hydrolysed the ester complex.[174]

The steric blocking of the oxy-anion hole, along with additional hydrogen-bonding interactions that could disrupt acid-base catalysis, appear to be the main factors contributing to the stability of the acyl-enzyme complex. Furthermore, unlike the acyl-enzyme complex between some SBLs and clavulanic acid where a protonated aldehyde or iminium provides an alternative electrophile for the hydrolytic water molecule,[175] the structurally analogous oxime of the **162** acyl-enzyme complex is shown not to be attacked by a water molecule. Thus, the deacylation of the BS3-**162** complex apparently proceeds in a fashion like that observed for the acyl-enzyme complex between BS3 and 6-β-iodopenicillinate.[174, 176]

1.6.10 Antibacterial activity of cycloserine analogues

D-Cycloserine (**190**), also called oxamycin, is a metabolic product first isolated from *Streptomyces orchidaceus*.[177] **190** was reported to be an effective antibacterial agent in mouse models against Gram-positive bacterial infections. In *S. aureus*, **190** induces accumulation of uridine nucleotide, indicating the disruption of cell wall biosynthesis.[178] **190** is structurally similar to D-alanine and acts as a competitive inhibitor of the bacterial enzyme alanine racemase, preventing the bacterial synthesis of D-alanine from the natural amino acid L-alanine.[160] Recently, **190** has been shown to disrupt cell wall biosynthesis in *M. tuberculosis* by competitively inhibiting *M. tuberculosis* D-alanine:D-alanine ligase.[179]

Analogues of L-cycloserine were synthesised to explore the importance of the γ-lactone carboxylate moiety for PBP inhibition (**Figure 1-38**).[129] Analogues of lactivicin with the lactone carboxylate moiety substituted for other electron-withdrawing groups such as; sulfonates (**191**);[180] alkyl chlorides and hemi-aminal ethers (**192** and **193**),[181] and fumarates (**194**)[181] were synthesised and screened for activity. While compounds **191**, **192**, and **194** showed some antibacterial activity, they were considerably less active than **168**.[180, 181] Compound **193** showed no antibacterial activity against tested *E. coli* or *S. aureus* strains.[181] These studies reveal that simply attaching an electron-withdrawing group to the lactam nitrogen is not sufficient to activate the carbonyl to nucleophilic attack, and that the γ-lactone ring is essential for the antibacterial activity of lactivicins.[181]

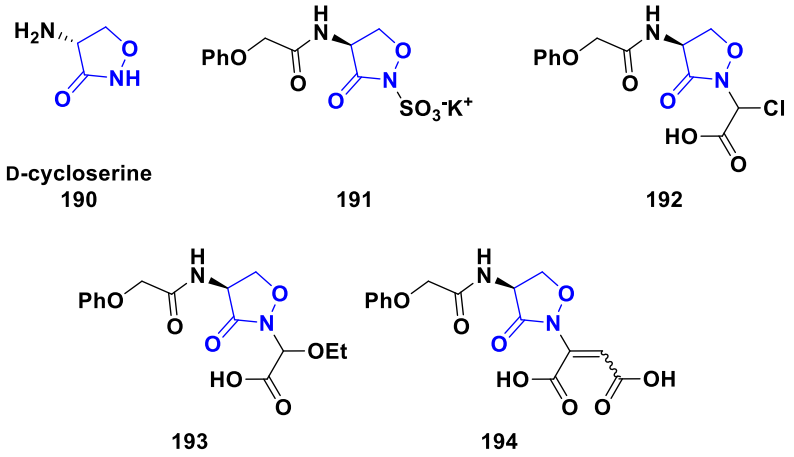

Figure 1-38 | Structures of D-cycloserine and cycloserines with various *N*-linked electron-withdrawing groups.

It is worth noting the structural similarity between the bicyclic pyrazolidinones **151** and the fumarate **194**, with the latter essentially being a ring-opened version of the

former, yet this subtle difference results in remarkably different antibacterial properties.

1.6.11 Bioisosteres of the lactivicin aminoisoxazolidinone ring

Since the discovery of **162**, numerous molecules with structurally related electrophilic cores have been developed for a range of applications. One such class of compounds is the benzisothiazolinones, which are used on a commercial scale as biocides in cosmetic products and paints,[182] and recent studies have also shown their potential as antimicrobials.[183, 184] The benzisoxazolidinone compound ebsulfur (**195**) displayed low MICs against clinically relevant strains of *H. pylori* and inhibit thioredoxin reductase (TrxR).[185] Analogues **196**, **197** and **198** showed antibacterial activity against MRSA.[186] EbsF (**199**) is a potent trypanothione reductase inhibitor (TryR).[183] Compound **200** was shown to inhibit MBLs via covalent modification of an active-site cysteine residue; against NDM-1 **200** exhibited nanomolar inhibition against NDM-1.[187] Compounds **201** and **202** also showed potent antifungal activity.[188, 189]

Ebselen (**203**) and analogues **204** and **205** show potent antibacterial activity against MRSA and VRE. These studies identified a correlation between ClogP and MIC whereby lower ClogP values corresponded to more potent MICs. Interestingly, the MICs for **204** and **205** were shown to be unaffected by expression of NDM-1, suggesting that these inhibitors are not susceptible to inactivation by MBLs and that the isoselenazolinone ring is not readily hydrolysed.[190, 191] The maintenance of

potency in the presence of MBLs for **204** and **205** appears to suggest they are not substrates for MBLs. In addition, **203** has been reported as a potent inhibitor of NDM-1 and, like the ebsulfur analogue **200**, **203** reacts covalently with an active-site cysteine that coordinates a zinc ion.[192] **203** was shown to inhibit Ldt_{mts} via covalent reaction of the selenium atom with the active site cysteine to give a thioselenide adduct.[193] **203** was shown in mice to be effective as a topical treatment of MRSA skin legions.[194] **203** was reported to exhibit micromolar inhibition of *S. aureus* TrxR and *B. anthracis* TrxR.[195, 196] **206** features an activated ester R group that is able to cross-link the MBL active site via the reaction with **206** an active-site lysine residue. Inhibitory activity was also reported for the B1 and B2 MBL subclasses.[197] From these studies it is clear that both benzisothiazolinone- and benzisoselenazolinone-based compounds show promise for further development as antimicrobial agents.

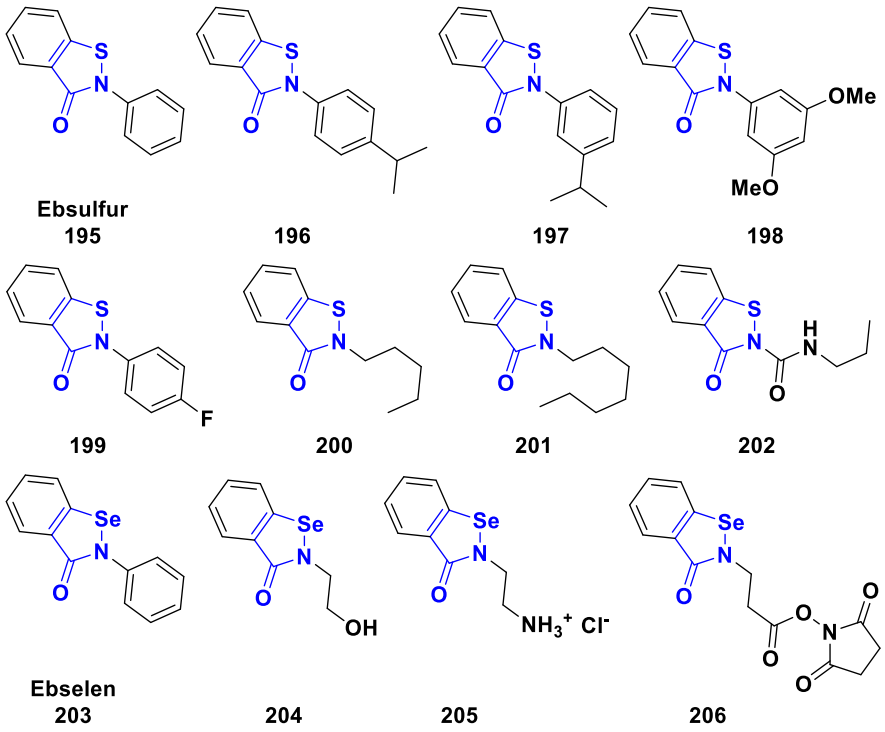

Figure 1-39 | Structures of benzisothiazolinone- and benzisoselenazolinone-based compounds with antimicrobial activity.

The monocyclic isoxazolidin-5-one **207** and bicyclic analogues **208** and **209** were synthesised as potential covalent inhibitors of bacterial transpeptidases and showed weak antibacterial activity against *S. aureus* and *E. coli*.[198] However, no inhibition of PBPs was observed.[198]

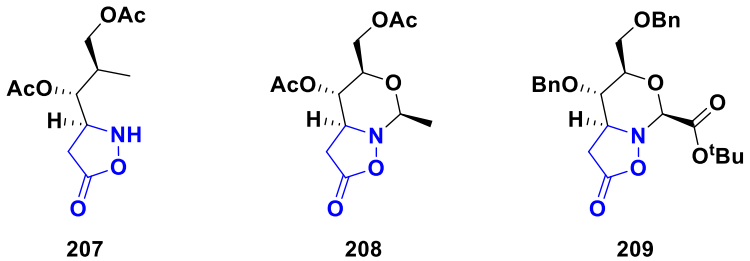

Figure 1-40 | Structures of isoxazolidin5-one analogues synthesised for antibacterial testing.

1.7 Summary of non-β-lactam-based antibacterials

This introduction has outlined in detail the historical precedent for non-β-lactam-based antibacterial agents. The cyclobutanones **78**, **79**, and **80**, synthesised as analogues of penem and penam antibacterials, demonstrated both modest antibacterial activity as well as micromolar inhibition of β-lactamases.[98] The β-thiolactam **91** exhibited reduced antibacterial activity compared to its penicillin analogue **5**, and the β-lactone **92** was reported to be a covalent inhibitor of PBPs with weak antibacterial activity.[105-107] The DBOs **96**, **97**, **99**, **102**, **103** all demonstrated potent antibacterial activity against β-lactamase-producing bacteria.[114, 116, 118, 121] Boronates **104**, **105**, **106**, **107**, and **108** were reported to be potent inhibitors of various PBPs. While **104** displayed moderate antibacterial activity, compounds **105**, **106**, **107** and **108** were not reported to exhibit antibacterial activity.[72, 122, 125]

The monocyclic γ-lactam analogues **113**, **114a-b**, and **115a-b** exhibited moderate antibacterial activity.[131-133] Of the bicyclic γ-lactam analogues outlined in this introduction, compounds **122-126**, **129d**, **133**, **134**, **135**, and **136** showed varying degrees of antibacterial activity, with **135** appearing to be the most therapeutically viable.[129, 137, 139, 141, 142, 199] The monocyclic aminopyrazolidinones **142**, **143**, **144**, and **145** were reported to show weak antibacterial activity.[147] Bicyclic aminopyrazolidinones with antibacterial activity include **150**, **151a-e**, **152**, **157**, **158a-b**, **159a-b**, **160a-b**, and **161**.[148-150, 152, 153, 157] Most notably, compounds **151a-e** and the siderophore-functionalised **157** were exceptionally potent antibacterial agents.[152, 153]

The lactivicins appear to be the most promising non-β-lactam class of transpeptidases inhibitors due to their broad spectrum of activity and their apparent stability to β-lactamases relative to comparable β-lactam antibiotics.[167, 174] Synthetic lactivicins **168**, **175a-h**, and the siderophore-conjugated **179** in particular are noteworthy for further development.[165, 167, 174] In addition, the identification of benzisothiazolinones **196**, **197**, and **198**, and benzisoselenazolinones **203**, **204**, and **205** as antibacterials against MRSA and, in the case of **203**, *M. tuberculosis* represent promising starting points for the development of future antibacterials.[186, 190, 191]

1.8 Project aims

The overall aim of this thesis was to further explore non-β-lactam-based ring systems as potentially new covalent inhibitors of bacterial transpeptidases. As discussed in **Section 1.7**, the lactivicins, benzisothiazolinones, and benzisoselenazolinones appear to be promising electrophilic warheads for the inhibition of nucleophilic serine and cysteine enzymes, hence these ring systems were selected for further development into potential antimicrobial agents. The aims of the work described in this thesis are outlined below:

1. Design and synthesise novel non-β-lactam analogues as potential transpeptidase inhibitors.
2. Explore the potential of benzisothiazolinone-based compounds as inhibitors of nucleophilic serine and cysteine enzymes.

3. Develop methodology for the modification of **2-OG** as precursors to γ-lactone-functionalised lactivicin analogues.
4. Evaluate the activity of synthesised compounds against their biological targets, in collaboration with others.

Chapter 2 Synthesis of lactivicin analogues

2.1 Introduction

The synthetic lactivicin analogues that were discussed in **Chapter 1** demonstrated potent and broad-spectrum antibacterial activity, clearly validating the lactivicin core as a promising electrophilic warhead for PBP inhibition.[165] These synthetic lactivicins also spurred efforts to identify other suitable non-β-lactam rings that are capable of inhibiting PBPs. Collectively, these studies provide a rudimentary SAR for PBP inhibition by lactivicin-type compounds. However, the SAR surrounding the lactivicin core remains relatively unexplored. Given the urgent need to develop novel antibacterial agents in an era of increasing bacterial resistance, and the efficacy demonstrated by reported synthetic lactivicin analogues, there is a clear need to further investigate the SAR for the inhibition of PBPs by lactivicin.

Therefore, the work described in this Chapter focused on the development of synthetic routes that would enable the preparation of novel lactivicin analogues bearing functionality in previously unexplored areas. The Chapter focuses first on the synthesis of reported lactivicins to facilitate the comparison of novel lactivicins to reported biological data. Then, lactivicin 'fragments' were synthesised to explore the specific contributions of specific areas on the molecule to the biological activity. Methods to allow for the introduction of modifications to the cycloserine ring of

lactivicin were explored, followed by the synthesis of tricyclic lactivicins initially disclosed in a patent filing by Yamawaki *et al*.[173]

2.2 Synthesis of reported lactivicin compounds

To enable direct biological comparison of new molecules to previously disclosed lactivicins and clinically used β-lactam antibiotics, syntheses of the reported lactivicins **168** and **180** were undertaken following reported procedures.[165, 167]

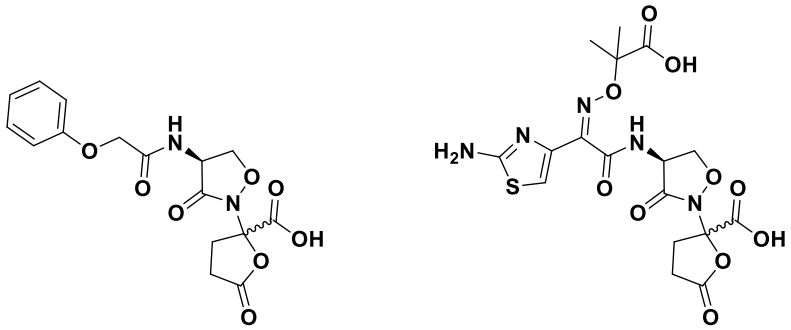

Figure 2-1 | Structures of reported lactivicin compounds **168** and **180**.[165, 174]

2.2.1 Synthesis of compound 168

The synthesis of **168** (**Figure 2-2**) was achieved, following a reported procedure,[174] in three linear steps from the readily available L-cycloserine, which was first reacted with phenoxyacetyl chloride in THF/pH 10 carbonate buffer to afford the cycloserine intermediate **210** in good yield (70%). The γ-lactone moiety was installed by reacting **210** with the **2-OG** ester **172** in the presence of dicyclohexylamine (DCC) in CH_2Cl_2 to give the lactone **211** in moderate yield (56%) as an approximately 1:1 mixture of diastereomers (by ^{1}H NMR). The 4-nitrobenzyl

ester was then removed by hydrogenation and the free acid purified using preparative high performance liquid chromatography (prep HPLC) to give **168** in a 56% yield as a ~1:1 mixture of diastereomers (by ^{1}H NMR). Note that the separation of the two diastereomers was not achieved using prep HPLC as **168** readily undergoes interconversion between the two diastereomers in solution.[159]

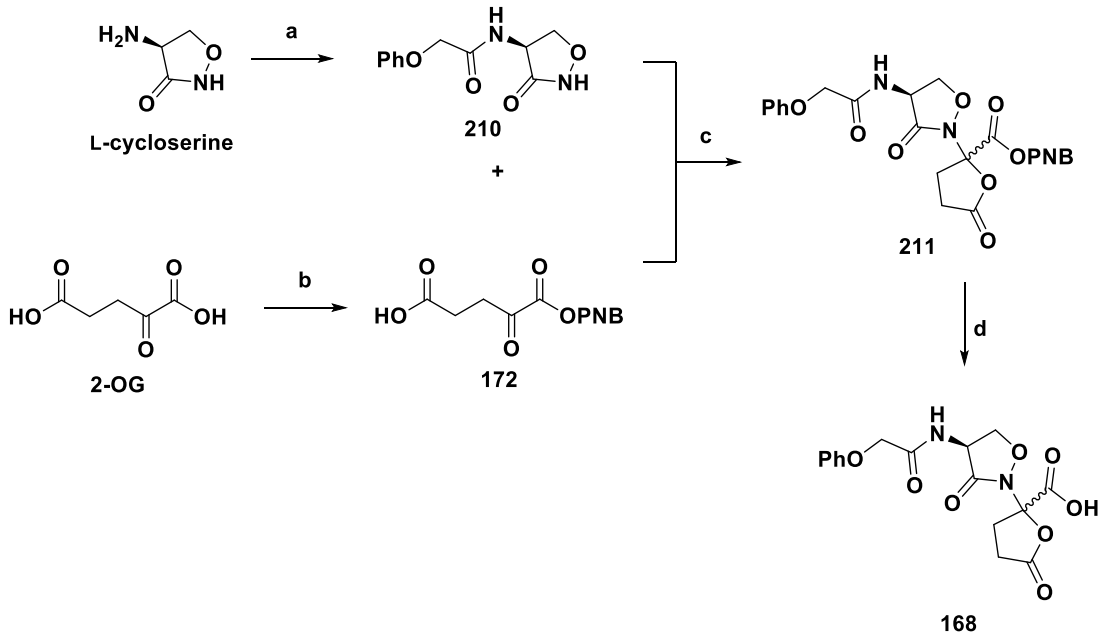

Figure 2-2 | Synthesis of **168**. Reagents and conditions: (**a**) phenoxyacetyl chloride, THF/pH 10 carbonate buffer, rt, o/n, 70%; (**b**) 4-nitrobenzyl bromide, DIPA, DMF, 70 °C, 2 h, 92%; (**c**) DCC, CH_2Cl_2, rt, o/n, 56%; (**d**) Pd/C, H_2, THF/H_2O (2:1 *v*/*v*), rt, 3 h, 56%.

The lactonisation reaction is a key synthetic step for the synthesis of all lactivicin-type molecules. A proposed mechanism for this transformation is shown in **Figure 2-3** and is thought to proceed via the initial formation of the activated isourea ester **212**. The ketone of the **2-OG** ester **212** then undergoes nucleophilic attack by the

ring nitrogen of the cycloserine **210** to reversibly form the hemiaminal **213**; the hemiaminal hydroxyl group then reacts with the activated ester to form the lactone ring.

The nucleophilic attack of the endocyclic nitrogen onto the **2-OG** ester **212** appears to be regioselective for the *C*-2 ketone over the activated *C*-5 ester; no evidence for the imide product **214** was observed in these reactions. The observed regioselectivity of the lactonisation reaction suggests that the activated ester of **212** is likely insufficiently electrophilic to enable the nucleophilic attack of the endocyclic nitrogen. The use of other coupling reagents might indeed result in the formation of the imide **214** by more strongly activating the ester.

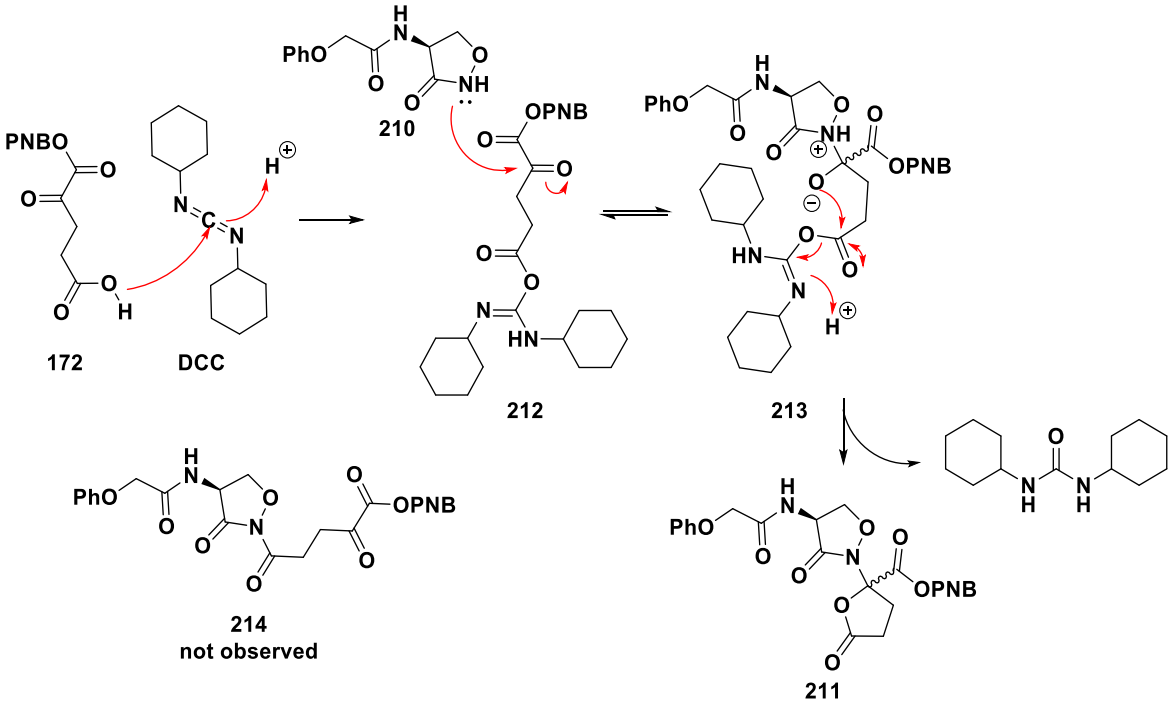

Figure 2-3 | Proposed mechanism for the lactonisation reaction to form **211**.

2.2.2 Synthesis of compound 180

The synthesis of **180** followed the same general route to that described for **168**, but utilized a different protecting group strategy (**Figure 2-4**). Following a reported procedure[167], the 'ATMO'-type sidechain **215** was first *N*-Boc protected to give **216** then reacted with *N*-hydroxylsuccinimide (NHS) and DCC to give the activated NHS ester **217**. The ester **217** was then coupled to L-cycloserine in refluxing EtOH to give the amide **218**, albeit in low yields (34%). Attempts to optimize the amide coupling using different coupling conditions (summarised in **Table 2-1**) were largely unproductive. While the conversion of the carboxylic acid **216** to the NHS ester **217** appeared to proceed efficiently, the poor solubility of L-cycloserine in organic solvents might hamper the formation of the amide bond in the subsequent step. The reaction was performed in solvents that dissolved L-cycloserine, such as aqueous solutions in THF or alcoholic solvents, but these conditions appeared to quench of the activated ester with little to no amide product formation. Thus, the reported low-yielding conditions were used to couple the ATMO-type sidechain onto cycloserine.[167]

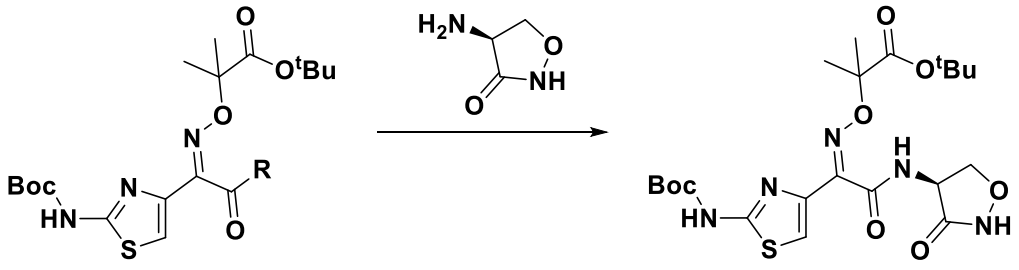

Entry	R	Coupling Reagent	Solvent	Base	T (°C)	Isolated Yield (%)
1*	NHS	n/a	EtOH	K_2CO_3	78 °C	34
2	Cl	n/a	DMF	DIPEA	rt	6
3	Cl	n/a	THF/H_2O	$NaHCO_3$	rt	0
4	OH	HATU	DMF	DIPEA	rt	0
5	OH	HATU	DMF	DIPEA	80 °C	0
6	OH	HATU	DMF/EtOH	DIPEA	rt	0
7	OH	EDCI/HOBt	DMF	DIPEA	rt	0
8	OH	DCC	CH_2Cl_2	DIPEA	rt	0
9	OPfp	n/a	DMF	DIPEA	rt	19

Table 2-1 | Reaction optimisation of the amide coupling between the 'ATMO' sidechain **216** and L-cycloserine. (*) Indicates the reported conditions.

Formation of the lactone ring was performed analogously to the method described previously for the preparation of **168** using the benzhydryl ester **219**, giving the protected lactivicin intermediate **220** in good yield (72%). The benzhydryl ester

protecting group was again removed by hydrogenation to give the corresponding free acid **221**. The final deprotection of the *N*-Boc and *tert*-butyl groups from the ATMO sidechain was achieved using BCl_3 (4 M solution in CH_2Cl_2). This step was challenging as the presence of even small amounts of water resulted in hydrolysis of either (or both) the cycloserine and lactone rings to give the ring-opened product **222** (as observed by LCMS). In addition, **180** was found to slowly hydrolyse during the work-up, so the time taken to work-up and purify the reaction was kept as short as possible. These factors were largely responsible for the significant variations observed in the isolated product yields (0-23%).

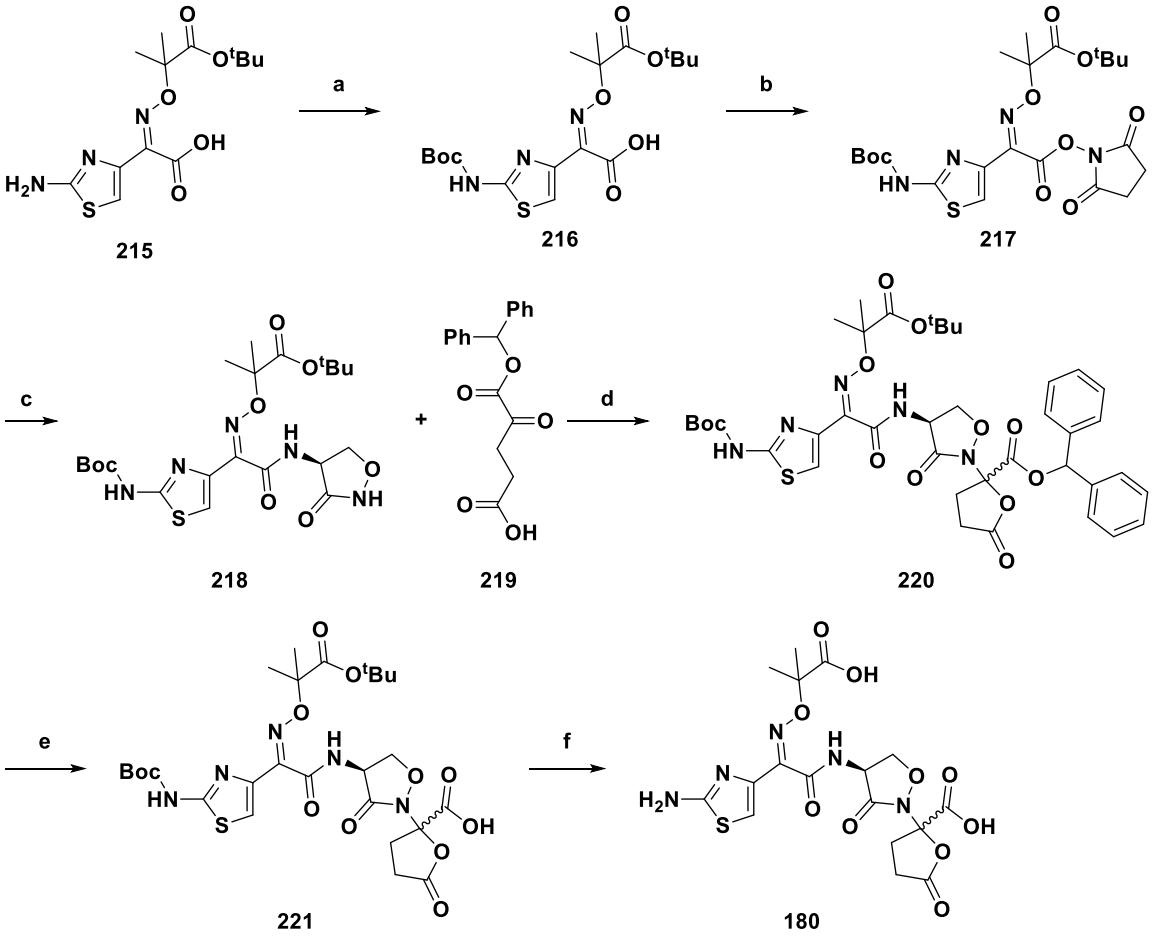

Figure 2-4 | Synthesis of **180**. Reagents and conditions: (**a**) Boc_2O, Et_3N, DMAP, $CHCl_3$, rt, 6 h, 42%; (**b**) NHS, DCC, CH_2Cl_2, rt, 90 min, used crude; (**c**) L-cycloserine, $NaHCO_3$, EtOH; reflux, 2 h, 34%

over 2 steps; (**d**) DCC, CH_2Cl_2, rt, o/n, 72%; (**e**) Pd/C, H_2, THF/ pH 7 phosphate buffer, 0 °C, 45 min, used crude; (**f**) BCl_3, CH_2Cl_2, -40 °C, 30 min, 0-23%.

2.3 Design and synthesis of substituted cycloserines

As discussed in **Section 1.6.3**, lactivicins functionalised with cephalosporin sidechains exhibit similar antibacterial activities with respect to their cephalosporin analogues, which suggests that the SAR of the β-lactam sidechains may be broadly transferrable onto the lactivicin core. It was therefore envisaged that other structural features of β-lactam antibiotics that improve their performance as PBP inhibitors should also translate onto the lactivicin core. Thus, cycloserine rings with novel modifications derived from selected β-lactam antibiotics and β-lactamase inhibitors were designed.

2.3.1 Design of 3-isoxazolidinone fragment 223

To investigate the contribution of the lactivicin sidechain to the antibacterial activity of the molecule, the analogue of lactivicin **223** lacking an amido sidechain on the cycloserine ring was envisaged. It was hypothesised that such an analogue might also be capable of β-lactamase inhibition, given that the structures of clinically used nucleophilic serine β-lactamase inhibitors (i.e. **41**, **42**, and **43**, **Figure 2-5**) all possess a bicyclic β-lactam ring system without a *C*-6 amido sidechain.

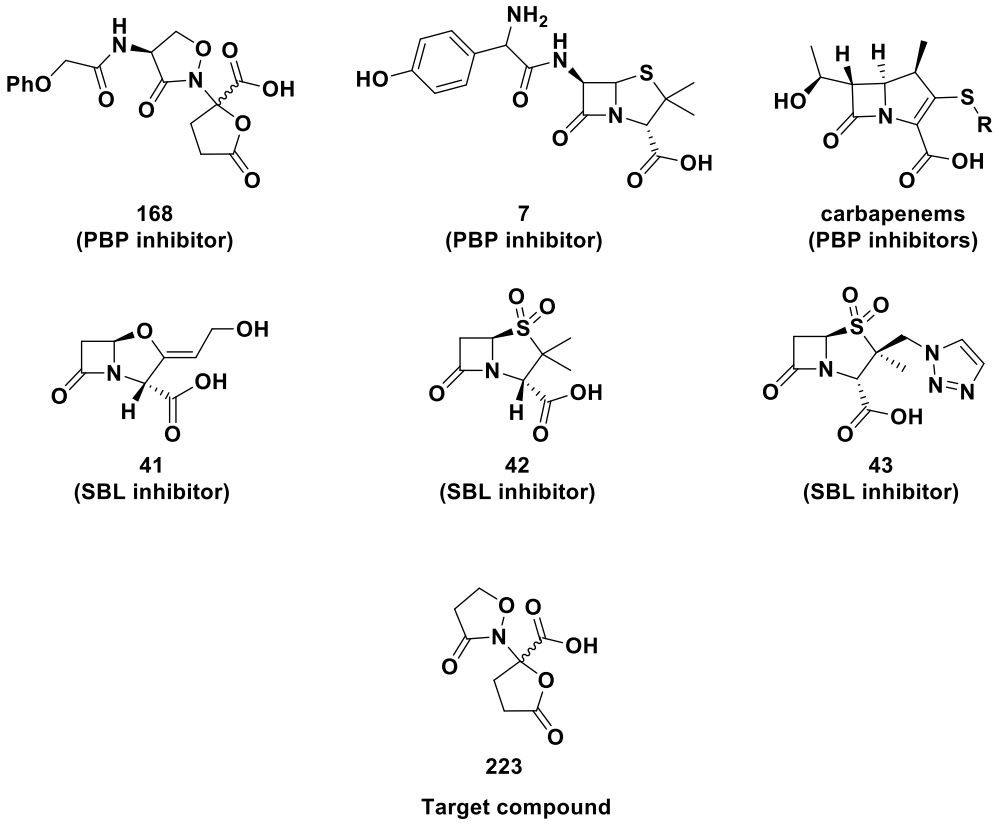

Figure 2-5 | Structures of PBP inhibitors bearing amido sidechains (**168** and **7**), SBL inhibitors lacking amido sidechains (**41**, **42**, **43**), carbapenems with hydroxyethyl sidechains, and target lactivicin analogue **223** with similar structural features.

Interestingly, a lactivicin analogue lacking any *C*-3 sidechain has not been previously reported. The synthesis of such analogues could be achieved following the route described for **168**, via the consecutive (i) preparation of the required oxa-γ-lactam, (ii) lactonisation, and (iii) ester deprotection. The synthesis of the isoxazolidinone intermediate **224** was achieved in two steps following a reported procedure[200] (**Figure 2-6)** that began from 3-chloropropionic acid, which was activated using ethyl chloroformate and then reacted with hydroxylamine to afford the hydroxamic acid **225** in 71% yield. The 5-*exo*-tet cyclisation of **225** was next performed in aqueous NaOH at 50 °C to give **224** in 71% yield. Evidence for the

formation of the 5-membered ring was observed in the IR spectrum with a carbonyl stretch at 1683 cm^{-1}, which is on the low end of the typical range for 5-membered lactams, and much lower than would be expected for a β-lactam.[201] The lactone ring was then installed in 89% yield to give **226** using DCC and the 4-nitrobenzyl ester removed by hydrogenation to give **223** in low isolated yields following troublesome purification by preparative HPLC. As with **168** and **180**, the stability of the lactone **223** to hydrolysis during deprotection and purification was poor, resulting in low isolated yields of the lactone **223** and substantial formation of the unwanted hydrolysed products.

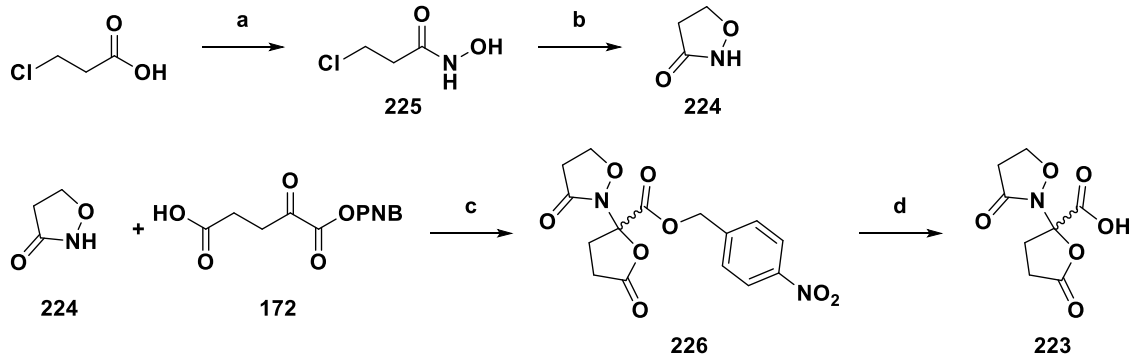

Figure 2-6 | Synthesis of **223**. Reagents and conditions: (**a**) ethyl chloroformate, NMM, Et_2O, 0 °C, 15 min then NH_2OH, MeOH/Et_2O, rt, 15 min, 71%; (**b**) 1 N NaOH, 50 °C, 15 min 72%; (**c**) DCC, CH_2Cl_2, rt, o/n, 89%; (**d**) Pd/C, H_2, THF/H_2O, rt, 1 h, 29%.

2.3.2 Synthesis of bicyclic cycloserine derivatives

While previously reported studies on lactivicin analogues explored different cycloserine ring sizes and arrangements, no investigations into fused bicyclic cycloserine analogues of lactivicin as antibacterial agents have been reported to date. Many such bicyclic systems are, however, known for other applications.

Benzisoxazolidinones have been investigated for the treatment of a wide range of disorders such as schizophrenia (**227**),[202] addiction (**228**),[203] depression (**229**),[204] and, recently, as antibacterials **230**.[205] As mentioned in the introduction, benzisothiazolinones (e.g. **195**, **197**, **198**, and **231**) are used on commercial scale as biocides in cosmetic products and paints,[182] and recent studies have shown their potential as antimicrobials,[183, 184] while analogous *S*-oxidised derivatives such as saccharin (**232**) are used as artificial sweeteners.[206] Molecules with an indazolinone core (e.g. **233**) have been studied as an anti-inflammatory agents ,[207] and the related compound phthalimide (**234**) is readily commercially available as it has multiple synthetic uses, for example as a nitrogen donor in the Gabriel amine synthesis.[208]

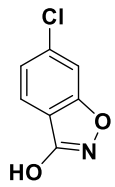

227

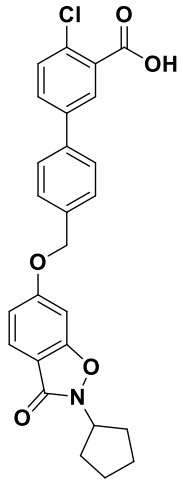

228

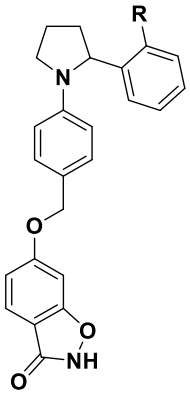

229

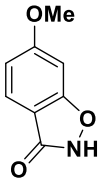

230

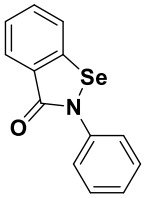

203

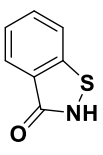

231

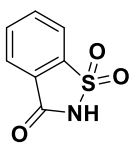

232

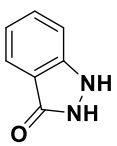

233

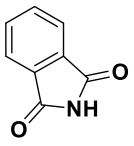

234

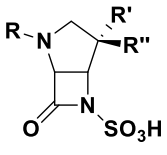

235

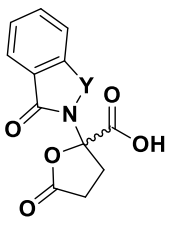

236

Figure 2-7 | Bicyclic ring systems structurally related to cycloserine and the target lactivicin analogues **236a-f**.

The bicyclic compounds shown in **Figure 2-7** also bear some structural similarity to the *C*-3/*C*-4 'bridged' monobactams (**235**) developed at Roche that were shown to possess potent inhibitory activity against SBLs.[107] The presence of a 5-membered ring at the *C*-3/*C*-4 positions of these monobactams may enable 'locking' of the conformation of the acyl-enzyme complex, via steric clashes with active site residues and additional non-covalent interactions, such that hydrolytic water molecules could not approach the ester, which would otherwise hydrolyse the acyl-enzyme complex and restore catalytic function.[107] Thus, the bicycles shown in **Figure 2-7** are potentially biologically relevant fragments whose starting materials are cheap and widely commercially available. The synthesis of bicyclic lactivicin analogues **236a-f** derived from the bicycles shown in **Figure 2-7** is summarised in **Table 2-2** and utilised the general synthetic route described for **168** (**Section 2.2.1**).

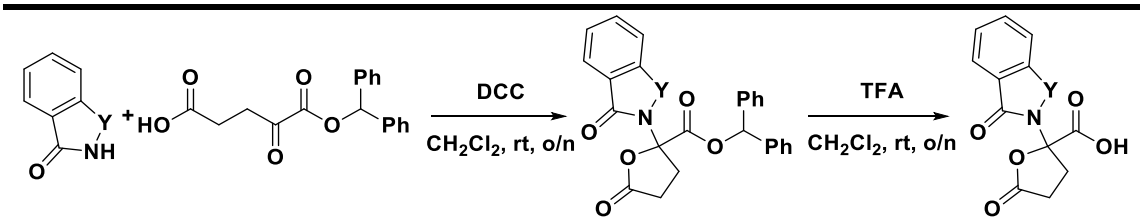

Compound	Y	Isolated yield (%) of 237	Isolated yield (%) of 236
236a	O	67	41
236b	S	54	38
236c	NH	0	-
236d	NMe	0	-
236e	SO_2	64	0
236f	CO	30	42

Table 2-2 | Synthesis of bicyclic cycloserine analogues.

Compound **219** was reacted with the appropriate bicyclic nucleophiles to form the protected lactone intermediates **237a-f**. Reaction of **219** with 3-indazolinone was observed to form the 6-membered hemiaminal **238**, analogous to the side product **239** observed by Tamura *et al*.[164], but none of the desired lactone **237c** (**Figure 2-8**). To circumvent the formation of the hemiaminal side product **238**, the β-amino group was protected with a methyl group via reductive amination using formaldehyde and sodium cyanoborohydride to give **240** in moderate yield (53%). The regiochemical identity of **241** was confirmed using heteronuclear multiple-bond correlation spectroscopy (HMBC), which identified a correlation between the hydrogens of the methyl group and the *C*-3 carbon (**Figure 2-9**). However, **240** did

not readily undergo cyclisation with **219** in the presence of DCC, and none of the desired lactone **237c** was isolated.

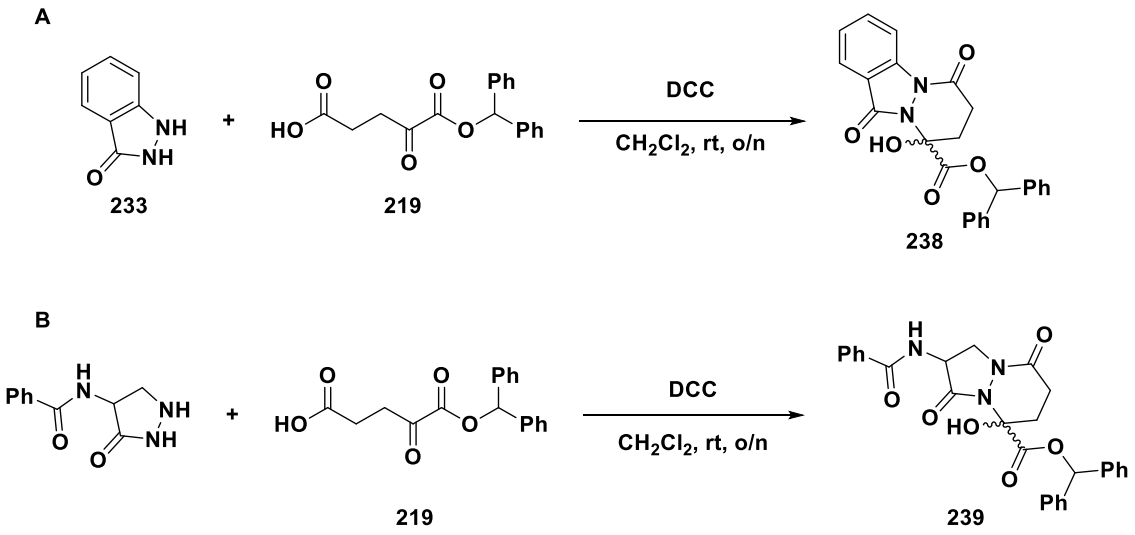

Figure 2-8 | Reaction of (**A**) indazolinone and (**B**) a pyrazolidinone (as reported by Tamura *et al.*[164]) with **219** to give 6-membered hemiaminal side products.

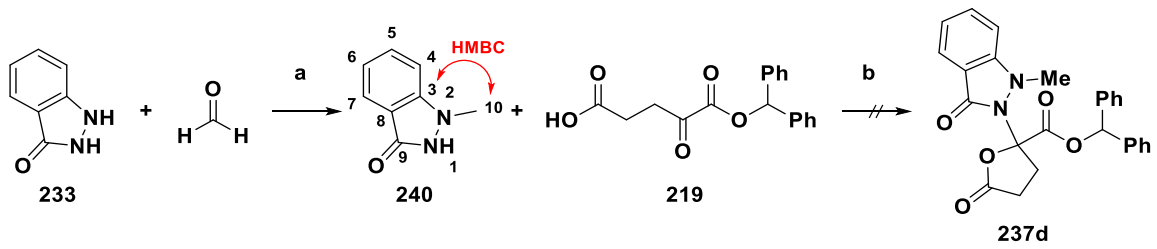

Figure 2-9 | Attempted synthesis of **237d**. Reagents and conditions: (**a**) $NaBH_3CN$, CH_2Cl_2, rt, 3 d, 53%; (**b**) DCC, CH_2Cl_2, rt, o/n.

The failure of these conditions to produce the desired lactone **237d** could be due to the increased steric bulk associated with the *N*-methyl group; however a previously reported synthesis on structurally related monocyclic analogues were successful,[164] and the lactonisation using phthalimide **234** (which has a carbonyl group at the

analogous position) successfully reacted to form the corresponding lactone **237f**, albeit in a low yield (30%). The lactonisation reaction of the **2-OG** ester **219** with **232** to form the lactone **237e** was achieved in moderate yield (64%).

Deprotection of the benzhydryl ester by hydrogenation was first attempted on the benzisothiazolidinone lactone **237b**. However, the reaction stalled repeatedly, requiring the addition of additional palladium catalyst, possibly due to poisoning of the Pd catalyst by the sulfur,[209] so an alternative deprotection strategy using trifluoroacetic acid was employed for all subsequent benzhydryl deprotections, and yielded compounds **236a**, **236b**, and **236f**.

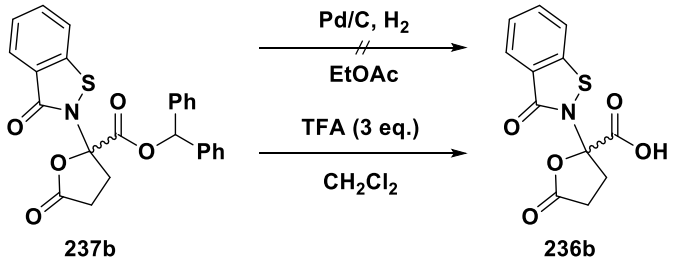

Figure 2-10 | Attempted deprotection of **237b**. The use of TFA avoided the issue of catalyst poisoning observed in the hydrogenation condition.

While the benzhydryl group of the saccharine intermediate **237e** was removed efficiently, the resulting lactone carboxylate **236e** was unstable to purification. Instead, the lactone moiety underwent a retro-lactonisation-type reaction to return **232** and **2-OG**. In summary, the bicyclic cycloserine lactivicin analogues **236a**, **236b**, and **236f** were synthesised successfully.

2.3.3 Synthesis of a "decarboxylactivicin" analogue

As described in **Section 1.3.1**, the presence of a carboxylate group at the *C*-2 position of β-lactam antibiotics plays a key role in substrate recognition and binding of β-lactams with PBPs. Similarly, mechanistic studies suggest that the carboxylate group is equally important for the inhibitory activity of the lactivicins.[162] However, β-lactamase inhibitors without a carboxylate group have also been reported.[210] To examine the importance of the carboxylate group for antibacterial activity, a decarboxylated analogue of **168**, **242**, was prepared. This analogue was synthesized in one step from **210** with levulinic acid (**243**) and DCC in moderate yield (65%) to give a ~1:1 mixture of diastereomers (by ^{1}H NMR).

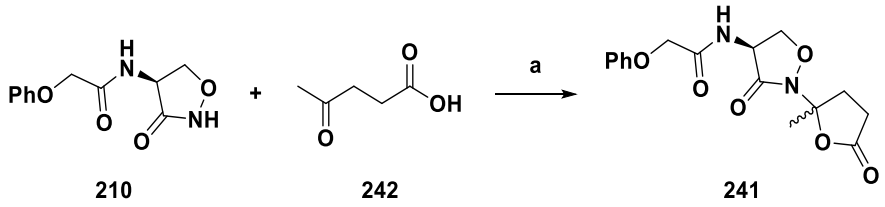

Figure 2-11 | Synthesis of **242**. Reagents and conditions: (**a**) DCC, CH_2Cl_2, rt, o/n, 65%.

2.4 Synthesis of *C*-3-modified cycloserines

The development of synthetic methods allowing the modification of the cycloserine ring would lead to the generation of new libraries of lactivicins containing novel functionalities, which may (i) impart greater stability of these molecules to β-lactamases, (ii) exhibit improved cellular uptake, and/or (iii) confer greater inhibitory activities against different bacterial transpeptidases. Installation of a

methyl group on the *C*-3 position of the β-lactam in monobactams (e.g. **33**) confers additional β-lactamase stability by disrupting the binding interaction between the β-lactam and the enzyme active site.[211] Similar modifications to the cycloserine core of lactivicin may therefore also confer increased levels of resistance to β-lactamase hydrolysis, hence methods enabling the installation of a methyl group to the *C*-3 position of the cycloserine ring were investigated.

The compound acinetobactin (**244**) (**Figure 2-12**) was found in a literature search for methodology to synthesise functionalized aminoisoxazolidinones. **244** is an iron-sequestering siderophore expressed by *Acinetobacter baumanii* under low-iron conditions.[212] At its core is a *C*-3-methylaminoisoxazlidinone ring – exactly the kind of functionality targeted for introduction into the lactivicin scaffold (**Figure 2-12**). Thus, it was proposed that methods to synthesise **244** could be used for the synthesis of *C*-3-modified lactivicins **245**.

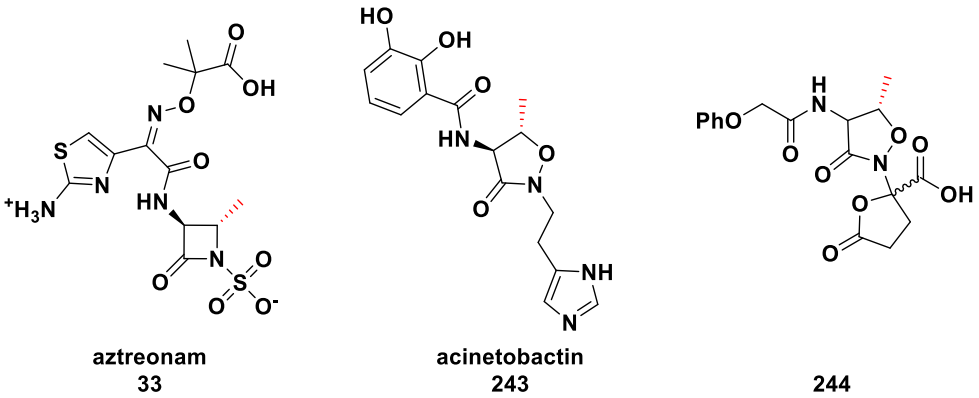

Figure 2-12 | Structures of aztreonam, acinetobactin, and the target compound **245**.

2.4.1 Biosynthesis of acinetobactin

The proposed biosynthesis of acinetobactin is shown in **Figure 2-13** and is facilitated by non-ribosomal peptide synthase (NRPS) catalysis.[213] The biosynthesis begins with the amide condensation of the catechol **246** with L-threonine to give the amide intermediate **247**, which then undergoes a dehydrative cyclisation to form the oxazoline **248**. Reaction with the hydroxylamine **249**, derived from histamine, then affords pre-acinetobactin (**250**), which is released from the NRPS domain and can undergo a pH dependent, enzyme-free rearrangement to form **244**.[214]

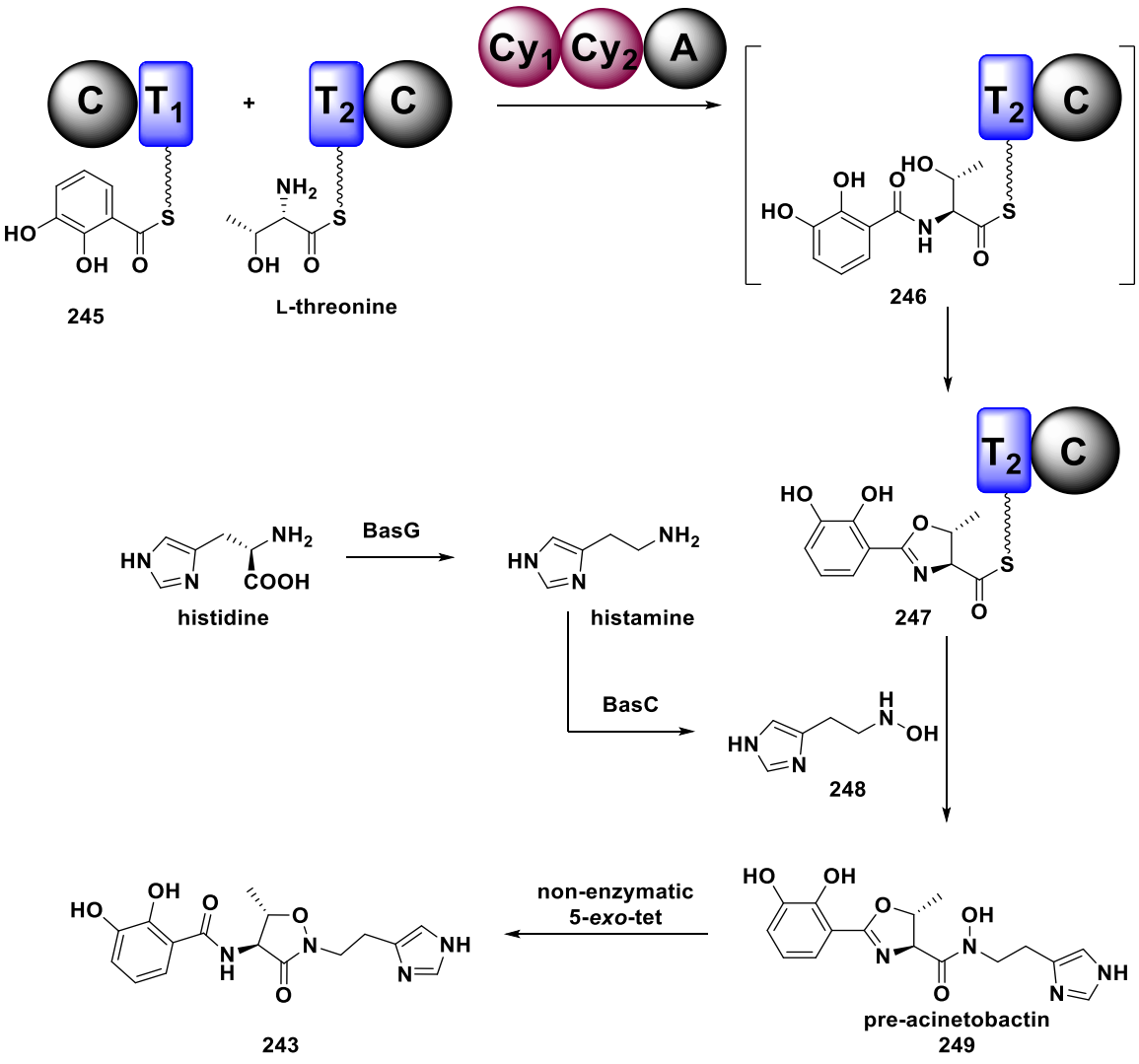

Figure 2-13 | Proposed biosynthesis of acinetobactin via non-ribosomal peptide synthase catalysis. Adapted from Wuest *et al*.[213] **Abbreviations:** A – adenylation domain; C – condensation domain; Cy – cyclisation domain; T – thiolation domain.

The key step in the biosynthesis of acinetobactin is the enzyme-free rearrangement of the oxazoline of **250** to the isoxazolidinone of **244** (**Figure 2-14**) via a 5-*exo*-tet ring closure reaction.[214] The rearrangement reaction occurs at pH values above 7 and is facilitated by the favourable protonation states of both the imidazole and the catechol moieties. At pH values below 7, the imidazole is protonated and positively charged and the cation coordinates to the hydroxamate, preventing the hydroxamate oxygen from attacking the oxazoline. At pH values above 7, the imidazole is neutral and does not coordinate to the hydroxamate, liberating the hydroxamate to act as a nucleophile. The oxazoline moiety is additionally activated

to undergo a nucleophilic attack under these conditions due to the tautomerisation that occurs between the oxazoline and the catechol.

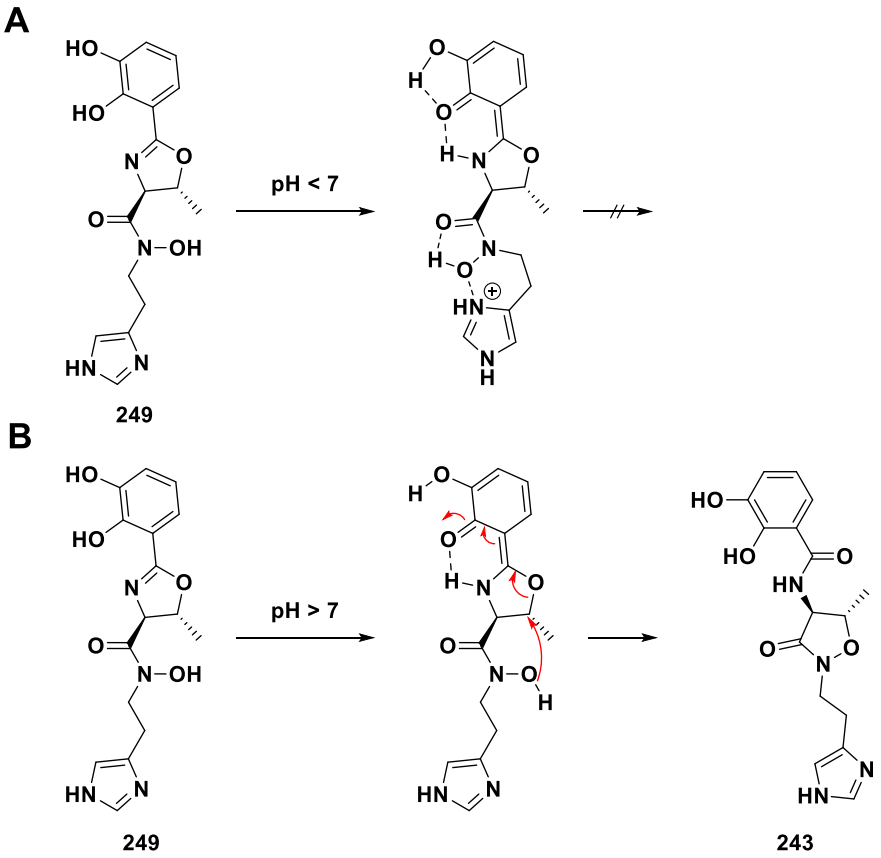

Figure 2-14 | Proposed mechanism for the pH-dependent 5-*exo*-tet cyclisation of pre-acinetobactin to acinetobactin at (**A**) low pH and (**B**) high pH conditions.

2.4.2 Synthesis of acinetobactin analogues

Song *et al.*[215] prepared analogues of acinetobactin to investigate their siderophoric properties (**Figure 2-15**). The reported synthesis began with an amide coupling between a methyl threoninate **251** and the appropriate 2-hydroxybenzoic acid **252** to form the target amide **253**. Subsequent dehydrative cyclisation yielded the oxazoline **254**, which was then saponified to give the carboxylic acid **255**. The *O*-

benzyl hydroxamate moiety was installed using a peptide coupling reagent to give **256**, then the *O*-benzyl group was hydrogenated to give the hydroxamate **257**. Finally, refluxing **257** in methanol yielded the rearranged isoxazolidinone product **258**. These synthetic conditions formed the basis of the route toward modified cycloserines for lactivicins that are described in this thesis.

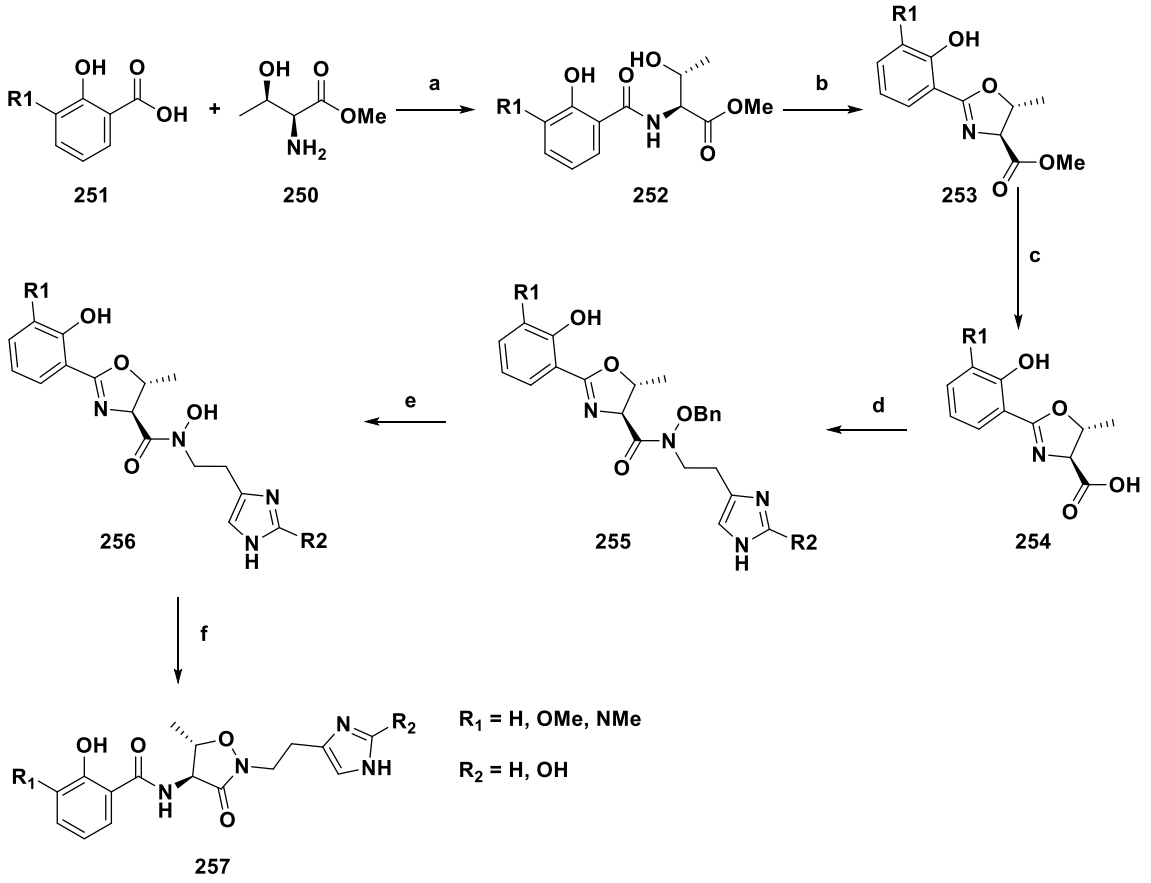

Figure 2-15 | Synthesis of acinetobactin as described by Song et al.[215] Reagents and conditions: (**a**) EDC, HOBt, DIPEA, DMF, rt, 95-96%; (**b**) $MoO_2(acac)_2$, tol, Dean-Stark then (**c**) Potassium trimethylsilanoate, Et_2O, rt, 74-82%; (**d**) HATU or PyBOP, K_2CO_3, DMF, rt then **e**) 55 psi H_2, Pd/C, MeOH, rt, quant.; **f**) MeOH, reflux, o/n.

Two key differences between the reported synthetic route to **258** and the planned synthetic route toward modified cycloserines **259** were the absence of the imidazole moiety on the hydroxamate precursor **260** and the use of the phenoxyacetamido

sidechain in place of the catechol amide due to concerns about removing selectively the catechol moiety at a later stage in the synthesis. However, as discussed above, the catechol moiety acts to activate the oxazoline ring to nucleophilic attack, so replacing it with the inert phenoxyacetyl moiety risked losing the ability to facilitate the 5-*exo*-tet rearrangement reaction.

The attempted synthetic route to **259** began with an amide condensation between **251** and phenoxyacetic acid using EDCI and HOBt, which gave the amide **261** in good yields (79%). To circumvent issues of oxazoline hydrolysis during saponification of the methyl ester, the hydroxamate moiety was installed prior to the oxazoline cyclisation. Hence, **261** was then saponified to the acid **262** with LiOH in good yield (80%). Coupling of the *O*-benzylhydroxylamine group to give the hydroxamate **263** was achieved in moderate yield (40%) using HATU. Then, the dehydrative cyclisation of **263** using catalytic $(NH_4)_2MoO_4$ as a Lewis acid in toluene under Dean-Stark conditions gave the oxazoline **264** in moderate yields (44%).[216] The *O*-benzylhydroxylamine group of **264** was deprotected by hydrogenation with Pd/C and H_2 to give the hydroxamate **260** in good yield (77%). The 5-*exo*-tet cyclisation was then attempted in refluxing methanol as previously described,[215] however, no cyclisation of the oxazoline to the desired isoxazolidinone **259** was observed under these conditions. This observation may be reflective of the absence of the catechol moiety, which has been shown to facilitate the

oxazoline/isoxazolidinone rearrangement through chelation of a proton between the *ortho*-hydroxyl group and the oxazoline nitrogen.[217]

To overcome the poor reactivity of the hydroxamate, it was proposed that the addition of a strong base (e.g., NaH), to deprotonate the hydroxyl group would sufficiently activate the nucleophile to complete the rearrangement. Another option could have been to first form the isoxazolidinone with the catechol amide sidechain, followed by the cleavage of the amide bond with PCl_5. However, since the isoxazolidinone ring would likely not have been stable to these conditions and given the time constraints induced by the COVID-19 restrictions, these conditions were not explored further.

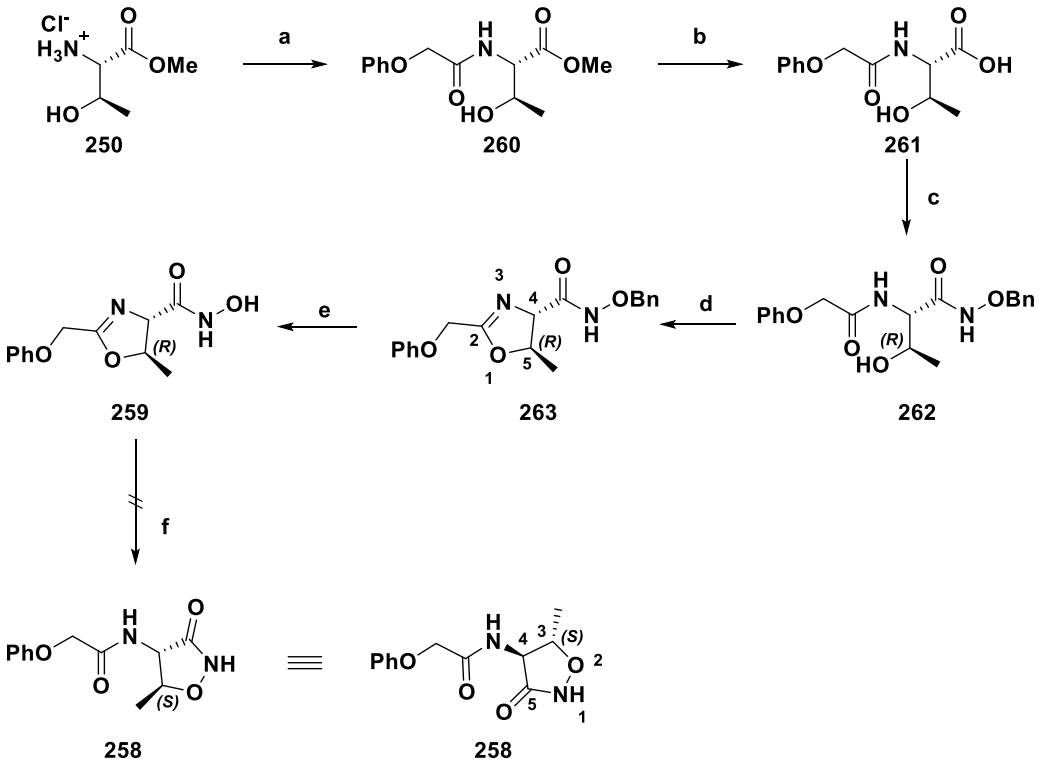

Figure 2-16 | Attempted synthesis of methylated cycloserine analogue **259**. (**a**) phenoxyacetic acid, EDCI, HOBt, DIPEA, DMF, rt, 2 h, 79% (**b**) LiOH, THF/H_2O (2:1 *v*/*v*), 30 °C, 6 h, 80%; (**c**) *O*-

benzylhydroxylamine hydrochloride, HATU, Et_3N, CH_2Cl_2, rt, o/n, 40%; (**d**) $(NH_4)_2MoO_4$ (cat.), tol, Dean-Stark, 16 h, 44%; (**e**) Pd/C, H_2, EtOAc, rt, 3 h, 77%; (**f**) MeOH, reflux, 2 d, 0%.

2.5 Synthesis of functionalized pyrazolidinones

3-Aminopyrazolidinones have been investigated as antibacterial agents by multiple research groups. In their initial publication of synthetic lactivicins, Tamura *et al.*[165] synthesised pyrazolidinone analogues of lactivicin **181** and **182**, though they did not observe any antibacterial activity. Aminopyrazolidinones are also found in the bicyclic pyrazolidinones (e.g., **151a,b**), as described by Eli-Lilly (**Section 1.5.10**), thus showing their potential to effectively acylate bacterial transpeptidases.[151] While **181** and **182** did not display antibacterial activity, it was proposed that the addition of a trifluoroacetyl group to the β-nitrogen of the pyrazolidinone ring may facilitate the covalent inhibition of bacterial transpeptidases. Thus, an attempt to synthesise the pyrazolidinone lactivicin derivative **265** was conducted.

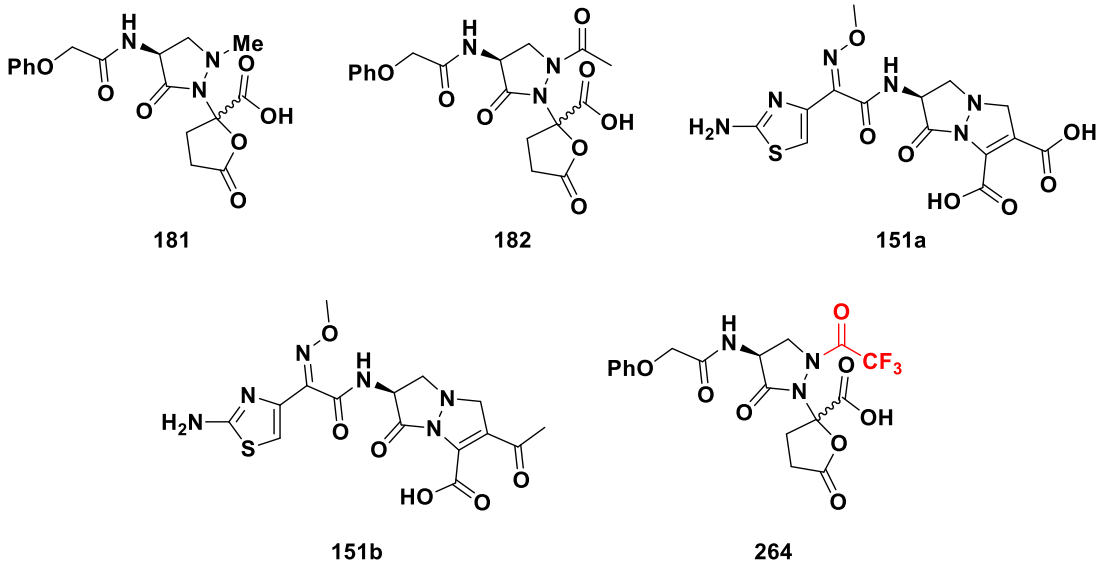

Figure 2-17 | Aminopyrazolidinones in the literature and the target compound **265**.[151, 164, 165]

2.5.1 Synthesis of aminopyrazolidinone precursor 266

The reported procedure for the synthesis of the *N*-Boc-protected pyrazolidinone **266** by Jungheim *et al*. [218] (**Figure 2-18**), which proceeds via the conversion of the serine methyl ester **267** to the tosylate (**268**), was attempted, but the final cyclisation step to give **266** via the reaction with hydrazine was unsuccessful.

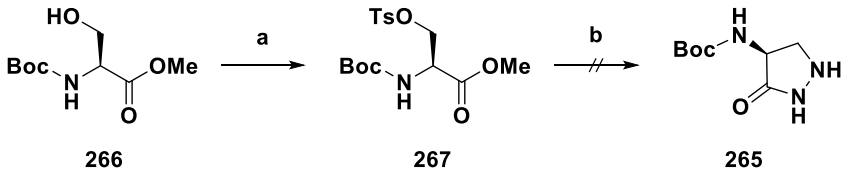

Figure 2-18 | Attempted synthesis of pyrazolidinone **266** using the procedure reported by Jungheim *et al*.[218] Reagents and conditions: (**a**) TsCl, pyr, CH_2Cl_2, rt, 2 h, 92%; (**b**) $N_2H_4 \bullet H_2O$, THF, rt, o/n.

Successful synthesis of the precursor **266** was then achieved following a modified procedure reported by Holmes *et al*.[219] (**Figure 2-19**), wherein the reaction of

hydrazine with **267** affords the hydrazide **269**, which is functionalised with an electron-withdrawing trifluoroacetyl group to give **270**, thereby increasing the acidity of the nitrogen and allowing for the cyclisation step to be performed under Mitsunobu conditions to give **271**.[220] Following the formation of the oxyphosphonium intermediate, the trifluoroacetyl hydrazide reacts via an S_N2-type reaction enabling the ring closure with a concurrent displacement of the phosphine oxide as a by-product.

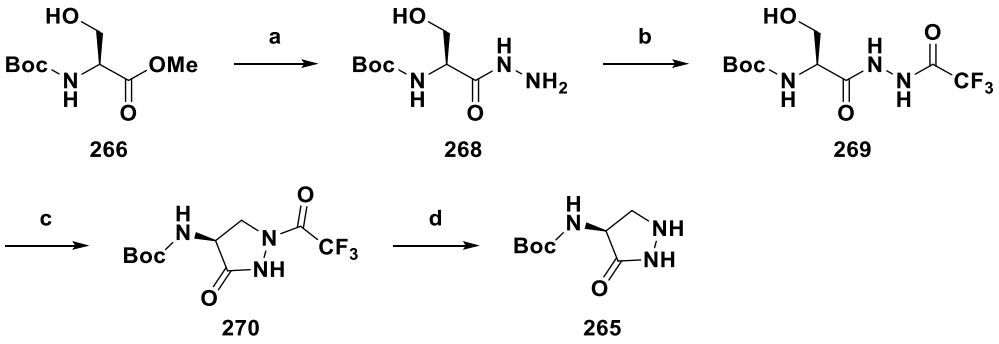

Figure 2-19 | Synthesis of **266** following a modified procedure reported by Holmes *et al*.[34] Reagents and conditions: (**a**) $N_2H_4 \bullet H_2O$, MeOH, rt, o/n, 95%; (**b**) *S*-ethyl trifluorothioacetate, EtOH, 30 °C, 2 d, 95%; (**c**) DIAD (1 M in CH_2Cl_2), PPh_3, THF, rt, o/n, 69%; (**d**) $N_2H_4 \bullet H_2O$, THF/H_2O (2:1 *v*/*v*) rt, o/n, 70%.

The trifluoroacetyl group was then deprotected to allow for further functionalisation of the β-nitrogen. After a brief screen of conditions for the cleavage of the trifluoroacetyl group, the *α*-effect[221] nucleophile hydrazine was found to be superior reagent for its deprotection, compared to the reported conditions using NaOH. (**Table 2-3**).[219]

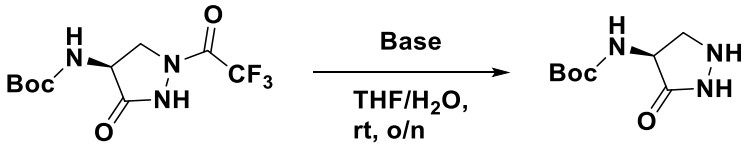

Entry	Base	Equivalents	% Isolated yield
1*	NaOH	2	16
2	NaOH	8	29
3	NH_2OH	2	17
4	N_2H_4	2	70

Table 2-3 | Condition screen for the deprotection of the trifluoroacetyl group of **271** to form **266.** (*) denotes the reported conditions.[219]

From the pyrazolidinone intermediate **266**, functionalization of the β-nitrogen is possible to create novel pyrazolidinone-based lactivicin analogues, though the inactivity of the *N*-methyl derivative reported by Tamura *et al.*[165] made this area of investigation less of a priority.

2.5.2 Attempted lactonisation of aminopyrazolidone 265

As mentioned in **Section 2.5**, while the *N*-acetyl lactivicin derivative **182**, reported by Tamura *et al.*,[165] did not show antibacterial activity, it was proposed that the lactivicin analogue **265**, functionalised with the additional electron-withdrawing nature of the trifluoroacetyl may increase the electrophilicity of the pyrazolidinone ring such that the compound is able to react covalently with transpeptidase enzymes. Hence lactonisation of the trifluoroacetyl pyrazolidinone intermediate

271 with **172** was attempted. However, the lactone product **272** seemed to decompose during flash chromatography, possibly due to the increased electrophilicity of the pyrazolidinone nitrogen due to the presence of the trifluoroacetyl group.

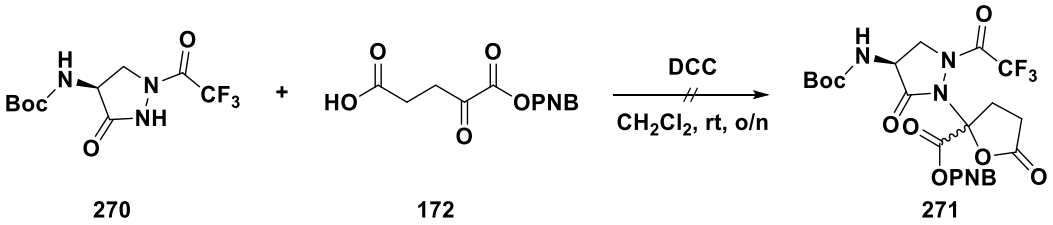

270 172 271

Figure 2-20 | Attempted lactonisation of pyrazolidinone **271** with **172** to form **272**.

2.5.3 Synthesis of *C*-3-functionalised aminopyrazolidinones

As discussed in **Section 1.3.5**, the addition of alkyl groups to the rings of monobactams is proposed to confer stability to SBL hydrolysis. It was envisaged that the method used for the synthesis of **266** could be applied to the L-threonine derivative **273** for the synthesis of the *C*-3-methyl pyrazolidinone analogue **274** (**Figure 2-21**). The synthesis of **274** was achieved in four linear steps beginning with the reaction of hydrazine with **273** to give **275** in excellent yield (91%), which was protected as the trifluoroacetyl hydrazide **276** in excellent yield (95%). Cyclisation under Mitsunobu conditions gave the pyrazolidinone **277** in good yield (72%), which was then deprotected, as for **271**, using hydrazine to give **274** in low yield (41%).

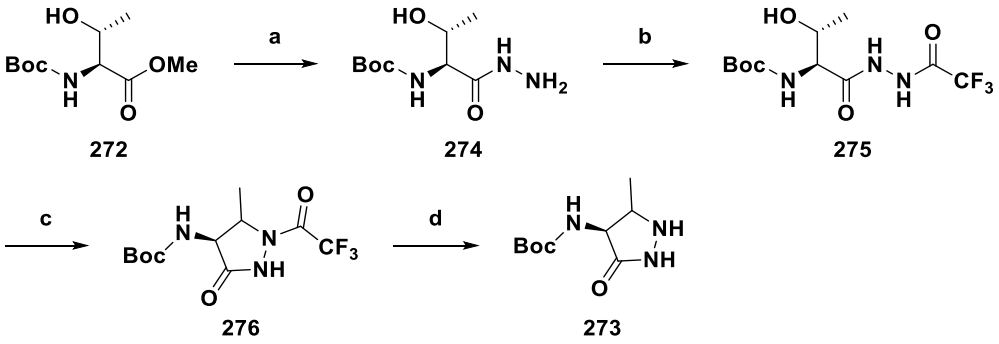

Figure 2-21 | Synthesis of **274**. Reagents and conditions: (**a**) $N_2H_4 \bullet H_2O$, MeOH, rt, o/n, 91%; (**b**) *S*-ethyl trifluorothioacetate, EtOH, 30 °C, 2 d, 95%; (**c**) DIAD (1 M in CH_2Cl_2), PPh_3, THF, rt, o/n, 72%; (**d**) $N_2H_4 \bullet H_2O$, THF/H_2O (2:1 *v*/*v*) rt, o/n, 41%.

Methods enabling the synthesis of *C*-3-functionalised aminopyrazolidinone **278** involving the cyclisation of a hydrazine moiety with various methyl acrylates were also attractive, given the ability to install a wide variety of olefins (using Horner-Wadsworth-Emmons conditions) onto the commercially readily available glycine phosphonate ester **279** (**Figure 2-22**). Moreover, there is a literature precedent for the cyclisation of hydrazine with dehydrovaline precursors **280** to give *C*-4-alkyl pyrazolidinones **278**.[222] The Horner-Wadsworth-Emmons reaction between **279** and acetone was attempted as a proof-of-concept reaction, affording **280** in moderate yield (59%). The subsequent reaction of hydrazine with **280** to give the cyclised pyrazolidinone **278** was attempted in refluxing EtOH as per literature conditions[222], but little conversion of the starting material was observed by TLC and LCMS and the isolated product yield was low (9%). When the reaction was repeated using *n*-BuOH as the reaction solvent to allow for a higher reflux temperature, the conversion of **280** to the desired product **278** was improved to 34% (**Figure 2-22**).

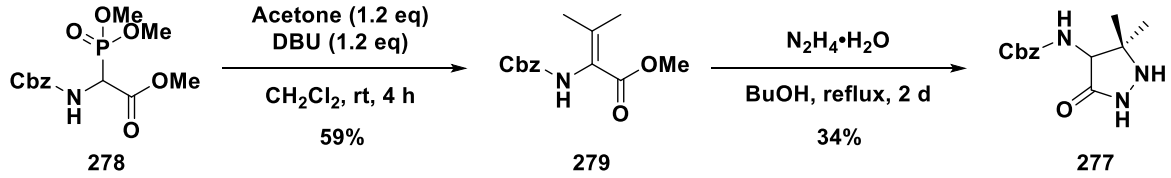

Figure 2-22 | Synthesis of *C*-alkyl aminopyrazolidinones following a modified procedure reported by Drev *et al*.[222]

2.6 Synthesis of a tricyclic lactivicin analogue

Shionogi Inc. recently disclosed structures of the tricyclic lactivicin analogues **189a-e** in a 2016 patent (**Figure 2-23**).[173] These tricyclic lactivicin analogues share the bicyclic pyrazolidinone core of the bicyclic pyrazolidinones (e.g., **151b**), developed by Eli-Lilly, except that a cis-fused γ-lactone replaces the enone moiety found on the Eli-Lilly pyrazolidinones (**Figure 2-23**). The replacement of the enone for a γ-lactone changes the hybridization of the *C*-7 and *C*-8 carbons from sp^2 to sp^3, resulting in the breaking of the electronic conjugation that extends from the γ-lactam to the *C*-7 ketone of the bicyclic pyrazolidinones. However, the γ-lactone moiety still provides an electron sink for the nitrogen anion formed following the nucleophilic attack onto the γ-lactam, which should sufficiently activate the pyrazolidinone carbonyl to attack by nucleophilic serine residues.

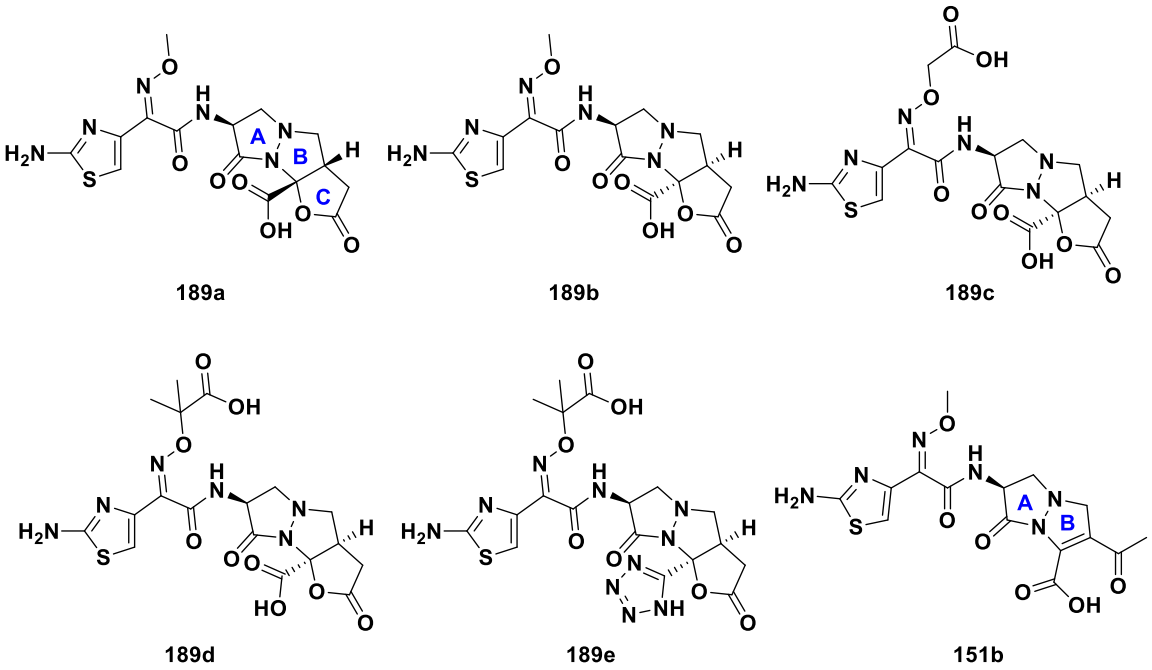

Figure 2-23 | Structures of Shionogi tricyclic lactivicin analogues **189a-e** and the related pyrazolidinone **151b**.

It was further hypothesised that the γ-lactone moiety of the tricyclic lactivicins would likely also have an important effect on the three-dimensional structure of these compounds, especially regarding the positioning of the *C*-8 carboxylate group which is, for lactivicins, crucial for binding to target proteins (as discussed later in Chapter 3). The *cis*-ring junction at *C*-7/*C*-8 positions generates two diastereomers. The *C*-8 carboxylate on diastereomer **189a** is oriented towards the *Si*-face of the γ-lactam, while the *C*-8 carboxylate on diastereomer **189b** is oriented toward the *Re*-face of the γ-lactam (**Figure 2-24**).

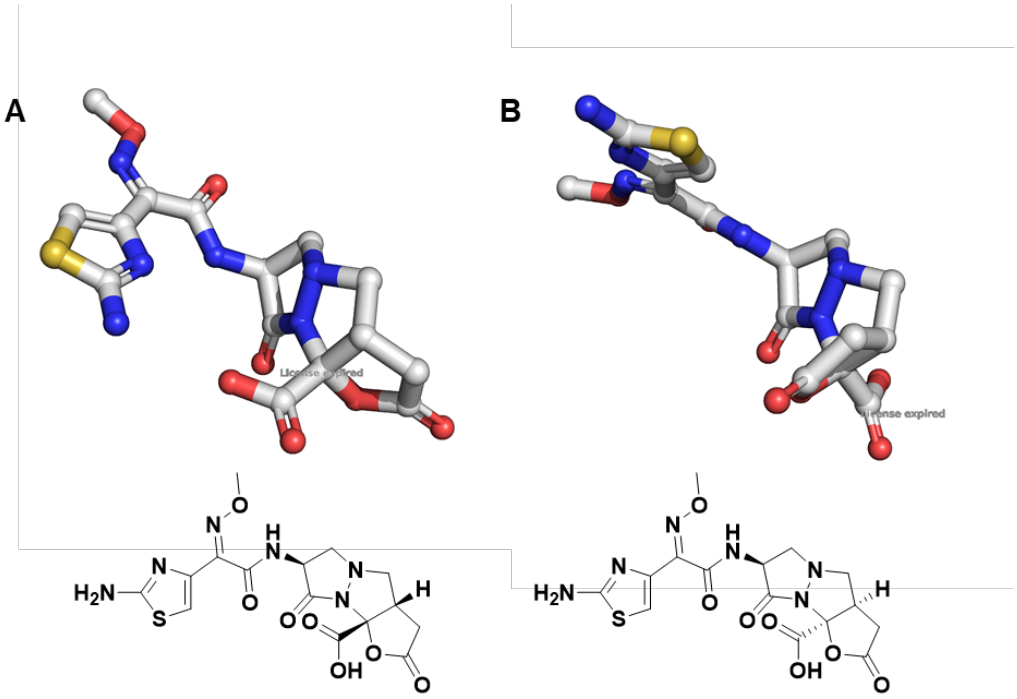

Figure 2-24 | Energy-minimised (MM2, Chem3D) conformations of (**A**) **189a** and (**B**) **189b**.

By contrast, the *C*-8 carboxylate of the bicyclic pyrazolidinones sits in the plane of the γ-lactam carbonyl and points away from the γ-lactam. Thus, the ring geometry of these tricyclic compounds is like both the flexible γ-lactone carboxylate of the lactivicins and the more rigid, conjugated bicyclic ring system of the Eli-Lilly pyrazolidinones (**Figure 2-23**). The additional rigidity conferred to the tricyclic lactivicins by the methylene bridge might further improve the hydrolytic stability of the tricyclic lactivicin analogue relative to lactivicins, as well as potentially reducing their susceptibility to β-lactamase hydrolysis.

2.6.1 Reported synthetic route for tricyclic lactivicins

The key steps required for the synthesis of tricyclic lactivicins are summarised as a retrosynthesis in **Figure 2-25** below. The 'ATMO' sidechain **281** was installed at a

late stage via an amide coupling with the amine **282** after the construction of the tricyclic ring system to avoid potential side reactions of the aminothiazole ring as well as to allow for late-stage diversification of the sidechains. In the reported synthesis[173], the γ-lactone ring was envisaged to be synthesised using conditions analogous to the lactonisation reaction required to form the γ-lactone of lactivicins (**Figure 2-2**); however the lactonisation reaction proceeds intramolecularly due to presence of a the methylene linker between the β-nitrogen of **283** and the 3-position of the **2-OG** ester. The precursor **283** could be prepared by the intermolecular aza-Michael addition of the aminopyrazolidinone **266** onto the Michael acceptor **284**.

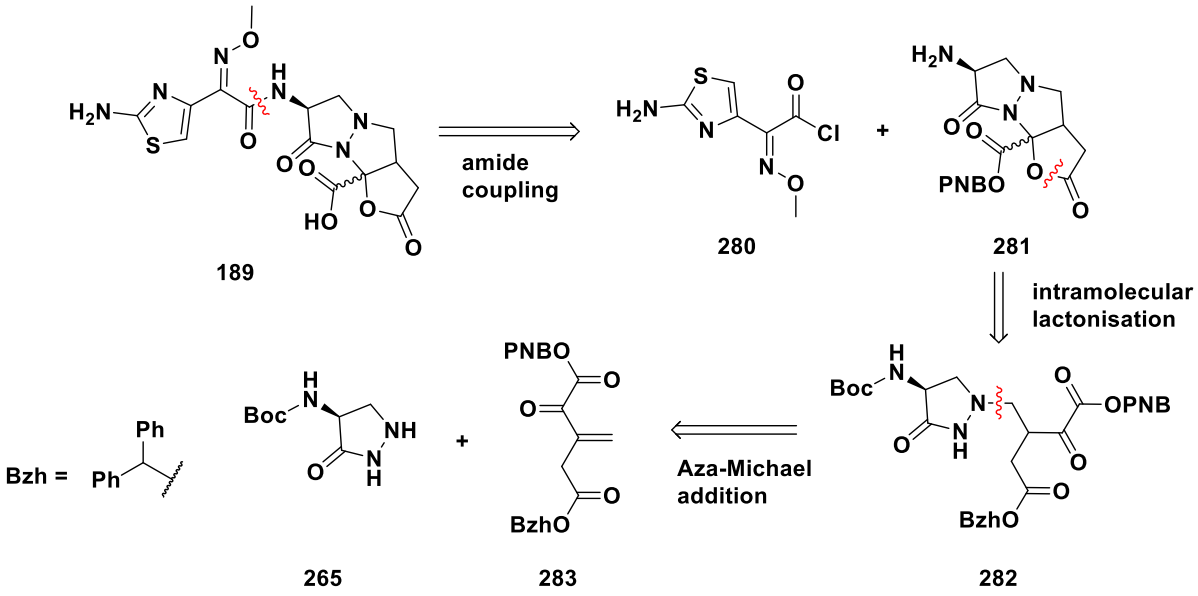

Figure 2-25 | Reported retrosynthesis of Shionogi tricyclic lactivicins.[173]

The syntheses of the aminopyrazolidinone **266** and the Michael acceptor **284** were not disclosed in the patent, however. Section **2.5.1** described the synthesis of the

aminopyrazolidinone precursor **266**, and the Michael acceptor **284** was readily prepared in two steps from the **2-OG** ester **172** (**Figure 2-26**).

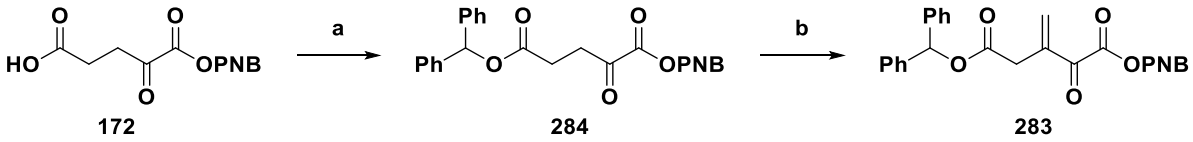

Figure 2-26 | Synthesis of the Michael acceptor **284**. Reagents and conditions: (**a**) diazobenzophenone, CH_2Cl_2, rt, o/n, 67%; (**b**) *N*,*N*,*N*',*N*'-tetramethyldiaminomethane, Ac_2O, AcOH, CH_2Cl_2, rt, 6 h, 78%.

Esterification of **172** with diazobenzophenone gave the di-ester **285** in moderate yield (67%). Aldol-type reaction using *N*,*N*,*N*′,*N*′-tetramethyldiaminomethane as the carbon source, which was performed in the presence of acetic anhydride and acetic acid, gave the Michael acceptor **284** in good yield (78%).

2.6.2 Synthesis of 283 via an *aza*-Michael addition

The aza-Michael addition of pyrazolidinone **266** onto the Michael acceptor **284** was the first reaction reported in the Shionogi patented synthesis of the tricyclic lactivicins.[173] The reported conditions for the Michael addition are outlined in **Figure 2-27**.

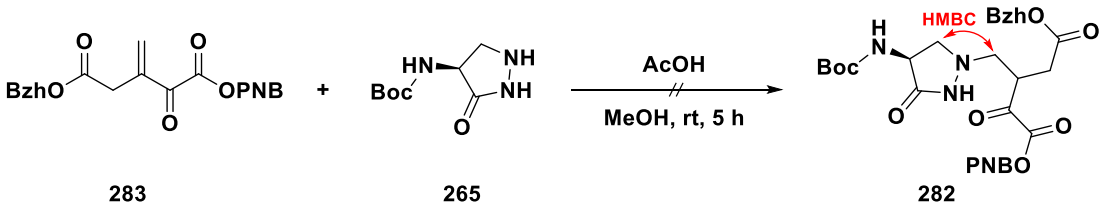

283 265 282

Figure 2-27 | Attempted synthesis of **283** using the reported conditions.[173]

All attempts to reproduce their results using the above conditions did not result in product formation. The Michael acceptor **284** was insoluble in the reported methanolic conditions, possibly due to the substantial lipophilicity of the benzhydryl and 4-nitrobenzyl esters, hence a condition screen was conducted to identify reaction conditions in which the Michael donor and acceptor were most soluble.

The Michael acceptor **284** remained insoluble in MeOH in the presence of Et_3N instead of AcOH (entry 2). At reflux in MeOH (entry 3), transesterification of the Michael acceptor **284** to give methyl esters was observed as evidenced by TLC and LCMS analyses. Next, whilst switching the solvent to DMF (entry 4) improved the solubility of the Michael acceptor **284**, the pyrazolidinone **266** was now insoluble and no formation of the expected product **283** was observed. The pyrazolidinone **266** was also insoluble in CH_2Cl_2 and AcOH (entry 5). However, when the reaction was run in CH_2Cl_2 without AcOH (entry 6), **266** became partially soluble and the Michael addition proceeded in excellent yield (90%). The regiochemical identity of

283 was confirmed by HMBC correlation between the methylene protons at position 6 and the *C*-2 ring carbon.

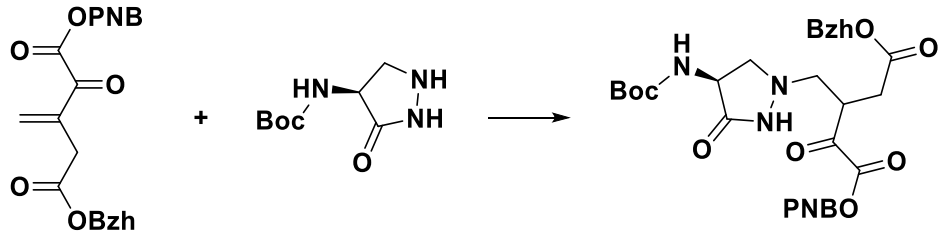

283 **265** **282**

Entry	Solvent	Additive	T (°C)	% Isolated yield	Notes
1*	MeOH	AcOH	25	0%	**284** insoluble
2	MeOH	Et_3N	25	0%	**284** insoluble
3	MeOH	AcOH	65	0%	Transesterification to methyl ester
4	DMF	AcOH	25	0%	**266** insoluble
5	CH_2Cl_2	AcOH	25	0%	**266** insoluble
6	CH_2Cl_2	-	25	90%	**266** partially soluble

Table 2-4 | Condition screen for the Michael addition to form **283**. (*) denotes the reported conditions.[173]

2.6.3 Benzhydryl deprotection and cyclisation of the Michael product 283

To enable the synthesis of the B and C rings of the tricyclic lactivicins **(Figure 2-23**), it was envisaged that the benzhydryl ester of the **283** must be selectively deprotected to give **286** over both the 4-nitrobenzyl group and the *N*-Boc group to allow the lactonisation reaction. The conditions for the benzhydryl deprotection reported by Shionogi used aluminium trichloride and nitromethane in anisole at -50 °C (**Figure 2-28**).[173] However, attempts to replicate these conditions on small scale resulted in the decomposition of **283**, and none of the product **286** was isolated upon chromatographic purification. Decomposition was observed by TLC even at early time points, suggesting that the problem could not be overcome by shorter reaction times. It is possible that the reaction stoichiometry effected the success of the reaction: when the reaction was attempted on a small scale (< 1 mmol) compared to the patent procedure (20 mmol) the addition of the reagents and the maintenance of anhydrous conditions were less easily controlled than on large scale.

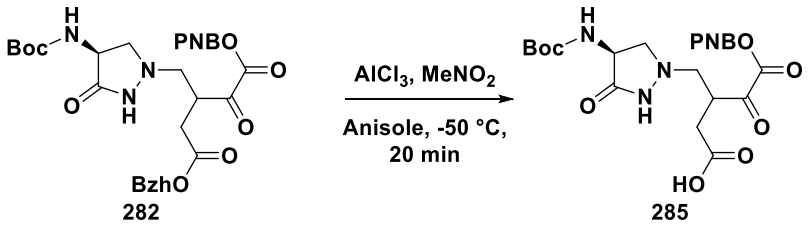

Figure 2-28 | Reported conditions for the benzhydryl deprotection of **286**.[173]

Following these attempts to replicate reported benzhydryl deprotection conditions, alternative conditions were sought. Typically, benzhydryl esters are removed either by hydrogenation or under acidic conditions.[223] However, selectively hydrogenating the benzhydryl ester in the presence of the 4-nitrobenzyl ester would likely result in the cleavage of both protecting groups. The presence of the *N*-Boc protecting group, which is also cleaved under acidic conditions (though typically stronger conditions than the acidic conditions needed for benzhydryl cleavage) was an important consideration.[224] For example, as shown in Section **2.3.2**, the benzhydryl esters of **237** can be cleaved in three equivalents of TFA while *N*-Boc groups typically require fifteen or more equivalents of TFA.[224] Thus the benzhydryl deprotection of **283** was initially carried out using analogous conditions for the deprotection of the bicyclic cycloserine analogues **237** (**Figure 2-29**). The results showed that the use of three equivalents of TFA did not selectively cleave the benzhydryl ester in the presence of the *N*-Boc group. Instead, a significant amount of the *N*-Boc-deprotected product **287** was also observed by LCMS, resulting in a poor isolated yield (5%) of the desired product **286**.

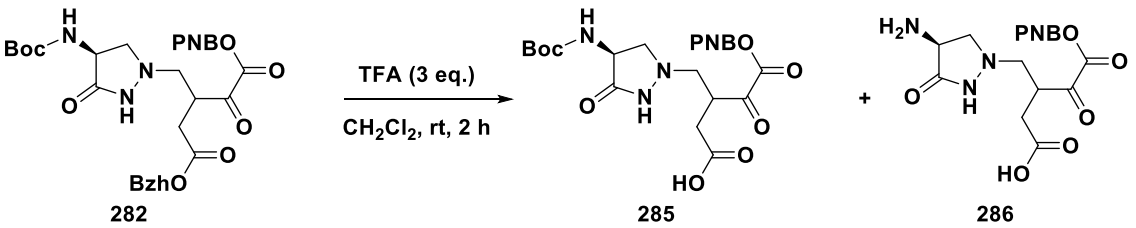

Figure 2-29 | Attempted benzhydryl deprotection of **283**. These conditions also cleaved the *N*-Boc group.

An alternative benzhydryl deprotection was therefore required to avoid the removal of the *N*-Boc group. A literature search identified formic acid in *m*-cresol as an effective condition for the mild benzhydryl deprotection of acid-sensitive cephalosporin precursors.[225] Thus, the benzhydryl deprotection of **283** was attempted using these reaction conditions. These deprotection conditions afforded the expected product **286** in low yields (24%) (**Figure 2-30**). Surprisingly, a small amount of the tricyclic lactonised product **288** was also generated under these conditions, without the need for a separate carbodiimide-mediated coupling step to facilitate the lactone ring formation, as is typically needed for lactivicins and was performed in the reported synthesis.[173]

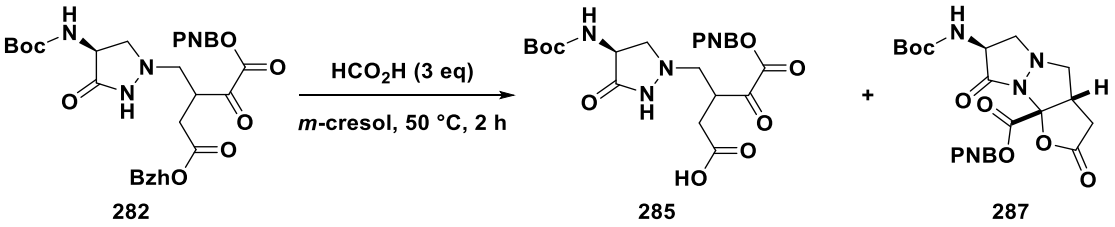

Figure 2-30 | Benzhydryl deprotection of **283** using formic acid in *m*-cresol generated the expected product **286** as well as a small amount of the lactonised product **288**.

2.6.4 Optimising the one-pot deprotection/lactonisation reaction

The unexpected discovery that the conditions used in the benzhydryl deprotection of **283** could also facilitate the subsequent ring closing reactions to form the tricyclic lactone **288** (therefore allowing a more concise synthesis) prompted efforts to identify conditions that favour the formation of the lactone product **288**. Such a one-

pot procedure would clearly be advantageous in terms of both reducing the overall synthetic steps, and avoiding the use of carbodiimide reagents, whose by-products are often difficult to separate from the lactone products. Hence, a study was conducted to identify conditions favouring the conversion of the starting material **283** to the target tricyclic lactone **288** (**Table 2-5**). As discussed previously, the reported[173] conditions (entry 1) and the use of TFA (entry 2) both resulted in minimal formation of either **286** or **288**. The use of anisole as a solvent with three equivalents of formic acid (entry 3) resulted in no reaction of the Michael product **283**. As mentioned above, three equivalents of formic acid in *m*-cresol (entry 4) resulted in **286** as the major product, with a small amount of **288** formed. The addition of trimethylsilane as a scavenger of the benzhydryl cation (entry 5) also produced **286** as the major product.

Different reaction solvents were then explored. It was clear from entries 4 and 5 that an acidic protic solvent was likely needed for the reaction, so hexafluoroisopropanol (HFIP) was selected. At room temperature in the presence of formic acid (entry 6), no conversion of the starting material was observed. Heating the reaction to 50 °C (entry 7) generated **286** as the major product, but significantly more of **288** was formed than was formed when *m*-cresol was used as the solvent. The use of acetic acid instead of formic acid (entry 8) improved the ratio of **288** to **286** further to almost 1:1, and increasing the equivalents of acetic acid to

3.5 equivalents (entry 9) further improved the isolated ratio of **288** to **286** to approximately 2:1, respectively.

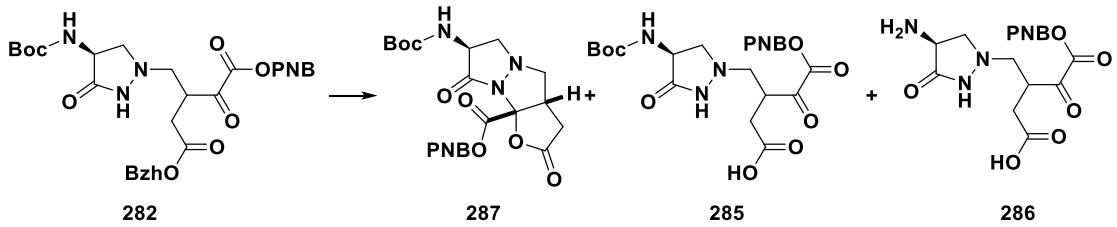

282 287 285 286

Entry	Solvent	acid (eq.)	T °C	Time	Additive	Major product‡
1*	Anisole	$AlCl_3$	-50	20 min	$MeNO_2$	Decomp.
2	CH_2Cl_2	TFA (3)	rt	2 h	-	**287**
3	anisole	HCO_2H (3)	50	24 h	-	no rxn
4	*m*-cresol	HCO_2H (3)	50	24 h	-	**286**
5	*m*-cresol	HCO_2H (3)	50	24 h	Et_3SiH	**286**
6	HFIP	HCO_2H (3)	rt	24 h	-	no rxn
7	HFIP	HCO_2H (3)	50	16 h	-	**286**
8	HFIP	AcOH (3)	50	16 h	-	**288**, **286** (~1:1)
9	HFIP	AcOH (3.5)	60	16 h	-	**288**

Table 2-5 | Optimisation of the one-pot deprotection/lactonisation reaction. (*) denotes the reported condition. ‡As observed by LCMS.

Thus, the conditions of entry 9 of **Table 2-5** was selected as the optimised condition for the one-pot conversion of the Michael product **283** to the tricyclic lactone **288**. The isolated yield of the lactone **288** on 1 mmol scale was low (38%); this could be increased by reacting the crude mixture of the acid **286** and the lactone **288** with DCC to convert the remaining **286** to the lactone **288**. This was achieved by dilution of the reaction in water and extracting the acid **286** and lactone **288** into ethyl acetate, followed by concentration *in vacuo* and dissolution into CH_2Cl_2 and addition of DCC. The product could then be purified by filtration and flash chromatography. This additional step increased the yield to 46% on 1 mmol scale.

Upon scale-up (7 mmol), however, the isolated yield of the lactone **288** decreased, and an increasing amount of the *N*-Boc-deprotected side product **287** was observed as indicated by LCMS. The only change to the experimental parameters between the 1 mmol and the 7 mmol-scale reactions was the switch from a sealed microwave vial to a round bottom flask fitted with a Liebig condenser. When the reaction was repeated on 7 mmol scale in sealed vials, the yield of the lactone **288** was comparable to the yields observed on a 1 mmol scale. It was postulated that the increased vapour pressure in the headspace of the heated sealed vial compared to the ambient pressure in the Liebig condenser probably disfavours the liberation of CO_2 that results from the Boc cleavage, thereby decreasing the amount of Boc cleavage. In the open flask, however, the pressure remains at ambient levels and it appeared that the Boc cleavage became a more viable reaction pathway.

2.6.5 N-Boc deprotection and amide coupling

The Boc group of **288** was removed using a large excess TFA in CH_2Cl_2 to give the amine **282** as the TFA salt (**Figure 2-31**). Trituration of the crude residue with Et_2O was effective in removing the excess TFA and allowed for the amide coupling to be performed without further purification of the amine **282**.

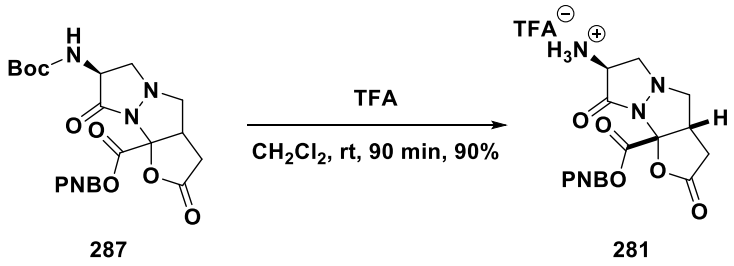

Figure 2-31 | *N*-Boc deprotection of **288**.

Unlike previous syntheses of lactivicins (**Section 2.2**), the strategy developed in this project allows for the introduction of unique sidechains much later in the synthesis, improving the synthetic efficiency of the route. Proof of feasibility of this route was also demonstrated by the installation of the phenoxyacetamido sidechain of **168** via an amide coupling between the free base of **282** and phenoxyacetyl chloride to give the amide **289**. Deprotection of the 4-nitrobenzyl ester was accomplished by hydrogenation to give the lactone carboxylic acid **290** as an approximately 1:1 mixture of two diastereomers by ^{1}H NMR (**Figure 2-32**). While no spectroscopic experiments were conducted to confirm that the diastereomers of **291** are both *cis*, the spectroscopic data matched those initially reported by Yamawaki *et al*.[173]

However, future spectroscopic experiments are needed to confirm the relative configuration of the ring junctions.

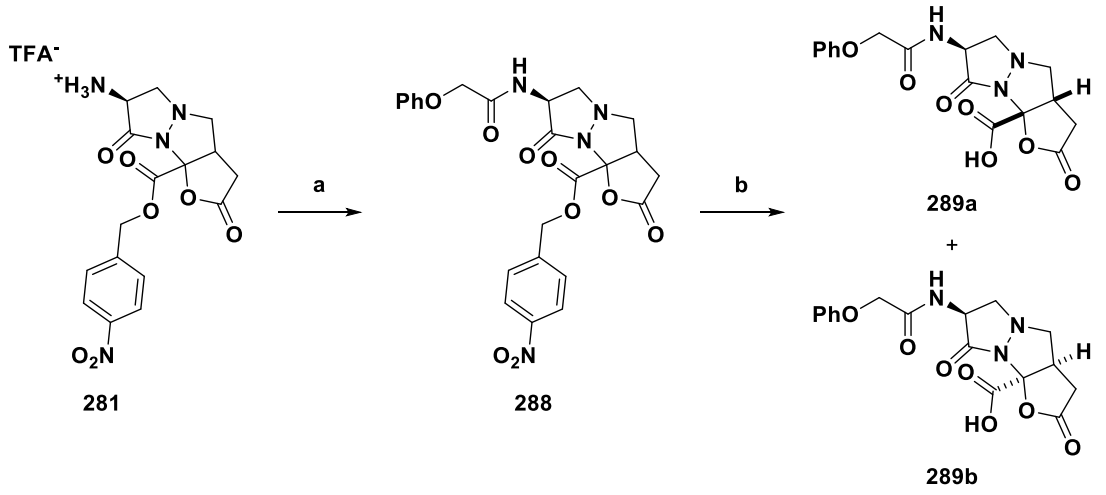

Figure 2-32 | Final stage of the tricyclic lactivicin synthesis. Reagents and conditions: (**a**) phenoxyacetyl chloride, Et_3N, CH_2Cl_2, rt, o/n, 75%; (**b**) Pd/C, H_2, THF/H_2O (2:1), rt, 3 h, 5% **290a**, 8% **290b**.

The separation of the two diastereomers of **290** was achieved using reverse-phase chromatography on a Biotage® Sfär C18 cartridge (**Figure 2-33**). Unlike the lactivicins, no interconversion of the isolated single diastereomers was observed by ^{1}H NMR, suggesting that the methylene bridge between the pyrazolidinone and γ-lactone rings stabilises the stereochemical configuration of the γ-lactone ring.

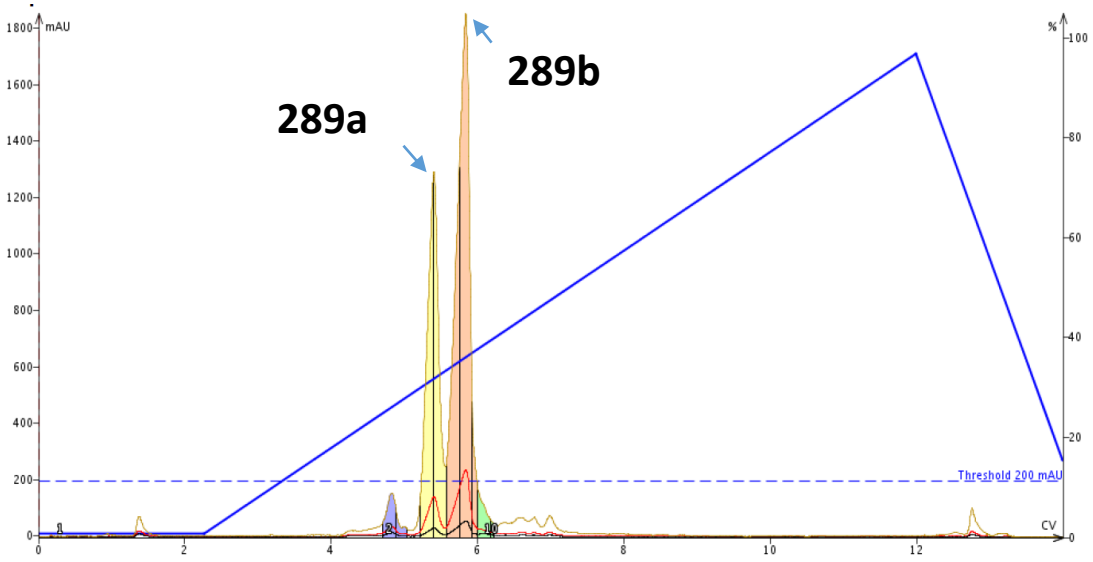

Figure 2-33 | Purification of **290** by reverse-phase chromatography. Conditions: Biotage Isolera using Biotage Sfar® C18 30 g cartridge, solvent A: H_2O + 0.1% formic acid, solvent B: MeCN + 0.1% formic acid, flow rate: 15 mL/min.

2.6.6 Variable-temperature NMR of 'diastereomer B'

Despite the structural similarity between diastereomers **290a** and **290b**, the ^{1}H NMR spectra of the two diastereomers showed substantial differences (**Figure 2-34**). Notably, the ^{1}H spectrum of **290b** was much less resolved than the spectrum **290a**, particularly for peaks corresponding to positions 3 and 10 adjacent to the β-nitrogen in the pyrazolidinone ring, which were so broad that they were barely visible under standard operating conditions. The presence and resolution of other characteristic peaks, such as the diastereotopic peaks of the lactone methylene protons, suggested that the ring system was intact and had not hydrolysed.

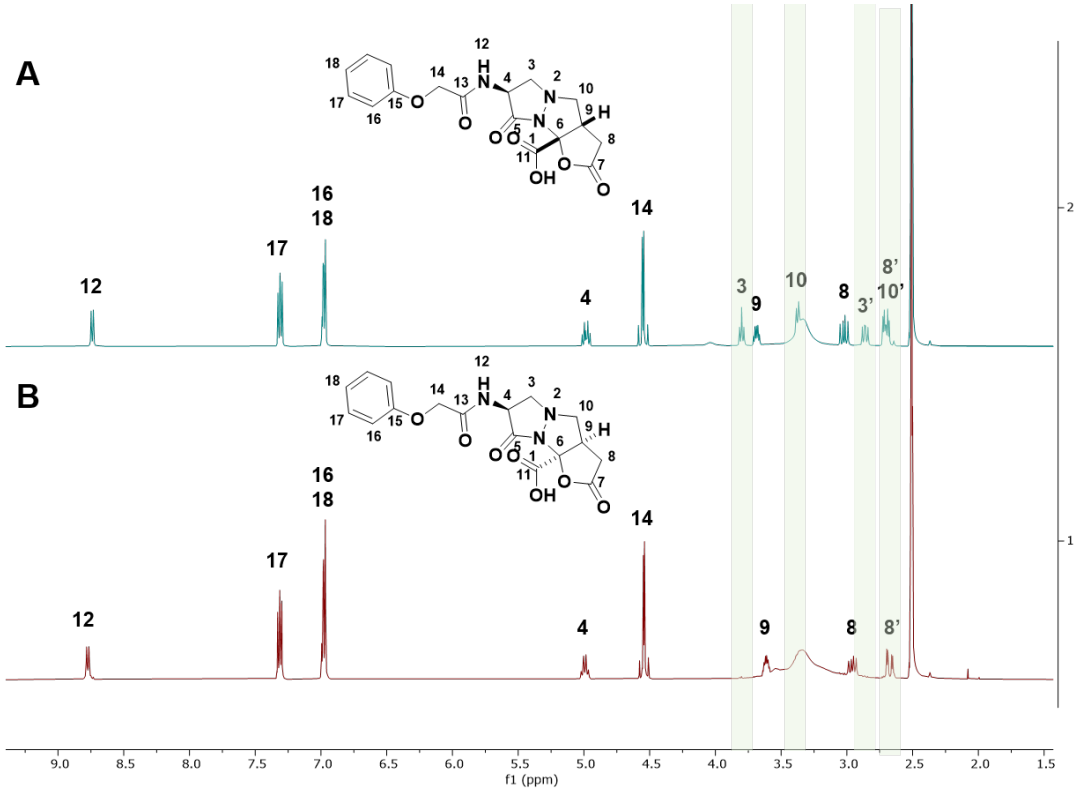

Figure 2-34 | ^{1}H NMR (500 MHz, d_6-DMSO) spectra of tricyclic diastereomers **290a** and **290b.** The spectrum for **290b** is missing peaks for positions 3 and 10. Note that the relative stereochemistry has not been assigned.

Thus, variable temperature NMR (vtNMR) experiments were conducted on **290b** to investigate whether the peak broadening was due to an exchange process (**Figure 2-35**). At 358 K the spectrum is fully resolved and the peaks corresponding to positions 3 and 10 are clearly visible. Given the proximity of positions 3 and 10 to the β ring nitrogen, the results of this experiment suggest that the exchange process responsible for the peak broadening is likely due to the inversion of the nitrogen lone pair that is slow on ^{1}H NMR timescales

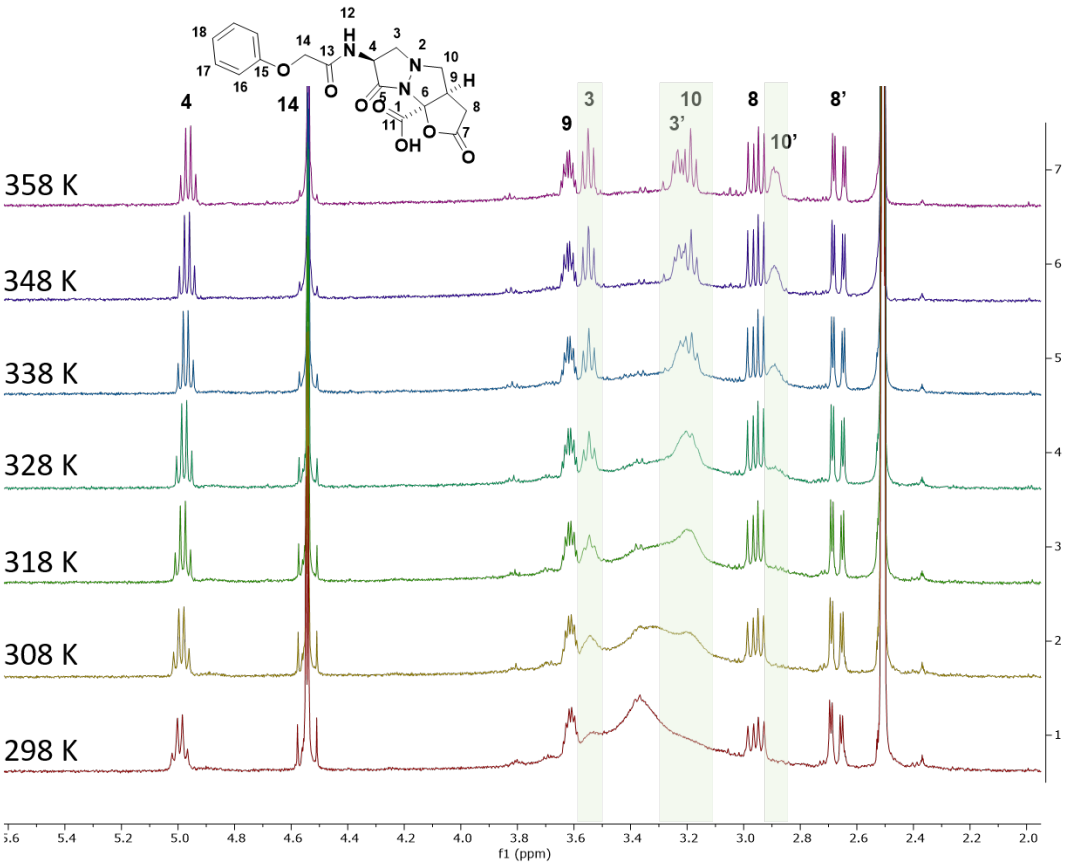

Figure 2-35 | ^{1}H (500 MHz, d_6-DMSO) vtNMR of **290b**.

Curiously, the peak broadening is only observed for diastereomer **290b**, implying that the two diastereomers exhibit different conformational behaviours at ambient temperatures. Thus, one diastereomer might adopt a conformation that is more reactive to bacterial transpeptidases.

2.7 Summary of work detailed in Chapter 2

The work described in Chapter 2 sought to explore the chemical space surrounding the lactivicin core and synthesise novel classes of lactivicin-inspired molecules. First, previously reported lactivicins were synthesized to serve as controls in

biochemical assays. Compounds **223** and **242** were next synthesised to evaluate the importance of the amido sidechain and the γ-lactone carboxylate, respectively, for antibacterial activity. The compound **242** might serve as a useful precursor to bioisosteres of the carboxylate group, either by functionalizing the ketone prior to cyclisation, or employing radical halogenation/C-H activation of the methyl group to install novel functionality. These experiments were not performed in the scope of this thesis due to time constraints but are an area for future work.

Bicyclic compounds **236a, 236b,** and **236f** were synthesised to evaluate alternative ring configurations, as well as to explore the impact of heteroatom variations at the 5-position of cycloserine. A synthetic route towards *C*-4 alkyl cycloserines inspired by the synthesis of acinetobactin was also explored, however, the crucial 5-*exo*-tet rearrangement could not be achieved.

Routes to novel pyrazolidinone-based analogues of lactivicins were explored, including the synthesis of the tricyclic lactivicin analogue **290**. The reported synthetic route required considerable optimisation, and a modified route was developed that enabled the preparation of such analogues with good overall yields. The separation of diastereomers was achieved using reverse-phase chromatography, and NMR characterization of **290b** showed that it undergoes an exchange process on NMR timescales, possibly caused by the inversion of the *C*-5 ring nitrogen lone pair. Variable-temperature NMR was conducted to confirm the identity of **290b**, and the absolute assignment of the two diastereomers was

attempted by NOESY experiments. Overall, a small but diverse set of novel lactivicin analogues was successfully synthesised. The studies involving these compounds as antibacterials against WHO 'priority 1' pathogens were investigated in Chapter 3.

Chapter 3 Efficacy of modified lactivicin analogues against *Mycobacterium tuberculosis*.

Forward

Recombinant Ldt_{mt1}, Ldt_{mt2}, Ldt_{mt3}, Ldt_{mt4}, Ldt_{mt5}, *and* Ldt_{fm} *proteins were produced by* Tika R. Malla *and, unless specified otherwise, were used with* N*-terminal His-tags attached. Protein-observed mass spectrometry assays were conducted by* Tika R. Malla. *X-ray crystallographic studies were conducted by* Tika R. Malla *and* Dr. Michael A. McDonough. *MIC assays were conducted in conjunction with* Dr. Karina A. Calvopiña.

3.1 Introduction

3.1.1 Structure and function of L,D-transpeptidases

As discussed in **Section 1.2.2**, most bacteria rely on D,D-transpeptidases to crosslink the peptidoglycan polymers that make up their cell walls. As their name suggests, D,D-transpeptidases crosslink at the D-Ala-D-Ala subunit of the peptidoglycan polypeptide chain.[226] In *Mycobacterium tuberculosis*, however, peptidoglycan crosslinking is also performed by Ldt enzymes, which install crosslinking between *m*-DAP (or L-lysine) and D-Ala, resulting in a different peptidoglycan composition (**Figure 3-1**).[22]

Structurally, the Ldt enzymes and PBPs differ at their active sites; whereas PBPs use a nucleophilic serine residue, the Ldt enzymes use a nucleophilic cysteine to enable their respective transpeptidation reactions.[23] The thiol of cysteine is a softer nucleophile than the oxygen of serine; this may promote covalent reaction of analogues of lactivicin with softer electrophilicity than lactivicin itself with the Ldts.[227] The use of a softer electrophilic warhead for Ldt inhibition could help enable improved selectivity and reduced sensitivity to nucleophilic serine enzymes, including SBLs (*M. tuberculosis* contains the BlaC SBL).

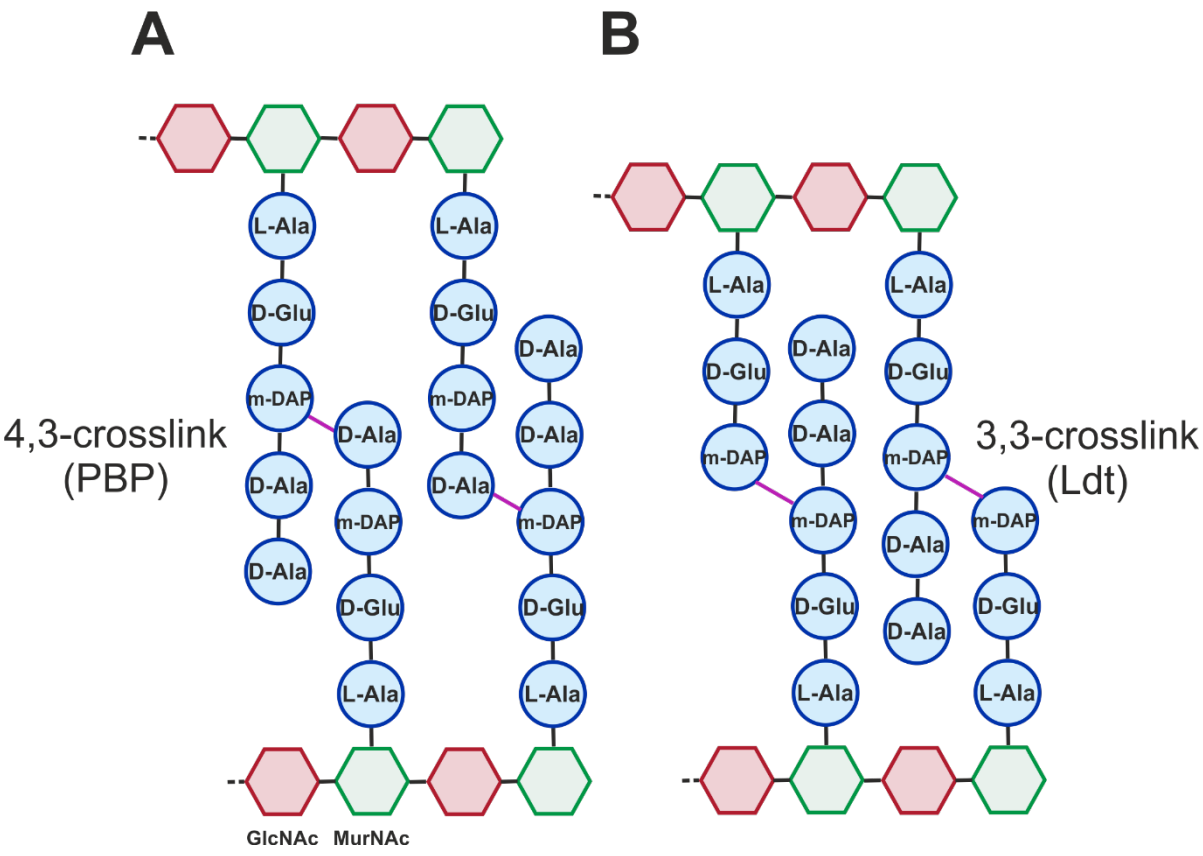

Figure 3-1 | Comparison of peptidoglycan crosslinking catalysed by (**A**) PBPs and (**B**) Ldt enzymes. Adapted from Pidgeon *et al*.[228]

3.2 Protein-observed mass spectrometry studies between Ldts and lactivicin analogues

Existing β-lactam antibiotics generally perform poorly against *M. tuberculosis*.[229] The decreased activity of β-lactams is at least in part due to their poor cellular uptake into *mycobacteriaceae*.[230, 231] *M. tuberculosis* can reside and multiply inside of the macrophages of the host immune system, meaning that any antibacterial molecule must also cross a eukaryotic cell membrane in addition to the bacterial cell membranes to access the periplasmic space.[232] β-Lactams from the penicillin and cephalosporin families generally exhibit low rates of Ldt acylation, faster rates of hydrolysis of the resulting thioester and, in the case of ampicillin, alternative fragmentation pathways that result in poor inhibition of the Ldt enzymes.[229]

Carbapenems, however, are potent inhibitors of Ldt enzymes and the resulting acyl-enzyme complexes from the reaction of the nucleophilic cysteine and the carbapenem β-lactam are not as readily hydrolysed.[233] The stability of the carbapenem acyl-enzyme complex relative to other β-lactam families might be explained by the structural differences in the bicyclic β-lactam ring systems. There is therefore a potential therapeutic role for novel lactivicin derivatives as Ldt inhibitors for the treatment of tuberculosis. Thus, a selection of compounds synthesised in **Chapter 2** were investigated for activity against Ldt enzymes. The compounds (**Figure 3-2**) used in the study happened to be the ones available at the

time the experiments were being conducted by Tika R. Malla as part of her DPhil project to characterise L,D-transpeptidases.

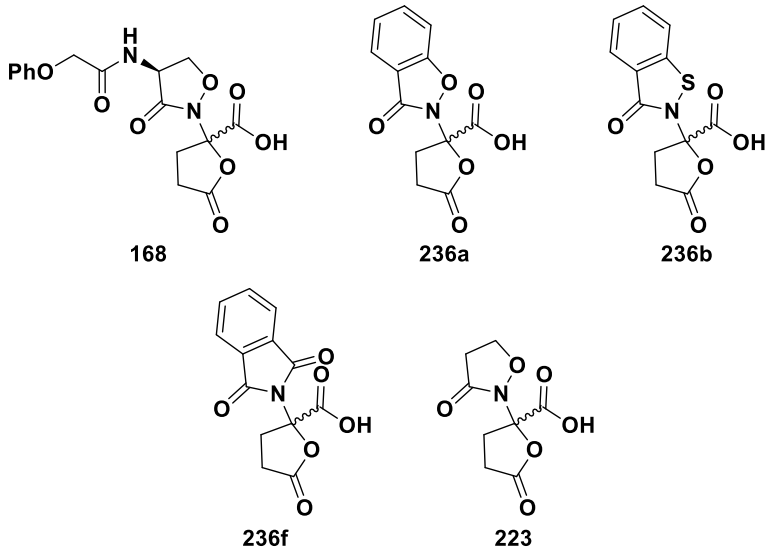

Figure 3-2 | Selected lactivicin analogues **168**, **236a**,**b**,**f**, and **223** screened for activity against the Ldt enzymes.

3.2.1 Inhibitor screen for covalent modification of Ldt enzymes.

To investigate the ability of the compounds shown in **Figure 3-2** to react covalently with Ldt enzymes, protein-observed mass-spectrometry (POMS) assays were conducted using a panel of Ldt enzymes from *M. tuberculosis* and *E. faecium* (as a cross-screen to investigate the spectrum of activity of these compounds). Ldt_{Mt2} is responsible for the majority of L,D-crosslinking in *M. tuberculosis* and is generally regarded as the most clinically relevant Ldt enzyme for inhibition.[234] Hence, Ldt_{Mt2} was chosen for the first POMS experiments (**Figure 3-3**).

Compound **168** was observed to fully react with Ldt_{Mt2} to give a stable covalent adduct after five minutes incubation. However, the structurally related compound **236a** did not appear to covalently modify Ldt_{Mt2} at all. Like **168**, compound **236b**, which differs from **236a** by the substitution of the endocyclic oxygen for a sulfur, showed complete covalent modification of Ldt_{Mt2} after five minutes. By contrast, the phthalimide derivative **236f**, like **236a,** showed no evidence of a covalent reaction with Ldt_{Mt2}. Finally, compound **223** reacted covalently with Ldt_{Mt2}, albeit at a considerably slower rate than **168** and **236b**.

The results from the POMS experiments shown in **Figure 3-3** reveal some unexpected reactivity trends amongst the tested compounds. The rapid reaction of **168** with Ldt_{Mt2} appears to confirm that the cycloserine ring is a suitable electrophile to react with the active site nucleophilic cysteine, suggesting that, unlike some classes of β-lactam antibiotics, appropriately derivatised lactivicins may be potent inhibitors of the Ldts. The apparent absence of covalent reaction between Ldt_{Mt2} and **236a**, which is structurally similar to **168**, may indicate that: the additional steric bulk of the fused benzene ring is not tolerated in the Ldt_{Mt2} active site; or that the acylamino sidechain of **168** may contribute to the initial substrate binding via non-covalent interactions with residues on Ldt_{Mt2}.

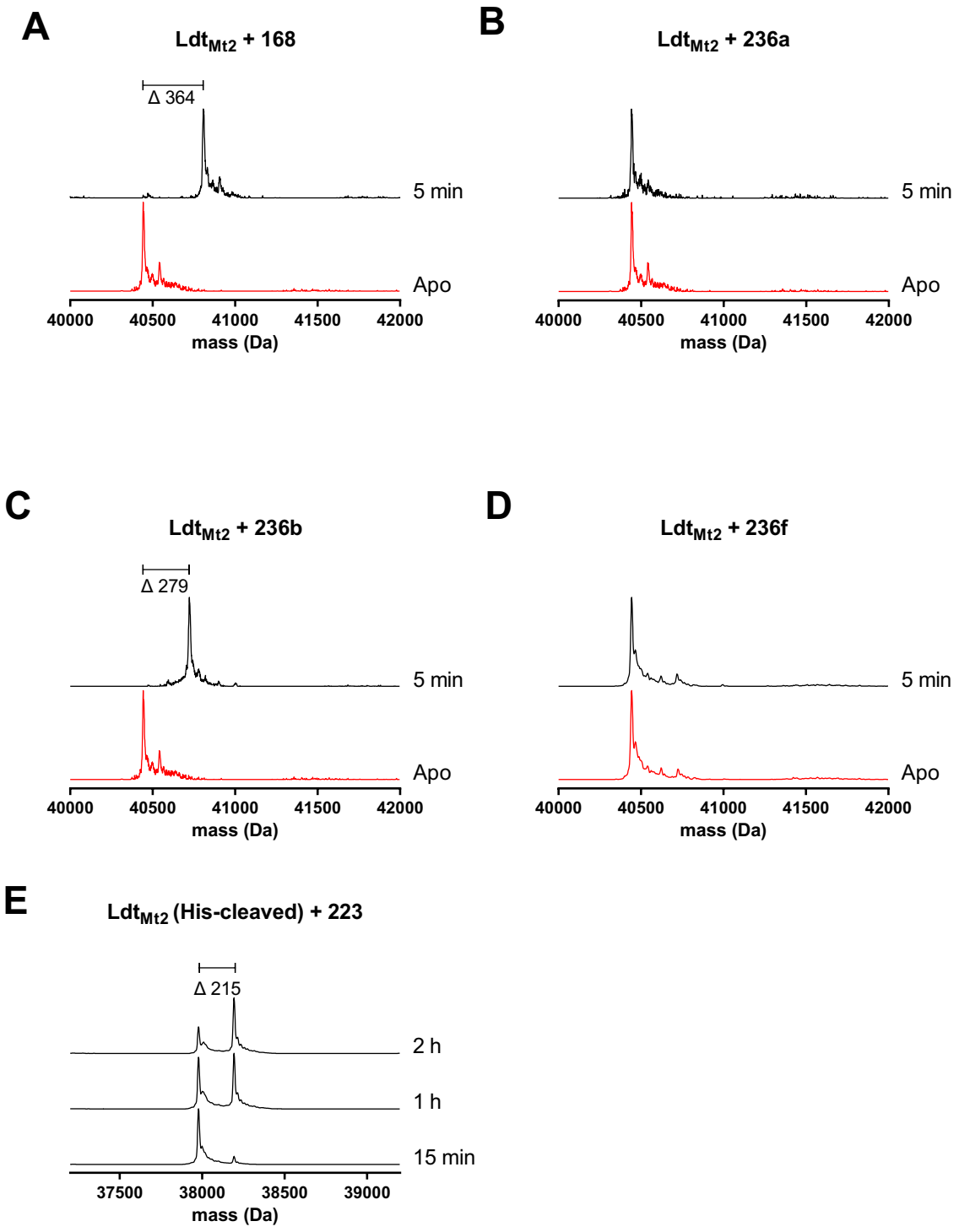

Figure 3-3 | POMS experiments of the reaction between Ldt$_{Mt2}$ and lactivicin analogues. (**A**) Ldt$_{Mt2}$ and **168**, (**B**) Ldt$_{Mt2}$ and **236a**, and (**C**) Ldt$_{Mt2}$ and **236b**, (**D**) Ldt$_{Mt2}$ and **236f**, (**E**) Ldt$_{Mt2}$ and **223**. Conditions: 2 μM enzyme, 40 μM inhibitor. These experiments were performed by *Tika R. Malla*.

The slower rate of reaction observed for **223**, which lacks any functionalisation of the cycloserine ring at the *C*-3 and *C*-4 positions, also seems to suggest that the acylamino sidechain of **168** promotes the covalent reaction with Ldt_{Mt2}. Like **236a**, the lack of reactivity for **236f** may be explained by the presence of the fused benzene ring. However, the presence of a benzene ring did not seem to affect the reactivity of the structurally analogous **236b**. Clearly, the reactivity of **236b** is incongruent with the reactivity observed for its structural analogues.

POMS experiments were also conducted on Ldt_{fm} from *E. faecium* to investigate the scope of Ldt inhibition by the lactivicin analogues (**Figure 3-4**), the results of which indicated that the reactivity of the selected lactivicin compounds with Ldt_{fm} was broadly similar to their reactivity with Ldt_{Mt2}.

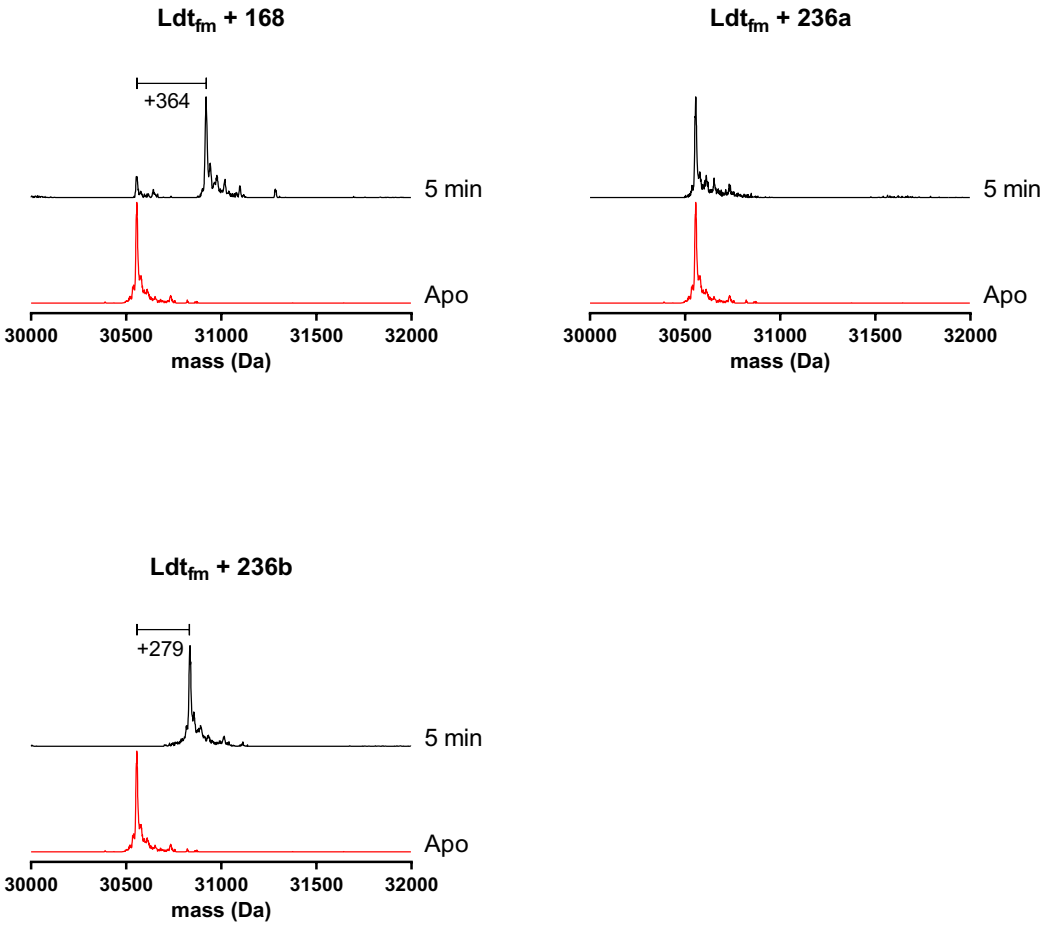

Figure 3-4 | Protein-observed mass spectrometry for the reaction of (**A**) Ldt_{fm} and **168**, (**B**) Ldt_{fm} and **236a**, and (**C**) Ldt_{fm} and **236b**. Conditions: 2 μM enzyme, 40 μM inhibitor. These experiments were performed by *Tika R. Malla*.

Together, the POMS experiments investigating the covalent reaction of selected lactivicin analogues with Ldt_{Mt2} and Ldt_{fm} indicate that, for the tested compounds, covalent reactions only occur for **168** and **236b**. Compound **168** is expected to react via its electrophilic carbonyl to form a thioester enzyme-inhibitor complex. The absence of covalent reaction for the benzisoxazolidinone analogue **236a** suggests that replacement of the amido sidechain with a benzene ring renders the

electrophilic carbonyl incompatible for productive reaction with the nucleophilic cysteine of the enzyme. The additional phenyl ring might clash sterically with residues in the active site, as it is known that β-lactams with larger amido sidechains generally show poorer inhibition of Ldt enzymes for this reason.[234] However, this explanation does not explain the rapid reaction of the sulfur analogue **236b** with Ldt_{Mt2}. Given that **236b** differs from **236a** simply by the replacement of oxygen for sulfur, no reaction between the compound and the enzyme should be observed if steric hindrance of the bicyclic ring is responsible for the lack of activity.

It was proposed that the covalent reaction between **236b** with Ldt_{Mt2} might occur between the nucleophilic cysteine residue and the endocyclic sulfur of **236b**, resulting in a disulfide-linked covalent adduct. Literature precedent for such a reaction exists for the structurally related organoselenium compound ebselen (**203**), which was reported to react via the selenium atom with the nucleophilic cysteines of Ldt enzymes. to give a selenosulfide bridge (**Figure 3-5**).[193]

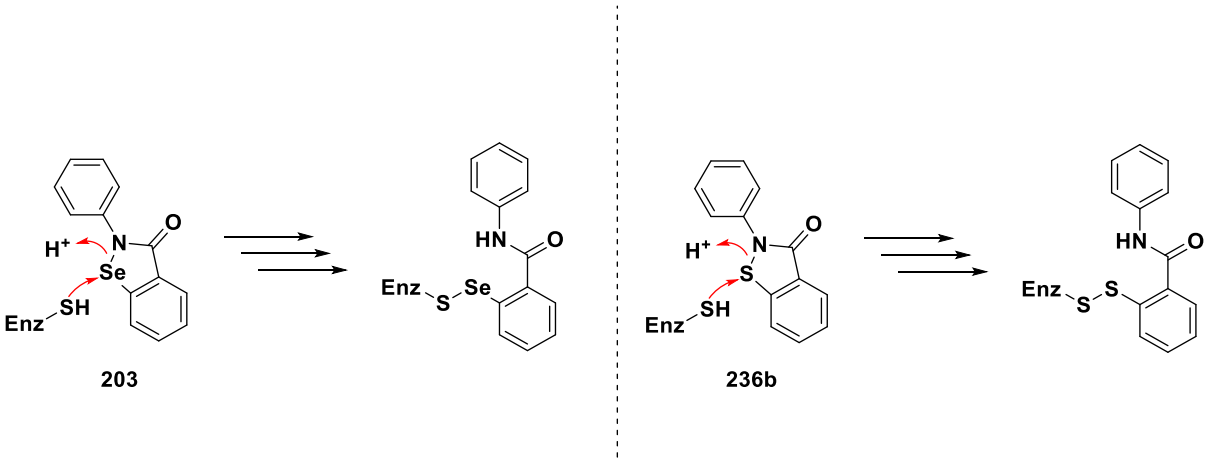

Figure 3-5 | Proposed mechanism for the covalent inhibition of Ldt enzymes by **203** and **236b**.[193]

3.2.2 The effect of dithiothreitol on the Ldt_{Mt2}-236b adduct

To investigate the nature of the POMS results for **168** and **236b**, experiments were conducted whereby the reducing agent dithiothreitol (DTT) was added following the incubation of Ldt_{Mt2} with the inhibitors. DTT reduces disulfide bonds in proteins, hence the addition of DTT to the reaction mixture containing the Ldt-**236b** covalent adduct the reaction should cleave the disulfide bond of the Ldt-**236b** complex, but should not reduce the thioester of the Ldt-**168** adduct.

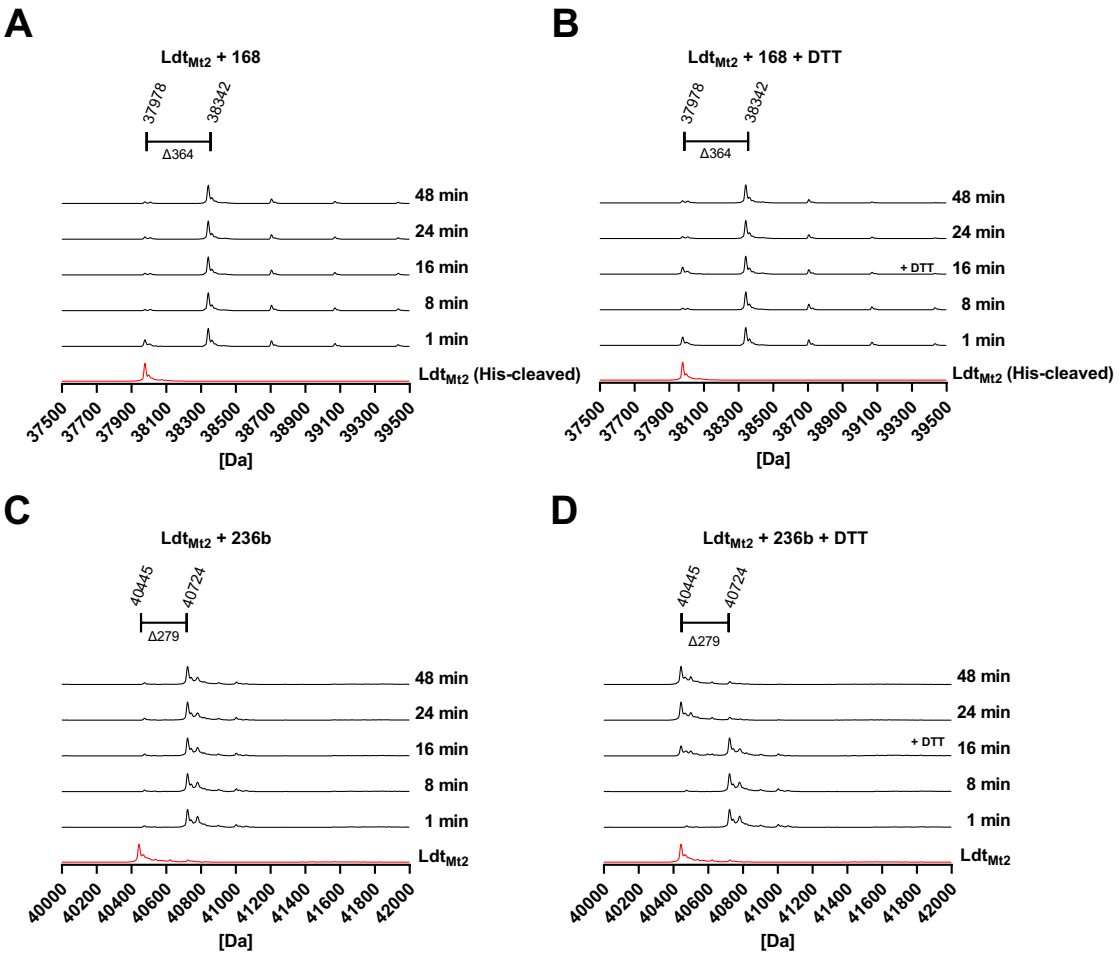

Figure 3-6 | POMS experiments of the reaction between Ldt_{Mt2} and inhibitors. (**A**) reaction with **168** under standard assay conditions; (**B**) reaction with **168** with the addition of DTT to the reaction at

16 min; (**C**) reaction with **236b** under standard assay conditions; (**D**) reaction with **236b** with the addition of DTT to the reaction at 16 min. Note: the additional peaks in the spectra of (**A**) and (**B**) are likely multiple adducts of **168**, however the nature of these additional adducts has not been explored Conditions: 2 μM enzyme, 40 μM inhibitor, 2 mM DTT. These experiments were performed by *Tika R. Malla.*

The apparent cleavage of the enzyme-inhibitor covalent adduct following the addition of DTT seems to validate the proposed mechanism of reaction between Ldt_{Mt2} and **236b**, whereby the nucleophilic cysteine reacts covalently with the sulfur to form a disulfide-linked adduct (**Figure 3-7**). This reaction mechanism relies on both the enzyme and inhibitor having a sulfur (II) atom, which likely confines the inhibitory activity of **236b**-type compounds to Ldt enzymes and not PBPs (as PBPs use an active site serine). However, this could be advantageous as these disulfide-forming inhibitors might not be as susceptible to β-lactamase hydrolysis, side-stepping one of the most formidable defences bacteria have against transpeptidase inhibitors. It is also unlikely that resistance will develop via mutation of the Ldt active site as cysteine to serine mutants of Ldt enzymes are not able to catalyse their natural L-Ala-D-Ala crosslinking reaction. Thus, the apparent divergence in reactivity between **168** and **236b** (**Figure 3-7**) suggests that benzisothiazolinone-based covalent inhibitors may be promising antituberculosis agents. However, their clinical value is uncertain due to the likelihood that these agents will react with other biological thiols (e.g. cysteines of other proteins or glutathione). Rigorous counterscreening would be required to demonstrate that these benzisothiazolinone-based inhibitors are selective for L,D-transpeptidases, and it is unlikely that this is

the case. Nevertheless, given the threat posed by β-lactamase resistance, the identification of a novel mechanism of covalent inhibition of transpeptidases merits further investigation.

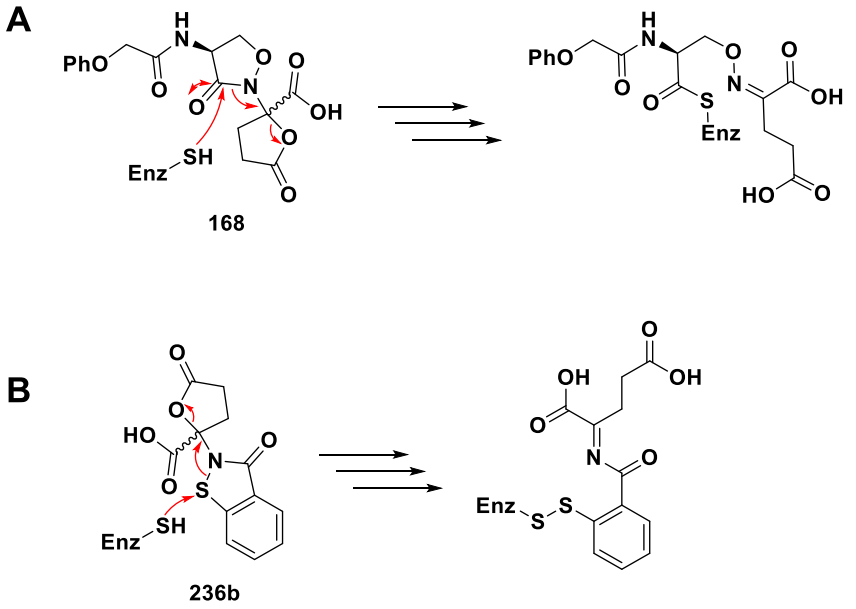

Figure 3-7 | Proposed mechanisms for the reactions of Ldt_{Mt2} with (**A**) **168** and (**B**) **236b**, highlighting the stark differences in the resultant covalent adducts.

3.2.3 Evaluating the scope of Ldt inhibition

To evaluate the scope of Ldt enzymes with which **168** and **236b** can react covalently, POMS experiments were conducted using a panel of Ldt enzymes from clinically relevant organisms *M. tuberculosis* (Ldt_{Mt1-5}) and *E. faecium* (Ldt_{fm}). The results of the experiments with **168** and the panel of Ldts are shown in **Figure 3-8**.

168 reacts at varying rates to form a stable covalent adduct with Ldt_{Mt1-4}; however, no covalent adduct was observed for the reaction between **168** and Ldt_{Mt5}. After five minutes, the reaction of **168** with Ldt_{Mt1} results in a roughly 1:1 ratio of reacted and

unreacted protein. The proportion of reacted enzyme increased over time to roughly 2:1 reacted and unreacted protein. The reaction of **168** and Ldt_{Mt2} proceeds rapidly, with the majority of protein reacting after five minutes. With Ldt_{Mt3}, **168** only partial reaction was observed after five minutes, and the ratio of reacted to unreacted protein did not change over three hours. The reaction of **168** with Ldt_{Mt4} is also apparently slower than for Ldt_{Mt2}; however, by contrast with respect to the results for Ldt_{Mt3}, product formation increases over time. While **168** exhibits varying rates of reaction with different Ldt enzymes, it is important to note that the rate of reaction of **168** with the clinically relevant Ldt_{Mt2} and Ldt_{fm} is rapid.

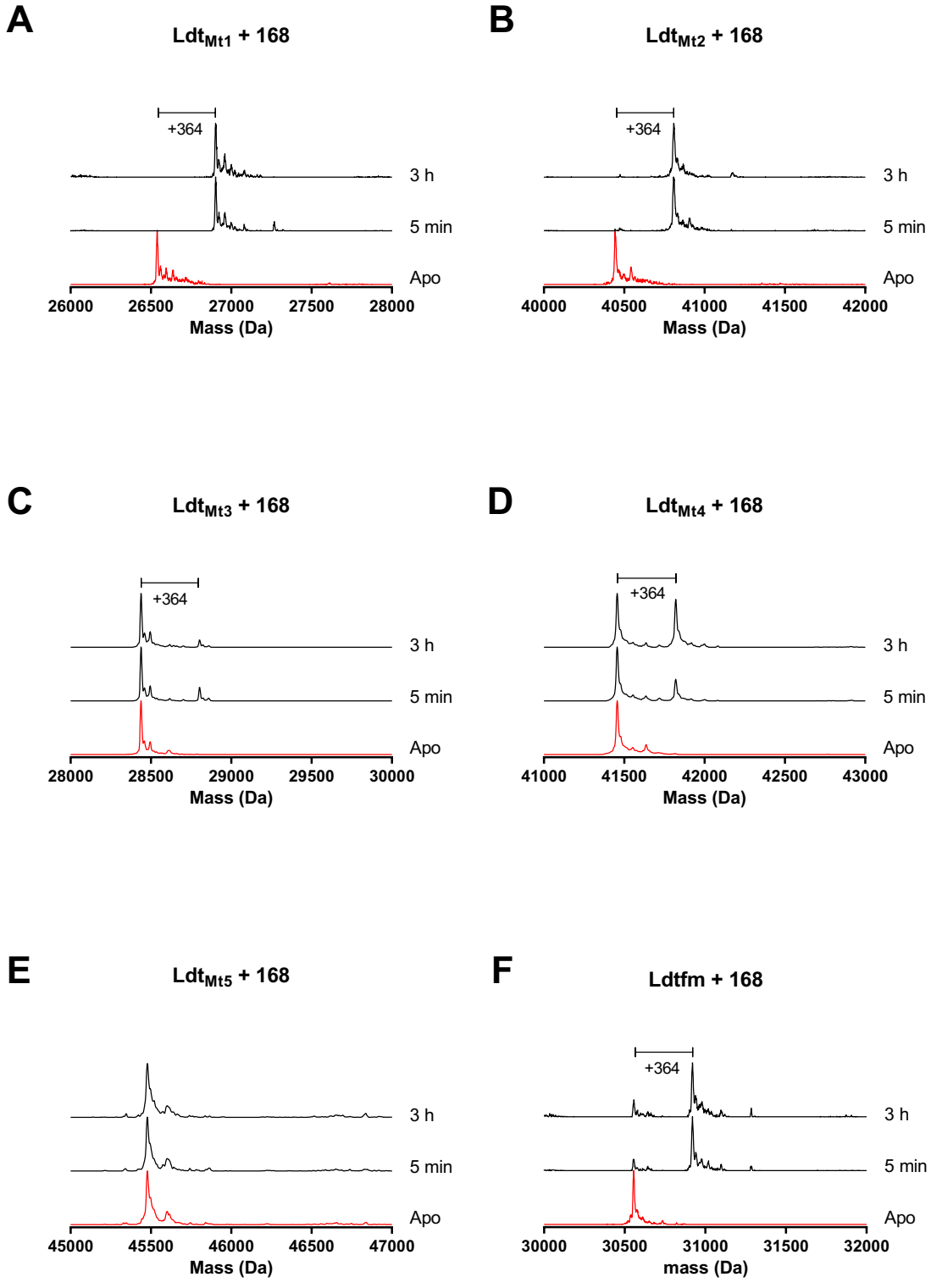

Figure 3-8 | Protein observed mass spectrometry of the reaction between **168** and (**A**) Ldt$_{Mt1}$, (**B**) Ldt$_{Mt2}$, (**C**) Ldt$_{Mt3}$, (**D**) Ldt$_{Mt4}$, (**E**) LdtMt$_5$, and (**F**) Ldt$_{fm}$. Conditions: 2 μM enzyme, 40 μM inhibitor. These experiments were performed by *Tika R. Malla.*

The POMS results for the reaction of **236b** and the panel of Ldt enzymes are summarised in **Figure 3-9**. The results indicate that, against a larger panel of Ldt enzymes, the similarity between the **168** and **236b** decreases. Like **168**, **236b** rapidly reacts to form stable covalent adducts with Ldt_{Mt1} and Ldt_{Mt2}. Unlike **168**, however, **236b** also reacts readily with Ldt_{Mt3}. Similarly, while **168** reacts with Ldt_{Mt4}, no formation of a covalent adduct was observed for Ldt_{Mt4} and **236b**.

Unexpectedly, the reaction between **236b** and Ldt_{Mt5} appears to generate a covalent adduct that forms rapidly but is not stable over longer time points. The apparent instability of the **236b**-Ldt_{Mt5} adduct is contrary to the results from other POMS experiments, where **236b** is observed to either rapidly form stable covalent adducts or not react at all. However, as with **168**, it is important to note that the covalent reaction of **236b** with the clinically relevant Ldt_{Mt2} and Ldt_{fm} is rapid.

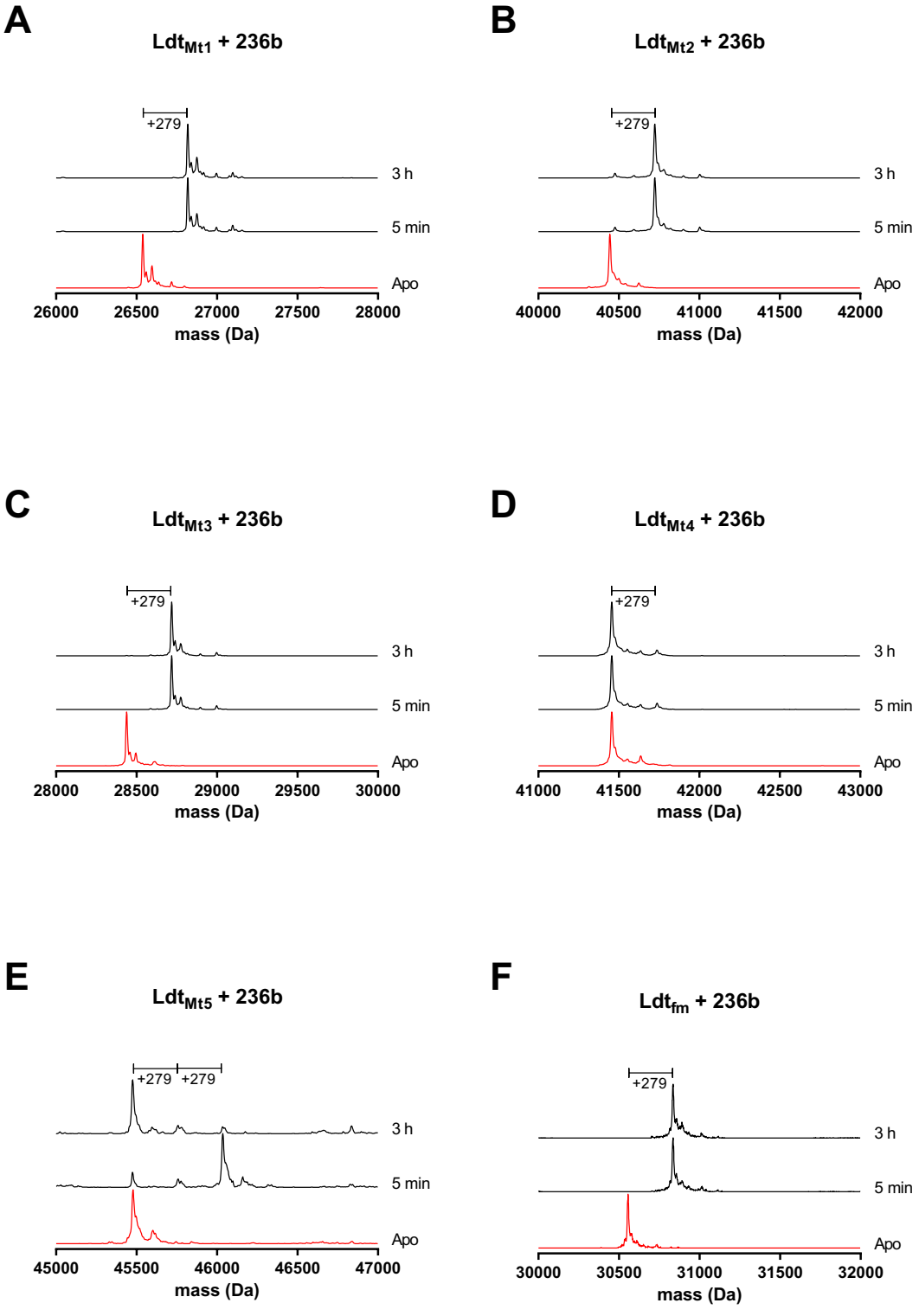

Figure 3-9 | Protein-observed mass spectrometry of the reaction between **236b** and (**A**) Ldt$_{Mt1}$, (**B**) Ldt$_{Mt2}$, (**C**) Ldt$_{Mt3}$, (**D**) Ldt$_{Mt4}$, (**E**) Ldt$_{Mt5}$, and (**F**) Ldt$_{fm}$. Conditions: 2 μM enzyme, 40 μM inhibitor. These experiments were performed by *Tika R. Malla.*

3.3 Protein crystallography of Ldt_{mt2} and inhibitors

Crystal structures of the acyl-enzyme complexes between Ldt enzymes and various β-lactams are reported,[235-237] as are structures of the acyl-enzyme complexes between lactivicins and selected PBPs and SBLs.[162, 167, 174] However, no structures have been reported for lactivicin-Ldt structures. Thus, attempts to solve a Ldt_{Mt2}-**168** complex were undertaken. Ldt_{Mt2} crystals were soaked with **168** to produce crystals of the acyl-enzyme complex, which were then analysed to produce a structure with 1.8 Å resolution. Though the active site occupancy of **168** is not full, the preliminary structure provides an initial characterization of the acyl-enzyme complex between Ldt_{Mt2} and **168** (**Figure 3-10**).

Although the current density map requires further refinement, the view from the crystal structure shown in **Figure 3-10** appears to show that **168** is covalently bound to the active site cysteine of Ldt_{Mt2} via a thioester bond. Like the crystal structures of **168** bound to PBPs,[162] the reaction at the cycloserine carbonyl appears to result in opening of the lactone ring. The terminal carboxylate moiety appears to present to the bulk solvent and the alkyl chain from the lactone ring is likely able to rotate freely, which may account for the poor electron density on that part of the molecule. The phenoxyacetyl sidechain of **168** appears to wrap around the sidechain of His336, which is part of the Ldt_{Mt2} catalytic dyad, potentially in a manner that hinders hydrolytic degradation of the thioester.

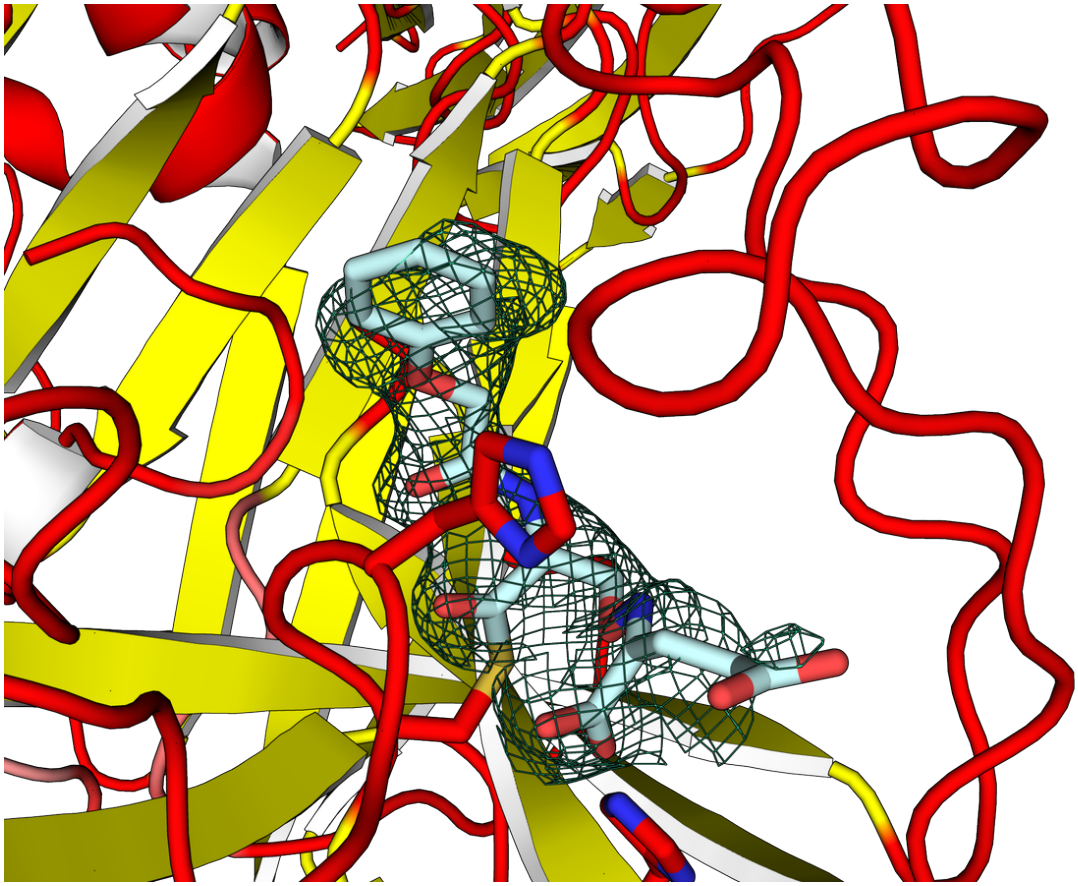

Figure 3-10 | View from a crystal structure (1.8 Å) of the acyl-enzyme complex formed from the reaction of **168** with Ldt_{Mt2}. Note that further refinement is necessary. Crystal soaking experiments were performed by *Tika R. Malla*. Data collection and structural refinements were performed by *Tika R. Malla* and *Dr. Michael A. McDonough*.

3.4 MIC results

Minimum inhibitory concentration assays were run in conjunction with Dr. Karina Calvopiña.

Minimum inhibitory concentration (MIC) assays were performed on select molecules described from this Chapter to determine their antibacterial activity. The compounds tested include: **6** – a representative first generation β-lactam antibiotic; **168**, which as a literature compound was used as a benchmark for the antibacterial

activity of the other lactivicins; bicyclic cycloserine analogues **236a**,**b**,**f** as described in **section 2.4**; the lactivicin analogue **223** lacking a *C*-4 amido sidechain described in **section 2.3**; compound **242**, which lacks a carboxylate moiety; and the tricyclic lactivicin analogues **290a** and **290b**.

Being a phenotypic assay, MICs are an excellent test of a compound's antibacterial activity; however, MIC values alone do not provide insight into the mechanism of antibacterial activity, nor do they define why a compound is not active. Inhibition assays against specific cellular targets and/or the identification of resistance mechanisms are used to identify a molecule's mechanism of action. The MIC activity screen was conducted using the standard *E. coli* strain BW25113 (**Table 3-1**).

Compound	MIC (μg/mL)
6	4
168	16
236a	> 256
236b	64
236f	> 256
223	> 128
242	> 256
290a	> 128
290b	> 128

Table 3-1 | MIC values of selected compounds against *E. coli* BW25118. Data gathered as technical duplicates.

Ampicillin (**6**) and **168** both displayed MICs consistent with previous reports.[129, 238] Compound **223**, which lacks the typical amido sidechain of lactivicins and antibiotics, did not show antibacterial activity, highlighting the apparent

importance of the amido sidechain for both substrate binding and cell entry. The benzisoxazolidinone-derived analogue **236a** showed no antibacterial activity, however, the sulfur analogue **236b** showed a clear increase in antibacterial activity (though its absolute activity is still low compared to ampicillin and **168**). The reason for the increased activity of **236b** over **236a** is not clear, as *E. coli* is not known to express nucleophilic cysteine transpeptidases. The nucleophilic serine-containing PBPs that are expressed in *E. coli* should not be capable of disulfide bond formation with the sulfur analogue **236b**. The activity of the sulfur analogue compared to the oxygen analogue **236a** could be indicative of an alternative mechanism of action for the sulfur analogue, such as the inhibition of an enzyme other than nucleophilic serine transpeptidases or the generation of ROS as was observed for **140**.[146]

3.5 Summary

The results described in this Chapter reveal differences in the reactivities of lactivicin analogues with Ldt enzymes. POMS experiments demonstrated that **168** is an effective covalent inhibitor of clinically relevant Ldt enzymes from *M. tuberculosis* (Ldt_{Mt1} and Ldt_{Mt2}) and *E. faecium* (Ldt_{fm}). POMS experiments on lactivicin analogues revealed that compound **223** can react covalently with Ldt_{Mt2}, however, in a manner substantially less efficient than **168**.

POMS experiments also showed that, of the bicyclic cycloserine lactivicin analogues, only compound **236b** is a covalent inhibitor of Ldt enzymes. Mechanistic studies using the reducing agent DTT provided evidence that **236b** reacts with the

enzyme cysteine via the sulfur atom, rather than the carbonyl (as is proposed for **168**), to form a disulfide-linked covalent adduct, suggesting that benzisothiazolinone-based covalent inhibitors may be promising future anti-tuberculosis agents with enhanced efficacy against resistant strains. Like **168**, **236b** demonstrated rapid covalent reactions with clinically relevant Ldt enzymes. However, it is likely that these benzisothiazolinone-based covalent inhibitors may exhibit high reactivity for other biological thiols, potentially leading to unwanted side effects that mitigate their clinical efficacy. Future studies should include evaluating the reactivity of these compounds towards other cysteine proteases, as well as small molecule thiols like glutathione.

The MICs for compounds described in this Chapter were determined against the susceptible *E. coli* strain BW25113. While ampicillin and **168** both displayed moderate inhibition (consistent with literature reports[129, 238]), only **236b** exhibited an MIC below 128 μg/mL. Disappointingly, neither compound **223**, nor the tricyclic lactivicins **290a** and **290b** displayed even modest antibacterial activity. The lack of antibacterial activity for compounds **223**, **290a**, and **290b**, along with the many structurally similar yet inactive compounds described in Section **1.5**, highlight the relatively narrow chemical space in which non-β-lactam transpeptidase inhibitors may exist. Nevertheless, the discovery of **236b** as a novel covalent inhibitor of Ldt enzymes is promising for the development of future non-β-lactam transpeptidase inhibitors.

Chapter 4 Methods for the modification of 2-oxoglutarate and their applications

4.1 Introduction

As discussed in **Chapter 1**, the studies of Baldwin *et al*. on cycloserine derivatives demonstrated the importance of the γ-lactone carboxylate moiety for the antibacterial activity of the lactivicin class of antibiotics.[181] Starr *et al.* demonstrated that functionalisation of the lactivicin lactone can be tolerated and can even contribute to additional non-covalent interactions between lactivicin and the transpeptidases.[167] Thus the γ-lactone of lactivicin is a logical place to further functionalise the lactivicin core. The work described in this Chapter aimed to improve reported synthetic methods and to develop novel methodology for the functionalisation of 2-OG to allow access to γ-lactone-modified lactivicin analogues.

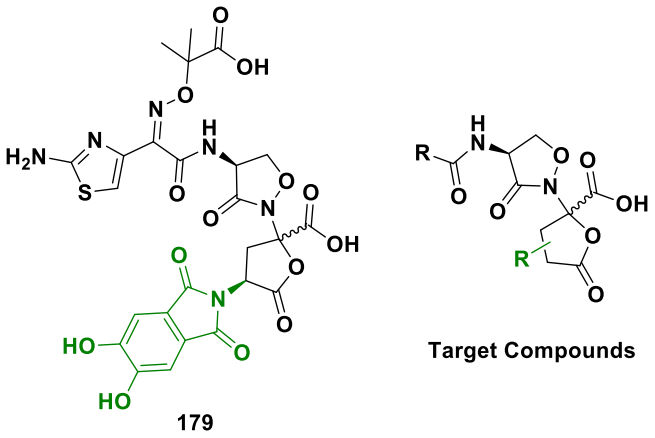

Figure 4-1 | Structures of **179**, with γ-lactone modification (green); and target lactivicins with novel γ-lactone modifications.

The methodology explored for the functionalisation of **2-OG** was also applied to the synthesis of a library of 3-mercaptomethyl 2-OG analogues (**Figure 4-2**). It was envisaged that this methodology would enable researchers to easily access functionalised **2-OG** analogues for biochemical and therapeutic applications. As a proof of concept, the library of *C*-3-functionalised **2-OG** analogues **292** was synthesised and screened for inhibitory activity against clinically relevant isocitrate dehydrogenase (IDH) variants.

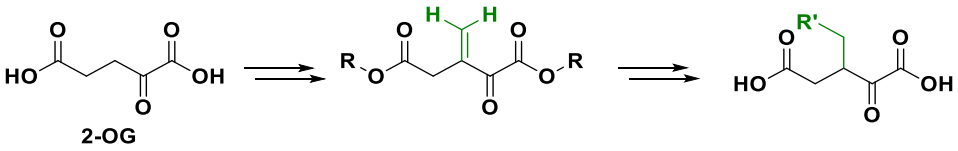

Figure 4-2 | General method for the facile functionalisation of **2-OG**.

4.1.1 PBPs can accommodate additional functionality to the lactivicin γ-lactone

Crystal structures of **162** and **168** bound to *S. pneumoniae* PBP1b as reported by Macheboeuf *et al.*[162] reveals that the γ-lactone carboxylate occupies a groove in the PBP active site that is occupied by the pentapeptide natural substrate during transpeptidation, suggesting that there is sufficient room in the active site to append additional functionality to the γ-lactone ring of lactivicin (**Figure 4-3**).

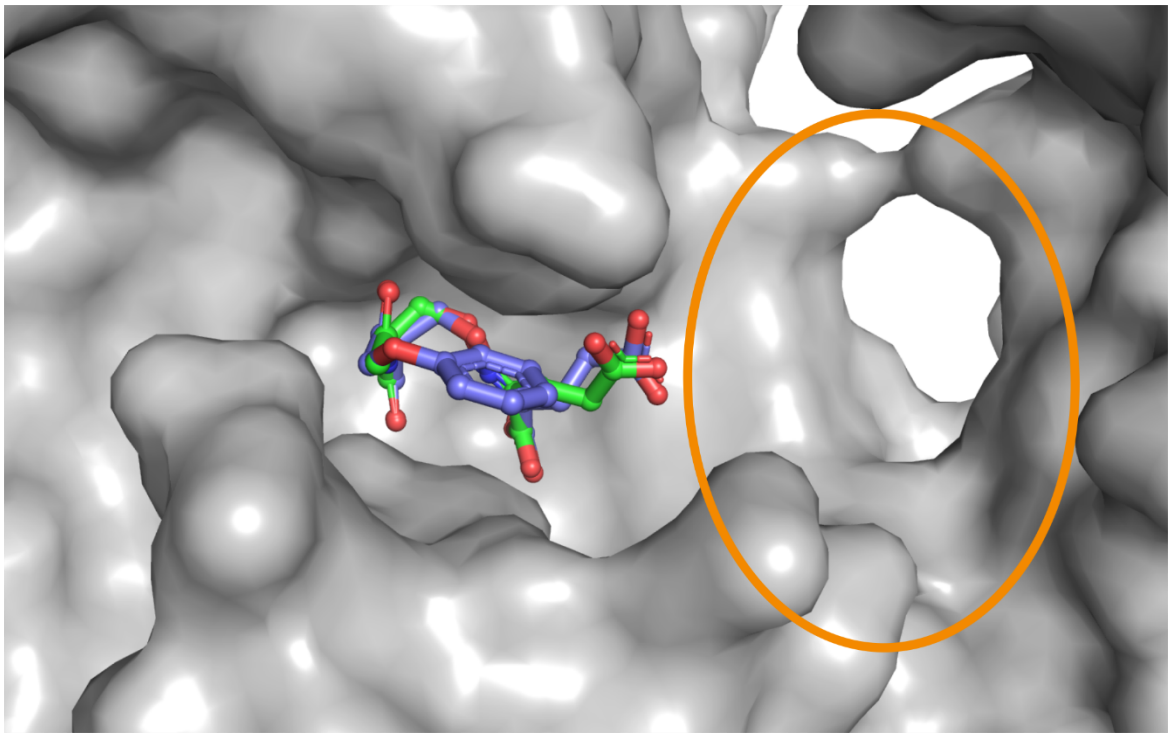

Figure 4-3 | 162 (green) and **168** (blue) in complex with *S. pneumoniae* PBP1b (grey). The carboxylic acid group of both molecules extends towards a sterically open region of the protein (orange oval), suggesting that the acyl-enzyme complexes of different lactivicins adopt similar conformations, and that additional functionality could be attached without introducing steric clashes with the protein. (PDB: 2BG4 and 2JCH).

4.1.2 Crystal structure of compound 179 with pae PBP1a

Starr *et al*. explored the potential for γ-lactone-functionalised lactivicins by synthesising derivatives of lactivicin with siderophores attached at the *C*-4 position of the γ-lactone.[167] The molecule **179**, which possesses a dihydroxyphthalimido group conjugated to the γ-lactone ring of lactivicin, showed potent antibacterial activity and nanomolar potency (as judged by IC_{50} values) for the PBPs. The potent antibacterial activity of **179** demonstrates that not only does the functionalisation of the lactivicin γ-lactone not affect the inhibitory action of lactivicin, but it provides opportunities to improve other parameters of the molecule, such as its uptake into bacterial cells.[155] A crystal structure of **179** in complex with *P. aeruginosa* PBP1a shows that the siderophoric moiety points out of the catalytic cleft and interacts with Tyr733 via π-π stacking.

It is important to note, however, that a primary limitation of IC_{50}s for covalent inhibitors is the inability to directly compare IC_{50} values between different experiments. Due to the time-dependent nature of IC_{50}s, differences in the incubation conditions of the inhibition assay can lead to variations in the measured IC_{50} of an inhibitor. A time-independent kinetic parameter k_{inact}/k_i is often used to evaluate the potency of covalent inhibitors, which takes into account the relative rates of covalent reactions between inhibitors and their targets.[239] Thus, the IC_{50} values reported by Starr et al. cannot be directly compared to IC_{50}s for other covalent inhibitors of other enzymes, however the relative improvement of **179** over

other screened lactivicins indicates an increase in potency, at least for *P. aeruginosa* PBP1a, provided the incubation conditions are long enough to allow for maximum inhibition to be observed.

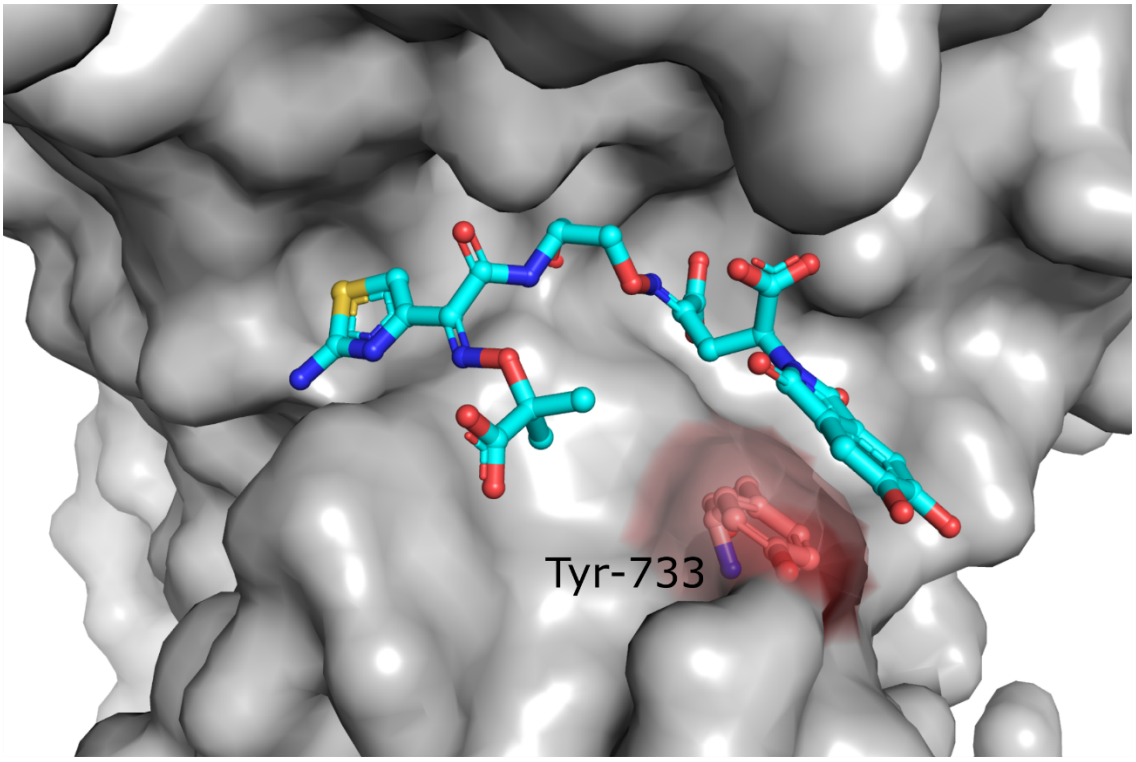

Figure 4-4 | Structure of **179** (cyan) in complex with *P. aeruginosa* PBP1a (PDB: 4OON).[167] The siderophore moiety is not sterically confined and interacts with Tyr733 (light pink), indicating modifications to the lactone are tolerated and can be used to generate additional non-covalent interactions between the enzyme and inhibitor.

4.1.3 Synthesis of the functionalised 2-OG precursor 299.

The synthetic route to the modified 2-OG precursors **293** reported by Starr *et al.* (**Figure 4-5**) began from enantiopure (L)-Cbz-Asp-OMe (**294**), which is activated by EDCI, enabling the nucleophilic attack of the triphenylphosphonium ylide **295** to form the triphenylphosphoranylidene intermediate **296**. Oxidation using ozone at -65 °C and trapping the resulting keto-acid as the allyl ester yielded the protected 4-

amino-2-oxoglutarate precursor **297**. The allyl ester was exchanged for a *tert*-butyl ester to give **298**, then the methyl ester was saponified to give the carboxylic acid **299**, the Cbz group of which was hydrogenated to yield the key intermediate **299**.

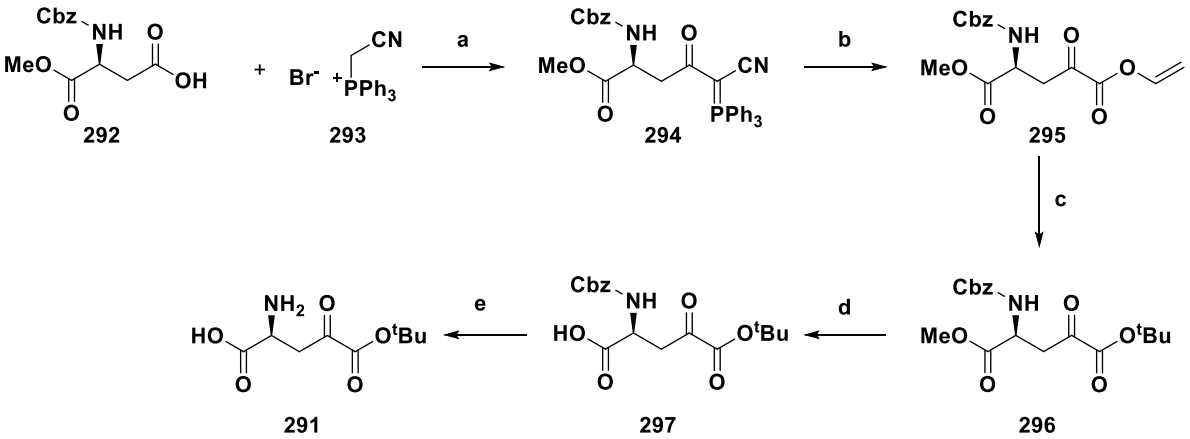

Figure 4-5 | Reported synthesis of γ-lactone-functionalised lactivicins by Starr *et al*.[167] Reagents and conditions: (**a**) (triphenylphosphoranylidene) acetonitrile, EDCI, rt, o/n, 74%; (**b**) O_3/O_2, CH_2Cl_2, -65 °C, then allyl alcohol, -65 °C, 2 h, 30%; (**c**) $Pd(PPh_3)_4$, morpholine, THF, rt, 45 min, then *tert*-butyl-*N*,*N*′-diisopropylimidate, THF, rt, 30 min, 50%; (**d**) LiOH, THF/H_2O, rt, 30 min, 29%; (**e**) Pd black, THF/HCl in 1,4-dioxane, H_2 (45 psi), rt, 25 h.

4.1.4 Drawbacks of the Pfizer route to compound 179

The synthesis of γ-lactone-functionalised lactivicins employed by Starr *et al.*[167] had some drawbacks. Firstly, the use of the phosphonium ylide **295** requires ozone to enable oxidation of the phosphonium intermediate **296** to the keto-acid **297**. Ozonolysis set-ups are dangerous and often not readily available to academic laboratories. These synthetic factors make it difficult to use the route reported by Starr *et al*. to synthesise siderophore-functionalised lactivicin analogues such as **179**. It was envisaged that the use of a cyanosulfur ylide to introduce the keto-acid

would allow for milder oxidising conditions to be used in place of ozone, as described by Ju *et al.*[240] in the synthesis of peptides with *C*-terminal α-keto acids (**Figure 4-6**).

4.2 Improving the Pfizer route

4.2.1 α-Keto-acid synthesis using a cyanosulfur ylide

Ju *et al*.[240] have reported the stereoretentive synthesis of *C*-terminal peptide α-keto acids using a cyanosulfur ylide that can be oxidatively cleaved using Oxone® (**Figure 4-6**). The cyanosulfur ylide **300** is conjugated to the *C*-terminus using HATU and the resulting product is stable to Boc deprotection and amide coupling conditions. Oxidative cleavage of the resulting compound **301** with Oxone® yielded the desired α-keto acid **302**. The conditions needed for this α-keto acid synthesis are milder than those used by Starr *et al.*[167], thus this chemistry was applied to the synthesis of amino-lactivicin analogues.

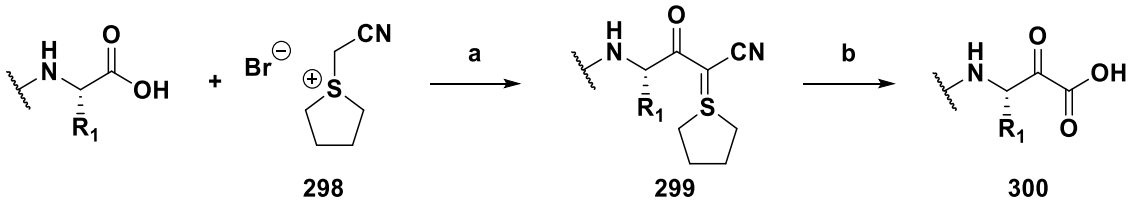

Figure 4-6 | Reported[240] synthesis of peptides with *C*-terminal α-keto acids using a cyanosulfur ylide and Oxone®. Reagents and conditions: (**a**) HATU, HOBt, DIPEA, DMF, 4 h; (**b**) Oxone®, DMF/H_2O, rt, 30 min.

The HATU-mediated coupling of the ylide **300** with **294** proceeded in good yield (70%) to give **303**. Like the reports of Ju *et al.*,[240] facile oxidation of **303** was achieved using Oxone® to give the keto-acid **304** (carried forward crude), which was esterified with *tert*-butyl-*N,N'*-diisopropylimidate to give the *tert*-butyl keto-ester **298** in moderate yield (44%). Finally, hydrolysis of the methyl ester with LiOH yielded the key intermediate **299**.

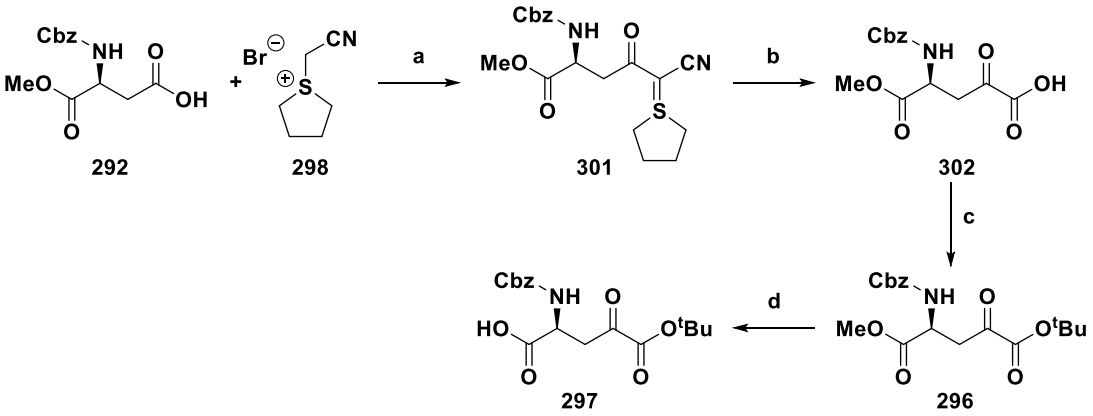

Figure 4-7 | Improved synthesis route to **299**. (**a**) HATU, DIPEA, DMA, rt, 4 h, 70%; (**b**) Oxone, THF/H_2O, 0 °C, 30 min, carried forward crude; (**c**) *tert*-butyl-*N,N'*-diisopropylimidate, THF, rt, 30 min, 44% over 2 steps; (**d**) LiOH, THF/H_2O, rt, 30 min, 68%.

4.3 Sulfide-functionalised lactivicin analogues

4.3.1 Functionalisation of Michael acceptor 284.

It was envisaged that the Michael acceptor **284** used in the synthesis of Shionogi-type tricyclic lactivicin analogues could be reacted with other nucleophiles to generate 2-oxoglutarate intermediates that could be used to synthesise lactivicins with additional functionality at the *C*-3 position of the γ-lactone (**Figure 4-8**).

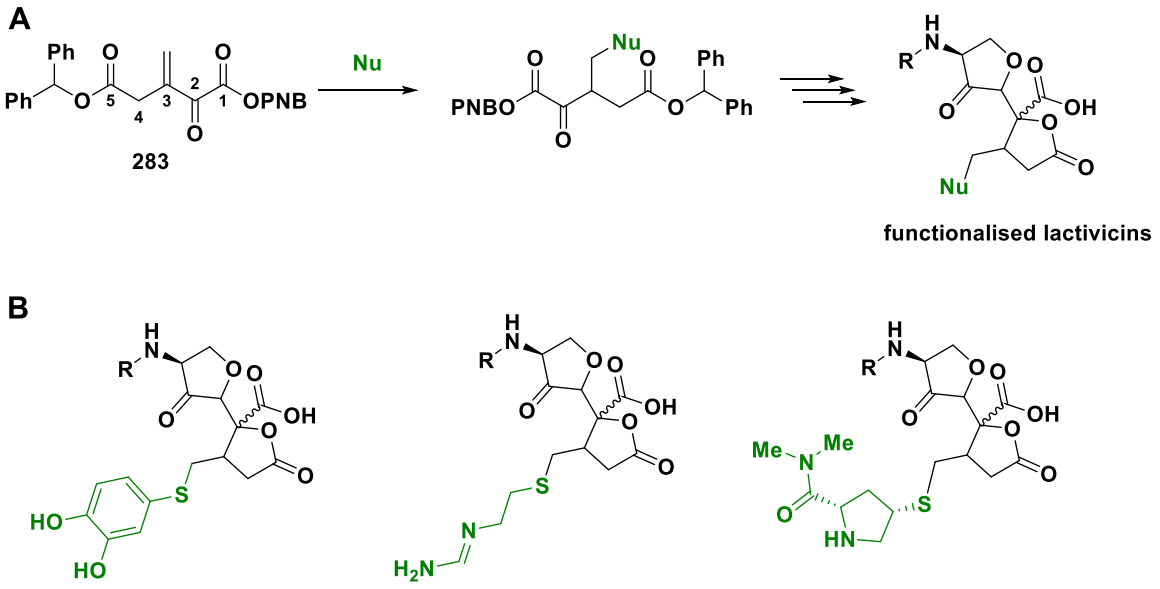

Figure 4-8 | (**A**) Michael Addition of nucleophiles with the Michael acceptor **284** to generate *C*-3-γ-lactone-functionalised lactivicins. (**B**) Target lactivicins with siderophoric or carbapenem-derived sidechains attached at *C*-3 via a sulfide.

The *C*-3 sulfido sidechains of carbapenems play a crucial role in mediating cellular uptake via ion channels.[241] It was proposed that the attachment of carbapenem *C*-3 sidechains onto the γ-lactone ring might confer similar cellular uptake benefits to lactivicins. Thus, thiols were a logical starting point for the functionalisation of the *C*-3 position of the lactivicin γ-lactone. However, simpler thiols were attempted as a proof of concept before committing to the more complex thiols derived from the *C*-3 sidechains of carbapenems.

4.3.2 Method exploration

The synthetic route outlined in **Figure 4-8A** was initially attempted using thiophenol as the nucleophile. The Michael addition of thiophenol onto the Michael acceptor **284** proceeded with good yields (87%) to give **305**, as did the removal of

the benzhydryl ester with TFA to give **306** in good yield (85%). However, the lactonisation reaction of the deprotected product with the cycloserine analogue **210** using DCC did not produce the expected γ-lactonised product **307**. The additional steric bulk introduced by the sulfide moiety may hinder the cyclisation of the hemi-aminal that results from the nucleophilic attack of the cycloserine onto the ketone of the precursor **306**. Alternatively, decomposition of the product **307** may have occurred under the reaction conditions.

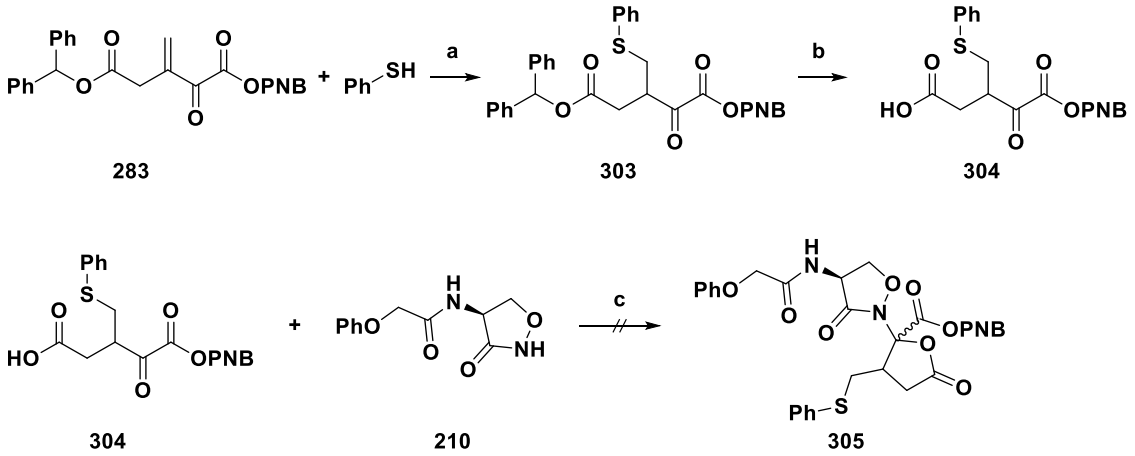

Figure 4-9 | Attempted synthesis of the *S*-phenyl-substituted γ-lactone lactivicin derivative **307**. Reagents and conditions: (**a**) PhSH, Et_3N (cat.), CH_2Cl_2, rt, 30 min, 87%; (**b**) TFA, CH_2Cl_2, rt, o/n, 85%; (**c**) DCC, CH_2Cl_2, rt, o/n.

To investigate whether the steric barrier to cyclisation could be overcome with higher temperatures, the reaction was repeated in refluxing CH_2Cl_2, though these conditions also did not form the desired product **307**. A brief condition screen was conducted (**Table 4-1**). The solvent was switched to $CHCl_3$ to allow for a higher reflux temperature, however decomposition of **306** was observed at these higher

temperatures. EDCI was also used as the coupling reagent instead of DCC; but its use also did not produce the desired lactone **307**.

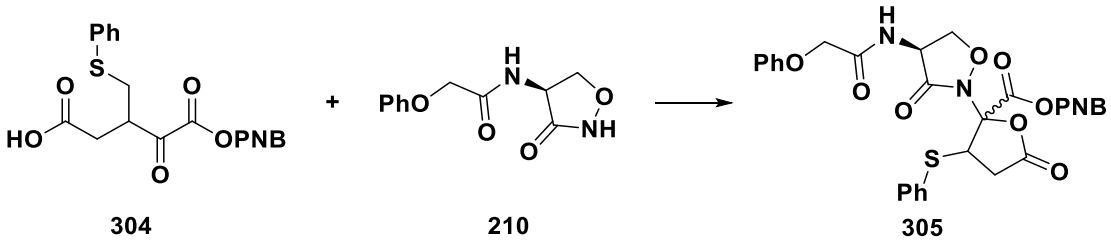

Entry	Coupling Reagent	Solvent	T (°C)	% isolated yield of 307
1	DCC	CH_2Cl_2	25	0
2	DCC	CH_2Cl_2	40	0
3	DCC	$CHCl_3$	61	0
4	EDCI	CH_2Cl_2	25	0

Table 4-1 | Condition screen for the lactonisation reaction to form **307**.

These results indicate that the addition of steric bulk at the *C*-3 position of the **2-OG** synthetic precursor to lactivicins prevents the lactonisation reaction to form the γ-lactone ring. Hence, the use of this synthetic route for the synthesis of sulfide-functionalised lactivicins was deemed unfeasible.

4.4 Synthesis of 3-sulfido 2-oxoglutarate analogues

While the chemistry developed above was not applicable to the functionalisation of the γ-lactone of lactivicins, this method for installing an alkene at the 3-position of **2-OG** derivatives allows for facile access to novel chemical space on the **2-OG** core.

Given the abundance of **2-OG** as both a metabolic intermediate and an enzymatic co-substrate, the ability to easily synthesise functionalised **2-OG** analogues could be a powerful tool for probing and inhibiting biological targets from a wide range of biochemical processes and disease states.

4.4.1 2-Oxoglutarate as a co-substrate in enzyme catalysis

2-OG is a ubiquitous small molecule in cells with a range of biochemical functions. **2-OG** is a key intermediate in the tricarboxylic acid (TCA) cycle, where its oxidative decarboxylation is coupled to the synthesis of nicotinamide adenine dinucleotide (NADH) – the primary electron transfer reagent in the oxidative phosphorylation of adenosine diphosphate (ADP) to adenosine triphosphate (ATP).[235] **2-OG** is a co-substrate for a class of oxidoreductases (EC1) collectively called 2-OG-dependent dioxygenases.[242] The 2-OG-dependent dioxygenase family is diverse and catalyses an equally wide range of reactions, including: hydroxylations;[243] demethylations (which proceed via an initial hydroxylation);[244] halogenations;[245] epoxidations;[246] and even ring-forming reactions;[247] and ring-expansion reactions.[248] Some of these 2-OG-dependent dioxygenases have emerged as therapeutic targets against human diseases such as anaemia and cancer.[249]

There have been many efforts to develop metal chelating inhibitors of 2-OG-dependent oxygenases that compete with **2-OG** for coordination to the catalytic metal ion. These compounds typically rely on polar moieties capable of bidentate coordination of the catalytic metal ion as the primary binding interaction. Some of

these inhibitors are clearly inspired by **2-OG**; however, a literature search revealed only one recent report of modified **2-OG**s developed as inhibitors and alternative substrates of a 2-OG-dependent oxygenase.[250] 2-OG-based inhibitors with alkyl or aryl functionalisation at the *C*-3 or *C*-4 position have been developed as inhibitors for aspartate/asparagine-β-hydroxylase (AspH).[250]

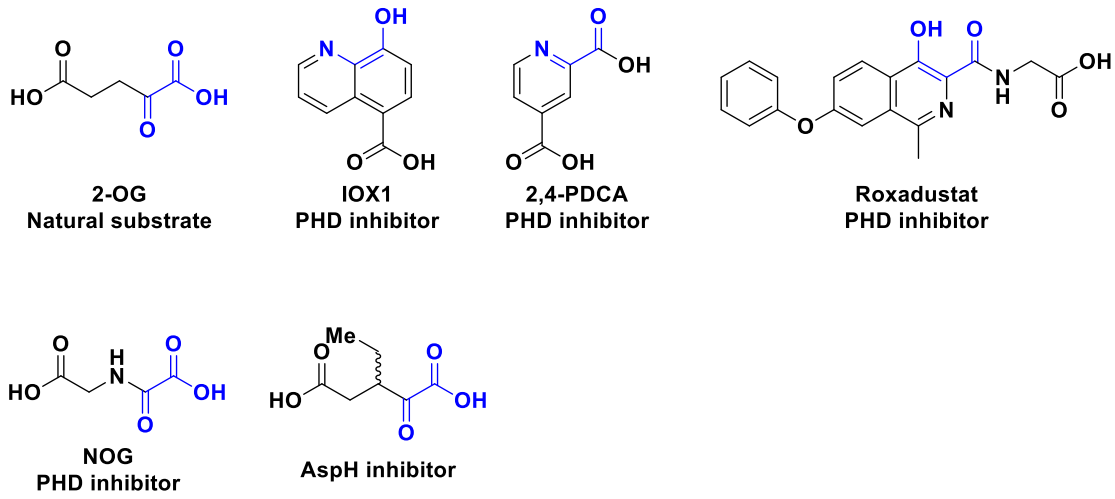

Figure 4-10 | Structures of competitive inhibitors of 2-OG-dependent dioxygenases with bidentate metal chelating moieties (blue).

2-OG therefore presents a rational starting point for the development of novel competitive inhibitors of **2-OG**-dependent dioxygenases. **2-OG** analogues could potentially inhibit any of the **2-OG**-dependent dioxygenases, so a library of *C*-3-functionalised **2-OG** analogues was synthesised for screening against panels of **2-OG**-dependent dioxygenases. Selective 'hit' compounds can then be developed into selective competitive inhibitors.

4.5 Synthesis of a library of 2-oxoglutarate inhibitors of Isocitrate dehydrogenase

4.5.1 Introduction to isocitrate dehydrogenase

Isocitrate dehydrogenases (IDH) are a class of enzymes that catalyse the oxidative decarboxylation of isocitrate to **2-OG**. IDH enzymes utilise the divalent cation magnesium (or manganese) in catalysis. IDH3, located in mitochondria, catalyses this reaction as part of the Krebs cycle under concomitant reduction of NAD^+ to NADH.[251] Cytosolic IDH1 and mitochondrial IDH2 have been shown to mitigate cellular damage by oxidative stress via their production of the reducing agent NADPH.[252]

The cytosolic isoform IDH1 is the primary source of NADPH production in the human brain.[253] In humans, $IDH1^{R132}$ variants are commonly observed in glioma tumours.[254] These IDH1 variants exhibit a gain-of-function to reduce **2-OG** to 2-hydroxyglutarate (**2-HG**) via the conversion NADPH to $NADP^+$. The decrease in cellular NAPDH levels leaves the cell more vulnerable to oxidative stress, potentially explaining the slightly improved life expectancies of glioma patients expressing $IDH1^{R132}$ variants relative to glioma patients expressing *wt* IDH. The increased concentration of **2-HG** in cells expressing mutant IDH1 is proposed to inhibit other **2-OG**-dependent dioxygenases such as Jumonji C (JmjC)-domain histone demethylases (KDMs) or ten-eleven translocation (TET) oxygenases that

control the methylation state of histones and DNA, respectively, and are hence involved in epigenetic regulation.[255] **2-HG** has been reported as a weak competitive inhibitor of some **2-OG**-dependendent dioxygenases.[256]

Since initial reports of the oncogenic effect of $IDH1^{R132}$ variants in cancer[257], selective inhibitors for $IDH1^{R132}$ variants have been disclosed.[258-264] Many of these inhibitors bind allosterically at the IDH1/2 dimer interface of the enzyme and interfere with the binding of Mg^{2+} and hence **2-OG**.[265] Recently, **ivosidenib** (IDH1 variant inhibitor) and **enasidenib** (IDH2 variant inhibitor) (**Figure 4-11**) have been approved by the FDA for the treatment of relapsed or refractory acute myeloid leukaemia (AML) where an IDH1 or IDH2 mutation is present. While these inhibitors potently reduce plasma **2-HG** levels (used for therapy control), there have been several reports of tumours gaining resistance to ivosidenib.[266, 267] The resistance of IDH1 variants to small molecule inhibition has been shown to be linked to a Ser-280 to phenylalanine second-site variation in $IDH1^{R132C}$ variants. The added steric bulk of the phenylalanine has been proposed to interfere with binding of **ivosidenib** at the dimer interface, restoring the oncogenic function of the enzyme.

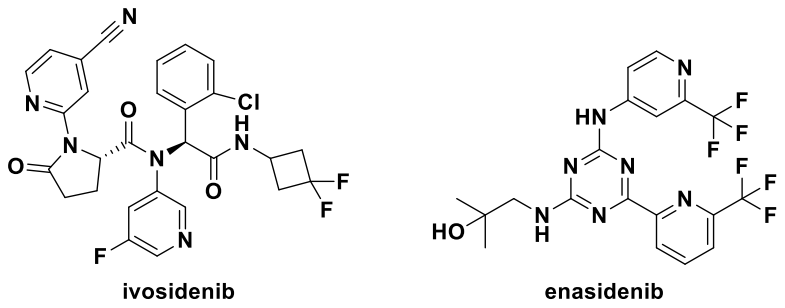

Figure 4-11 | Reported structures of $IDH1^{R132H}$ inhibitors **ivosidenib** and **enasidenib**.

It is proposed that the development of a competitive inhibitor based on the structure of **2-OG** for IDH1^{R132} variants might be less susceptible to the development of resistance as it would require a change to the active site that not only prevents the inhibitor from binding, but also maintains the gain-of-function R132 substitution. Considering that the active site of the IDH1^{R132} variants is already relatively confined, it may be considered less likely that such a variation to the active site would be able to fulfil both of those requirements for resistance compared to variations at the dimer interface.

4.5.2 Structure of the IDH1^{R132H} active site

Wild-type (*wt*) IDH1 is homodimeric with two active sites per dimer. Each active site can bind a divalent cation, $NADP^+$/NADPH, and the substrate (isocitrate). IDH1 uses a Mg(II) ion as a co-factor, to which one of the *C*-1 carboxylate group of isocitrate chelates during catalysis; the *C*-3 carboxylate of isocitrate coordinates to arginine 132 (Arg-132) and other residues. The nicotinamide moiety of NADP/H binds close to the *C*-3 carbon of isocitrate (~3 Å).[268]

Like the *wt* IDH1, the IDH1^{R132H} variant is homodimeric with two active sites, each of which can bind a Mg(II) ion and NADP/H. However, as discussed above, IDH1^{R132H} loses affinity for isocitrate. The substitution of the Arg-132 residue to histidine results in structural changes to the IDH1^{R132H} active site that disfavour binding of isocitrate compared to **2-OG** (**Figure 4-12**). Principally, the *C*-3 carboxylate of isocitrate is unable to form a salt bridge to the histidine in the

IDH1^{R132H} variant. The loss of the salt bridge between the *C*-3 carboxylate of isocitrate and the enzyme reduces the affinity for isocitrate in IDH1^{R132} variants. Upon binding of **2-OG** to IDH1^{R132H} mutants, the Tyr-139 residue is proposed to rotate towards the active site and contribute additional binding interactions to **2-OG**. [268] Since **2-OG** chelates the Mg(II) ion similarly to isocitrate, the distance from the 2-keto-group of **2-OG** to the reducing nicotinamide moiety of NADP/H is similarly close, allowing for the reduction of **2-OG** to **2-HG**.

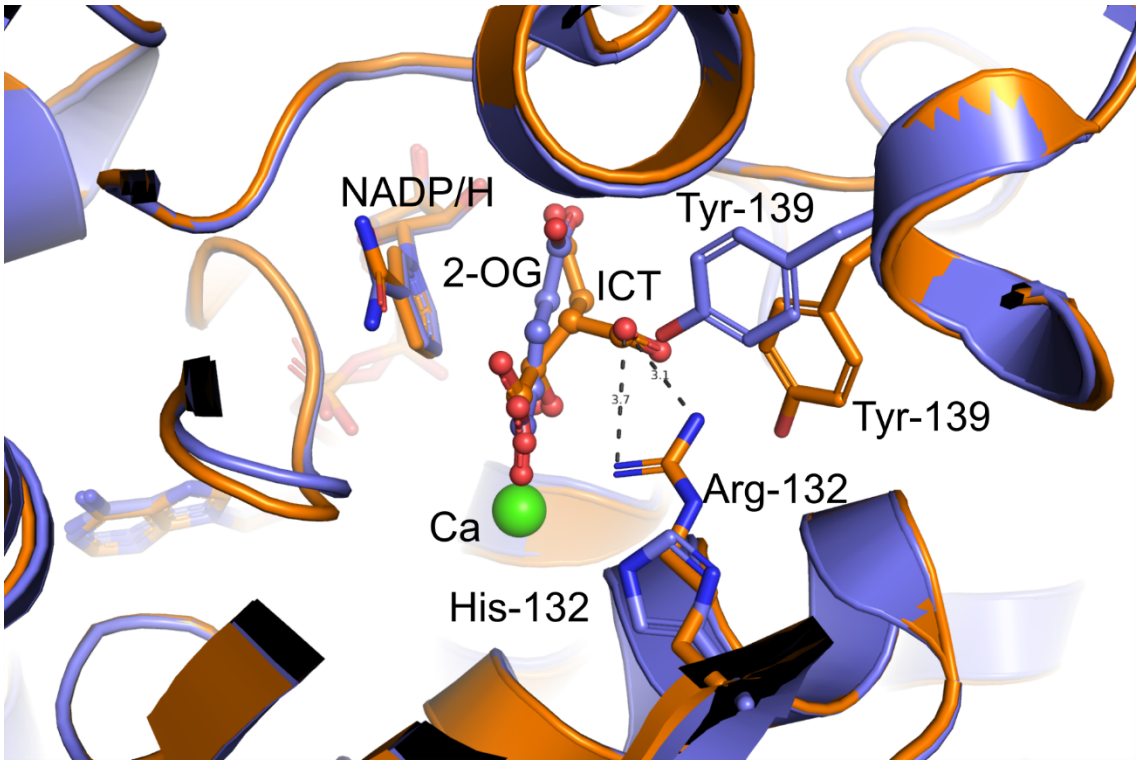

Figure 4-12 | Comparison of the active sites of *wt*IDH1 (orange) (PDB: 1T0L) and IDH1^{R132H} (purple) (PDB: 4KZO). Isocitrate (ICT) has a lower binding affinity for IDH1^{R132H} due to the loss of the interaction with the R132 residue.

It was proposed that inhibition of the IDH1^{R132H} variant by functionalised **2-OG** derivatives could be achieved by attaching substituents to **2-OG** that interfere with

the binding of NADPH in the active site. If the additional functionality introduced onto the **2-OG** backbone were to occupy the same binding site as NADPH, the nicotinamide moiety would not be close enough to reduce the **2-OG** ketone. Thus, an initial series of sulfide-functionalised 2-OG derivatives (**292a-g**) was conceived that included compounds with a variety of functional groups (**Figure 4-13**).

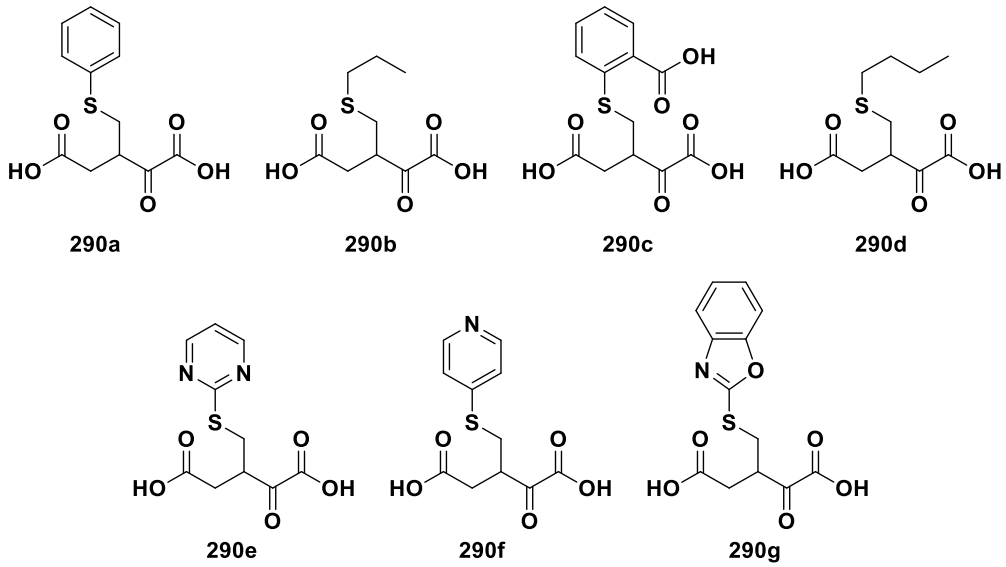

Figure 4-13 | Structures of proposed 3-sulfido-2-OG derivatives **292a-g** for inhibition studies against $IDH1^{R132H}$.

4.5.3 Optimisation of the general synthetic route to 3-sulfido-2-OG analogues

The general synthetic route to these compounds is shown as a retrosynthesis in **Figure 4-14**. By contrast with the syntheses of the key Michael acceptor intermediate **284** for Shionogi-type tricyclic lactivicins and modified γ-lactones, the ability to selectively deprotect the α-keto ester in the presence of the *C*-5 ester is not needed for the synthesis of sulfido-2-oxoglutaric acid derivatives. Thus, the same protecting

group can be used on both esters, allowing for a single deprotection step to yield the desired 2-oxoglutaric acid derivatives.

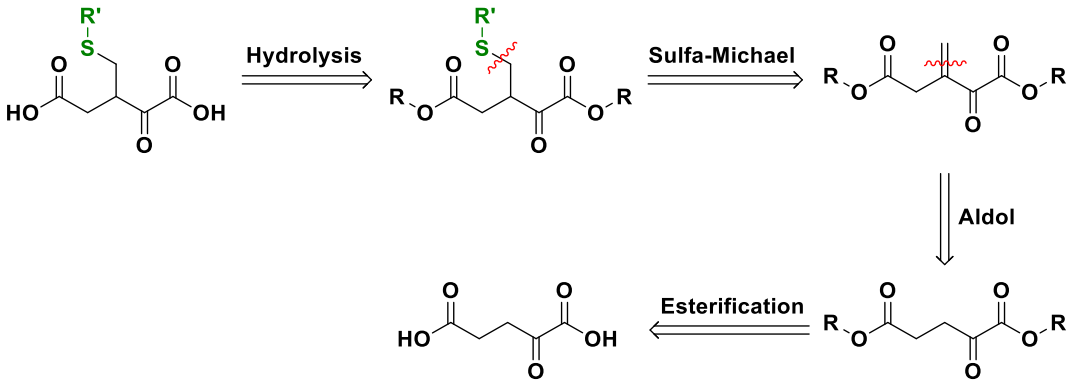

Figure 4-14 | General synthetic route to *C*-3 functionalised 2-OG analogues.

Initially, methyl esters were used to protect the carboxyl groups of (**Figure 4-15**). The methylene alkene moiety was installed as described previously via reaction with **308** to give the Michael acceptor **309** in a 37% yield. As before, thiophenol was used as the model thiol to validate the subsequent chemistry. The sulfa-Michael reaction between the Michael acceptor **309** and thiophenol in the presence of catalytic triethylamine proceeded with excellent (98%) yields to give the sulfide product **310**. Deprotection of the methyl esters using LiOH, however yielded a complex mixture of products that could not be readily separated. It is likely that the aqueous alkaline conditions facilitated some retro-Michael elimination of the thiophenol, as well as potential Claisen condensation-type reactions.

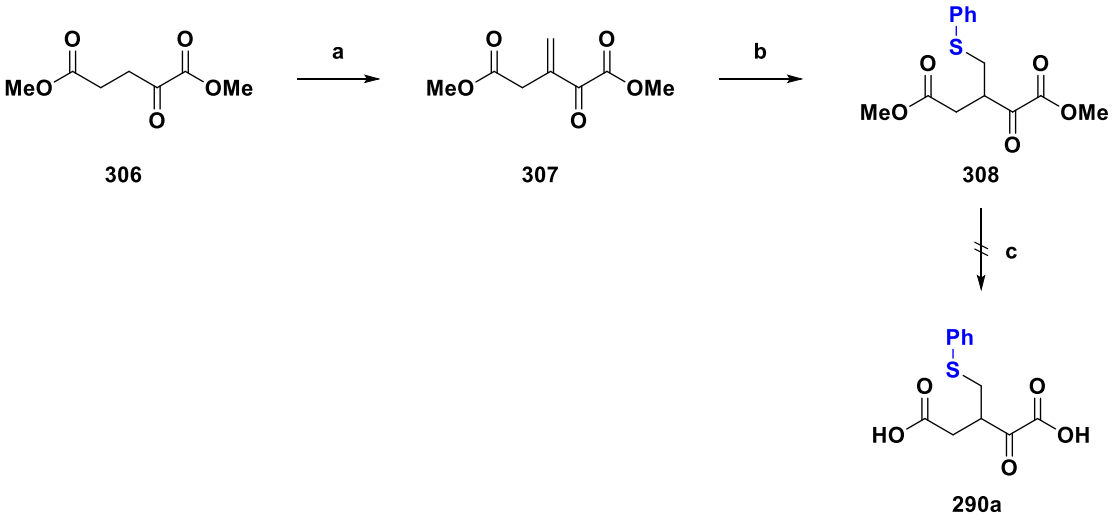

Figure 4-15 | Attempted synthesis of **292a** using methyl ester protecting groups. Reagents and conditions: (**a**) *N*,*N*,*N*′,*N*′-tetramethylenediaminomethane, Ac_2O, AcOH, CH_2Cl_2, rt, 5 h, 37%; (**b**) thiophenol, Et_3N (cat.), CH_2Cl_2, rt, o/n, 98%; (**c**) LiOH, THF/H_2O, rt.

It was apparent from this synthetic attempt that methyl esters were not suitable protecting groups for the carboxyl groups of **2-OG**, so acid-labile *tert*-butyl ester protection was attempted (**Figure 4-16**). The di-*tert*-butyl 2-oxoglutarate **311** was synthesised in 68% yield by transesterification of **2-OG** with *tert*-butyl acetate and sulfuric acid. The alkene was introduced, in an analogous fashion as for the di-methyl **2-OG** intermediate **309**, to give **312**, and a Michael addition with thiophenol was performed to give the sulfide **313a**. Deprotection of the *tert*-butyl esters was accomplished by titration of TFA until both *tert*-butyl groups were fully cleaved. Deprotection of the first ester (presumed to be the α-keto ester) was observed by TLC with nine equivalents of TFA, and full deprotection was achieved at twenty equivalents of TFA. Thus, subsequent *tert*-butyl deprotections were performed using twenty equivalents of TFA.

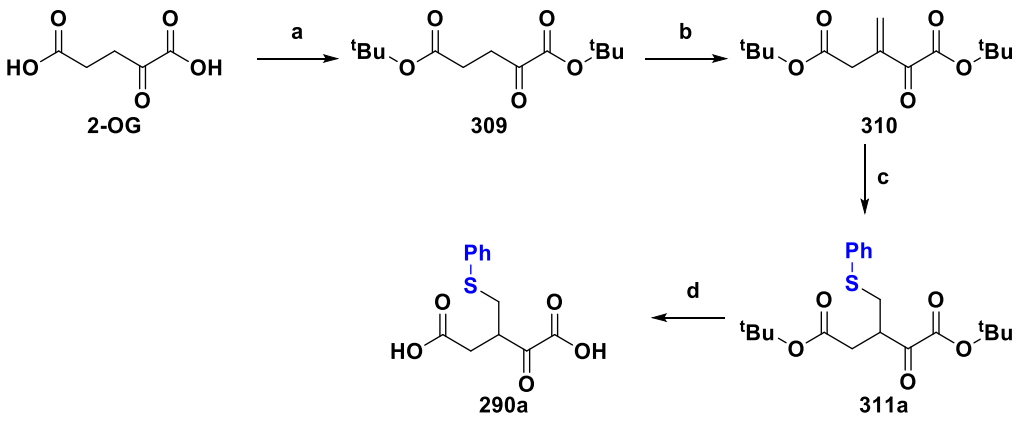

Figure 4-16 | Successful synthesis of **292a** using *tert*-butyl ester protecting groups. Reagents and conditions: (**a**) H_2SO_4, *tert*-butyl acetate, rt, o/n, 68%; (**b**) *N*,*N*,*N*′,*N*′-tetramethylenediaminomethane, Ac_2O, AcOH, CH_2Cl_2, rt, 5 h, 43%; (**c**) thiophenol, Et_3N (cat.), CH_2Cl_2, rt, o/n, 99%; (**d**) TFA, CH_2Cl_2, rt, o/n, 46%.

Having established the synthetic conditions for the sulfa-Michael addition and *tert*-butyl ester deprotection reactions, the synthesis of a library of *C*-3-functionalised **2-OG** analogues **313b-g** was commenced.

4.5.4 Synthesis of the initial series of 3-sulfido-2-OG analogues

The general procedure developed for the synthesis of a 3-sulfido-2-oxoglutaric acid analogues from the Michael acceptor **312** is shown in **Figure 4-17**. An initial set of seven compounds (**313a-g**) was synthesised for screening against $IDH1^{R132H}$ (**Table 4-2**).

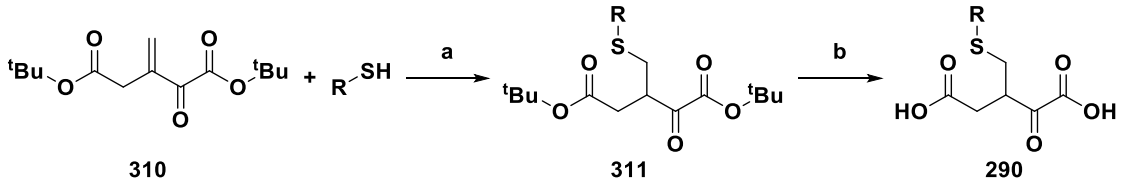

Figure 4-17 | General procedure for library synthesis. Reagents and conditions: (**a**) Et_3N (cat.), CH_2Cl_2, rt, o/n; (**b**) TFA, CH_2Cl_2, rt, o/n.

The first series of compounds included a mixture of aliphatic and aromatic residues, including heteroaromatic rings. The heteroaromatic residues were intended to mimic structurally the nicotinamide ring of the NADPH co-substrate given the proximity of NADPH to **2-OG** in the crystal structure of IDH^{R132H} (**Figure 4-12**).

The sulfa-Michael reactions to form **313a-e** and **313g** proceeded with good to excellent isolated yields (72-99%). The synthesis of the 4-pyridyl compound **313f**, however, was achieved with a lower isolated yield, possibly due to interactions between the pyridine moiety and the silica column that resulted in streaking of the product. The *tert*-butyl deprotections to give compounds **292a-g** proceeded with moderate yields (27-64%).

Compound	R	% isolated yield of 313	% isolated yield of 292
292a	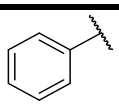	99	46
292b	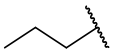	72	59
292c	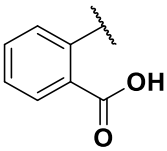	95	27
292d	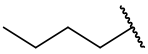	72	54
292e	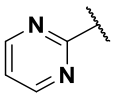	73	39
292f	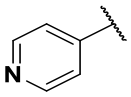	33	36
292g	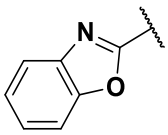	99	64

Table 4-2 | Synthesis of the first series of 3-sulfido-2-OG compounds.

4.5.5 IDH1^{132H} activity screen for the first series of compounds

The first series of compounds **292a-g** were screened for inhibitory activity against IDH1^{R132H}. The compounds were initially screened at fixed concentrations (10 mM) as a first pass to test for inhibitory activity (**Figure 4-18**). At 10 mM, compounds **292b-d** showed no inhibitory activity, while compounds **292a** and **292g** showed some inhibition of IDH1^{R132H} (76% and 28%, respectively). Compounds **292e** and

292f appeared to absorb UV light at 340 nm (the wavelength used to monitor the consumption of NADPH), resulting in errant data at high concentrations. Compounds **292b-d** showed no inhibition at 10 mM, so their inhibitory activity was not evaluated at lower concentrations.

The compounds that showed inhibition at 10 mM were screened for inhibition at 1 mM, 100 μM, 10 μM, and 1 μM (**Table 4-3**). At 1 mM, **292a** showed roughly the same level of inhibition compared to its activity at 10 mM, however the inhibitory activity of **292a** decreased significantly at 100 μM. Compound **292g** showed negligible inhibition at concentrations below 10 mM. Compounds **292e** and **292f** continued to show assay interference at 1 mM and 100 μM, but accurate measurements could be taken at 10 μM. At 10 μM, **292e** and **292f** showed 12% and 32% inhibition, respectively. The inhibitory activity of compounds **292e** and **292f**.

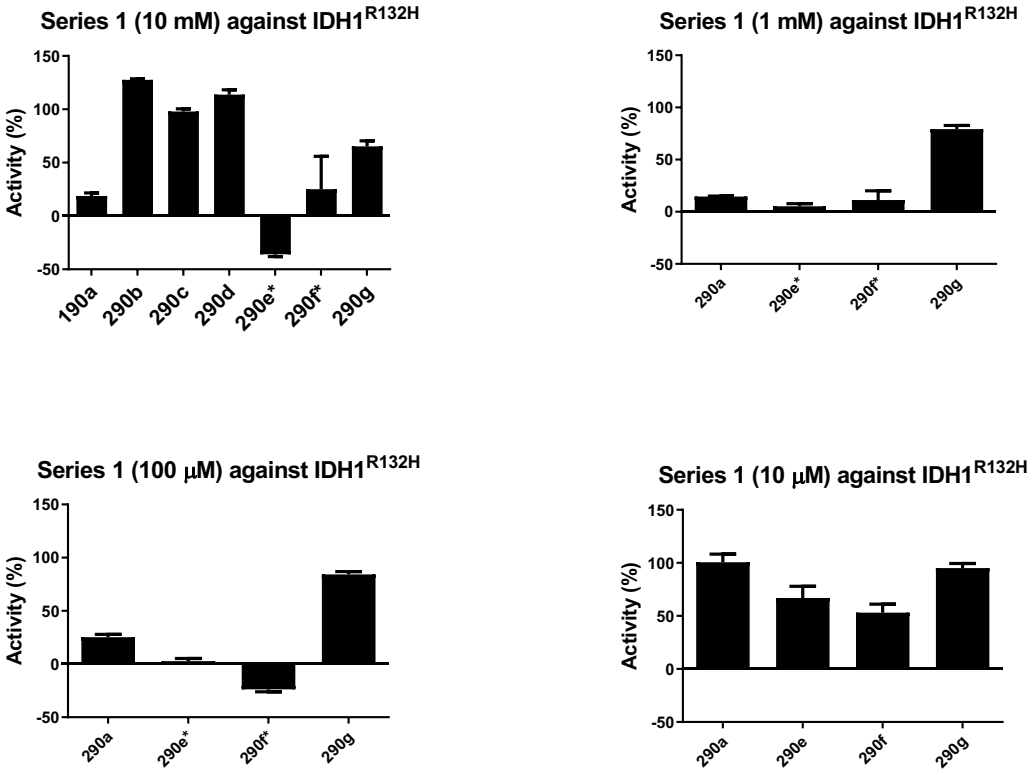

Figure 4-18 | Activity screen of series 1 compounds against IDH1^{R132H} variants. (*) indicates the absorbance values were skewed by the presence of the inhibitor. Data are normalised to a no-inhibitor positive control (100%) and a no-enzyme negative control (0%), and were measured in triplicate; error bars represent the standard error of the mean. Experiments run by *Raphael Reinbold*.

The inhibitory activity against IDH1^{R132H} of this initial series of 3-mercaptomethyl 2-OG compounds generated a general structure-activity relationship for the effect of the sidechain on the inhibition of IDH^{R132H}. The key findings are that none of the *S*-alkyl derivatives showed inhibitory activity against IDH1^{R132H}, while *S*-aryl derivatives possessed varying levels of inhibitory activity against IDH1^{R132H}. Compounds with heteroaryl rings also out-performed the unsubstituted phenyl ring of compound **292a**. The higher IDH1 inhibition of the heteroaryl derivatives might be due to their similarity to the nicotinamide ring of NADPH. Monocyclic

moieties also appeared to perform better than the bicyclic ring of compound **292g**, possibly because of poor compatibility with the active site of IDH1. Curiously, compound **292b** did not show inhibition of IDH1. **292b** differs structurally from **292a** by an *ortho*-carboxylic acid suggesting that the *ortho*-substitution is not tolerated by the $IDH1^{R132H}$ mutant.

Compound	R	% activity at 10 mM	% activity at 1 mM	% activity at 100 μM	% activity at 10 μM
292a	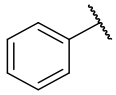	24	15	> 100	> 100
292b	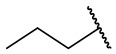	128	nt	nt	nt
292c	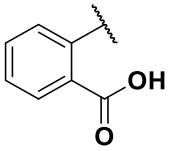	96	nt	nt	nt
292d	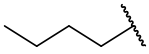	107	nt	nt	nt
292e	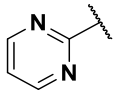	-	-	-	89
292f	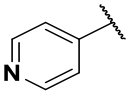	-	-	-	52
292g	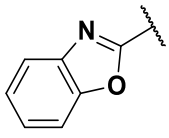	72	79	86	98

Table 4-3 | Activity of the first series of compounds against IDH^{R132H} variant. *nt* = not tested.

4.5.6 Synthesis of the second series of 3-sulfido-2-oxoglutarate analogues

From the first series of compounds, compounds with *N*-heteroaryl sidechains appeared to exhibit the highest potency. Building on the $IDH1^{R132H}$ inhibition data from the first series of, the R-groups in this series exclusively featured *N*-heteroaryl rings (**Table 4-4**). The synthesis of the second series of 3-mercaptomethyl 2-OG analogues **292h-l** was then carried out using the same general procedure as for the first series of compounds.

Compounds **313h-j** were synthesised in moderate to excellent yields. For compounds **313k** and **313l**, the solubility of the thiols was poor in CH_2Cl_2 and no conversion of the Michael acceptor was observed. The reactions were repeated in DMF in an attempt to improve the solubility of the thiols, however no product was observed for these reactions either. The *tert*-butyl deprotection of **313h-j** proceeded with moderate yields (34-60%).

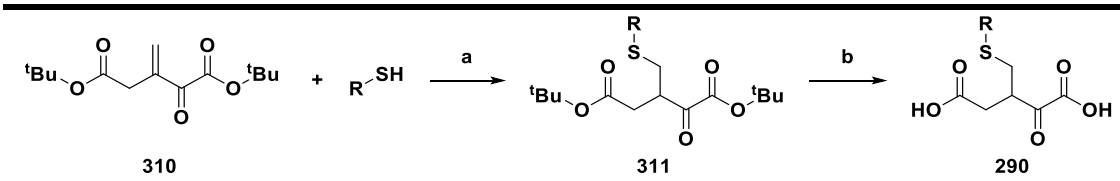

310 311 290

Compound	R	% isolated yield of 313	% isolated yield of 292
292h	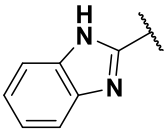	30	43
292i	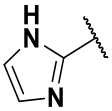	94	60
292j	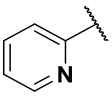	75	34
292k	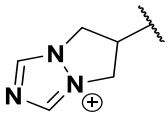	0	n/a
292l	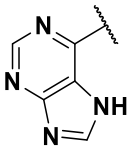	0	n/a

Table 4-4 | Synthesis of *N*-containing *S*-heteroaryl 2-OG analogues. Reagents and conditions: (**a**) Et_3N (cat.), CH_2Cl_2; (**b**) TFA, CH_2Cl_2.

4.5.7 Activity of the second series of 3-sulfido-2-OG analogues

The *N*-heteroaryl-3-sulfido-2-OG analogues **292h-l** from the second series were screened for inhibitory activity against $IDH1^{R132H}$ (**Figure 4-19**). Like the first series compounds **292e** and **292f**, inhibitors in the second series also appeared to exhibit some interference with the absorbance-based assay at concentrations above 100 μM.

At 100 μM, compounds **292h** and **292i** showed no inhibitory activity, while compound **292j** showed roughly 50% inhibition. Given the relative structural similarity of the second series compounds to the hits identified in the series 1 screen (**292e** and **292f**), it is perhaps surprising that the second series of compounds do not show stronger inhibitory activity against $IDH1^{R132H}$. The active site of $IDH1^{R132H}$ thus appears to be sensitive to small changes in the structure of the 3-sulfido sidechain. This is shown clearly in the comparison between **292f** and **292j**, which differ only by the position of the pyridine nitrogen. Moving the nitrogen from the *para*-position of **292f** to the *ortho*-position of **292j** resulted in a roughly six-fold decrease in enzyme inhibition (activity at 100 μM: **292f** ~7.56, **292j** ~45.1). In a similar comparison, **292e** and **292h** both possess aromatic heterocycles containing two nitrogen atoms, however, the sidechain of **292e** is a six-membered pyrazine ring, while **292h** is a 5-membered imidazole. The contraction of the sidechain ring by a carbon atom resulted in a roughly 30-fold decrease in activity (activity at 100 μM: **292e** ~33.8; **292h** ~93.1).

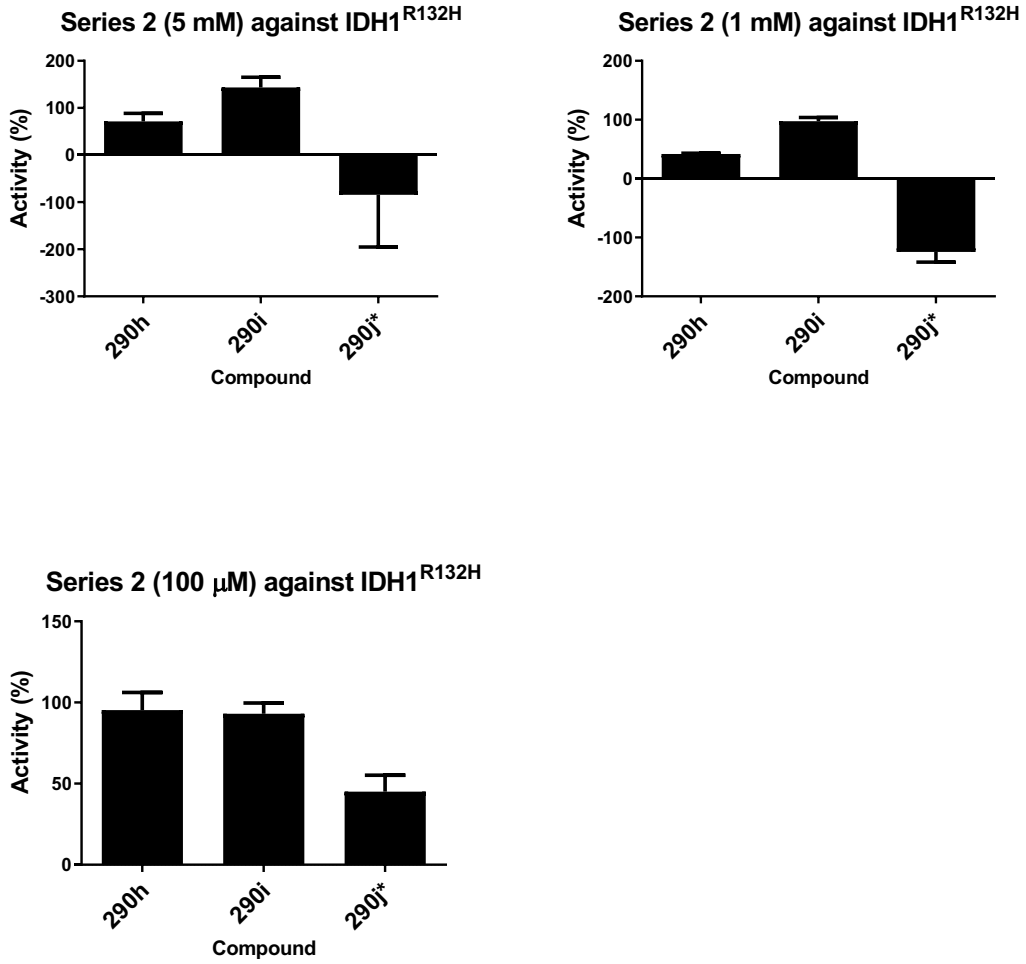

Figure 4-19 | Inhibitory activity of compounds from the second series against IDH1^{R132H}. Data are normalised to a no-inhibitor positive control (100%) and a no-enzyme negative control (0%), and were measured in triplicate; error bars represent the standard error of the mean. Experiments run by *Raphael Reinbold*.

4.5.8 Synthesis of a third series of 3-sulfido-2-OG analogues

A third series of 3-mercaptomethyl 2-OG analogues was synthesised as potential inhibitors of IDH1^{R132H} using the general procedure described above (**Figure 4-16**). The structures of compounds in this series consist of substituted phenyl rings with varying steric and electronic characteristics to further probe the SAR of the

sidechain for inhibition of $IDH1^{R132H}$ (**Table 4-5**). Compounds **313n**, **313o**, **313q-s** were synthesised in moderate to good yields (52-81%). With the exception of **313s**, the deprotections of these compounds proceeded with moderate to excellent yields (52-91%). As expected, the acid-labile trityl group was cleaved under the strongly acidic TFA deprotection conditions but attempts to purify the free thiol were unsuccessful. In the reaction of Michael acceptor **312** with pentafluorothiophenol to form **313p**, conversion of the Michael acceptor was observed, however no product could be isolated following column chromatography. It is plausible that the highly electron-withdrawing character of the pentofluorophenyl group facilitated a retro-Michael reaction to eliminate the thiol during purification.

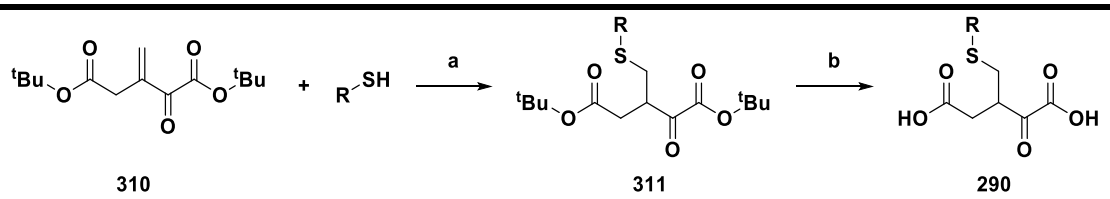

Compound	R	% isolated yield of 313	% isolated yield of 292
292m	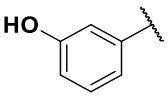	0	n/a
292n	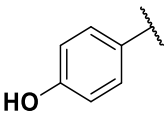	81	52
292o	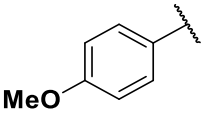	74	54
292p	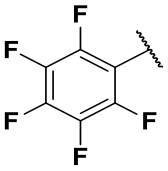	0	n/a
292q	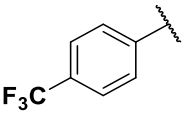	52	92
292r	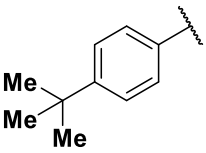	69	64
292s	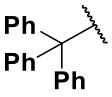	80	0

Table 4-5 | Synthesis of the third series of 3-sulfido-2-OG analogues. Reagents and conditions: (**a**) Et_3N (cat.), CH_2Cl_2; (**b**) TFA, CH_2Cl_2.

The reaction of Michael acceptor **312** with 3-hydroxythiophenol did not form the expected Michael product **313m**. Instead, **313m** appeared to undergo an intramolecular cyclisation to give the bicyclic compound **314** (**Figure 4-20**). As hydroxy and sulfide groups are both electron donating, the aromatic ring is more electron rich and nucleophilic as a result. And as electron-donating groups are *ortho*/*para*-directing the S_EAr cyclised product is only observed for analogues where the electron donating groups are *meta* to the sulfide (as they are then *ortho* to the 2-position of the aryl ring).

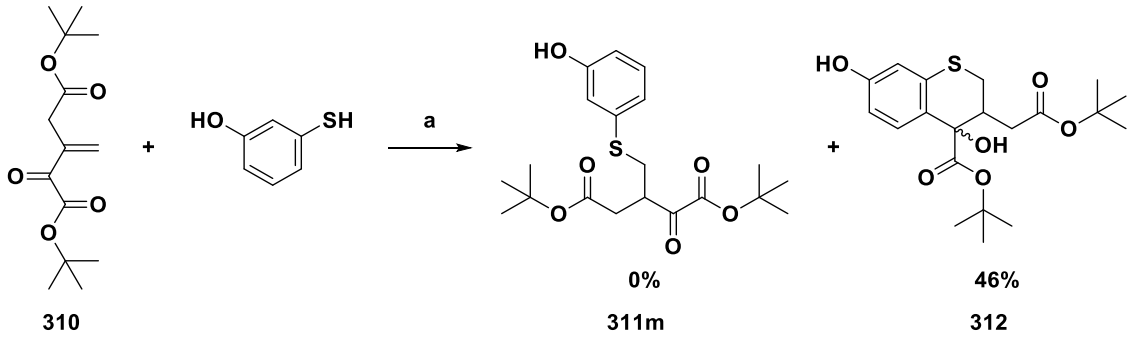

Figure 4-20 | Reaction of 3-hydroxythiophenol with Michael acceptor **312**. Reagents and conditions: (**a**) Et_3N (cat.), CH_2Cl_2, rt, 5 h.

Evidence for the formation of **314** can be found in the ^1H spectra of the product (**Figure 4-21**). The aromatic region shows three peaks corresponding to the protons at the 2, 4, and 5 positions, but no peak for the proton at position 6 was observed. The multiplicity of the peaks is consistent with a 1,3,6-trisubstituted benzene ring: position 2 is a doublet with a coupling constant in the range expected for 3*J* couplings (*J* = 2.6 Hz); position 4 is a doublet of doublets (*J* = 8.6, 2.6 Hz) with coupling constants in the range expected for a 2*J* and 3*J* coupling, respectively;

position 5 is a doublet with a 2*J* coupling constant (*J* = 8.6 Hz). The ^{1}H spectrum also shows an additional broad singlet that does not couple to a carbon in HSQC, consistent with the presence of a tertiary alcohol. Additionally, the ^{13}C spectra shows the disappearance of the ketone carbonyl peak, which usually resides around 194 ppm for compounds in this series, and the appearance of a peak at 75 ppm consistent with a tertiary alcohol.

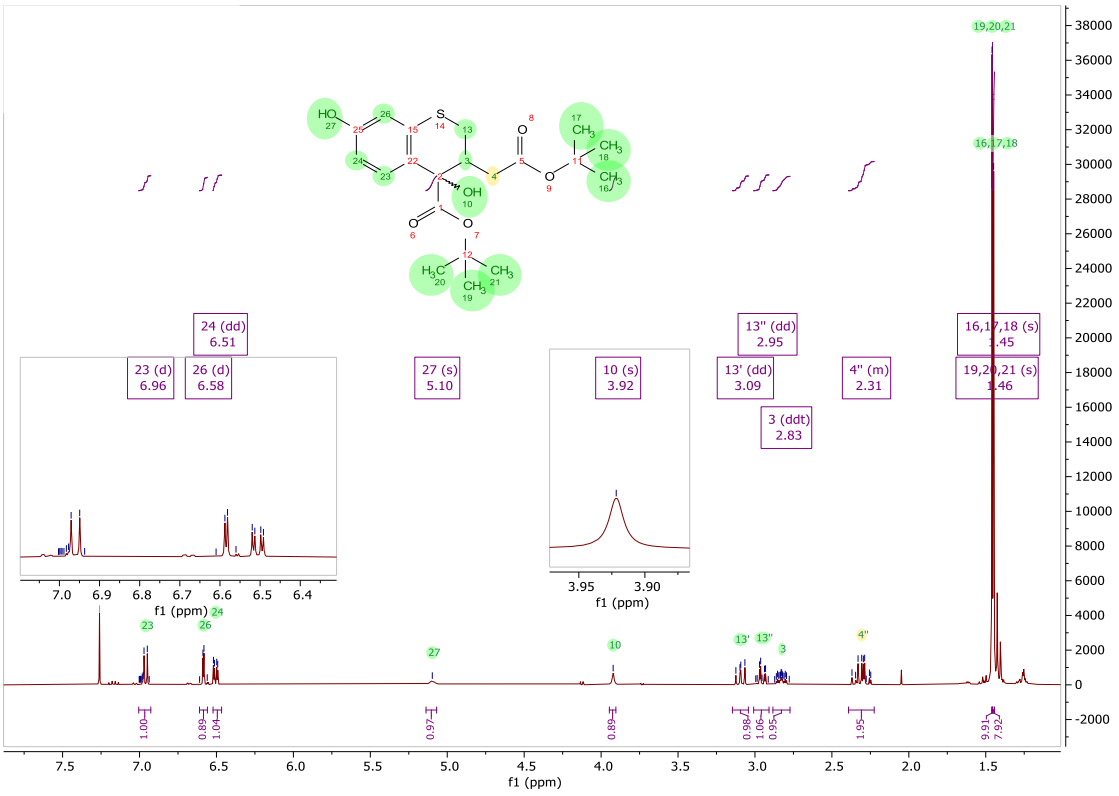

Figure 4-21 | ^{1}H NMR (400 MHz) spectrum of the cyclised product **314**.

4.5.9 Series 3 activity

The inhibitory activity against IDH1^{R132H} was evaluated for the series 3 compounds (**Figure 4-22**). These compounds showed poor inhibitory activity against IDH1^{R132H}.

Compounds **292n** and **292r** showed roughly 50% inhibition at 1 mM. Compounds **292o** and **292q** seemed to show interference with the assay.

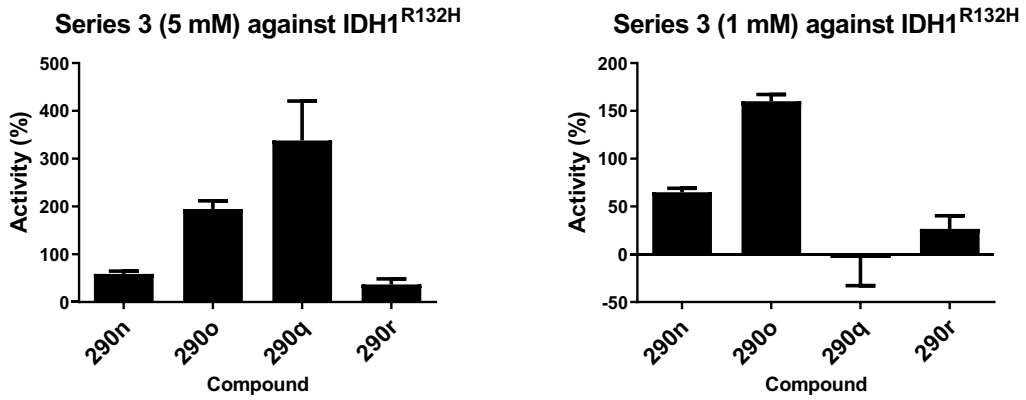

Figure 4-22 | Inhibitory activity of third-series compounds against IDH1^{R132H}. Data are normalised to a no-inhibitor positive control (100%) and a no-enzyme negative control (0%), and were measured in triplicate; error bars represent the standard error of the mean. Experiments run by *Raphael Reinbold*.

4.5.10 Determination of IC_{50}s for hit compounds against IDH1^{R132H}

From these three series of 3-sulfido-2-OG analogues, compounds **292e** and **292f** showed the greatest inhibition. The IC_{50}s of **292e** and **292f** was determined by the same absorbance-based assay (**Figure 4-23**). While the IC_{50}s for **292e** and **292f** are approximately 100- to 500-fold higher than the most potent reported allosteric inhibitors that bind at the dimer interface, the fact that they appear to bind to the active site sets them apart from dimer-face inhibitors.[258, 259, 264] Additionally, there is likely scope to augment the inhibitory activity of 3-sulfido-functionlaised 2-OG inhibitors. Further modifications to improve the inhibitory activity of these compounds could include the attachment of additional functionality to the pyridine

ring to mimic the structure of NADPH more closely. Additionally, the use of an enantioselective Michael addition to synthesise single enantiomers might also improve the activity of single enantiomers over the racemic mixture of compounds.

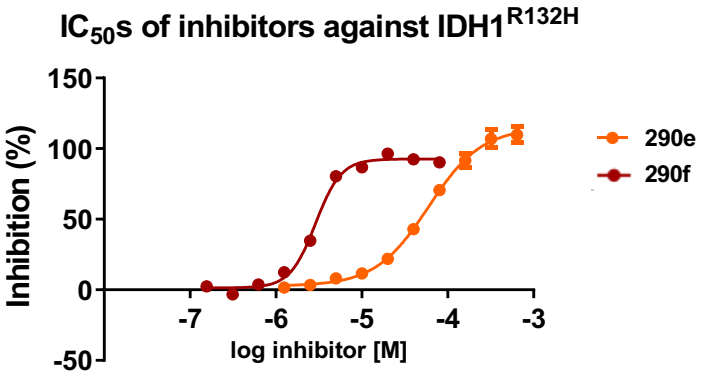

Figure 4-23 | IC_{50} curves for **292e** and **292f** against $IDH1^{R132H}$. Data are normalised to a no-inhibitor positive control (100%) and a no-enzyme negative control (0%), and were measured in triplicate; error bars represent the standard error of the mean. Experiments run by *Raphael Reinbold*.

Cpd	R	$IDH1^{R132H}$ IC_{50} (μM)
292e	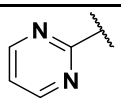	59.75
292f	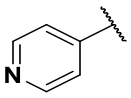	2.89

Figure 4-24 | Calculated IC_{50} values for **292e** and **292f** against $IDH1^{R132H}$

4.5.11 Evaluation of modified 2-OG analogues as IDH1 alternative substrates

To investigate whether 3-sulfido-2-OG analogues could act as alternative substrates for IDH1^{R132H}, an NADPH/NADP$^+$ assay was conducted using only the modified **2-OG** analogue as the substrate instead of **2-OG**. The conversion of NADPH/NADP$^+$ in the presence of the **2-OG** analogue would indicate that the enzyme accepts the **2-OG** analogue as a substrate (**Figure 4-25**).

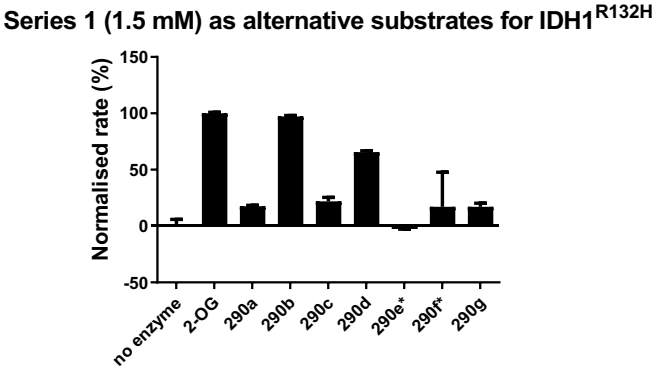

Figure 4-25 | Activity of compounds from the first series as alternative substrates of IDH1^{R132H}. Data are normalised to a no-inhibitor positive control (100%) and a no-enzyme negative control (0%), and were measured in triplicate; error bars represent the standard error of the mean. Experiments run by *Raphael Reinbold*.

These results imply a general trend that compounds with aromatic R-groups (**292a**,**c**,**e**-**g**), which showed varying degrees of inhibition, do not act as substrates of IDH1 in the presence of NADPH. These results also imply that compounds with aliphatic R-groups (**292b** and **292d**) can act as alternative substrates of IDH1^{R132H}. In particular, the *S*-propyl-functionalised compound **292b** showed comparable rates

of reaction to **2-OG** itself. The *S*-butyl-functionalised compound **292d** also acted as an alternative substrate, though not as effectively as compound **292b**. As before, the *N*-heteroaryl compounds **292e** and **292f** caused interference with the absorbance assay at the high concentrations used for the turnover conditions.

4.5.12Synthesis of an aliphatic series of 3-sulfido-2-OGs as alternative substrates

Building on the alternative substrate assay results for compounds from the first series, a new series of **2-OG** analogues functionalised with aliphatic sidechains was synthesised in poor to fair yields (26-74%) (**Table 4-6**).

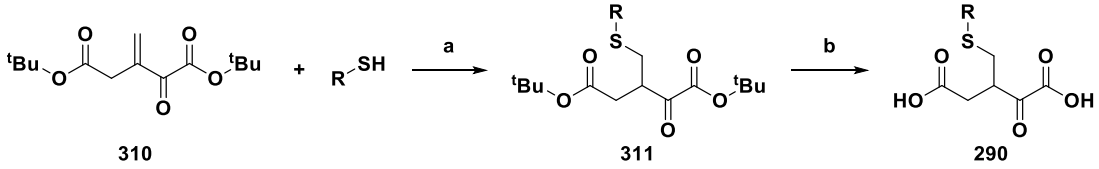

Compound	R	% isolated yield of 313	% isolated yield of 292
292t	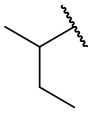	58	63
292u	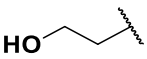	53	43
292v		26	74
292w		60	69

292x	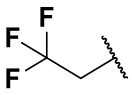	42	44

Table 4-6 | Synthesis of aliphatic 2-OG analogues. Reagents and conditions: (**a**) Et_3N (cat.), CH_2Cl_2; (**b**) TFA, CH_2Cl_2.

4.5.13 Activity of the aliphatic series as alternative substrates for IDH1

The activity data for the aliphatic series as a substrate of $IDH1^{R132H}$ are shown in **Figure 4-26**. Compounds **292t**, **292v** and **292w** exhibited roughly 50% of the activity exhibited by the natural substrate **2-OG**, while compounds **292u** and **292x** were roughly a third as active as **2-OG**. These results imply that these compounds can act as alternative substrates for $IDH1^{R132H}$, though they are not as effective as **292b** and **292d** from the first series of compounds.

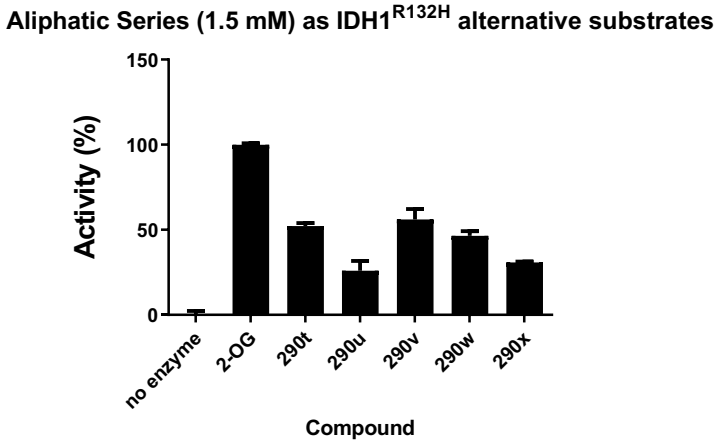

Figure 4-26 | Activity of aliphatic series compounds as $IDH1^{R132H}$ alternative substrates. Data are normalised to a no-inhibitor positive control (100%) and a no-enzyme negative control (0%), and were measured in triplicate; error bars represent the standard error of the mean. Experiments run by *Raphael Reinbold*.

4.5.14 Counter screen of inhibitors as alternative substrates

Selected aromatic compounds from the second and third series that showed inhibitory activity against IDH1^{R132H} were screened for activity as alternative substrates (**Figure 4-27**).

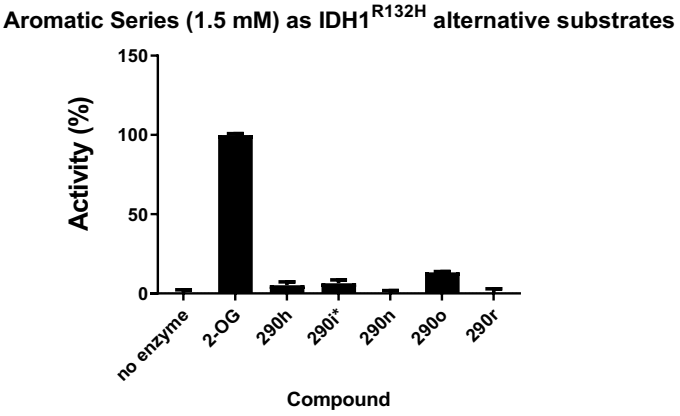

Figure 4-27 | Alternative substrate turnover assay for aromatic 2-OG analogues. Data were measured in triplicate; error bars represent the standard error of the mean. Experiments run by *Raphael Reinbold*.

Compounds **292r** and **292n** showed no evidence for turnover, while compounds **292h**, **292i**, and **292o** showed some turnover. These data support the hypothesis that modified **2-OG**s either inhibit IDH1^{R132H} or are turned over by IDH1^{R132H} as alternative substrates.

4.5.15 Inhibitory activity of the aliphatic series

The modified **2-OG**s with aliphatic sidechains that acted as IDH1^{R132H} alternative substrates were counter-screened for inhibitory activity (**Figure 4-28**).

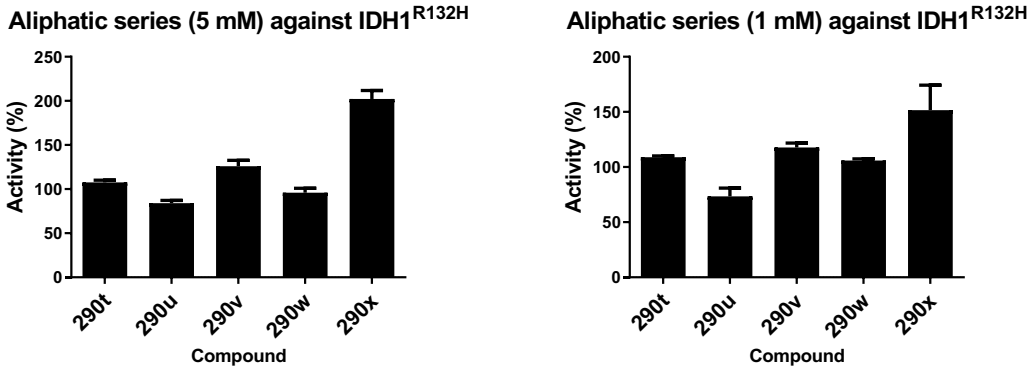

Figure 4-28 | Inhibitory activities against IDH1^{R132H} for 3-mercaptomethyl 2-OGs bearing aliphatic R-groups. Experiments run by *Raphael Reinbold*.

From these compounds, only **292u** showed slight inhibitory activity. It is plausible that the hydroxyethyl sidechain of **292u** could interact via hydrogen bonding with active-site residues. These additional binding interactions might increase the affinity of **292u** for the IDH1^{R132H} active site, resulting in slight inhibition compared to analogous compounds such as **292b** that possess hydrocarbon sidechains. These data also seem to show that **292x** acts as an enhancer of IDH1^{R132H} at high concentrations.

4.5.16 Counter screen against *wt* IDH1

A key parameter of IDH1^{R132} inhibitors for the treatment of cancer is that the inhibitors demonstrate high selectivity for the IDH1^{R132} variants over *wt* IDH1, as

inhibition of *wt* IDH1 would have serious off-target side effects that would negate any therapeutic benefit from the inhibition of tumour cells expressing IDH1^{R132} variants. Thus, the library of synthesised 3-sulfido-2-OG analogues was screened for inhibitory activity against *wt* IDH1 (**Figure 4-29**).

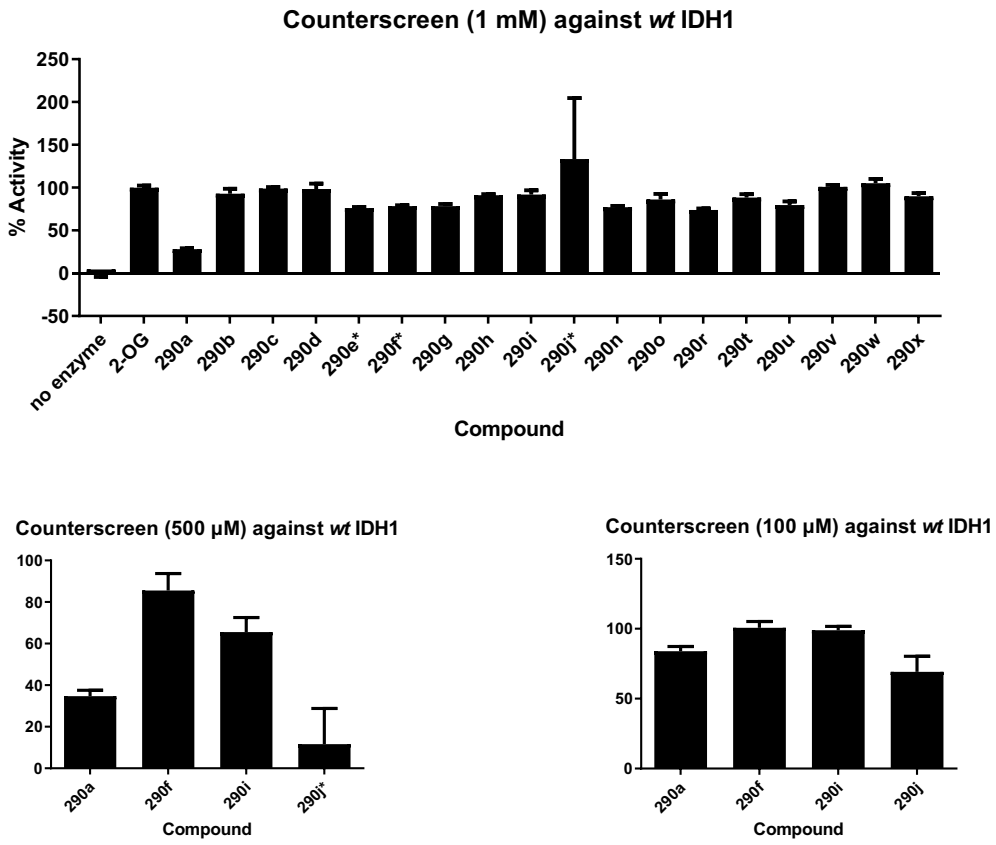

Figure 4-29 | Counter screen of 3-sulfido-2-OG analogues against *wt*IDH1. Data are normalised to a no-inhibitor positive control (100%) and a no-enzyme negative control (0%), and were measured in triplicate; error bars represent the standard error of the mean. Experiments run by *Raphael Reinbold*.

These results imply that all but one of the modified **2-OG** analogues do not inhibit *wt*IDH1. Interestingly, some inhibition was observed for the *S*-phenyl-substituted compound **292a** (roughly 65% inhibition at 500 µM). Crucially, the hit compounds

292e and **292f** did not inhibit *wt* IDH1, confirming that competitive inhibitors of $IDH1^{R132H}$ that mimic the structure of **2-OG** can be developed with high selectivity for the mutant enzyme over the wild type. Conceptually, this result is consistent with the substrate affinities of the two enzymes. **2-OG** is the product of the *wt* IDH1 enzymatic reaction and the affinity of *wt*IDH1 is low. However, as discussed above, R132 variants of IDH1 catalyse the reduction of **2-OG** to **2-HG**. Thus, **2-OG** is a substrate of $IDH1^{R132}$ variants, which have a higher affinity for **2-OG** compared to the *wt* IDH1. Thus, it is therefore possible that modified **2-OG** compounds may exhibit selective inhibition of $IDH1^{R132}$ variants.

4.5.17Stability studies on 292f and 292d

During spectroscopic characterisation of **292f** by NMR, it was observed to decompose in solution over time, possibly by a retro-Michael-type reaction. An NMR time course experiment was conducted to evaluate the stability of **292f** (**Figure 4-30**). The time course shows that peaks corresponding to the olefin of the retro-Michael product **315**, which has not been previously described, can be detected after ten minutes, and that, after 24 h, nearly all of the **292f** species had decomposed. For comparison, an NMR time course experiment was performed on the *S*-butyl analogue **292d** (**Figure 4-31**). The results for the time course experiment show that **292d** is relatively stable under the experimental conditions, with the olefin peaks corresponding to retro-Michael product **315** only being detected after 2 h. The stability of **292d** over **292f** may be explained by the pK_a values of their

respective thiols; the pyridylthiol moiety should have a lower pK_a compared to the *S*-butylthiol moiety due to the electron-withdrawing nature of the pyridine ring, which has the effect of facilitating the retro-Michael reaction.

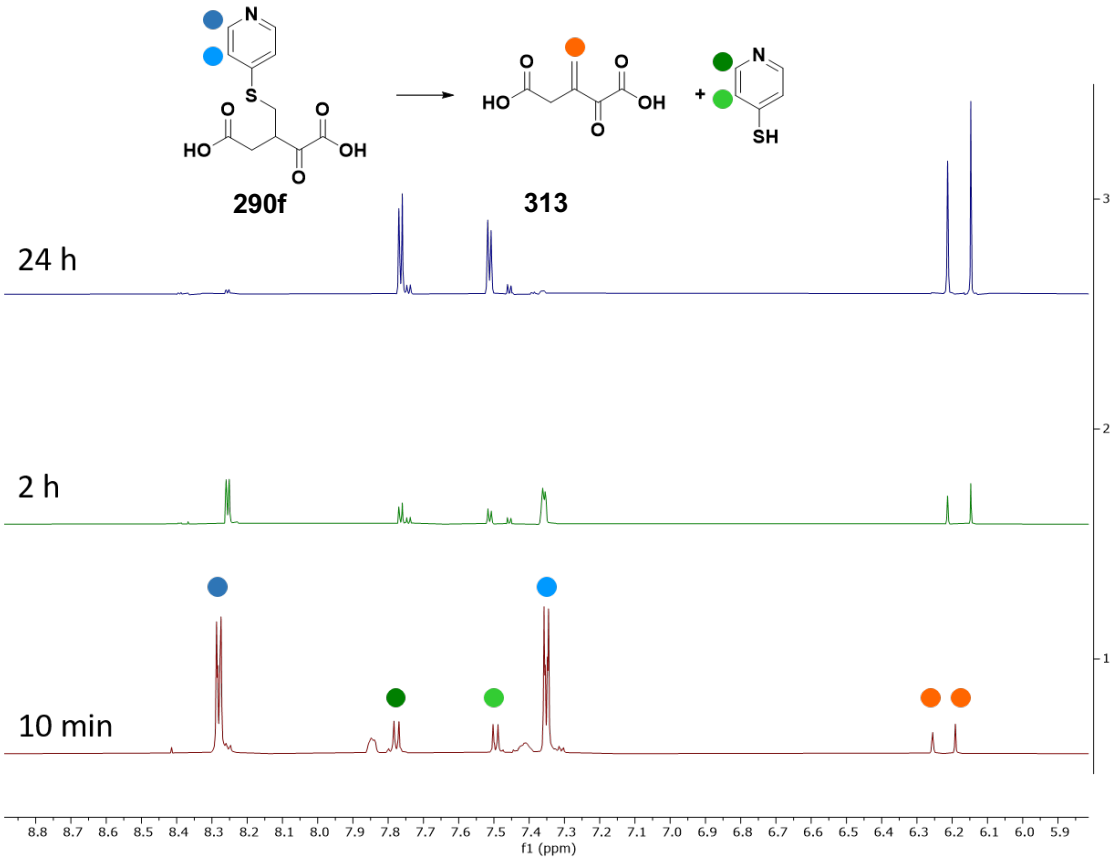

Figure 4-30 | ^{1}H NMR (500 MHz, 10% D_2O in pH 7.4 phosphate buffer) time course of **292f**.

The observation that **292f** is unstable in the assay buffer raised questions about whether its potency was derived from either the retro-Michael product **315** or the eliminated thiol. However, it seems likely that the sulfide **292f** is the main inhibitory species. Firstly, the fact that **292f** does not inhibit *wt* IDH1 suggests that inhibition is not due to the complexation of the thiol to the metal ion, as if it were, both enzymes would likely be inhibited. Secondly, the incubation time for the inhibition

assay is only twelve minutes. While some of the retro-Michael product **315** likely forms in this time, it is likely that its concentration is much less than **292f**. In addition, the incubation time allows for **292f** to bind to the protein, which may act to stabilise **292f** to the retro-Michael reaction pathway. To further investigate the interaction of **290f** with IDH variants, future experiments should include inhibition assays run after longer inhibition times, as well as isolating and evaluating the inhibitory activity of the proposed retro-Michael elimination product **315**.

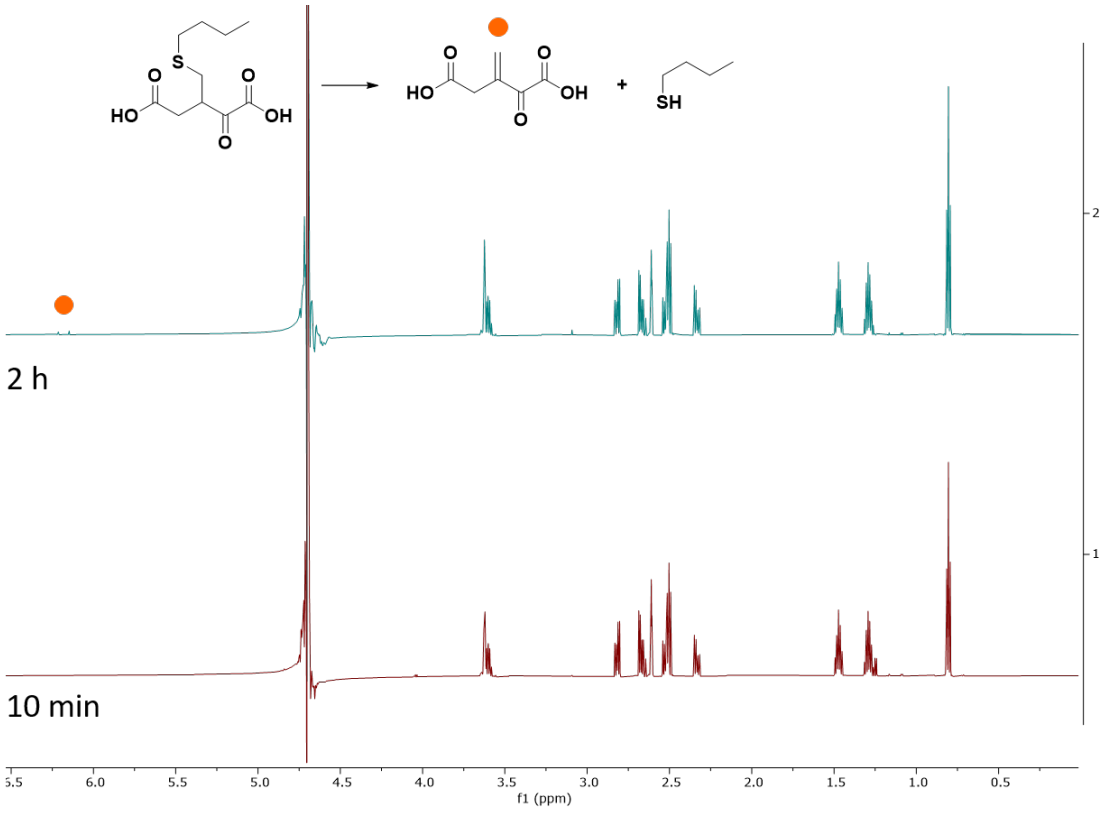

Figure 4-31 | ^{1}H NMR (500 MHz, 10% D_2O in pH 7.4 phosphate buffer) time course of **292d**.

4.5.18 Development of conditions for C-C couplings

The α,β-unsaturated keto-ester moiety of the Michael acceptor **312** is a versatile handle for the functionalisation of the **2-OG** core. As discussed above, these Michael acceptors readily undergo sulfa-Michael additions with thiols to give 3-sulfido-modified **2-OG** analogues. However, some of these compounds underwent retro-Michael eliminations. A different linker that enables diverse functionalisation of the 3-position, but with greater stability than a sulfide linker, is desirable.

Rhodium(I)-catalysed conjugate additions of boronic acids is an appealing methodology to install functionality via a C-C bond. Unlike Grignard reagents, which tend to react via 1,2-addition into the carbonyl of Michael acceptors rather than via the desired 1,4-addition, the Rh(I) catalysed conjugate additions favour addition to the alkene.[269] The Rh(I) catalyst also provides a mechanism for introducing stereocontrol of the Michael addition by using chiral ligands. However, achiral ligands were used for the validation of the chemistry. Thus, a brief investigation of Rh(I)-catalysed Michael additions onto the **2-OG** alkene **312** was conducted.

4.5.19 Synthesis and validation of the Rh(I) catalyst

The $[Rh(COD)Cl]_2$ dimer **316** was prepared by a reported procedure,[270] via the reaction of $RhCl_3 \bullet xH_2O$ with 1,5-cyclooctadiene in ethanol/H_2O under reflux. The activity of **316** was validated by reacting phenylboronic acid (**317**) with cyclohexen-

3-one (**318**) to give the arylcyclohexanone **319** following a reported procedure (**Figure 4-32**).

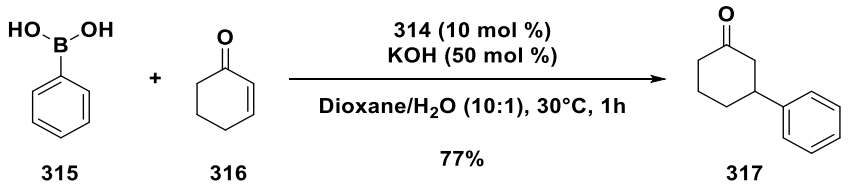

Figure 4-32 | Validation of the catalytic activity of the $[Rh(COD)Cl]_2$ dimer **316** for conjugate additions.

With the activity of the **316** validated, investigations into Rh(I)-catalysed conjugate additions onto **2-OG** analogues were undertaken.

4.5.20Reaction optimisation for the 2-OG Michael acceptor

A brief conditions screen was conducted to identify optimal conditions for the conjugate addition of **317** onto the Michael acceptor **312** to form the desired product **320** (**Table 4-7**). Initial attempts to form **320** by conjugate addition were based on reported conditions.[271] These conditions utilised half an equivalent of potassium hydroxide and a 10:1 (*v*/*v*) ratio of dioxane to H_2O, per the reported conditions. The initial condition (**Table 4-7**, entry 1) resulted in no conversion of the starting materials. Increasing the temperature to 80 °C resulted in significant consumption of the **317** (possibly by deborylation), but no formation of the expected product. The catalyst loading was decreased, which reduced the decomposition of the **317**, however none of the expected product **320** was observed under these conditions either.

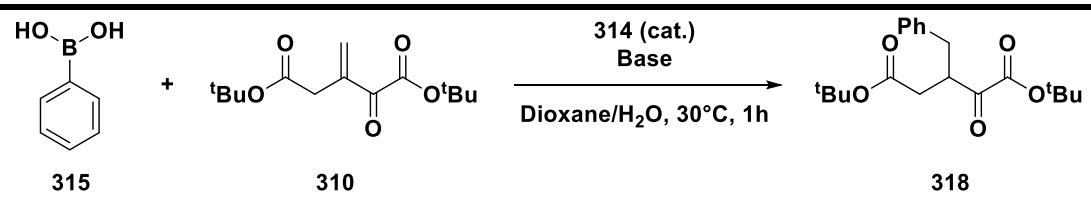

Entry	Base (eq.)	Solvent	Catalyst loading (mol %)	T (°C)	% Isolated yield
1	KOH (0.5)	Dioxane/H_2O (10:1)	10	30	0
2	KOH (0.5)	Dioxane/H_2O (6:1)	10	80	0
3	KOH (0.5)	Dioxane/H_2O (6:1)	2.5	80	0
4	Et_3N (1)	Dioxane/H_2O (6:1)	2.5	30	81

Table 4-7 | Condition screen for Rh(I)-catalysed conjugate additions onto **312**.

Significant improvements in the isolated yield of **320** occurred after changing the base from potassium hydroxide to triethylamine, resulting in a clean conversion of the starting materials to the desired product. Triethylamine is a weaker and less nucleophilic base compared to potassium hydroxide, which may reduce unwanted side reaction of the Michael acceptor with hydroxide ions.

The establishment of reaction conditions for the conjugate addition of aryl boronates onto the Michael acceptor **312** will allow for further exploration of the chemical space surrounding the **2-OG** core. Due to time constraints the synthesis of a library of conjugate-addition-functionalised **2-OG**s was not undertaken, however it is an important area for future work. Further development of this chemistry should also include an investigation into asymmetric Michael additions using chiral BINAP ligands, as described by Hayashi *et al*.[271]. Although, the diastereoselectivity of these methods is predicted to be low due to the propensity for the keto-ester to tautomerise at the *C*-3 position.

4.6 Summary

The work described in this Chapter aimed to develop and improve methods for functionalising **2-OG** as a synthetic precursor for the synthesis of lactivicins and as novel **2-OG**-dependent dioxygenase inhibitors. Improvements were made to the synthesis of key intermediates for the 4-amino-γ-lactone lactivicin derivatives initially pioneered by Star *et al*;[167] the use of a sulfur ylide in place of a phosphonium ylide for the synthesis of α-keto ester **298** enabled milder oxidative cleavage using Oxone®.

The Michael acceptor **284** was reacted with thiophenol to generate a 3-sulfido-2-OG ester for the synthesis of *C*-3-functionalised lactivicins. However, none of the

expected lactone product **307** was formed. It is plausible that the additional steric bulk of the *C*-3 functionalisation disfavours the cyclisation step in the lactonisation reaction. Thus, lactivicin analogues with functionalisation at the *C*-3 position cannot be (at least readily) accessed via this synthetic route, and other alternatives need development.

The methodology to functionalise **2-OG** with sulfides at the *C*-3 position was used for the synthesis of a library of **2-OG** analogues **292**. This library of compounds could function as the starting point for the development of competitive active-site inhibitors for the many **2-OG** dependent enzymes. As a proof of concept, a series of *C*-3-functionalised **2-OG** analogues were synthesised and screened against $IDH1^{R132H}$. From these data, two general activity trends emerged: compounds bearing heteroaromatic sidechains generally inhibited $IDH1^{R132H}$, while compounds bearing aliphatic sidechains generally could act as alternative substrates to **2-OG**. In addition, the inhibitory compounds from this library showed selectivity for the mutant IDH1 over the *wt* variant.

Both the inhibitors and alternative substrates from this series have potential applications as tools to elucidate the structure and function of IDH1 variants. Inhibitors could enable competition assays with other small molecules while tagged alternative substrates could be developed as chemical probes,[272, 273] *in-vitro* biotin labelling,[274] or assay development.[275] The ease of synthesis would allow researchers to quickly optimise the scaffold to suit their scientific objectives.

Initial investigations were made into the conjugate addition of other nucleophiles into the Michael acceptor **312**. These studies demonstrated that the Rh(I)-catalysed addition of aryl boronates onto the Michael acceptor was possible, adding an additional method by which the Michael acceptor **312** can be functionalised. Future work on the development of enantioselective Michael additions/α-protonations of aryl boronates into **312** would be of value for the asymmetric synthesis of competitive inhibitors of **2-OG**-dependent oxygenases.

Chapter 5 Synthesis of benzisothiazolinone inhibitors of SARS-CoV-2 Main Protease

Forward

The synthesis described in this Chapter was conducted in tandem with Siegfried Thun-Hohenstein*, who was a Master's student under the author's laboratory supervision. Compounds prepared by* Siegfried Thun-Hohenstein *are denoted with an asterisk and a table of spectroscopic data for these compounds is included in the experimental section. The biological assays described in this Chapter were conducted either by* Siegfried Thun-Hohenstein, Tika R. Malla, *or* Dr. Anthony Tumber*, and are referenced appropriately in the text. M^{pro} was expressed and purified by* Eidarus Salah.

5.1 Introduction

The results from **Chapter 3** demonstrated the ability of the benzisothiazolinone-γ-lactone carboxylate **236b** to covalently inhibit Ldt enzymes via disulfide bond formation, indicating that the benzisothiazolinone (BIT) core could be used as a potent electrophilic warhead for the inhibition of other nucleophilic cysteine enzymes. In early 2020, when the Severe Acute Respiratory Syndrome Coronavirus 2 (SARS-CoV-2) virus emerged as a global threat to human health,[276] the attention of the Schofield Group turned towards the development of covalent inhibitors of SARS-CoV-2 Main Protease (M^{pro}), a crucial enzyme for viral replication. The

proposed mechanism of M^{pro} inhibition by some of these inhibitors was based in part on the mechanism of reaction of compound **236b** with Ldt_{mts} as discussed in Chapter **3**.

Ebselen (**203**) was identified by high-throughput screening as a potent covalent inhibitor of M^{pro}.[277] **203** is proposed to react with M^{pro} cysteines via covalent reaction of its Se-N bond to form a catalytically inactive thioselenide adduct (**Figure 5-1**).[277, 278] However, despite its reported high potency against M^{pro} (< 100 nM),[277] **203** has been shown by MS to react promiscuously with biological cysteines, raising concerns about potential off-target toxicity and prompting a search for alternative covalent inhibitors.[279-281] Due to the similarity between the reactions of **203** with cysteine-containing enzymes and the proposed reactivity of the BIT-γ-lactone carboxylate **236b** with Ldt_{mts}, it was proposed that 'ebsulfur'[282] compounds **321** containing the BIT core might exhibit milder and therefore more selective reactivity for M^{pro} active site cysteine. The work in this Chapter describes the development of ebsulfur-based covalent inhibitors of M^{pro}.

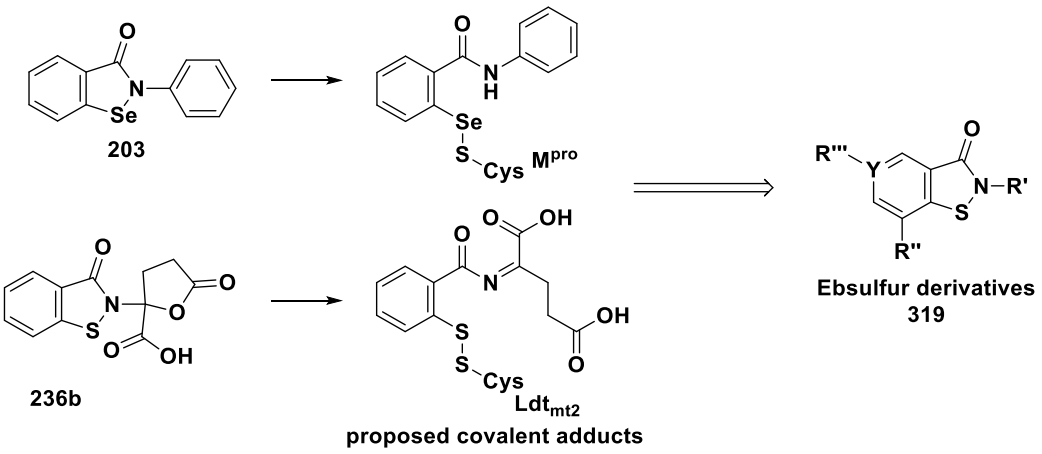

Figure 5-1 | Overview of the development of 'ebsulfur' M^{pro} inhibitors based on the structures and reactivity of **203** and compound **236b**.

5.1.1 Structure and function of the SARS-CoV-2 main protease

The genome of the SARS-CoV-2 virus consists of nearly 30,000 nucleotides that code for two overlapping polyproteins (pp1a and pp1b).[276] Post-translational proteolytic cleavage of the SARS-CoV-2 polyprotein produces the functional proteins needed for viral replication.[283] This proteolytic cleavage is catalysed by the 34 kDa 3*C*-like protease called M^{pro}, and the papaein-like protease called PL^{pro}. M^{pro} catalyses the proteolytic cleavage of the polyproteins at no less than 11 conserved sites, making it an attractive therapeutic target for the prevention of viral replication.[277]

The M^{pro} proteolysis reaction proceeds initially via the formation of a non-covalent enzyme-substrate complex. Then, a catalytic dyad consisting of His-41 and Cys-145 reacts covalently with the targeted amide bond to form a labile thioester, which is hydrolysed by a water molecule.[277, 284] The use of a nucleophilic cysteine in the active

site of M^{pro} provides an opportunity for covalent inhibition of M^{pro} by thiophilic electrophiles.

5.1.2 Reported inhibitors of the SARS-CoV-2 main protease

Early in the coronavirus (COVID-19) pandemic, a high-throughput inhibitor screen was conducted by Jin *et al*. to identify small molecule inhibitors of M^{pro}.[277] The screening identified six 'hit' compounds, consisting of clinically approved drugs (carmofur (**322**)[285] and disulfiram (**323**),[286] **Figure 5-2**) and pre-clinical candidates (ebselen (**203**),[287] shikonin (**324**),[288] tideglusib (**325**),[289] and PX-12 (**326**),[290] **Figure 5-2**).

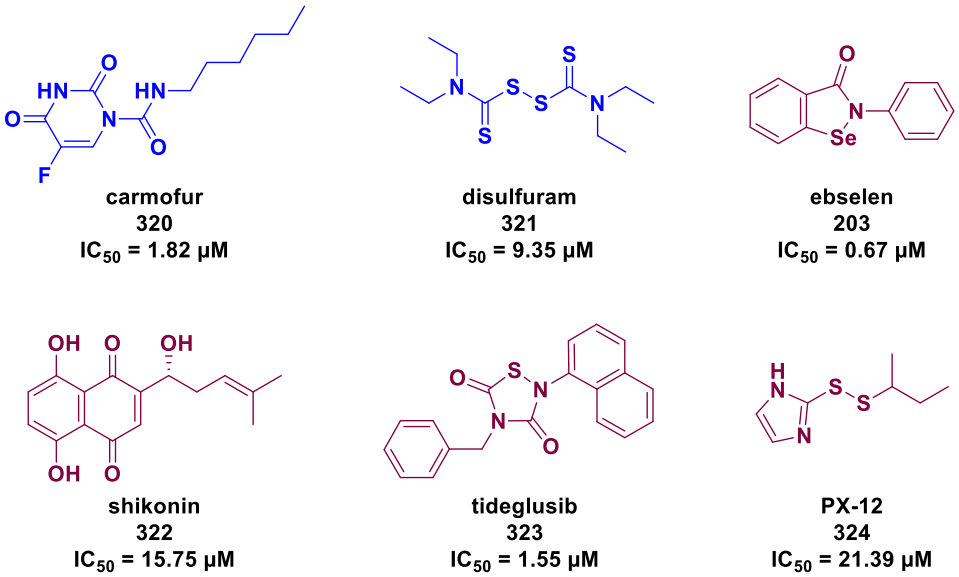

Figure 5-2 | Structures and IC$_{50}$s of clinical (blue) and preclinical (maroon) compounds identified by high-throughput screening as M^{pro} inhibitors.[277]

The high-throughput screen identified that the selenium-containing compound **203** was the most potent inhibitor. POMS experiments showed that **203** is a covalent

inhibitor of M^{pro} that reacts to form a stable covalent adduct with cysteine residues.[277]

As mentioned in **Section 1.6.11**, **203** is currently under investigation as a therapeutic agent for several conditions, where it appears to act as a scavenger of reactive oxygen species (ROS).[291] **203** is also able to react with cysteines to form a thioselenide bridge with the active site cysteines of the Ldt_{mt} enzymes, and it is proposed that the reaction of **203** with active site cysteines is the mechanism by which **203** inhibits M^{pro}.[193, 292] Indeed, **203** is now in clinical trials as a therapy against SARS-CoV-2 infections.[293] However, **203** exhibits cellular toxicity via several mechanisms; some of which stem from the presence of a selenium atom in the ring.[291] Though the IC_{50} of **203** for M^{pro} is low (~0.67 μM),[277] in-house experiments revealed that **203** reacts non-selectively with all twelve cysteines of M^{pro}.[278] These factors raise questions about the viability of **203** as a clinically useful therapy against SARS-CoV-2.

5.1.3 Mechanistic studies on the inhibition of M^{pro} by compound 203

Recent crystallographic studies into the mechanism of M^{pro} inhibition by **203** show that, under the reported conditions, **203** undergoes fragmentation following reaction with the catalytic cysteine that results in a free selenium atom bound to cysteine in the M^{pro} active site.[284]

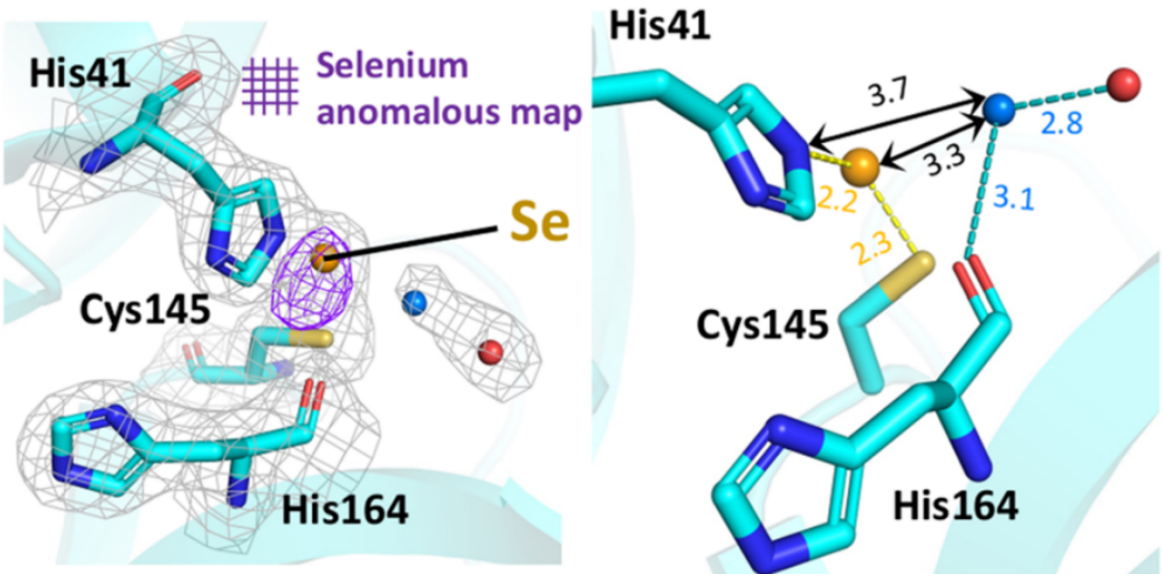

Figure 5-3 | View from a crystal structure of M^{pro} following reaction with **203**. Figure adapted from Amporndanai *et al.*[284] and used with permission under the terms of the Creative Commons CC BY license.

Amporndanai *et al.* proposed that the fragmentation mechanism proceeds via the S$_N$Ar-type reaction of a water molecule on the *C*-1 carbon, which displaces the selenium atom to give the observed selenium-functionalised M^{pro} and the benzamide **327** (**Figure 5-4**).[284] The identity of the benzamide **327** was confirmed by HPLC elution times as compared to a standard.

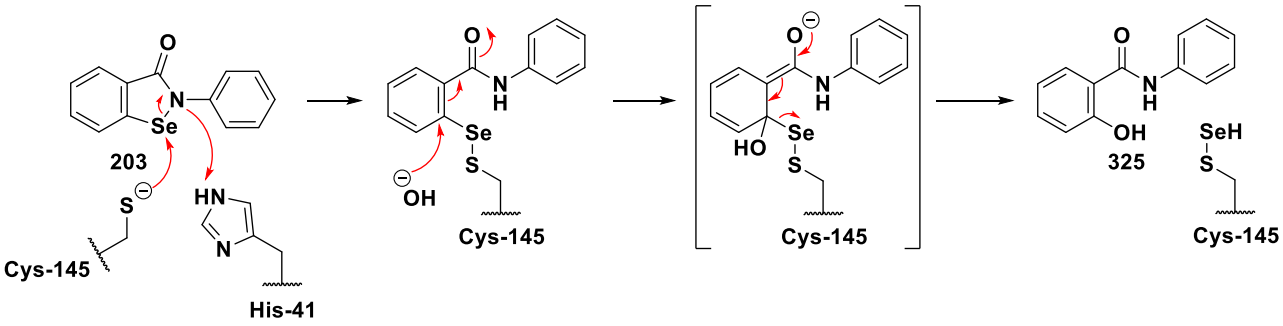

Figure 5-4 | Proposed mechanism for the fragmentation of the M^{pro}-**203** complex.

While crystallographic evidence suggests that the selenosulfide formed from the reaction of **203** with M^{pro} Cys-145 is not hydrolytically stable, the protein-observed mass spectrometry assays conducted by Jin *et al.*[277] and in-house clearly show the formation of stable covalent adducts. Thus, the nature of products formed from the reaction between **203** and M^{pro} are likely condition dependent.

5.1.4 Development of ebsulfur inhibitors against M^{pro}

'Ebsulfur'-type compounds present an electrophilic scaffold for the covalent inhibition of nucleophilic cysteine-containing enzymes without the potential toxicities associated with the presence of the selenium of **203**. **Section 3.2** showed the BIT ring of compound **236b** can act as a cysteine-selective electrophilic warhead against Ldt_{mts}, and other literature reports show the BIT ring can react covalently with other cysteine-containing enzymes.[183, 187, 188] Hence, the BIT core was selected as the starting point for the development of 'ebsulfur'-based covalent M^{pro} inhibitors.

With the BIT core as the starting point for molecular design, areas for functionalisation of the molecule were considered based on their assumed position in the enzyme active site and their ease of synthesis. It was envisaged that the functionalisation of the amide nitrogen might mimic the P1 or P1' residues of the M^{pro} natural substrate, while functionalisation of the *C*-6 or *C*-8 positions might allow for interactions within the P2 binding site for the M^{pro} natural substrate (**Figure 5-5**).

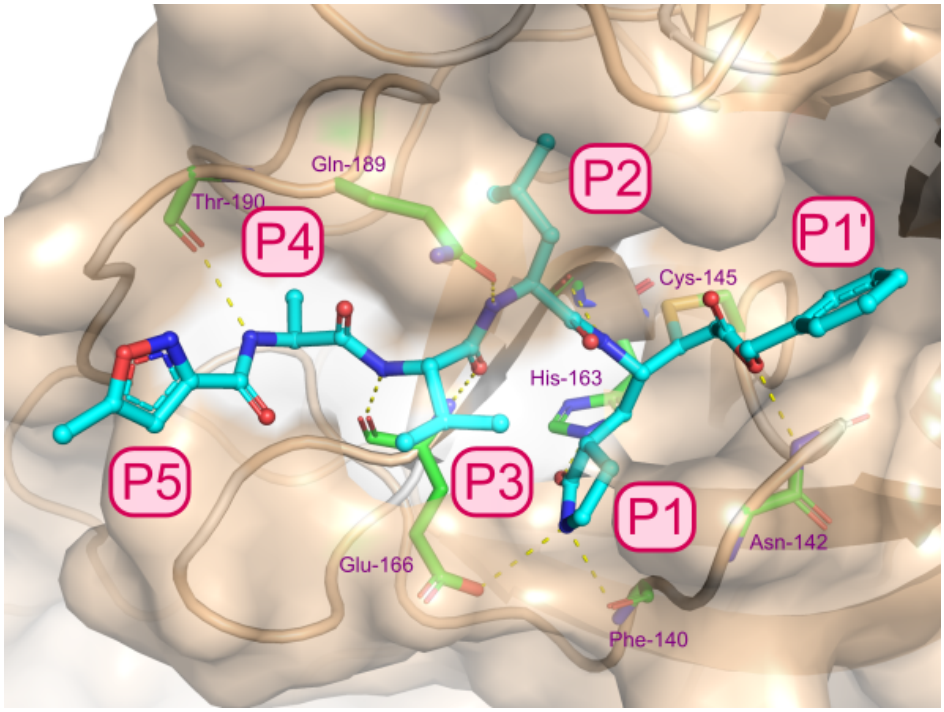

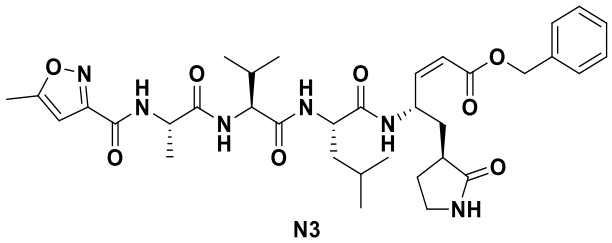

Figure 5-5 | View from a crystal structure of N3 (cyan) covalently bound to Cys-145 of M^{pro} (wheat). (PDB: 6LU7).[277]

Thus, four primary areas on the BIT core were identified for modification (**Figure 5-6**).

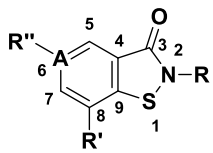

Figure 5-6 | Overview of the modification sites on the BIT core considered for the development of covalent M^{pro} inhibitors.

5.2 Synthesis of first generation ebsulfur inhibitors

The initially proposed series of compounds (**321a-i**) sought to vary the structure of the R-group attached to the isothiazolinone nitrogen (**Figure 5-6**). A wide range of R-groups were selected, ranging from aromatic rings to long alkyl chains, and more complex sidechains like the 4-(aminomethyl)pyrrolidine-2-one moiety of compound **321g**. Based on the structure of the covalent adduct formed from the reaction of **N3** with M^{pro}, it was thought that the R-group might occupy the same location in the active site as the P1 glutamine residue of the natural substrate (though no modelling was performed to support this hypothesis).[277] Indeed, the 4-(aminomethyl)pyrrolidine-2-one residue present in the peptide-based covalent M^{pro} inhibitor **N3** is shown to provide a key non-covalent interaction to M^{pro} in the P1 binding site (**Figure 5-5**).[277] The first series of compounds prepared, varying solely in the structure of the *N*-linked R-group, therefore aimed to explore the chemical space around this binding pocket.

5.2.1 Overview of the synthetic route

The targeted ebsulfur analogues were prepared via a two-step synthesis consisting of an amide formation reaction between the acyl chloride **328** and an appropriate primary amine to give the amide **329**, followed by the reaction of **329** via a copper-mediated oxidative sulfur insertion and ring-closing reaction to give the ebsulfur compound **321** (**Figure 5-7**).

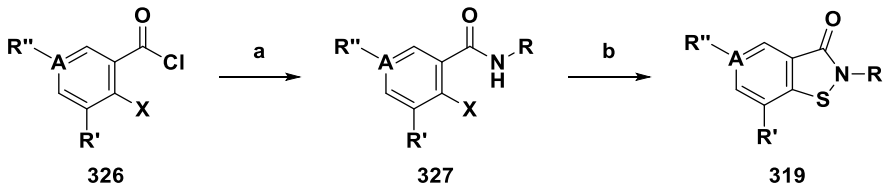

Figure 5-7 | General route for the synthesis of ebsulfur analogues. Conditions: (**a**) R-NH_2, Et_3N, CH_2Cl_2, rt, o/n, 13-74%; (**b**) S_8, K_2CO_3, CuI, 1,10-phenanthroline, DMF, 110 °C, 30 min-o/n, 17-81%.

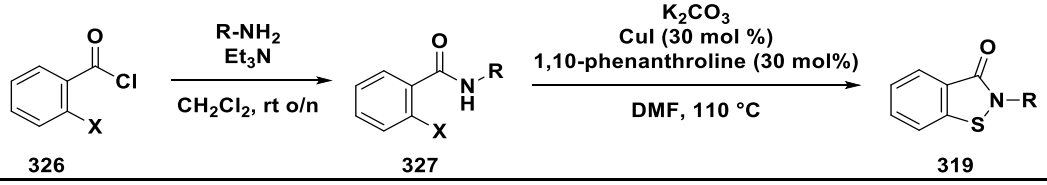

Compound	Structure	329 Isolated Yield (%)	321 Isolated Yield (%)
321a	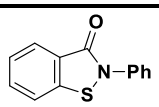	74	70
321b	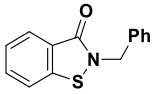	63	49
321c	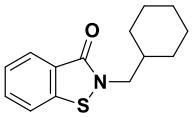	61	20
321d	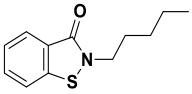	64	81
321e	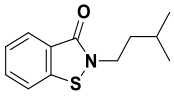	65	28
321f	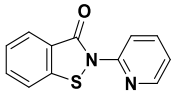	13	65
321g	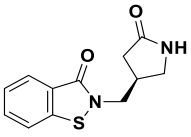	33	17
321h	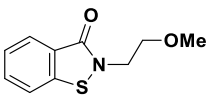	34	62
321i	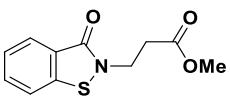	59	80

Table 5-1 | Synthesis of the first generation of ebsulfur derivatives.

This straightforward synthetic route enabled the facile synthesis of a library of ebsulfur compounds **321a-i** (**Table 5-1**).

5.2.2 Determination of IC_{50}s for first generation compounds against M^{pro}

The FRET IC_{50} assays were performed by Siegfried Thun-Hohenstein. *The SPE-MS IC_{50} assays were performed by* Tika R. Malla *and* Dr. Anthony Tumber.

The IC_{50}s for the first generation compounds were determined by two orthogonal methods: a solid-phase extraction – mass-spectrometry (SPE-MS)-based inhibition assay developed by researchers in the Schofield Group (**Figure 5-8**),[292] and a modified fluorescence resonance energy transfer (FRET)-based inhibition assay described by Jin *et al.* (**Figure 5-9**).[277] The SPE-MS assay monitors the proteolysis of a peptide fragment based on the glutamine-serine cleavage site of the pp1a polypeptide.[292] Inhibition of M^{pro} can be quantified by the relative abundances of the uncleaved and cleaved peptide fragments compared to positive and negative controls. The FRET-based inhibition assay utilises a modified substrate peptide functionalised with fluorophores near the *C*- and *N*-termini. When the substrate peptide is intact, the excitation of the 5-FAM fluorophore can be quenched by the nearby dabcyl group, resulting in no fluorescent emission.[294] Upon peptide cleavage, however, the fluorophore and quencher are no longer tethered to each other and the FRET from the fluorophore to the quencher is not as likely. Thus, cleavage of the substrate peptide will result in the appearance of fluorescent emission.

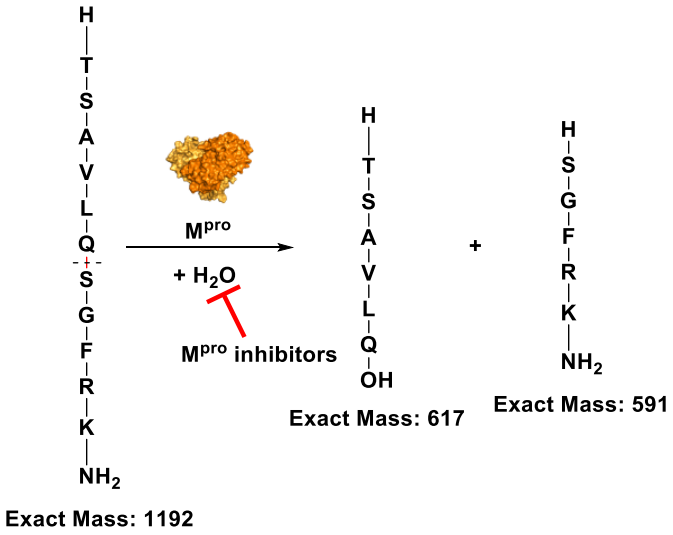

Figure 5-8 | Overview of the SPE-MS Mpro inhibition assay.

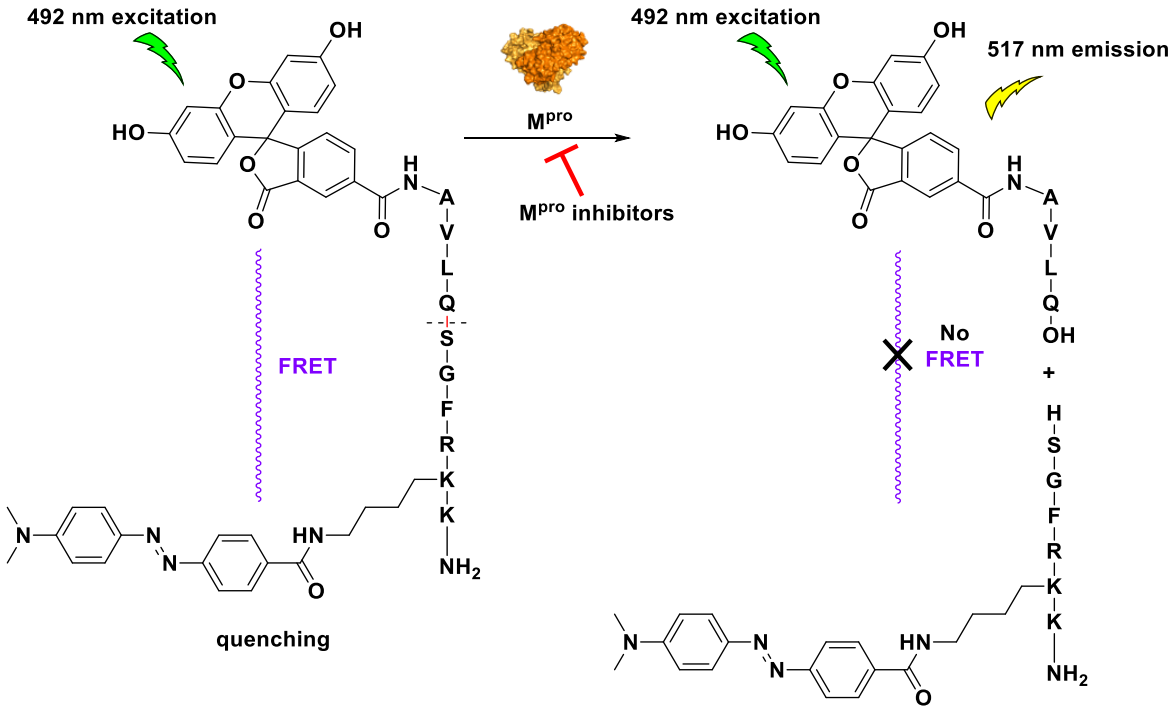

Figure 5-9 | Overview of the FRET-based Mpro inhibition assay.

The results of both the SPE-MS- and FRET-based IC_{50} assays for the first-generation compounds against Mpro are shown in **Table 5-2**. The first generation ebsulfur

compounds manifested micromolar to sub-micromolar potency as judged by IC_{50} values versus M^{pro}. The ebselen analogue **321a** showed the most potent IC_{50} by both the FRET assay (~0.13 μM) and SPE-MS assay (~0.34 μM). These data showed that compounds with non-polar alkyl and aryl R-groups (**321a-e**) generally exhibited higher potency against M^{pro} compared to compounds with more polar R-groups (**321f-i**). This result suggests that the R-group might occupy a hydrophobic pocket in the M^{pro} active site, such as the P2 site occupied by the leucine residue of **N3**.[277] Alternatively, the R-group of the first generation compounds might occupy the relatively open P1′ of the M^{pro} active site occupied by the benzyl ester of **N3**.

Compound	Structure	IC_{50} (SPE-MS) (μM)	IC_{50} (FRET) (μM)
ebselen (**203**)	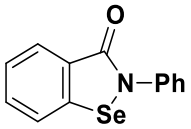	0.26 ± 0.15	0.04 ± 0.01
321a	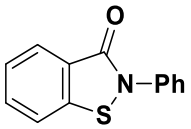	0.34 ± 0.06	0.13 ± 0.04
321b	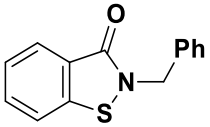	0.43 ± 0.03	0.19 ± 0.04
321c	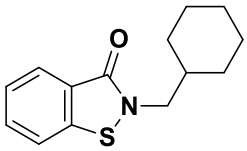	0.53± 0.05	1.00 ± 0.50
321d	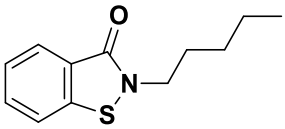	0.47 ± 0.02	0.41 ± 0.12
321e	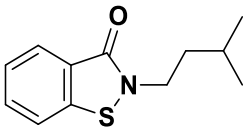	0.42 ± 0.03	0.32 ± 0.04
321f	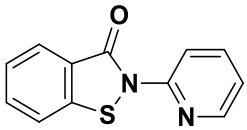	0.79 ± 0.09	0.22 ± 0.10
321g	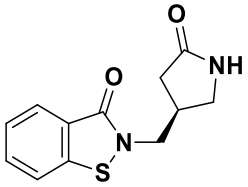	2.55 ± 0.57	0.51± 0.02
321h	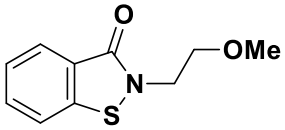	0.78 ± 0.18	0.95 ± 0.04
321i	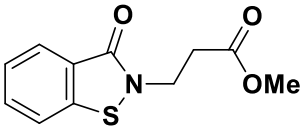	0.39 ± 0.05	0.25 ± 0.02

Table 5-2 | IC_{50} values for first generation compounds against M^{pro}. Data shown are the mean of triplicate measurements from two independent repeats. Errors shown are the standard error of the mean.

Together, these IC_{50} experiments show that the ebsulfur compounds are slightly weaker inhibitors of M^{pro} as compared to ebselen, though ebsulfur compounds **321a-e** bearing non-polar *N*-linked R-groups still retain considerable potency. However, more refined statistical analysis is needed to determine whether there is a statistically significant difference in potency between polar and non-polar R groups.

5.2.3 Protein-observed mass spectrometry of first-generation compounds with M^{pro}

Protein-observed mass spectrometry assays were carried out by Tika R. Malla.

As discussed previously, **203** has been reported to react in a non-selective manner with all twelve cysteines of M^{pro}, implying that **203** does not exhibit selectivity for the M^{pro} active site.[292] Considering that as **203** exhibits potent inhibition against other nucleophilic cysteine enzymes such as Ldt_{mt2}, it is likely that **203** will react with any biological thiol. Ebselen, therefore, should be expected to undergo substantial off-target reactions regardless of its therapeutic application, raising doubts about the safety of **203** as a potential medicine. It was proposed that the stronger S-N bond of the ebsulfur compounds compared to the Se-N bond of ebselen[295] would help confer selectivity towards reaction with the active site Cys-145, where activation by other active-site residues (His-41) would help to overcome the decreased electrophilicity of the inhibitor.

To test the hypothesis that ebsulfur compounds would react less promiscuously with M^{pro} cysteines, POMS experiments were conducted (**Figure 5-10**). These experiments involved the incubation of M^{pro} with a covalent inhibitor followed by mass spectrometric analysis of the covalent adducts. In these experiments, non-selective inhibitors would be expected to react multiple times with M^{pro} to produce adducts with multiple covalent modifications, while selective compounds ideally react once. Data were measured at two time points (2 min and 35 min of incubation).

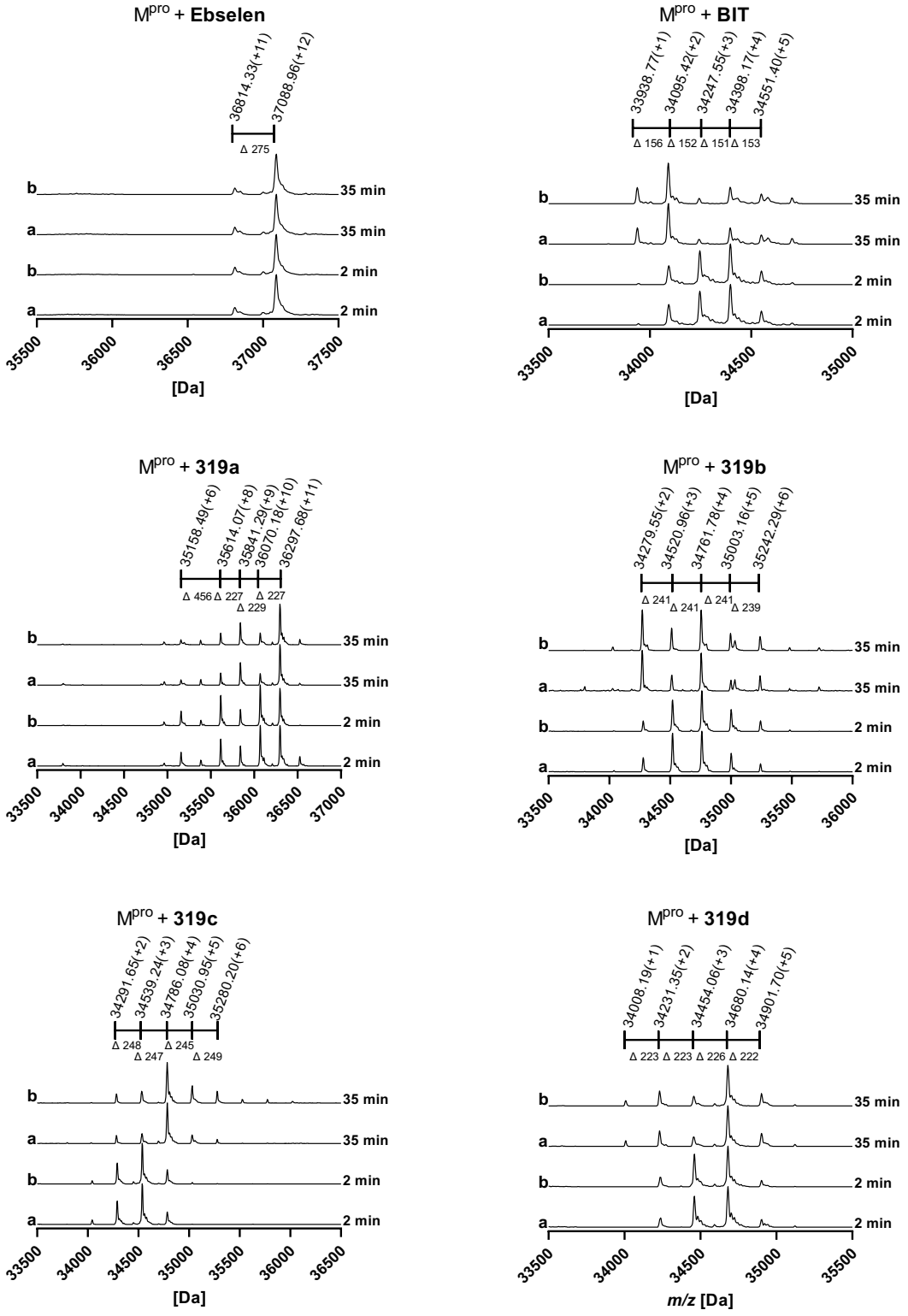

Figure 5-10 | POMS experiments using first generation ebsulfur compounds **321a-d** with M^{pro}. (a) and (b) denote technical repeats. Experiments run by *Tika R. Malla*.

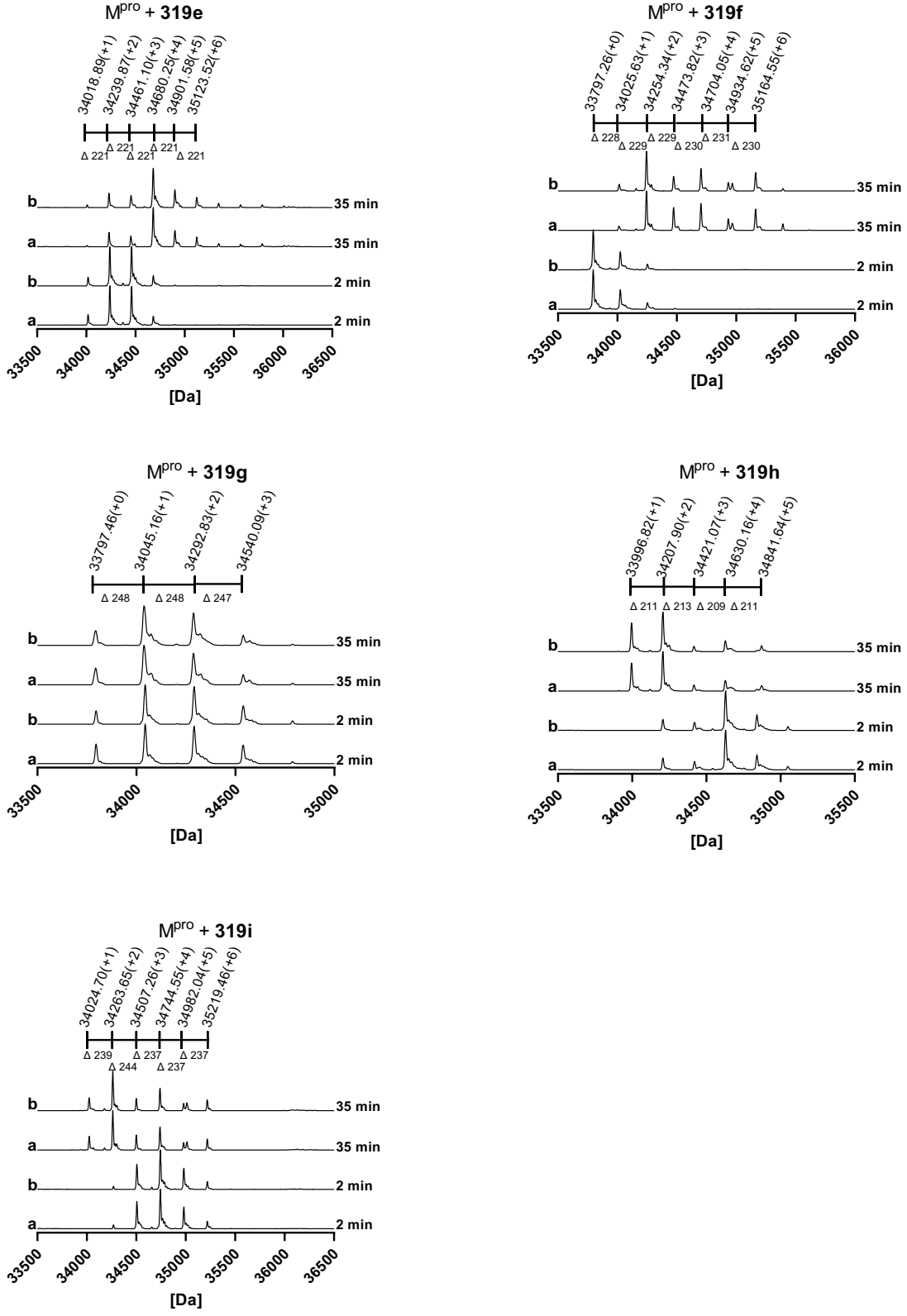

Figure 5-11 | POMS experiments of first generation ebsulfur compounds **321e-i** with M^{pro}. Experiments run by *Tika R. Malla*.

Compound **321a**, the ebsulfur analogue of **203**, was observed to react up to eleven times with M^{pro}. Thus, **321a** exhibits similar reactivity to **203**, which is observed to react up to twelve times with M^{pro}. The other first generation compounds, however, showed lower numbers of covalent reactions with M^{pro}: Compounds **321b-f** and **321i** reacted up to six times with M^{pro}, though the dominant number of reactions was lower; compound **321g** reacted up to three times; and compound **321h** initially reacted up to five times, but the dominant number of reactions was two after 35 minutes. Thus, the POMS experiments demonstrated that, with the exception of **321**a, the ebsulfur compounds appear to show less reactivity to M^{pro} cysteines as compared to **203**. However, it is important to note that the number of covalent modifications is likely dependent on the MS conditions employed in the assay, and that these compounds still react more than once, indicating they do not react exclusively with the active site cysteine of M^{pro}. Thus, while these ebsulfur compounds may avoid the toxicities associated with selenium, they have the potential to undergo undesired reactions with other biological thiols, such as the cysteines of endogenous proteins or glutathione.

While the potency of these ebsulfur compounds is lower than **203** (as discussed in **Section 5.2.2**), they react considerably fewer times than **203** with M^{pro}. It was thought that a useful parameter for the optimisation of ebsulfur compounds as M^{pro} inhibitors might be the ratio of the inhibitor's pIC_{50} value to the number of observed

covalent reactions (**Table 5-3**). The higher the value of this parameter, referred to as "relative potency", the better the inhibitor.

Cpd	Structure	FRET pIC_{50}	Max. no. of reactions	Relative potency (pIC_{50} / max. no. of reactions)
ebselen (203)	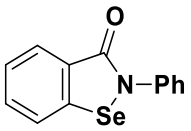	7.40	12	0.6
321a	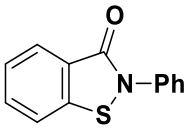	6.89	11	0.6
321b	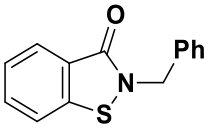	6.75	6	1.1
321c	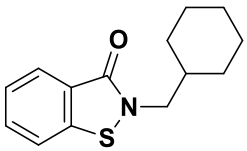	6.03	6	1.0
321d	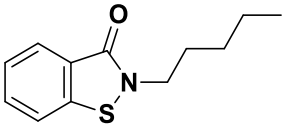	6.39	5	1.3
321e	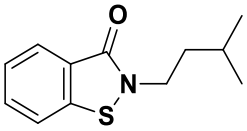	6.50	6	1.1
321f*	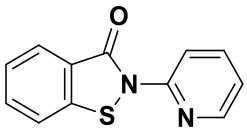	6.67	6	1.1
321g*	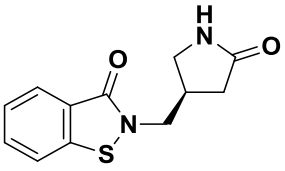	6.29	3	2.1
321h	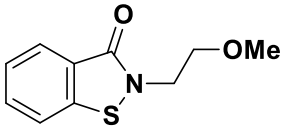	6.11	5	1.2

321i*	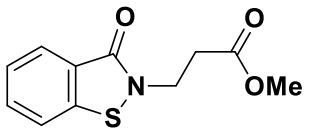	6.61	6	1.1

Table 5-3 | Relative potencies of first-generation compounds.

By comparing the relative potency parameter for these ebsulfur compounds, it is clear that **321g**, bearing a 4-(aminomethyl)pyrrolidine-2-one R-group, exhibits the greatest potency for a given number of covalent reactions, while **203** and its analogue **321a** actually exhibit the lowest potency for a given number of covalent reactions.

5.2.4 Ebsulfur paper by Sun *et al.*

As the ebsulfur analogues synthesised in the Chapter were being evaluated against M^{pro}, Sun *et al.* published a report covering a similar idea to screen ebsulfur derivatives as M^{pro} inhibitors.[296] In their publication, Sun *et al.* described the biological evaluation of a panel of ebsulfur derivatives as M^{pro} inhibitors (**Table 5-4**). Like the first generation of ebsulfur inhibitors synthesised in-house, the ebsulfur derivatives disclosed by Sun *et al.* varied solely in the nature of the *N*-linked R-group. The IC_{50}s were determined using the FRET assay described by Jin *et al.*[277]

There was little overlap in structures between those synthesised in the first generation reported here and those reported by Sun *et al.*[296] Compounds **321a** and **321b**, however, were synthesised by Sun *et al.*, and the reported FRET IC_{50}s for these compounds are in agreement with those measured in-house. The reproducibility of the FRET IC_{50}s for identical compounds synthesised by different research groups

not only validates the accuracy of the assay, but it also allows for a direct comparison between the results obtained in-house and the results reported by Sun *et al.*[296]

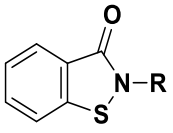

Cpd	R =	IC_{50} (μM)[296]	Cpd	R =	IC_{50} (μM)[296]
330		0.66	**331**	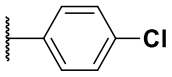	0.39
332		0.78	**333**	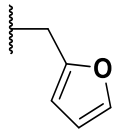	0.11
334	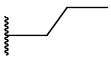	0.73	**335**	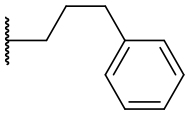	0.41
336	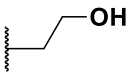	0.41	**337**	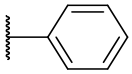	0.49
338	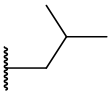	0.48	**339**	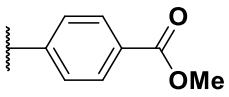	0.36
340	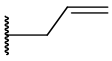	0.63	**341**	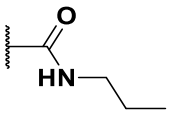	0.23
342		0.13	**343**	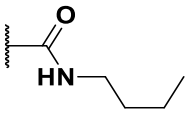	0.91
344	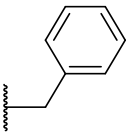	0.17	**345**	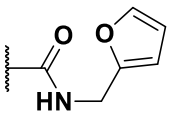	0.38
346	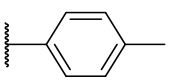	0.33			

Table 5-4 | IC_{50}s of ebsulfur-based M^{pro} inhibitors reported by Sun *et al*.[296]

The ebsulfur compounds reported by Sun *et al.* exhibited sub-micromolar IC_{50}s against M^{pro}. The most potent inhibitors generally bear aromatic R-groups, while compounds bearing aliphatic R-groups generally had higher IC_{50}s. The most potent compound (**333**) possesses a furan R-group, which is structurally similar to the 4-(aminomethyl)pyrrolidine-2-one moiety of the first generation 'hit' **321g**. The results of these inhibition studies are generally consistent with the reactivity trends observed for the first generation ebsulfur compounds.

As mentioned above, the selectivity of the covalent reactions of inhibitors with M^{pro} cysteines is probably of importance with respect to the safety of an ebsulfur-type inhibitor. However, the report by Sun *et al.* does not investigate the selectivity of their ebsulfur compounds. Further investigations into the development of ebsulfur compounds as M^{pro} inhibitors should certainly include compounds with the *N*-linked R-groups from the potent compounds reported by Sun *et al.* However, investigations into the selectivity of their reactions with M^{pro} and the determination of their relative potencies are needed to fully evaluate the potential of these compounds as efficacious M^{pro} inhibitors.

5.3 Second-generation ebsulfur inhibitors

The compounds in this series were synthesised by Siegfried Thun-Hohenstein *under the laboratory supervision of the author.*

5.3.1 Design of second-generation compounds

The data from the first series of ebsulfur compounds imply that the selectivity of M^{pro} inhibition via the covalent reactions with cysteine residues can be improved while retaining potency. Thus, a second series of compounds was synthesised with the aim of investigating whether further active site selectivity could be imparted via the functionalisation of the BIT core at other positions.

To allow for pairwise comparisons of modifications to the benzene ring, the *N*-linked R-groups were kept constant. While compound **321g** was identified by the relative potency parameter to be the best-performing ebsulfur compound from first generation, the cost of the amine precursor to **321g** was prohibitively expensive to be used for library generation (~£500 / 100 mg). Instead, the sidechains from **321a** and **321e** were selected as the standard sidechains for the second-generation ebsulfur compounds. These compounds showed high potency (~0.13 μM and ~0.32, respectively) and their starting materials were more readily available. In addition, the selection of the sidechains from **321a** and **321e** allowed for comparison between an ebsulfur derivative that reacts non-selectively (**321a** – eleven observed reactions) and one that shows some improvement in selectivity (**321e** – six observed reactions). It was envisaged that once beneficial functionalisation to the benzene ring was identified, ebsulfur compounds with these optimised functionalities could be synthesised bearing the 4-(aminomethyl)pyrrolidine-2-one sidechain of **321g**.

The functionalisation of the *C*-6 and *C*-8 positions of the BIT core intended to access additional binding interactions within the M^{pro} active site with the aim of improving the selectivity of ebsulfur compounds for the active site cysteine of M^{pro}. It was proposed that *C*-6 modifications would enable interactions with M^{pro} residues in the P2 and, possibly, P3 binding pockets (**Figure 5-5**). To investigate whether increasing the steric bulk near the reactive sulfur atom would improve selectivity, a series of *C*-8-functionalised ebsulfur derivatives were synthesised.

5.3.2 Synthesis of second-generation ebsulfur compounds

The synthesis of second-generation ebsulfur compounds was achieved via the extension of the synthetic route used for the synthesis of the first generation of ebsulfur compounds (**Figure 5-12**). The introduction of bromines at the *C*-6 or *C*-8 position allow for the attachment of additional functionality to the BIT core via Pd(0)-catalysed cross coupling reactions.[297-299] Alternatively, functional groups at the *C*-6 or *C*-8 positions were introduced at the beginning of the synthesis by using the appropriate 2-halobenzoyl chloride.

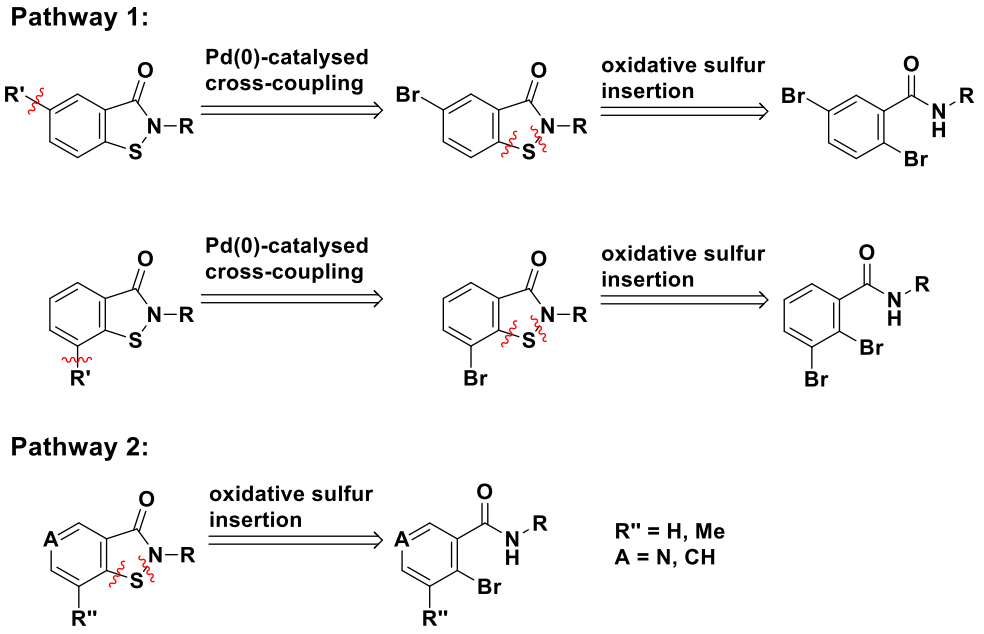

Figure 5-12 | Retrosynthesis of second-generation ebsulfur compounds. Functionalisation of the *C*-6 and/or *C*-8 positions can be achieved either by Pd(0)-catalysed cross-coupling (**Pathway 1**) or by starting from the appropriate halobenzamide (**Pathway 2**).

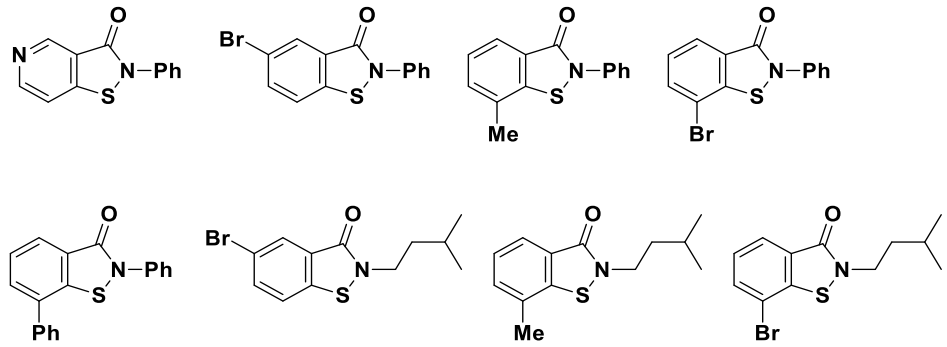

Figure 5-13 | Structures of second-generation compounds.

Efforts to functionalise the *C*-6-bromo group of compounds **321k** and **321o** via Pd(0) cross-coupling reactions are currently under investigation by *Siegfried Thun-Hohenstein* at the time of writing this thesis.

5.3.3 Inhibitory activity of second-generation ebsulfur compounds against M^{pro}

The FRET IC_{50} assays were performed by Siegfried Thun-Hohenstein. *The RFMS IC_{50} assays were performed by* Anthony Tumber *and* Tika R. Malla.

The IC_{50}s for second-generation compounds were evaluated in the same manner as for the first-generation compounds (**Table 5-5**). Compounds **321j**, **321k**, and **321o**, which bear functionality on the *C*-6 position of the BIT core, exhibit comparable potency to the analogous compounds **321a** and **321e**. Conversely, compounds **321l-m**, **321p**, and **321q**, which bear functionality on the *C*-8 position of the BIT core, show negligible inhibition of M^{pro}. These results indicate that while modifications to the *C*-6 position are tolerated, *C*-8 functionalisation of the BIT core leads to a substantial loss in potency.

It is proposed that the loss of potency for M^{pro} for *C*-8-functionalised ebsulfur analogues can be explained by steric hindrance of the electrophilic sulfur by the adjacent functional group, rather than the influence of the functional group on the electronic nature of the BIT core. As the *C*-6 and *C*-8 positions are *para* and *ortho*, respectively, to the sulfur atom, any electronic influence on the sulfur atom from these substituents should be similar due to the similar inductive and mesomeric effects of *ortho* and *para* substitution of benzenes.[300]

Compound	Structure	IC_{50} (SPE-MS) (μM)	IC_{50} (FRET) (μM)
321j*	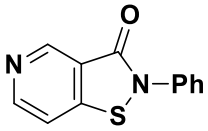	0.43 ± 0.01	0.48 ± 0.09
321k*	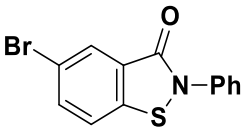	0.34 ± 0.01	0.03 ± 0.01
321l*	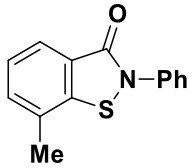	> 100	> 100
321m*	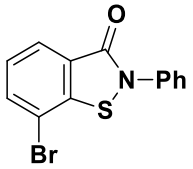	10.88 ± 0.82	> 100
321n*	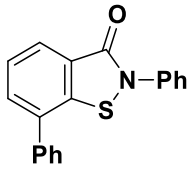	> 100	> 100
321o*	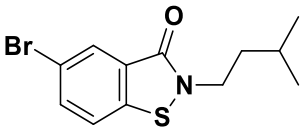	0.43 ± 0.01	0.21 ± 0.13
321p*	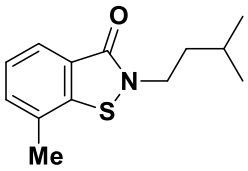	> 100	> 100
321q*	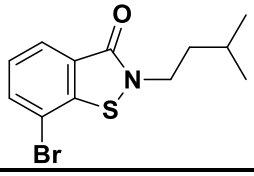	> 100	94.50 ± 8.22

Table 5-5 | IC_{50}s for second-generation analogues. Data shown are the mean of triplicate measurements from two independent repeats. Errors shown are the standard error of the mean.

Thus, if the loss of potency against M^{pro} was due to changes in the electronic character, it would be expected that *C*-6- and *C*-8 functionalisation would produce

similarly (un)reactive ebsulfur compounds. However, functionalisation of the BIT core with the same functional groups at *C*-6 as *C*-8 results in ebsulfur compounds with high potency (cf. **321k** and **321o** to **321m** and **321q**, respectively). In addition, the pyridine-containing compound **321j**, which would be expected to have significantly different electronic character to the other ebsulfur compounds, maintains similar potency to the related compound **321a**. Hence, the steric hindrance of the electrophilic sulfur to nucleophilic attack of M^{pro} cysteines by substituents at *C*-8 is a plausible explanation for the loss of potency. Future modifications of the ebsulfur compounds will therefore be focused on areas of the molecule that do not interfere sterically with the electrophilic sulfur.

5.3.4 Protein-observed mass spectrometry of second-generation compounds with M^{pro}

As for the first generation of ebsulfur M^{pro} inhibitors, POMS experiments were conducted with M^{pro} and the second-generation of ebsulfur M^{pro} inhibitors (**Figure 5-14**). These experiments sought to evaluate the effect of *C*-6 or *C*-8 functionalisation of the BIT core on the selectivity of these compounds in the reaction with M^{pro} cysteines. These experiments reveal that ebsulfur compounds (**321l-n**, **321p**, and **321q**) bearing *C*-8 functionalisation do not react with M^{pro} to form stable covalent adducts, at least under the tested conditions.

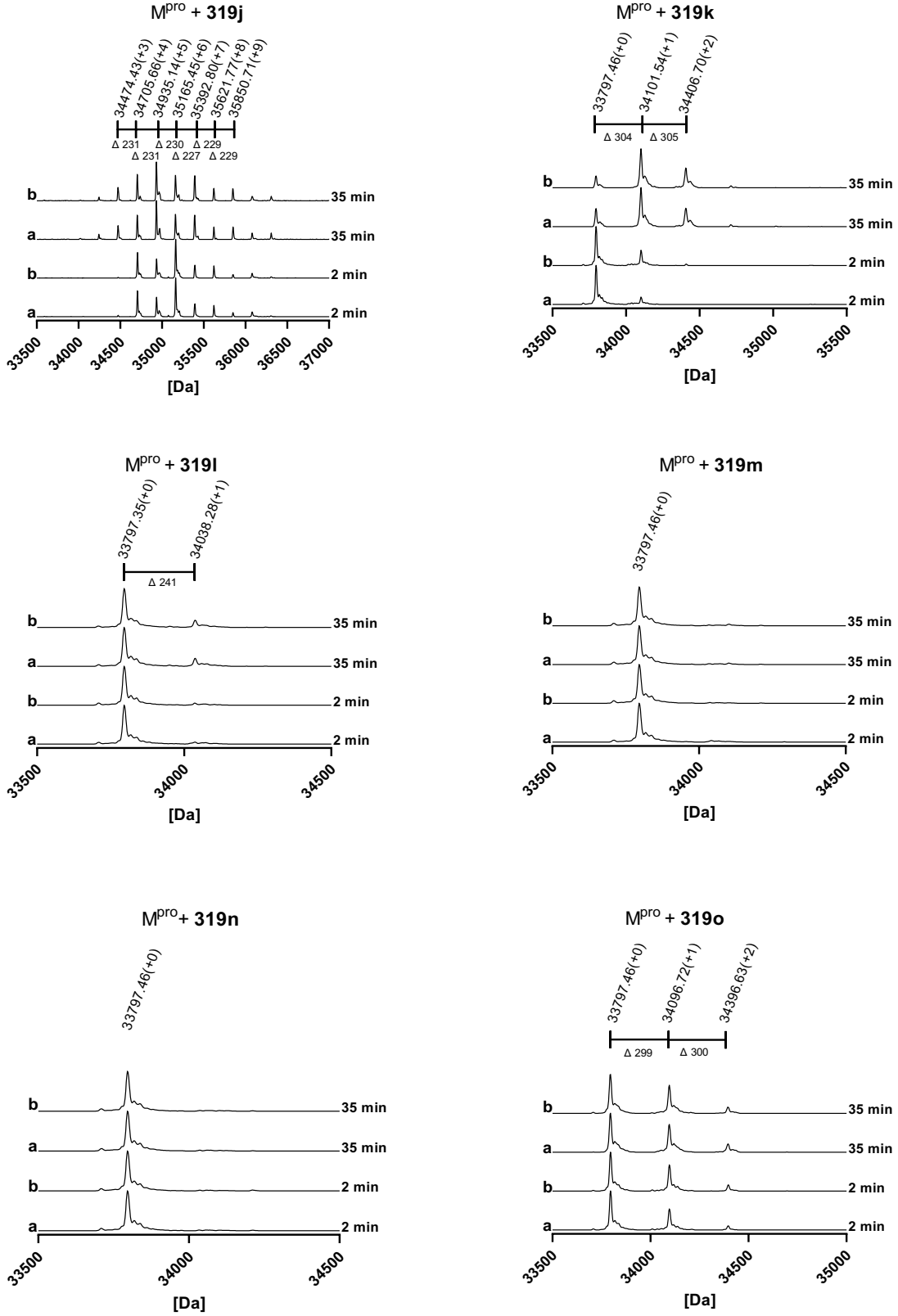

Figure 5-14 | POMS experiments using second-generation ebsulfur compounds **321j-o** with M^{pro} (a and b indicate technical repeats**.** Experiments run by *Tika R. Malla*.

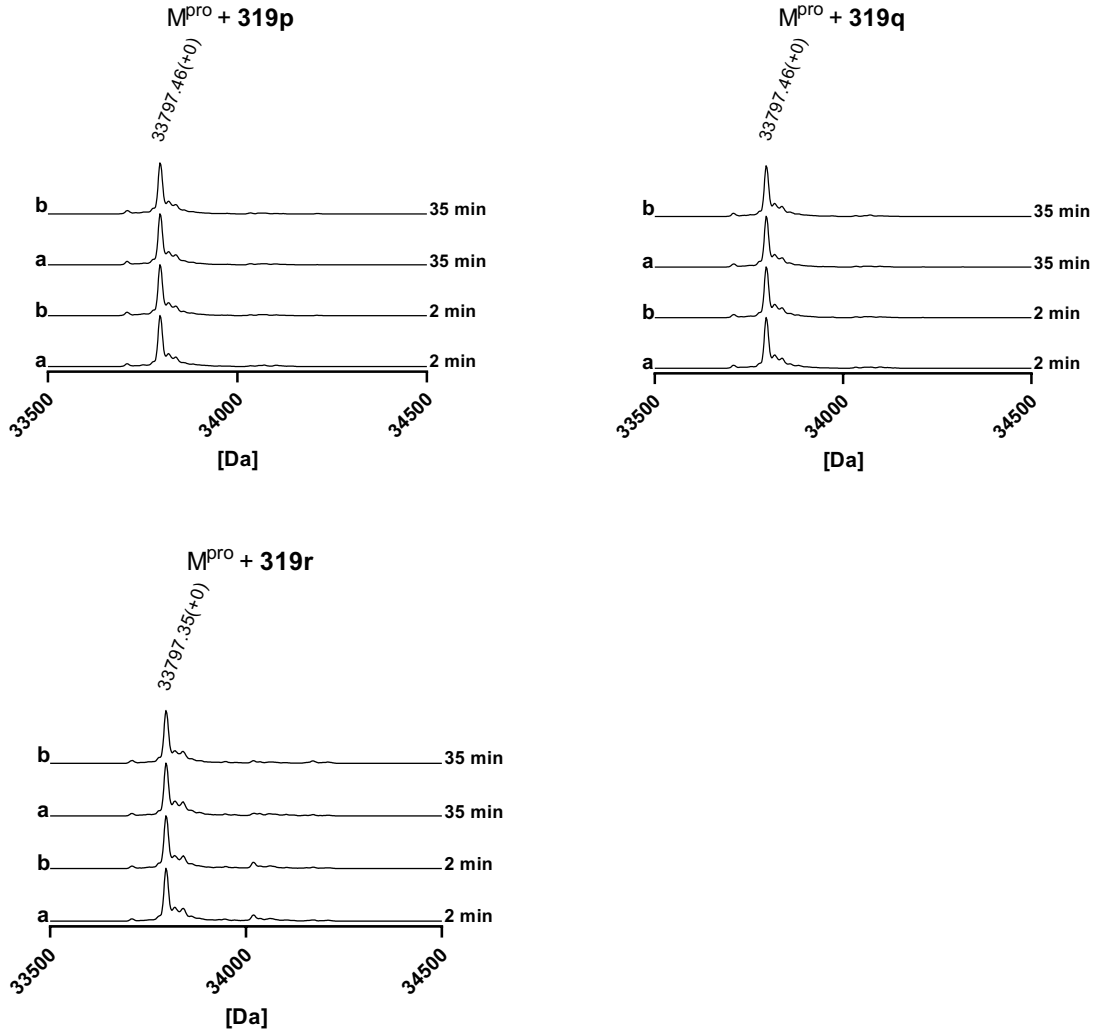

Figure 5-15 | POMS experiments using second-generation ebsulfur compounds **321p-r** with M^{pro} (continued). Experiments run by *Tika R. Malla*.

These experiments also show that compound **321j**, which has a nitrogen in the aromatic ring at the *C*-6 position, reacts in a relatively non-selective manner compared to the structurally similar **321a** (cf. nine observed reactions for **321j** and eleven observed reactions for **321a**). Unexpectedly, simple substitution of a bromine

for a hydrogen at the *C*-6 position resulted in a significant decrease in the number of observed covalent reactions between M^{pro} and the ebsulfur compounds **321k** and **321o**, as compared to the unsubstituted analogues **321a** and **321e**.

The relative potency parameter for the second-generation compounds with *C*-6 functionalisation reveals a substantial improvement over the first generation ebsulfur compounds and ebselen. Compounds **321k** and **321o**, bearing 6-bromo substituents, both had relative potencies over three (Error! Reference source not found.: relative potency 3.8 and 3.3, respectively) – an improvement over the first generation hit compound **321g** (**Table 5-3**: relative potency 2.1) and a substantial improvement over ebsulfur **321a** and **203** (relative potency 0.6 and 0.6, respectively). The improvement in relative potency apparently does not come from an increase in the pIC_{50}s relative to the first generation hit **321g,** but from a substantial decrease in the number of observed covalent reactions between the compounds and M^{pro}. Whether the decrease in the number of covalent reactions is due to a change in electrophilicity of the sulfur (thereby changing the rates of reaction for disulfide formation) or from the induction of steric clashes when reacting with other cysteines cannot be determined from these POMS and IC_{50} assays. Given the time-dependent nature of IC_{50} measurements and POMS experiments, it is plausible that the *C*-6-functionalised ebsulfur derivatives are no more selective than the unfunctionalised analogues, but have slower rates of covalent reaction. POMS and IC_{50} values measured at longer incubation times may show whether the

functionalisation at *C*-6 truly reduces the number of observed covalent reactions or whether the rate of subsequent reactions has been slowed. From these initial observations, however, compounds **321k** and **321o** appear to be the best compounds from the second generation of ebsulfur M^{pro} inhibitors.

Table 5-6 | *Results from the POMS experiments between M^{pro} and second-generation ebsulfur derivatives.*

Cpd	Structure	FRET pIC_{50}	Max. no. of reactions	Relative potency (pIC_{50} / max. no. of reactions)
321j*	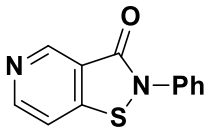	6.32	9	0.7
321k*	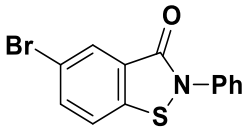	7.51	2	3.8
321l*	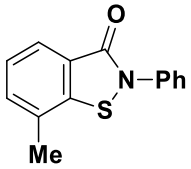	< 3	0	-
321m*	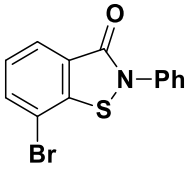	< 3	0	-
321n*	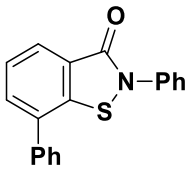	< 3	0	-
321o*	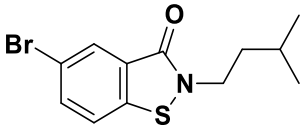	6.68	2	3.3
321p*	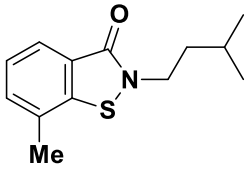	< 3	0	-
321q*	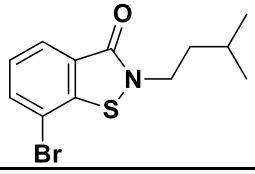	3.02	0	-

5.3.5 Future development of ebsulfur M^{pro} inhibitors

The work described above details the initial development of ebsulfur compounds as M^{pro} inhibitors. The first generation of ebsulfur compounds varied solely in the nature of the *N*-linked R group. Of the first generation ebsulfur compounds, compound **321g**, bearing a 4-(aminomethyl)pyrrolidine-2-one moiety, was observed to react fewer times with M^{pro} while still retaining sub-micromolar potency. The *C*-6-bromo-functionalised compounds **321k** and **321o** from the second generation of ebsulfur compounds demonstrated a significant improvement in the relative potency over other ebsulfur compounds and ebselen (**203**). The combination of the 4-(aminomethyl)pyrrolidine-2-one moiety of **321g** with the *C*-6-bromo functionalisation of **321k** and **321o** would be expected to further improve the selectivity of the covalent reactions with M^{pro}. In addition, further exploration of the functionalisation of the *C*-6 position might lead to additional non-covalent binding interactions between the inhibitor and the enzyme that could improve the affinity and selectivity of ebsulfur compounds for the active site of M^{pro}.

Structural studies are of interest for the reaction of ebsulfur compounds with M^{pro} to identify the cysteines at which these ebsulfur compounds react with M^{pro}. In addition, X-ray crystallographic studies on covalent adducts of M^{pro} and ebsulfur compounds might reveal the binding conformation of the ebsulfur compound in the M^{pro} active site. A crystal structure would facilitate the design of future

generations of ebsulfur compounds to allow for additional non-covalent interactions.

5.4 Ebsulfur compounds as inhibitors of Ldts

As discussed in **Chapter 3** and **Section 5.1.2**, ebsulfur compounds have been shown to act as covalent inhibitors of other cysteine-containing enzymes. Consistent with the overall focus of the work described in this thesis concerning the inhibition of nucleophilic cysteine/serine enzymes, the potential of these ebsulfur compounds as potential antimicrobial agents was evaluated. As the Ldt_{Mt} enzymes from *M. tuberculosis* utilise a nucleophilic cysteine in the enzyme active site, they are promising biological targets for the ebsulfur warhead.[23]

Whilst, like M^{pro}, Ldt_{Mt2} utilises a catalytic dyad consisting of a cysteine and a histidine, the overall size and shape of the active site is considerably different to the active site of M^{pro}. The M^{pro} active site is designed to accommodate the large polyprotein chains produced by the SARS-CoV-2 mRNA strand, while the Ldt_{Mt2} active site accommodates the apparently shorter polypeptide chains of peptidoglycan sub-units. In addition, the residue sequences at the cleavage / transpeptidation sites of both M^{pro} and Ldt_{Mt2} are highly conserved, providing an opportunity to impart selectivity onto the ebsulfur ring via the addition of structural modifications complementary to the targeted active site. The work in this section will briefly discuss the efficacy of synthesised ebsulfur compounds as inhibitors of Ldt_{Mt2}.

5.4.1 Protein Observed Mass Spectrometry experiments with Ldt_{Mt2}

The ebsulfur compounds were investigated for covalent binding to Ldt_{Mt2} by POMS (**Figure 5-16**). Unlike M^{pro}, Ldt_{Mt2} has only a single cysteine, meaning that the ebsulfur compounds are much less likely to react covalently with non-active residues. Thus, covalent reaction of ebsulfur compounds with Ldt_{Mt2} should only produce a single covalent adduct.

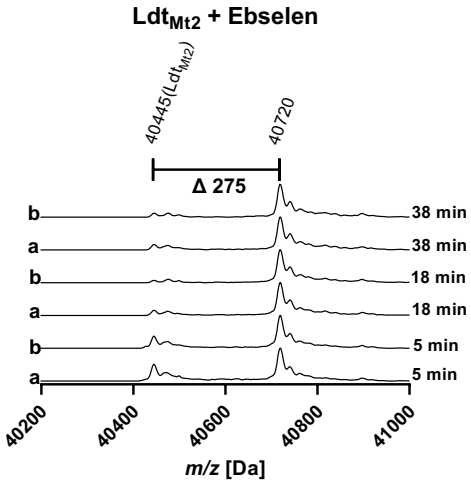
Ldt$_{Mt2}$ + Ebselen
40445(Ldt$_{Mt2}$)
40720
Δ 275
b 38 min
a 38 min
b 18 min
a 18 min
b 5 min
a 5 min
40200
40400
40600
40800
41000
m/z [Da]

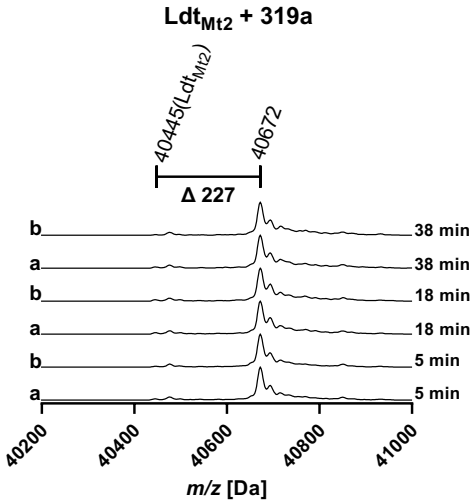
Ldt$_{Mt2}$ + 319a
40445(Ldt$_{Mt2}$)
40672
Δ 227
b 38 min
a 38 min
b 18 min
a 18 min
b 5 min
a 5 min
40200
40400
40600
40800
41000
m/z [Da]

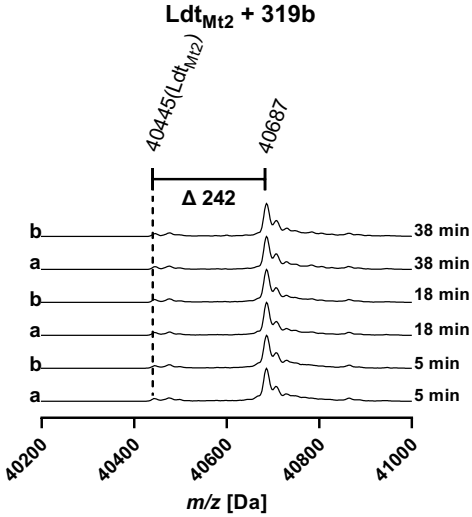
Ldt$_{Mt2}$ + 319b
40445(Ldt$_{Mt2}$)
40687
Δ 242
b 38 min
a 38 min
b 18 min
a 18 min
b 5 min
a 5 min
40200
40400
40600
40800
41000
m/z [Da]

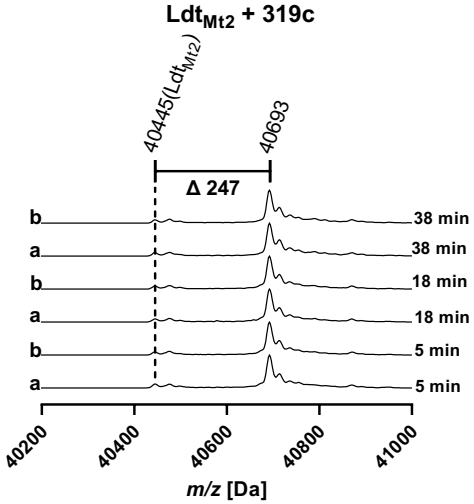
Ldt$_{Mt2}$ + 319c
40445(Ldt$_{Mt2}$)
40693
Δ 247
b 38 min
a 38 min
b 18 min
a 18 min
b 5 min
a 5 min
40200
40400
40600
40800
41000
m/z [Da]

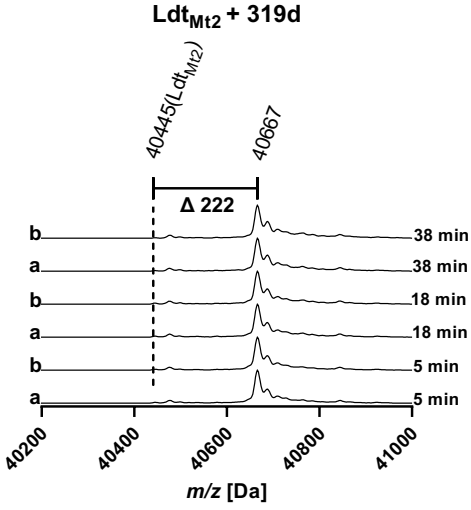
Ldt$_{Mt2}$ + 319d
40445(Ldt$_{Mt2}$)
40667
Δ 222
b 38 min
a 38 min
b 18 min
a 18 min
b 5 min
a 5 min
40200
40400
40600
40800
41000
m/z [Da]

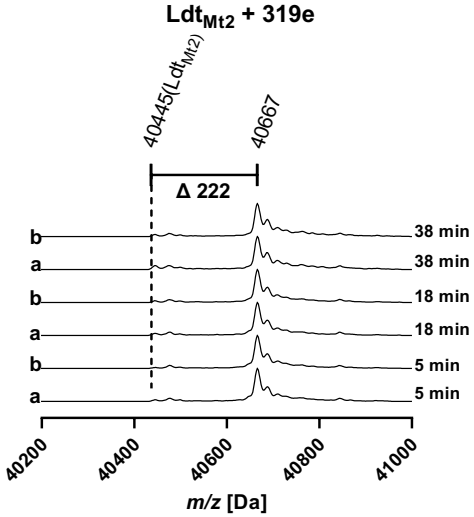
Ldt$_{Mt2}$ + 319e
40445(Ldt$_{Mt2}$)
40667
Δ 222
b 38 min
a 38 min
b 18 min
a 18 min
b 5 min
a 5 min
40200
40400
40600
40800
41000
m/z [Da]

Figure 5-16 | POMS experiments on the reaction of first generation ebsulfur compounds **321a-e** with Ldt_{Mt2}. Note the shoulder on both the unmodified and modified adducts is likely due to formylation.[301] ([a]) and ([b]) denote technical repeats. Experiments run by *Tika R. Malla*.

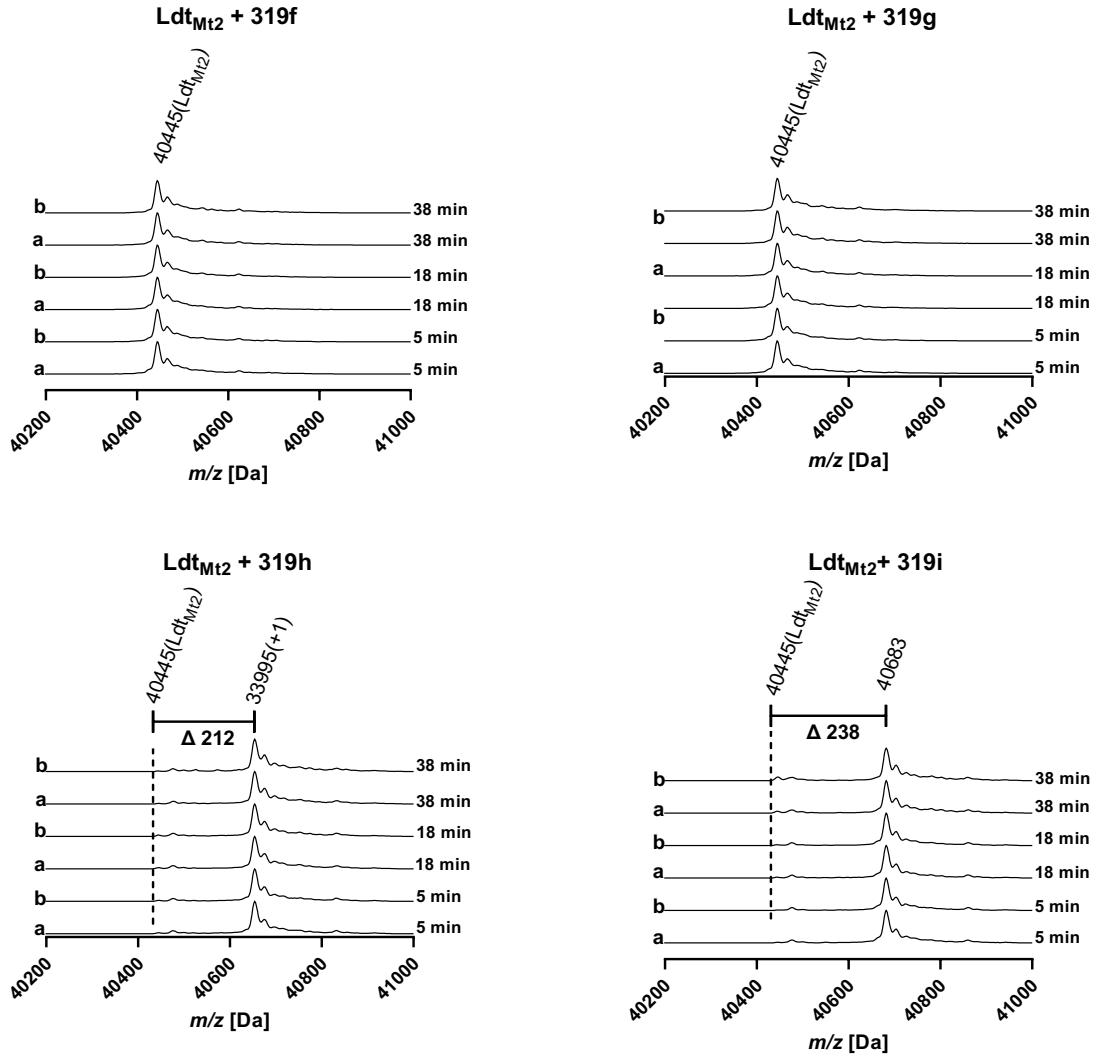

Figure 5-17 | POMS experiments on the reaction of first generation ebsulfur compounds **321f-i** with Ldt_{Mt2}. Note the shoulder on both the unmodified and modified adducts is likely due to formylation.[301] ([a]) and ([b]) denote technical repeats. Experiments run by *Tika R. Malla*.

Of the first generation of ebsulfur compounds, **321a-e** and **321h-i** reacted fully with Ldt_{Mt2} after five minutes to give a single stable covalent adduct. Intriguingly, compounds **321f** and **321g** did not react at all with Ldt_{Mt2}. The R-groups of **321f** and

321g appear to prevent the nucleophilic active-site cysteine from attacking the electrophilic sulfur of the BIT core, but more detailed structural experiments are needed to determine exactly why those R-groups inhibit covalent reaction. Nevertheless, the absence of a covalent reaction of **321f** and **321g** with Ldt_{Mt2} is evidence that the selectivity of the ebsulfur electrophilic warhead can be tailored to specific enzyme active sites. Indeed, the fact that **321g** in particular exhibits high potency against M^{pro} but not Ldt_{mt2} further emphasises the importance of the 4-(aminomethyl)pyrrolidine-2-one R-group for M^{pro} selectivity.

POMS experiments were also conducted on the reaction of the second-generation ebsulfur compounds with Ldt_{Mt2} (**Figure 5-18**). The pyridine-containing compound **321j** reacts fully with Ldt_{Mt2}, though the rate of its reaction is slower than for the analogous benzene-containing compound **321a**. After five minutes, **321j** had reacted with roughly half of the Ldt_{Mt2}, whereas **321a** had fully reacted with Ldt_{Mt2} after five minutes. This result suggests that the change in electronic character resulting from the addition of a nitrogen into the aromatic ring of the BIT core may have a detrimental impact on the compound's reactivity towards Ldt_{Mt2}, although additional pyridine-based ebsulfur compounds would need to be synthesised to validate this hypothesis. Interestingly, none of the other second-generation ebsulfur compounds bearing functionalisation of the BIT core (**321l-r**) were observed to react covalently with Ldt_{Mt2}. While *C*-8-functionalised ebsulfur compounds (**321l-n**, **321p-r**) did not react covalently with M^{pro}, *C*-6-functionalised ebsulfur compounds

reacted readily with M^{pro} (albeit fewer times than unfunctionalised ebsulfur derivatives).

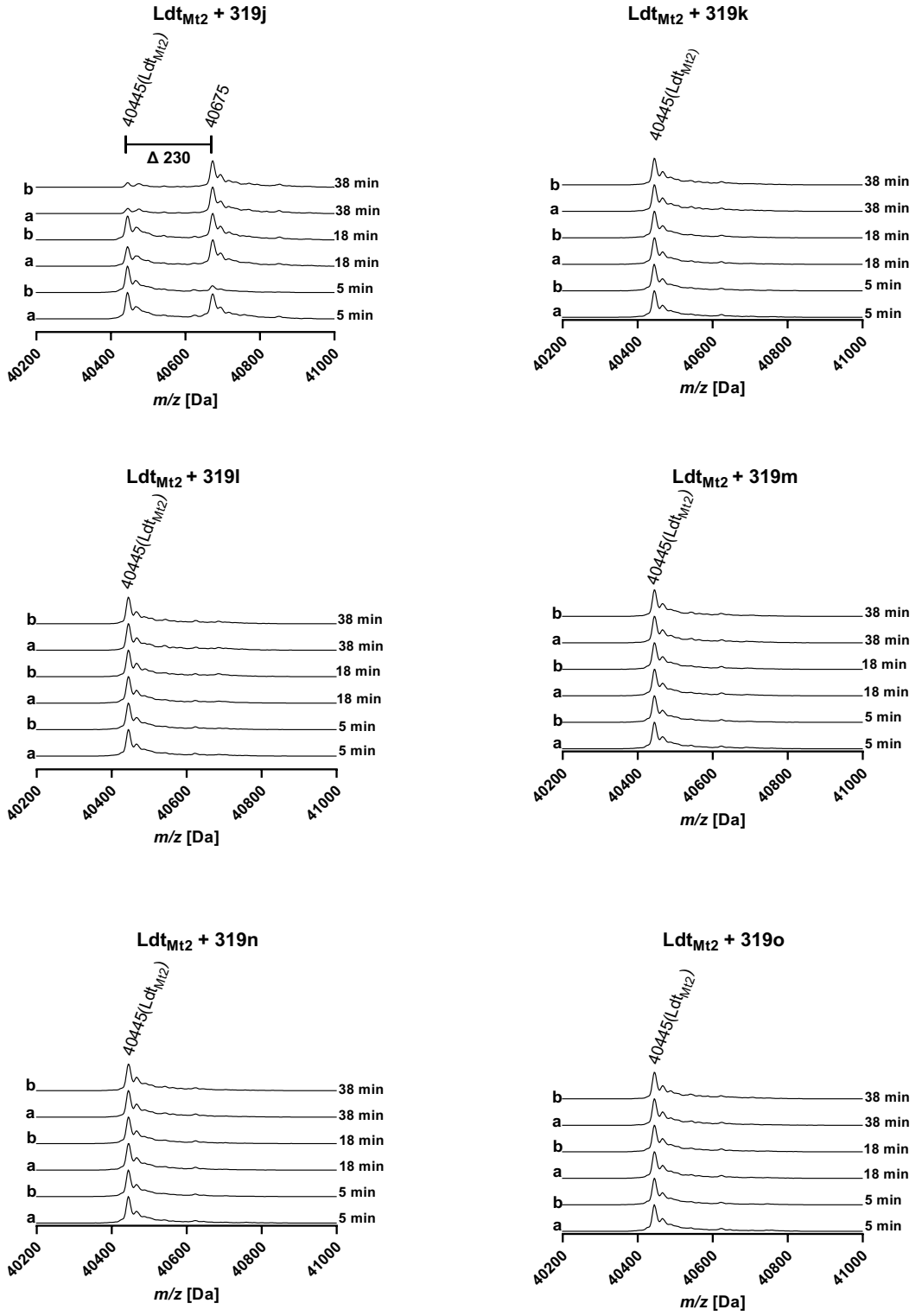

Figure 5-18 | POMS experiments on the reaction of second-generation ebsulfur compounds **321j-o** with Ldt_{Mt2}. Note the shoulder on both the unmodified and modified adducts is likely due to formylation.[301] ([a]) and ([b]) denote technical repeats. Experiments run by *Tika R. Malla*.

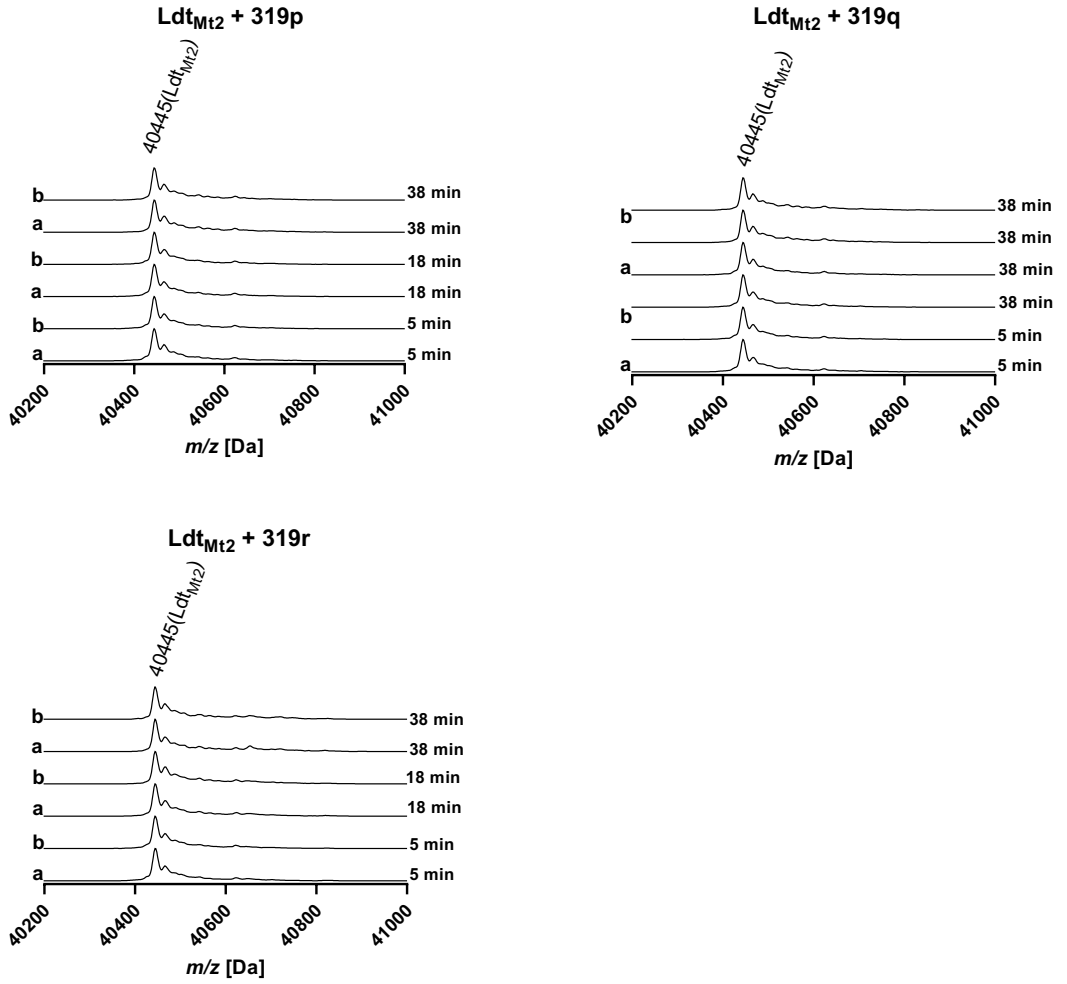

Figure 5-19 | POMS experiments on the reaction of second-generation ebsulfur compounds **321p-r** with Ldt$_{Mt2}$. Note the shoulder on both the unmodified and modified adducts is likely due to formylation.[301] ([a]) and ([b]) denote technical repeats. Experiments run by *Tika R. Malla*.

The reactivity trend for functionalised ebsulfur compounds towards Ldt$_{Mt2}$ is therefore distinct from their reactivity trend towards M^{pro}, lending further support to the idea that ebsulfur compounds can be developed with selectivity for specific cysteine-containing enzymes.

5.5 Multi-drug-resistant *M. tuberculosis* cellular assays

5.5.1 Introduction

A collaboration with Dr. Chris Moon and Dr. Joanna Bacon *et al.* from Public Health England allowed for the screening of selected ebsulfur compounds in a whole-cell assay against *M. tuberculosis*. As these compounds possess the same BIT core as compound **236b** and react covalently with the nucleophilic cysteine of M^{pro}, it was hypothesised that the ebsulfur compounds might also inhibit Ldt_{mts}.

5.5.2 Flow Cytometry Assay

Flow cytometry enables the spectrophotometric analysis of individual cells by measuring the transmittance of light from a laser as it irradiates each cell.[302] The flow cytometer allows for single cells to be exposed to a laser beam, and the light scattered by each cell can be quantified to reveal characteristics about that cell's phenotype.[303]

Cells are often labelled with fluorescent tags to aid in the differentiation of the light-scattering properties depending on the characteristics of the cells.[303] In the assay for *M. tuberculosis*, cell proliferation is measured by the fluorescence of calcein violet (CV). This fluorophore is supplied to cells as the non-fluorescent acetoxy-methyl ester derivative (CV-AM), allowing the fluorophore to enter cells where the esters are hydrolysed, and CV fluorescence is observed. The intensity of the fluorescence is indicative of the growth rate of the cell. *M. tuberculosis* cells are also stained with

Sytox green (SG), which stains nucleic acids but cannot permeate cell membranes. Thus, the staining of cells with SG indicates disruption of the cell wall and cell membrane of *M. tuberculosis* cells.[302]

5.5.3 Results for ebsulfur compounds

The results of the flow cytometry assay used to test selected ebsulfur compounds against a resistant strain of *M. tuberculosis* are shown in **Figure 5-20**. Dead cells should exhibit low CV fluorescence and inhibitors that act via disruption of the bacterial cell wall should cause a large portion of cells to exhibit high SG fluorescence (indicating the cell membrane is ruptured).[302]

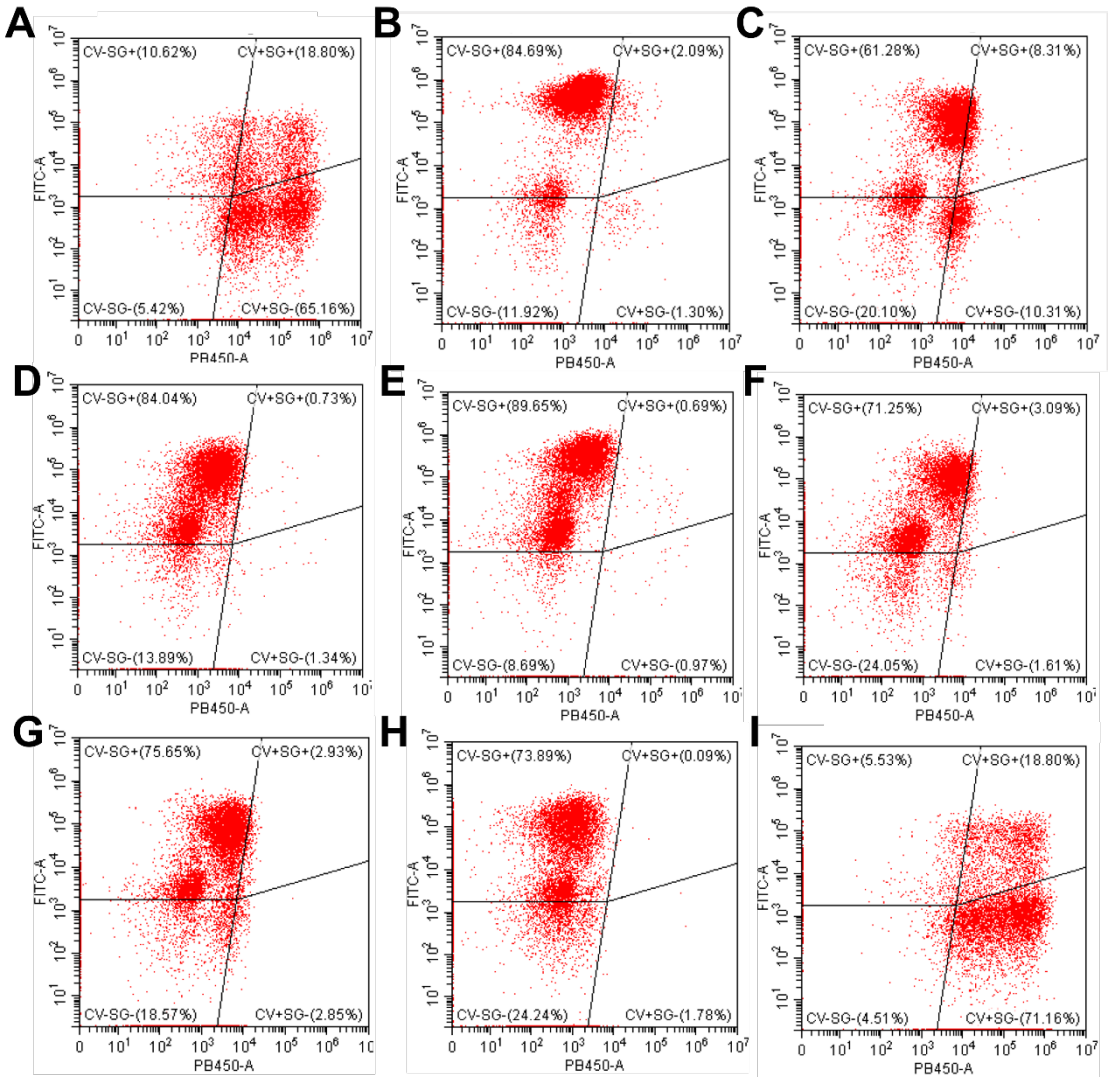

Figure 5-20 | Flow cytometry experiments of: (**A**) vehicle control; (**B**) imipenem (an inhibitor of cell wall biosynthesis); (**C**) SQ109 (an intracellular inhibitor)[304]; (**D**) **319a**; (**E**) **319b**; (**F**) **319f**; (**G**) **319i**; (**H**) **319k**; (**I**) **319r** against MDR *M. tuberculosis.* The x-axes represent CV fluorescent intensity and the y-axes represent SG fluorescence intensityExperiments performed by the research groups of *Dr. Chris Moon* and *Dr. Joanna Bacon* from Public Health England.

Ebsulfur compounds **321a**, **321b**, and **321i** exhibited MICs in the ~30 μM range (**Table 5-7**), while compounds **321f**, **321k**, and **321r** exhibited MICs above 100 μM. The flow cytometry results at inhibitor concentrations of 100 μM show that compounds **321a**, **321b**, **321f**, **321k** and **321i** resulted in a large proportion of cells (> 70%) in the upper left quadrant, indicating these compounds compromise the

viability of the bacterial cell wall, but do not appear to disrupt cellular metabolic activity (as evidenced by the high fluorescence from SG and low fluorescence from CV). Compound **321r** exhibited a MIC above 100 μM and the flow cytometry assay showed only ~5% occupation of the upper left quadrant, implying the compound did not affect the permeability of the bacterial cell wall.

Cpd	Structure	MIC (μM)	% cells in upper left quadrant
321a	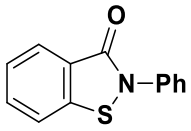	37.04 ± 10.70	84.44
321b	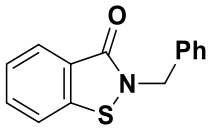	38.25 ± 10.20	89.65
321f	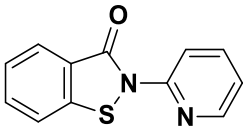	>100	71.25
321k	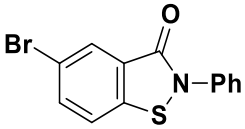	>100	73.89
321i	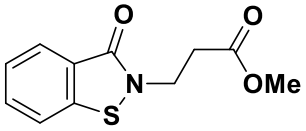	30.80 ± 6.23	75.65
321r	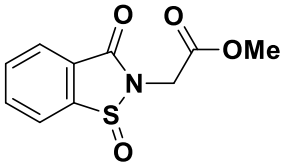	>100	5.53

Table 5-7 | Results from the MIC and flow cytometry assays on ebsulfur compounds against *M. tuberculosis*.

These results further support the hypothesis that ebsulfur compounds can act as antibacterial agents by compromising the integrity of the bacterial cell wall. . Together with the POMS experiments demonstrating covalent reaction with Ldt enzymes, these experiments suggest that certain first generation ebsulfur compounds may exert their antibacterial activity against resistant *M. tuberculosis* by disrupting the biosynthesis of the bacterial cell wall. Further investigations are necessary to confirm the antibacterial mechanism of action of these ebsulfur compounds. While certain ebsulfur compounds reacted covalently with Ldt_{Mt2}, the POMS experiment does not reveal whether the enzyme was inhibited. Thus, inhibition assays must be conducted to confirm that certain ebsulfur compounds do indeed inhibit Ldts. Additionally, experiments to monitor the uptake of labelled peptidoglycan subunits into the cell wall would provide crucial evidence that ebsulfur compounds exert their antibacterial activity via the disruption of cell wall biosynthesis.[305]

5.6 Summary

The work described in this Chapter detailed the development of benzisothiazolinone-based 'ebsulfur' compounds as inhibitors of M^{pro}. The design of these compounds was based on the mechanism of reaction of compound **236b** with the nucleophilic cysteine of Ldts, as well as the nanomolar inhibition displayed by ebselen (**203**) for M^{pro}. The ebsulfur inhibitors sought to reduce the number of

observed covalent reactions between the inhibitor and M^{pro}, as the promiscuity of **203**, which is observed to react with M^{pro} up to twelve times, raised concerns about potentially toxic off-target interactions.

From the investigations detailed in this chapter, the hit compounds **321g** and **321k** were identified as potent inhibitors of M^{pro} that apparently react in a more selective manner towards enzyme cysteines. Substantial work would be required to develop these compounds into clinical therapeutic agents; however, they clearly demonstrate scope for the optimisation of the benzisothiazolinone core as an inhibitor of nucleophilic cysteine enzymes.

Chapter 6 Summary

The primary objective of the work described in this thesis was to enable the development of non-β-lactam-based antimicrobial small molecules as inhibitors of nucleophilic serine and cysteine enzymes. As outlined in **Chapter 1**, there is established literature precedent for covalent inhibitors of bacterial transpeptidases that do not contain a β-lactam ring. Of these, the lactivicins are a particularly attractive class of compounds for further development. The recent reports on the potential antibacterial activities of benzisothiazolinones and benzisoselenazolinones and the similarities of these ring systems to that of lactivicin inspired investigations into their development as antimicrobial agents.

The work described in **Chapter 2** focused on the synthesis of novel analogues of lactivicin – a naturally occurring non-β-lactam antibacterial agent. Previously reported lactivicins **168** and **180** were synthesized to serve as controls in biochemical assays. Compounds **223** and **242** were synthesised to evaluate the importance of the amido sidechain and the γ-lactone carboxylate, respectively, for antibacterial activity. The synthetic route used in the preparation of compound **242** would allow access to previously explored chemical space surrounding the lactivicin core and is envisaged to be a useful method for preparing bioisosteres of the carboxylate group. These experiments were not performed in the scope of this thesis but are an area for future work.

In addition to exploring the antibacterial activity of these two compounds, future analogues should be screened as inhibitors of other nucleophilic enzymes. Given the lack of acylamido sidchains on covalent SBL inhibitors such as clavulanic acid and sulbactam, the lack of a sidechain on compound **223** may also allow for covalent SBL inhibiton. Future analogues of compound **241** lacking a carboxylate moiety could be explored as inhibitors of other nucleophilic serine enzymes, such human neutrophil elastase, which is implicated in various inflammatory disease states[306], or proteases associated with cancer.[307] Bicyclic compounds **236a, 236b,** and **236d** were synthesised to evaluate the viability of fused bicyclic ring configurations, as well as to explore the impact of heteroatom variations at the β-position of cycloserine.

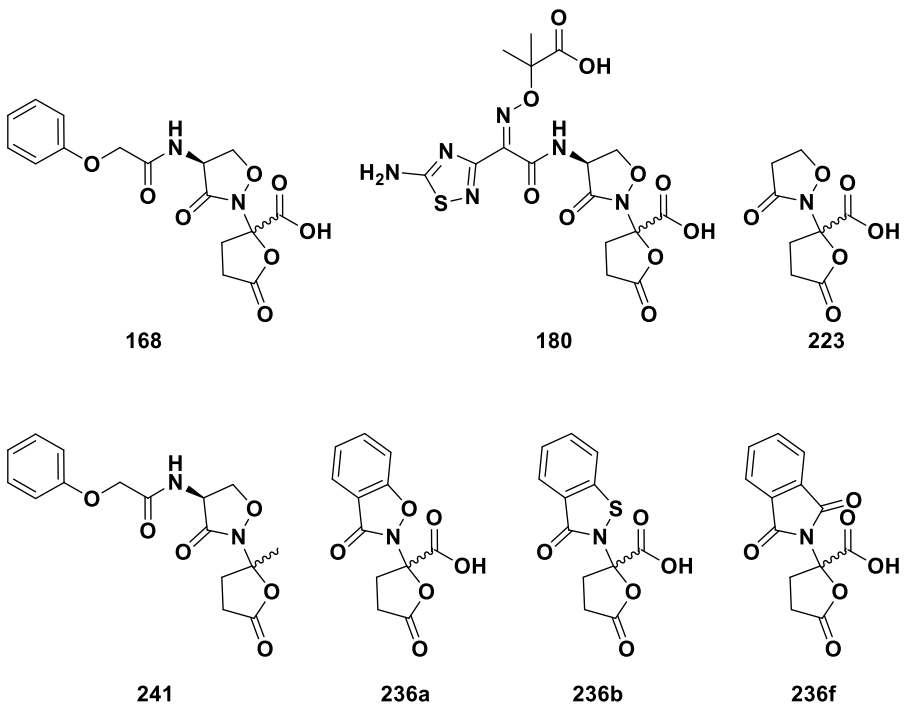

Figure 6-1 | Structures of novel lactivicin analogues synthesised in **Chapter 2**.

A synthetic route towards *C*-4 alkyl cycloserines, inspired by the synthesis of acinetobactin was also explored, however, the crucial 5-*exo*-tet rearrangement could not be achieved. Further investigations of the rearrangement reaction using more forcing conditions or alternative functionalisation strategies are worth exploring to access *C*-4-alkyl lactivicin analogues. Functionalisation of the *C*-4 position of the lactivicin core may lead to increased resistance to β-lactamase hydrolysis, as is observed for the analogous functionalisation of monobactams and is therefore a key priority for future exploration. The synthesis of pyrazolidinone-based analogues of lactivicins featuring electron-withdrawing functionality on the β-nitrogen were explored. While the pyrazolidinone precursors were synthesised successfully, the subsequent lactone products could not be successfully isolated.

The tricyclic lactivicin analogue **290**, which was disclosed in the patent literature, was synthesised for the purposes of evaluating the antibacterial activity of this novel class of lactivicins. Following validation and substantial optimisation of the reported synthetic route, such analogues were prepared with good overall yields. The separation of diastereomers was achieved using reverse-phase chromatography, and NMR characterization of **290b** showed that it undergoes an exchange process on NMR timescales, possibly caused by the inversion of the *C*-5 ring nitrogen lone pair. Variable-temperature NMR was conducted to confirm the identity of **290b**, though the absolute stereochemical assignments of the two diastereomers was not determined.

The successful synthesis of **289** lays the foundation for future studies to synthesise and test libraries of tricyclic lactivicin analogues with diverse functionalities on both ends of the molecule. Future tricyclic lactivicins should combine elements from the different avenues of investigation covered herein, as well as others that were outside the scope of this thesis. Of particular interest are analogues featuring clinically-relevant 'ATMO'-type amido sidechains, which may demonstrate substantially higher potency against bacteria than the phenoxyacetyl sidechain employed in the validation of the synthetic route. Similarly, the attachment of siderophores to the lactone of these tricyclic lactivicin analogues should be undertaken in an effort to enhance the cellular permeability of these compounds.

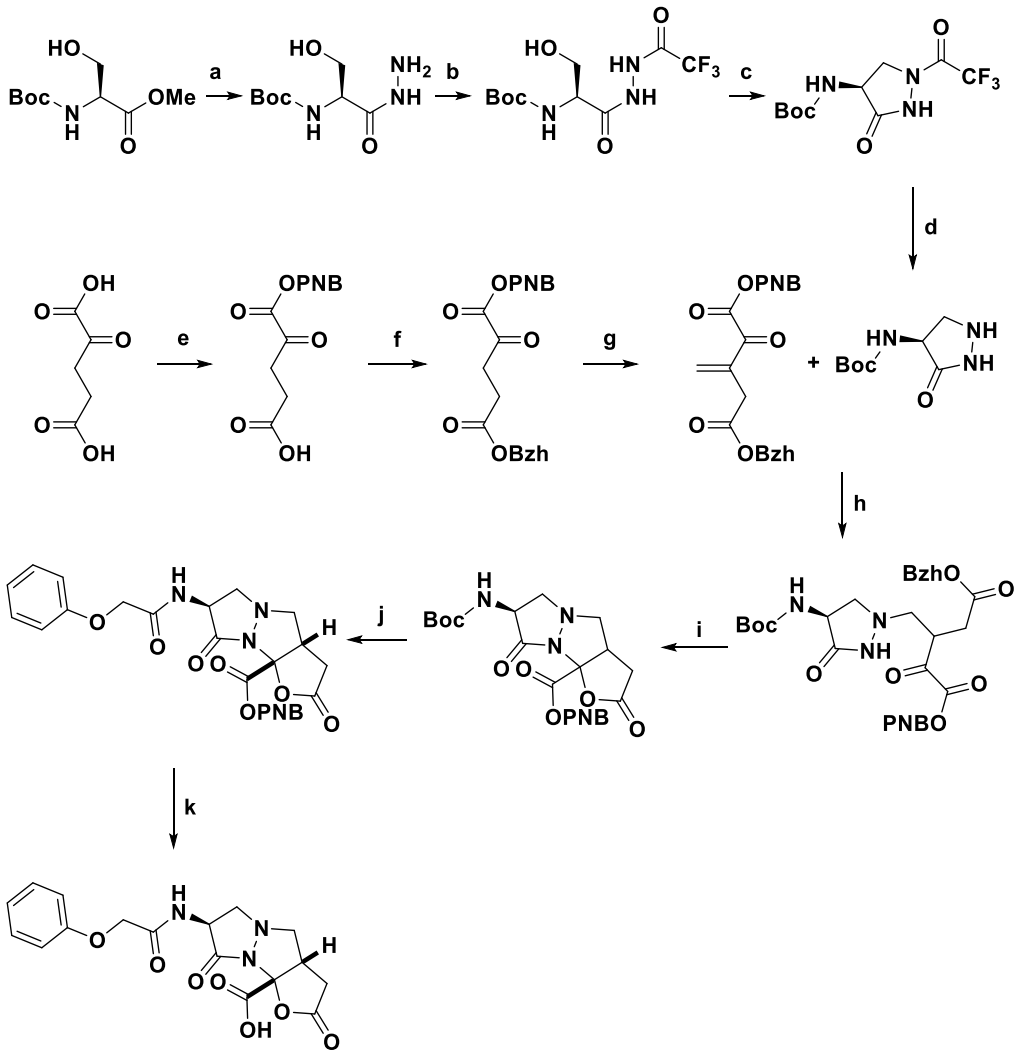

Figure 6-2 | Total synthesis of tricyclic lactivicins **290**. Reagents and conditions: (**a**) N_2H_4•H_2O, MeOH, rt, o/n, 95%; (**b**) *S*-ethyl trifluorothioacetate, EtOH, 30 °C, 2 d, 95%; (**c**) DIAD (1 M in CH_2Cl_2), PPh_3, THF, rt, o/n, 69%; (**d**) N_2H_4•H_2O, THF/H_2O (2:1 *v*/*v*) rt, o/n, 70%. (**e**) 4-nitrobenzyl bromide, DIPA, DMF, 70 °C, 2 h, 92%; (**f**) diazobenzophenone, CH_2Cl_2, rt, o/n, 67%; (**g**) *N*,*N*,*N*',*N*'-tetramethydiaminomethane, Ac_2O, AcOH, CH_2Cl_2, rt, 6 h, 78%; (**h**) CH_2Cl_2, rt, o/n, 92%; (**i**) AcOH, HFIP, 60 °C (sealed vial), 16 h, then EDCI, CH_2Cl_2, rt, 2 h; 46%; (**j**) TFA, CH_2Cl_2, rt, 1 h, then phenoxyacetyl chloride, Et_3N, CH_2Cl_2, rt, o/n, 75%; (**k**) Pd/C, H_2, THF/H_2O (2:1), 5% (**290a**), 8% (**290b**).

Overall, the work described in **Chapter 2** detailed the synthesis of a small but diverse set of novel lactivicin analogues, which were then evaluated as antibacterial agents in **Chapter 3**. MIC experiments on susceptible *E.coli* and *S. aureus* strains revealed that compounds **236a** and **236d** did not possess antibacterial activity. However, **236b** demonstrated weak antibacterial activity against both Gram-

positive and Gram-negative strains tested. Surprisingly, neither isomer of **290** showed antibacterial activity against tested strains, suggesting either that the compounds were substantially less cell-permeable than the analogous **168**, or that their inhibitory effect on PBPs was greatly diminished by the presence of the additional ring. Futher studies are needed to better characterise the performance of these molecules as transpeptidase inhibitors. Biochemical inhibition assays would offer great insight into their capacity to inhibit PBPs, while POMS studies would indicate whether they can react to form stable covalent adducts. The stability of these lactivicin analogues to hydrolysis by β-lactamases should also be evaluated, as should a screen for SBL inhibition. Cell permeability and efflux studies could be undertaken to study whether the compounds can penetrate bacteria, and whether bacteria can effectively pump out the molecules before they can react.

The lactivicin analogues synthesised in **Chapter 2** were investigated for inhibitory activity of Ldts from *M. tuberculosis* and *E. faecium*. POMS studies revealed that **168** reacts rapidly with Ldt_{mt1}, Ldt_{mt2}, Ldt_{mt3} and Ldt_{fm} to form stable covalent adducts, indicating the lactivicin core is a suitable electrophilic warhead for the inhibition of cysteine transpeptidases. However, the fused bicyclic cycloserine analogue **236a** was not observed to covalently react with any of the tested Ldts. Conversely, the compound **236b**, which has an endocyclic sulfur atom in place of oxygen, was observed to readily react with Ldt enzymes to give stable covalent adducts. The covalent adduct between Ldts and **236b** was cleaved by the addition of DTT,

suggesting that **236b** inhibits Ldts by a novel mechanism to form a disulfude-linked covalent adduct to the active site cysteine. The apparent tendency for **236b** to react via the sulfur atom rather than the carbonyl suggests that similar compounds might exhibit increased stability to β-lactamases, which generally react at the carbonyl. Future work is needed to confirm the proposed mechanism of inhibition. Higher quality crystal structures should be obtained to confirm the structure of the formed covalent adduct. POMS experiments using a Ldt variant with a cysteine to serine mutation at the active site would also provide insight into the mechanism of action, as it is unlikely that the oxygen of the serine atom would react with the endocyclic sulfur in a similar manner.

The utility of **236b** as a therapeutic is questionable due to the likelihood of reactions with other biological nucleophiles. It is recommended that these compounds, as well as the ebsulfur compounds described in **Chapter 5**, are screened for covalent reactivity against a panel of other cysteine-containing enzymes as well as small molecule thiols such as cysteine and glutathione. While it is likely that **236b** and other related benzisothiazolinone-containing compounds will demonstrate undesired reactivity with these targets, the identification of a potentially novel mechanism of inhibition of a bacterial transpeptidase is at least useful from an academic perspective. It is conceivable that a future analogue of **236b** could be developed as a chemical probe or suicide inhibitor used to study the mechanisms

of action of other Ldt inhibitors, and may eventually lead to a new promising anti-tuberculosis agent.

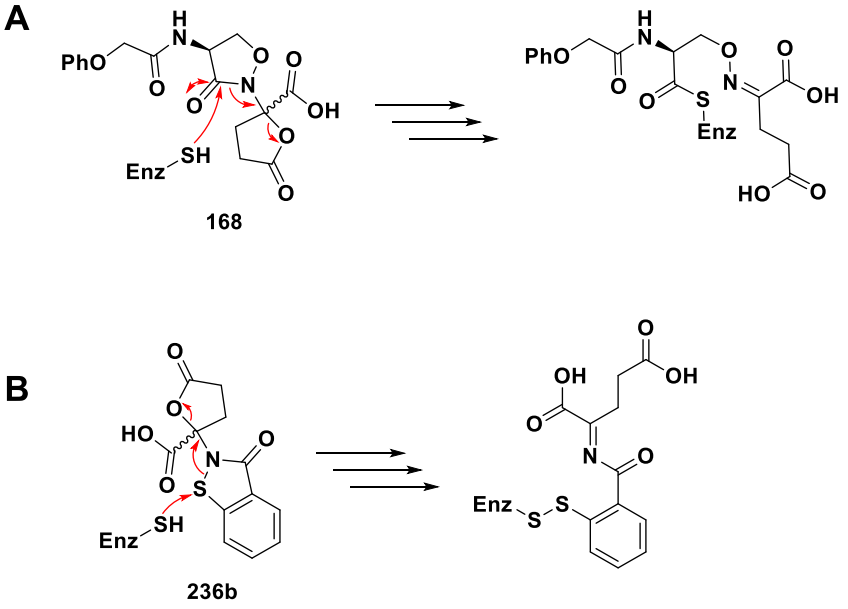

Figure 6-3 | Proposed mechanisms for the reactions of Ldt_{Mt2} with (**A**) **168** and (**B**) **236b**.

The work described in Chapter 4 focused on the modification of **2-OG** for various biological applications, including the synthesis of γ-lactone-functionalised analogues of lactivicin as well as the development of selective competitive inhibitors of $IDH1^{R132H}$ mutants. Improvements were made to the synthesis of key intermediates for the 4-amino-γ-lactone lactivicin derivatives initially pioneered by Star *et al*;[167] the use of a sulfur ylide in place of a phosphonium ylide for the synthesis of α-keto ester **303** enabled milder oxidative cleavage using Oxone®.

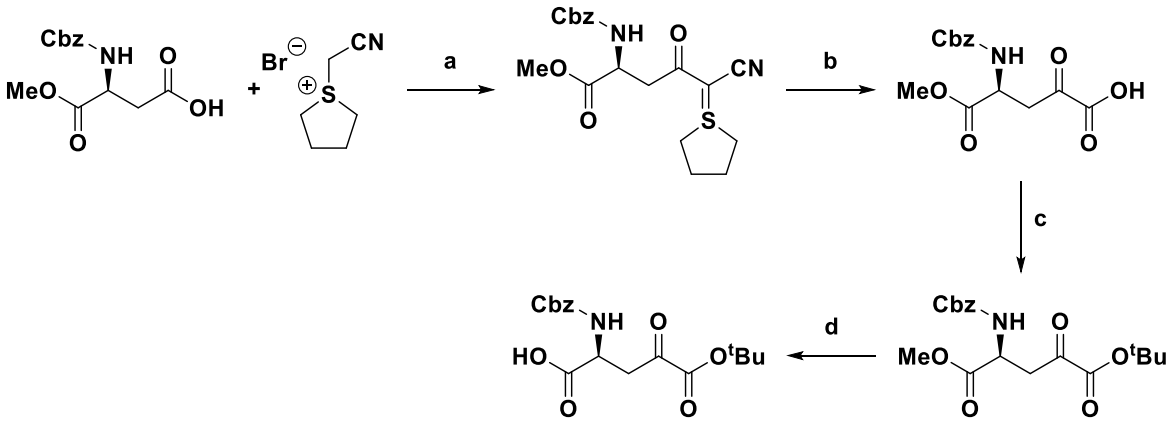

Figure 6-4 | Facile synthesis of the key intermediate **299.** Reagents and conditions: (**a**) HATU, DIPEA, DMA, rt, 4 h, 70%; (**b**) Oxone, THF/H_2O, 0 °C, 30 min, carried forward crude; (**c**) *tert*-butyl-N,N′-diisopropylimidate, THF, rt, 30 min, 44%; (**d**) LiOH, THF/H_2O, rt, 30 min, 68%.

The attachment of carbapenem *C*-3 sidechains to the γ-lactone of lactivicin was attempted via sulfa-Michael reactions of thiols onto the Michael acceptor **284**. While the sulfa-Michael reaction of **284** with thiophenol and subsequent benzhydryl ester deprotection proceeded with excellent yields, no formation of the expected lactone **307** was observed following the lactonisation of the **2-OG** precursor **306** onto the cycloserine **210**. While the functionalisation of lactivicin γ-lactones via sulfa-Michael addition were unsuccessful, the methodology remained a powerful tool for the functionalisation of **2-OG** and was used for the synthesis of a library of **2-OG** analogues **292** that were screened for inhibition of $IDH1^{R132H}$ variants. The initial inhibitory data revealed a general SAR for 3-mercaptomethyl 2-OG analogues: compounds with heteroaromatic sidechains generally inhibited $IDH1^{R132H}$, while compounds bearing aliphatic sidechains generally could act as alternative substrates to **2-OG**.

Initial investigations were made into the conjugate addition of other nucleophiles into the Michael acceptor **312**. These studies demonstrated that the Rh(I)-catalysed addition of aryl boronates onto the Michael acceptor was possible, adding an additional method by which the Michael acceptor **312** can be functionalised. These results support the notion that the facile functionalisation of **2-OG** using the described methodology is a versatile tool with many scientific applications. Future work on the functionaisation of **310** via aza-Michael reactions and Heck couplings, and the development of enantioselective Michael additions of aryl boronates into **312** would be of value for the asymmetric synthesis of competitive inhibitors of **2-OG**-dependent oxygenases, and would grant access to a vast chemical space around a small molecular scaffold with countless biological roles.

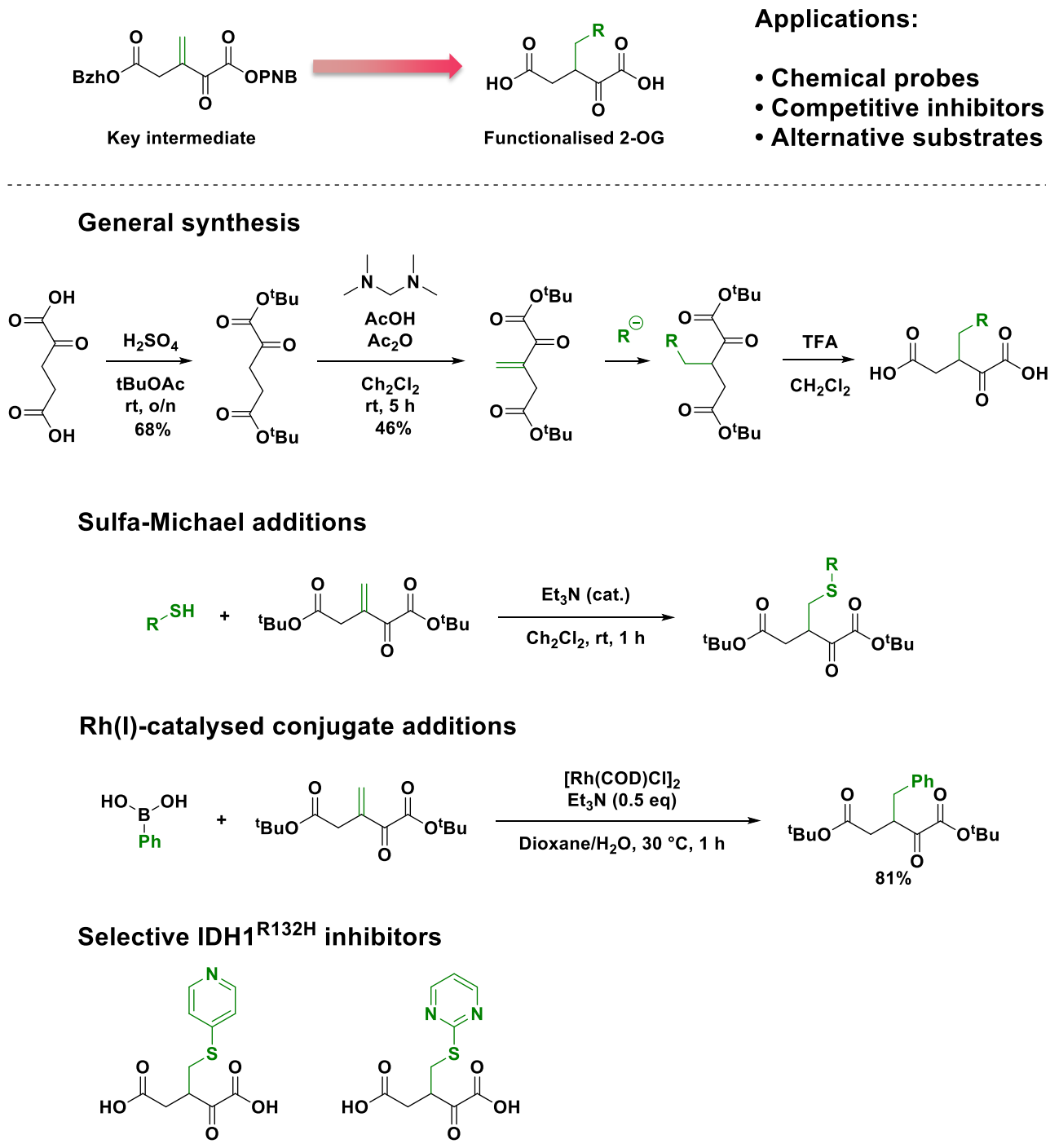

Figure 6-5 | Overview of the work described in **Chapter 4**.

Finally, **Chapter 5** detailed the development of ebsulfur-based inhibitors of M^{pro}. From the mechanistic studies on the reaction of **236b** with Ldt enzymes, as well as the identification of **203** as a potent inhibitor of M^{pro}, the benzisothiazolinone core

was an attractive electrophilic warhead for the potential inhibition of M^{pro} as, like the Ldts, M^{pro} utilises a nucleophilic cysteine residue to catalyse its proteolysis reactions. The ebsulfur compounds developed in **Chapter 5** showed high potency against M^{pro} while also demonstrating apparent improvements in selectivity over ebselen (**203**).

However, the ebsulfur molecules still demonstrated multiple covalent reactions by POMS experiments, indicating they were not truly selective for the M^{pro} active site. Further work is needed to identify the locations of these covalent modifications. Crystallographic studies and competition experiments using inhibitors proven to be selective for the active site would help to answer these questions. As discussed for the lactivicin analogue **236b**, the evidence of multiple reactions for these compounds suggests that these ebsulfur compounds may react with many other biological thiols, thus a thorough cross-screen should be conducted to identify any potential side reactions that these compounds may undergo. Additional studies on Ldt enzymes revealed that the functionalisation of the *C*-6 position of the BIT core apparently conferred selectivity for M^{pro} over Ldts.

In summary, the work described in this thesis made substantial progress in developing strategies for the synthesis of novel non-β-lactam-based covalent inhibitors of bacterial transpeptidase inhibitors, which will be used to combat antimicrobial resistance, and pioneered facile methodology for the synthesis of functionalised 2-OG analogues with diverse biochemical applications.

Chapter 6

Chapter 7 Experimental

7.1 General Information

Commercially available reagents and solvents were from Merck, Fluorochem, or Activate Scientific, and were used as received. All manipulations with air- and moisture-sensitive compounds were carried out under a positive pressure of argon in oven-dried glassware.

Reactions were monitored by TLC on Merck aluminium-backed sheets coated with Merck Kieselgel 60 F254 (230-400 mesh) fluorescent treated silica, and visualised under ultra-violet light (254 nm or 365 nm) and/or stained with ninhydrin, permanganate, or cerium ammonium molybdate (CAM) stain. Flash chromatographic separation/purifications were performed using a Biotage® Isolera system equipped with a Sfär HC Duo cartridge (5 g, 10 g, 25 g, 50 g, or 100 g). Reverse-phase purifications were performed a Biotage® Isolera system equipped with a Sfär C_{18} Duo cartridge (12 g or 30 g). HPLC purifications were conducted using an ACE® AQ 10 (C_{18}) column (250 × 21.2 mm i.d.) on a Shimadzu HPLC equipped with a DGU-20A degassing unit; a CBM-20A control module; two LC20-AR pumps; and an SPD20-A UV/Vis detector.

NMR-spectra were acquired using: a 2-channel Bruker AVIIIHD 400 machine equipped with a 5 mm BBFO probe (400 MHz for ^{1}H and 101 MHz for ^{13}C); a Brucker AVIIIHD 500 machine (500 MHz for ^{1}H and 126 for ^{13}C); or a Bruker AVIIIHD 600

with Prodigy broadband cryoprobe (600 MHz for ^{1}H and 151 MHz for ^{13}C). Chemical shifts are reported in ppm and were referenced to residual protio- and perdeuterio-solvent resonances (δ_H 7.26 and δ_C 77.16 for $CDCl_3$; δ_H 2.50 and δ_C 39.52 for DMSO; δ_H 3.31 and δ_C 49.00 for MeOD) as internal standards for ^{1}H NMR and ^{13}C NMR spectra, respectively. All NMR spectra were processed with MestReNova software v. 14.1.

LCMS (liquid chromatography/mass spectrometry) data were obtained using an Agilent 1200 series LC machine connected to an Agilent 6120 Quadrupole MS using electrospray ionization (ESI) machine. High resolution mass spectra were obtained using a Bruker μTOF (ESI) spectrometer. *m/z* Values are reported in Daltons. Specific rotations were measured using a Schmidt-Haensch UniPol polarimeter. Values are expressed in 10^{-1} deg cm^2 g^{-1}; concentrations (c) are quoted in g/100 mL; and D refers to the D-line of sodium (589 nm). Melting points were taken using a Stuart® SMP40 automatic melting point instrument. Lyophilisation was done using a Scanvac Coolsafe™ instrument. Infrared spectra were recorded on a Bruker Tensor27 FTIR spectrometer.

7.2 General Procedures

7.2.1 General Procedure A – Sulfa-Michael addition

To a stirred solution of 1,5-di-alkyl 3-methylidene-2-oxopentanedioate (1.00 eq.) in CH_2Cl_2 (0.2M) was added the appropriate thiol (1.10 eq.) and triethylamine (0.05 eq.). The reaction was stirred at rt o/n then diluted with CH_2Cl_2. The organic layer

was washed with sat. aq. $NaHCO_3$ then brine. The organic layer was dried over Na_2SO_4 then concentrated *in vacuo*. Purification by flash chromatography yielded the desired compound.

7.2.2 General Procedure B – *tert*-Butyl deprotection

The appropriate di-*tert*-butyl 3-alkyl/arylsulfido-2-oxopentanedioate (1.00 eq.) was dissolved in CH_2Cl_2 (0.20 M). TFA (20.0 eq.) was added, and the reaction was stirred until full conversion to the double-deprotected product was observed by TLC analysis. The solvent was removed *in vacuo,* then the residue dissolved in H_2O/MeCN and subjected to purification by reverse-phase chromatography to give the desired compound. NMR samples were prepared by converting a sample of the product to the disodium salt via dissolution in 100 mM NaOH (2 eq.), then lyophilising to dryness. The sample was then dissolved in D_2O and analysed by NMR.

7.2.3 General Procedure C – Amide coupling

Triethylamine (2 eq.) was added to the requisite acyl chloride (1 eq.) in CH_2Cl_2 (0.30 M), followed by addition of the requisite primary amine (1.1 eq.). The mixture was stirred at rt o/n. The reaction was then diluted with EtOAc; the resultant solution was washed with 1 N HCl, then brine. The organic phase was dried over Na_2SO_4, then concentrated *in vacuo*. Purification was achieved using flash chromatography to yield the desired compound.

7.2.4 General Procedure D – Oxidative sulfur insertion and ring closure[308]

Following a modified literature procedure,[308] a reaction vial was charged with CuI (0.3 eq.) and 1,10-phenanthroline (0.3 eq.). The atmosphere was purged with argon and anhydrous DMF (0.4 M) was added. The suspension was stirred at rt for 15 min, then the *N*-alkyl/aryl-2-halobenzamide (1 eq.), S_8 (1.3 eq.), and K_2CO_3 (1.3 eq.) were added. The suspension was stirred for a further 15 min at rt, then heated to 110 °C until full conversion of the starting material was observed (TLC, MS). The reaction was cooled to rt and diluted in brine. The resulting mixture was extracted with EtOAc. The combined organic phases were dried over Na_2SO_4, then concentrated *in vacuo*. Purification by flash chromatography yielded the desired compound.

7.3 Compound Synthesis

_N_-[(4_S_)-3-Oxo-1,2-oxazolidin-4-yl]-2-phenoxyacetamide (210)

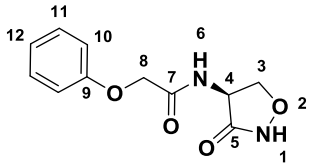

Following a modified version of a reported procedure[174], a solution of 2-phenoxyacetyl chloride (3.79 mL; 27.4 mmol) in THF (19.6 mL) was added drop-wise to a solution of (4*S*)-4-amino-1,2-oxazolidin-3-one (2.00 g; 19.6 mmol) in carbonate buffer (pH 10.3; 100 mM) (19.6 mL) that had been cooled to 0 °C. The reaction was allowed to warm to rt and stirred for 5 h. The mixture was extracted with EtOAc (3 × 50 mL). The combined organic phases were washed with brine (30 mL), then dried over Na_2SO_4. The organic phases were

concentrated *in vacuo* then purified by flash chromatography (0→60% EtOAc in cyclohexane, 0.1% formic acid) to give 3.23 g (70%) of **210** as a white solid.

Mp: 121-124 °C. **R_f**: 0.25 (3:2 EtOAc/cyclohexane). **$[\alpha]_D^{25}$** = 36.1 (c = 0.35, $CHCl_3$). **IR (neat): ν_{max} (cm^{-1})** 3317, 3183, 2971, 1720, 1696, 1444, 1242. **^{1}H NMR** (400 MHz, $CDCl_3$) δ 7.35 – 7.27 (m, 3H, H10, N*H*), 7.07 – 7.01 (m, 1H, H12), 6.95 – 6.90 (m, 2H, H11), 4.94 – 4.82 (m, 2H, H3), 4.53 (ABq, *J* = 14.0 Hz, 2H, H8), 4.15 – 4.08 (m, 1H, H4). **^{13}C NMR** (126 MHz, $CDCl_3$) δ 170.6 (C=O), 169.3 (C=O), 157.0 (C9), 129.9 (C10), 122.4 (C12), 114.8 (C11), 74.3 (C8), 67.1 (C3), 51.3 (C4). **HRMS** (ESI^+) *m*/*z* for $[C_{11}H_{13}N_2O_4]^+$ $[M+H]^+$ calculated 237.0870, found 237.0871. The spectroscopic data match those reported in the literature.[174]

5-[(4-Nitrophenyl)methoxy]-2,5-dioxopentanoic acid (172)

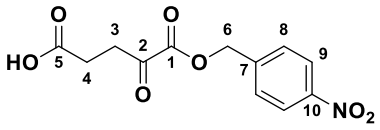

Following a reported procedure,[174] 2-oxopentanedioic acid (5.00 g; 34.0 mmol) and diisopropylamine (DIPA) (4.76 mL; 34.0 mmol) were dissolved in DMF (68.0 mL; 0.50 M) and heated to 50 °C. 1-(Bromomethyl)-4-nitrobenzene (9.00 g; 38.0 mmol) was added and the reaction was heated to 70 °C. The reaction was stirred for 2 h before being cooled to 40 °C. The reaction was diluted in sat. aq. NH_4Cl (100 mL), then extracted with EtOAc (3 × 100 mL). The combined organic phases were dried with Na_2SO_4 and concentrated *in vacuo*. Purification by flash chromatography (0→60% EtOAc in

cyclohexane, 0.1% formic acid) yielded 7.03 g (74%) of the desired compound as a pale-yellow solid.

Mp: 89-91 °C. **R_f.** 0.65 (1:1 EtOAc/cyclohexane, 1% formic acid). **IR (neat): ν_{max} (cm^{-1})** 3115, 3085, 2970, 2937, 2863, 1731, 1706, 1521, 1344, 1276, 1220, 1085. **^{1}H NMR** (400 MHz, DMSO) δ 8.29 – 8.25 (m, 2H, H9), 7.74 – 7.69 (m, 2H, H8), 5.42 (s, 2H, H6), 3.12 – 3.06 (m, 2H, H3), 2.55 – 2.52 (m, 2H, H4). **^{13}C NMR** (101 MHz, DMSO) δ 192.59 (C2), 173.8 (C=O), 163.5 (C=O), 147.8 (C10), 143.3 (C7), 129.3 (C8), 124.1 (C9), 66.2 (C6), 34.4 (C3), 28.0 (C4). **HRMS** (ESI^-) *m*/*z* for $[C_{12}H_{10}NO_7]^-$ $[M-H]^-$ calculated 280.0463, found 280.0462. The spectroscopic data match those reported in the literature.[174]

(4-Nitrophenyl)methyl 5-oxo-2-[(4*S*)-3-oxo-4-(2-phenoxyacetamido)-1,2-oxazolidin-2-yl]oxolane-2-carboxylate (211)[174]

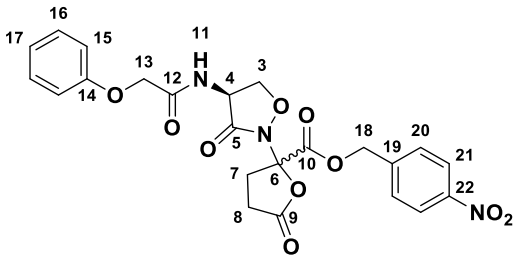

Following a reported procedure,[174] *N*-[(4*S*)-3-oxo-1,2-oxazolidin-4-yl]-2-phenoxyacetamide (200 mg; 0.85 mmol) and 5-[(4-nitrophenyl)methoxy]-2,5-dioxopentanoic acid (287 mg; 1.02 mmol) were dissolved in anhydrous CH_2Cl_2 (4.25 mL; 0.20 M) and cooled to 0 °C. *N*,*N*'-dicyclohexylmethanediimine (DCC) (210 mg; 1.02 mmol) was added and the reaction was allowed to warm to rt. The reaction was stirred at rt for 3 h, then filtered through a short plug of Celite®. The

filtrate was concentrated *in vacuo* then purified by flash chromatography (0→40% EtOAc in cyclohexane) to give 291 mg (57%) of **211** as a colourless oil.

R_f. 0.25 (1:1 EtOAc/cyclohexane). **IR (neat): ν_{max} (cm^{-1})** 2980, 2932, 1800, 1737, 1679, 1519, 1347, 1176, 1053. **^{1}H NMR** (500 MHz, DMSO) (1:1 mixture of diastereomers) δ 8.87 – 8.79 (m, 1H, NH), 8.26 (m, 2H, H21), 7.69 (d, J = 8.5 Hz, 2H, H20), 7.31 (m, 2H, H16), 7.01 – 6.96 (m, 3H, H17, H15), 5.50 – 5.37 (m, 2H, H18), 5.19 – 4.85 (m, 1H, H4), 4.71 – 4.53 (m, 2H, H13), 4.22 – 4.06 (m, 2H, H3), 3.04 – 2.96 (m, 1H, H7'), 2.84 – 2.65 (m, 3H, H7'', H8). **^{13}C NMR** (1:1 mixture of diastereomers) (126 MHz, DMSO) δ 175.0 (C=O), 172.4 (C=O), 170.3 (C=O), 168.9 (C=O), 158.0 (C14), 147.8 (C22), 143.1 (C18), 130.0 (C16), 129.3 (C21), 124.1 (C20), 121.8 (C17), 115.2 (C18), 91.8 (C6), 71.4 (C3), 67.2 (C18), 67.1 (C13), 51.3 (C4), 28.9 (C8), 27.7 (C7). **HRMS** (ESI^+) *m/z* calculated for $[C_{23}H_{22}N_3O_{10}]^+$ $(M+H)^+$ 500.1300, found 500.1301. The spectroscopic data match those reported in the literature.[174]

5-Oxo-2-[(4*S*)-3-oxo-4-(2-phenoxyacetamido)-1,2-oxazolidin-2-yl]oxolane-2-carboxylic acid (168)

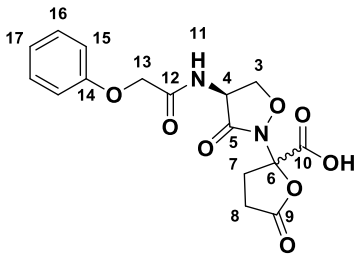

Following a modified version of a reported procedure, (4-nitrophenyl)methyl 5-oxo-2-[(4*S*)-3-oxo-4-(2-phenoxyacetamido)-1,2-oxazolidin-2-yl]oxolane-2-carboxylate (300 mg; 0.60 mmol) was dissolved in a 1:1 mixture of THF and H_2O (6 mL). The flask was purged with argon, then 10% Pd/C (150 mg) was added. H_2

was introduced into the mixture via a balloon and the reaction was stirred at rt for 30 min. $NaHCO_3$ (31 mg; 0.38 mmol) in H_2O (0.50 mL) was added and the reaction was stirred for a further 5 min. The mixture was filtered through Celite® and the filtrate was washed with H_2O (2 × 5 mL) Et_2O (2 × 5 mL). The aqueous phase was lyophilised to give 122 mg (56%) of the desired compound as a white solid.

Mp: 162-165 °C. **IR (neat): ν_{max} (cm^{-1})** 3059, 2941, 1780, 1723, 1649, 1493, 1378, 1192. (1:1 Mixture of diastereomers) **^{1}H NMR** (500 MHz, DMSO) δ 7.32 (m, 2H, H16), 7.07 – 6.94 (m, 3H, H17, H15), 4.99 – 4.86 (m, 1H, H4), 4.62 – 4.49 (m, 2H, H13), 4.45 – 4.35 (m, 1H, H3'), 4.14 – 3.89 (m, 1H, H3''), 2.99 – 2.86 (m, 1H, H7'), 2.57 – 2.44 (m, 2H, H8), 2.38 – 2.22 (m, 1H, H7''). **^{13}C NMR** (126 MHz, DMSO) δ 176.6 (C=O), 174.1 (C=O), 168.7 (C=O), 166.7 (C=O), 156.9 (C14), 130.0 (C15), 121.7 (C16), 115.2 (C17), 98.4 (C6), 71.3 (C3), 67.1 (C13), 52.7 (C4), 29.8 (C8), 28.8 (C7). **HRMS** (ESI$^-$) *m*/*z* for $[C_{16}H_{15}N_2O_8]^-$ [M-Na]$^-$ calculated 363.0834, found 363.0839. The spectroscopic data match those reported in the literature.[174]

(2*Z*)-2-([[1-(*tert*-Butoxy)-2-methyl-1-oxopropan-2-yl]oxy]imino)-2-(2-[[(*tert*-butoxy)carbonyl]amino]-1,3-thiazol-4-yl)acetic acid (216)

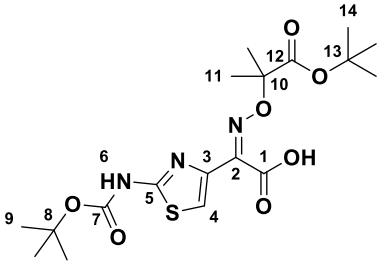

Following a modified version of a reported procedure[167], (2*Z*)-2-(2-amino-1,3-thiazol-4-yl)-2-([(1-(*tert*-butoxy)-2-methyl-1-oxopropan-2-yl)oxy]imino)acetic acid (4.00 g; 12.1 mmol),

triethylamine (3.38 mL; 24.3 mmol), and *N*,*N*-dimethylpyridin-4-amine (DMAP) (297 mg; 2.43 mmol) were dissolved in anhydrous $CHCl_3$ (12.1 mL) under an argon atmosphere. A solution of di-*tert*-butyl dicarbonate (5.30 g; 24.3 mmol) in anhydrous $CHCl_3$ (4 mL) was added drop-wise and the mixture was stirred at rt for 1 h. This addition was repeated every hour until 6 eq. of di-*tert*-butyl dicarbonate had been added. The mixture was then stirred at rt for 6 h. The reaction mixture was diluted in CH_2Cl_2 and washed with 0.1 N HCl (2 × 30 mL). The aqueous layer was acidified to pH 3 with 2 N HCl and back-extracted with CH_2Cl_2 (3 × 50 mL). The combined organic phases were washed with brine (20 mL) and dried over Na_2SO_4 before being concentrated *in vacuo*. Purification by flash chromatography (0→30% EtOAc/cyclohexane then 30→80% EtOAc in cyclohexane, 1% formic acid) yielded 2.16 g (42%) of **216** as a white solid.

Mp: 181-184 °C. **R_f**. 0.35 (1:1 EtOAc/cyclohexane, 1% formic acid). **IR (neat): ν_{max} (cm^{-1})** 2980, 2888, 1768, 1715, 1549, 1355, 1248, 1151. **^{1}H NMR** (400 MHz, $CDCl_3$) δ 8.11 (s, 1H, NH), 7.39 (s, 1H, H4), 1.60 (s, 6H, H11), 1.54 (s, 9H, C(CH_3)$_3$), 1.44 (s, 9H, C(CH_3)$_3$). **^{13}C NMR** (126 MHz, $CDCl_3$) δ 175.7 (C=O), 163.9 (C=O), 161.5 (C=O), 148.9 (C3), 140.9 (C2), 116.2 (C4), 83.7 (C10), 83.5 (C(CH_3)$_3$), 82.0 (C(CH_3)$_3$), 28.5 (C(CH_3)$_3$), 28.2 (C(CH_3)$_3$), 24.1 (C11). **HRMS** (ESI^+) *m*/*z* for $[C_{18}H_{28}O_7N_3S]^+$ $[M+H]^+$ calculated 430.1642, found 430.1638. The spectroscopic data match those reported in the literature.[167]

tert-Butyl 2-([(_Z_)-[(2-([(_tert_-butoxy)carbonyl]amino)-1,3-thiazol-4-yl)(([(4_S_)-3-oxo-1,2-oxazolidin-4-yl]carbamoyl))methylidene]amino]oxy)-2-methylpropanoate (218)[167]

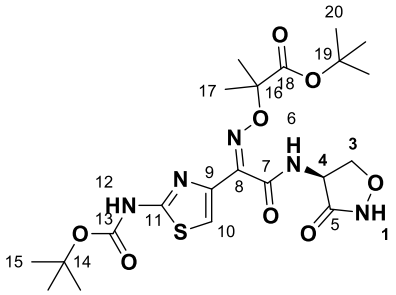

Following a modified reported procedure,[167] (_Z_)-2-(((1-(_tert_-butoxy)-2-methyl-1-oxopropan-2-yl)oxy)imino)-2-(2-((_tert_-butoxycarbonyl)-amino)thiazol-4-yl)acetic acid (2.10 g; 4.89 mmol) and _N_-hydroxysuccinimide (NHS) (619 mg; 5.38 mmol) were dissolved in anhydrous $CHCl_3$ (24.5 mL) and placed under an argon atmosphere. A solution of DCC (1.11 g; 5.38 mmol) in anhydrous $CHCl_3$ (5 mL) was added drop-wise. The reaction was stirred at rt for 90 min, before being filtered through a short plug of Celite®. The filtrate was concentrated _in vacuo_, then re-dissolved in anhydrous EtOH (24.5 mL). To this solution was added (4_S_)-4-amino-1,2-oxazolidin-3-one (549 mg; 5.38 mmol) and $NaHCO_3$ (456 mg; 5.43 mmol). The suspension was heated to reflux for 2 h before being hot-filtered through a short plug of Celite®. The filtrate was washed with sat. aq. $NaHCO_3$ (2 × 30 mL). The combined aqueous phases were acidified to pH 2 with 2 N HCl, then back-extracted with EtOAc (3 × 50 mL). The combined organic phases were washed with brine (20 mL) and dried over Na_2SO_4 then concentrated _in vacuo_. Purification by flash chromatography (0→50% EtOAc in CH_2Cl_2) yielded 856 mg (34% over 2 steps) of **218** as a white solid.

Mp: 207-211 °C. **R_f**. 0.20 (2:1 EtOAc/cyclohexane). **$[\alpha]_D^{25}$** = -13.0 (c = 0.25, $CHCl_3$). **IR (neat): ν_{max} (cm^{-1})** 2980, 2889, 1719, 1705, 1680, 1559, 1248, 1149. **^{1}H NMR** (400 MHz, DMSO) δ 11.80 (s, 1H, NH), 11.58 (s, 1H, NH), 8.97 (d, J = 8.5 Hz, 1H, NH), 7.41 (s, 1H, H10), 4.97 – 4.84 (m, 1H, H4), 4.59 (app. t, *J* = 8.5 Hz, 1H, H3'), 4.07 (app. t, *J* = 8.5 Hz, 1H, H3''), 1.47 (s, 9H, $C(CH_3)_3$), 1.40 (s, 6H, H17), 1.39 (s, 9H, $C(CH_3)_3$). **^{13}C NMR** (151 MHz, DMSO) δ 172.4 (C=O), 170.5 (C=O), 162.9 (C=O), 160.8 (C=O), 149.9 (C8), 142.5 (C9), 115.8 (C10), 82.4 (C16), 81.8 ($C(CH_3)_3$), 81.0 ($C(CH_3)_3$), 72.3 (C3), 51.7 (C4), 28.3 ($C(CH_3)_3$), 28.1 ($C(CH_3)_3$), 24.2 (C17). **HRMS** (ESI$^+$) *m/z* for $[C_{21}H_{32}O_8N_5S]^+$ $[M+H]^+$ calculated 514.1966, found 514.1965. The spectroscopic data match those reported in the literature.[167]

5-(Diphenylmethoxy)-4,5-dioxopentanoic acid (219)[167]

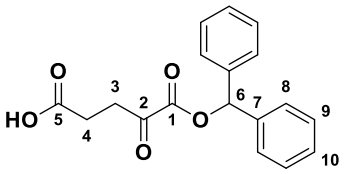

Following a reported procedure,[167] 2-oxopentanedioic acid (5.00 g; 34.0 mmol) and dicyclohexylamine (6.76 mL; 34.0 mmol) were dissolved in anhydrous DMF (34.0 mL; 1 M) and heated to 50 °C. Bromodiphenylmethane (9.39 g; 38.0 mmol) was added and the solution was heated to 70 °C for 2 h. The reaction mixture was filtered through Celite® then the filtrate was diluted in EtOAc (100 mL). The organic phase was washed with sat. aq. NH_4Cl (2 × 100 mL) followed by saturated brine solution (50 mL). The organic layer was dried over anhydrous $MgSO_4$ and then concentrated

in vacuo. Purification by flash chromatography (0→40% EtOAc in cyclohexane, 0.1% formic acid) gave 7.59 g (72%) of **219** as an off-white solid.

Mp: 107-110 °C. **R_f**. 0.60 (1:1 EtOAc/cyclohexane, 1% formic acid). **IR (neat): ν_{max} (cm^{-1})** 3063, 2995, 2914, 1827, 1732, 1448, 1243, 1189. **^{1}H NMR** (400 MHz, $CDCl_3$) δ 7.48 – 7.30 (m, 10 H, Ar-H), 6.98 (s, 1H, H6), 3.28 – 3.12 (m, 2H, H3), 2.85 – 2.65 (m, 2H, H4). **^{13}C NMR** (101 MHz, $CDCl_3$) δ 191.9 (C2), 177.4 (C=O), 159.5 (C=O), 138.8 (C7), 128.8 (Ar-CH), 128.5 (Ar-CH), 127.2 (Ar-CH), 79.3 (C6), 34.1 (C3), 27.3 (C4). **HRMS** (ESI$^+$) *m/z* for $[C_{18}H_{16}O_5Na]^+$ [M+Na]$^+$ calculated 335.0890, found 335.0892. The spectroscopic data match those reported in the literature.[167]

Diphenylmethyl 2-[(4*S*)-4-[(2*Z*)-2-([[1-(*tert*-butoxy)-2-methyl-1-oxopropan-2-yl]oxy]imino)-2-(2-[[(*tert*-butoxy)carbonyl]amino]-1,3-thiazol-4-yl)acetamido]-3-oxo-1,2-oxazolidin-2-yl]-5-oxooxolane-2-carboxylate (220)

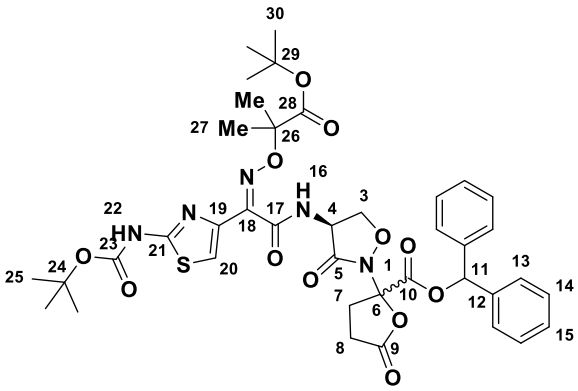

A reaction vial was charged with *tert*-Butyl 2-([(*Z*)-[(2-([(*tert*-butoxy)carbonyl]amino)-1,3-thiazol-4-yl)(([(4*S*)-3-oxo-1,2-oxazolidin-4-yl]carbamoyl))methylidene]amino]oxy)-2-methylpropanoate (850 mg; 1.66 mmol) and 5-(diphenylmethoxy)-4,5-dioxopentanoic acid (622 mg; 1.99 mmol) then the atmosphere was purged with argon. Anhydrous CH_2Cl_2 (16.6 mL; 0.10 M) was

added then the solution was cooled to 0 °C. A solution of DCC (411 mg; 1.99 mmol) in anhydrous CH_2Cl_2 (2 mL) was added drop-wise. The reaction was allowed to warm to rt and stirred for 3 h. The resulting mixture was filtered through a short plug of Celite® then the filtrate was concentrated *in vacuo*. Purification by flash chromatography (0→40% EtOAc in cyclohexane) yielded 962 mg (72%) of **220** as a pale-yellow solid.

Mp: 118-122 °C. **R_f**. 0.65 (1:1 EtOAc/cyclohexane). **IR (neat): ν_{max} (cm^{-1})** 3065, 2979, 2930, 1779, 1721, 1651, 1494, 1372, 1241, 1192. (1:1 mixture of diastereomers) **^{1}H NMR** (400 MHz, $CDCl_3$) δ 8.11 (s, 1H, NH), 7.95 (m, 1H, NH), 7.34 – 7.21 (m, 11H, Ar-H, H20), 6.92 (d, *J* = 5.5 Hz, 1H, H11), 5.07 – 4.60 (m, 2H, H3), 4.16 – 4.00 (m, 1H, H4), 3.29 – 3.12 (m, 1H, H7'), 2.79 – 2.65 (m, 1H, H8'), 2.52 – 2.39 (m, 1H, H8''), 2.34 – 2.24 (m, 1H, H7''), 1.51 (s, 6H, H27), 1.46 (s, 9H, $C(CH_3)_3$), 1.36 (s, 9H, $C(CH_3)_3$). **^{13}C NMR** (151 MHz, $CDCl_3$) δ 173.9 (C=O), 173.6 (C=O), 171.2 (C=O), 170.1 (C=O), 164.6 (C=O), 163.0 (Ar-C), 162.9 (C=O), 159.6 (C18), 148.7 (Ar-C), 138.6 (Ar-C), 128.7 (Ar-C), 128.4 (Ar-CH), 127.4 (Ar-CH), 127.0 (Ar-CH), 92.8 (C6), 83.2 (C26), 83.1 ($C(CH_3)_3$), 82.4 ($C(CH_3)_3$), 80.0 (C11), 71.4 (C3), 52.4 (C4), 28.6 (C8), 28.2 ($C(CH_3)_3$), 28.0 ($C(CH_3)_3$), 27.4 (C7), 23.9 (C27). **HRMS** (ESI^+) *m*/*z* for $[C_{39}H_{46}O_{12}N_5S]^+$ $[M+H]^+$ calculated 808.2858, found 808.2847.

2-[(4*S*)-4-[(2*Z*)-2-(2-amino-1,3-thiazol-4-yl)-2-[(1-carboxy-1-methylethoxy)imino]acetamido]-3-oxo-1,2-oxazolidin-2-yl]-5-oxooxolane-2-carboxylic acid (180)[167]

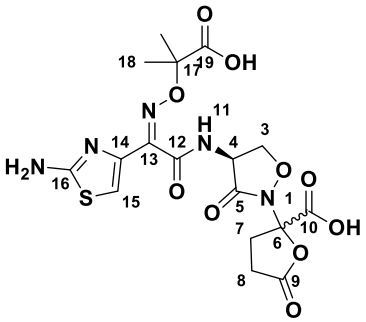

Following a modified reported procedure,[167] diphenylmethyl 2-[(4*S*)-4-[(2*Z*)-2-([[1-(*tert*-butoxy)-2-methyl-1-oxopropan-2-yl]oxy]imino)-2-(2-[[(*tert*-butoxy)carbonyl]amino]-1,3-thiazol-4-yl)acetamido]-3-oxo-1,2-oxazolidin-2-yl]-5-oxooxolane-2-carboxylate (200 mg; 248 μmol) was dissolved in a mixture of THF (5.00 mL) and phosphate buffer (100 mM; pH 7) (2.50 mL). The mixture was cooled to 0 °C and 10% (*w*/*w*) Pd/C (180 mg) was added to the mixture. The reaction flask was then purged with argon. H_2 was introduced into the mixture via a balloon, and the reaction was stirred at 0 °C for 45 min. The mixture was diluted in H_2O and filtered through Celite®. The filtrate was acidified to pH 2 with 1 N HCl and extracted with EtOAc (3 × 15 mL). The combined organic phases were washed with brine (5 mL) and dried over Na_2SO_4. The solvent was removed *in vacuo* to give a pale-yellow oil, which was placed under high-vacuum o/n. The oil was then placed under an argon atmosphere and re-dissolved in anhydrous CH_2Cl_2 (3.54 mL). The solution was cooled to -40 °C, then BCl_3 (1 M in CH_2Cl_2) (496 L; 496 μmol) was added drop-wise. The reaction was stirred at -40 °C for 2 h and then was allowed to warm to 0 °C. A solution of $NaHPO_4$ (500 μL; 0.25 M) was added to the mixture followed by a solution of $NaHCO_3$ (500 μL; 0.25 M). The mixture was stirred at 0 °C for 3 min then the aqueous and organic

phases were separated. The organic phases were washed with H_2O (2 × 1 mL) and then the combined aqueous phase was lyophilised. Purification by HPLC (solvent A: 0.1% (*v*/*v*) TFA in acetonitrile, solvent B: 0.1% (*v*/*v*) TFA in H2O. Flow rate: 17 mL min^{-1}. Gradient: 2%→40% A/B over 30 min, then 40%→99% A/B over 10 min. Elution at 12 min) yielded 27 mg (23% over 2 steps) of **180** as a lyophilised white solid.

IR (neat): ν_{max} (cm^{-1}) 2988, 2928, 1780, 1724, 1372, 1241, 1192. **^{1}H NMR** (400 MHz, D_2O) (1:1 mixture of diastereomers) δ 7.10 (s, 1H, H15), 5.22 – 5.09 (m, 1H, H3), 4.82 – 4.58 (m, 1H, H3'), 4.32 – 4.20 (m, 1H, H4), 3.03 (m, 1H, H7'), 2.92 – 2.78 (m, 1H, H8'), 2.71 – 2.58 (m, 1H, H8''), 2.44 (m, 1H, H7''), 1.48 (s, 6H, H18). **^{13}C NMR** (101 MHz, D_2O) δ 177.5 (C=O), 174.9 (C=O) 174.4 (C=O), 172.5 (C=O), 168.8 (C16), 161.6 (C=O), 145.8 (C13), 142.0 (C14), 111.8 (C15), 95.8 (C6), 81.0 (C17), 72.6 (C3), 49.8 (C4), 30.7 (C8), 27.7 (C7), 24.3 (C18). **HRMS** (ESI^+) *m*/*z* for $[C_{17}H_{20}O_{10}N_5S]^+$ $[M+H]^+$ calculated 486.0925, found 486.0926. The spectroscopic data match those reported in the literature.[167]

1,2-Oxazolidin-3-one (224)[170]

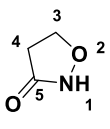

Following a modified reported procedure,[170] 3-chloropropionic acid (1.09 g; 10 mmol) was dissolved in Et_2O (30.0 mL) and cooled to 0 °C. *N*-methylmorpholine (NMM) (1.43 ml; 13.0 mmol) was added followed by the drop-wise addition of ethyl chloroformate (1.15 mL; 12.0 mmol). The reaction was stirred

at 0 °C for 15 min and then filtered through sintered glass. To the filtrate was added freshly prepared[200] hydroxylamine (495 mg; 15.0 mmol) in MeOH (14.0 mL). The reaction was stirred for 15 min before being concentrated *in vacuo*. The residue was dissolved in aq. NaOH (0.25 M; 80.0 mL) and heated to 50 °C for 15 min. The mixture was concentrated *in vacuo* to 10% of its original volume and acidified to pH 1 with 2N HCl. The aqueous layer was extracted with EtOAc and dried over $MgSO_4$. The organic layer was concentrated *in vacuo* to give 561 mg (72%) of **224** as a colourless oil, which was used without further purification.

R_f. 0.30 (1:1 EtOAc/cyclohexane). **IR (neat): ν_{max} (cm^{-1})** 2965, 2912, 1683, 1559, 1540, 1507, 1287. **^{1}H NMR** (400 MHz, DMSO) δ 11.03 (s, 1H, NH), 4.28 (t, *J* = 8.5 Hz, 2H, H3), 2.62 (t, *J* = 8.5 Hz, 2H, H4). **^{13}C NMR** (101 MHz, DMSO) δ 174.3 (C5), 69.0 (C3), 33.4 (C4). **HRMS** (ESI^+) *m/z* for $[C_3H_5NO_2]^+$ $[M+H]^+$ calculated 88.0393, found 88.0397. The spectroscopic data match those reported in the literature.[170]

(4-Nitrophenyl)methyl 5-oxo-2-(3-oxo-1,2-oxazolidin-2-yl)oxolane-2-carboxylate (226)

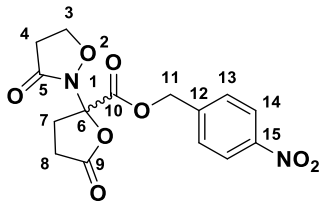

1,2-Oxazolidin-3-one (50.0 mg; 0.57 mmol) and 5-[(4-nitrophenyl)methoxy]-2,5-dioxopentanoic acid (177 mg; 0.63 mmol) were dissolved in anhydrous CH_2Cl_2 under argon. DCC (130 mg; 0.63 mmol) was added then the reaction was stirred at rt o/n. The reaction was filtered through a short plug of Celite® then the filtrate was

concentrated *in vacuo*. Purification by flash chromatography (0→45% EtOAc in cyclohexane) yielded 168 mg (89%) of **226** as a colourless oil.

R_f. 0.40 (1:1 EtOAc/cyclohexane). **IR (neat): ν_{max} (cm^{-1})** 3043, 2944, 2685, 1729, 1699, 1608, 1520, 1347. **^{1}H NMR** (400 MHz, $CDCl_3$) δ 8.27 – 8.19 (m, 2H, H13), 7.60 – 7.51 (m, 2H, H14), 5.43 – 5.33 (m, 2H, H11), 4.41 (t, *J* = 8.0 Hz, 2H, H3), 3.08 (m, 1H, 7'), 2.92 – 2.77 (m, 3H, H4, H8'), 2.59 (m, 1H, 8''), 2.44 (m, 1H, 7''). **^{13}C NMR** (101 MHz, $CDCl_3$) δ 173.8 (C=O), 173.7 (C=O), 165.4 (C=O), 148.1 (C15), 141.5 (C12), 128.9 (C14), 123.9 (C13), 91.6 (C6), 67.3 (C11), 67.1 (C3), 33.9 (C4) 29.5 (C7), 27.5 (C8). **HRMS** (ESI^+) *m*/*z* for $[C_{15}H_{15}N_2O_8]^+$ $[M+H]^+$ calculated 351.0823, found 351.0823.

5-Oxo-2-(3-oxo-1,2-oxazolidin-2-yl)oxolane-2-carboxylic acid (223)

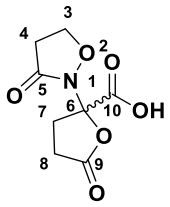

(4-Nitrophenyl)methyl 5-oxo-2-(3-oxo-1,2-oxazolidin-2-yl)oxolane-2-carboxylate (74.0 mg; 0.21 mmol) was dissolved in THF/H_2O (1:1, 2.1 mL) and the atmosphere was purged with argon. 10% (*w*/*w*) Pd/C (70.0 mg) was added, then H_2 was introduced under balloon pressure into the reaction at rt for 4 h. A solution of $NaHCO_3$ (18.0 mg; 0.21 mmol) in H_2O (500 μL) was added and the reaction was stirred vigorously for 5 min. The reaction was filtered through a short plug of Celite® then the filtrate was diluted in Et_2O. The aqueous layer was separated then the organic layer washed with H_2O (2 × 2 mL). The combined aqueous layers were lyophilised and purified by reverse-phase

chromatography (0→100% MeCN + 0.1% formic acid in H_2O + 0.1% formic acid) to give 13 mg (29%) of **223** as a colourless oil.

IR (neat): ν_{max} (cm^{-1}), 2982, 2685, 1761, 1731, 1671, 1595, 1517, 1347. **^{1}H NMR** (400 MHz, D_2O) δ 3.93 – 3.85 (m, 2H, H3), 3.25 – 3.19 (m, 2H, H4), 2.80 – 2.66 (m, 2H, H7', H8'), 2.62 – 2.46 (m, 1H, H7'', H8''). **^{13}C NMR** (101 MHz, $CDCl_3$) δ 177.4 (C=O), 173.2 (C=O), 172.4 (C=O), 96.1 (C6) 66.6 (C3), 33.0 (C4), 30.9 (C7), 27.7 (C8). **HRMS** (ESI^+) *m/z* for $[C_9H10NO_7]^+$ $[M+H]^+$ calculated 216.0503, found 216.0503.

Diphenylmethyl 5-oxo-2-(3-oxo-2,3-dihydro-1,2-benzoxazol-2-yl)oxolane-2-carboxylate (237a)

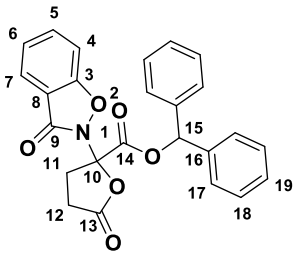

2,3-Dihydro-1,2-benzoxazol-3-one (300 mg; 2.22 mmol) and 5-(diphenylmethoxy)-4,5-dioxopentanoic acid (830 mg; 2.66 mmol) were dissolved in anhydrous CH_2Cl_2 (11.0 mL) then cooled to 0 °C. DCC (549 mg; 2.66 mmol) was added then the reaction was allowed to warm to rt. The reaction was stirred at rt for 4 h before being filtered through a short plug of Celite®. The filtrate was concentrated *in vacuo* and purified by flash chromatography (0→30% EtOAc in cyclohexane) to give 642 mg (67%) of **237a** as a viscous white gum.

R_f. 0.75 (1:1 EtOAc/cyclohexane). **IR (neat): ν_{max} (cm^{-1})** 3033, 2932, 1802, 1731, 1520, 1237, 1177, 1053. **^{1}H NMR** (400 MHz, DMSO) δ 7.92 – 7.83 (m, 1H, Ar-H), 7.53 – 7.18 (m, 13H, Ar-H), 6.93 (s, 1H, H15), 3.57 – 3.45 (m, 1H, H11'), 3.31 – 3.25 (m, 1H, H12'),

3.04 – 2.89 (m, 1H, H12''), 2.84 – 2.67 (m, 1H, H11''). **^{13}C NMR** (101 MHz, DMSO) δ 174.7 (C=O), 166.5 (C=O), 162.3 (C=O), 139.6 (Ar-C), 139.5 (Ar-C), 137.0 (Ar-C), 129.2 (Ar-CH), 129.1 (Ar-CH), 128.6 (Ar-CH), 128.6 (Ar-CH), 127.1 (Ar-CH), 127.0 (Ar-CH), 126.8 (Ar-CH), 93.5 (C10), 80.0 (C15), 29.2 (C11), 27.5 (C12). **HRMS** (ESI$^+$) *m*/*z* for $[C_{19}H_{20}NO_6]^+$ $[M+H]^+$ calculated 430.1285, found 430.1286.

Diphenylmethyl 5-oxo-2-(3-oxo-2,3-dihydro-1,2-benzothiazol-2-yl)oxolane-2-carboxylate (237b)

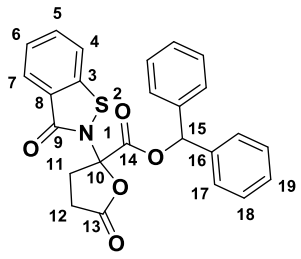

2,3-Dihydro-1,2-benzothiazol-3-one (500 mg; 3.30 mmol) and 5-(diphenylmethoxy)-4,5-dioxopentanoic acid (1.24 g; 4.00 mmol) were dissolved in anhydrous CH_2Cl_2 (16.0 mL) and cooled to 0 °C. DCC (825 mg; 4.00 mmol) was added and the reaction was allowed to warm to rt. The reaction was stirred o/n before being filtered through a short plug of Celite®. The filtrate was concentrated *in vacuo* and purified by flash chromatography (0→35% EtOAc in cyclohexane) to give 798 mg (54%) of **237b** as an off-white solid.

Mp: 173-176°C. **R$_f$**. 0.46 (1:2 EtOAc/cyclohexane). **IR (neat): ν_{max} (cm^{-1})** 3124, 2998, 2922, 1797, 1765, 1685, 1452, 1301, 1183, 1046. **^{1}H NMR** (600 MHz, DMSO) δ 8.07 (dt, *J* = 8.2, 0.9 Hz, 1H, H4), 7.90 (dt, *J* = 7.8, 1.0 Hz, 1H, H7), 7.79 (ddd, *J* = 8.3, 7.1, 1.3 Hz, 1H, H5), 7.51 (ddd, *J* = 8.0, 7.1, 1.0 Hz, 1H, H6), 7.36 – 7.21 (m, 10H, Ar-H), 6.90 (s, 1H, H15), 3.18 – 3.09 (m, 1H, H11'), 2.96 – 2.85 (m, 2H, H12), 2.77 – 2.70 (m, 1H,

H11''). **^{13}C NMR** (151 MHz, DMSO) δ 174.4 (C=O), 165.8 (C=O), 165.7 (C=O), 141.8 (Ar-C), 139.8 (Ar-C), 133.6 (C5), 128.9 (Ar-CH), 126.9 (Ar-CH), 126.7 (Ar-CH), 126.6 (Ar-C), 126.4 (C7), 124.4 (C6), 122.8 (C4), 91.8 (C10), 79.4 (C15), 31.4 (C11), 27.60 (C12). **HRMS** (ESI$^+$) *m/z* for $[C_{25}H_{20}NO_5S]^+$ $[M+H]^+$ calculated 446.1057, found 446.1056.

Diphenylmethyl 5-oxo-2-(1,1,3-trioxo-2,3-dihydro-1λ^6,2-benzothiazol-2-yl)oxolane-2-carboxylate (237e)

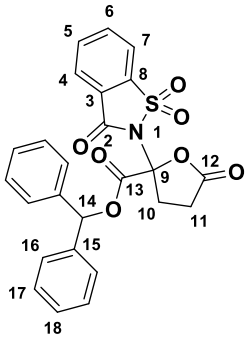

Saccharin (200 mg; 1.10 mmol) and 5-(diphenylmethoxy)-4,5-dioxopentanoic acid (286 mg; 0.92 mmol) were dissolved in anhydrous DMF (1.3 mL; 0.75 M) then cooled to 0 °C. DCC (208 mg; 1.01 mmol) was added then the reaction was stirred at rt o/n. The reaction was filtered through a short plug of Celite® then the filtrate was concentrated *in vacuo*. Purification by flash chromatography (0→30% EtOAc in cyclohexane) yielded 334 mg (70%) of **237e** as a colourless oil.

R_f. 0.75 (EtOAc/cyclohexane). **IR (neat): ν_{max} (cm^{-1})** 3058, 2979, 2886, 1804, 1761, 1730, 1510, 1366, 1182, 1124, 1060. **^{1}H NMR** (400 MHz, $CDCl_3$) δ 7.94 – 7.88 (m, 1H, Ar-H), 7.86 – 7.80 (m, 2H, Ar-H), 7.79 – 7.73 (m, 1H, Ar-H), 7.37 – 7.21 (m, 10H, Ar-H), 6.90 (s, 1H, H14), 3.41 – 3.31 (m, 1H, H10'), 3.28 (ddd, *J* = 6.7, 5.0, 1.4 Hz, 1H, H11'), 3.12 (t, *J* = 6.5 Hz, 1H, H11''), 2.64 (dd, *J* = 8.2, 4.5 Hz, 1H, H10''). **^{13}C NMR** (101 MHz, DMSO) δ 175.9 (C=O), 167.4 (C=O), 158.3 (C=O), 140.5 (Ar-C), 139.3 (Ar-C),

134.8 (Ar-CH), 133.3 (Ar-CH), 128.7 (Ar-CH), 128.6 (Ar-C), 126.9 (Ar-CH), 125.7 (Ar-CH), 123.4 (Ar-CH), 94.5 (C9), 78.8 (C14), 31.6 (C10), 27.3 (C11). **HRMS** (ESI^+) *m*/*z* for $[C_{25}H_{20}NO_7S]^+$ $[M+H]^+$ calculated 478.0955, found 478.0956.

1-Methyl-2,3-dihydro-1*H*-indazol-3-one (240)[309]

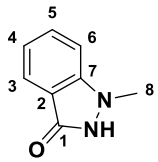

To a stirred solution of 3-indazolinone (100 mg; 0.74 mmol) in THF/H_2O (2:1 *v*/*v*; 7.40 mL; 0.10 M) was added formaldehyde (2 M in H_2O; 3.70 mL; 7.4 mmol). The reaction was cooled to 0 °C then sodium cyanoborohydride (47 mg; 0.74 mmol) was added. The reaction was stirred at rt for 3 days, then quenched with sat. aq. NH_4Cl (15 mL). The aqueous phase was extracted with CH_2Cl_2 (3 × 20 mL) then the combined organic phases were dried over Na_2SO_4 then concentrated *in vacuo*. Purification by flash chromatography (0→8% MeOH in CH_2Cl_2) yielded 58 mg (53%) of **240** as a white solid.

R_f. 0.45 (7% MeOH in CH_2Cl_2). **^{1}H NMR** (400 MHz, $CDCl_3$) δ 7.78 (d, *J* = 8.1 Hz, 1H, Ar-H), 7.45 – 7.41 (m, 1H, Ar-H), 7.29 – 7.21 (m, 1H, Ar-H), 7.12 – 7.06 (m, 1H, Ar-H), 3.85 (s, 3H, H8). **^{13}C NMR** (101 MHz, $CDCl_3$) δ 156.5 (C1), 142.2 (Ar-C), 128.6 (Ar-CH), 121.2 (Ar-CH), 112.7 (Ar-C), 108.8 (Ar-CH), 34.8 (C8). **HRMS** (ESI^+) *m*/*z* for $[C_8H_9N_2O]^+$ $[M+H]^+$ calculated 149.0710, found 149.0709. The spectroscopic data match those reported in the literature.[309]

Diphenylmethyl 2-(1,3-dioxo-2,3-dihydro-1*H*-isoindol-2-yl)-5-oxooxolane-2-carboxylate (237f)

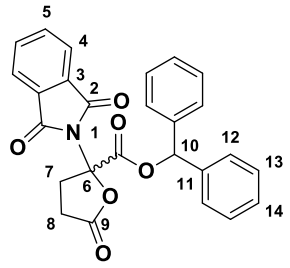

Phthalimide (200 mg; 1.36 mmol) and 5-(diphenylmethoxy)-4,5-dioxopentanoic acid (635 mg; 2.04 mmol) were dissolved in anhydrous CH_2Cl_2 (6.80 mL; 0.2 M) then cooled to 0 °C. DCC (421 mg; 2.04 mmol) was added then the reaction was allowed to warm to rt. The reaction was stirred o/n then filtered through a short plug of Celite®. The filtrate was concentrated *in vacuo* then purified by flash chromatography (0→45% EtOAc in cyclohexane) to give 539 mg (90%) of **237f** as a white solid.

Mp: 181-184°C. **IR (neat): ν_{max} (cm^{-1})** 3063, 2981, 2889, 1801, 1765, 1729, 1507, 1369, 1182, 1140, 1054. ^{1}H NMR (400 MHz, $CDCl_3$) δ 7.85 – 7.72 (m, 2H, Ar-H), 7.41 – 7.16 (m, 12H, Ar-H), 7.02 (s, 1H, H10), 3.77 – 3.65 (m, 1H, H7'), 3.13 – 2.95 (m, 1H, H8'), 2.74 – 2.50 (m, 1H, H8''), 2.44 – (m, 1H, H7''). ^{13}C NMR (101 MHz, $CDCl_3$) δ 174.3 (C=O), 166.7 (C=O), 166.2 (C=O), 138.8 (Ar-C), 135.0 (Ar-CH), 131.2 (Ar-C), 128.6(Ar-CH), 127.6 (Ar-CH), 127.1 (Ar-CH), 124.0 (Ar-CH), 88.5 (C6), 79.7 (C10), 28.7 (C7), 27.9 (C8). **HRMS** (ESI$^+$) *m*/*z* for $[C_{26}H_{20}NO_6]^+$ $[M+H]^+$ calculated 442.1285, found 442.1283.

5-Oxo-2-(3-oxo-2,3-dihydro-1,2-benzoxazol-2-yl)oxolane-2-carboxylic acid (236a)

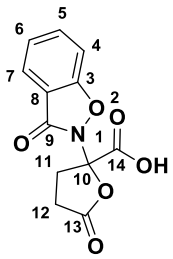

Diphenylmethyl 5-oxo-2-(3-oxo-2,3-dihydro-1,2-benzoxazol-2-yl)oxolane-2-carboxylate (100 mg; 0.23 mmol) was dissolved in CH_2Cl_2 (1.15 mL; 0.20 M). TFA (54.0 μL; 0.69 mmol) was added and the reaction was stirred at rt for 7 h. The solvent and TFA were removed *in vacuo* and the crude residue purified by HPLC (ACE AQ 10 (C18), flow rate 15 mL/min, 10→55% MeCN + 0.1% formic acid/H_2O + 0.1% formic acid) to give 25 mg (41%) of **236a** as a while lyophilised powder.

IR (neat): ν_{max} (cm^{-1}) 2981, 2972, 1716, 1643, 1553, 1406, 1276, 1255, 1288. **^{1}H NMR** (600 MHz, DMSO) δ 8.02 (dd, *J* = 8.2, 0.9 Hz, 1H, H4), 7.89 (dt, *J* = 7.9, 1.0 Hz, 1H, H6), 7.76 (dd, *J* = 8.3, 7.1, Hz, 1H, H7), 7.49 (ddd, *J* = 8.0, 7.1, 1.0 Hz, 1H, H5), 3.00 (ddd, *J* = 13.2, 9.4, 7.7 Hz, 1H, H11'), 2.93 – 2.82 (m, 2H, H12), 2.77 (ddd, *J* = 17.7, 9.5, 7.7 Hz, 1H, H11''). **^{13}C NMR** (151 MHz, DMSO) δ 174.9 (C=O), 172.8 (C=O) 165.5 (C=O), 141.7 (Ar-C), 133.5 (Ar-C), 126.5 (Ar-CH), 126.3 (Ar-CH), 124.6 (Ar-CH), 122.6 (Ar-CH), 99.7 (C10), 31.7 (C12), 28.0 (C11). **HRMS** (ESI$^+$) *m*/*z* for $[C_{12}H_9NO_6]^+$ $[M+H]^+$ calculated 264.0514, found 264.0509.

5-Oxo-2-(3-oxo-2,3-dihydro-1,2-benzothiazol-2-yl)oxolane-2-carboxylic acid (236b)

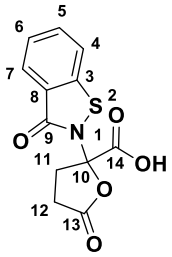

Diphenylmethyl 5-oxo-2-(3-oxo-2,3-dihydro-1,2-benzothiazol-2-yl)oxolane-2-carboxylate (150 mg; 0.33 mmol) was dissolved in CH_2Cl_2 (3.30 mL; 0.10 M). TFA (76.0 μL; 0.99 mmol) was added and the solution stirred at rt for 3 h. The solvent and TFA were removed *in vacuo* and the crude residue was purified by HPLC (ACE AQ 10 (C18), flow rate 15 mL/min, 10→60% MeCN + 0.1% formic acid/H_2O + 0.1% formic acid) to give 35 mg (38%) of **236b** as a while lyophilised powder.

IR (neat): ν_{max} (cm^{-1}) 3011, 2980, 2934, 1716, 1682, 1201, 1141. **^{1}H NMR** (400 MHz, DMSO) δ 8.87 (dd, *J* = 7.7, 1.6 Hz, 1H, H4), 7.58 (dd, *J* = 7.3, 1.8 Hz, 1H, H7), 7.49 (td, *J* = 7.3, 1.7 Hz, 1H, H6), 7.42 (td, *J* = 7.5, 1.8 Hz, 1H, H5), 2.80 (m, 1H, H11'), 2.63 (m, 1H, H12'), 2.63 – 2.51 (m, 2H, H11'', H12''). **^{13}C NMR** (101 MHz, DMSO) δ 177.3 (C=O), 171.0 (C=O), 168.5 (C=O), 143.2 (Ar-C), 132.9 (Ar-C), 127.3 (Ar-CH), 126.2 (Ar-CH), 125.7 (Ar-CH), 121.1 (Ar-CH), 99.9 (C10), 32.1 (C12), 27.9 (C11). **HRMS** (ESI$^+$) *m*/*z* for $[C_{12}H_{10}NO_5S]^+$ $[M+H]^+$ calculated 280.0274, found 280.0274.

2-(1,3-Dioxo-2,3-dihydro-1*H*-isoindol-2-yl)-5-oxooxolane-2-carboxylic acid (236f)

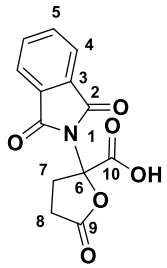

Diphenylmethyl 2-(1,3-dioxo-2,3-dihydro-1*H*-isoindol-2-yl)-5-oxooxolane-2-carboxylate (250 mg; 0.57 mmol) was dissolved in CH_2Cl_2 (5.70 mL; 0.10 M). TFA (87.0 μL; 1.14 mmol) was added and the solution was stirred at rt for 5 h. The solvent and TFA were removed *in vacuo* and the crude residue was purified by HPLC (ACE AQ 10 (C18), flow rate 15 mL/min, 10→60% MeCN + 0.1% formic acid/H_2O + 0.1% formic acid) to give 66 mg (42%) of **236f** as a white lyophilised powder.

IR (neat): ν_{max} (cm^{-1}) 3093, 2981, 1803, 1784, 1621, 1396, 1347, 1210, 1138. **^{1}H NMR** (600 MHz, DMSO) δ 7.99 – 7.90 (m, 4H, Ar-H), 3.60 (ddd, *J* = 13.8, 9.7, 5.0 Hz, 1H, Ar-H), 2.87 (ddd, *J* = 17.6, 9.6, 8.0 Hz, 1H, H7'), 2.78 – 2.63 (m, 2H, H7'', H8'), 2.58 (ddd, *J* = 13.8, 9.6, 8.0, 2Hz, 1H, H8''). **^{13}C NMR** (151 MHz, DMSO) δ 175.6 (C=O), 168.6 (C=O), 167.2 (C=O), 135.9 (Ar-C), 131.2 (Ar-CH), 124.2 (Ar-CH), 89.2 (C6), 28.9 (C7), 28.2 (C8). **HRMS** (ESI^+) *m*/*z* for $[C_{13}H_{19}NO_6Na]^+$ $[M+Na]^+$ calculated 298.0322, found 298.0323.

***N*-[(4*S*)-2-(2-methyl-5-oxooxolan-2-yl)-3-oxo-1,2-oxazolidin-4-yl]-2-phenoxyacetamide (242)**

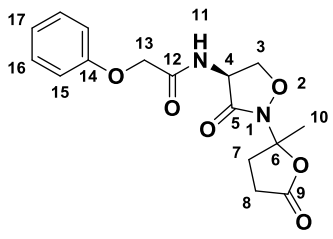

(*S*)-*N*-(3-Oxoisoxazolidin-4-yl)-2-phenoxyacetamide (118 mg; 0.50 mmol) and levulinic acid (64 mg; 0.55 mmol) were dissolved in anhydrous CH_2Cl_2 (2.50 mL; 0.20 M).

DCC (113 mg; 0.55 mmol) was added and the reaction was stirred at rt for 2 h. The reaction was filtered through a short plug of Celite® and the filtrate was concentrated *in vacuo*. Purification by flash chromatography (0→40% EtOAc in cyclohexane) yielded 92 mg (65%) of **242** as an amber oil.

R_f. 0.45 (1:2 EtOAc/cyclohexane). **IR (neat): ν_{max} (cm^{-1})** 3318, 2980, 2933, 2859, 1742, 1707, 1663, 1537, 1362, 1281, 1220, 1169. **^{1}H NMR** (400 MHz, $CDCl_3$, 1:1 mixture of diastereomers) δ 7.39 – 7.27 (m, 2H, H16), 7.05 (tt, *J* = 7.5, 1.1 Hz, 1H, H17), 6.98 – 6.89 (m, 2H, H15), 5.04 – 5.00 (m, 2H, H3), 4.90 (t, *J* = 8.5 Hz, 1H, H4), 4.56 (ABq, *J* = 12.5 Hz, 2H, H13), 4.22 (dd, *J* = 11.3, 8.5 Hz, 1H, H8'), 3.14 – 2.95 (m, 2H, H7), 2.90 – 2.79 (m, 1H, H8''), 2.21 (s, 3H, H10). **^{13}C NMR** (101 MHz, $CDCl_3$) δ 174.4 (C=O), 169.1 (C=O), 166.1 (C=O), 156.9 (C14), 129.9 (Ar-CH), 122.5 (Ar-CH), 114.7 (Ar-CH), 93.9 (C6), 71.9 (C4), 67.1 (C13), 52.3 (C3), 36.8 (C8), 29.8 (C7), 29.4 (C10). **HRMS** (ESI^+) *m*/z for $[C_{16}H_{19}N_2O_6]^+$ $[M+H]^+$ calculated 335.1238, found 335.1238.

Methyl (2*S*,3*R*)-3-hydroxy-2-(2-phenoxyacetamido)butanoate (261)

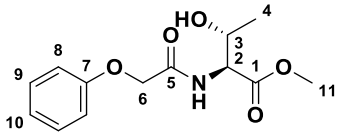

2-Phenoxyacetic acid (5.00 g; 32.9 mmol) and DIPEA (17.2 mL; 98.6 mmol) were dissolved in anhydrous DMF (66.0 mL; 0.50 M). HOBt (6.66 g; 49.3 mmol) and EDCI (9.45 g; 39.4 mmol) were added then the reaction was stirred at rt for 5 min. Methyl (2*S*,3*R*)-2-amino-3-hydroxybutanoate hydrochloride (6.69 g; 39.4 mmol) was added then the reaction was stirred for 4 h. The reaction was diluted in EtOAc (150 mL) and washed with

1 N HCl (3 × 100 mL), then sat. aq. $NaHCO_3$ (2 × 100 mL), then brine (50 mL). The organic layer was dried over Na_2SO_4 and concentrated *in vacuo*. Purification by flash chromatography (0→75% EtOAc in cyclohexane) yielded 6.94 g (79%) of **261** as a colourless oil.

R_f. 0.30 (1:1 EtOAc/cyclohexane). **$[\alpha]_D^{25}$** = 5.8 (c = 0.7, $CHCl_3$) **IR (neat): ν_{max} (cm^{-1})** 2979, 1741, 1663, 1527, 1493, 1209. **^{1}H NMR** (400 MHz, $CDCl_3$) δ 7.35 – 7.28 (m, 3H, Ar-H, NH), 7.01 (tt, J = 7.0, 1.0 Hz, 1H, Ar-H), 6.97 – 6.93 (m, 2H, Ar-H), 4.64 (dd, J = 9.0, 2.5 Hz, 1H, H2), 4.56 (s, 2H, H6), 4.42 – 4.34 (m, 1H, H3), 3.74 (s, 3H, H11), 2.59 (d, J = 5.0 Hz, 1H, OH), 1.17 (d, J = 6.5 Hz, 3H, H4). **^{13}C NMR** (101 MHz, $CDCl_3$) δ 171.1 (C=O), 169.2 (C=O), 157.3 (C7), 129.9 (Ar-CH), 122.3 (Ar-CH), 115.0 (Ar-CH), 67.8 (C6), 67.4 (C11), 57.0 (C3), 52.7 (C6), 20.0 (C4). **HRMS** (ESI$^+$) *m/z* for $[C_{13}H_{18}O_5N]^+$ $[M+H]^+$ calculated 268.1180, found 268.1181.

(2*S*,3*R*)-3-Hydroxy-2-(2-phenoxyacetamido)butanoic acid (262)

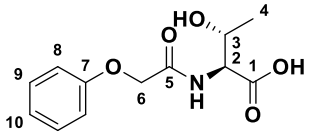

Methyl (2*S*,3*R*)-3-hydroxy-2-(2-phenoxyacetamido)butanoate (500 mg; 1.87 mmol) and LiOH•H_2O (94.0 mg; 2.24 mmol) were dissolved in THF/H_2O (1:1; 9.35 mL) then stirred at 50 °C o/n. The THF was removed *in vacuo* then the aqueous layer was washed with EtOAc (30 mL). The aqueous layer was acidified to pH 2 with 1 N HCl then extracted with EtOAc (3 × 30 mL). The combined organic layers were dried over Na_2SO_4 then concentrated *in vacuo* to give 375 mg (79%) of **262** as a white solid.

Mp. 156-150 °C. **R_f**. 0.25 (1:1 EtOAc/cyclohexane + 1% Formic Acid). **$[\alpha]_D^{25}$** = 4.99 (c = 0.5, MeOH) **IR (neat): ν_{max} (cm^{-1})** 3310, 2981, 2936, 2921, 1717, 1700, 1621, 1557, 1497, 1269, 1232, 1062. **^{1}H NMR** (400 MHz, $CDCl_3$) δ 7.76 (d, *J* = 8.8 Hz, 1H, NH), 7.37 – 7.23 (m, 2H, H16), 6.98 (m, 3H, H15, H17), 4.61 (s, 2H, H6), 4.27 (dd, *J* = 8.8, 2.9 Hz, 1H, H2), 4.18 (qd, *J* = 6.3, 3.0 Hz, 1H, H3), 1.05 (d, *J* = 6.4 Hz, 3H, H4). **^{13}C NMR** (101 MHz, $CDCl_3$) δ 177.0 (C=O), 173.3 (C=O), 162.8 (C7), 134.8 (Ar-CH), 126.5 (Ar-CH), 120.0 (Ar-CH), 71.9 (C6), 71.4 (C2), 62.4 (C3), 25.7 (C4). **HRMS** (ESI^-) *m*/*z* for $[C_{12}H_{14}NO_5]^-$ $(M-H)^-$ calculated 252.0877 found 252.0876.

(2*S*,3*R*)-*N*-(Benzyloxy)-3-hydroxy-2-(2-phenoxyacetamido)butanamide (263)

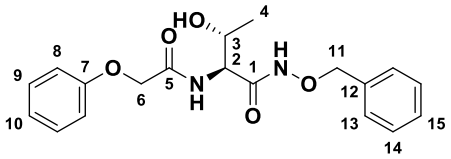

(2*S*,3*R*)-3-Hydroxy-2-(2-phenoxyacetamido)butanoic acid (1.82 g; 7.20 mmol) and HOBt (1.17 g; 8.64 mmol) were dissolved in anhydrous DMF (18.0 mL; 0.4 M) under argon. DIPEA (5.02 mL; 28.8 mmol) and EDCI (1.66 g; 8.64 mmol) were added then the reaction was stirred for 5 minutes. *O*-benzylhydroxylamine hydrochloride (1.38 g; 8.64 mmol) was added then the reaction was stirred at rt o/n. The reaction was diluted with EtOAc (50 mL) then washed with 1 N HCl (2 × 50 mL), followed by sat. aq. $NaHCO_3$ (2 × 50 mL). The organic layer was washed with brine (25 mL) then dried over Na_2SO_4. Purification by flash chromatography (0→80% EtOAc in cyclohexane) yielded 1.29 g (49%) of **263** as a colourless oil.

IR (neat): ν_{max} (cm^{-1}) 3032, 2980, 1655, 1599, 1525, 1495, 1240. **$[\alpha]_D^{25}$** = 7.30 (c = 1, $CHCl_3$). **^{1}H NMR** (400 MHz, $CDCl_3$) δ 9.46 (s, 1H, NH), 7.52 (d, *J* = 7.9 Hz, 1H, NH), 7.42 – 7.28 (m, 5H, Ar-H), 7.03 (tt, *J* = 7.2, 1.0 Hz, 2H, 16), 6.97 – 6.88 (m, 3H, H15, H17), 4.96 – 4.84 (m, 2H, H11), 4.60 – 4.37 (m, 2H, H6), 4.34 (dd, *J* = 6.2, 2.7 Hz, 1H, H2), 4.23 (m, 1H, H3), 3.67 (d, *J* = 3.0 Hz, 1H, OH), 1.07 (d, *J* = 6.5 Hz, 3H, H4). **^{13}C NMR** (101 MHz, $CDCl_3$) δ 169.9 (C=O), 168. 5 (C=O), 156.9 (C7), 134.9 (C11), 129.9 (Ar-CH), 129.2 (Ar-CH), 128.9 (Ar-CH), 128.6 (Ar-CH), 114.8 (Ar-CH), 78.3 (C11), 67.0 (C2), 66.0 (C6), 54.1 (C3), 18.2 (C4). **HRMS** (ESI$^+$) *m*/*z* for $[C_{19}H_{23}N_2O_5]^+$ $[M+H]^+$ calculated 359.1601, found 359.1601.

(4*S*,5*R*)-*N*-(Benzyloxy)-5-methyl-2-(phenoxymethyl)-4,5-dihydro-1,3-oxazole-4-carboxamide (264)

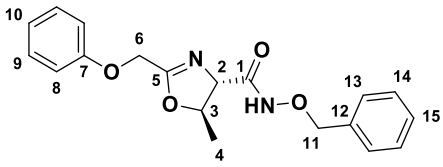

(2*S*,3*R*)-*N*-(Benzyloxy)-3-hydroxy-2-(2-phenoxyacetamido)butanamide (124 mg; 0.35 mmol) and $(NH_4)_2MoO_4$ (4.00 mg; 0.02 mmol) were suspended in. toluene (5 mL) in a round bottom flask fitted with a Dean Stark trap pre-filled with toluene. The reaction was heated to 160 °C and stirred for 28 h. The reaction was cooled to rt then concentrated *in vacuo*. Purification by flash chromatography (0→50% EtOAc in cyclohexane) yielded 52 mg (44%) of **264** as a colourless oil.

R$_f$. 0.65 (2:1 EtOAc/cyclohexane). **IR (neat): ν_{max} (cm^{-1})** 3276, 3031, 2980, 2937, 1732, 1652, 1599, 1495, 1374, 1221, 1046. **$[\alpha]_D^{25}$** = 86.7 (c = 0.5, $CHCl_3$). **^{1}H NMR** (400 MHz,

$CDCl_3$) δ 8.78 (s, 1H, NH), 7.42 – 7.33 (m, 5H, Ar-H), 7.32 – 7.27 (m, 2H, H9), 7.05 – 6.97 (m, 1H, H10), 6.97 – 6.87 (m, 2H, H8), 4.95 – 4.80 (m, 3H, H3, H11), 4.66 – 4.60 (m, 2H, H6), 4.18 (dt, *J* = 7.4, 1.3 Hz, 1H, H2), 1.49 (d, *J* = 6.3 Hz, 3H, H4). **^{13}C NMR** (101 MHz, $CDCl_3$) δ 167.9 (C1), 165.6 (C5), 157.7 (C7), 134.9 (C12), 129.7 (Ar-CH), 129.3 (Ar-CH), 128.9 (Ar-CH), 128.6 (Ar-CH), 122.0 (Ar-CH), 114.7 (Ar-CH), 80.4 (C3), 78.4 (C11), 73.8 (C2), 62.4 (C6), 21.6 (C4). **HRMS** (ESI^+) *m*/*z* for $[C_{19}H_{21}N_2O_4]^+$ $[M+H]^+$ calculated 341.1496, found 341.1495.

(4*S*,5*R*)-*N*-hydroxy-5-methyl-2-(phenoxymethyl)-4,5-dihydro-1,3-oxazole-4-carboxamide (260)

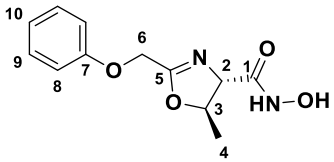

Benzyl (4*S*,5*R*)-5-methyl-2-(phenoxymethyl)-4,5-dihydro-1,3-oxazole-4-carboxylate (20.0 mg; 59.0 μmol) was dissolved in EtOAc (590 μL; 0.10 M) and the flask was purged with argon. 10% (*w*/*w*) Pd/C (20.0 mg) was added then H_2 was bubbled into the suspension for 1 h. The reaction mixture was filtered through Celite® then the filtrate concentrated *in vacuo* to give 12 mg (83%) of **263** as a pale-yellow oil, which was used without further purification.

^{1}H NMR (400 MHz, $CDCl_3$) δ 7.35 – 7.25 (m, 2H, H9), 7.05 – 6.93 (m, 3H, H8, H10), 4.97 (app. p, *J* = 6.2 Hz, 1H, H3), 4.75 – 4.62 (m, 2H, H6), 4.53 (d, *J* = 6.4 Hz, 1H, H2), 1.33 (d, *J* = 6.1 Hz, 3H, H4). ^{13}C NMR (101 MHz, $CDCl_3$) δ 169.1 (C1), 160.3 (C6),

158.9 (C7), 129.9 (C8), 121.6 (C10), 115.1 (C9), 81.2 (C3), 69.7 (C2), 61.3 (C6), 20.0 (C4). **HRMS** (ESI$^+$) *m*/*z* for $[C_{12}H_{15}N_2O_4]^+$ $[M+H]^+$ calculated 251.1027, found 251.1029.

Methyl (2*S*)-2-([(*tert*-butoxy)carbonyl]amino)-3-[(4-methylbenzenesulfonyl)oxy]propanoate (268)[310]

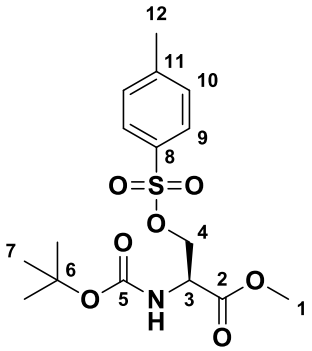

Following a modified reported procedure, to a stirred solution of methyl (2*S*)-2-([(*tert*-butoxy)carbonyl]amino)-3-hydroxypropanoate (2.20 g; 10.0 mmol) and pyridine (886 μL; 11 mmol) in Et_2O (33 mL; 0.30 M) was added tosyl chloride (2.09 g; 11 mmol). The reaction was stirred at rt o/n then concentrated washed with H_2O (3 × 20 mL), sat. aq. $NaHCO_3$ (3 × 20 mL), then brine (10 mL). The organic phase was dried over Na_2SO_4. Purification by flash chromatography (0→20% EtOAc in cyclohexane) yielded 3.43 g (92%) of **268** as a white solid.

R_f. 0.85 (1:2 EtOAc/cyclohexane). **^{1}H NMR** (400 MHz, $CDCl_3$) δ 7.75 (d, J = 7.9 Hz, 2H, Ar-H), 7.34 (d, J = 7.9 Hz, 2H, Ar-H), 5.30 (d, J = 7.6 Hz, 1H, NH), 4.50 – 4.47 (m, 1H, H3), 4.39 (dd, J = 10.1, 1.5 Hz, 1H, H4'), 4.28 (dd, J = 10.0, 1.9 Hz, 1H, H4''), 3.69 (s, 3H, H1), 2.44 (s, 3H, H12), 1.41 (s, 9H, H7). **^{13}C NMR** (101 MHz, $CDCl_3$) δ 169.0 (C2), 155.0 (C5), 145.2 (C8), 132.4 (C11), 129.9 (Ar-CH), 128.0 (Ar-CH), 80.5 (C6), 69.5 (C4), 53.0 (C1), 52.9 (C3), 28.2 (C7), 21.7 (C12). **HRMS** (ESI$^+$) *m*/*z* for $[C_{16}H_{24}NO_7S]^+$ $[M+H]^+$

calculated 374.1268, found 374.1268. The spectroscopic data match those reported in the literature.[310]

2-Methyl-2-propanyl[(2*S*)-1-hydrazino-3-hydroxy-1-oxo-2-propanyl]carbamate (269)[219]

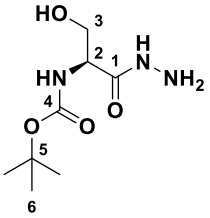

Following a modified version of a reported procedure,[219] methyl (2*S*)-2-([(*tert*-butoxy)carbonyl]amino)-3-hydroxypropanoate (11.1 g; 50.6 mmol) was dissolved in MeOH (110 mL; 0.50 M) then cooled to 0 °C. $N_2H_4 \bullet H_2O$ (7.13 mL; 55.7 mmol) was added drop-wise, then the reaction was stirred at rt o/n. The solvent was removed *in vacuo* then the residue was triturated with Et_2O (3 × 50 mL) to give 11.0 g (95%) of **269** as a white amorphous powder.

^{1}H NMR (500 MHz, MeOD) δ 4.12 (d, *J* = 5.5 Hz, 1H, H2), 3.77 – 3.71 (m, 2H, H3), 1.47 (s, 9H, H6). **^{13}C NMR** (126 MHz, MeOD) δ 171.1 (C1), 156.3 (C4), 79.5 (C5), 61.9 (C2), 55.5 (C3), 27.3 (C6). **HRMS** (ESI^+) *m*/*z* for $[C_8H_{17}N_3O_4Na]^+$ $[M+Na]^+$ calculated 242.1110, found 242.1112. The spectroscopic data match those reported in the literature.[219]

tert-Butyl _N_-[(1_S_)-2-hydroxy-1-[_N_'-(2,2,2-trifluoroacetyl)hydrazinecarbonyl]ethyl]carbamate (270)[219]

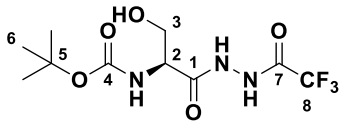

Following a modified reported procedure,[219] *tert*-butyl *N*-[(1*S*)-1-(hydrazinecarbonyl)-2-hydroxyethyl]carbamate (11.0 g; 50.1 mmol) was dissolved in EtOH (170 mL; 0.30 M) at rt. *S*-ethyl trifluorothioacetate (7.06 mL; 55.1 mmol) was added. The reaction was heated to 30 °C then stirred for 2 d. The solvent was removed *in vacuo* to yield 15.0 g (95%) of **270** as a white gum, which was used without further purification.

R$_f$. 0.50 (1:1 (EtOAc + 1% formic acid)/cyclohexane). **IR (neat): ν_{max} (cm^{-1})** 2979, 2931, 1698, 1652, 1558, 1541, 1395, 1261. **^{1}H NMR** (500 MHz, MeOD) δ 4.26 (app. t, *J* = 5.6 Hz, 1H), 3.80 (q, *J* = 6.3 Hz, 2H), 1.48 (s, 9H). **^{13}C NMR** (126 MHz, MeOD) δ 170.5 (C1), 156.3 (C4), 156.1 (q, *J* = 36.0 Hz, C7) 117.1 (q, *J* = 284.0 Hz, C8), 79.5 (C5), 61.8 (C2), 55.6 (C3), 27.3 (C6). **^{19}F NMR** (470 MHz, MeOD) δ -76.6. **HRMS** (ESI$^+$) *m*/*z* for $[C_{10}H_{17}F_3N_3O_5]^+$ $[M+H]^+$ calculated 316.1115, found 316.1115. The spectroscopic data match those reported in the literature.[219]

tert-Butyl _N_-[(4_S_)-3-oxo-1-(2,2,2-trifluoroacetyl)pyrazolidin-4-yl]carbamate (271)[219]

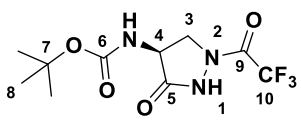

Following a modified reported procedure[219], *tert*-butyl *N*-[(1*S*)-2-hydroxy-1-[*N*'-(2,2,2-trifluoroacetyl)hydrazinecarbonyl]ethyl]carbamate (15.0 g; 47.6 mmol) and PPh_3

(13.7 g; 52.3 mmol) were dissolved in THF (164 mL; 0.20 M) and cooled to 0 °C. DIAD (10.3 mL; 52.3 mmol) was added slowly over 15 minutes. The reaction was allowed to warm to rt and stirred o/n. The reaction was concentrated *in vacuo* then the resulting residue was re-dissolved in EtOAc (100 mL). The solution was extracted with sat. aq. $NaHCO_3$ (5 × 50 mL). The combined aqueous phases were washed with Et_2O (50 mL) then acidified to pH 3 using 4 N HCl with vigorous stirring. The acidified aqueous phase was extracted with EtOAc (3 × 100 mL). The organic phase was dried over Na_2SO_4 then concentrated *in vacuo* to give 9.70 g (69%) of **271** as a colourless oil, which was used without further purification.

R_f. 0.55 (1:1 (EtOAc + 1% formic acid)/cyclohexane). **IR (neat): ν_{max} (cm^{-1})** 2957, 2920, 2851, 1697, 1684, 1507, 1457, 1370, 1258, 1166. **$[\alpha]_D^{25}$** = -90.1 (c = 1, MeOH). **^{1}H NMR** (400 MHz, DMSO, 1:1 mixture of rotamers) δ 7.59 (dd, *J* = 14.3, 8.3 Hz, 1H), 4.90 – 4.83 (m, 0.5H), 4.64 (q, *J* = 8.7 Hz, 0.5H), 4.55 (t, *J* = 10.1 Hz, 0.5H), 4.27 (t, *J* = 11.8 Hz, 0.5H), 3.91 (t, *J* = 9.3 Hz, 0.5H), 3.69 (dd, *J* = 12.4, 6.9 Hz, 0.5H), 1.44 (s, 9H). **^{13}C NMR** (101 MHz, DMSO) δ 175.8 (C5), 156.7 (q, *J* = 33.3 Hz) (C9), 155.1 (C6), 115.3 (q, *J* = 283.9 Hz), 79.9 (C7), 55.0 (C2), 48.6 (C3), 28.3 (C8). **HRMS** (ESI^-) *m*/*z* for $[C_{10}H_{13}F_3N_3O_4]^-$ $[M-H]^-$ calculated 296.0864, found 296.0857. The spectroscopic data match those reported in the literature.[219]

tert-Butyl _N_-[(4_S_)-3-oxopyrazolidin-4-yl]carbamate (266)

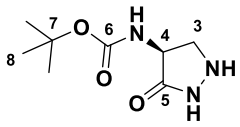

tert-Butyl _N_-[(4_S_)-3-oxo-1-(2,2,2-trifluoroacetyl)pyrazolidin-4-yl]carbamate (9.62 g; 32.4 mmol) was dissolved in THF/H_2O (2:1 _v_/_v_; 162 mL; 0.20 M) and cooled to 0 °C. $N_2H_4 \bullet H_2O$ (1.31 mL; 32.4 mmol) was added then the reaction was stirred at rt o/n. The solvent was removed _in vacuo_, then trituration with Et_2O (3 × 50 mL) yielded 4.55 g (70%) of **266** as a white amorphous solid.

IR (neat): ν_{max} (cm^{-1}) 3264, 2973, 1710, 1672, 1541, 1666, 1284, 1256, 1176. **^{1}H NMR** (400 MHz, DMSO) δ 9.23 (s, 1H), 7.03 (d, _J_ = 8.9 Hz, 1H), 5.26 (s, 1H), 4.24 (dt, _J_ = 10.8, 8.3 Hz, 1H), 3.44 – 3.35 (m, 1H), 2.89 (t, _J_ = 11.0 Hz, 1H), 1.39 (s, 9H). **^{13}C NMR** (101 MHz, DMSO) δ 174.2 (C=O), 155.9 (C=O), 78.6 (C7), 52.3 (C4), 51.8 (C3), 28.7 (C8). **HRMS** (ESI^+) _m_/_z_ for $[C_8H_{16}N_3O_3]^+$ $[M+H]^+$ calculated 202.1186, found 202.1186.The spectroscopic data match those reported in the literature.[219]

Methyl (2_S_,3_R_)-2-([(_tert_-butoxy)carbonyl]amino)-3-hydroxybutanoate (273)[311]

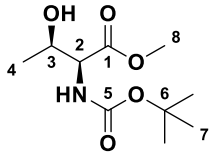

Methyl (2_S_,3_R_)-2-amino-3-hydroxybutanoate hydrochloride (4.00 g; 23.7 mmol) and Et_3N (7.16 mL; 51.5 mmol) were dissolved in CH_2Cl_2 (36.8 mL; 0.5 M). Di-_tert_-butyl dicarbonate (5.68 g; 26.0 mmol) was added portion-wise then the reaction was stirred at rt o/n. The reaction was diluted in CH_2Cl_2 (50 mL). The organic layer was washed with 1 N HCl (50 mL), sat. aq. $NaHCO_3$ (50 mL), then brine (25 mL). The organic layer was dried over Na_2SO_4 and

concentrated *in vacuo*. Purification by flash chromatography (0→5 % MeOH in CH_2Cl_2) yielded 4.42 g (80%) of **273** as a colourless oil.

R_f. 0.65 (5% MeOH in CH_2Cl_2). **^{1}H NMR** (400 MHz, $CDCl_3$) δ 5.42 (d, *J* = 9.3 Hz, 1H, H2), 4.31 – 4.18 (m, 1H, H3), 3.73 (s, 3H, H8), 2.72 (s, 1H, OH), 1.41 (s, 9H, H7), 1.20 (d, *J* = 6.3 Hz, 3H, H4). **^{13}C NMR** (101 MHz, $CDCl_3$) δ 172.1 (C=O), 156.2 (C=O), 80.1 (C6), 68.0 (C8), 58.8 (C2), 52.4 (C3), 28.3 (C7), 19.8 (C4). **HRMS** (ESI^+) *m*/*z* for $[C_{10}H_{19}NO_5Na]^+$ $[M+Na]^+$ calculated 256.1155, found 256.1154. The spectroscopic data match those reported in the literature.[311]

***tert*-Butyl *N*-[(1*S*,2*R*)-1-(hydrazinecarbonyl)-2-hydroxypropyl]carbamate (275)**

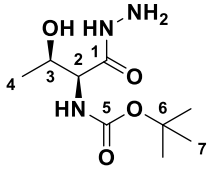

Methyl (2*S*,3*R*)-2-([(*tert*-butoxy)carbonyl]amino)-3-hydroxybutanoate (3.30 g; 14.1 mmol) was dissolved in MeOH (28.2 mL; 0.50 M) and cooled to 0 °C. $N_2H_4 \bullet H_2O$ (1.37 mL; 28.2 mmol) was added slowly and the reaction was allowed to warm to rt. The reaction was stirred at rt o/n then concentrated *in vacuo*. The residue was triturated with Et_2O (3 × 30 mL) to give 3.01 g (91%) of **275** as a white amorphous powder.

R_f. 0.35 (5% MeOH/CH_2Cl_2). **IR (neat): ν_{max} (cm^{-1})** 3331, 3283, 2980, 2889, 1683, 1656, 1524, 1367, 1248, 1167. **$[\alpha]_D^{25}$** = -15.44 (c = 0.3, MeOH). **^{1}H NMR** (400 MHz, $CDCl_3$) δ 9.53 (s, 1H, NH), 9.30 (s, 1H, N, NH), 5.68 (d, *J* = 8.1 Hz, 1H, H2), 4.35 (dt, *J* = 7.8, 4.1 Hz, 1H, H3), 4.27 – 4.20 (m, 1H, OH), 1.45 (s, 9H, H7), 1.30 – 1.18 (m, 3H, H4). **^{13}C NMR** (101 MHz, DMSO) δ 170.8 (C=O), 156.0 (C=O), 79.8 (C6), 67.2 (C2),

59.4 (C3), 28.3 (C7), 19.5 (C4). **HRMS** (ESI$^+$) *m*/*z* for $[C_9H_{29}N_2O_4]^+$ $[M+H]^+$ calculated 234.1449, found 234.1449.

tert-Butyl _N_-[(1_S_,2_R_)-2-hydroxy-1-[_N_'-(2,2,2-trifluoroacetyl)hydrazinecarbonyl]propyl]carbamate (276)

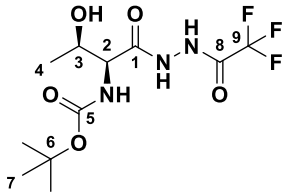

tert-Butyl *N*-[(1*S*,2*R*)-1-(hydrazinecarbonyl)-2-hydroxypropyl]carbamate (3.00 g; 12.9 mmol) was dissolved in ethanol (43.0 mL; 0.30 M). *S*-ethyl trifluorothioacetate (2.47 mL; 19.3 mmol) was added then the reaction was stirred at 30 °C for 48 h. The solvent was removed *in vacuo* to give 3.99 g (95%) of **276** as a pale-yellow oil, which was used without further purification.

R$_f$. 0.35 (5% MeOH/CH_2Cl_2). **IR (neat): ν_{max} (cm^{-1})** 3326, 2981, 2918, 2851, 1671, 1626, 1541, 1507, 1395, 1202, 1140. **$[\alpha]_D^{25}$** = -1.93 (c = 1, $CHCl_3$). **^{1}H NMR** (500 MHz, MeOD) δ 4.29 (app. t, *J* = 5.4 Hz, 1H, H2), 3.80 (m, 1H, H3), 1.48 (s, 9H, H7), 1.12 (d, *J* = 6.3 Hz, 3H, H4). **^{13}C NMR** (125 MHz, MeOD) δ 170.3 (C1), 157.4 (q, *J* = 37.0 Hz, C8), 156.0 (C5), 117.7 (q, *J* = 284.6 Hz, C9), 79.8 (C6), 67.0 (C2), 60.1 (C3), 28.3 (C7), 19.5 (C4). **^{19}F NMR** (377 MHz, $CDCl_3$) δ -73.4. **HRMS** (ESI$^-$) *m*/*z* for $[C_{11}H_{17}N_3O_3F_3]^-$ $[M-H]^-$ calculated 328.1126, found 328.1126.

tert-Butyl _N_-[(4_S_,5_S_)-5-methyl-3-oxo-1-(2,2,2-trifluoroacetyl)pyrazolidin-4-yl]carbamate (277)

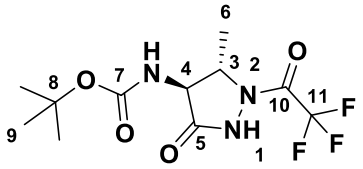

tert-Butyl _N_-[(1_S_,2_R_)-2-hydroxy-1-[_N_'-(2,2,2-trifluoroacetyl)hydrazinecarbonyl]propyl]carbamate (3.30 g; 10.0 mmol) and triphenylphosphine (2.89 g; 11.0 mmol) were dissolved in THF (50.0 mL; 0.20 M) then cooled to 0 °C. DIAD (2.17 mL; 11.0 mmol) was added over 15 min, then the reaction was stirred at rt o/n. The reaction was concentrated _in vacuo_ then the residue was re-dissolved in EtOAc (50 mL). The solution was washed with sat. aq. $NaHCO_3$ (3 × 30 mL). The combined aqueous layers were washed with Et_2O (2 × 30 mL), then acidified to pH 3 with 4 N HCl. The aqueous layer was extracted with EtOAc (3 × 50 mL) then the combined organic layers were washed with brine (10 mL) and dried over Na_2SO_4. Purification by flash chromatography (0→60% (EtOAc + 1% formic acid) in cyclohexane) yielded 2.23 g (72%) of **277** as a colourless oil.

R_f. 0.55 (1:1 (EtOAc + 1% formic acid)/cyclohexane). **IR (neat): ν_{max} (cm^{-1})** 3444, 2981, 1765, 1710, 1684, 1506, 1307, 1206, 1166, 1140. **$[\alpha]_D^{25}$** = -30.27 (c = 0.5, $CHCl_3$). **^{1}H NMR** (400 MHz, $CDCl_3$) δ 5.63 (s, 1H, NH), 4.59 (m, 1H, H3), 3.99 (app. s, 1H, H4), 1.55 (d, _J_ = 6.7 Hz, 3H, H6), 1.44 (s, 9H, H9). **^{13}C NMR** (101 MHz, $CDCl_3$) δ 171.8 (C5), 155.2 (C7), 153.7 (q, _J_ = 39.3 Hz, C10), 116.3 (q, _J_ = 283.8 Hz, C11), 79.8 (C8), 57.5 (C3), 51.9 (C4), 28.3 (C9), 15.4 (C6). **^{19}F NMR** (377 MHz, $CDCl_3$) δ -70.1. **HRMS** (ESI^-) _m/z_ for $[C_{11}H_{15}N_3O_3F_3]^-$ $[M-H]^-$ calculated 310.1020, found 310.1009.

tert-Butyl _N_-[(3_S_,4_S_)-3-methyl-5-oxopyrazolidin-4-yl]carbamate (274)

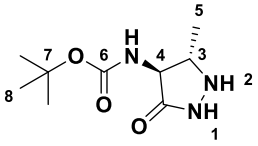

tert-Butyl _N_-[(4_S_,5_S_)-5-methyl-3-oxo-1-(2,2,2-trifluoroacetyl)pyrazolidin-4-yl]carbamate (1.50 g; 4.80 mmol) was dissolved in THF/H_2O (2:1 _v_/_v_; 2.40 mL; 2.00 M) and cooled to 0 °C. $N_2H_4 \bullet H_2O$ (233 μL; 4.80 mmol) was added slowly then the reaction was stirred at rt o/n. The solvent was removed _in vacuo_, then trituration with Et_2O (3 × 10 mL) yielded 422 mg (41%) of **274** as a white gum.

IR (neat): ν_{max} (cm^{-1}) 3256, 2981, 1724, 1697, 1522, 1533, 1253, 1169. **$[\alpha]_D^{25}$** = -50.17 (c = 1, $CHCl_3$). **^{1}H NMR** (400 MHz, DMSO) δ 9.12 (s, 1H, N<u>H</u>), 6.91 (d, _J_ = 9.2 Hz, 1H, N<u>H</u>), 3.78 (dd, _J_ = 11.1, 9.3 Hz, 1H, H4), 3.08 (dq, _J_ = 12.5, 6.4 Hz, 1H, H3), 1.32 (s, 9H, H8), 1.04 (d, _J_ = 6.4 Hz, 3H, H5). **^{13}C NMR** (101 MHz, DMSO) δ 174.2 (<u>C</u>=O), 155.7 (<u>C</u>=O), 78.0 (C7), 59.1 (C4), 58.0 (C3), 28.1 (C8), 15.2 (C5). **HRMS** (ESI$^+$) _m_/_z_ for $[C_9H_{18}N_3O_3]^+$ $[M+H]^+$ calculated 216.1343, found 216.1344.

Methyl 2-([(benzyloxy)carbonyl]amino)-3-methylbut-2-enoate (280)

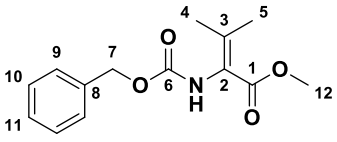

Following a modified version of a reported procedure,[312] methyl 2-([(benzyloxy)carbonyl]amino)-2-(dimethoxyphosphoryl)acetate (662 mg; 2.00 mmol) and acetone (154 μL; 2.40 mmol) were dissolved in anhydrous CH_2Cl_2 (8.00 mL; 0.25 M) then the atmosphere was purged with argon. The reaction was cooled to 0 °C, then DBU

(328 μL; 2.20 mmol) was added drop-wise. The reaction was stirred at rt for 5 h, then the reaction was diluted in sat. aq. NH_4Cl (25 mL) and extracted with CH_2Cl_2 (3 × 20 mL). The combined organic layers were washed with brine (10 mL), dried over Na_2SO_4, then concentrated *in vacuo*. Purification by flash chromatography (0→5% MeOH in CH_2Cl_2) yielded 312 mg (59%) of **280** as a colourless oil.

IR (neat): ν_{max} (cm^{-1}) 3033, 2951, 1795, 1708, 1500, 1312, 1250, 1218, 1048.**^{1}H NMR** (400 MHz, $CDCl_3$) δ 7.43 – 7.30 (m, 5H, Ar-H), 5.97 (s, 1H, NH), 5.14 (s, 2H, H7), 3.75 (s, 3H, H12), 2.16 (s, 3H, CH_3), 1.88 (s, 3H, CH_3). **^{13}C NMR** (101 MHz, $CDCl_3$) δ 166.6 (C1), 154.8 (C6), 136.3 (C8), 128.4 (Ar-CH), 128.0 (Ar-CH), 127.5 (Ar-CH), 124.5 (C3), 67.1 (C7), 52.0 (C12), 21.0 (CCH_3), 20.7 (CCH_3). **HRMS** (ESI^+) *m/z* for $[C_{14}H_{18}NO_4]^+$ $[M+H]^+$ calculated 264.1230, found 264.1230. The spectroscopic data match those reported in the literature.[312]

Benzyl *N*-(3,3-dimethyl-5-oxopyrazolidin-4-yl)carbamate (278)[222]

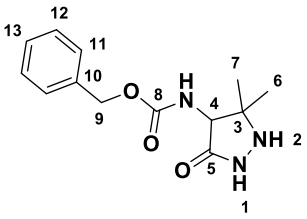

Methyl 2-([(benzyloxy)carbonyl]amino)-3-methylbut-2-enoate (100 mg; 0.38 mmol) was dissolved in *n*-BuOH (633 μL; 0.60 M), then $N_2H_4 \bullet H_2O$ (76 μL; 1.52 mmol) was added drop-wise. The reaction was refluxed for 16 h then cooled to rt. The reaction was concentrated *in vacuo*, then trituration with Et_2O (2 × 5 mL) yielded 34 mg (34%) of **278** as a white amorphous solid.

IR (neat): ν_{max} (cm^{-1}) 3278, 3185, 3058, 2980, 1649, 1582, 1534, 1258, 1126. **^{1}H NMR** (400 MHz, $CDCl_3$) δ 8.01 (d, *J* = 7.0 Hz, 1H, NH), 7.41 – 7.29 (m, 5H, Ar-H), 5.47 (s, 1H, NH), 5.20 – 5.06 (m, 2H, H8), 4.35 (d, *J* = 7.1 Hz, 1H, H4), 3.86 (d, *J* = 6.0 Hz, 1H, NH), 1.40 (s, 3H, CH_3), 1.06 (s, 3H, CH_3). **^{13}C NMR** (101 MHz, $CDCl_3$) δ 175.8 (C5), 157.0 (C8), 136.1 (C10), 128.7 (Ar-CH), 128.5 (Ar-CH), 128.3 (Ar-CH), 67.6 (C9), 64.7 (C4), 61.5 (C3), 24.9 (CH_3), 19.5, (CH_3). **HRMS** (ESI^+) *m/z* for $[C_{13}H_{18}N_3O_3]^+$ $[M+H]^+$ calculated 264.1343, found 264.1342. The spectroscopic data match those reported in the literature.[222]

5-Diphenylmethyl 1-(4-nitrophenyl)methyl 2-oxopentanedioate (285)

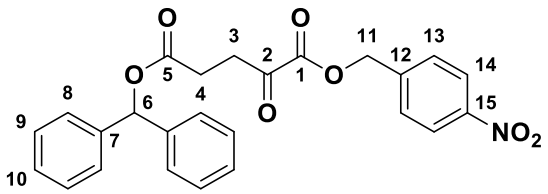

(Diphenylmethylidene)hydrazine (10.8 g; 55.0 mmol) was dissolved in CH_2Cl_2 (138 mL; 0.40 M) and cooled to 0 °C. $MgSO_4$ (5.00 g) was added then the suspension stirred for 5 min. MnO_2 (10.3 g; 117 mmol) was added portion-wise then the reaction was stirred at rt o/n. The reaction was filtered through sintered glass and the filtrate was reserved. 5-[(4-Nitrophenyl)methoxy]-4,5-dioxopentanoic acid (14.1 g; 50.0 mmol) was dissolved in CH_2Cl_2 (125 mL; 0.40 M) then the filtrate was added slowly over 10 min. The reaction was stirred at rt for 2 h then concentrated *in vacuo*. Purification by flash chromatography (0→30% EtOAc in cyclohexane) yielded 11.2 g (50%) of **285** as a yellow oil.

R_f. 0.35 (1:3 EtOAc/cyclohexane). **IR (neat): ν_{max} (cm^{-1})** 3032, 3018, 2971, 2917, 1734, 1718, 1653, 1558, 1541, 1347, 1168, 1115. **^{1}H NMR** (400 MHz, $CDCl_3$) δ 8.17 – 8.10 (m, 2H, H14), 7.52 – 7.44 (m, 2H, H13), 7.42 – 7.36 (m, 2H, Ar-H), 7.33 – 7.21 (m, 8H, Ar-H), 6.85 (s, 1H, H6), 5.25 (m, 2H, H11), 3.03 (dd, *J* = 8.2, 7.1 Hz, 2H, H3), 2.78 (dd, *J* = 8.2, 7.1 Hz, 2H, H4). **^{13}C NMR** (101 MHz, $CDCl_3$) δ 184.7 (C2), 171.3 (C=O), 163.8 (C=O), 147.7 (Ar-C), 140.1 (Ar-C), 137.2 (Ar-C), 134.5 (Ar-CH), 128.7 (Ar-CH), 128.1 (Ar-CH), , 127.7 (Ar-CH), 127.2 (Ar-CH), 123.8 (Ar-CH), 65.3 (C11), 30.4 (C3), 23.8 (C4). **HRMS** (ESI$^+$) *m*/*z* for $[C_{25}H_{21}NO_7Na]^+$ [M+Na]$^+$ calculated 470.1210, found 470.1210.

5-Diphenylmethyl 1-(4-nitrophenyl)methyl 3-methylidene-2-oxopentanedioate (284)

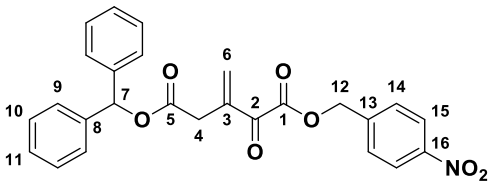

5-Diphenylmethyl 1-(4-nitrophenyl)methyl 2-oxopentanedioate (6.78 g; 15.2 mmol) was dissolved in CH_2Cl_2 (38.0 mL; 0.40 M); the solution was cooled to 0 °C, then [(dimethylamino)methyl]dimethylamine (8.27 mL; 60.7 mmol) was added, then acetic acid (6.07 mL; 106.1 mmol), and acetic anhydride (7.15 mL; 75.8 mmol). The reaction was warmed to rt and stirred for 5 h. The reaction mixture was diluted with ice-cold H_2O (50 mL) then the organic layer was separated. The organic layer was washed with H_2O (3 × 30 mL) then brine

(15 mL), then dried over Na_2SO_4. Purification by flash chromatography (0→20% EtOAc in cyclohexane) yielded 4.65 g (68%) of **284** as a yellow oil.

R_f. 0.55 (1:2 EtOAc/cyclohexane). **IR (neat): ν_{max} (cm^{-1})** 3063, 3033, 2968, 2927, 2851, 1734, 1607, 1252, 1347, 1282, 1148. **^{1}H NMR** (400 MHz, $CDCl_3$) δ 8.27 – 8.18 (m, 2H, H15), 7.57 – 7.49 (m, 2H, H14), 7.37 – 7.24 (m, 10H, Ar-H), 6.86 (s, 1H, H7), 6.36 (app. s, 1H, H6'), 6.26 (app. t, *J* = 1.2 Hz, 1H, H6''), 5.36 (s, 2H, H12), 3.53 (d, *J* = 1.2 Hz, 2H, H4). **^{13}C NMR** (101 MHz, $CDCl_3$) δ 185.7 (C2), 169.1 (C=O), 162.3 (C=O), 148.2 (C3), 141.6 (Ar-C), 139.9 (Ar-C), 138.0 (Ar-C), 134.9 (Ar-CH), 128.8 (Ar-CH), 128.7 (Ar-CH), 128.2 (Ar-CH), 127.2 (Ar-CH), 124.1 (C6), 78.0 (C7), 66.1 (C12), 36.3 (C4). **HRMS** (ESI^-) *m/z* for $[C_{26}H_{20}NO_7]^-$ [M-H]$^-$ calculated 458.1245, found 458.1245.

Diphenylmethyl 3-([(4S)-4-([(tert-butoxy)carbonyl]amino)-3-oxopyrazolidin-1-yl]methyl)-5-[(4-nitrophenyl)methoxy]-4-oxopentanoate (283)

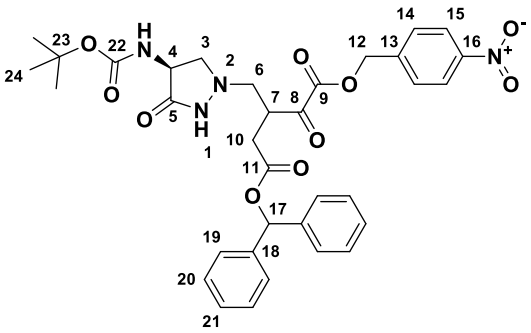

5-Diphenylmethyl 1-(4-nitrophenyl)methyl 3-methylidene-2-oxopentanedioate (9.20 g; 20.0 mmol) was dissolved in CH_2Cl_2 (100 mL; 0.20 M) *tert*-butyl *N*-[(4*S*)-3-oxopyrazolidin-4-yl]carbamate (4.02 g; 20.0 mmol) was added and the reaction was stirred at rt o/n. The solvent was removed *in vacuo* then the residue was purified by flash chromatography (0→70% EtOAc in cyclohexane) to give 11.9 g (90%) of 276 as a yellow oil.

R_f. 0.40 (5% MeOH in CH_2Cl_2). **IR (neat): ν_{max} (cm^{-1})** 3031, 2981, 2937, 1791, 1769, 1719, 1689, 1520, 1347, 1282, 1346, 1194, 1068. **^{1}H NMR** (400 MHz, $CDCl_3$, 1:1 mixture of diastereomers) δ 8.25 – 8.09 (m, 2H, H15), 7.58 – 7.42 (m, 2H, H14), 7.38 – 7.22 (m, 10H, Ar-H), 6.82 (s, 1H, H17), 5.40 – 5.21 (m, 3H), 4.79 – 4.54 (m, 1H, NH), 4.12 – 4.03 (m, 1H, H4), 3.56 – 3.37 (m, 2H, H3), 3.13 – 2.40 (m, 4H, H6, H10). **^{13}C NMR** (126 MHz, $CDCl_3$) (1:1 mixture of diastereomers) δ 171.0 (C=O), 170.3 (C=O), 168.7 (C=O), 164.0 (C=O), 155.4 (C=O), 148.0 (C16), 141.6 (Ar-C), 139.8 (Ar-C), 139.7 (Ar-C), 139.6 (Ar-CH), 128.9 (Ar-CH), 128.6 (Ar-CH), 128.6 (Ar-CH), 128.3 (Ar-CH), 127.2 (Ar-CH), 126.9 (Ar-CH), 123.8 (Ar-CH), 83.4 (C17), 81.0 (C23), 67.2 (C12), 58.0 (C4), 49.1 (C6), 47.0 (C3), 34.6 (C10), 29.7 (C7), 28.3 (C24). **HRMS** (ESI$^+$) *m*/*z* for $[C_{34}H_{37}N_4O_{10}]^+$ $[M+H]^+$ calculated 661.2504, found 661.2501.

(4-Nitrophenyl)methyl (10*S*)-10-([(*tert*-butoxy)carbonyl]amino)-4,11-dioxo-3-oxa-1,8-diazatricyclo[6.3.0.0^{2,6}]undecane-2-carboxylate (288)

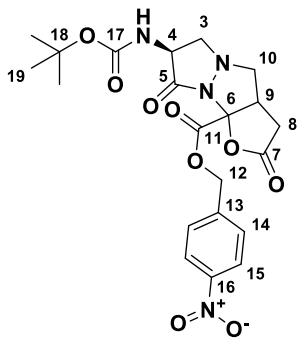

Diphenylmethyl 3-([(4*S*)-4-([(*tert*-butoxy)carbonyl]amino)-3-oxopyrazolidin-1-yl]methyl)-5-[(4-nitrophenyl)methoxy]-4-oxopentanoate (4.58 g; 6.93 mmol) was dissolved in HFIP (34.6 mL; 0.20 M) and sealed in a microwave vial. Acetic acid (1.39 mL; 24.3 mmol) was added then the reaction was stirred at 60 °C for 16 h. The reaction was cooled to rt and concentrated *in vacuo*. The residue was subjected to high-vacuum for 4 h before being re-dissolved in CH_2Cl_2 (34.6 mL; 0.20 M). Et_3N

(241 μL; 1.73 mmol) and EDCI (332 mg; 1.73 mmol) were then added and the reaction was stirred at rt for 3 h. The solvent was removed *in vacuo* and the residue was purified by flash chromatography (0→75% EtOAc/cyclohexane) to give 1.52 g (46%) of **288** as an off-white powder.

IR (neat): ν_{max} (cm^{-1}) 3132, 3081, 2981, 2888, 1791, 1769, 1719, 1687, 1522, 1348, 1167, 1076. **^{1}H NMR** (400 MHz, DMSO, 1:1 mixture of diastereomers) δ 8.30 – 8.21 (m, 2H, H15), 7.76 – 7.63 (m, 2H, H14), 5.50 – 5.27 (m, 2H, H12), 4.59 (q, *J* = 9.4 Hz, 1H, H4), 3.90 – 3.69 (m, 2H, H3', H9), 3.44 – 3.38 (m, 1H, H10'), 3.05 – 2.90 (m, 1H, H8'), 2.84 – 2.64 (m, 3H, H3'', H8'', H10''), 1.41 – 1.31 (m, 9H, H19). **^{13}C NMR** (101 MHz, DMSO) δ 175.0 (C=O), 164.7 (C=O), 163.0 (C=O), 155.5 (C17), 147.8 (C16), 143.1 (C13), 129.2 (Ar-CH), 124.1 (Ar-CH), 104.1 (C6), 89.44 (C6) 79.2 (C18), 67.0 (C12), 61.5 (C10), 60.2 (C3), 55.4 (C4), 48.3 (C9), 33.2 (C8), 28.6 (C19). **HRMS** (ESI^+) *m*/*z* for $[C_{21}H_{25}N_4O_9]^+$ $[M+H]^+$ calculated 477.1616, found 477.1618.

(4-Nitrophenyl)methyl (10*S*)-4,11-dioxo-10-(2-phenoxyacetamido)-3-oxa-1,8-diazatricyclo[6.3.0.0^{2,6}]undecane-2-carboxylate (289)

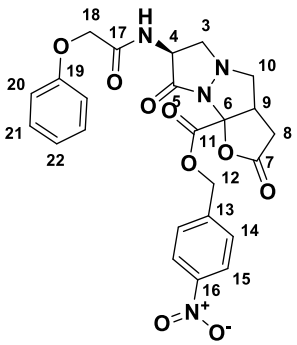

(4-Nitrophenyl)methyl (10*S*)-10-([(*tert*-butoxy)carbonyl]amino)-4,11-dioxo-3-oxa-1,8-diazatricyclo[6.3.0.0^{2,6}]undecane-2-carboxylate (480 mg; 1.01 mmol) was dissolved in CH_2Cl_2 (5.05 mL; 0.20 M). TFA (1.55 mL; 20.2 mmol) was added and the reaction was stirred at rt for 1 h. The

reaction was then concentrated *in vacuo* and the residue was triturated with Et_2O (3 × 10 mL). The residue was then re-dissolved in CH_2Cl_2 (5.05 mL; 0.20 M) then Et_3N (422 μL; 3.03 mmol) was added. 2-Phenoxyacetyl chloride (153 μL; 1.11 mmol) was then added drop-wise then the reaction was stirred at rt o/n. The solvent was removed *in vacuo* and the residue was purified via flash chromatography (0→100% EtOAc in cyclohexane) to give 386 mg (75%) of **289** as an amber oil.

^{1}H NMR (400 MHz, $CDCl_3$, 1:1 mixture of diastereomers) δ 8.26 – 8.17 (m, 2H, H15), 7.63 – 7.49 (m, 2H, H14), 7.38 – 7.24 (m, 2H, H21), 7.02 (dtt, J = 9.4, 7.4, 1.0 Hz, 1H, H22), 6.95 – 6.86 (m, 2H, H20), 5.53 – 5.28 (m, 2H, H12), 4.90 (ddd, J = 12.1, 8.2, 6.1 Hz, 1H, H4), 4.51 (d, J = 2.0 Hz, 2H, H18), 4.17 (t, J = 8.5 Hz, 1H, H3'), 3.60 – 3.58 (m, 1H, H9), 3.36 (d, J = 9.2 Hz, 2H, H10'), 3.05 – 2.66 (m, 4H, H3'', H8, H10''). **^{13}C NMR** (101 MHz, CDCl3) δ 172.8 (C=O), 169.0 (C=O), 164.8 (C=O), 161.6 (C=O), 157.0 (C19), 148.1 (C16), 141.3 (C13), 129.8 (Ar-CH), 128.8 (Ar-CH), 124.0 (Ar-CH), 122.3 (Ar-CH), 114.8 (Ar-CH), 89.1 (C6), 67.5 (C12), 67.2 (C18), 60.9 (C10), 58.7 (C3), 54.4 (C4), 48.9 (C9), 32.7 (C8). **HRMS** (ESI^+) *m/z* for $[C_{24}H_{23}N_4O_9]^+$ $[M+H]^+$ calculated 511.1460, found 511.1460.

(10*S*)-4,11-Dioxo-10-(2-phenoxyacetamido)-3-oxa-1,8-diazatricyclo[6.3.0.0^{2,6}]undecane-2-carboxylicacid (290**)**

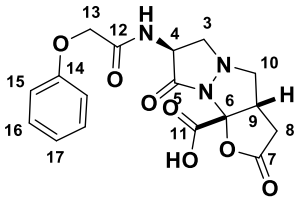

(4-Nitrophenyl)methyl (10S)-4,11-dioxo-10-(2-phenoxyacetamido)-3-oxa-1,8-diazatricyclo[6.3.0.0^{2,6}]undecane-2-carboxylate (362 mg; 0.71 mmol) was dissolved in THF/H_2O (2:1 *v*/*v*, 7.10 mL; 0.10 M). The flask was purged with argon, then 10% (*w*/*w*) Pd/C (180 mg) was added. H_2 was introduced into the suspension under balloon pressure at rt for 3 h. $NaHCO_3$ (6.00 mg; 0.71 mmol) was added and the reaction was stirred vigorously for a further 5 min. The reaction was filtered through a short plug of Celite® then plug was washed with H_2O (3 × 5 mL). The filtrate was washed with Et_2O (3 × 10 mL) then the aqueous layer was lyophilised to give the title compound as a white lyophilised powder with a crude yield of 102 mg (36%). Purification by HPLC (ACE 10 AQ column (i.d. 250 ×21.2 mm) flow rate 15 mL/min. A solvent: H_2O + 0.1 % (*v*/*v*) HCO_2H; B solvent: MeCN + 0.1% HCO_2H. Gradient: 5%→10% B over 3 mins, 10%→45% B over 17 min, 45%→98% B over 3 min, 98% over 2 min, 98% → 5% over 1 min. Diastereomer A elution at 16 min; diastereomer B elution at 18 min) gave 14 mg (5%) of diastereomer A as a white lyophilised powder and 22 mg (8%) of diastereomer B as a white lyophilised powder.

Diastereomer A:

^{1}H NMR (700 MHz, D_2O) δ 7.31 – 7.28 (m, 2H, H16), 6.99 (d, *J* = 7.3 Hz, 1H, H17), 6.94 (d, *J* = 8.0 Hz, 2H, H15), 5.18 (dd, *J* = 12.4, 8.4 Hz, 1H, H4), 3.92 – 3.90 (m, 2H, H13), 3.59 (dq, *J* = 11.7, 5.6 Hz, 1H, H3'), 3.40 – 3.38 (m, 1H, H9), 3.10 – 2.99 (m, 1H, H8'), 2.89 – 2.86 (m, 1H,), 2.82 (app. t, *J* = 11.0 Hz, 1H, H3''), 2.72 – 2.66 (m, 2H, H8'', H10''). **^{13}C NMR** (176 MHz, D_2O) δ 177.9 (C=O), 171.6 (C=O), 168.9 (C=O), 162.5 (C=O), 157.0 (C14), 129.9 (Ar-CH), 122.2 (Ar-CH), 114.7 (Ar-CH), 91.6 (C6), 61.0 (C13), 60.5 (C3), 57.1 (C10), 53.8 (C4), 47.8 (C9), 33.0 (C8). **HRMS** (ESI^+) *m*/*z* for $[C_{17}H_{17}N_3O_7]^+$ $[M+H]^+$ calculated 376.1139, found 376.1139.

Diastereomer B:

^{1}H NMR (500 MHz, DMSO, 385 K) δ 8.50 (d, *J* = 8.4 Hz, 1H, NH), 7.34 – 7.27 (m, 2H, H16), 7.02 – 6.95 (m, 3H, H15, H17), 4.96 (app. q, *J* = 8.9 Hz, 1H, H4), 4.54 (d, *J* = 1.2 Hz, 2H, H14), 3.66 – 3.59 (m, 1H, H9), 3.58 – 3.52 (m, 1H, H3'), 3.27 – 3.15 (m, 2H, H3'', H10'), 3.01 – 2.92 (m, 1H, H8'), 2.91 – 2.86 (m, 1H, H10''), 2.70 – 2.63 (m, 1H, H8''). **^{13}C NMR** (176 MHz, D_2O) δ 174.2 (C=O), 170.1 (C=O), 166.7 (C=O), 162.3 (C=O), 157.0 (C14), 129.2 (Ar-CH), 121.5 (Ar-CH), 114.5 (Ar-CH), 61.0 (C13), 53.8 (C4), 48.4 (C9), 33.0 (C8). **HRMS** (ESI^+) *m*/*z* for $[C_{17}H_{17}N_3O_7]^+$ $[M+H]^+$ calculated 376.1139, found 376.1140.

Methyl (2*S*)-2-[[(benzyloxy)carbonyl]amino]-5-cyano-5-(1λ4-thiolan-1-ylidene)-4-oxopentanoate (303)

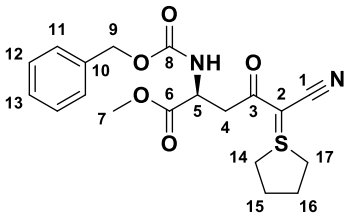

(3*S*)-3-([(Benzyloxy)carbonyl]amino)-4-methoxy-4-oxobutanoic acid (1.4 g; 5.00 mmol) was dissolved in CH_2Cl_2 (25 mL; 0.2 M) then DIPEA (2.61 mL; 15.0 mmol) and HATU (2.28 g; 6 mmol) were added. The reaction was stirred for 10 min then 1-(cyanomethyl)thiolan-1-ium bromide (1.04 g; 1.00 mmol) was added. The reaction was stirred at rt for 2 h then diluted in CH_2Cl_2 (25 mL) then washed with sat. aq. NH_4Cl (2 × 25 mL). The organic phase was washed with brine (10 mL) then dried over Na_2SO_4. Purification by flash chromatography (0→100% EtOAc in cyclohexane then 0→50% acetone in EtOAc) yielded 1.35 g (70%) of **303** as a red oil.

^{1}H NMR (400 MHz, $CDCl_3$) δ 7.51 – 7.28 (m, 5H, Ar-H), 5.93 (d, *J* = 9.0 Hz, 1H, NH), 5.17 – 5.05 (m, 2H, H9), 4.62 (dt, *J* = 9.2, 4.6 Hz, 1H, H5), 3.73 (s, 3H, H7), 3.42 – 3.10 (m, 4H, H4', 3 × CH_2), 2.98 – 2.86 (m, 1H, H4''), 2.53 (dtq, *J* = 15.1, 7.2, 3.6 Hz, 2H, CH_2), 2.13 – 1.96 (m, 3H, CH_2). **^{13}C NMR** (101 MHz, $CDCl_3$) δ 187.9 (C3), 172.1 (C6), 156.1 (C8), 136.5 (C10), 128.5 (Ar-CH), 128.1 (Ar-CH), 128.0 (Ar-CH), 119.8 (C1), 108.0 (C2), 66.9 (C9), 55.3 (C7), 52.5 (C5), 50.9 (C14), 45.4 (C17), 45.1 (C4), 28.6 (C15), 28.5 (C16). **HRMS** (ESI$^+$) *m/z* for $[C_{19}H_{23}N_2O_5S]^+$ $[M+H]^+$ calculated 391.1322, found 391.1322.

1-*tert*-Butyl 5-methyl (4*S*)-4-[[(benzyloxy)carbonyl]amino]-2-oxopentanedioate (298**)**

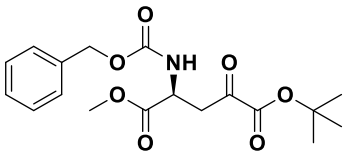

Methyl (2*S*)-2-[[(benzyloxy)carbonyl]amino]-5-cyano-5-(1λ4-thiolan-1-ylidene)-4-oxopentanoate (200 mg; 0.52 mmol) was dissolved in THF/H_2O (1:1 *v*/*v*; 10.2 mL; 0.05 M) then Oxone® (640 mg; 1.04 mmol) was added. The reaction was stirred at rt for 30 min then diluted in H_2O (10 mL) and extracted with EtOAc (3 × 15 mL). The combined organic phases were washed with brine (10 mL), dried over Na_2SO_4, and concentrated *in vacuo*. The residue was dissolved in THF (1.7 mL; 0.5 M) then a solution of *N*,*N*'-bis(propan-2-yl)(*tert*-butoxy)methanimidamide (198 μL; 0.84 mmol). The reaction was stirred at rt o/n then concentrated *in vacuo*. Purification by flash chromatography (0→30% EtOAc in cyclohexane) yielded 83 mg (44%) of **298** as a colourless oil.

^{1}H NMR (400 MHz, $CDCl_3$) δ 7.33 – 7.22 (m, 5H), 5.67 – 5.63 (m, 1H), 5.10 (s, 2H), 4.73 – 4.68 (m, 1H), 3.72 (s, 3H), 3.50 – 3.37 (m, 2H), 1.53 (s, 9H).

The spectroscopic data match those reported in the literature.[167]

(2*S*)-2-[[(Benzyloxy)carbonyl]amino]-5-(*tert*-butoxy)-4,5-dioxopentanoic acid (299)

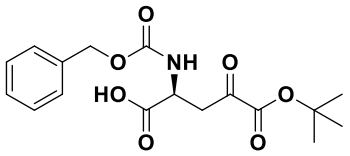

1-*tert*-Butyl 5-methyl (4*S*)-4-[[(benzyloxy)carbonyl]amino]-2-oxopentanedioate (75 mg; 0.21 mmol) was dissolved in THF/H_2O (2:1 *v*/*v*; 1 mL; 0.20 M) then LiOH•H_2O (18 mg; 0.42 mmol) was added. The reaction was stirred at 30 °C o/n then concentrated *in vacuo*. The residue was dissolved in EtOAc (10 mL) then washed with sat. aq. $NaHCO_3$ (3 × 5 mL). The combined aqueous phases were acidified to pH 2 with 1 N HCl then the aqueous phases were extracted with EtOAc (3 × 5 mL). The combined organic phases were washed with brine (5 mL), dried over Na_2SO_4, and concentrated *in vacuo* to give 49 mg (68%) of **299** as a white solid.

^{1}H NMR (400 MHz, DMSO) δ 7.61 (d, J = 7.6 Hz, 1H), 7.26 – 7.39 (m, 5H), 5.02 (s, 2H), 4.42 – 4.40 (m, 1H),3.24 – 3.22 (m, 1H), 3.07 – 3.05 (m, 1H), 1.47 (s, 9H).

The spectroscopic data match those reported in the literature.[167]

5-Diphenylmethyl 1-(4-nitrophenyl)methyl 2-oxo-3-[(phenylsulfanyl)methyl]pentanedioate (305)

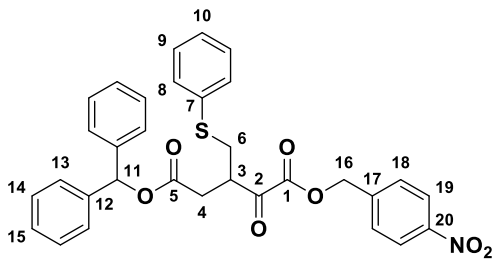

General Procedure A was followed using 5-diphenylmethyl 1-(4-nitrophenyl)methyl 3-methylidene-2-oxopentanedioate (1.00 g; 2.18 mmol), benzenethiol (244 μL; 2.39 mmol),

and triethylamine (16.0 μL; 120 μmol). Purification by flash chromatography (0→30% EtOAc in cyclohexane) yielded 1.10 g (87%) of **305** as a yellow oil.

R_f. 0.50 (1:3 EtOAc/cyclohexane). **IR (neat): ν_{max} (cm^{-1})** 3059, 3033, 2955, 2919, 2851, 1714, 1658, 1603, 1251, 1449, 1347, 1278, 1199. **^{1}H NMR** (400 MHz, $CDCl_3$) δ 8.21 – 8.11 (m, 2H, H19), 7.51 – 7.43 (m, 2H, H18), 7.37 – 7.18 (m, 15H, Ar-H), 6.79 (s, 1H, H11), 5.26 (s, 2H, H16), 3.92 (m, 1H, H3), 3.29 (dd, *J* = 13.6, 6.5 Hz, 1H, H6'), 3.12 – 2.91 (m, 3H, H6'', H4', H4''). **^{13}C NMR** (101 MHz, $CDCl_3$) δ 193.62 (C2), 170.6 (C=O), 159.8 (C=O), 141.6 (Ar-C), 139.5 (Ar-C), 134.4 (Ar-C), 130.3 (Ar-C), 129.2 (Ar-CH), 128.6 (Ar-CH), 128.5 (Ar-CH), 128.2 (Ar-CH), 128.1 (Ar-CH), 127.1 (Ar-CH), 126.9 (Ar-CH), 123.9 (Ar-CH), 78.0 (C11), 66.2 (C16), 43.0 (C3), 35.8 (C4), 35.0 (C6). **HRMS** (ESI$^+$) *m*/*z* for $[C_{32}H_{27}NO_7SNa]^+$ $[M+Na]^+$ calculated 592.1400, found 592.1399.

5-[(4-Nitrophenyl)methoxy]-4,5-dioxo-3-[(phenylsulfanyl)methyl]pentanoic acid (306)

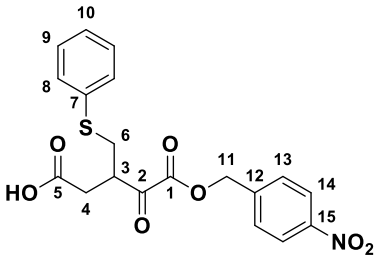

5-diphenylmethyl 1-(4-nitrophenyl)methyl 2-oxo-3-[(phenylsulfanyl)methyl]pentanedioate (575 mg; 1.01 mmol) was dissolved in CH_2Cl_2 (10.1 mL; 0.10 M). TFA (230 μL; 3.03 mmol) was added then the reaction was stirred at rt o/n. The reaction was concentrated *in vacuo* then purified by flash

chromatography (0→35% EtOAc in cyclohexane) to give 347 mg (85%) of **276** as a yellow oil.

R_f. 0.4 (1:2 EtOAc/cyclohexane + 1% formic acid). **IR (neat): ν_{max} (cm^{-1})** 3079, 3058, 2971, 2920, 2850, 1793, 1770, 1743, 1473, 1347, 1154, 1926. **^{1}H NMR** (400 MHz, $CDCl_3$) δ 8.16 (d, *J* = 8.3 Hz, 2H, H14), 7.36 (d, *J* = 8.2 Hz, 2H, H13), 7.31 – 7.16 (m, 5H, Ar-H), 5.29 (m, 2H, H11), 3.37 – 3.12 (m, 3H, H3, H6', H6''), 2.77 (dd, *J* = 17.2, 8.3 Hz, 1H, H4'), 2.58 (dd, *J* = 17.4, 11.7 Hz, 1H, H4''). **^{13}C NMR** (101 MHz, $CDCl_3$) δ 196.3 (C2), 175.8 (C=O), 163.4 (C=O), 147.7 (Ar-C), 141.0 (Ar-C), 135.8 (Ar-C), 131.0 (Ar-CH), 128.3 (C13), 127.4 (Ar-CH), 126.9 (Ar-CH), 123.8 (C14), 66.8 (C11), 44.7 (C3), 36.6 (C4), 34.9 (C5). **HRMS** (ESI^+) *m/z* for $[C_{19}H_{18}NO_7S]^+$ $[M+H]^+$ calculated 404.0798, found 404.0798.

1,5-Dimethyl 3-methylidene-2-oxopentanedioate (309)

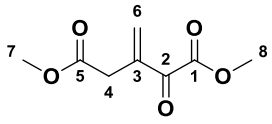

1,5-Dimethyl 2-oxopentanedioate (145 μL; 1.00 mmol) was dissolved in CH_2Cl_2 (2.50 mL; 0.40 M) then cooled to 0 °C. [(Dimethylamino)methyl]dimethylamine (546 μL; 4.00 mmol) was added, followed by acetic acid (420 μL; 7.00 mmol) and acetic anhydride (510 μL; 5.00 mmol). The reaction was allowed to warm to rt, then stirred for 5 h. The reaction mixture was diluted with ice-cold H_2O (10 mL) then the organic layer was separated. The organic layer was washed with H_2O (3 × 5 mL) then brine (5 mL), then dried over Na_2SO_4.

Purification by flash chromatography (0→35% EtOAc in cyclohexane) yielded 70 mg (37%) of **309** as a colourless oil.

R_f. 0.50 (1:2 EtOAc/cyclohexane). **IR (neat): ν_{max} (cm^{-1})** 2958, 2919, 2849, 1803, 1739, 1662, 1439, 1297, 1211, 1151, 1057. **^{1}H NMR** (400 MHz, $CDCl_3$) δ 6.41 (s, 1H, H6'), 6.29 (t, *J* = 1.2 Hz, 1H, H6''), 3.90 (s, 3H, C$\underline{H}_3$), 3.69 (s, 3H, C$\underline{H}_3$), 3.39 (d, *J* = 1.2 Hz, 2H, H4). **^{13}C NMR** (101 MHz, $CDCl_3$) δ 186.4 (C2), 170.4 ($\underline{C}$=O), 163.2 ($\underline{C}$=O), 138.0 C3), 134.7 (C6), 52.8 ($\underline{C}H_3$), 52.2 ($\underline{C}H_3$), 35.7 (C4). **HRMS** (ESI^+) *m*/*z* for $[C_8H_{11}O_5]^+$ $[M+H]^+$ calculated 187.0601, found 187.0602.

1,5-Dimethyl 2-oxo-3-[(phenylsulfanyl)methyl]pentanedioate (310)

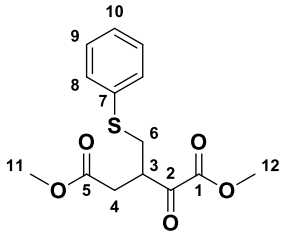

General Procedure A was followed using 1,5-dimethyl 3-methylidene-2-oxopentane (60.0 mg; 0.32 mmol), benzenethiol (33.0 μL; 0.32 mmol), and triethylamine (2.00 μL; 16.0 μmol). Purification by flash chromatography (0→35% EtOAc in cyclohexane) yielded 193 mg (98%) of **310** as a colourless oil.

R_f. 0.60 (1:2 EtOAc/cyclohexane). **IR (neat): ν_{max} (cm^{-1})** 3058, 2980, 2957, 1798, 1732, 1582, 1480, 1439, 1219, 1154, 1024. **^{1}H NMR** (400 MHz, $CDCl_3$) δ 7.42 – 7.36 (m, 2H, Ar-$\underline{H}$), 7.34 – 7.29 (m, 2H, Ar-$\underline{H}$), 7.26 – 7.21 (m, 1H, H10), 3.95 – 3.85 (m, 1H, H3), 3.85 (s, 3H, C$\underline{H}_3$), 3.63 (s, 3H, C$\underline{H}_3$), 3.34 (dd, *J* = 13.7, 6.0 Hz, 1H, H6'), 3.05 – 2.79 (m, 3H, H6'', H4', H4''). **^{13}C NMR** (101 MHz, $CDCl_3$) δ 194.0 (C2), 171.9 ($\underline{C}$=O), 160.7 ($\underline{C}$=O), 134.6 (C7), 130.4 (Ar-$\underline{C}$H), 129.2 (Ar-$\underline{C}$H), 127.0 (Ar-$\underline{C}$H), 53.1 ($\underline{C}H_3$),

52.1 (<u>C</u>H$_3$), 43.1 (C3), 35.0 (C4), 34.9 (C6). **HRMS** (ESI$^+$) *m*/*z* for [C$_{14}$H$_{16}$O$_5$SNa]$^+$ [M+Na]$^+$ calculated 319.0611, found 319.0611.

1,5-Di-*tert*-butyl 2-oxopentanedioate (311)[313]

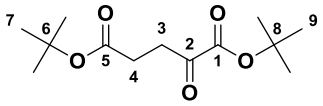

Following a modified reported procedure,[313] 2-oxopentanedioic acid (8.00 g; 45.9 mmol) was dissolved in *tert*-butyl acetate (230 mL; 0.20 M) then cooled to 0 °C. H_2SO_4 (4.92 mL; 91.8 mmol) was added drop-wise, then the reaction was allowed to warm to rt. The reaction was stirred at rt o/n, then poured over ice-cold 4 N NaOH (100 mL). The aqueous phase was separated, then the organic phase washed with 1 N NaOH (2 × 100 mL) then brine (50 mL). The organic phase was dried over Na_2SO_4, then concentrated *in vacuo*. Purification by flash chromatography (0→30% EtOAc in cyclohexane) yielded 8.09 g (68%) of **311** as a colourless oil.

R$_f$. 0.65 (1:3 EtOAc/cyclohexane). **IR (neat): ν_{max} (cm^{-1})** 2981, 2934, 2851, 1725, 1395, 1369, 1297, 1257, 1156, 1081. **^{1}H NMR** (400 MHz, $CDCl_3$) δ 3.03 (t, *J* = 6.6 Hz, 2H, H3), 2.54 (t, *J* = 6.6 Hz, 2H, H4), 1.53 (s, 9H, C(C<u>H</u>$_3$)$_3$), 1.42 (s, 9H, C(C<u>H</u>$_3$)$_3$). **^{13}C NMR** (101 MHz, $CDCl_3$) δ 193.9 (C2), 171.4 (<u>C</u>=O), 160.2 (<u>C</u>=O), 84.1 (<u>C</u>(CH$_3$)$_3$), 81.0 (<u>C</u>(CH$_3$)$_3$), 34.3 (C3), 28.9 (C4), 28.1 (C(<u>C</u>H$_3$)$_3$), 27.9 (C(<u>C</u>H$_3$)$_3$). **HRMS** (ESI$^+$) *m*/*z* for [C$_{13}$H$_{22}$O$_5$Na]$^+$ [M+Na]$^+$ calculated 281.1359, found 281.1360. The spectroscopic data match those reported in the literature.[313]

1,5-Di-*tert*-butyl 3-methylidene-2-oxopentanedioate (312)

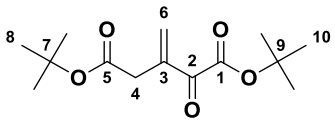

1,5-Di-*tert*-butyl 2-oxopentanedioate (2.64 g; 10.2 mmol) was dissolved in CH_2Cl_2 (25.6 mmol: 0.40 M), then cooled to 0 °C. [(Dimethylamino)methyl]dimethylamine (5.59 mL; 40.9 mmol) was added, followed by acetic acid (4.09 mL; 71.5 mmol) and acetic anhydride (4.82 mL; 51.1 mmol). The reaction was warmed to rt, then stirred for 5 h. The reaction mixture was diluted with ice-cold H_2O (30 mL), then the organic layer was separated. The organic layer was washed with H_2O (3 × 30 mL) then brine (15 mL), the organic layer was dried over Na_2SO_4 then concentrated *in vacuo*. Purification by flash chromatography (0→20% EtOAc in cyclohexane) yielded 1.19 g (43%) of **312** as a colourless oil.

R_f. 0.55 (1:4 EtOAc/cyclohexane). **IR (neat): ν_{max} (cm^{-1})** 2979, 2936, 1805, 1733, 1370, 1251, 1221, 1150. **^{1}H NMR** (400 MHz, $CDCl_3$) δ 6.18 (s, 1H, H6'), 6.13 (t, *J* = 1.2 Hz, 1H, H6''), 3.21 (d, *J* = 1.2 Hz, 2H, H4), 1.51 (s, 9H, C(C$\underline{H}_3$)$_3$), 1.37 (s, 9H, C(C$\underline{H}_3$)$_3$). **^{13}C NMR** (101 MHz, $CDCl_3$) δ 187.5 (C2), 169.2 (C=O), 163.0 (C=O), 138.7 (C3), 133.1 (C6), 84.6 (C(CH$_3$)$_3$), 81.4 (C(CH$_3$)$_3$), 37.1 (C4), 28.0 (C(CH$_3$)$_3$), 27.9 (C(CH$_3$)$_3$). **HRMS** (ESI^+) *m*/*z* for $[C_{14}H_{22}O_5Na]^+$ $[M+Na]^+$ calculated 293.1359, found 293.1359.

1,5-Di-*tert*-butyl 2-oxo-3-[(phenylsulfanyl)methyl]pentanedioate (313a)

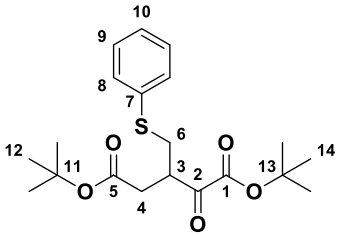

General procedure A was followed using 1,5-di-*tert*-butyl 3-methylidene-2-oxopentanedioate (100 mg; 0.37 mmol), benzenethiol (40.0 μL; 0.39 mmol), and triethylamine (2.50 μL; 19.0 μmol) in CH_2Cl_2 (1.85 mL). Purification by flash chromatography (0→30% EtOAc in cyclohexane) yielded 140 mg (99%) of **313a** as a colourless oil.

R_f. 0.65 (1:4 EtOAc/cyclohexane). **IR (neat): ν_{max} (cm^{-1})** 3059, 2980, 2921, 2850, 1724, 1370, 1296, 1258, 1155. **^{1}H NMR** (400 MHz, $CDCl_3$) δ 7.41 – 7.34 (m, 2H, Ar-H), 7.34 – 7.27 (m, 2H, Ar-H), 7.26 – 7.17 (m, 1H, Ar-H), 3.74 – 3.71 (m, 1H, H3), 3.31 (dd, *J* = 13.6, 6.1 Hz, 1H, H6'), 2.96 (dd, *J* = 13.7, 7.9 Hz, 1H, H6''), 2.85 – 2.68 (m, 2H, H4), 1.52 (s, 9H, C(CH_3)$_3$), 1.39 (s, 9H, C(CH_3)$_3$). **^{13}C NMR** (101 MHz, $CDCl_3$) δ 195.3 (C2), 170.4 (C=O), 159.9 (C=O), 135.2 (C7), 130.1 (Ar-CH), 129.1 (Ar-CH), 126.8 (Ar-CH), 84.1 (C(CH_3)$_3$), 81.5 (C(CH_3)$_3$), 43.2 (C3), 36.3 (C4), 34.7 (C6), 28.0 (C(CH_3)$_3$), 27.8 (C(CH_3)$_3$). **HRMS** (ESI$^+$) *m*/*z* for $[C_{20}H_{28}O_5SNa]^+$ [M+Na]$^+$ calculated 453.1550, found 453.1549.

1,5-Di-*tert*-butyl 2-oxo-3-[(propylsulfanyl)methyl]pentanedioate (313b)

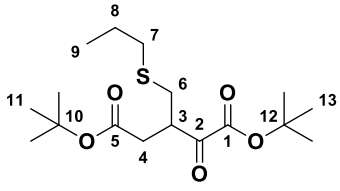

General procedure A was followed using 1,5-di-*tert*-butyl 3-methylidene-2-oxopentanedioate (100 mg; 0.37 mmol), propane thiol (36.0 μL; 0.39 mmol), and triethylamine

(2.50 μL; 19.0 μmol) in CH_2Cl_2 (1.85 mL). Purification by flash chromatography (0→30% EtOAc in cyclohexane) yielded 92 mg (72%) of **313b** as a colourless oil.

R_f. 0.70 (1:4 EtOAc/cyclohexane). **IR (neat): ν_{max} (cm^{-1})** 2979, 2931, 2874, 1800, 1772, 1731, 1371, 1227, 1151. **^{1}H NMR** (400 MHz, $CDCl_3$) δ 3.77 – 3.74 (m, 1H, H3), 2.82 (dd, *J* = 13.5, 6.4 Hz, 1H, H6'), 2.76 (dd, *J* = 16.9, 8.8 Hz, 1H, H6''), 2.66 (dd, *J* = 16.9, 5.2 Hz, 1H, H4'), 2.61 – 2.49 (m, 3H, H4'', H7), 1.67 – 1.55 (m, 2H, H8), 1.56 (s, 9H, $C(C\underline{H}_3)_3$), 1.41 (s, 9H, $C(C\underline{H}_3)_3$), 0.98 (t, *J* = 7.3 Hz, 3H, H9). **^{13}C NMR** (101 MHz, $CDCl_3$) δ 195.8 (C2), 170.6 ($\underline{C}$=O), 160.0 ($\underline{C}$=O), 84.0 ($\underline{C}(CH_3)_3$), 81.3 ($\underline{C}(CH_3)_3$), 43.2 (C3), 36.4 (C4), 34.6 (C7), 32.6 (C6), 28.0 ($C(\underline{C}H_3)_3$), 27.8 ($C(\underline{C}H_3)_3$), 22.7, 13.4 (C9). **HRMS** (ESI^+) *m*/*z* for $[C_{17}H_{30}O_5SNa]^+$ $[M+Na]^+$ calculated 369.1706, found 369.1707.

2-([4-(*tert*-Butoxy)-2-[2-(*tert*-butoxy)-2-oxoethyl]-3,4-dioxobutyl]sulfanyl)benzoic acid (313c)

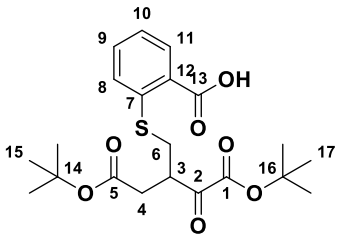

General procedure A was followed using 1,5-di-*tert*-butyl 3-methylidene-2-oxopentanedioate (100 mg; 0.37 mmol), 2-thiosalicylic acid (60.0 mg; 0.39 mmol), and triethylamine (2.50 μL; 19.0 μmol) in CH_2Cl_2 (1.85 mL). Purification by flash chromatography (0→35% EtOAc in cyclohexane) yielded 150 mg (95%) of **313c** as a white solid.

Mp. 137-140 °C. **R_f**. 0.25 (1:4 EtOAc/cyclohexane). **IR (neat): ν_{max} (cm^{-1})** 2981, 2932, 1721, 1688, 1466, 1370, 1294, 1256, 1155. **^{1}H NMR** (400 MHz, $CDCl_3$) δ 8.12 (dd,

J = 7.8, 1.6 Hz, 1H, H11), 7.55 (ddd, *J* = 8.2, 7.2, 1.6 Hz, 1H, H9), 7.47 (dd, *J* = 8.2, 1.2 Hz, 1H, H8), 7.29 – 7.20 (m, 1H, H10), 3.86– 3.82 (m, 1H, H3), 3.38 (dd, *J* = 13.3, 5.7 Hz, 1H, H6'), 2.95 (dd, *J* = 13.3, 8.6 Hz, 1H, H6''), 2.85 (d, *J* = 6.9 Hz, 2H, H4), 1.55 (s, 9H, C(C<u>H</u>$_3$)$_3$), 1.41 (s, 9H, C(C<u>H</u>$_3$)$_3$). **^{13}C NMR** (101 MHz, $CDCl_3$) δ 195.2 (C2), 170.6 (<u>C</u>=O), 170.4 (<u>C</u>=O), 159.9 (<u>C</u>=O), 141.2 (C7), 133.5 (C9), 132.6 (C11), 126.7 (C12), 126.0 (C8), 124.6 (C10), 84.3 (<u>C</u>(CH$_3$)$_3$), 81.6 (<u>C</u>(CH$_3$)$_3$), 42.2 (C3), 36.7 (C4), 32.6 (C6), 28.0 (C(<u>C</u>H$_3$)$_3$), 27.8 (C(<u>C</u>H$_3$)$_3$). **HRMS** (ESI$^+$) *m*/*z* for $[C_{21}H_{28}O_7SNa]^+$ [M+Na]$^+$ calculated 447.1448, found 447.1448.

1,5-Di-*tert*-butyl 3-[(butylsulfanyl)methyl]-2-oxopentanedioate (313d)

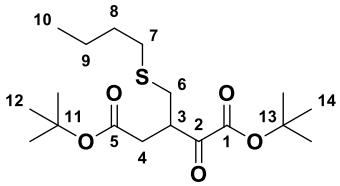

General procedure A was followed using 1,5-di-*tert*-butyl 3-methylidene-2-oxopentanedioate (100 mg; 0.37 mmol), butane thiol (42.0 μL; 0.39 mmol), and triethylamine (2.50 μL; 19.0 μmol) in CH_2Cl_2 (1.85 mL). Purification by flash chromatography (0→25% EtOAc in cyclohexane) yielded 96 mg (72%) of **313d** as a colourless oil.

R$_f$. 0.75 (1:4 EtOAc/cyclohexane). **IR (neat): ν$_{max}$ (cm^{-1})** 2980, 2931, 2874, 1800, 1772, 1731, 1371, 1227, 1151. **^{1}H NMR** (400 MHz, $CDCl_3$) δ 3.78– 7.75 (m, 1H, H3), 2.82 (dd, *J* = 13.5, 6.4 Hz, 1H, H6'), 2.76 (dd, *J* = 16.9, 8.9 Hz, 1H, H4'), 2.66 (dd, *J* = 16.9, 5.2 Hz, 1H, H4''), 2.60 – 2.51 (m, 3H, H6'', H7), 1.65 – 1.49 (m, 11H, C<u>H</u>$_2$, C(C<u>H</u>$_3$)$_3$), 1.48 – 1.32 (m, 11H, C<u>H</u>$_2$, C(C<u>H</u>$_3$)$_3$), 0.91 (t, *J* = 7.3 Hz, 3H, H10). **^{13}C NMR** (101 MHz, $CDCl_3$) δ 195.8 (C2), 170.6 (<u>C</u>=O), 160.0 (<u>C</u>=O), 84.0 (<u>C</u>(CH$_3$)$_3$), 81.3 (<u>C</u>(CH$_3$)$_3$), 43.1 (C3),

36.4 (<u>C</u>H$_2$), 32.6 (<u>C</u>H$_2$), 32.3 (<u>C</u>H$_2$), 31.4 (<u>C</u>H$_2$), 28.0 (C(<u>C</u>H$_3$)$_3$), 27.8 (C(<u>C</u>H$_3$)$_3$), 21.9 (C9), 13.7 (C10). **HRMS** (ESI$^+$) *m*/*z* for [C$_{18}$H$_{33}$O$_5$S]$^+$ [M+H]$^+$ calculated 383.1863, found 383.1864.

1,5-Di-*tert*-butyl 2-oxo-3-[(pyrimidin-2-ylsulfanyl)methyl]pentanedioate (313e)

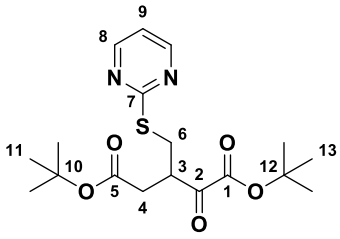

General procedure A was followed using 1,5-di-*tert*-butyl 3-methylidene-2-oxopentanedioate (100 mg; 0.37 mmol), 2-mercaptopyrimidine (44.0 mg; 0.39 mmol), and triethylamine (2.50 μL; 19.0 μmol) in CH_2Cl_2 (1.85 mL). Purification by flash chromatography (0→35% EtOAc in cyclohexane) yielded 103 mg (73%) of **313e** as a colourless oil.

R$_f$. 0.50 (1:2 EtOAc/cyclohexane). **IR (neat): ν_{max} (cm^{-1})** 3032, 2919, 2850, 1719, 1682, 1631, 1464, 1369, 1261, 1154, 1099. **^{1}H NMR** (400 MHz, $CDCl_3$) δ 8.47 (d, *J* = 4.9 Hz, 2H, H8), 6.97 (t, *J* = 4.8 Hz, 1H, H9), 3.95 (ddt, *J* = 8.4, 6.6, 5.6 Hz, 1H, H3), 3.55 (dd, *J* = 14.3, 5.8 Hz, 1H, H6'), 3.42 (dd, *J* = 14.3, 6.7 Hz, 1H, H6''), 2.87 (dd, *J* = 16.9, 8.4 Hz, 1H, H4'), 2.70 (dd, *J* = 16.9, 5.4 Hz, 1H, H4''), 1.56 (s, 9H, C(C<u>H</u>$_3$)$_3$), 1.41 (s, 9H, C(C<u>H</u>$_3$)$_3$). **^{13}C NMR** (101 MHz, $CDCl_3$) δ 194.4 (C2), 171.3 (<u>C</u>=O), 170.5 (<u>C</u>=O), 159.5 (C7), 157.1 (C8), 116.8 (C9), 83.8 (<u>C</u>(CH$_3$)$_3$), 81.4 (<u>C</u>(CH$_3$)$_3$), 43.3 (C3), 36.1 (C4), 31.4 (C6), 28.0 (C(<u>C</u>H$_3$)$_3$), 27.9 (C(<u>C</u>H$_3$)$_3$). **HRMS** (ESI$^+$) *m*/*z* for [C$_{18}$H$_{27}$N$_2$O$_5$S]$^+$ [M+H]$^+$ calculated 383.1635, found 383.1633.

1,5-Di-*tert*-butyl 2-oxo-3-[(pyridin-4-ylsulfanyl)methyl]pentanedioate (313f)

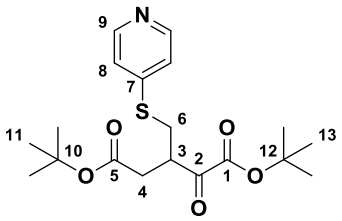

General procedure A was followed using 1,5-di-*tert*-butyl 3-methylidene-2-oxopentanedioate (100 mg; 0.37 mmol), pyridine-4-thiol (43.0 mg; 0.39 mmol), and triethylamine (2.50 μL; 19.0 μmol) in CH_2Cl_2 (1.85 mL). Purification by flash chromatography (0→45% EtOAc in cyclohexane) yielded 47 mg (33%) of **313f** as a pale-yellow oil.

R_f. 0.20 (1:2 EtOAc/cyclohexane). **IR (neat): ν_{max} (cm^{-1})** 2961, 2919, 2850, 1719, 1681, 1464, 1369, 1261, 1153, 1099. **^{1}H NMR** (400 MHz, $CDCl_3$) δ 8.40 – 8.34 (m, 2H, H9), 7.18 – 7.12 (m, 2H, H8), 3.77– 3.73 (m, 1H, H3), 3.32 (dd, *J* = 13.8, 6.4 Hz, 1H, H6'), 2.98 (dd, *J* = 13.8, 7.8 Hz, 1H, H6''), 2.80 – 2.60 (m, 2H, H4', H4''), 1.47 (s, 9H, C($C\underline{H}_3$)$_3$), 1.34 (s, 9H, C($C\underline{H}_3$)$_3$). **^{13}C NMR** (101 MHz, $CDCl_3$) δ 194.8 (C2), 170.1 ($\underline{C}$=O), 159.8 ($\underline{C}$=O), 149.2 (C7), 148.1 (C9), 121.0 (C8), 84.5 ($\underline{C}(CH_3)_3$), 81.9 ($\underline{C}(CH_3)_3$), 42.5 (C3), 36.5 (C4), 31.0 (C6), 28.0 (C($\underline{C}H_3$)$_3$), 27.8 (C($\underline{C}H_3$)$_3$). **HRMS** (ESI^+) *m*/*z* for $[C_{19}H_{28}NO_5S]^+$ $[M+H]^+$ calculated 382.1683, found 382.1683.

1,5-Di-*tert*-butyl 3-[(1,3-benzoxazol-2-ylsulfanyl)methyl]-2-oxopentanedioate (313g)

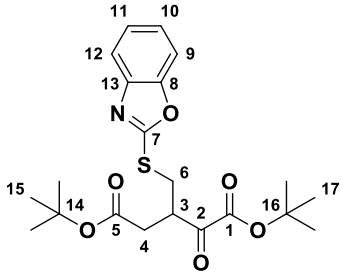

General procedure A was followed using 1,5-di-*tert*-butyl 3-methylidene-2-oxopentanedioate (98.0 mg; 0.36 mmol), 1,3-benzoxazole-2-thiol (65.0 μL; 0.43 mmol), and triethylamine (2.50 μL; 19.0 μmol) in CH_2Cl_2

(1.80 mL). Purification by flash chromatography (0→40% EtOAc in cyclohexane) yielded 163 mg (99%) of **313g** as a white solid.

Rf. 0.40 (1:2 EtOAc/cyclohexane). **IR (neat): ν_{max} (cm^{-1})** 2980, 2937, 1717, 1698, 1558, 1507, 1396, 1262, 1153, 1079. **^{1}H NMR** (400 MHz, $CDCl_3$) δ 7.37 – 7.22 (m, 4H, Ar-H), 4.41 (dd, *J* = 6.8, 1.2 Hz, 2H, H6), 4.21 – 4.17 (m, 1H, H3), 2.82 (dd, *J* = 6.6, 3.4 Hz, 2H, H4), 1.47 (s, 9H, C(CH$_3$)$_3$), 1.41 (s, 9H, C(CH$_3$)$_3$). **^{13}C NMR** (101 MHz, $CDCl_3$) δ 194.4 (C2), 180.6 (C7), 170.1 (C=O), 159.4 (C=O), 147.1 (Ar-C), 131.9 (Ar-C), 125.2 (Ar-CH), 124.5 (Ar-CH), 110.4 (Ar-CH), 110.1 (Ar-CH), 84.5 (C(CH$_3$)$_3$), 82.1 (C(CH$_3$)$_3$), 46.0 (C6), 41.9 (C3), 35.6 (C4), 28.0 (C(CH$_3$)$_3$), 27.7 (C(CH$_3$)$_3$). **HRMS** (ESI$^+$) *m*/*z* for $[C_{21}H_{28}NO_6S]^+$ $[M+H]^+$ calculated 422.1632, found 422.1632.

1,5-Di-*tert*-butyl 3-[(1*H*-1,3-benzodiazol-2-ylsulfanyl)methyl]-2-oxopentanedioate (313h)

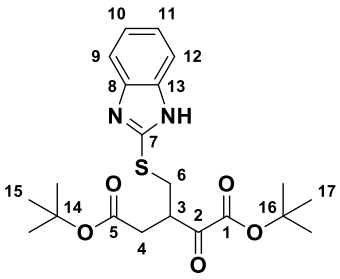

General procedure A was followed using 1,5-di-*tert*-butyl 3-methylidene-2-oxopentanedioate (270 mg; 1.00 mmol), 1*H*-1,3-benzodiazole-2-thiol (165 mg; 1.10 mmol), and triethylamine (7.00 μL; 50.0 μmol) in CH_2Cl_2 (5.00 mL; 0.20 M). Purification by flash chromatography (0→35% EtOAc in cyclohexane) yielded 126 mg (30%) of **313h** as a yellow oil.

Rf. 0.55 (1:2 EtOAc/cyclohexane). **IR (neat): ν_{max} (cm^{-1})** 3222, 3012, 2981, 2886, 1771, 1969, 1558, 1507, 1387, 1340, 1153. **^{1}H NMR** (400 MHz, $CDCl_3$) δ 7.33 – 7.22 (m, 4H,

Ar-H), 4.58 (dd, *J* = 14.2, 6.9 Hz, 1H, H6'), 4.46 (dd, *J* = 14.1, 6.8 Hz, 1H, H6''), 4.22 (m, 1H, H3), 2.87 (dd, *J* = 17.4, 8.4 Hz, 1H, H4'), 2.74 (dd, *J* = 17.4, 5.2 Hz, 1H, H4''), 1.46 (s, 9H, C(CH$_3$)$_3$), 1.40 (s, 9H, C(CH$_3$)$_3$). **^{13}C NMR** (126 MHz, $CDCl_3$) δ 194.8 (C2), 170.5 (C=O), 169.4 (C7), 159.7 (C=O), 133.0 (Ar-C), 130.4 (Ar-C), 123.8 (Ar-CH), 123.4 (Ar-CH), 110.0 (Ar-CH), 109.9 (Ar-CH), 84.3 (C(CH$_3$)$_3$), 82.0 (C(CH$_3$)$_3$), 44.6 (C6), 42.9 (C3), 35.6 (C4), 28.1 (C(CH$_3$)$_3$), 27.8 (C(CH$_3$)$_3$). **HRMS** (ESI$^+$) *m*/*z* for $[C_{21}H_{29}N_2O_5S]^+$ $[M+H]^+$ calculated 421.2333, found 421.2334.

1,5-Di-*tert*-butyl 3-[(1*H*-imidazol-2-ylsulfanyl)methyl]-2-oxopentanedioate (313i)

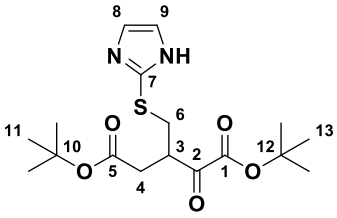

General procedure A was followed using 1,5-di-*tert*-butyl 3-methylidene-2-oxopentanedioate (270 mg; 1.00 mmol), 1*H*-imidazole-2-thiol (110 mg; 1.10 mmol), and triethylamine (7.00 μL; 50.0 μmol) in CH_2Cl_2 (5.00 mL; 0.20 M). Purification by flash chromatography (0→35% EtOAc in cyclohexane) yielded 350 mg (94%) of **313i** as a yellow oil.

R$_f$. 0.35 (1:2 EtOAc/cyclohexane). **IR (neat): ν_{max} (cm^{-1})** 3198, 2978, 2932, 2875, 1722, 1482, 1457, 1370, 1275, 1258, 1157, 1111, 1014. **^{1}H NMR** (400 MHz, $CDCl_3$) δ 6.77 (d, *J* = 2.4 Hz, 1H, Ar-H), 6.68 (d, *J* = 2.4 Hz, 1H. Ar-H), 4.36 – 4.22 (m, 2H, H6), 4.10 – 3.97 (m, 1H, H3), 2.84 (dd, *J* = 16.9, 5.4 Hz, 1H, H4'), 2.74 (dd, *J* = 17.0, 7.2 Hz, 1H, H4''), 1.54 (s, 9H, C(CH$_3$)$_3$), 1.40 (s, 9H, C(CH$_3$)$_3$). **^{13}C NMR** (101 MHz, $CDCl_3$) δ 194.4 (C2), 170.2 (C=O), 159.5 (C=O), 150.9 (C7), 119.5 (Ar-CH), 114.0 (Ar-CH),

84.3 (<u>C</u>(CH_3)$_3$), 82.0 (<u>C</u>(CH_3)$_3$), 46.9 (C6), 43.6 (C3), 35.3 (C4), 28.0 (C(<u>C</u>H_3)$_3$), 27.8 (C(<u>C</u>H_3)$_3$). **HRMS** (ESI^+) *m/z* for $[C_{17}H_{27}N_2O_5S]^+$ $[M+H]^+$ calculated 371.1635, found 371.1635.

1,5-Di-*tert*-butyl 2-oxo-3-[(pyridin-2-ylsulfanyl)methyl]pentanedioate (313j)

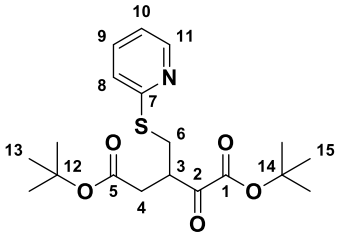

General procedure A was followed using 1,5-di-*tert*-butyl 3-methylidene-2-oxopentanedioate (270 mg; 1.00 mmol), pyridine-2-thiol (122 mg; 1.10 mmol), and triethylamine (7.00 μL; 50.0 μmol) in CH_2Cl_2 (5.00 mL; 0.20 M). Purification by flash chromatography (0→20% EtOAc in cyclohexane) yielded 288 mg (75%) of **313j** as a colourless oil.

R_f. 0.45 (1:5 EtOAc/cyclohexane). **IR (neat): ν_{max} (cm^{-1})** 2980, 2932, 1723, 1579, 1456, 1417, 1369, 1257, 1155. **^{1}H NMR** (400 MHz, $CDCl_3$) δ 8.37 (dd, *J* = 5.1, 1.9, 1H, H11), 7.47 (ddd, *J* = 8.1, 7.3, 1.9 Hz, 1H, H9), 7.16 (d, *J* = 8.1 Hz, 1H, H8), 7.02 – 6.95 (m, 1H, H10), 3.92 – 3.88 (m, 1H, H3), 3.62 (dd, *J* = 14.1, 5.7 Hz, 1H, H6'), 3.44 (dd, *J* = 14.1, 6.8 Hz, 1H, H6''), 2.85 (dd, *J* = 16.9, 8.5 Hz, 1H, H4'), 2.68 (dd, *J* = 16.9, 5.4 Hz, 1H, H4''), 1.55 (s, 9H, C(C<u>H</u>$_3$)$_3$), 1.40 (s, 9H, C(C<u>H</u>$_3$)$_3$). **^{13}C NMR** (101 MHz, $CDCl_3$) δ 194.5 (C2), 170.6 (<u>C</u>=O), 159.6 (<u>C</u>=O), 157.5 (C7), 148.9 (C11), 136.3 (C9), 122.3 (C8), 119.7 (C10), 83.7 (<u>C</u>(CH_3)$_3$), 81.3 (<u>C</u>(CH_3)$_3$), 43.5 (C3), 36.1 (C4), 30.3 (C6), 28.1 (C(<u>C</u>H_3)$_3$), 27.8 (C(<u>C</u>H_3)$_3$). **HRMS** (ESI^+) *m/z* for $[C_{19}H_{28}NO_5S]^+$ $[M+H]^+$ calculated 382.1683, found 382.1682.

1,5-Di-*tert*-butyl 3-([(4-hydroxyphenyl)sulfanyl]methyl)-2-oxopentanedioate (313n)

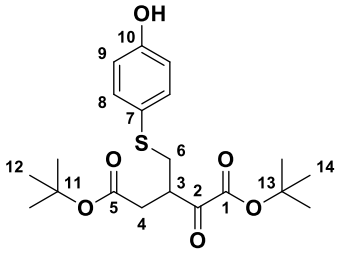

General procedure A was followed using 1,5-di-*tert*-butyl 3-methylidene-2-oxopentanedioate (270 mg; 1.00 mmol), 4-hydroxythiophenol (139 mg; 1.10 mmol), and triethylamine (7.00 μL; 50.0 μmol) in CH_2Cl_2 (5.00 mL; 0.20 M). Purification by flash chromatography (0→50% EtOAc in cyclohexane) yielded 320 mg (81%) of **313n** as a white solid.

R_f. 0.20 (1:2 EtOAc/cyclohexane). **IR (neat): ν_{max} (cm^{-1})** 2980, 2933, 1800, 1723, 1600, 1584, 1496, 1370, 1262, 1154. **^{1}H NMR** (400 MHz, $CDCl_3$) δ 7.36 – 7.27 (m, 2H, Ar-H), 6.82 – 6.74 (m, 2H, Ar-H), 3.68 – 3.65 (m, 1H, H3), 3.18 (dd, *J* = 13.6, 6.2 Hz, 1H, H6'), 2.91 – 2.65 (m, 3H, H4', H4'', H6''), 1.51 (s, 9H, $C(CH_3)_3$), 1.39 (s, 9H, $C(CH_3)_3$). **^{13}C NMR** (101 MHz, $CDCl_3$) δ 195.6 (C2), 170.7 (C=O), 159.9 (C=O), 155.8 (Ar-C), 134.3 (Ar-C), 125.1 (Ar-CH), 116.3 (Ar-CH), 84.2 ($C(CH_3)_3$), 81.6 ($C(CH_3)_3$), 43.5 (C3), 36.9 (C4), 36.2 (C6), 28.0 ($C(CH_3)_3$), 27.8 ($C(CH_3)_3$). **HRMS** (ESI$^+$) *m*/*z* for $[C_{20}H_{29}O_6S]^+$ $[M+H]^+$ calculated 397.1679, found 397.1681.

1,5-Di-*tert*-butyl 3-([(4-methoxyphenyl)sulfanyl]methyl)-2-oxopentanedioate (313o)

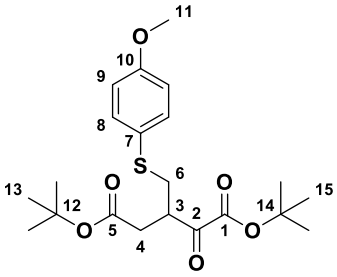

General procedure A was followed using 1,5-di-*tert*-butyl 3-methylidene-2-oxopentanedioate (270 mg; 1.00 mmol), 4-methoxythiophenol (135 μL; 1.10 mmol), and triethylamine (7.00 μL; 50.0 μmol) in CH_2Cl_2 (5.00 mL; 0.20 M). Purification by flash chromatography (0→40% EtOAc in cyclohexane) yielded 305 mg (74%) of **313o** as a colourless oil.

R_f. 0.45 (1:2 EtOAc/cyclohexane). **IR (neat): ν_{max} (cm^{-1})** 2980, 2931, 2850, 1727, 1592, 1495, 1369, 1296, 1257, 1155. **^{1}H NMR** (400 MHz, $CDCl_3$) δ 7.43 – 7.33 (m, 2H, Ar-H), 6.89 – 6.81 (m, 2H, Ar-H), 3.79 (s, 3H, H11), 3.67 – 3.63 (m, 1H, H3), 3.19 (dd, *J* = 13.6, 6.2 Hz, 1H, H6'), 2.90 – 2.66 (m, 3H, H4', H4'', H6''), 1.51 (s, 9H, C(CH_3)$_3$), 1.39 (s, 9H, C(CH_3)$_3$). **^{13}C NMR** (101 MHz, $CDCl_3$) δ 195.5 (C2), 170.4 (C=O), 159.9 (C=O), 159.5 (Ar-C), 134.0 (Ar-C), 125.2 (Ar-CH), 114.8 (Ar-CH), 84.00 (C(CH_3)$_3$), 81.4 (C(CH_3)$_3$), 55.4 (C11), 43.4 (C3), 36.8 (C4), 36.2 (C6), 28.0 (C(CH_3)$_3$), 27.8 (C(CH_3)$_3$). **HRMS** (ESI^+) *m*/*z* for $[C_{21}H_{30}O_6SNa]^+$ [M+Na]$^+$ calculated 433.1655, found 433.1656.

1,5-Di-*tert*-butyl 2-oxo-3-(([4-(trifluoromethyl)phenyl]sulfanyl)methyl)pentanedioate (313q)

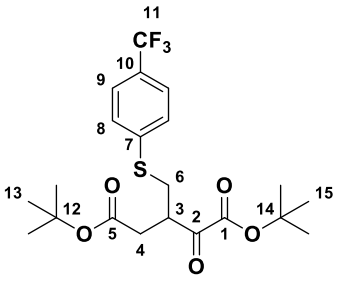

General procedure A was followed using 1,5-di-*tert*-butyl 3-methylidene-2-oxopentanedioate (270 mg; 1.00 mmol), 4-(trifluoromethyl)benzene-1-thiol (196 mg; 1.10 mmol), and triethylamine (7.00 μL; 50.0 μmol) in CH_2Cl_2 (5.00 mL; 0.20 M). Purification by flash chromatography (0→25% EtOAc in cyclohexane) yielded 231 mg (52%) of **313q** as a colourless oil.

R_f. 0.70 (1:2 EtOAc/cyclohexane). **IR (neat): ν_{max} (cm^{-1})** 3044, 2981, 2972, 1792, 1761, 1734, 1607, 1327, 1217, 1164, 1121, 1063. **^{1}H NMR** (400 MHz, $CDCl_3$) δ 7.58 – 7.50 (m, 2H, Ar-H), 7.47 – 7.39 (m, 2H, Ar-H), 3.79 (tdd, *J* = 8.1, 6.3, 5.6 Hz, 1H, H3), 3.37 (dd, *J* = 13.7, 6.3 Hz, 1H, H6'), 3.03 (dd, *J* = 13.7, 7.8 Hz, 1H, H6''), 2.86 – 2.67 (m, 2H, H4), 1.53 (s, 9H, C(CH$_3$)$_3$), 1.40 (s, 9H, C(CH$_3$)$_3$). **^{13}C NMR** (101 MHz, $CDCl_3$) δ 195.1 (C2), 170.3 (C=O), 160.0 (C=O), 140.9 (C7), 128.4 (C8), 126.0 (q, *J* = 3.8 Hz, C9), 124.0 (q, *J* = 272.0 Hz, C11) 84.5 (C(CH$_3$)$_3$), 81.8 (C(CH$_3$)$_3$), 43.0 (C3), 36.6 (C4), 33.4 (C6), 28.1 (C(CH$_3$)$_3$), 27.9 (C(CH$_3$)$_3$). **HRMS** (ESI$^+$) *m*/*z* for $[C_{16}H_{25}F_3O_5SNa]^+$ [M+Na]$^+$ calculated 409.1267, found 409.1270.

1,5-Di-*tert*-butyl 3-([(4-tert-butylphenyl)sulfanyl]methyl)-2-oxopentanedioate (313r)

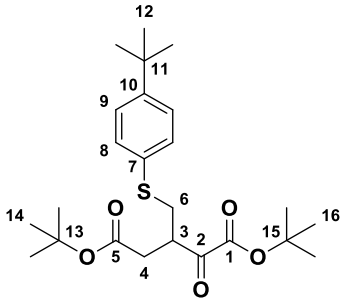

General procedure A was followed using 1,5-di-*tert*-butyl 3-methylidene-2-oxopentanedioate (270 mg; 1.00 mmol), 4-tert-butylbenzene-1-thiol (181 μL; 1.05 mmol), and triethylamine (7.00 μL; 50.0 μmol) in CH_2Cl_2 (5 mL; 0.20 M). Purification by flash chromatography (0→15% EtOAc in cyclohexane) yielded 300 mg (69%) of **313r** as a colourless oil.

R_f. 0.60 (1:4 EtOAc/cyclohexane). **IR (neat): ν_{max} (cm^{-1})** 2969, 2933, 2871, 1724, 1458, 1369, 1296, 1259, 1156. **^{1}H NMR** (400 MHz, $CDCl_3$) δ 7.32 (app. s, 4H, Ar-H), 3.73 (app. tt, *J* = 8.2, 5.8 Hz, 1H, H3), 3.28 (dd, *J* = 13.6, 6.0 Hz, 1H, H6'), 2.91 (dd, *J* = 13.6, 8.0 Hz, 1H H6''), 2.85 – 2.68 (m, 2H, H4), 1.51 (s, 9H, $C(CH_3)_3$), 1.39 (s, 9H, $C(CH_3)_3$), 1.30 (s, 9H, $C(CH_3)_3$). **^{13}C NMR** (101 MHz, $CDCl_3$) δ 195.5 (C2), 170.5 (C=O), 159.9 (C=O), 150.2 (C7), 131.5 (C10), 130.4 (Ar-CH), 126.2 (Ar-CH), 84.0 ($C(CH_3)_3$), 81.4 ($C(CH_3)_3$), 43.4 (C3), 36.3 (C4), 35.2 (C6), 34.5 (C11), 31.3 ($C(CH_3)_3$), 28.0 ($C(CH_3)_3$), 27.8 ($C(CH_3)_3$). **HRMS** (ESI^+) *m*/*z* for $[C_{24}H_{37}O_5S]^+$ $[M+H]^+$ calculated 437.2356, found 437.2358.

1,5-Di-*tert*-butyl 2-oxo-3-([(triphenylmethyl)sulfanyl]methyl)pentanedioate (313s)

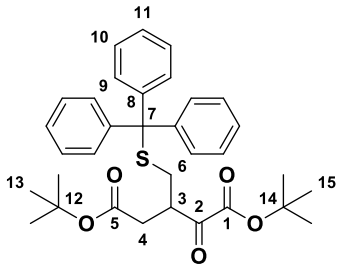

General procedure A was followed using 1,5-di-*tert*-butyl 3-methylidene-2-oxopentanedioate (270 mg; 1.00 mmol), triphenylmethanethiol (304 mg; 1.10 mmol), and triethylamine (7.00 μL; 50.0 μmol) in CH_2Cl_2 (5.00 mL; 0.20 M). Purification by flash chromatography (0→10% EtOAc in cyclohexane) yielded 461 mg (80%) of **313s** as a colourless oil.

R_f. 0.65 (1:5 EtOAc/cyclohexane). **IR (neat): ν_{max} (cm^{-1})** 2983, 2911, 1767, 1734, 1606, 1329, 1232, 1210, 1154, 1122, 1110.**^{1}H NMR** (400 MHz, $CDCl_3$) δ 7.33 – 7.28 (m, 6H, Ar-H), 7.27 – 7.17 (m, 6H, Ar-H), 7.15 (t, *J* = 1.4 Hz, 3H, H11), 3.33 – 3.29 (m, 1H, H3), 2.54 (dd, *J* = 16.9, 8.7 Hz, 1H, H6'), 2.45 (dd, *J* = 16.9, 4.9 Hz, 1H, H6''), 2.38 (dd, *J* = 11.9, 6.0 Hz, 1H, H4'), 2.12 (dd, *J* = 11.9, 7.8 Hz, 1H, H4''), 1.43 (s, 9H, C(CH_3)$_3$), 1.29 (s, 9H, C(CH_3)$_3$). **^{13}C NMR** (101 MHz, $CDCl_3$) δ 194.9 (C2), 170.2 (C=O), 159.7 (C=O), 144.3 (C8), 129.5 (Ar-CH), 128.0 (Ar-CH), 126.8 (Ar-CH), 83.9 (C(CH_3)$_3$), 81.3 (C(CH_3)$_3$), 67.0 (C7), 43.0 (C3), 36.4 (C4), 32.1 (C6), 28.0 (C(CH_3)$_3$), 27.8 (C(CH_3)$_3$). **HRMS** (ESI$^+$) *m*/*z* for $[C_{33}H_{38}O_5SNa]^+$ [M+Na]$^+$ calculated 569.2332, found 569.2331.

1,5-Di-*tert*-butyl 3-[(butan-2-ylsulfanyl)methyl]-2-oxopentanedioate (313t)

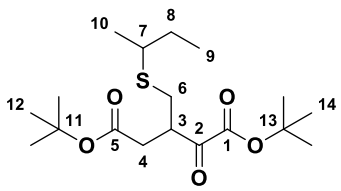

General procedure A was followed using 1,5-di-*tert*-butyl 3-methylidene-2-oxopentanedioate (270 mg; 1.00 mmol), butane-2-thiol (120 μL; 1.10 mmol), and triethylamine

(7.00 μL; 50.0 μmol) in CH_2Cl_2 (5.00 mL; 0.20 M). Purification by flash chromatography (0→15% EtOAc in cyclohexane) yielded 208 mg (58%) of **313t** as a colourless oil.

R_f. 0.65 (1:5 EtOAc/cyclohexane). **IR (neat): ν_{max} (cm^{-1})** 2976, 2932, 2876, 1726, 1457, 1369, 1277, 1258, 1158, 1116. **^{1}H NMR** (400 MHz, $CDCl_3$, 1:1 mixture of diastereromers) δ 3.80 – 3.69 (m, 1H, H3), 2.83– 2.54 (m, 5H, H4', H4'', H6', H6'', H7), 1.67 – 1.48 (m, 11H, H8, C(C<u>H</u>$_3$)$_3$), 1.41 (s, 9H, C(C<u>H</u>$_3$)$_3$), 1.24 (dd, *J* = 6.8, 2.1 Hz, 3H, H10), 0.95 (td, *J* = 7.4, 2.1 Hz, 3H, H9). **^{13}C NMR** (101 MHz, $CDCl_3$ 1:1 mixture of diastereomers) δ 195.8 (C2), 170.6 (<u>C</u>=O), 170.6 (<u>C</u>=O), 160.0 (<u>C</u>=O), 84.0 (<u>C</u>$(CH_3)_3$), 83.9 (<u>C</u>$(CH_3)_3$), 81.3 (<u>C</u>$(CH_3)_3$), 43.4 (C3), 43.4 (C3), 42.1 (C15), 42.0 (C15), 36.5 (C4), 36.4 (C4), 30.8 (C6), 30.7 (C6), 29.5 (C8), 28.0 (C(<u>C</u>H_3)$_3$), 27.8 (C(<u>C</u>H_3)$_3$), 20.6 (C10), 20.5 (C10), 11.3 (C9), 11.2 (C9). **HRMS** (ESI$^+$) *m*/*z* for $[C_{18}H_{32}O_5SNa]^+$ [M+Na]$^+$ calculated 383.1863, found 383.1864.

1,5-Di-*tert*-butyl 3-([(2-hydroxyethyl)sulfanyl]methyl)-2-oxopentanedioate (313u)

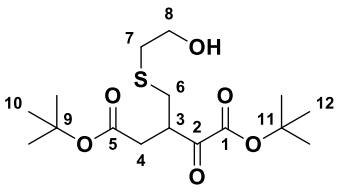

General procedure A was followed using 1,5-di-*tert*-butyl 3-methylidene-2-oxopentanedioate (270 mg; 1.00 mmol), 2-sulfanylethan-1-ol (77.0 μL; 1.10 mmol), and triethylamine (7.00 μL; 50.0 μmol) in CH_2Cl_2 (5.00 mL; 0.20 M). Purification by flash

chromatography (0→15% EtOAc in cyclohexane) yielded 186 mg (53%) of **313u** as a colourless oil.

R$_f$. 0.10 (1:5 EtOAc/cyclohexane). **IR (neat): ν_{max} (cm^{-1})** 2980, 2933, 2889, 1726, 1685, 1458, 1394, 1370, 1259, 1158, 1125, 1051. **^{1}H NMR** (400 MHz, $CDCl_3$) δ 3.86 – 3.72 (m, 3H, H3, H8), 2.87 (dd, *J* = 13.5, 6.9 Hz, 1H, H6'), 2.79 – 2.72 (m, 3H, H4', H7), 2.69 – 2.58 (m, 2H, H4'', H6''), 1.56 (s, 9H, C(C$\underline{H}_3$)$_3$), 1.41 (s, 9H, C(C$\underline{H}_3$)$_3$). **^{13}C NMR** (101 MHz, $CDCl_3$) δ 195.6 (C2), 170.5 (C=O), 160.1 (C=O), 84.3 (C(CH$_3$)$_3$), 81.6 (C(CH$_3$)$_3$), 60.5 (C8), 43.2 (C3), 36.5 (C7), 35.8 (C4), 32.2 (C6), 28.0 (C(CH$_3$)$_3$), 27.8 (C(CH$_3$)$_3$). **HRMS** (ESI$^+$) *m*/*z* for $[C_{16}H_{28}O_6SNa]^+$ [M+Na]$^+$ calculated 371.1499, found 371.1501.

1,5-Di-*tert*-butyl 3-[(ethylsulfanyl)methyl]-2-oxopentanedioate (313v)

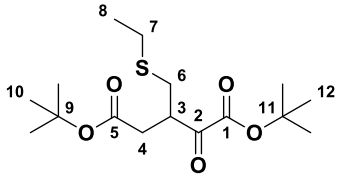

General procedure A was followed using 1,5-di-*tert*-butyl 3-methylidene-2-oxopentanedioate (270 mg; 1.00 mmol), ethanethiol (82.0 μL; 1.10 mmol), and triethylamine (7.00 μL; 50.0 μmol) in CH_2Cl_2 (5.00 mL; 0.20 M). Purification by flash chromatography (0→10% EtOAc in cyclohexane) yielded 86 mg (26%) of **313v** as a colourless oil.

R$_f$. 0.65 (1:5 EtOAc/cyclohexane). **IR (neat): ν_{max} (cm^{-1})** 2976, 2920, 2850, 1724, 1699, 1558, 1457, 1370, 1260, 1157. **^{1}H NMR** (400 MHz, $CDCl_3$) δ 3.78 – 3.74 (m, 1H, H3), 2.84– 2.54 (m, 6H, H4, H6, H7), 1.56 (s, 9H, C(C$\underline{H}_3$)$_3$), 1.41 (s, 9H, C(C$\underline{H}_3$)$_3$), 1.25 (t,

J = 7.4 Hz, 3H, H8). **^{13}C NMR** (101 MHz, $CDCl_3$) δ 195.8 (C2), 170.6 (C=O), 160.0 (C=O), 84.0 ($C(CH_3)_3$), 81.3 ($C(CH_3)_3$), 43.0 (CH_2), 36.4 (CH_2), 32.1 (CH_2), 28.0 ($C(CH_3)_3$), 27.8 ($C(CH_3)_3$), 26.3 (CH_2), 14.4 (C8). **HRMS** (ESI^+) *m*/*z* for $[C_{16}H_{28}O_5SNa]^+$ $[M+Na]^+$ calculated 355.1550, found 355.1551.

1,5-Di-*tert*-butyl 2-oxo-3-[(propan-2-ylsulfanyl)methyl]pentanedioate (313w)

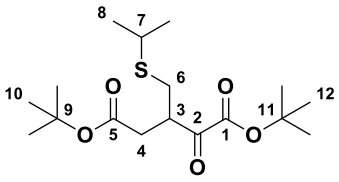

General procedure A was followed using 1,5-di-*tert*-butyl 3-methylidene-2-oxopentanedioate (270 mg; 1.00 mmol), propane-2-thiol (102 μL; 1.10 mmol), and triethylamine (7.00 μL; 50.0 μmol) in CH_2Cl_2 (5.00 mL; 0.20 M). Purification by flash chromatography (0→10% EtOAc in cyclohexane) yielded 207 mg (60%) of **313w** as a colourless oil.

R_f. 0.65 (1:5 EtOAc/cyclohexane). **IR (neat): ν_{max} (cm^{-1})** 2979, 2926, 2869, 1801, 1724, 1685, 1458, 1369, 1257, 1156. **^{1}H NMR** (400 MHz, $CDCl_3$) δ 3.77 – 3.74 (m, 1H, H3), 2.95 (hept, *J* = 6.7 Hz, 1H, H7), 2.84 (dd, *J* = 13.4, 6.4 Hz, 1H, H6'), 2.79 – 2.63 (m, 2H, H4), 2.58 (dd, *J* = 13.4, 7.9 Hz, 1H, H6''), 1.56 (s, 9H, $C(CH_3)_3$), 1.41 (s, 9H, $C(CH_3)_3$), 1.29 – 1.22 (m, 6H, H8). **^{13}C NMR** (101 MHz, $CDCl_3$) δ 195.8 (C2), 170.6 (C=O), 160.0 (C=O), 84.0 ($C(CH_3)_3$), 81.3 ($C(CH_3)_3$), 43.3 (C3), 36.5 (C4), 35.2 (C7), 31.0 (C6), 28.0 ($C(CH_3)_3$), 27.8 ($C(CH_3)_3$), 23.2 (C8). **HRMS** (ESI^+) *m*/*z* for $[C_{17}H_{30}O_5SNa]^+$ $[M+Na]^+$ calculated 369.1706, found 369.1708.

1,5-Di-*tert*-butyl 2-oxo-3-([(2,2,2-trifluoroethyl)sulfanyl]methyl)pentanedioate (313x)

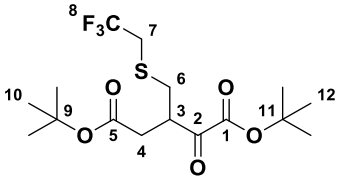

General procedure A was followed using 1,5-di-*tert*-butyl 3-methylidene-2-oxopentanedioate (270 mg; 1.00 mmol), 2,2,2-trifluoroethane-1-thiol (145 μL; 1.05 mmol), and triethylamine (7.00 μL; 50.0 μmol) in CH_2Cl_2 (5.00 mL; 0.20 M). Purification by flash chromatography (0→20% EtOAc in cyclohexane) yielded 162 mg (42%) of **313x** as a colourless oil.

R_f. 0.55 (1:4 EtOAc/cyclohexane). **IR (neat): ν_{max} (cm^{-1})** 2981, 2937, 1802, 1724, 1371, 1313, 1260, 1154, 1125, 1080. **^{1}H NMR** (400 MHz, $CDCl_3$) δ 3.79 (dtd, *J* = 8.5, 7.1, 5.4 Hz, 1H, H3), 3.13 (qd, *J* = 9.8, 4.9 Hz, 2H, H7), 2.95 (dd, *J* = 13.6, 7.0 Hz, 1H, H6'), 2.81 – 2.70 (m, 2H, H4', H6''), 2.63 (dd, *J* = 16.9, 5.4 Hz, 1H, H4''), 1.55 (s, 9H, C(C$\underline{H}_3$)$_3$), 1.41 (s, 9H, C(C$\underline{H}_3$)$_3$). **^{13}C NMR** (101 MHz, $CDCl_3$) δ 195.1 (C2), 170.2 ($\underline{C}$=O), 159.9 ($\underline{C}$=O), 125.7 (q, *J* = 276.4 Hz, C8), 84.4 ($\underline{C}(CH_3)_3$), 81.7 ($\underline{C}(CH_3)_3$), 42.7 (C3), 36.4 (C4), 34.4 (q, *J* = 32.9 Hz, C7), 33.1 (C6), 28.0 (C($\underline{C}H_3$)$_3$), 27.7 (C($\underline{C}H_3$)$_3$). **HRMS** (ESI^+) *m*/*z* for $[C_{16}H_{25}F_3O_5SNa]^+$ $[M+Na]^+$ calculated 409.1267, found 409.1270.

2-Oxo-3-[(phenylsulfanyl)methyl]pentanedioic acid (292a)

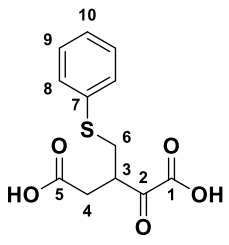

General procedure B was followed using 1,5-di-*tert*-butyl 2-oxo-3-[(phenylsulfanyl)methyl]pentanedioate (59.0 mg; 155 μmol) and TFA (237 μL; 3.10 mmol) in CH_2Cl_2 (310 μL). Purification by

reverse-phase chromatography (0→100% MeCN + 0.1% formic acid/H_2O + 0.1% formic acid) yielded 19 mg (46%) of **292a** as a yellow oil.

IR (neat): ν_{max} (cm^{-1}) 3074, 2981, 2972, 1791, 1773, 1726, 1482, 1439, 1219, 1024. **^{1}H NMR** (500 MHz, D_2O) δ 7.32 – 7.29 (m, 2H, Ar-H), 7.25 – 7.21 (m, 2H, Ar-H), 7.17 – 7.13 (m, 1H, H10), 3.51 (qd, *J* = 7.2, 5.8 Hz, 1H, H3), 3.17 (dd, *J* = 13.6, 7.2 Hz, 1H, H6'), 3.04 (dd, *J* = 13.7, 5.9 Hz, 1H, H6''), 2.46 (dd, *J* = 15.6, 6.7 Hz, 1H, H4'), 2.27 (dd, *J* = 15.6, 7.6 Hz, 1H, H4''). **^{13}C NMR** (126 MHz, D_2O) δ 206.0 (C2), 179.4 (C=O), 169.3 (C=O), 134.8 (C7), 129.3 (Ar-CH), 128.3 (Ar-CH), 126.8 (Ar-CH), 45.1 (C3), 37.5 (C4), 33.5 (C6). **HRMS** (ESI^+) *m/z* for $[C_{12}H_{13}O_5SNa]^+$ $[M+Na]^+$ calculated 291.0298, found 291.0298.

2-Oxo-3-[(propylsulfanyl)methyl]pentanedioic acid (292b)

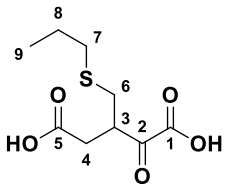

General procedure B was followed using 1,5-di-*tert*-butyl 2-oxo-3-[(propylsulfanyl)methyl]pentanedioate (40.0 mg; 115 μmol) and TFA (176 μL; 2.30 mmol) in CH_2Cl_2 (230 μL). Purification by reverse-phase chromatography (0→100% MeCN + 0.1% formic acid/H_2O + 0.1% formic acid) yielded 16 mg (59%) of **292b** as a yellow oil.

IR (neat): ν_{max} (cm^{-1}) 2964, 2931, 2874, 1749, 1732, 1653, 1419, 1213, 1154. **^{1}H NMR** (500 MHz, D_2O) δ 3.65 – 3.61 (m, 1H, H3), 2.81 (d, *J* = 13.5 Hz, 1H, H6'), 2.67 (d, *J* = 13.6 Hz, 1H, H6''), 2.54 – 2.46 (m, 3H, H4', H7), 2.31 (d, *J* = 15.7 Hz, 1H, H4''), 1.50 (m, 2H, H8), 0.86 (t, *J* = 7.4 Hz, 3H, H9). **^{13}C NMR** (126 MHz, D_2O) δ 206.5 (C2),

179.7 (C=O), 169.5 (C=O), 45.4 (C3), 37.5 (C4), 34.1 (C7), 31.2 (C6), 22.1 (C8), 12.6 (C9). **HRMS** (ESI$^-$) *m*/*z* for $[C_9H_{13}O_5S]^-$ $[M-H]^-$ calculated 233.0489, found 233.0484.

3-([(2-Carboxyphenyl)sulfanyl]methyl)-2-oxopentanedioic acid (292c)

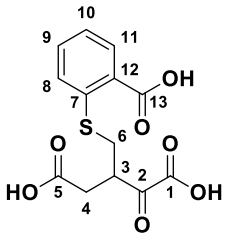

General procedure B was followed using 2-([4-(*tert*-butoxy)-2-[2-(*tert*-butoxy)-2-oxoethyl]-3,4-dioxobutyl]sulfanyl)benzoic acid (75.0 mg; 177 μmol) and TFA (270 μL; 3.54 mmol) in CH_2Cl_2 (354 μL). Purification by reverse-phase chromatography (0→100% MeCN + 0.1% formic acid/H_2O + 0.1% formic acid) yielded 15 mg (27%) of **292c** as a colourless oil.

IR (neat): ν_{max} (cm^{-1}) 3014, 2980, 2921, 2890, 1792, 1774, 1699, 1465, 1285, 1245, 1227, 1148, 1045, 1023. **^{1}H NMR** (500 MHz, D_2O) δ 7.35 (dd, *J* = 8.1, 1.1 Hz, 1H, H11), 7.26 (m, 2H, H8, H9), 7.11 (td, *J* = 7.5, 1.2 Hz, 1H, H10), 3.53 (app. p, *J* = 6.8 Hz, 1H, H3), 3.21 – 3.16 (m, 1H, H6'), 2.94 (dd, *J* = 13.2, 7.3 Hz, 1H, H6''), 2.48 (dd, *J* = 15.8, 6.9 Hz, 1H, H4'), 2.38 – 2.32 (m, 1H, H4''). **^{13}C NMR** (126 MHz, D_2O) δ 205.9 (C2), 179.5 (C=O), 176.6 (C=O), 169.4 (C=O), 139.9 (C7), 132.5 (C9), 129.5 (C11), 128.4 (C8), 127.4 (C10), 125.9 (C12), 44.9 (C3), 37.5 (C4), 32.9 (C6). **HRMS** (ESI$^+$) *m*/*z* for $[C_{13}H_{13}O_7S]^+$ $[M+H]^+$ calculated 313.0376, found 313.0378.

3-[(Butylsulfanyl)methyl]-2-oxopentanedioic acid (292d)

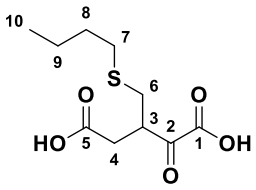

General procedure B was followed using 1,5-di-*tert*-butyl 3-[(butylsulfanyl)methyl]-2-oxopentanedioate (85.0 mg; 240 μmol) and TFA (360 μL; 4.70 mmol) in CH_2Cl_2 (1.20 mL). Purification by reverse-phase chromatography (0→100% MeCN + 0.1% formic acid/H_2O + 0.1% formic acid) yielded 32 mg (54%) of **292d** as a colourless oil.

^{1}H NMR (500 MHz, D_2O) δ 3.65 – 3.56 (m, 1H, H3), 2.82 (dd, *J* = 13.5, 7.0 Hz, 1H, H6'), 2.68 (dd, *J* = 13.5, 5.8 Hz, 1H, H6''), 2.57 – 2.47 (m, 3H, H4', H7), 2.32 (dd, *J* = 15.7, 7.5 Hz, 1H, H4''), 1.48 (tt, *J* = 7.6, 6.4 Hz, 2H, H8), 1.29 (h, *J* = 7.4 Hz, 2H, H9), 0.81 (t, *J* = 7.4 Hz, 3H, H10). **^{13}C NMR** (126 MHz, D_2O) δ 206.5 (C2), 179.7 (C=O), 169.6 (C=O), 45.3 (C3), 37.5 (C4), 31.7 (C7), 31.3 (C6), 30.8 (C8), 21.2 (C9), 12.9 (C10). **HRMS** (ESI^+) *m*/*z* for $[C_{10}H_{16}O_5SNa]^+$ $[M+Na]^+$ calculated 271.0383, found 271.0380.

2-Oxo-3-[(pyrimidin-2-ylsulfanyl)methyl]pentanedioic acid (292e)

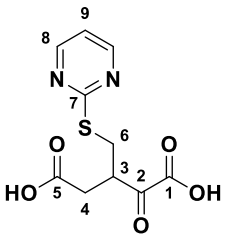

General procedure B was followed using 1,5-di-*tert*-butyl 2-oxo-3-[(pyrimidin-2-ylsulfanyl)methyl]pentanedioate (93.0 mg; 240 μmol) and TFA (360 μL; 4.7 mmol) in CH_2Cl_2 (1.20 mL). Purification by reverse-phase chromatography (0→100% MeCN + 0.1% formic acid/H_2O + 0.1% formic acid) yielded 25 mg (39%) of **292e** as a colourless oil.

IR (neat): ν_{max} (cm^{-1}) 2981, 2972, 2891, 1792, 1772, 1712, 1567, 1555, 1384, 1206, 1024, 988.**^{1}H NMR** (500 MHz, D_2O) δ 8.47 (d, *J* = 4.9 Hz, 2H, H8), 7.13 (t, *J* = 5.0 Hz, 1H,

H9), 3.87 – 3.78 (m, 1H, H3), 3.53 (dd, *J* = 14.1, 5.1 Hz, 1H, H6'), 3.42 (dd, *J* = 14.0, 6.7 Hz, 1H, H6''), 2.60 (dd, *J* = 15.9, 6.9 Hz, 1H, H4'), 2.39 (dd, *J* = 15.9, 7.2 Hz, 1H, H4''). **^{13}C NMR** (126 MHz, D_2O) δ 198.2 (C2), 179.5 (C=O), 170.1 (C=O), 168.8 (C7), 157.8 (C8), 117.5 (C9), 44.6 (C3), 37.4 (C4), 30.7 (C6). **HRMS** (ESI^-) *m*/*z* for $[C_{10}H_9N_2O_5S]^-$ $[M-H]^-$ calculated 269.0238, found 269.0234.

2-Oxo-3-[(pyridin-4-ylsulfanyl)methyl]pentanedioic acid (292f)

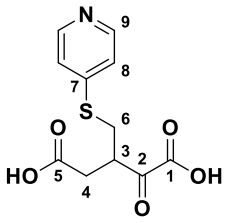

General procedure B was followed using 1,5-di-*tert*-butyl 2-oxo-3-[(pyridin-4-ylsulfanyl)methyl]pentanedioate (38.0 mg; 100 μmol) and TFA (153 μL; 2.00 mmol) in CH_2Cl_2 (500 μL). Purification by reverse-phase chromatography (0→100% MeCN + 0.1% formic acid/H_2O + 0.1% formic acid) yielded 10 mg (36%) of **292f** as a yellow oil.

IR (neat): ν_{max} (cm^{-1}) 2981, 2864, 1771, 1716, 1623, 1542, 1482, 1387, 1209, 1110, 985. **^{1}H NMR** (500 MHz, D_2O) δ 8.27 – 8.22 (m, 2H, H9), 7.33 – 7.30 (m, 2H, H8), 3.71 (tt, *J* = 7.6, 6.1 Hz, 1H, H3), 3.32 (dd, *J* = 13.8, 7.5 Hz, 1H, H6'), 3.22 (dd, *J* = 13.8, 5.8 Hz, 1H, H6''), 2.61 (dd, *J* = 15.9, 6.4 Hz, 1H, H4'), 2.37 (dd, *J* = 15.9, 7.8 Hz, 1H, H4''). **^{13}C NMR** (126 MHz, D_2O) δ 205.6 (C2), 179.1 (C=O), 169.3 (C=O), 148.1 (C7), 134.6 (C8), 121.4 (C9), 44.5 (C3), 37.6 (C4), 30.1 (C6). **HRMS** (ESI^+) *m*/*z* for $[C_{11}H_{12}NO_5S]^+$ $[M+H]^+$ calculated 270.0431, found 270.0431.

3-[(1,3-Benzoxazol-2-ylsulfanyl)methyl]-2-oxopentanedioic acid (292g)

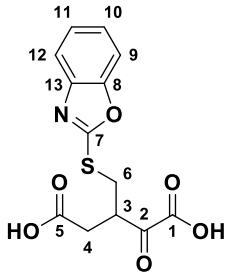

General procedure B was followed using 1,5-di-*tert*-butyl 3-[(1,3-benzoxazol-2-ylsulfanyl)methyl]-2-oxopentanedioate (152 mg; 360 μmol) and TFA (549 μL; 7.2 mmol) in CH_2Cl_2 (1.8 mL). Purification by reverse-phase chromatography (0→100% MeCN + 0.1% formic acid/H_2O + 0.1% formic acid) yielded 71 mg (64%) of **292g** as a colourless oil.

IR (neat): ν_{max} (cm^{-1}) 3064, 2981, 2889, 1793, 1779, 1717, 1478, 1449, 1399, 1285, 1241, 1023.**^{1}H NMR** (500 MHz, D_2O) δ 7.41 – 7.25 (m, 4H, Ar-H), 4.46 (dd, *J* = 14.3, 7.8 Hz, 1H, H6'), 4.31 (dd, *J* = 14.3, 6.4 Hz, 1H, H6''), 4.14 – 4.07 (m, 1H, H3), 2.59 (dd, *J* = 16.5, 7.3 Hz, 1H, H4'), 2.48 (dd, *J* = 16.5, 6.5 Hz, 1H, H4''). **^{13}C NMR** (126 MHz, D_2O) δ 204.8 (C2), 180.3 (C7), 178.7 (C=O), 168.0 (C=O), 147.0 (Ar-C), 139.9 (Ar-C), 125.3 (Ar-CH), 124.8 (Ar-CH), 110.9 (Ar-CH), 110.4 (Ar-CH), 46.1 (C3), 42.9 (C4), 36.6 (C6). **HRMS** (ESI$^+$) *m*/*z* for $[C_{13}H_{12}NO_6S]^+$ $[M+H]^+$ calculated 310.0380, found 310.0380.

3-[(1*H*-1,3-Benzodiazol-2-ylsulfanyl)methyl]-2-oxopentanedioic acid (292h)

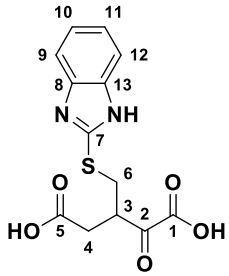

General procedure B was followed using 1,5-di-*tert*-butyl 3-[(1*H*-1,3-benzodiazol-2-ylsulfanyl)methyl]-2-oxopentanedioate (116 mg; 280 μmol) and TFA (421 μL; 9.85 mmol) in CH_2Cl_2 (2.45 mL). Purification by reverse-phase chromatography

(0→100% MeCN + 0.1% formic acid/H_2O + 0.1% formic acid) yielded 37 mg (43%) of **292h** as a yellow oil.

IR (neat): ν_{max} (cm^{-1}) 3101, 2980, 2890, 1792, 1770, 1733, 1717, 1684, 1507, 1458, 1396, 1329, 1215, 1159. **^{1}H NMR** (500 MHz, D_2O) δ 7.34 – 7.31 (m, 1H, Ar-H), 7.27 – 7.16 (m, 2H, Ar-H), 4.48 (dd, *J* = 14.3, 7.7 Hz, 1H, Ar-H), 4.34 (dd, *J* = 14.3, 7.0 Hz, 1H, H6'), 4.09 – 4.01 (m, 1H, H3), 2.58 – 2.48 (m, 1H, H4'), 2.46 – 2.38 (m, 1H, H4''). **^{13}C NMR** (126 MHz, D_2O) δ 205.3 (C2), 179.0 (C=O), 168.2, (C=O), 166.0 (C6), 132.8 (Ar-C), 131.0 (Ar-C), 123.6 (Ar-CH), 123.0 (Ar-CH), 122.5 (Ar-CH), 110.8 (Ar-CH), 46.8 (C6), 42.1 (C3), 36.5 (C4). **HRMS** (ESI^+) *m/z* for $[C_{13}H_{13}N_2O_5S]^+$ $[M+H]^+$ calculated 309.0540, found 309.0540.

3-[(1*H*-Imidazol-2-ylsulfanyl)methyl]-2-oxopentanedioic acid (292i)

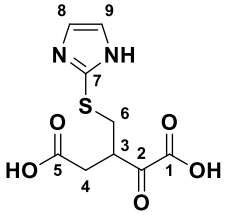

General procedure B was followed using 1,5-di-*tert*-butyl 3-[(1*H*-imidazol-2-ylsulfanyl)methyl]-2-oxopentanedioate (336 mg; 910 μmol) and TFA (1.40 mL; 18.2 mmol) in CH_2Cl_2 (4.55 mL). Purification by reverse-phase chromatography (0→100% MeCN + 0.1% formic acid/H_2O + 0.1% formic acid) yielded 142 mg (60%) of **292i** as a pale-yellow lyophilised powder.

IR (neat): ν_{max} (cm^{-1}) 3136, 2980, 2931, 1721, 1577, 1459, 1278, 1257, 1158. **^{1}H NMR** (500 MHz, D_2O) δ 6.91 (d, *J* = 2.4 Hz, 1H, Ar-H), 6.83 (d, *J* = 2.3 Hz, 1H, Ar-H), 4.76-4.65 (m, 1H, H3 (under D_2O peak)), 4.33 – 4.23 (m, 1H, H6'), 4.19 – 4.08 (m, 1H, H6'),

2.52 – 2.33 (m, 2H, H4). **^{13}C NMR** (126 MHz, D_2O) δ 205.0 (C2), 178.8 (C=O), 168.5 (C=O), 156.7 (C7), 120.0 (Ar-CH), 116.1 (Ar-CH), 46.8 (C6), 44.7 (C3), 36.2 (C4). **HRMS** (ESI^+) *m*/*z* for $[C_9H_{11}N_2O_5S]^+$ $[M+H]^+$ calculated 259.0383, found 259.0382.

2-Oxo-3-[(pyridin-2-ylsulfanyl)methyl]pentanedioic acid (292j)

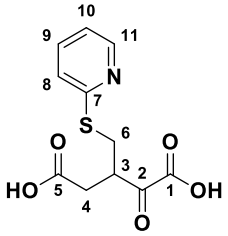

General procedure B was followed using 1,5-di-*tert*-butyl 2-oxo-3-[(pyridin-2-ylsulfanyl)methyl]pentanedioate (276 mg; 720 μmol) and TFA (1.10 mL; 14.5 mmol) in CH_2Cl_2 (3.60 mL). Purification by reverse-phase chromatography (0→100% MeCN + 0.1% formic acid/H_2O + 0.1% formic acid) yielded 65 mg (34%) of **292j** as a colourless oil.

IR (neat): ν_{max} (cm^{-1}) 3103, 3043, 2943, 1772, 1719, 1614, 1580, 1455, 1417, 1275, 1211, 1138, 986. **^{1}H NMR** (500 MHz, D_2O) δ 8.28 (ddd, *J* = 5.0, 2.0, 0.9 Hz, 1H, H11), 7.65 (td, *J* = 7.8, 1.9 Hz, 1H, H9), 7.36 (d, *J* = 8.1 Hz, 1H, H8), 7.13 (ddd, *J* = 7.5, 5.0, 1.1 Hz, 1H, H10), 3.75 – 3.66 (m, 1H, H3), 3.40 – 3.30 (m, 2H, H6), 2.57 (dd, *J* = 15.8, 6.7 Hz, 1H, H4'), 2.37 (dd, *J* = 15.8, 7.5 Hz, 1H, H4''). **^{13}C NMR** (126 MHz, D_2O) δ 205.6 (C2), 179.3 (C=O), 173.1 (C=O), 149.1 (C7), 140.4 (C11), 134.5 (C9), 132.3 (C8), 116.4 (C10), 44.9 (C3), 37.5 (C4), 30.9 (C6). **HRMS** (ESI^+) *m*/*z* for $[C_{11}H_{12}NO_5S]^+$ $[M+H]^+$ calculated 270.0431, found 270.0431.

3-([(4-Hydroxyphenyl)sulfanyl]methyl)-2-oxopentanedioic acid (292n)

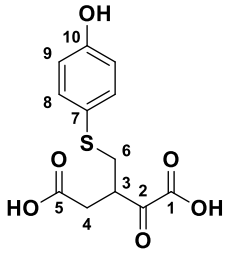

General procedure B was followed using 1,5-di-*tert*-butyl 3-([(4-hydroxyphenyl)sulfanyl]methyl)-2-oxopentanedioate (307 mg; 770 μmol) and TFA (1.19 mL; 15.5 mmol) in CH_2Cl_2 (3.85 mL). Purification by reverse-phase chromatography (0→100% MeCN + 0.1% formic acid/H_2O + 0.1% formic acid) yielded 113 mg (52%) of **292n** as a colourless oil.

IR (neat): ν_{max} (cm^{-1}) 3354, 2980, 2972, 2930, 1749, 1733, 1585, 1495, 1429, 1220, 1173. **^{1}H NMR** (500 MHz, D_2O) δ 7.30 – 7.26 (m, 2H, Ar-H), 6.76 – 6.72 (m, 2H, Ar-H), 3.52 – 3.46 (m, 1H, H3), 3.15 – 3.08 (m, 1H, H6'), 2.99 – 2.92 (m, 1H, H6''), 2.51 (dd, *J* = 15.7, 7.0 Hz, 1H, H4'), 2.34 (dd, *J* = 15.7, 7.3 Hz, 1H, H4''). **^{13}C NMR** (126 MHz, D_2O) δ 206.2 (C2), 179.5 (C=O), 169.3 (C=O). 158.1 (C10), 134.2 (C7), 122.5 (Ar-CH), 117.1 (Ar-CH), 45.2 (C3), 37.5 (C4), 35.9 (C6). **HRMS** (ESI$^+$) *m*/*z* for $[C_{12}H_{13}O_6S]^+$ $[M+H]^+$ calculated 285.0427, found 285.0428.

3-([(4-Methoxyphenyl)sulfanyl]methyl)-2-oxopentanedioic acid (292o)

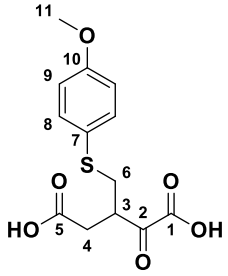

General procedure B was followed using 1,5-di-*tert*-butyl 3-([(4-methoxyphenyl)sulfanyl]methyl)-2-oxopentanedioate (292 mg; 710 μmol) and TFA (1.09 mL; 14.2 mmol) in CH_2Cl_2 (3.55 mL). Purification by reverse-phase chromatography (0→100% MeCN + 0.1% formic acid/H_2O + 0.1% formic acid) yielded 114 mg (54%) of **292o** as a colourless oil.

IR (neat): ν_{max} (cm^{-1}) 2980, 2971, 2839, 1792, 1759, 1733, 1592, 1494, 1286, 1243, 1179, 1026. **^{1}H NMR** (500 MHz, D_2O) δ 7.37 (d, *J* = 8.9 Hz, 2H, Ar-H), 6.91 (d, *J* = 8.8 Hz, 2H, Ar-H), 3.76 (s, 3H, H11), 3.53 – 3.47 (m, 1H, H3), 3.16 (dd, *J* = 13.6, 7.1 Hz, 1H, H6'), 3.01 (dd, *J* = 13.6, 5.8 Hz, 1H, H6''), 2.51 (dd, *J* = 15.7, 6.8 Hz, 1H, H4'), 2.33 (dd, *J* = 15.7, 7.4 Hz, 1H, H4''). **^{13}C NMR** (126 MHz, D_2O) δ 206.1 (C2), 179.5 (C=O), 169.3 (C=O), 158.6 (C10), 133.5 (C7), 125.4 (Ar-CH), 115.0 (Ar-CH), 55.5 (C11), 45.2 (C3), 37.5 (C4), 35.4 (C6). **HRMS** (ESI^+) *m/z* for $[C_{13}H_{14}O_6S]^+$ $[M+H]^+$ calculated 299.0658, found 299.0566.

2-Oxo-3-(([4-(trifluoromethyl)phenyl]sulfanyl)methyl)pentanedioic acid (292q)

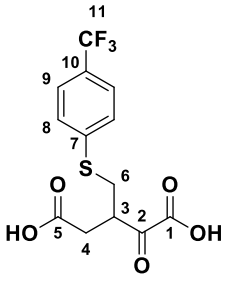

General procedure B was followed using 1,5-di-*tert*-butyl 2-oxo-3-(([4-(trifluoromethyl)phenyl]sulfanyl)methyl)pentanedioate (221 mg; 490 μmol) and TFA (1.13 mL; 9.85 mmol) in CH_2Cl_2 (2.45 mL). Purification by reverse-phase chromatography (0→100% MeCN + 0.1% formic acid/H_2O + 0.1% formic acid) yielded 152 mg (92%) of **292q** as a colourless oil.

IR (neat): ν_{max} (cm^{-1}) 3019, 2980, 2972, 1791, 1760, 1734, 1607, 1327, 1217, 1122, 1064. **^{1}H NMR** (400 MHz, D_2O) δ 7.59 (d, *J* = 8.1 Hz, 2H, H9), 7.49 (d, *J* = 8.0 Hz, 2H, H9), 3.65 (tt, *J* = 7.4, 5.9 Hz, 1H, H3), 3.32 (dd, *J* = 13.7, 7.3 Hz, 1H, H6'), 3.20 (dd, *J* = 13.7, 5.8 Hz, 1H, H6''), 2.58 (dd, *J* = 15.7, 6.5 Hz, 1H, H4'), 2.37 (dd, *J* = 15.7, 7.7 Hz, 1H, H4''). **^{13}C NMR** (^{19}F decoupled) (126 MHz, D_2O) δ 205.8 (C2), 179.3 (C=O),

169.2 (C=O), 140.7 (C7), 132.9 (C10), 128.2(C8), 125.8 (C9), 124.5 (C11), 38.3 (C3), 37.5 (C4), 32.1 (C6). **^{19}F NMR** (471 MHz, D_2O) δ -62.2. **HRMS** (ESI^-) *m/z* for $[C_{13}H_{10}F_3O_5S]^-$ $[M-H]^-$ calculated 335.0207, found 335.0197.

3-([(4-*tert*-Butylphenyl)sulfanyl]methyl)-2-oxopentanedioic acid (292r)

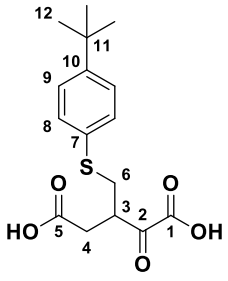

General procedure B was followed using 1,5-di-*tert*-butyl 3-([(4-*tert*-butylphenyl)sulfanyl]methyl)-2-oxopentanedioate (288 mg; 660 μmol) and TFA (1.01 mL; 13.2 mmol) in CH_2Cl_2 (3.30 mL). Purification by reverse-phase chromatography (0→100% MeCN + 0.1% formic acid/H_2O + 0.1% formic acid) yielded 137 mg (64%) of **292r** as a yellow oil.

IR (neat): ν_{max} (cm^{-1}) 2964, 2904, 2870, 1760, 1733, 1488, 1396, 1363, 1267, 1218, 1161, 1122, 1013. **^{1}H NMR** (500 MHz, D_2O) δ 7.40 (d, *J* = 8.6 Hz, 2H, Ar-H), 7.34 (d, *J* = 8.5 Hz, 2H, Ar-H), 3.61 – 3.52 (m, 1H, H3), 3.23 (dd, *J* = 13.6, 7.2 Hz, 1H, H6'), 3.07 (dd, *J* = 13.6, 6.0 Hz, 1H, H6''), 2.54 (dd, *J* = 15.7, 6.8 Hz, 1H, H4'), 2.36 (dd, *J* = 15.7, 7.3 Hz, 1H, H4''), 1.22 (s, 9H, H12). **^{13}C NMR** (126 MHz, D_2O) δ 206.0 (C2), 179.4 (C=O), 169.4 (C=O), 150.7 (C7), 131.4 (C10), 130.0 (Ar-CH), 126.5 (Ar-CH), 77.2 (C11), 45.1 (C3), 37.6 (C4), 33.9 (C6), 30.4 (C12). **HRMS** (ESI^-) *m/z* for $[C_{16}H_{19}O_5S]^-$ $[M-H]^-$ calculated 323.0959, found 323.0953.

3-[(Butan-2-ylsulfanyl)methyl]-2-oxopentanedioic acid (292t)

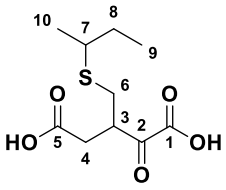

General procedure B was followed using 1,5-di-*tert*-butyl 3-[(butan-2-ylsulfanyl)methyl]-2-oxopentanedioate (198 mg; 530 μmol) and TFA (809 mL; 10.6 mmol) in CH_2Cl_2 (2.65 mL). Purification by reverse-phase chromatography (0→100% MeCN + 0.1% formic acid/H_2O + 0.1% formic acid) yielded 82 mg (62%) of **292t** as a colourless oil.

IR (neat): ν_{max} (cm^{-1}) 2967, 2932, 2877, 1757, 1730, 1455, 1420, 1389, 1217, 1148. **^{1}H NMR** (500 MHz, D_2O) (1:1 mixture of diastereomers) δ 2.87 – 2.65 (m, 3H, H3, H6', H6''), 2.52 – 2.47 (m, 1H, H3), 2.31 (app dd, *J* = 15.7, 8.7 Hz, 1H, H4'), 1.57 – 1.35 (m, 3H, H4'', H8), 1.16 (app dd, *J* = 6.7, 2.0 Hz, 3H, H10), 0.85 (app td, *J* = 7.4, 2.8 Hz, 3H, H9). **^{13}C NMR** (151 MHz, D_2O) (1:1 mixture of diastereomers) δ 206.4 (C2), 179.7 (C=O), 169.5 (C=O), 45.5 (C3), 42.1 (C7), 37.4 (C4), 29.4 (C6), 29.0 (C8), 19.8 (C10), 10.6 (C9). **HRMS** (ESI^+) *m/z* for $[C_{10}H_{16}O_5SNa]^+$ $[M+Na]^+$ calculated 271.0611, found 271.0611.

3-([(2-Hydroxyethyl)sulfanyl]methyl)-2-oxopentanedioic acid (292u)

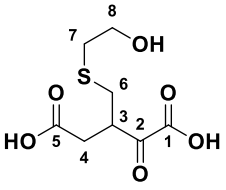

General procedure B was followed using 1,5-di-*tert*-butyl 3-([(2-hydroxyethyl)sulfanyl]methyl)-2-oxopentanedioate (175 mg; 500 μmol) and TFA (765 μL; 10.0 mmol) in CH_2Cl_2 (2.50 mL). Purification by reverse-phase chromatography (0→100% MeCN + 0.1% formic acid/H_2O + 0.1% formic acid) yielded 51 mg (43%) of **292u** as a colourless oil.

IR (neat): ν_{max} (cm^{-1}) 2978, 2926, 1293, 1731, 1418, 1213, 1154, 987. **^{1}H NMR** (500 MHz, D_2O) δ 3.69 – 3.57 (m, 3H, H3, H8), 2.85 (dd, *J* = 13.5, 7.1 Hz, 1H, H6'), 2.76 – 2.64 (m, 3H, H6'', H7), 2.54 (dd, *J* = 15.6, 6.7 Hz, 1H, H4'), 2.33 (dd, *J* = 15.7, 7.6 Hz, 1H, H4''). **^{13}C NMR** (126 MHz, D_2O) δ 206.4 (C2), 179.6 (C=O), 169.7 (C=O), 60.1 (C8), 45.4 (C3), 37.5 (C4), 34.2 (C7), 31.3 (C6). **HRMS** (ESI^-) *m/z* for $[C_8H_{11}O_6S]^-$ $[M-H]^-$ calculated 235.0282, found 235.0277.

3-[(Ethylsulfanyl)methyl]-2-oxopentanedioic acid (292v)

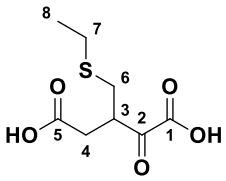

General procedure B was followed using 1,5-di-*tert*-butyl 3-[(ethylsulfanyl)methyl]-2-oxopentanedioate (74.0 mg; 220 μmol) and TFA (341 μL; 4.45 mmol) in CH_2Cl_2 (1.10 mL). Purification by reverse-phase chromatography (0→100% MeCN + 0.1% formic acid/H_2O + 0.1% formic acid) yielded 36 mg (74%) of **292v** as a colourless oil.

IR (neat): ν_{max} (cm^{-1}) 2979, 2933, 2876, 1796, 1729, 1421, 1215, 1154. **^{1}H NMR** (500 MHz, D_2O) δ 3.52 – 3.45 (m, 1H, H3), 2.81 (d, *J* = 13.5 Hz, 1H, H6'), 2.67 (d, *J* = 13.6 Hz, 1H, H6''), 2.54 – 2.46 (m, 2H, H4', H7), 2.31 (d, *J* = 15.7 Hz, 1H, H4''), 1.14 (t, *J* = 7.4 Hz, 3H, H8). **^{13}C NMR** (126 MHz, D_2O) δ 206.5 (C2), 179.7 (C=O), 169.5 (C=O), 37.5 (C3), 34.1 (C4), 31.2 (C6), 22.2 (C7), 12.6 (C8). **HRMS** (ESI^+) *m/z* for $[C_8H_{12}O_5SNa]^+$ $[M+Na]^+$ calculated 243.0298, found 243.0299.

2-Oxo-3-[(propan-2-ylsulfanyl)methyl]pentanedioic acid (292w)

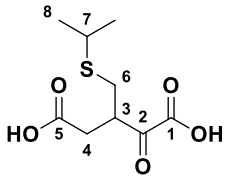

General procedure B was followed using 1,5-di-*tert*-butyl 2-oxo-3-[(propan-2-ylsulfanyl)methyl]pentanedioate (197 mg; 570 μmol) and TFA (870 μL; 11.4 mmol) in CH_2Cl_2 (2.85 mL). Purification by reverse-phase chromatography (0→100% MeCN + 0.1% formic acid/H_2O + 0.1% formic acid) yielded 92 mg (69%) of **292w** as a colourless oil.

IR (neat): ν_{max} (cm^{-1}) 2969, 2927, 2869, 1792, 1749, 1732, 1457, 1419, 1216, 1155. **^{1}H NMR** (600 MHz, D_2O) δ 3.47 – 3.41 (m, 1H, H3), 2.95 – 2.87 (m, 1H, H7), 2.87 – 2.77 (m, 2H, H6), 2.72 – 2.61 (m, 2H, H4), 1.18 (dd, *J* = 6.8, 2.5 Hz, 6H, H8). **HRMS** (ESI$^+$) *m*/*z* for $[C_9H_{14}O_5SNa]^+$ $[M+Na]^+$ calculated 257.0454, found 257.0454.

2-Oxo-3-([(2,2,2-trifluoroethyl)sulfanyl]methyl)pentanedioic acid (292x)

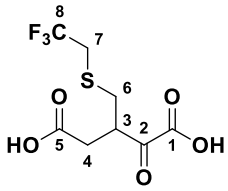

General procedure B was followed using 1,5-di-*tert*-butyl 2-oxo-3-([(2,2,2-trifluoroethyl)sulfanyl]methyl)pentanedioate (149 mg; 390 μmol) and TFA (590 μL; 7.70 mmol) in CH_2Cl_2 (2.00 mL). Purification by reverse-phase chromatography (0→100% MeCN + 0.1% formic acid/H_2O + 0.1% formic acid) yielded 58 mg (44%) of **292x** as a yellow oil.

IR (neat): ν_{max} (cm^{-1}) 2975, 2943, 2910, 2866, 1761, 1732, 1636, 1471, 1416, 1220, 1128. **^{1}H NMR** (500 MHz, D_2O) δ 3.66 – 3.58 (m, 1H, H3), 3.30 – 3.21 (m, 2H, H7), 3.00 – 2.96 (m, 1H, H6'), 2.86 – 2.82 (m, 1H, H6''), 2.56 (dd, *J* = 15.8, 6.6 Hz, 1H, H4'), 2.33 (dd, *J* = 15.7, 7.6 Hz, 1H, H4''). **^{19}F NMR** (470 MHz, D_2O) δ -66.5. **^{13}C NMR** (126 MHz,

D_2O) δ 206.0 (C2), 179.3 (C=O), 169.5 (C=O), 127.2 (q, *J* = 275.1 Hz, C8), 45.2 (C3), 37.4 (C4), 33.9 (q, *J* = 32.4 Hz, C7), 32.5 (C6). **HRMS** (ESI^+) *m/z* for $[C_8H_9F_3O_5S]^+$ $[M+H]^+$ calculated 273.0050, found 273.0047.

3-Phenylcyclohexan-1-one (319)[314]

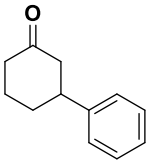

Following a modified reported procedure,[271] a reaction vial was charged with bis(1,5-cyclooctadiene)dirhodium(I) dichloride (26.0 mg; 52.0 μmol) and phenylboronic acid (95.0 mg; 0.78 mmol) then the atmosphere was purged with argon. A solution of degassed dioxane/H_2O (10:1, 1.73 mL; 0.30 M) was added, followed by degassed 1.5 N KOH (17.0 μL; 0.26 mmol). The solution was stirred for 5 min, then cyclohex-2-en-1-one (50.0 μL; 0.52 mmol) was added. The reaction was stirred at 30 °C for 1 h, then diluted in Et_2O (10 mL). The organic layer was separated and washed with sat. aq. $NaHCO_3$ (5 mL) then brine (5 mL). The organic layer was dried over Na_2SO_4 and concentrated *in vacuo*. Purification by flash chromatography (0→10% EtOAc in cyclohexane) yielded 85 mg (95%) of **319** as a colourless oil.

^{1}H NMR (400 MHz, $CDCl_3$) δ 7.36 (t, *J* = 8.2 Hz, 2H), 7.29-7.24 (m, 3H), 3.05-3.01 (m, 1H), 2.65-2.40 (m, 4H), 2.16-2.07 (m, 2H), 1.90-1.78 (m, 2H). **^{13}C NMR** (101 MHz, $CDCl_3$) δ 221.1, 144.4, 128.6, 126.6, 49.1, 44.8, 41.2, 32.8 25.5. **HRMS** (ESI^+) *m/z* for $[C_{12}H_{14}O]^+$ $[M+H]^+$ calculated 175.1117, found 175.1119. The spectroscopic data match those reported in the literature.[314]

1,5-Di-*tert*-butyl 3-benzyl-2-oxopentanedioate (320)

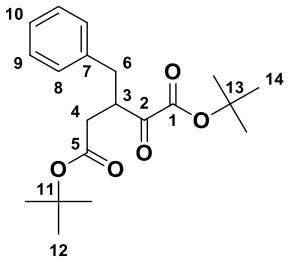

A reaction vial was charged with *bis*-(1,5-cyclooctadiene)dirhodium(I) dichloride (2.00 mg; 4.50 μmol) and phenylboronic acid (33.0 mg; 0.27 mmol) and purged with argon. A solution of degassed dioxane/H_2O (6:1 *v*/*v*, 660 μL; 0.30 M) was added, followed by triethylamine (25.0 μL; 0.18 mmol). The solution was stirred at rt for 5 min, then cyclohex-2-en-1-one (50.0 μL; 0.52 mmol) was added. The reaction was stirred at 30 °C for 1 h, then diluted in Et_2O (5 mL). The organic layer was separated and washed with sat. aq. $NaHCO_3$ (2 mL) then brine (2 mL). The organic layer was dried over Na_2SO_4 and concentrated *in vacuo*. Purification by flash chromatography (0→10% EtOAc in cyclohexane) yielded 56 mg (89%) of **320** as a colourless oil.

IR (neat): ν_{max} (cm^{-1}) 3064, 2917, 2849, 1749, 1684, 1653, 1456, 1211, 1130, 988. **^{1}H NMR** (400 MHz, $CDCl_3$) δ 7.35 – 7.13 (m, 5H, Ar-H), 3.84 (m, 1H, H3), 3.10 – 2.99 (m, 1H, H6'), 2.74 – 2.52 (m, 2H, H4), 2.40 (dd, *J* = 16.9, 4.6 Hz, 1H, H6''), 1.52 (s, 9H, $C(CH_3)_3$), 1.38 (s, 9H, $C(CH_3)_3$). **^{13}C NMR** (101 MHz, $CDCl_3$) δ 196.6 (C2), 170.7 (C=O), 160.0 (C=O), 137.9 (C7), 129.2 (Ar-CH), 128.7 (Ar-CH), 126.8 (Ar-CH), 83.9 ($C(CH_3)_3$), 81.2 ($C(CH_3)_3$), 45.1 (C3), 36.8 (C6), 36.2 (C4), 28.0 ($C(CH_3)_3$), 27.8 ($C(CH_3)_3$). **HRMS** (ESI^+) *m*/*z* for $[C_{20}H_{29}O_5]^+$ $[M+H]^+$ calculated 349.2010, found 349.2011.

2-Iodo-*N*-phenylbenzamide (329a)[315]

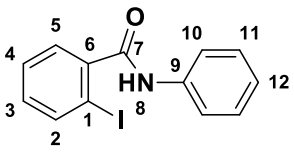

General procedure C was followed using 2-iodobenzoyl chloride (267 mg, 1.00 mmol), triethylamine (278 μL; 2.00 mmol), and aniline (100 μL, 1.10 mmol). Purification by flash chromatography (0→30% EtOAc in cyclohexane) yielded 250 mg (74%) of **329a** as a colourless oil.

Rf. 0.60 (1:2 EtOAc/cyclohexane). **IR (neat): ν_{max} (cm^{-1})** 3058, 2921, 1655, 1619, 1540, 1440, 1325. **^{1}H NMR** (400 MHz, $CDCl_3$) δ 7.91 (dd, J = 8.0, 1.0 Hz, 1H, Ar-H), 7.67 – 7.60 (m, 2H, Ar-H), 7.53 (dd, J = 7.5, 1.5 Hz, 1H, Ar-H), 7.46-7.36 (m, 4H, Ar-H, NH), 7.23 – 7.11 (m, 2H, Ar-H). **^{13}C NMR** (101 MHz, $CDCl_3$) δ 167.2 (C=O), 142.2 (Ar-C), 140.1 (Ar-CH), 137.5 (Ar-C), 131.5 (Ar-CH), 129.2 (Ar-CH), 128.6 (Ar-CH), 128.4 (Ar-CH), 125.0 (Ar-CH), 120.1 (Ar-CH), 92.4 (C1). **HRMS** (ESI^+) *m*/*z* calculated for $[C_{13}H_{10}INO+Na]^+$ $[M+Na]^+$ 345.9699, found: 345.9699. The spectroscopic data match those reported in the literature.[315]

***N*-Benzyl-2-iodobenzamide (329b)**[316]

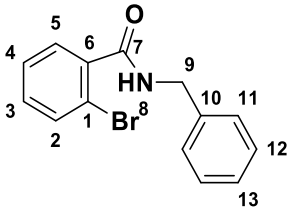

General procedure C was followed using 2-bromobenzoyl chloride (219 mg, 1.00 mmol), triethylamine (278 μL; 2.00 mmol), and benzylamine (120 μL, 1.10 mmol). Purification by flash chromatography (0→30% EtOAc in cyclohexane) yielded 184 mg (63%) of **329b** as an off-white solid.

Mp 115-116°C. **R**$_f$. 0.30 (1:4 EtOAc/cyclohexane). **IR (neat): ν_{max} (cm^{-1})** 3065, 2923, 1639, 1539, 1360. **^{1}H NMR** (400 MHz, $CDCl_3$) δ 7.49 (m, 2H, Ar-H), 7.41 – 7.09 (m, 7H, Ar-H), 6.20 (br. s, 1H, NH), 4.58 (d, J = 5.5 Hz, 2H, H9). **^{13}C NMR** (101 MHz, $CDCl_3$) δ 167.6 (C=O), 137.8 (Ar-C), 137.6 (Ar-C), 133.5 (Ar-CH), 131.5 (Ar-CH), 129.8 (Ar-CH), 128.9 (Ar-CH), 128.2 (Ar-CH), 127.8 (Ar-CH), 127.7 (Ar-CH), 119.4 (Ar-C), 44.4 (C9). **HRMS** (ESI$^+$) *m/z* calculated for $[C_{14}H_{12}BrNO+H]^+$: 290.0715, found 290.0717. The spectroscopic data match those reported in the literature.[316]

***N*-(Cyclohexylmethyl)-2-iodobenzamide (329c)**

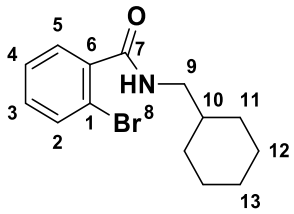

General procedure C was followed using 2-bromobenzoyl chloride (219 mg, 1.00 mmol), triethylamine (278 μL; 2.00 mmol), and cyclohexylmethylamine (143 μL, 1.10 mmol). Purification by flash chromatography (0→25% EtOAc in cyclohexane) yielded 180 mg (61%) of **329c** as a yellow oil.

R$_f$. 0.50 (1:2 EtOAc/Cyclohexane). **IR (neat): ν_{max} (cm^{-1})** 3068, 2921, 2850, 1641, 1541, 1367. **^{1}H NMR** (400 MHz, $CDCl_3$) δ 7.62 – 7.49 (m, 2H, Ar-H), 7.34 (td, J = 7.5, 1.0 Hz, 1H, Ar-H), 7.30 – 7.21 (m, 1H, Ar-H), 6.03 (br. s, 1H, NH), 3.30 (dd, J = 6.5, 6.0 Hz, 2H, H9), 2.01 – 1.52 (m, 6H, H10, CH_2), 1.42 – 1.11 (m, 3H, CH_2), 1.02 (m, 2H, CH_2). **^{13}C NMR** (101 MHz, $CDCl_3$) δ 167.7 (C=O), 138.3 (Ar-C), 133.5 (Ar-CH), 131.3 (Ar-CH), 129.8 (Ar-CH), 127.7 (Ar-CH), 119.3 (Ar-C), 46.5 (C9), 38.0 (C10), 31.1 (CH_2),

26.5 (<u>C</u>H$_2$), 26.0 (<u>C</u>H$_2$). **HRMS** (ESI$^+$) *m*/*z* calculated for [C$_{14}$H$_{18}$BrNO+H]$^+$: 296.0645, found 296.0646.

2-Iodo-*N*-pentylbenzamide (329d)[237, 317]

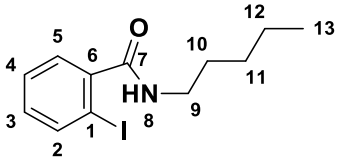

General procedure C was followed using 2-iodobenzoyl chloride (267 mg, 1.00 mmol), triethylamine (278 μL; 2.00 mmol), and pentylamine (128 μL, 1.10 mmol). Purification by flash chromatography (0→25% EtOAc in cyclohexane) yielded 203 mg (64%) of **329d** as a white solid.

Mp 98-100 °C**. R$_f$**. 0.45 (1:2 EtOAc/Cyclohexane). **IR (neat): ν_{max} (cm^{-1})** 3066, 2926, 1634, 1546. **^{1}H NMR** (400 MHz, CDCl$_3$) δ 7.88 – 7.81 (m, 1H, Ar-<u>H</u>), 7.43 – 7.32 (m, 2H, Ar-<u>H</u>), 7.08 (ddd, J = 8.0, 6.5, 3.0 Hz, 1H, Ar-<u>H</u>), 5.78 (br. s, 1H, N<u>H</u>), 3.44 (td, J = 7.0, 6.0 Hz, 2H, H9), 1.70 – 1.56 (m, 2H, H10), 1.46 – 1.30 (m, 4H, H11, H12), 0.99 – 0.82 (m, 3H, H13). **^{13}C NMR** (101 MHz, CDCl$_3$) δ 169.3 (<u>C</u>=O), 142.6 (Ar-<u>C</u>), 139.8 (Ar-<u>C</u>H), 131.0 (Ar-<u>C</u>H), 128.3 (Ar-<u>C</u>H), 128.2 (Ar-<u>C</u>H), 92.4 (C1), 40.1 (C9), 29.2 (C11), 29.1 (C10), 22.4 (C12), 14.0 (C13). **HRMS** (ESI$^+$) *m*/*z* calculated for [C$_{12}$H$_{16}$INO+H]$^+$: 318.0349, found 318.0349. The spectroscopic data match those reported in the literature.[317]

2-Iodo-*N*-(2-methoxyethyl)benzamide (329h)

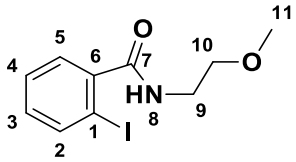

General procedure C was followed using 2-iodobenzoyl chloride (267 mg, 1.00 mmol), triethylamine (278 μL; 2.00 mmol), and 2-methoxyethan-1-amine (96.0 μL, 1.10 mmol). Purification by flash chromatography (0→40% EtOAc in cyclohexane) yielded 105 mg (34%) of **329h** as a white wax.

R_f. 0.40 (1:2 EtOAc/Cyclohexane). **IR (neat): ν_{max} (cm^{-1})** 3058, 2924, 1647, 1537, 1360, 1120, 1014. **^{1}H NMR** (400 MHz, $CDCl_3$) δ 7.92 – 7.83 (m, 1H, Ar-H), 7.45 – 7.33 (m, 2H, Ar-H), 7.09 (m, 1H, Ar-H), 6.16 (br. s, 1H, NH), 3.70 – 3.62 (m, 2H, H10), 3.59 (ddd, J = 5.5, 4.6, 1.1 Hz, 2H, H9), 3.39 (s, 3H, H11). **^{13}C NMR** (101 MHz, $CDCl_3$) δ 169.5 (C=O), 142.4 (Ar-C), 140.0 (Ar-CH), 131.2 (Ar-CH), 128.4 (Ar-CH), 128.3 (Ar-CH), 92.6 (C1), 71.1 (C10), 58.9 (C11), 39.8 (C9). **HRMS** (ESI^+) *m*/*z* calculated for $[C_{10}H_{12}INO_2+Na]^+$: 327.9805, found 327.9804.

Methyl 2-[(2-iodophenyl)formamido]acetate (329r)

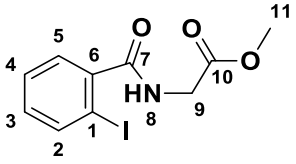

General procedure C was followed using 2-iodobenzoyl chloride (267 mg, 1.00 mmol), triethylamine (278 μL; 2.00 mmol), and methyl 2-aminoacetate hydrochloride (138 mg, 1.10 mmol). Purification by flash chromatography (0→45% EtOAc in cyclohexane) yielded 231 mg (71%) of **329r** as a white solid.

Mp 96-98°C. **R**f. 0.25 (1:2 EtOAc/cyclohexane). **IR (neat): ν_{max} (cm^{-1})** 3058, 2920, 1749, 1654, 1532, 1211, 1017; **^{1}H NMR** (400 MHz, CDCl3) δ 7.88 (dd, J = 7.9, 1.1 Hz, 1H, Ar-H), 7.44 (dd, J = 7.6, 1.9 Hz, 1H, Ar-H), 7.38 (td, J = 7.5, 1.1 Hz, 1H, Ar-H), 7.11 (ddd, J = 8.0, 7.3, 1.9 Hz, 1H, Ar-H), 6.37 (br. s, 1H, NH), 4.25 (d, J = 5.1 Hz, 2H, H9), 3.80 (s, 3H, H11). **^{13}C NMR** (101 MHz, $CDCl_3$) δ 170.0 (C=O), 169.2 (C=O), 141.3 (Ar-C), 140.1 (Ar-CH), 131.4 (Ar-CH), 128.5 (Ar-CH), 128.2 (Ar-CH), 92.4 (C1), 52.5 (C11), 41.7 (C9). **HRMS** (ESI$^+$) *m*/*z* calculated for $[C_{10}H_{10}INO_3+Na]^+$: 341.9598, found 341.9598.

2-Phenyl-2,3-dihydro-1,2-benzothiazol-3-one (321a)[308]

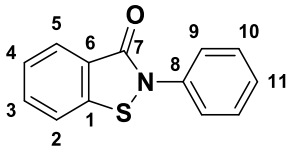

General procedure D was followed using CuI (42.0 mg, 0.22mmol), 1,10-phenanthroline (40.0 mg, 0.22 mmol), 2-iodo-*N*-phenylbenzamide (239 mg, 0.74 mmol), S_8 (32.5 mg, 0.96 mmol), and K_2CO_3 (131.5 mg, 0.96 mmol). Purification by flash chromatography (0→25% EtOAc in cyclohexane) yielded 117 mg (70%) of **321a** as a white solid.

Mp 141-143°C. **R**f. 0.70 (1:2 EtOAc/cyclohexane). **IR (neat): ν_{max} (cm^{-1})** 3064, 2921, 1663, 1593, 1488, 1448, 1299; **^{1}H NMR** (400 MHz, $CDCl_3$) δ 8.11 (ddd, J = 7.9, 1.2, 0.8 Hz, 1H, Ar-H), 7.76 – 7.69 (m, 2H, Ar-H), 7.67 (ddd, J = 8.2, 7.1, 1.2 Hz, 1H, Ar-H), 7.59 (dt, J = 8.1, 0.9 Hz, 1H, Ar-H), 7.52 – 7.41 (m, 3H, Ar-H), 7.37 – 7.28 (m, 1H, Ar-H). **^{13}C NMR** (101 MHz, $CDCl_3$) δ 164.3 (C=O), 140.0 (Ar-C), 137.4 (Ar-C), 132.5 (Ar-C), 129.5 (Ar-CH), 127.4 (Ar-CH), 127.2 (Ar-CH), 125.9 (Ar-CH), 125.0 (Ar-

CH), 124.7 (Ar-CH), 120.2 (Ar-CH). **HRMS** (ESI$^+$) *m*/*z* calculated for [$C_{13}H_9NOS+H]^+$: 228.0480, found: 228.0478. The spectroscopic data match those reported in the literature.[308]

2-Benzyl-2,3-dihydro-1,2-benzothiazol-3-one (321b)[308]

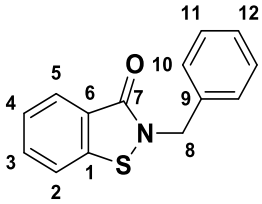

General procedure D was followed using CuI (29.0 mg, 0.15 mmol), 1,10-phenanthroline (27.0 mg, 0.15 mmol), *N*-benzyl-2-iodobenzamide (145 mg, 0.50 mmol), S_8 (22.0 mg, 0.65 mmol), and K_2CO_3 (89.0 mg, 0.65 mmol). Purification by flash chromatography (0→25% EtOAc/cyclohexane) yielded 59 mg (49%) of **321b** as a white solid.

Mp 140-142°C. **R**$_f$. 0.40 (1:3 EtOAc/cyclohexane). **IR (neat): ν_{max} (cm^{-1})** 3063, 2920, 1654, 1447, 1333. **^{1}H NMR** (400 MHz, $CDCl_3$) δ 8.07 (dt, J = 7.9, 1.0 Hz, 1H), 7.59 (ddd, J = 8.3, 7.1, 1.3 Hz, 1H), 7.49 (dt, J = 8.2, 0.9 Hz, 1H), 7.40 (ddd, J = 8.0, 7.1, 1.0 Hz, 1H), 7.37 – 7.29 (m, 5H), 5.06 (s, 2H). **^{13}C NMR** (101 MHz, $CDCl_3$) δ 165.5 (C=O), 140.6 (Ar-C), 136.3 (Ar-C), 132.0 (Ar-C), 129.0 (Ar-CH), 128.6 (Ar-CH), 128.4 (Ar-CH), 127.0 (Ar-CH), 125.7 (Ar-CH), 124.7 (Ar-CH), 120.5 (Ar-CH), 47.7 (C8). **HRMS** (ESI$^+$) *m*/*z* calculated for [$C_{14}H_{11}NOS+Na]^+$: 264.0454, found: 264.0454. The spectroscopic data match those reported in the literature.[308]

2-(Cyclohexylmethyl)-2,3-dihydro-1,2-benzothiazol-3-one (321c)

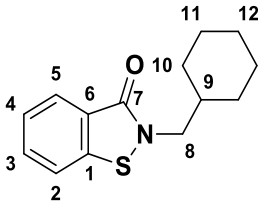

General procedure D was followed using CuI (29.0 mg, 0.15 mmol), 1,10-phenanthroline (27.0 mg, 0.15 mmol), 2-bromo-*N*-(cyclohexyl-methyl)benzamide (148 mg, 0.50 mmol), S_8 (22.0 mg, 0.65 mmol), and K_2CO_3 (89.0 mg, 0.65 mmol). Purification by flash chromatography (0→25% EtOAc in cyclohexane) yielded 22 mg (20%) of **321c** as a colourless oil.

R_f. 0.45 (1:3 EtOAc/cyclohexane). **IR (neat): ν_{max} (cm^{-1})** 3065, 2922, 1652, 1447, 1330. **^{1}H NMR** (400 MHz, $CDCl_3$) δ 8.03 (dt, J = 7.9, 1.0 Hz, 1H, Ar-H), 7.64 – 7.50 (m, 2H, Ar-H), 7.39 (ddd, J = 8.0, 7.0, 1.2 Hz, 1H, Ar-H), 3.73 (d, J = 7.3 Hz, 2H, H8), 1.88 – 1.61 (m, 6H, H9, CH_2), 1.29 – 1.14 (m, 3H, CH_2), 1.11 – 0.99 (m, 2H, CH_2). **^{13}C NMR** (101 MHz, $CDCl_3$) δ 165.7 (C=O), 140.4 (Ar-C), 131.8 (Ar-C), 126.9 (Ar-CH), 125.5 (Ar-CH), 124.9 (Ar-CH), 120.3 (Ar-CH), 50.2 (C8), 38.3 (C9), 30.7 (CH_2), 26.4 (CH_2), 25.8 (CH_2). **HRMS** (ESI^+) *m*/*z* calculated for $[C_{14}H_{17}NOS+H]^+$: 248.1104, found: 248.1104.

2-Pentyl-2,3-dihydro-1,2-benzothiazol-3-one (321d)[188]

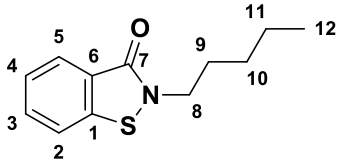

General procedure D was followed using CuI (32.0 mg, 0.18 mmol), 1,10-phenanthroline (34.0 mg, 0.18 mmol), 2-iodo-*N*-pentylbenzamide (190 mg, 0.60 mmol), S_8 (26.0 mg, 0.78 mmol), and K_2CO_3

(89.0 mg, 0.78 mmol). Purification by flash chromatography (0→30% EtOAc in cyclohexane) yielded 108 mg (81%) of **321d** as a colourless oil.

R_f. 0.65 (1:2 EtOAc/cyclohexane). **IR (neat): ν_{max} (cm^{-1})** 3066, 2955, 1650, 1446, 1336. **^{1}H NMR** (400 MHz, $CDCl_3$) δ 8.03 (dt, J = 7.9, 1.0 Hz, 1H, Ar-H), 7.64 – 7.50 (m, 2H, Ar-H), 7.39 (ddd, J = 8.0, 6.9, 1.2 Hz, 1H, Ar-H), 3.93 – 3.85 (m, 2H, H8), 1.82 – 1.71 (m, 2H, H9), 1.40 – 1.33 (m, 4H, H10, H11), 0.94 – 0.87 (m, 3H, H12). **^{13}C NMR** (101 MHz, $CDCl_3$) δ 165.4 (C=O), 140.3 (Ar-C), 131.7 (Ar-C), 126.8 (Ar-CH), 125.5 (Ar-CH), 125.0 (Ar-CH), 120.4 (Ar-CH), 44.1 (C8), 29.4 (C9), 28.8 (C10), 22.4 (C11), 14.1 (C12). **HRMS** (ESI^+) *m/z* calculated for $[C_{12}H_{15}NOS+H]^+$: 222.0947, found: 222.0949. The spectroscopic data match those reported in the literature.[188]

2-(2-Methoxyethyl)-2,3-dihydro-1,2-benzothiazol-3-one (321h)[318]

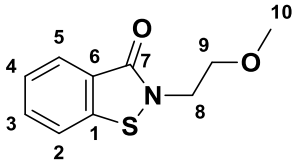

General procedure D was followed using CuI (17.0 mg, 0.09 mmol), 1,10-phenanthroline (18.0 mg, 0.09 mmol), 2-iodo-*N*-(2-methoxy-ethyl)benzamide (95.0. mg, 0.31 mmol), S_8 (103 mg, 0.40 mmol), and K_2CO_3 (55.0 mg, 0.40 mmol). Purification by flash chromatography (0→35% EtOAc in cyclohexane) yielded 40 mg (62%) of **321h** as a white solid.

Mp. 136-138°C. **R_f**. 0.30 (1:2 EtOAc/cyclohexane). **IR (neat): ν_{max} (cm^{-1})** 2961, 2923, 2852, 1750, 1653, 1637, 1558, 1541, 1458, 1260, 1090. **^{1}H NMR** (400 MHz, $CDCl_3$) δ 8.03 (dt, J = 7.9, 1.0 Hz, 1H, Ar-H), 7.59 (ddd, J = 8.2, 7.0, 1.3 Hz, 1H, Ar-H), 7.55 – 7.51 (m, 1H, Ar-H), 7.38 (ddd, J = 8.0, 7.0, 1.1 Hz, 1H, Ar-H), 4.09 (dd, J = 5.5, 4.7 Hz,

2H, H9), 3.69 (dd, J = 5.5, 4.7 Hz, 2H, H8), 3.40 (s, 3H, H10). **^{13}C NMR** (101 MHz, $CDCl_3$) δ 165. 7 (C=O), 141.2 (Ar-C), 131.9 (Ar-C), 126.7 (Ar-CH), 125.4 (Ar-CH), 124.3 (Ar-CH), 120.3 (Ar-CH), 71.3 (C9), 59.0 (C10), 44.0 (C8). **HRMS** (ESI^+) *m*/*z* calculated for $[C_{10}H_{11}NO_2S+H]^+$: 210.0583 found 210.0584. The spectroscopic data match those reported in the literature.[318]

Methyl 2-(1,3-dioxo-2,3-dihydro-1λ^4,2-benzothiazol-2-yl)acetate (321r)

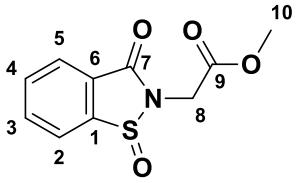

General procedure D was followed using CuI (36.0 mg, 0.20 mmol), 1,10-phenanthroline (39.0 mg, 0.20 mmol), methyl 2-[(2-iodophenyl)formamido]acetate (217 mg, 0.68 mmol), S_8 (29.0 mg, 0.88 mmol), and K_2CO_3 (122 mg, 0.88 mmol). Purification by flash chromatography (0→50% EtOAc/cyclohexane) yielded 25 mg (15%) of **321r** as a colourless oil.

R_f. 0.35 (1:1 EtOAc/cyclohexane). **IR (neat): ν_{max} (cm^{-1})** 3058, 2921, 1751, 1649, 1530, 1465, 1209, 746. **^{1}H NMR** (400 MHz, $CDCl_3$) δ 7.64 (dd, J = 7.6, 1.6 Hz, 1H, Ar-H), 7.47 – 7.37 (m, 1H, Ar-H), 7.34 (dd, J = 8.0, 1.3 Hz, 1H, Ar-H), 7.08 – 6.95 (m, 1H, Ar-H), 4.28 (d, J = 5.1 Hz, 2H, H8), 3.80 (s, 3H, H10). **^{13}C NMR** (151 MHz, $CDCl_3$) δ 168.2 (C=O), 165.8 (C=O), 140.8 (Ar-C), 132.3 (Ar-C), 127.0 (Ar-CH), 125.7 (Ar-CH), 123.4 (Ar-CH), 120.4 (Ar-CH), 52.7 (C10), 44.5 (C8). **HRMS** (ESI^+) *m*/*z* calculated for $[C_{10}H_9NO_4S+H]^+$ 240.0324, found 240.0325.

7.3.1 Characterisation Table for compounds synthesised by Siegfried Thun-Hohenstein

Cpd	^{1}H NMR	^{13}C NMR	IR	HRMS
321j	(400 MHz, $CDCl_3$) δ 9.29 (s, 1H), 8.75 (d, J = 5.4 Hz, 1H), 7.71 – 7.63 (m, 2H), 7.60 (d, J = 5.4 Hz, 1H), 7.56 – 7.45 (m, 2H), 7.44 – 7.33 (m, 1H).	(151 MHz, $CDCl_3$) δ 162.8, 149.9, 149.3, 149.1, 136.4, 129.8, 128.0, 125.0, 121.0, 115.2	2922, 2846, 1670, 1584, 1440, 1287, 1031	calcd. for $[C_{12}H_8N_2OS+H]^+$: 229.0430, found: 229.0432.
321k	(400 MHz, $CDCl_3$) δ 7.91 – 7.84 (m, 1H), 7.41 – 7.30 (m, 2H), 3.96 – 3.90 (m, 2H), 2.36 (s, 3H), 1.67 (pd, J = 4.6, 2.3 Hz, 3H), 1.03 – 0.93 (m, 6H)	(101 MHz, $CDCl_3$) δ 166.1, 140.4, 131.9, 130.0, 126.1, 124.8, 124.2, 42.5, 38.5, 25.8, 22.6, 18.8	3092, 2981, 2884, 1642, 1493, 1444, 1337	calcd. for $[C_{13}H_{17}NOS+H]^+$: 236.1104, found: 236.1105.
321l	(400 MHz, C_2D_6OS) δ 7.97 (dd, J = 7.7, 1.0 Hz, 1H), 7.94 (dd, J = 7.8, 1.0 Hz, 1H), 7.46 (t, J = 7.8 Hz, 1H), 3.90 (t, J = 7.0 Hz, 2H), 1.64 – 1.48 (m, 3H), 0.97 – 0.87 (m, 6H)	(101 MHz, C_2D_6OS) δ 164.1, 141.6, 134.4, 127.9, 126.4, 125.1, 113.7, 41.6, 37.7, 25.0, 22.2	2999, 2956, 2917, 1665, 1541, 1377, 1133, 1024	calcd. for $[C_{12}H_{14}BrNOS+H]^+$: 300.0052, found: 300.0054
321m	(400 MHz, $CDCl_3$) δ 8.16 (d, J = 1.9 Hz, 1H), 7.69 (dd, J = 8.5, 2.0 Hz, 1H), 7.42 (d, J = 8.4 Hz, 1H), 3.93 – 3.88 (m, 2H), 1.65 (ddd, J = 7.9, 4.2, 2.6 Hz, 3H), 0.96 (dd, J = 7.0, 3.8 Hz, 7H)	(101 MHz, $CDCl_3$) δ 164.1, 138.9, 134.8, 129.6, 126.8, 121. 9, 119.4, 42.7, 38.4, 29.8, 25.8, 22.5	2961, 2918, 2849, 1669, 1488, 1403, 1298, 1072	calcd. for $[C_{12}H_{14}BrNOS+H]^+$: 300.0052, found 300.0053

321n	(400 MHz, $CDCl_3$) δ 8.24 (d, J = 2.0 Hz, 1H), 7.76 (dd, J = 8.5, 2.0 Hz, 1H), 7.68 (dd, J = 7.7, 1.6 Hz, 2H), 7.48 (t, J = 7.5 Hz, 3H), 7.34 (t, J = 7.4 Hz, 1H)	(101 MHz, $CDCl_3$) δ 162.9, 138.7, 137.0, 135.6, 130.1, 129.6, 127.6, 124.8, 121.7, 119.8	3055, 2918, 2850, 1675, 1495, 1327, 1174	calcd. for $[C_{13}H_8BrNOS+H]^+$: 305.9582, found 305.9584
321o	(400 MHz, $CDCl_3$) δ 7.95 (ddd, J = 7.6, 1.3, 0.7 Hz, 1H), 7.78 – 7.69 (m, 2H), 7.51 – 7.42 (m, 3H), 7.39 (t, J = 7.5 Hz, 1H), 7.35 – 7.29 (m, 1H), 2.39 (d, J = 0.8 Hz, 3H)	(101 MHz, $CDCl_3$) δ 164.9, 140.1, 137.6, 132.7, 129.8, 129.5, 127.1, 126.5, 124.9, 124.8, 18.8	3093, 2947, 2849, 1650, 1453, 1308, 1078	calcd. for $[C_{14}H_{11}NOS+H]^+$: 242.0634, found: 242.0636
321p	(400 MHz, $CDCl_3$) δ 8.09 (dd, J = 7.8, 1.0 Hz, 1H), 7.78 (dd, J = 7.8, 1.0 Hz, 1H), 7.74 – 7.68 (m, 2H), 7.53 – 7.46 (m, 2H), 7.41 – 7.31 (m, 2H)	(101 MHz, $CDCl_3$) δ 164.1, 142.4, 137.1, 134.8, 129.6, 127.6, 127.5, 127.2, 126.1, 124.9, 114.0	3066, 2957, 1662, 1478, 1385, 1211	calcd. for $[C_{13}H_8BrNOS+H]^+$: 305.9583, found: 305.9583
321q	(400 MHz, $CDCl_3$) δ 8.11 (dd, J = 7.8, 1.2 Hz, 1H), 7.76 – 7.68 (m, 3H), 7.62 – 7.43 (m, 8H), 7.31 (ddt, J = 7.9, 6.9, 1.1 Hz, 1H)	(101 MHz, $CDCl_3$) δ 164.6, 139.2, 138.4, 137.4, 134.5, 131.9, 129.6, 129.5, 129.0, 127.3, 127.0, 126.1, 126.0, 124.7	2962, 2917, 2849, 1669, 1488, 1328. 1089	calcd. for $[C_{19}H_{13}NOS+H]^+$: 304.0791, found: 304.0792

Table 7-1 | Spectroscopic table of final compounds synthesised by *Siegfried Thun-Hohenstein*.

7.4 Biochemical Assays

7.4.1 General information

M^{pro} assays were performed exclusively using freshly purified recombinant M^{pro} solution, prepared as reported.[292] Refrozen M^{pro} samples exhibited reduced activity and were not used. LCMS (Merck, Supelco) grade solvents were used for MS analyses and to prepare buffers. The peptide substrate and M^{pro} solution were

diluted in freshly prepared reaction buffer (defined below) to prepare stock solutions. Compound stock solutions were prepared to 10mM in DMSO and diluted using the reaction buffer.

7.4.2 Fluorescence assays

The inhibitory activities of compounds against M^{pro} were determined using a spectroscopic assay, monitoring M^{pro} catalysed hydrolysis of the fluorogenic substrate ([5-FAM]-AVLQSGFR-[Lys(Dabcyl)]-K-amide) as reported.[277] In brief, assays were conducted at room temperature in clear-bottomed Greiner 384 black well microplates using a ClarioStar or PHERAstar FS microplate reader (BMG LabTech). Compound dilutions were transferred in quadruplicate from a 96 well plate to a 384 well plate (5 μL/well) using a CyBio Liquid Handler (Analytik Jena AG). M^{pro} (5 μl/well) and substrate (10 μL/well) were dispensed across 384 well plates using a Multidrop Combi dispenser (Thermo Scientific), the plates were then centrifuged (500 g, 15 s, Axygen Plate Spinner Centrifuge, Corning). Final reaction concentrations were 50 nM M^{pro}, 375 nM substrate, 20 mM HEPES, pH 7.3, 50 mM NaCl, 10% glycerol, 1% DMSO, 0.01% (*v*/*v*) Triton X-100. The initial rates of reaction (measured after 15 min pre-incubation of the inhibitor with the enzyme) were assessed by monitoring the fluorescence intensity at λ_{ex} = 485 nm and λ_{em} = 520 nm. Following the determination of initial rates of reaction, data were fitted using a four-parameter function: log (inhibitor) vs. response, variable slope in GraphPad Prism 5 to obtain IC_{50} values.

7.4.3 Solid-phase extraction coupled to MS assays

The inhibitory activity of compounds against M^{pro} was also determined using a RapidFire (RF) 365 high-throughput sampling robot (Agilent) connected to an iFunnel Agilent 6550 accurate mass quadrupole time-of-flight (Q-TOF) mass spectrometer as reported.[292] In brief, compounds were dispensed in an 11-point, 3-fold dilution series (100 μM top concentration) across 384-well plates using an acoustic Echo Dispenser (LabCyte). Ebselen and DMSO were used as positive and negative controls, respectively. M^{pro} (0.3 μM) was dispensed across 384-well plates (25 μL/well) using a Multidrop Combi dispenser (Thermo Scientific) and incubated for 15 min at rt. TSAVLQ/SGFRK-NH_2 peptide solution (4 μM) was then dispensed to the mixture (25 μL/well). Reactions were incubated (10 minutes), then quenched by addition of 10% (*v*/*v*) aqueous formic acid (5 μL/well). Data was extracted and processed as reported.[292]

7.4.4 Protein observed mass spectrometry assays

The reactions of compounds with recombinant M^{pro} were investigated using protein observed mass spectrometry coupled to solid phase extraction purification as reported.[16] In brief, the compounds were dispensed across 384 well plates using an acoustic Echo Dispenser (LabCyte). M^{pro} was dispensed across 384-well plates using a Multidrop Combi dispenser (Thermo Scientific). The plates were then centrifuged (500 g, 15 s, Axygen Plate Spinner Centrifuge, Corning). Final reaction conditions:

40 μM compound, 2 μM M^{pro}, 20 mM HEPES, pH 7.5, 50 mM NaCl, 50μL final volume/well.

7.4.5 IDH1 expression and purification

IDH1 variants were produced by *Raphael Reinbold* following reported protocols.[319]

7.4.6 Absorbance-based spectrophotometric IDH1 activity assay

Enzyme activity was quantified spectrophotometrically based on changes in concentration of NADPH and measured by its absorption at 340 nm (ε = 6,220 $M^{-1}\cdot cm^{-1}$). Analyses were conducted in 96-well half area clear microtiter plates (Greiner Bio-One 675001) using a PHERAstar FS Microplate Reader at 25°C in a reaction volume of 100 μL. This assay was used to study substrate turnover and inhibition of reactions catalysed by IDH1 variants. The assay buffer was 100 mM tris, 10 mM $MgCl_2$, enzyme 400nM, 0.2 mM dithiothreitol (DTT), 0.005 % Tween 20, and 0.1 mg mL-1 bovine serum albumin (BSA) (pH 8.0). For inhibition assays, IDH1 variants were incubated with inhibitor for 12 minutes before the reaction was initiated by substrate addition. The assay conditions were: 2-OG 1.5 mM; NADPH 300 μM. For alternative substrate turnover assays, the alternative substrate concentration was: 1.5 mM; 300 μM NADPH.

Chapter 8 Bibliography

1. Vandamme, P.; Pot, B.; Gillis, M.; De Vos, P.; Kersters, K.; Swings, J., Polyphasic taxonomy, a consensus approach to bacterial systematics. *Microbiol. Rev.* **1996,** *60* (2), 407-438.
2. Shapiro, J. A., Thinking about bacterial populations as multicellular organisms. *Ann. Rev. Microbiol.* **1998,** *52* (1), 81-104.
3. Madigan, M. T., Bacterial habitats in extreme environments. In *Journey to diverse microbial worlds*, Springer: 2000; pp 61-72.
4. Van Veen, J.; Kuikman, P., Soil structural aspects of decomposition of organic matter by micro-organisms. *Biogeochemistry* **1990,** *11* (3), 213-233.
5. Franche, C.; Lindström, K.; Elmerich, C., Nitrogen-fixing bacteria associated with leguminous and non-leguminous plants. *Plant Soil* **2009,** *321* (1), 35-59.
6. Cummings, J. H.; Englyst, H. N., Fermentation in the human large intestine and the available substrates. *Am. J. Clin. Nutr.* **1987,** *45* (5), 1243-1255.
7. Chilloux, J.; Neves, A. L.; Boulangé, C. L.; Dumas, M.-E., The microbial-mammalian metabolic axis, a critical symbiotic relationship. *Curr. Opin. Clin. Nutr. Metab. Care* **2016,** *19* (4), 250.
8. Morens, D. M.; Folkers, G. K.; Fauci, A. S., The challenge of emerging and re-emerging infectious diseases. *Nature* **2004,** *430* (6996), 242-249.
9. Lister, J., On the antiseptic principle in the practice of surgery. *Br. Med. J.* **1867,** *2* (351), 246.
10. Walker, T. J., The treatment of syphilis by the hypodermic injection of the salts of mercury. *Br. Med. J.* **1869,** *2* (466), 605.
11. Jones, H. W., Report of a series of cases of syphilis treated by Ehrlich's arsenobenzol at the Walter Reed General Hospital, District of Columbia. *Boston Med. Surg. J.* **1911,** *164* (11), 381-383.
12. Colebrook, L.; Kenny, M., Treatment of human puerperal infections, and of experimental infections in mice, with prontosil. *Lancet* **1936,** *227* (5884), 1279-1281.
13. Fleming, A., On the antibacterial action of cultures of a penicillium, with special reference to their use in the isolation of *B. influenzae*. *Br. J. Exp. Pathol.* **1929,** *10* (3), 226.
14. Nicolaou, K. C.; Rigol, S., A brief history of antibiotics and select advances in their synthesis. *J. Antibiot.* **2018,** *71* (2), 153-184.
15. Kong, K.-F.; Schneper, L.; Mathee, K., Beta-lactam Antibiotics: From Antibiosis to Resistance and Bacteriology. *APMIS* **2010,** *118* (1), 1-36.
16. Dmitriev, B.; Toukach, F.; Ehlers, S., Towards a comprehensive view of the bacterial cell wall. *Trends Microbiol.* **2005,** *13* (12), 569-574.
17. Gram, C., The differential staining of Schizomycetes in tissue sections and in dried preparations. *Fortschr. Med.* **1884,** *2* (6), 185-189.

18. Seltmann, G.; Holst, O., *The bacterial cell wall*. Springer Science & Business Media: 2002.
19. Lovering, A. L.; Safadi, S. S.; Strynadka, N. C., Structural perspective of peptidoglycan biosynthesis and assembly. *Ann. Rev. Biochem.* **2012,** *81*, 451-478.
20. Sauvage, E.; Kerff, F.; Terrak, M.; Ayala, J. A.; Charlier, P., The penicillin-binding proteins: structure and role in peptidoglycan biosynthesis. *FEMS Mircobiol. Rev.* **2008,** *32* (2), 234-258.
21. Frère, J. M.; Joris, B.; Shockman, G. D., Penicillin-sensitive enzymes in peptidoglycan biosynthesis. *Crit. Rev. Microbiol.* **1984,** *11* (4), 299-396.
22. Lavollay, M.; Arthur, M.; Fourgeaud, M.; Dubost, L.; Marie, A.; Veziris, N.; Blanot, D.; Gutmann, L.; Mainardi, J.-L., The peptidoglycan of stationary-phase *Mycobacterium tuberculosis* predominantly contains cross-links generated by L, D-transpeptidation. *J. Bacteriol.* **2008,** *190* (12), 4360-4366.
23. Böth, D.; Steiner, E. M.; Stadler, D.; Lindqvist, Y.; Schnell, R.; Schneider, G., Structure of LdtMt2, an L, D-transpeptidase from *Mycobacterium tuberculosis*. *Acta Crystallogr. D* **2013,** *69* (3), 432-441.
24. Waxman, D. J.; Strominger, J. L., Penicillin-binding proteins and the mechanism of action of beta-lactam antibiotics. *Ann. Rev. Biochem.* **1983,** *52* (1), 825-869.
25. Wright, A. J., The penicillins. *Mayo Clin. Proc.* **1999,** *74* (3), 290-307.
26. Marshall, W. F.; Blair, J. E., The cephalosporins. *Mayo Clin. Proc.* **1999,** *74* (2), 187-195.
27. Papp-Wallace, K. M.; Endimiani, A.; Taracila, M. A.; Bonomo, R. A., Carbapenems: past, present, and future. *Antimicrob. Agents Chemother.* **2011,** *55* (11), 4943-4960.
28. Brewer, N. S.; Hellinger, W. C., The monobactams. *Mayo Clin. Proc.* **1991,** *66* (11), 1152-1157.
29. Yocum, R. R.; Rasmussen, J. R.; Strominger, J. L., The mechanism of action of penicillin. Penicillin acylates the active site of Bacillus stearothermophilus D-alanine carboxypeptidase. *J. Biol. Chem.* **1980,** *255* (9), 3977-3986.
30. Tipper, D. J.; Strominger, J. L., Mechanism of action of penicillins: a proposal based on their structural similarity to acyl-D-alanyl-D-alanine. *Proc. Natl. Acad. Sci.* **1965,** *54* (4), 1133.
31. Boyd, D. B.; Herron, D. K.; Lunn, W.; Spitzer, W. A., Electronic structures of cephalosporins and penicillins. 11. Parabolic relationships between antibacterial activity of cephalosporins and β-lactam reactivity predicted from molecular orbital calculations. *J. Am. Chem. Soc.* **1980,** *102* (6), 1812-1814.
32. Miller, E. L., The penicillins: A review and update. *J. Midwifery & Women's Health* **2002,** *47* (6), 426-434.
33. Eriksen, N. L.; Blanco, J. D., Extended-spectrum (second-and third-generation) cephalosporins. *Obstet. Gynecol. Clin. North Am.* **1992,** *19* (3), 461-474.
34. Zhanel, G. G.; Golden, A. R.; Zelenitsky, S.; Wiebe, K.; Lawrence, C. K.; Adam, H. J.; Idowu, T.; Domalaon, R.; Schweizer, F.; Zhanel, M. A., Cefiderocol:

a siderophore cephalosporin with activity against carbapenem-resistant and multidrug-resistant Gram-negative bacilli. *Drugs* **2019,** *79* (3), 271-289.
35. Zhanel, G. G.; Lam, A.; Schweizer, F.; Thomson, K.; Walkty, A.; Rubinstein, E.; Gin, A. S.; Hoban, D. J.; Noreddin, A. M.; Karlowsky, J. A., Ceftobiprole. *Am. J. Clin. Dermatol.* **2008,** *9* (4), 245-254.
36. Zhanel, G. G.; Sniezek, G.; Schweizer, F.; Zelenitsky, S.; Lagacé-Wiens, P. R.; Rubinstein, E.; Gin, A. S.; Hoban, D. J.; Karlowsky, J. A., Ceftaroline. *Drugs* **2009,** *69* (7), 809-831.
37. Albers-Schoenberg, G.; Arison, B. H.; Hensens, O. D.; Hirshfield, J.; Hoogsteen, K.; Kaczka, E. A.; Rhodes, R. E.; Kahan, J. S.; Kahan, F. M., Structure and absolute configuration of thienamycin. *J. Am. Chem. Soc.* **1978,** *100* (20), 6491-6499.
38. Kahan, F. M.; Kropp, H.; Sundelof, J. G.; Birnbaum, J., Thienamycin: development of imipenem-cilastatin. *J. Antimicrob. Chemother.* **1983,** *12* (suppl_D), 1-35.
39. Solomkin, J. S.; Dellinger, E. P.; Christou, N. V.; Busuttil, R. W., Results of a multicenter trial comparing imipenem/cilastatin to tobramycin/clindamycin for intra-abdominal infections. *Ann. Surg.* **1990,** *212* (5), 581.
40. Watanabe, M.; Iyobe, S.; Inoue, M.; Mitsuhashi, S., Transferable imipenem resistance in *Pseudomonas aeruginosa*. *Antimicrob. Agents Chemother.* **1991,** *35* (1), 147-151.
41. Clissold, S. P.; Todd, P. A.; Campoli-Richards, D. M., Imipenem/Cilastatin. *Drugs* **2012,** *33*, 183-241.
42. Nadler, H.; Pitkin, D.; Sheikh, W., The postantibiotic effect of meropenem and imipenem on selected bacteria. *J. Antimicrob. Chemother.* **1989,** *24* (suppl_A), 225-231.
43. Bax, R.; Bastain, W.; Featherstone, A.; Wilkinson, D.; Hutchison, M., The pharmacokinetics of meropenem in volunteers. *J. Antimicrob. Chemother.* **1989,** *24* (suppl_A), 311-320.
44. Livermore, D. M.; Sefton, A. M.; Scott, G. M., Properties and potential of ertapenem. *J. Antimicrob. Chemother.* **2003,** *52* (3), 331-344.
45. Ji, X.-w.; Xue, F.; Kang, Z.-s.; Zhong, W.; Hui-san Kuan, I.; Yang, X.-p.; Zhu, X.; Li, Y.; Lv, Y., Model-informed drug development of benapenem: Pharmacokinetic/Pharmacodynamic cutoff value determination and antibacterial efficacy against *enterobacteriaceae*. *Antimicrob. Agents Chemother.* **2019**.
46. Ednie, L. M.; Appelbaum, P. C., Antianaerobic activity of sulopenem compared to six other agents. *Antimicrob. Agents Chemother.* **2009,** *53* (5), 2163-2170.
47. Sykes, R.; Cimarusti, C.; Bonner, D.; Bush, K.; Floyd, D.; Georgopapadakou, N.; Koster, W.; Liu, W.; Parker, W.; Principe, P., Monocyclic β-lactam antibiotics produced by bacteria. *Nature* **1981,** *291* (5815), 489-491.
48. Asai, M.; Haibara, K.; Muroi, M.; Kintaka, K.; Kishi, T., Sulfazecin, a novel β-lactam antibiotic of bacterial origin: isolation and chamical characterisation. *J. Antibiot.* **1981,** *34* (6), 621-627.

49. Sykes, R.; Bonner, D., Aztreonam: the first monobactam. *Am. J. Med.* **1985,** *78* (2), 2-10.
50. Fuchs, P. C.; Jones, R. N.; Barry, A. L., In vitro antimicrobial activity of tigemonam, a new orally administered monobactam. *Antimicrob. Agents Chemother.* **1988,** *32* (3), 346-349.
51. Mushtaq, S.; Warner, M.; Livermore, D., Activity of the siderophore monobactam BAL30072 against multiresistant non-fermenters. *J. Antimicrob. Chemother.* **2010,** *65* (2), 266-270.
52. Brown, M. F.; Mitton-Fry, M. J.; Arcari, J. T.; Barham, R.; Casavant, J.; Gerstenberger, B. S.; Han, S.; Hardink, J. R.; Harris, T. M.; Hoang, T.; Huband, M. D.; Lall, M. S.; Lemmon, M. M.; Li, C.; Lin, J.; McCurdy, S. P.; McElroy, E.; McPherson, C.; Marr, E. S.; Mueller, J. P.; Mullins, L.; Nikitenko, A. A.; Noe, M. C.; Penzien, J.; Plummer, M. S.; Schuff, B. P.; Shanmugasundaram, V.; Starr, J. T.; Sun, J.; Tomaras, A.; Young, J. A.; Zaniewski, R. P., Pyridone-Conjugated Monobactam Antibiotics with Gram-Negative Activity. *J. Med. Chem.* **2013,** *56* (13), 5541-5552.
53. Dean, C. R.; Barkan, D. T.; Bermingham, A.; Blais, J.; Casey, F.; Casarez, A.; Colvin, R.; Fuller, J.; Jones, A. K.; Li, C., Mode of action of the monobactam LYS228 and mechanisms decreasing in vitro susceptibility in *Escherichia coli* and *Klebsiella pneumoniae*. *Antimicrob. Agents Chemother.* **2018,** *62* (10), e01200-18.
54. Sun, Y.; Liao, X.; Huang, Z.; Xie, Y.; Liu, Y.; Ma, C.; Jiang, B.; Zhang, L.; Yan, Y.; Li, G., Therapeutic effect and mechanisms of the novel monosulfactam 0073. *Antimicrob. Agents Chemother.* **2020,** *64* (10), e00529-20.
55. Freischem, S.; Grimm, I.; López-Pérez, A.; Willbold, D.; Klenke, B.; Vuong, C.; Dingley, A. J.; Weiergräber, O. H., Interaction Mode of the Novel Monobactam AIC499 Targeting Penicillin Binding Protein 3 of Gram-Negative Bacteria. *Biomolecules* **2021,** *11* (7), 1057.
56. James, C.; Winterhalter, M., The porin and the permeating antibiotic: a selective diffusion barrier in Gram-negative bacteria. *Nat. Rev. Microbiol.* **2008,** *6*, 893-903.
57. Kumar, A.; Schweizer, H. P., Bacterial resistance to antibiotics: active efflux and reduced uptake. *Adv. Drug Deliv. Rev.* **2005,** *57* (10), 1486-1513.
58. Frère, J. M., Beta-lactamases and bacterial resistance to antibiotics. *Mol. Microbiol.* **1995,** *16* (3), 385-395.
59. Kolář, M.; Urbánek, K.; Látal, T., Antibiotic selective pressure and development of bacterial resistance. *Int. J. Antimicrob. Agents* **2001,** *17* (5), 357-363.
60. Hall, B. G.; Barlow, M., Revised Ambler classification of β-lactamases. *J. Antimicrob. Chemother.* **2005,** *55* (6), 1050-1051.
61. Sawa, T.; Kooguchi, K.; Moriyama, K., Molecular diversity of extended-spectrum β-lactamases and carbapenemases, and antimicrobial resistance. *J. Intensive Care* **2020,** *8* (1), 13.
62. Walther-Rasmussen, J.; Høiby, N., OXA-type carbapenemases. *J. Antimicrob. Chem.* **2006,** *57* (3), 373-383.

63. Cahill, S. T.; Cain, R.; Wang, D. Y.; Lohans, C. T.; Wareham, D. W.; Oswin, H. P.; Mohammed, J.; Spencer, J.; Fishwick, C. W.; McDonough, M. A.; Schofield, C. J., Cyclic boronates inhibit all classes of β-lactamases. *Antimicrob. Agents Chemother.* **2017,** *61* (4), e02260-16.
64. Tooke, C. L.; Hinchliffe, P.; Bragginton, E. C.; Colenso, C. K.; Hirvonen, V. H.; Takebayashi, Y.; Spencer, J., β-Lactamases and β-Lactamase Inhibitors in the 21st Century. *J. Mol. Biol.* **2019,** *431* (18), 3472-3500.
65. Saudagar, P. S.; Survase, S. A.; Singhal, R. S., Clavulanic acid: a review. *Biotechnol. Adv.* **2008,** *26* (4), 335-351.
66. Reading, C.; Cole, M., Structure-Activity Relationships Amongst β-Lactamase Inhibitors. *J. Enzym. Inhib.* **1986,** *1* (2), 83-104.
67. Sulton, D.; Pagan-Rodriguez, D.; Zhou, X.; Liu, Y.; Hujer, A. M.; Bethel, C. R.; Helfand, M. S.; Thomson, J. M.; Anderson, V. E.; Buynak, J. D., Clavulanic acid inactivation of SHV-1 and the inhibitor-resistant S130G SHV-1 β-lactamase: insights into the mechanism of inhibition. *J. Biol. Chem.* **2005,** *280* (42), 35528-35536.
68. Sawai, T.; Yamaguchi, A., Mechanism of beta-lactamase inhibition: differences between sulbactam and other inhibitors. *Diagn. Microbiol. Infect. Dis.* **1989,** *12* (4), 121-129.
69. Pagan-Rodriguez, D.; Zhou, X.; Simmons, R.; Bethel, C. R.; Hujer, A. M.; Helfand, M. S.; Jin, Z.; Guo, B.; Anderson, V. E.; Ng, L. M., Tazobactam inactivation of SHV-1 and the inhibitor-resistant Ser130→ Gly SHV-1 β-lactamase: insights into the mechanism of inhibition. *J. Biol. Chem.* **2004,** *279* (19), 19494-19501.
70. Papp-Wallace, K. M.; Bonomo, R. A., New β-lactamase inhibitors in the clinic. *Infect. Dis. Clin.* **2016,** *30* (2), 441-464.
71. King, D. T.; King, A. M.; Lal, S. M.; Wright, G. D.; Strynadka, N. C., Molecular mechanism of avibactam-mediated β-lactamase inhibition. *ACS Infect. Dis.* **2015,** *1* (4), 175-184.
72. Brem, J.; Cain, R.; Cahill, S.; McDonough, M. A.; Clifton, I. J.; Jiménez-Castellanos, J.-C.; Avison, M. B.; Spencer, J.; Fishwick, C. W. G.; Schofield, C. J., Structural basis of metallo-β-lactamase, serine-β-lactamase and penicillin-binding protein inhibition by cyclic boronates. *Nat. Commun.* **2016,** *7*, 12406.
73. Lomovskaya, O.; Sun, D.; Rubio-Aparicio, D.; Nelson, K.; Tsivkovski, R.; Griffith, D. C.; Dudley, M. N., Vaborbactam: spectrum of beta-lactamase inhibition and impact of resistance mechanisms on activity in *Enterobacteriaceae*. *Antimicrob. Agents Chemother.* **2017,** *61* (11), e01443-17.
74. Brem, J.; Panduwawala, T.; Hansen, J. U.; Hewitt, J.; Liepins, E.; Donets, P.; Espina, L.; Farley, A. J. M.; Shubin, K.; Campillos, G. G.; Kiuru, P.; Shishodia, S.; Krahn, D.; Leśniak, R. K.; Schmidt, J.; Calvopiña, K.; Turrientes, M.-C.; Kavanagh, M. E.; Lubriks, D.; Hinchliffe, P.; Langley, G. W.; Aboklaish, A. F.; Eneroth, A.; Backlund, M.; Baran, A. G.; Nielsen, E. I.; Speake, M.; Kuka, J.; Robinson, J.; Grinberga, S.; Robinson, L.; McDonough, M. A.; Rydzik, A. M.; Leissing, T. M.; Jimenez-Castellanos, J. C.; Avison, M. B.; Da Silva Pinto, S.; Pannifer, A. D.; Martjuga, M.; Widlake, E.; Priede, M.; Hopkins Navratilova, I.;

Gniadkowski, M.; Belfrage, A. K.; Brandt, P.; Yli-Kauhaluoma, J.; Bacque, E.; Page, M. G. P.; Björkling, F.; Tyrrell, J. M.; Spencer, J.; Lang, P. A.; Baranczewski, P.; Cantón, R.; McElroy, S. P.; Jones, P. S.; Baquero, F.; Suna, E.; Morrison, A.; Walsh, T. R.; Schofield, C. J., Imitation of β-lactam binding enables broad-spectrum metallo-β-lactamase inhibitors. *Nat. Chem.* **2021**, https://doi.org/10.1038/s41557-021-00831-x.

75. O'Daniel, P. I.; Peng, Z.; Pi, H.; Testero, S. A.; Ding, D.; Spink, E.; Leemans, E.; Boudreau, M. A.; Yamaguchi, T.; Schroeder, V. A.; Wolter, W. R.; Llarrull, L. I.; Song, W.; Lastochkin, E.; Kumarasiri, M.; Antunes, N. T.; Espahbodi, M.; Lichtenwalter, K.; Suckow, M. A.; Vakulenko, S.; Mobashery, S.; Chang, M., Discovery of a New Class of Non-β-lactam Inhibitors of Penicillin-Binding Proteins with Gram-Positive Antibacterial Activity. *J. Am. Chem. Soc.* **2014,** *136* (9), 3664-3672.

76. Janardhanan, J.; Meisel, J. E.; Ding, D.; Schroeder, V. A.; Wolter, W. R.; Mobashery, S.; Chang, M., In vitro and in vivo synergy of the oxadiazole class of antibacterials with β-lactams. *Antimicrob. Agents Chemother.* **2016,** *60* (9), 5581-5588.

77. Miller, A. A.; Bundy, G. L.; Mott, J. E.; Skepner, J. E.; Boyle, T. P.; Harris, D. W.; Hromockyj, A. E.; Marotti, K. R.; Zurenko, G. E.; Munzner, J. B., Discovery and characterization of QPT-1, the progenitor of a new class of bacterial topoisomerase inhibitors. *Antimicrob. Agents Chemother.* **2008,** *52* (8), 2806-2812.

78. Shetnev, A.; Baykov, S.; Kalinin, S.; Belova, A.; Sharoyko, V.; Rozhkov, A.; Zelenkov, L.; Tarasenko, M.; Sadykov, E.; Korsakov, M., 1, 2, 4-Oxadiazole/2-imidazoline hybrids: multi-target-directed compounds for the treatment of infectious diseases and cancer. *Int. J. Mol. Sci.* **2019,** *20* (7), 1699.

79. Janardhanan, J.; Bouley, R.; Martínez-Caballero, S.; Peng, Z.; Batuecas-Mordillo, M.; Meisel, J. E.; Ding, D.; Schroeder, V. A.; Wolter, W. R.; Mahasenan, K. V., The quinazolinone allosteric inhibitor of PBP 2a synergizes with piperacillin and tazobactam against methicillin-resistant *Staphylococcus aureus*. *Antimicrob. Agents Chemother.* **2019,** *63* (5), e02637-18.

80. Turk, S.; Verlaine, O.; Gerards, T.; Živec, M.; Humljan, J.; Sosič, I.; Amoroso, A.; Zervosen, A.; Luxen, A.; Joris, B.; Gobec, S., New Noncovalent Inhibitors of Penicillin-Binding Proteins from Penicillin-Resistant Bacteria. *PloS One* **2011,** *6* (5), e19418.

81. Podoll, J. D.; Liu, Y.; Chang, L.; Walls, S.; Wang, W.; Wang, X., Bio-inspired synthesis yields a tricyclic indoline that selectively resensitizes methicillin-resistant *Staphylococcus aureus* (MRSA) to β-lactam antibiotics. *Proc. Natl. Acad. Sci.* **2013,** *110* (39), 15573-15578.

82. Qiao, Y.; Zhang, X.; He, Y.; Sun, W.; Feng, W.; Liu, J.; Hu, Z.; Xu, Q.; Zhu, H.; Zhang, J.; Luo, Z.; Wang, J.; Xue, Y.; Zhang, Y., Aspermerodione, a novel fungal metabolite with an unusual 2,6-dioxabicyclo[2.2.1]heptane skeleton, as an inhibitor of penicillin-binding protein 2a. *Sci. Rep.* **2018,** *8* (1), 5454.

83. Bessa, L. J.; Palmeira, A.; Gomes, A. S.; Vasconcelos, V.; Sousa, E.; Pinto, M.; Martins da Costa, P., Synergistic effects between thioxanthones and oxacillin

against methicillin-resistant *Staphylococcus aureus*. *Microb. Drug Resist.* **2015,** *21* (4), 404-415.
84. Lv, N.; Kong, Q.; Zhang, H.; Li, J., Discovery of novel *Staphylococcus aureus* penicillin binding protein 2a inhibitors by multistep virtual screening and biological evaluation. *Bioorg. Med. Chem. Lett.* **2021,** *41*, 128001.
85. Li, Z.-Z.; Tangadanchu, V. K. R.; Battini, N.; Bheemanaboina, R. R. Y.; Zang, Z.-L.; Zhang, S.-L.; Zhou, C.-H., Indole-nitroimidazole conjugates as efficient manipulators to decrease the genes expression of methicillin-resistant *Staphylococcus aureus*. *Eur. J. Med. Chem.* **2019,** *179*, 723-735.
86. Negi, B.; Kumar, D.; Kumbukgolla, W.; Jayaweera, S.; Ponnan, P.; Singh, R.; Agarwal, S.; Rawat, D. S., Anti-methicillin resistant *Staphylococcus aureus* activity, synergism with oxacillin and molecular docking studies of metronidazole-triazole hybrids. *Eur. J. Med. Chem.* **2016,** *115*, 426-437.
87. Dingsdag, S. A.; Hunter, N., Metronidazole: an update on metabolism, structure–cytotoxicity and resistance mechanisms. *J. Antimicrob. Chemother.* **2018,** *73* (2), 265-279.
88. Hirai, I.; Okuno, M.; Katsuma, R.; Arita, N.; Tachibana, M.; Yamamoto, Y., Characterisation of anti-*Staphylococcus aureus* activity of quercetin. *Int. J. Food Sci. Tech.* **2010,** *45* (6), 1250-1254.
89. Rani, N.; Vijayakumar, S.; PTV, L.; Arunachalam, A., Allosteric site-mediated active site inhibition of PBP2a using Quercetin 3-O-rutinoside and its combination. *J. Biomol. Struct. Dyn.* **2016,** *34* (8), 1778-1796.
90. Shiota, S.; Shimizu, M.; Sugiyama, J. i.; Morita, Y.; Mizushima, T.; Tsuchiya, T., Mechanisms of Action of Corilagin and Tellimagrandin I That Remarkably Potentiate the Activity of β-Lactams against Methicillin-Resistant *Staphylococcus aureus*. *Microbiol. Immunol.* **2004,** *48* (1), 67-73.
91. Durand, T.; Marchand-Brynaert, J.; Ghosez, L., Cyclopentenones as potential inhibitors of penicillin sensitive enzymes. *Bioorg. Med. Chem. Lett.* **1993,** *3* (11), 2309-2312.
92. Zervosen, A.; Lu, W.-P.; Chen, Z.; White, R. E.; Demuth Jr, T. P.; Frère, J.-M., Interactions between penicillin-binding proteins (PBPs) and two novel classes of PBP inhibitors, arylalkylidene rhodanines and arylalkylidene iminothiazolidin-4-ones. *Antimicrob. Agents Chemother.* **2004,** *48* (3), 961-969.
93. Tomašić, T.; Peterlin Mašič, L., Rhodanine as a scaffold in drug discovery: a critical review of its biological activities and mechanisms of target modulation. *Expert Op. Drug Disc.* **2012,** *7* (7), 549-560.
94. Lowe, G.; Swain, S., Synthesis of 7β-phenylacetamido-6-oxo-2-oxabicyclo [3.2.0] heptane-4α-carboxylic acid, a cyclobutanone analogue of a β-lactam antibiotic. *J. Chem. Soc. Chem. Commun.* **1983,** (22), 1279-1281.
95. Gordon, E.; Pluščec, J.; Ondetti, M., Carbacyclic isosteres of penicillanic and carbapenemic acids. Synthesis of bicyclo [3.2.0] Heptan-6-ones as potential enzyme inhibitors. *Tetrahedron Lett.* **1981,** *22* (20), 1871-1874.

96. Meth-Cohn, O.; Reason, A. J.; Roberts, S. M., Carbocyclic analogues of penicllin. *J. Chem. Soc. Chem. Commun.* **1982,** (1), 90-92.
97. Johnson, J. W.; Gretes, M.; Goodfellow, V. J.; Marrone, L.; Heynen, M. L.; Strynadka, N. C.; Dmitrienko, G. I., Cyclobutanone analogues of β-lactams revisited: insights into conformational requirements for inhibition of serine-and metallo-β-lactamases. *J. Am. Chem. Soc.* **2010,** *132* (8), 2558-2560.
98. Tanner, C. Biochemical and Microbiological Investigations of Inhibitors for β-Lactamases from Human Pathogenic Bacteria. University of Waterloo, 2019.
99. Cocuzza, A.; Boswell, G., Cyclobutanone analogs of β-lactam antibiotics: Sythesis of N-acetyldeazathienamycin. *Tetrahedron Lett.* **1985,** *26* (44), 5363-5366.
100. Cavagna, F.; Koller, W.; Linkies, A.; Rehling, H.; Reuschling, D., Synthesis of Bicyclic β-Sultams. *Angew. Chem. Int. Ed.* **1982,** *21* (7), 548-549.
101. Llinás, A.; Ahmed, N.; Cordaro, M.; Laws, A. P.; Frere, J.-M.; Delmarcelle, M.; Silvaggi, N. R.; Kelly, J. A.; Page, M. I., Inactivation of bacterial DD-peptidase by β-sultams. *Biochemistry* **2005,** *44* (21), 7738-7746.
102. Page, M. I., β-Sultams mechanism of reactions and use as inhibitors of serine proteases. *Acc. Chem. Res.* **2004,** *37* (5), 297-303.
103. Beardsell, M.; Hinchliffe, P. S.; Wood, J. M.; Wilmouth, R. C.; Schofield, C. J.; Page, M. I., β-Sultams—A novel class of serine protease inhibitors. *Chem. Commun.* **2001,** (5), 497-498.
104. Hinchliffe, P. S.; Wood, J. M.; Davis, A. M.; Austin, R. P.; Beckett, R. P.; Page, M. I., Structure–reactivity relationships in the inactivation of elastase by β-sultams. *Org. Biol. Chem.* **2003,** *1* (1), 67-80.
105. Wojtkowski, P. W.; Dolfini, J. E.; Kocy, O.; Cimarusti, C. M., β-Thionolactam analogs of cephalosporins and penicillins. *J. Am. Chem. Soc.* **1975,** *97* (19), 5628-5630.
106. Wells, J. S.; Trejo, W. H.; Principe, P. A.; Sykes, R. B., Obafluorin, a novel β-lactone produced by *Pseudomonas fluorescens*. Taxonomy, fermentation and biological properties. *J. Antibiot.* **1984,** *37* (7), 802-803.
107. Heinze-Krauss, I.; Angehrn, P.; Charnas, R. L.; Gubernator, K.; Gutknecht, E.-M.; Hubschwerlen, C.; Kania, M.; Oefner, C.; Page, M. G. P.; Sogabe, S.; Specklin, J.-L.; Winkler, F., Structure-Based Design of β-Lactamase Inhibitors. 1. Synthesis and Evaluation of Bridged Monobactams. *J. Med. Chem.* **1998,** *41* (21), 3961-3971.
108. Pu, Y.; Lowe, C.; Sailer, M.; Vederas, J. C., Synthesis, Stability, and Antimicrobial Activity of (+)-Obafluorin and Related. β-Lactone Antibiotics. *J. Org. Chem.* **1994,** *59* (13), 3642-3655.
109. Feling, R. H.; Buchanan, G. O.; Mincer, T. J.; Kauffman, C. A.; Jensen, P. R.; Fenical, W., Salinosporamide A: A Highly Cytotoxic Proteasome Inhibitor from a Novel Microbial Source, a Marine Bacterium of the New Genus *Salinospora*. *Angew. Chem. Int. Ed.* **2003,** *42* (3), 355-357.
110. Imming, P.; Klar, B.; Dix, D., Hydrolytic stability versus ring size in lactams: Implications for the development of lactam antibiotics and other serine protease inhibitors. *J. Med. Chem.* **2000,** *43* (22), 4328-4331.

111. Imming, P., Synthesis of the First Penicillin Derivatives with Medium-Sized Lactam Ring and of Related Thiazolidines. *Arch. Pharm.* **1995,** *328* (3), 207-215.
112. Hanessian, S. M.-S., Grant; Lombart, Henry-Georges, Lubell, William D., Design and Synthesis of Conformatinoally Constrained Amino Acids as Versatile Scaffolds and Peptide Mimetics. *Tetrahedron* **1997,** *53* (38), 12789-12484.
113. Aszodi, J.; Rowlands, D. A.; Mauvais, P.; Collette, P.; Bonnefoy, A.; Lampilas, M., Design and synthesis of bridged γ-lactams as analogues of β-lactam antibiotics. *Bioorg. Med. Chem. Lett.* **2004,** *14* (10), 2489-2492.
114. Morinaka, A.; Tsutsumi, Y.; Yamada, M.; Suzuki, K.; Watanabe, T.; Abe, T.; Furuuchi, T.; Inamura, S.; Sakamaki, Y.; Mitsuhashi, N., OP0595, a new diazabicyclooctane: mode of action as a serine β-lactamase inhibitor, antibiotic and β-lactam 'enhancer'. *J. Antimicrob. Chemother.* **2015,** *70* (10), 2779-2786.
115. Coleman, K., Diazabicyclooctanes (DBOs): a potent new class of non-β-lactam β-lactamase inhibitors. *Curr. Opin. Microbiol.* **2011,** *14* (5), 550-555.
116. Livermore, D. M.; Mushtaq, S.; Warner, M.; Vickers, A.; Woodford, N., In vitro activity of cefepime/zidebactam (WCK 5222) against Gram-negative bacteria. *J. Antimicrob. Chemother.* **2017,** *72* (5), 1373-1385.
117. Durand-Réville, T. F.; Guler, S.; Comita-Prevoir, J.; Chen, B.; Bifulco, N.; Huynh, H.; Lahiri, S.; Shapiro, A. B.; McLeod, S. M.; Carter, N. M., ETX2514 is a broad-spectrum β-lactamase inhibitor for the treatment of drug-resistant Gram-negative bacteria including *Acinetobacter baumannii*. *Nat. Microbiol.* **2017,** *2* (9), 1-10.
118. Miller, A. A.; Shapiro, A. B.; McLeod, S. M.; Carter, N. M.; Moussa, S. H.; Tommasi, R.; Mueller, J. P., In Vitro Characterization of ETX1317, a Broad-Spectrum β-Lactamase Inhibitor That Restores and Enhances β-Lactam Activity against Multi-Drug-Resistant *Enterobacteriales,* Including Carbapenem-Resistant Strains. *ACS Infect. Dis.* **2020,** *6* (6), 1389-1397.
119. Durand-Réville, T. F.; Comita-Prevoir, J.; Zhang, J.; Wu, X.; May-Dracka, T. L.; Romero, J. A. C.; Wu, F.; Chen, A.; Shapiro, A. B.; Carter, N. M.; McLeod, S. M.; Giacobbe, R. A.; Verheijen, J. C.; Lahiri, S. D.; Sacco, M. D.; Chen, Y.; O'Donnell, J. P.; Miller, A. A.; Mueller, J. P.; Tommasi, R. A., Discovery of an Orally Available Diazabicyclooctane Inhibitor (ETX0282) of Class A, C, and D Serine β-Lactamases. *J. Med. Chem.* **2020,** *63* (21), 12511-12525.
120. Reck, F.; Bermingham, A.; Blais, J.; Casarez, A.; Colvin, R.; Dean, C. R.; Furegati, M.; Gamboa, L.; Growcott, E.; Li, C.; Lopez, S.; Metzger, L.; Nocito, S.; Ossola, F.; Phizackerley, K.; Rasper, D.; Shaul, J.; Shen, X.; Simmons, R. L.; Tang, D.; Tashiro, K.; Yue, Q., IID572: A New Potentially Best-In-Class β-Lactamase Inhibitor. *ACS Infect. Dis.* **2019,** *5* (7), 1045-1051.
121. Durand-Reville, T. F.; Miller, A. A.; O'Donnell, J. P.; Wu, X.; Sylvester, M. A.; Guler, S.; Iyer, R.; Shapiro, A. B.; Carter, N. M.; Velez-Vega, C., Rational design of a new antibiotic class for drug-resistant infections. *Nature* **2021,** *597* (7878), 698-702.
122. Zervosen, A.; Bouillez, A.; Herman, A.; Amoroso, A.; Joris, B.; Sauvage, E.; Charlier, P.; Luxen, A., Synthesis and evaluation of boronic acids as inhibitors

of Penicillin Binding Proteins of classes A, B and C. *Bioorg. Med. Chem.* **2012,** *20* (12), 3915-3924.
123. Krajnc, A.; Lang, P. A.; Panduwawala, T. D.; Brem, J.; Schofield, C. J., Will morphing boron-based inhibitors beat the β-lactamases? *Curr. Opin. Chem. Biol.* **2019,** *50*, 101-110.
124. Kumar, V.; Viviani, S. L.; Ismail, J.; Agarwal, S.; Bonomo, R. A.; van den Akker, F., Structural analysis of the boronic acid β-lactamase inhibitor vaborbactam binding to *Pseudomonas aeruginosa* penicillin-binding protein 3. *PLoS one* **2021,** *16* (10), e0258359.
125. Newman, H.; Krajnc, A.; Bellini, D.; Eyermann, C. J.; Boyle, G. A.; Paterson, N. G.; McAuley, K. E.; Lesniak, R.; Gangar, M.; von Delft, F.; Brem, J.; Chibale, K.; Schofield, C. J.; Dowson, C. G., High-Throughput Crystallography Reveals Boron-Containing Inhibitors of a Penicillin-Binding Protein with Di- and Tricovalent Binding Modes. *J. Med. Chem.* **2021,** *64* (15), 11379-11394.
126. Contreras-Martel, C.; Amoroso, A.; Woon, E. C. Y.; Zervosen, A.; Inglis, S.; Martins, A.; Verlaine, O.; Rydzik, A. M.; Job, V.; Luxen, A.; Joris, B.; Schofield, C. J.; Dessen, A., Structure-Guided Design of Cell Wall Biosynthesis Inhibitors That Overcome β-Lactam Resistance in *Staphylococcus aureus* (MRSA). *ACS Chem. Biol.* **2011,** *6* (9), 943-951.
127. Schönherr, H.; Cernak, T., Profound Methyl Effects in Drug Discovery and a Call for New C-H Methylation Reactions. *Angew. Chem. Int. Ed.* **2013,** *52* (47), 12256-12267.
128. Woon, E. C.; Zervosen, A.; Sauvage, E.; Simmons, K. J.; Zivec, M.; Inglis, S. R.; Fishwick, C. W.; Gobec, S.; Charlier, P.; Luxen, A., Structure guided development of potent reversibly binding penicillin binding protein inhibitors. *ACS Med. Chem. Lett.* **2011,** *2* (3), 219-223.
129. Baldwin, J. E.; Lynch, G. P.; Pitlik, J., γ-Lactam analogues of β-lactam antibiotics. *J. Antibiot.* **1991,** *44* (1), 1-24.
130. Crossley, M. J.; Crumbie, R. L.; Fung, Y. M.; Potter, J. J.; Pegler, M. A., γ-lactam analogues of monocyclic β-lactam antibiotics. *Tetrahedron Lett.* **1987,** *28* (25), 2883-2886.
131. Kar, G. K.; Roy, B. C.; Das Adhikari, S.; Ray, J. K.; Brahma, N. K., Synthesis of some thieno gamma lactam monocarboxylic acids with high antibacterial activity: A new look at an old molecular system. *Bioorg. Med. Chem.* **1998,** *6* (12), 2397-2403.
132. Ray, J. K.; Sami, I.; Kar, G. K.; Roy, B. C.; Brahma, N. K., Structurally designed novel furogamma lactams as inhibitors for bacterial propagations. *Bioorg. Med. Chem.* **1994,** *2* (12), 1417-1421.
133. Patra, P.; Kar, G. K.; Sarkar, A.; Ray, J. K.; Dasgupta, T.; Ghosh, M.; Bhattacharya, S., N-Aryl Modification in γ-Lactam: Design and Synthesis of Novel Monocyclic γ-Lactam Derivatives as Inhibitor for Bacterial Propagation. *Synth. Commun.* **2012,** *42* (20), 3031-3041.

134. Baldwin, J. E.; Adlington, R. M.; Jones, R. H.; Schofield, C. J.; Zaracostas, C.; Greengrass, C. W., γ-Lactam analogues of carbapenicillanic acids. *Tetrahedron* **1986,** *42* (17), 4879-4888.
135. Heck, J. V. 3-amino-6-substituted thio-1-azabicyclo(3.2.0)hept-6-en-2-one-7-carboxylic acids. US4428960A, 1984.
136. Baldwin, J. E.; Adlington, R. M.; Jones, R. H.; Schofield, C. J.; Zarocostas, C.; Greengrass, C. W., γ-Lactam analogues of carbapenicillanic acids. *J. Chem. Soc. Chem. Commun.* **1985,** (4), 194-196.
137. Baldwin, J. E.; Lowe, C.; Schofield, C. J.; Lee, E., A γ-lactam analogue of penems possessing antibacterial activity. *Tetrahedron Lett.* **1986,** *27* (30), 3461-3464.
138. Boyd, D. B.; Elzey, T. K.; Hatfield, L. D.; Kinnick, M. D.; Morin, J. M., γ-Lactam analogues of the penems. *Tetrahedron Lett.* **1986,** *27* (30), 3453-3456.
139. Boyd, D.; Foster, B.; Hatfield, L.; Hornback, W.; Jones, N.; Munroe, J.; Swartzendruber, J., γ-Lactam analogues of carbapenems. *Tetrahedron Lett.* **1986,** *27* (30), 3457-3460.
140. Coulton, S.; Southgate, R., Synthesis of novel 2-oxo-4-thia-1-azabicyclo [3.3.0] oct-7-ene-8-carboxylic acid derivatives. *J. Chem. Soc. Perkin Trans. 1* **1992,** (8), 961-967.
141. Baldwin, J. E.; Freeman, R. T.; Schofield, C., Synthesis of a novel bicyclic γ-lactam analogue of the 1-oxapenams. *Tetrahedron Lett.* **1989,** *30* (30), 4019-4020.
142. Hashiguchi, S.; Natsugari, H.; Ochiai, M., Synthesis of γ-Lactam Analogues of Carbapenems with Substituted-thio Groups at the C-3 Position. *J. Chem. Soc. Perkin Trans. 1* **1988,** (8), 2345-2352.
143. Hanessian, S.; Buckle, R.; Bayrakdarian, M., Design and Synthesis of a Novel Class of Constrained Tricyclic Pyrrolizidinone Carboxylic Acids as Carbapenem Mimics. *J. Org. Chem.* **2002,** *67* (10), 3387-3397.
144. Davies, G. M.; Hitchcock, P. B.; Loakes, D.; Young, D. W., Synthesis of reactive γ-lactams related to penicillins and cephalosporins. *Tetrahedron Lett.* **1996,** *37* (31), 5601-5604.
145. Fong, A.; Ross, M.; Boudreau, J.; Nokhbeh, R.; Tilbe, K.; Lee, H., Raja 42, a novel gamma lactam compound, is effective against *Clostridioides difficile*. *PLoS One* **2021,** *16* (9), e0257143.
146. Fong, A. Characterization of the novel 4-chloro-1-piperidin-1ylmethyl-1H-indole-2,3-dione compound (Raja 42) for its antibacterial activity against *Escherichia coli, Clostridium difficile, Staphylococcus aureus* and *Helicobacter pylori*. Laurentian University of Sudbury, 2020.
147. Couloigner, E.; Cartier, D.; Labie, R., Synthesis of pyrazolidinone antibacterial agents. *Bioorg. Med. Chem. Lett.* **1999,** *9* (15), 2205-2206.
148. Ternansky, R. J.; Draheim, S. E., Structure-activity relationship within a series of pyrazolidinone antibacterial agents. 1. Effect of nuclear modification on in vitro activity. *J. Med. Chem.* **1993,** *36* (22), 3219-3223.

149. Jungheim, L. N.; Sigmund, S. K.; Fisher, J. W., Bicyclic pyrazolidinones, a new class of antibacterial agent based on the β-lactam model. *Tetrahedron Lett.* **1987,** *28* (3), 285-288.
150. Indelicato, J. M.; Pasini, C. E., The acylating potential of γ-lactam antibacterials: base hydrolysis of bicyclic pyrazolidinones. *J. Med. Chem.* **1988,** *31* (6), 1227-1230.
151. Allen, N. E.; Hobbs, J. N.; Preston, D. A.; Turner, J. R.; Wu, C. Y. E., Antibacterial properties of the bicyclic pyrazolidinones. *J. Antibiot.* **1990,** *43* (1), 92-99.
152. Ternansky, R. J.; Draheim, S. E.; Pike, A. J.; Counter, F. T.; Eudaly, J. A.; Kasher, J. S., Structure-activity relationship within a series of pyrazolidinone antibacterial agents. 2. Effect of side-chain modification on in vitro activity and pharmacokinetic parameters. *J. Med. Chem.* **1993,** *36* (22), 3224-3229.
153. Goldberg, J. A.; Nguyen, H.; Kumar, V.; Spencer, E. J.; Hoyer, D.; Marshall, E. K.; Cmolik, A.; O'Shea, M.; Marshall, S. H.; Hujer, A. M.; Hujer, K. M.; Rudin, S. D.; Domitrovic, T. N.; Bethel, C. R.; Papp-Wallace, K. M.; Logan, L. K.; Perez, F.; Jacobs, M. R.; van Duin, D.; Kreiswirth, B. M.; Bonomo, R. A.; Plummer, M. S.; van den Akker, F., A γ-Lactam Siderophore Antibiotic Effective against Multidrug-Resistant Gram-Negative *Bacilli*. *J. Med. Chem.* **2020,** *63* (11), 5990-6002.
154. WHO Global Tuberculosis Report 2017. http://www.who.int/news-room/detail/27-02-2017-who-publishes-list-of-bacteria-for-which-new-antibiotics-are-urgently-needed (accessed 10/10/2021).
155. Calvopiña, K.; Umland, K.-D.; Rydzik, A. M.; Hinchliffe, P.; Brem, J.; Spencer, J.; Schofield, C. J.; Avison, M. B., Sideromimic Modification of Lactivicin Dramatically Increases Potency against Extensively Drug-Resistant *Stenotrophomonas maltophilia* Clinical Isolates. *Antimicrob. Agents Chemother.* **2016,** *60* (7), 4170-4175.
156. Papp-Wallace, K. M.; Senkfor, B.; Gatta, J.; Chai, W.; Taracila, M. A.; Shanmugasundaram, V.; Han, S.; Zaniewski, R. P.; Lacey, B. M.; Tomaras, A. P., Early insights into the interactions of different β-lactam antibiotics and β-lactamase inhibitors against soluble forms of *Acinetobacter baumanni*i PBP1a and *Acinetobacter sp.* PBP3. *Antimicrob. Agents Chemother.* **2012,** *56* (11), 5687-5692.
157. Jungheim, L. N., Bicyclic pyrazolidinone antibacterial agents. Synthesis of side chain analogues of carbapenems PS-5 and thienamycin. *Tetrahedron Lett.* **1989,** *30* (15), 1889-1892.
158. Panfil, I.; Urbańczyk-Lipkowska, Z.; Suwińska, K.; Solecka, J.; Chmielewski, M., Synthesis of pyrazolidinone analogs of β-lactam antibiotics. *Tetrahedron* **2002,** *58* (6), 1199-1212.
159. Harada, S.; Tsubotani, S.; Hida, T.; Ono, H.; Okazaki, H., Structure of lactivicin, an antibiotic having a new nucleus and similar biological activities to β-lactam antibiotics. *Tetrahedron Lett.* **1986,** *27* (51), 6229-6232.
160. Lambert, M. P.; Neuhaus, F. C., Mechanism of D-cycloserine action: alanine racemase from *Escherichia coli J. Bacteriol.* **1972,** *110* (3), 978-987.

161. Harada, S.; Tsubotani, S.; Hida, T.; Koyana, K.; Kondo, M.; Ono, H., Chemistry of a new antibiotic: Lactivicin. *Tetrahedron* **1988,** *44* (21), 6589-6606.
162. Macheboeuf, P.; Fischer, D. S.; Brown Jr, T.; Zervosen, A.; Luxen, A.; Joris, B.; Dessen, A.; Schofield, C. J., Structural and mechanistic basis of penicillin-binding protein inhibition by lactivicins. *Nat. Chem. Biol.* **2007,** *3*, 565.
163. Natsugari, H.; Kawano, Y.; Morimoto, A.; Yoshioka, K.; Ochiai, M., Synthesis of lactivicin and its derivatives. *J. Chem. Soc. Chem. Commun.* **1987,** (2), 62-63.
164. Tamura, N.; Matsushita, Y.; Yoshioka, K.; Ochiai, M., Synthesis of lactivicin analogues. *Tetrahedron* **1988,** *44* (11), 3231-3240.
165. Tamura, N.; Matsushita, Y.; Kawano, Y.; Yoshioka, K., Synthesis and antibacterial activity of lactivicin derivatives. *Chem. Pharm. Bull.* **1990,** *38* (1), 116-122.
166. Crast, L. B.; Graham, R. G.; Cheney, L. C., Synthesis of cephapirin and related cephalosporins from 7-(α-bromoacetamido)cephalosporanic acid. *J. Med. Chem.* **1973,** *16* (12), 1413-1415.
167. Starr, J.; Brown, M. F.; Aschenbrenner, L.; Caspers, N.; Che, Y.; Gerstenberger, B. S.; Huband, M.; Knafels, J. D.; Lemmon, M. M.; Li, C.; McCurdy, S. P.; McElroy, E.; Rauckhorst, M. R.; Tomaras, A. P.; Young, J. A.; Zaniewski, R. P.; Shanmugasundaram, V.; Han, S., Siderophore Receptor-Mediated Uptake of Lactivicin Analogues in Gram-Negative Bacteria. *J. Med. Chem.* **2014,** *57* (9), 3845-3855.
168. Calvopiña, K.; Dulyayangkul, P.; Heesom, K. J.; Avison, M. B., TonB-dependent uptake of β-lactam antibiotics in the opportunistic human pathogen *Stenotrophomonas maltophilia*. *Mol. Microbiol.* **2020,** *113* (2), 492-503.
169. Fisher, J.; Belasco, J. G.; Khosla, S.; Knowles, J. R., β-Lactamase proceeds via an acyl-enzyme intermediate. Interaction of the Escherichia coli RTEM enzyme with cefoxitin. *Biochemistry* **1980,** *19* (13), 2895-2901.
170. Wolfe, S.; Wilson, M.-C.; Cheng, M.-H.; Shustov, G. V.; Akuche, C. I., Cyclic hydroxamates, especially multiply substituted [1,2]oxazinan-3-ones. *Can. J. Chem.* **2003,** *81* (8), 937-960.
171. Wolfe, S.; Akuche, C.; Ro, S.; Wilson, M.-C.; Kim, C.-K.; Shi, Z., 5-Hydroxy [1,2] oxazinan-3-ones as potential carbapenem and D-ala-D-ala surrogates. *Can. J. Chem.* **2003,** *81* (8), 915-936.
172. Wolfe, S.; Akuche, C.; Ro, S. Oxazinones having antibacterial activity. US6399600B1, 2002.
173. Yamawaki, K.; Kusano, H.; Aoki, T. Tricyclic compounds and uses thereof. WO2016175223A1, 2016.
174. Brown, T.; Charlier, P.; Herman, R.; Schofield, C. J.; Sauvage, E., Structural Basis for the Interaction of Lactivicins with Serine β-Lactamases. *J. Med. Chem.* **2010,** *53* (15), 5890-5894.

175. Brown, R. P.; Aplin, R. T.; Schofield, C. J., Inhibition of TEM-2 β-lactamase from Escherichia coli by clavulanic acid: observation of intermediates by electrospray ionization mass spectrometry. *Biochemistry* **1996,** *35* (38), 12421-12432.
176. Sauvage, E.; Zervosen, A.; Dive, G.; Herman, R.; Amoroso, A.; Joris, B.; Fonzé, E.; Pratt, R. F.; Luxen, A.; Charlier, P., Structural basis of the inhibition of class A β-lactamases and penicillin-binding proteins by 6-β-iodopenicillanate. *J. Am. Chem. Soc.* **2009,** *131* (42), 15262-15269.
177. Hidy, P. H.; Hodge, E.; Young, V. V.; Harned, R. L.; Brewer, G. A.; Phillips, W.; Runge, W.; Stavely, H. E.; Pohland, A.; Boaz, H., Structure and reactions of cycloserine. *J. Am. Chem. Soc.* **1955,** *77* (8), 2345-2346.
178. Park, J. T.; Strominger, J. L., Mode of action of penicillin. Biochemical basis for the mechanism of action of penicillin and for its selective toxicity. *Science* **1957,** *125* (3238), 99-101.
179. Prosser, G. A.; de Carvalho, L. P. S., Kinetic mechanism and inhibition of *M ycobacterium tuberculosis* d-alanine: d-alanine ligase by the antibiotic d-cycloserine. *FEBS J.* **2013,** *280* (4), 1150-1166.
180. Baldwin, J. E.; Ng, S. C.; Pratt, A. J., Synthesis of phenoxyacetyl-N-sulphonyl cycloserine. *Tetrahedron Lett.* **1987,** *28* (37), 4319-4320.
181. Baldwin, J. E.; Lowe, C.; Schofield, C. J., The synthesis of potential γ-lactam antibiotics containing a cycloserine nucleus. *Tetrahedron Lett.* **1990,** *31* (15), 2211-2212.
182. Silva, V.; Silva, C.; Soares, P.; Garrido, E. M.; Borges, F.; Garrido, J., Isothiazolinone biocides: chemistry, biological, and toxicity profiles. *Molecules* **2020,** *25* (4), 991-991.
183. Lu, J.; Vodnala, S. K.; Gustavsson, A.-L.; Gustafsson, T. N.; Sjöberg, B.; Johansson, H. A.; Kumar, S.; Tjernberg, A.; Engman, L.; Rottenberg, M. E., Ebsulfur is a benzisothiazolone cytocidal inhibitor targeting the trypanothione reductase of *Trypanosoma brucei*. *J. Biol. Chem.* **2013,** *288* (38), 27456-27468.
184. Jin, W. B.; Xu, C.; Cheung, Q.; Gao, W.; Zeng, P.; Liu, J.; Chan, E. W. C.; Leung, Y.-C.; Chan, T. H.; Wong, K.-Y.; Chen, S.; Chan, K.-F., Bioisosteric investigation of ebselen: Synthesis and in vitro characterization of 1,2-benzisothiazol-3(2H)-one derivatives as potent New Delhi metallo-β-lactamase inhibitors. *Bioorg. Chem.* **2020,** *100*, 103873.
185. Lu, J.; Vlamis-Gardikas, A.; Kandasamy, K.; Zhao, R.; Gustafsson, T. N.; Engstrand, L.; Hoffner, S.; Engman, L.; Holmgren, A., Inhibition of bacterial thioredoxin reductase: an antibiotic mechanism targeting bacteria lacking glutathione. *FASEB J.* **2013,** *27* (4), 1394-1403.
186. Ngo, H. X.; Shrestha, S. K.; Green, K. D.; Garneau-Tsodikova, S., Development of ebsulfur analogues as potent antibacterials against methicillin-resistant *Staphylococcus aureus*. *Bioorg. Med. Chem.* **2016,** *24* (24), 6298-6306.
187. Su, J.; Liu, J.; Chen, C.; Zhang, Y.; Yang, K., Ebsulfur as a potent scaffold for inhibition and labelling of New Delhi metallo-β-lactamase-1 in vitro and in vivo. *Bioorg. Chem.* **2019,** *84*, 192-201.

188. Ngo, H. X.; Shrestha, S. K.; Garneau-Tsodikova, S., Identification of ebsulfur analogues with broad-spectrum antifungal activity. *ChemMedChem* **2016,** *11* (14), 1507.
189. Thangamani, S.; Eldesouky, H. E.; Mohammad, H.; Pascuzzi, P. E.; Avramova, L.; Hazbun, T. R.; Seleem, M. N., Ebselen exerts antifungal activity by regulating glutathione (GSH) and reactive oxygen species (ROS) production in fungal cells. *Biochim. Biophys. Acta Gen. Subj.* **2017,** *1861* (1), 3002-3010.
190. AbdelKhalek, A.; Abutaleb, N. S.; Mohammad, H.; Seleem, M. N., Repurposing ebselen for decolonization of vancomycin-resistant *enterococci* (VRE). *PloS one* **2018,** *13* (6), e0199710.
191. Chen, C.; Yang, K., Ebselen bearing polar functionality: Identification of potent antibacterial agents against multidrug-resistant Gram-negative bacteria. *Bioorg. Chem.* **2019,** *93*, 103286.
192. Chiou, J. W., Shengbiao; Chan, Kin-Fai; So, Pui-Kin; He, Dandan; Chan, Edward Wai-Chi; Chan, Tak-hang; Wong, Kwok-yin; Tao, Jiang; Chen, Sheng, Ebselen as a potent covalent inhibitor of New Delhi metallo-β-lactamase (NDM-1). *Chem. Commun.* **2015,** *51* (46), 9543-9546.
193. de Munnik, M.; Lohans, C. T.; Lang, P. A.; Langley, G. W.; Malla, T. R.; Tumber, A.; Schofield, C. J.; Brem, J., Targeting the *Mycobacterium tuberculosis* transpeptidase Ldt Mt2 with cysteine-reactive inhibitors including ebselen. *Chem. Commun.* **2019,** *55* (69), 10214-10217.
194. Mohammad, H.; Abutaleb, N. S.; Dieterly, A. M.; Lyle, L. T.; Seleem, M. N., Evaluation of ebselen in resolving a methicillin-resistant *Staphylococcus aureu*s infection of pressure ulcers in obese and diabetic mice. *PloS one* **2021,** *16* (2), e0247508.
195. Dong, C.; Zhou, J.; Wang, P.; Li, T.; Zhao, Y.; Ren, X.; Lu, J.; Wang, J.; Holmgren, A.; Zou, L., Topical therapeutic efficacy of ebselen against multidrug-resistant *Staphylococcus aureus* LT-1 targeting thioredoxin reductase. *Front. Microbiol.* **2020,** *10*, 3016.
196. Gustafsson, T. N.; Osman, H.; Werngren, J.; Hoffner, S.; Engman, L.; Holmgren, A., Ebselen and analogs as inhibitors of *Bacillus anthracis* thioredoxin reductase and bactericidal antibacterials targeting *Bacillus* species, *Staphylococcus aureus* and *Mycobacterium tuberculosis*. *Biochim. Biophys. Acta Gen. Subj.* **2016,** *1860* (6), 1265-1271.
197. Chen, C.; Xiang, Y.; Yang, K.-W.; Zhang, Y.; Wang, W.-M.; Su, J.-P.; Ge, Y.; Liu, Y., A protein structure-guided covalent scaffold selectively targets the B1 and B2 subclass metallo-β-lactamases. *Chem. Commun.* **2018,** *54* (38), 4802-4805.
198. Panfil, I.; Urbańczyk-Lipkowska, Z.; Chmielewski, M., Isoxazolidin-5-one analogs of β-lactam antibiotics. *Carbohydr. Res.* **1998,** *306* (4), 505-515.
199. Boyd, D. B.; Elzey, T. K.; Hatfield, L. D.; Kinnick, M. D.; Morin Jr, J. M., γ-Lactam analogues of the penems. *Tetrahedron letters* **1986,** *27* (30), 3453-3456.
200. Reddy, A. S.; Kumar, M. S.; Reddy, G. R., A convenient method for the preparation of hydroxamic acids. *Tetrahedron Lett.* **2000,** *41* (33), 6285-6288.

201. Pretsch, E.; Bühlmann, P.; Affolter, C.; Pretsch, E.; Bhuhlmann, P.; Affolter, C., *Structure determination of organic compounds*. Springer: 2009; Vol. 13.
202. Ferraris, D.; Duvall, B.; Ko, Y.-S.; Thomas, A. G.; Rojas, C.; Majer, P.; Hashimoto, K.; Tsukamoto, T., Synthesis and biological evaluation of D-amino acid oxidase inhibitors. *J. Med. Chem.* **2008,** *51* (12), 3357-3359.
203. Dhanya, R.-P.; Sidique, S.; Sheffler, D. J.; Nickols, H. H.; Herath, A.; Yang, L.; Dahl, R.; Ardecky, R.; Semenova, S.; Markou, A., Design and synthesis of an orally active metabotropic glutamate receptor subtype-2 (mGluR2) positive allosteric modulator (PAM) that decreases cocaine self-administration in rats. *J. Med. Chem.* **2011,** *54* (1), 342-353.
204. He, G.; Song, Q.; Wang, J.; Xu, A.; Peng, K.; Zhu, Q.; Xu, Y., Design, synthesis and biological evaluation of N-hydroxy-aminobenzyloxyarylamide analogues as novel selective κ opioid receptor antagonists. *Bioorg. Med. Chem. Lett.* **2020,** *30* (13), 127236-127236.
205. Deering, R. W.; Whalen, K. E.; Alvarez, I.; Daffinee, K.; Beganovic, M.; LaPlante, K. L.; Kishore, S.; Zhao, S.; Cezairliyan, B.; Yu, S., Identification of a bacteria-produced benzisoxazole with antibiotic activity against multi-drug resistant *Acinetobacter baumannii*. *J. Antibiot.* **2021,** *74* (6), 370-380.
206. Chattopadhyay, S.; Raychaudhuri, U.; Chakraborty, R., Artificial sweeteners–a review. *J. Food Sci. Technol.* **2014,** *51* (4), 611-621.
207. Tse, E.; Butner, L.; Huang, Y.; Hall, I. H., The Anti-inflammatory Activity of N-Substituted Indazolones in Mice. *Arch. Pharm.* **1996,** *329* (1), 35-40.
208. Gabriel, S., Ueber eine Darstellungsweise primärer Amine aus den entsprechenden Halogenverbindungen. *Ber. Dtsch. Chem.* **1887,** *20* (2), 2224-2236.
209. Baltzly, R., Catalytic hydrogenation. II. Poisoning by nucleophiles. *J. Org. Chem.* **1976,** *41* (6), 928-933.
210. Ehmann, D. E.; Jahić, H.; Ross, P. L.; Gu, R.-F.; Hu, J.; Kern, G.; Walkup, G. K.; Fisher, S. L., Avibactam is a covalent, reversible, non–β-lactam β-lactamase inhibitor. *Proc. Natl. Acad. Sci.* **2012,** *109* (29), 11663-11668.
211. Decuyper, L.; Deketelaere, S.; Vanparys, L.; Jukič, M.; Sosič, I.; Sauvage, E.; Amoroso, A. M.; Verlaine, O.; Joris, B.; Gobec, S.; D'Hooghe, M., In Silico Design and Enantioselective Synthesis of Functionalized Monocyclic 3-Amino-1-carboxymethyl-β-lactams as Inhibitors of Penicillin-Binding Proteins of Resistant Bacteria. *Chem. Eur. J.* **2018,** *24* (57), 15254-15266.
212. Gaddy, J. A.; Arivett, B. A.; McConnell, M. J.; López-Rojas, R.; Pachón, J.; Actis, L. A., Role of acinetobactin-mediated iron acquisition functions in the interaction of *Acinetobacter baumannii* ATCC 19606T with human lung epithelial cells, Galleria mellonella caterpillars and mice. *Inf. Immun.* **2012**, IAI. 06279-11.
213. Wuest, W. M.; Sattely, E. S.; Walsh, C. T., Three siderophores from one bacterial enzymatic assembly line. *J. Am. Chem. Soc.* **2009,** *131* (14), 5056-5057.
214. Shapiro, J. A.; Wencewicz, T. A., Acinetobactin Isomerization Enables Adaptive Iron Acquisition in *Acinetobacter baumannii* through pH-Triggered Siderophore Swapping. *ACS Infect. Dis.* **2016,** *2* (2), 157-168.

215. Song, W. Y.; Jeong, D.; Kim, J.; Lee, M. W.; Oh, M. H.; Kim, H. J., Key Structural Elements for Cellular Uptake of Acinetobactin, a Major Siderophore of *Acinetobacter baumannii*. *Org. Lett.* **2017,** *19* (3), 500-503.
216. Sakakura, A.; Kondo, R.; Ishihara, K., Molybdenum Oxides as Highly Effective Dehydrative Cyclization Catalysts for the Synthesis of Oxazolines and Thiazolines. *Org. Lett.* **2005,** *7* (10), 1971-1974.
217. Shapiro, J. A.; Wencewicz, T. A., Structure-function studies of acinetobactin analogs. *Metallomics* **2017,** *9* (5), 463-470.
218. Jungheim, L. N.; Sigmund, S. K., 1, 3-Dipolar cycloaddition reactions of pyrazolidinium ylides with acetylenes. Synthesis of a new class of antibacterial agents. *J. Org. Chem.* **1987,** *52* (18), 4007-4013.
219. Holmes, R. E.; Neel, D. A., Asymmetric synthesis of 4-[(t-butoxycarbonyl)amino]-pyrazolidin-3-one: Precursor to bicyclic pyrazolidinone antibacterials. *Tetrahedron Lett.* **1990,** *31* (39), 5567-5570.
220. Mitsunobu, O.; Yamada, M., Preparation of Esters of Carboxylic and Phosphoric Acid via Quaternary Phosphonium Salts. *Bull. Chem. Soc. Jpn.* **1967,** *40* (10), 2380-2382.
221. Fina, N. J.; Edwards, J. O., The alpha effect. A review. *Int. J. Chem. Kinet.* **1973,** *5* (1), 1-26.
222. Drev, M.; Grošelj, U.; Svete, J., Transformations of β-aryl-N-Cbz-α,β-didehydro-α-amino esters with hydrazine hydrate. *Z. Naturforsch. B* **2016,** *71* (6), 623-631.
223. Greene, T. W.; Wuts, P. G. M., *Greene's Protective Groups in Organic Synthesis*. 2006; p 533-646.
224. Greene, T. W.; Wuts, P. G. M., *Greene's Protective Groups in Organic Synthesis*. 2006; p 696-926.
225. Torii, S.; Tanaka, H.; Taniguchi, M.; Kameyama, Y.; Sasaoka, M.; Shiroi, T.; Kikuchi, R.; Kawahara, I.; Shimabayashi, A.; Nagao, S., Deprotection of carboxylic esters of. beta.-lactam homologs. Cleavage of p-methoxybenzyl, diphenylmethyl, and tert-butyl esters effected by a phenolic matrix. *J. Org. Chem.* **1991,** *56* (11), 3633-3637.
226. Vollmer, W.; Bertsche, U., Murein (peptidoglycan) structure, architecture and biosynthesis in *Escherichia coli*. *Biochim. Biophys. Acta Biomembr.* **2008,** *1778* (9), 1714-1734.
227. Martin, J. S.; MacKenzie, C. J.; Fletcher, D.; Gilbert, I. H., Characterising covalent warhead reactivity. *Bioorg. Med. Chem.* **2019,** *27* (10), 2066-2074.
228. Pidgeon, S. E.; Apostolos, A. J.; Nelson, J. M.; Shaku, M.; Rimal, B.; Islam, M. N.; Crick, D. C.; Kim, S. J.; Pavelka, M. S.; Kana, B. D.; Pires, M. M., L,D-Transpeptidase Specific Probe Reveals Spatial Activity of Peptidoglycan Cross-Linking. *ACS Chem. Biol.* **2019,** *14* (10), 2185-2196.
229. Triboulet, S.; Dubée, V.; Lecoq, L.; Bougault, C.; Mainardi, J.-L.; Rice, L. B.; Ethève-Quelquejeu, M.; Gutmann, L.; Marie, A.; Dubost, L.; Hugonnet, J.-E.;

Simorre, J.-P.; Arthur, M., Kinetic Features of L,D-Transpeptidase Inactivation Critical for β-Lactam Antibacterial Activity. *PLoS One* **2013,** *8* (7), e67831.
230. Jarlier, V.; Gutmann, L.; Nikaido, H., Interplay of cell wall barrier and beta-lactamase activity determines high resistance to beta-lactam antibiotics in *Mycobacterium chelonae*. *Antimicrob. Agents Chemother.* **1991,** *35* (9), 1937-1939.
231. Quinting, B.; Reyrat, J.-M.; Monnaie, D.; Amicosante, G.; Pelicic, V.; Gicquel, B.; Frère, J.-M.; Galleni, M., Contribution of β-lactamase production to the resistance of *mycobacteria* to β-lactam antibiotics. *FEBS Lett.* **1997,** *406* (3), 275-278.
232. Keane, J.; Balcewicz-Sablinska, M. K.; Remold, H. G.; Chupp, G. L.; Meek, B. B.; Fenton, M. J.; Kornfeld, H., Infection by *Mycobacterium tuberculosis* promotes human alveolar macrophage apoptosis. *Inf. Immun.* **1997,** *65* (1), 298-304.
233. Dubée, V.; Triboulet, S.; Mainardi, J.-L.; Ethève-Quelquejeu, M.; Gutmann, L.; Marie, A.; Dubost, L.; Hugonnet, J.-E.; Arthur, M., Inactivation of *Mycobacterium tuberculosis* L, D-transpeptidase LdtMt1 by carbapenems and cephalosporins. *Antimicrob. Agents Chemother.* **2012,** *56* (8), 4189-4195.
234. Gokulan, K.; Khare, S.; Cerniglia, C. E.; Foley, S. L.; Varughese, K. I., Structure and inhibitor specificity of L, D-transpeptidase (LdtMt2) from *Mycobacterium tuberculosis* and antibiotic resistance: calcium binding promotes dimer formation. *AAPS J.* **2018,** *20* (2), 1-14.
235. Kim, H. S.; Kim, J.; Im, H. N.; Yoon, J. Y.; An, D. R.; Yoon, H. J.; Kim, J. Y.; Min, H. K.; Kim, S. J.; Lee, J. Y., Structural basis for the inhibition of *Mycobacterium tuberculosis* L, D-transpeptidase by meropenem, a drug effective against extensively drug-resistant strains. *Acta Crystallogr. Sect. D: Biol. Crystallogr.* **2013,** *69* (3), 420-431.
236. Zhao, F.; Hou, Y.-J.; Zhang, Y.; Wang, D.-C.; Li, D.-F., The 1-β-methyl group confers a lower affinity of l, d-transpeptidase LdtMt2 for ertapenem than for imipenem. *Biochem. Biophys. Res. Commun.* **2019,** *510* (2), 254-260.
237. Kumar, P.; Kaushik, A.; Lloyd, E. P.; Li, S.-G.; Mattoo, R.; Ammerman, N. C.; Bell, D. T.; Perryman, A. L.; Zandi, T. A.; Ekins, S., Non-classical transpeptidases yield insight into new antibacterials. *Nat. Chem. Biol.* **2017,** *13* (1), 54-61.
238. Guo, X.; Murray, M.; Xiong, C.; Zhu, S., Treatment of *Eschericia coli* BW25113 with subinhibitory levels of kanamycin results in antibiotic cross-resistance and TolC upregulation. *J. Exp. Microbiol. Immun.* **2013,** *17*, 19-23.
239. Mah, R.; Thomas, J. R.; Shafer, C. M., Drug discovery considerations in the development of covalent inhibitors. *Bioorganic & medicinal chemistry letters* **2014,** *24* (1), 33-39.
240. Ju, L.; Bode, J. W., A general strategy for the preparation of C-terminal peptide α-ketoacids by solid phase peptide synthesis. *Org. Biol. Chem.* **2009,** *7* (11), 2259-2264.
241. Soundararajan, G.; Bhamidimarri, S. P.; Winterhalter, M., Understanding Carbapenem Translocation through OccD3 (OpdP) of *Pseudomonas aeruginosa*. *ACS Chem. Biol.* **2017,** *12* (6), 1656-1664.

242. Islam, M. S.; Leissing, T. M.; Chowdhury, R.; Hopkinson, R. J.; Schofield, C. J., 2-Oxoglutarate-dependent oxygenases. *Ann. Rev. Biochem.* **2018,** *87*, 585-620.
243. Hausinger, R. P., Fe (II)/α-ketoglutarate-dependent hydroxylases and related enzymes. *Crit. Rev. Biochem. Mol. Biol.* **2004,** *39* (1), 21-68.
244. Walport, L. J.; Hopkinson, R. J.; Schofield, C. J., Mechanisms of human histone and nucleic acid demethylases. *Curr. Opin. Chem. Biol.* **2012,** *16* (5-6), 525-534.
245. Blasiak, L. C.; Vaillancourt, F. H.; Walsh, C. T.; Drennan, C. L., Crystal structure of the non-haem iron halogenase SyrB2 in syringomycin biosynthesis. *Nature* **2006,** *440* (7082), 368-371.
246. Li, J.; Liao, H.-J.; Tang, Y.; Huang, J.-L.; Cha, L.; Lin, T.-S.; Lee, J. L.; Kurnikov, I. V.; Kurnikova, M. G.; Chang, W.-c.; Chan, N.-L.; Guo, Y., Epoxidation Catalyzed by the Nonheme Iron(II)- and 2-Oxoglutarate-Dependent Oxygenase, AsqJ: Mechanistic Elucidation of Oxygen Atom Transfer by a Ferryl Intermediate. *J. Am. Chem. Soc.* **2020,** *142* (13), 6268-6284.
247. Baldwin, J. E.; Bradley, M., Isopenicillin N synthase: mechanistic studies. *Chem. Rev.* **1990,** *90* (7), 1079-1088.
248. Lloyd, M. D.; Lee, H.-J.; Harlos, K.; Zhang, Z.-H.; Baldwin, J. E.; Schofield, C. J.; Charnock, J. M.; Garner, C. D.; Hara, T.; Terwisscha van Scheltinga, A. C.; Valegård, K.; Viklund, J. A. C.; Hajdu, J.; Andersson, I.; Danielsson, Å.; Bhikhabhai, R., Studies on the active site of deacetoxycephalosporin C synthase. *J. Mol. Biol.* **1999,** *287* (5), 943-960.
249. Rose, N. R.; McDonough, M. A.; King, O. N. F.; Kawamura, A.; Schofield, C. J., Inhibition of 2-oxoglutarate dependent oxygenases. *Chem. Soc. Rev.* **2011,** *40* (8), 4364-4397.
250. Brewitz, L.; Nakashima, Y.; Schofield, C. J., Synthesis of 2-oxoglutarate derivatives and their evaluation as cosubstrates and inhibitors of human aspartate/asparagine-β-hydroxylase. *Chem. Sci.* **2021,** *12* (4), 1327-1342.
251. Haselbeck, R. J.; McAlister-Henn, L., Function and expression of yeast mitochondrial NAD-and NADP-specific isocitrate dehydrogenases. *J. Biol. Chem.* **1993,** *268* (16), 12116-12122.
252. Jo, S.-H.; Son, M.-K.; Koh, H.-J.; Lee, S.-M.; Song, I.-H.; Kim, Y.-O.; Lee, Y.-S.; Jeong, K.-S.; Kim, W. B.; Park, J.-W., Control of mitochondrial redox balance and cellular defense against oxidative damage by mitochondrial NADP+-dependent isocitrate dehydrogenase. *J. Biol. Chem.* **2001,** *276* (19), 16168-16176.
253. Bleeker, F. E.; Atai, N. A.; Lamba, S.; Jonker, A.; Rijkeboer, D.; Bosch, K. S.; Tigchelaar, W.; Troost, D.; Vandertop, W. P.; Bardelli, A., The prognostic IDH1 R132 mutation is associated with reduced NADP+-dependent IDH activity in glioblastoma. *Acta Neuropathol.* **2010,** *119* (4), 487-494.
254. Sanson, M.; Marie, Y.; Paris, S.; Idbaih, A.; Laffaire, J.; Ducray, F.; El Hallani, S.; Boisselier, B.; Mokhtari, K.; Hoang-Xuan, K., Isocitrate dehydrogenase 1 codon 132 mutation is an important prognostic biomarker in gliomas. *J. Clin. Oncol.* **2009,** *27* (25), 4150-4154.

255. Liu, X.; Ling, Z.-Q., Role of isocitrate dehydrogenase 1/2 (IDH 1/2) gene mutations in human tumors. *Histol. Histopathol.* **2015,** *30* (10), 1155-1160.
256. Xu, W.; Yang, H.; Liu, Y.; Yang, Y.; Wang, P.; Kim, S.-H.; Ito, S.; Yang, C.; Wang, P.; Xiao, M.-T., Oncometabolite 2-hydroxyglutarate is a competitive inhibitor of α-ketoglutarate-dependent dioxygenases. *Cancer Cell* **2011,** *19* (1), 17-30.
257. Mardis, E. R.; Ding, L.; Dooling, D. J.; Larson, D. E.; McLellan, M. D.; Chen, K.; Koboldt, D. C.; Fulton, R. S.; Delehaunty, K. D.; McGrath, S. D., Recurring mutations found by sequencing an acute myeloid leukemia genome. *N. Engl. J. Med.* **2009,** *361* (11), 1058-1066.
258. Popovici-Muller, J.; Lemieux, R. M.; Artin, E.; Saunders, J. O.; Salituro, F. G.; Travins, J.; Cianchetta, G.; Cai, Z.; Zhou, D.; Cui, D., Discovery of AG-120 (Ivosidenib): a first-in-class mutant IDH1 inhibitor for the treatment of IDH1 mutant cancers. *ACS Med. Chem. Lett.* **2018,** *9* (4), 300-305.
259. Pusch, S.; Krausert, S.; Fischer, V.; Balss, J.; Ott, M.; Schrimpf, D.; Capper, D.; Sahm, F.; Eisel, J.; Beck, A.-C., Pan-mutant IDH1 inhibitor BAY 1436032 for effective treatment of IDH1 mutant astrocytoma in vivo. *Acta Neuropathol.* **2017,** *133* (4), 629-644.
260. Zhao, Q.; Manning, J. R.; Sutton, J.; Costales, A.; Sendzik, M.; Shafer, C. M.; Levell, J. R.; Liu, G.; Caferro, T.; Cho, Y. S., Optimization of 3-pyrimidin-4-yl-oxazolidin-2-ones as orally bioavailable and brain penetrant mutant IDH1 inhibitors. *ACS Med. Chem. Lett.* **2018,** *9* (7), 746-751.
261. Zheng, B.; Yao, Y.; Liu, Z.; Deng, L.; Anglin, J. L.; Jiang, H.; Prasad, B. V.; Song, Y., Crystallographic investigation and selective inhibition of mutant isocitrate dehydrogenase. *ACS Med. Chem. Lett.* **2013,** *4* (6), 542-546.
262. Deng, G.; Shen, J.; Yin, M.; McManus, J.; Mathieu, M.; Gee, P.; He, T.; Shi, C.; Bedel, O.; McLean, L. R., Selective inhibition of mutant isocitrate dehydrogenase 1 (IDH1) via disruption of a metal binding network by an allosteric small molecule. *J. Biol. Chem.* **2015,** *290* (2), 762-774.
263. Okoye-Okafor, U. C.; Bartholdy, B.; Cartier, J.; Gao, E. N.; Pietrak, B.; Rendina, A. R.; Rominger, C.; Quinn, C.; Smallwood, A.; Wiggall, K. J., New IDH1 mutant inhibitors for treatment of acute myeloid leukemia. *Nat. Chem. Biol.* **2015,** *11* (11), 878-886.
264. Law, J. M.; Stark, S. C.; Liu, K.; Liang, N. E.; Hussain, M. M.; Leiendecker, M.; Ito, D.; Verho, O.; Stern, A. M.; Johnston, S. E., Discovery of 8-membered ring sulfonamides as inhibitors of oncogenic mutant isocitrate dehydrogenase 1. *ACS Med. Chem. Lett.* **2016,** *7* (10), 944-949.
265. Liu, S.; Cadoux-Hudson, T.; Schofield, C. J., Isocitrate dehydrogenase variants in cancer—Cellular consequences and therapeutic opportunities. *Curr. Opin. Chem. Biol.* **2020,** *57*, 122-134.
266. Oltvai, Z. N.; Harley, S. E.; Koes, D.; Michel, S.; Warlick, E. D.; Nelson, A. C.; Yohe, S.; Mroz, P., Assessing acquired resistance to IDH1 inhibitor therapy by full-exon IDH1 sequencing and structural modeling. *Cold Spring Harb. Mol. Case Stud.* **2021,** *7* (2), a006007.

267. Choe, S.; Wang, H.; DiNardo, C. D.; Stein, E. M.; de Botton, S.; Roboz, G. J.; Altman, J. K.; Mims, A. S.; Watts, J. M.; Pollyea, D. A., Molecular mechanisms mediating relapse following ivosidenib monotherapy in IDH1-mutant relapsed or refractory AML. *Blood Adv.* **2020,** *4* (9), 1894-1905.
268. Rendina, A. R.; Pietrak, B.; Smallwood, A.; Zhao, H.; Qi, H.; Quinn, C.; Adams, N. D.; Concha, N.; Duraiswami, C.; Thrall, S. H.; Sweitzer, S.; Schwartz, B., Mutant IDH1 Enhances the Production of 2-Hydroxyglutarate Due to Its Kinetic Mechanism. *Biochemistry* **2013,** *52* (26), 4563-4577.
269. Edwards, H. J.; Hargrave, J. D.; Penrose, S. D.; Frost, C. G., Synthetic applications of rhodium catalysed conjugate addition. *Chem. Soc. Rev.* **2010,** *39* (6), 2093-2105.
270. Pohl, M.; Lyon, D. K.; Mizuno, N.; Nomiya, K.; Finke, R. G., Polyoxoanion-Supported Catalyst Precursors. Synthesis and Characterization of the Iridium (I) and Rhodium (I) Precatalysts [(n-C4H9)4N]5Na3[(1,5-COD) M•P2W15Nb3O62] (M= Ir, Rh). *Inorg. Chem.* **1995,** *34* (6), 1413-1429.
271. Hayashi, T.; Ueyama, K.; Tokunaga, N.; Yoshida, K., A chiral chelating diene as a new type of chiral ligand for transition metal catalysts: Its preparation and use for the rhodium-catalyzed asymmetric 1, 4-addition. *J. Am. Chem. Soc.* **2003,** *125* (38), 11508-11509.
272. Müller, S.; Brown, P. J., Epigenetic chemical probes. *Clin. Pharm. Therap.* **2012,** *92* (6), 689-693.
273. Liu, X.; Chen, H.; Laurini, E.; Wang, Y.; Dal Col, V.; Posocco, P.; Ziarelli, F.; Fermeglia, M.; Zhang, C.-C.; Pricl, S.; Peng, L., 2-Difluoromethylene-4-methylenepentanoic Acid, A Paradoxical Probe Able To Mimic the Signaling Role of 2-Oxoglutaric Acid in *Cyanobacteria*. *Org. Lett.* **2011,** *13* (11), 2924-2927.
274. Bruick, R. K.; McKnight, S. L., A conserved family of prolyl-4-hydroxylases that modify HIF. *Science* **2001,** *294* (5545), 1337-1340.
275. Lei, Y.; Hu, T.; Wu, X.; Wu, Y.; Bao, Q.; Zhang, L.; Xia, H.; Sun, H.; You, Q.; Zhang, X., Affinity-Based Fluorescence Polarization Assay for High-Throughput Screening of Prolyl Hydroxylase 2 Inhibitors. *ACS Med. Chem. Lett.* **2015,** *6* (12), 1236-1240.
276. Wu, F.; Zhao, S.; Yu, B.; Chen, Y.-M.; Wang, W.; Song, Z.-G.; Hu, Y.; Tao, Z.-W.; Tian, J.-H.; Pei, Y.-Y., A new coronavirus associated with human respiratory disease in China. *Nature* **2020,** *579* (7798), 265-269.
277. Jin, Z.; Du, X.; Xu, Y.; Deng, Y.; Liu, M.; Zhao, Y.; Zhang, B.; Li, X.; Zhang, L.; Peng, C., Structure of M pro from SARS-CoV-2 and discovery of its inhibitors. *Nature* **2020,** *582* (7811), 289-293.
278. Thun-Hohenstein, S. T. D.; Suits, T. F.; Malla, T. R.; Tumber, A.; Brewitz, L.; Salah, E.; Choudhry, H.; Schofield, C. J., Structure-Activity Studies Reveal Scope for Optimisation of Ebselen-Type Inhibition of SARS-COV-2 Main Protease. *ChemMedChem* **2021**, https://doi.org/10.1002/cmdc.202100582.

279. Meotti, F. C.; Borges, V. C.; Zeni, G.; Rocha, J. B. T.; Nogueira, C. W., Potential renal and hepatic toxicity of diphenyl diselenide, diphenyl ditelluride and Ebselen for rats and mice. *Toxicol. Lett.* **2003,** *143* (1), 9-16.
280. Jacob, C.; Maret, W.; Vallee, B. L., Ebselen, a selenium-containing redox drug, releases zinc from metallothionein. *Biochem. Biophys. Res. Commun.* **1998,** *248* (3), 569-573.
281. Rose, N. R.; Thalhammer, A.; Seden, P. T.; Mecinović, J.; Schofield, C. J., Inhibition of the histone lysine demethylase JMJD2A by ejection of structural Zn (II). *Chem. Commun.* **2009,** (42), 6376-6378.
282. Briviba, K.; Roussyn, I.; Sharov, V. S.; Sies, H., Attenuation of oxidation and nitration reactions of peroxynitrite by selenomethionine, selenocystine and ebselen. *Biochem. J.* **1996,** *319* (1), 13-15.
283. Ziebuhr, J.; Snijder, E. J.; Gorbalenya, A. E., Virus-encoded proteinases and proteolytic processing in the *Nidovirales*. *Microbiology* **2000,** *81* (4), 853-879.
284. Amporndanai, K.; Meng, X.; Shang, W.; Jin, Z.; Rogers, M.; Zhao, Y.; Rao, Z.; Liu, Z.-J.; Yang, H.; Zhang, L.; O'Neill, P. M.; Samar Hasnain, S., Inhibition mechanism of SARS-CoV-2 main protease by ebselen and its derivatives. *Nat. Commun.* **2021,** *12* (1), 3061.
285. Sakamoto, J.; Oba, K.; Matsui, T.; Kobayashi, M., Efficacy of Oral Anticancer Agents for Colorectal Cancer. *Dis. Colon Rectum* **2006,** *49* (1), S82-S91.
286. Meraz-Torres, F.; Plöger, S.; Garbe, C.; Niessner, H.; Sinnberg, T., Disulfiram as a Therapeutic Agent for Metastatic Malignant Melanoma—Old Myth or New Logos? *Cancers* **2020,** *12* (12), 3538.
287. Sharpley, A. L.; Williams, C.; Holder, A. A.; Godlewska, B. R.; Singh, N.; Shanyinde, M.; MacDonald, O.; Cowen, P. J., A phase 2a randomised, double-blind, placebo-controlled, parallel-group, add-on clinical trial of ebselen (SPI-1005) as a novel treatment for mania or hypomania. *Psychopharmacology* **2020,** *237* (12), 3773-3782.
288. Boulos, J. C.; Rahama, M.; Hegazy, M.-E. F.; Efferth, T., Shikonin derivatives for cancer prevention and therapy. *Cancer Lett.* **2019,** *459*, 248-267.
289. Lovestone, S.; Boada, M.; Dubois, B.; Hüll, M.; Rinne, J. O.; Huppertz, H.-J.; Calero, M.; Andres, M. V.; Gómez-Carrillo, B.; Leon, T., A phase II trial of tideglusib in Alzheimer's disease. *J. Alzheimer's Dis.* **2015,** *45* (1), 75-88.
290. Baker, A. F.; Adab, K.; Raghunand, N.; Chow, H.; Stratton, S. P.; Squire, S.; Boice, M.; Pestano, L.; Kirkpatrick, D.; Dragovich, T., A phase IB trial of 24-hour intravenous PX-12, a thioredoxin-1 inhibitor, in patients with advanced gastrointestinal cancers. *Invest. New Drugs* **2013,** *31* (3), 631-641.
291. Azad, G. K.; Tomar, R. S., Ebselen, a promising antioxidant drug: mechanisms of action and targets of biological pathways. *Mol. Biol. Rep.* **2014,** *41* (8), 4865-4879.
292. Malla, T. R.; Tumber, A.; John, T.; Brewitz, L.; Strain-Damerell, C.; Owen, C. D.; Lukacik, P.; Chan, H. T. H.; Maheswaran, P.; Salah, E., Mass spectrometry

reveals potential of β-lactams as SARS-CoV-2 M pro inhibitors. *Chem. Commun.* **2021,** *57* (12), 1430-1433.
293. Haritha, C.; Sharun, K.; Jose, B., Ebselen, a new candidate therapeutic against SARS-CoV-2. *International Journal of Surgery (London, England)* **2020,** *84*, 53.
294. Li, H.; Zhang, D.; Gao, M.; Huang, L.; Tang, L.; Li, Z.; Chen, X.; Zhang, X., Highly specific C–C bond cleavage induced FRET fluorescence for in vivo biological nitric oxide imaging. *Chem. Sci.* **2017,** *8* (3), 2199-2203.
295. Davis, F. A.; Kluger, E. W., Chemistry of the sulfur-nitrogen bond. X. Barriers to planar inversion in N-(4, 4'-dimethylbenzophenylidene) arenesulfenamides and-selenenamides. *J. Am. Chem. Soc.* **1976,** *98* (1), 302-303.
296. Sun, L.-Y.; Chen, C.; Su, J.; Li, J.-Q.; Jiang, Z.; Gao, H.; Chigan, J.-Z.; Ding, H.-H.; Zhai, L.; Yang, K.-W., Ebsulfur and Ebselen as highly potent scaffolds for the development of potential SARS-CoV-2 antivirals. *Bioorg. Chem.* **2021,** *112*, 104889-104889.
297. Jagtap, S., Heck reaction—state of the art. *Catalysts* **2017,** *7* (9), 267.
298. Beletskaya, I. P.; Alonso, F.; Tyurin, V., The Suzuki-Miyaura reaction after the Nobel prize. *Coord. Chem. Rev.* **2019,** *385*, 137-173.
299. Dorel, R.; Grugel, C. P.; Haydl, A. M., The Buchwald–Hartwig amination after 25 years. *Angew. Chem. Int. Ed.* **2019,** *58* (48), 17118-17129.
300. Clark, D.; Murrell, J.; Tedder, J., The magnitudes and signs of the inductive and mesomeric effects of the halogens. *J. Chem. Soc.* **1963**, 1250-1253.
301. Lenčo, J.; Khalikova, M. A.; Švec, F., Dissolving Peptides in 0.1% Formic Acid Brings Risk of Artificial Formylation. *J. Proteome Res.* **2020,** *19* (3), 993-999.
302. Hendon-Dunn, C. L.; Doris, K. S.; Thomas, S. R.; Allnutt, J. C.; Marriott, A. A. N.; Hatch, K. A.; Watson, R. J.; Bottley, G.; Marsh, P. D.; Taylor, S. C., A flow cytometry method for rapidly assessing *Mycobacterium tuberculosis* responses to antibiotics with different modes of action. *Antimicrob. Agents Chemother.* **2016,** *60* (7), 3869-3883.
303. Adan, A.; Alizada, G.; Kiraz, Y.; Baran, Y.; Nalbant, A., Flow cytometry: basic principles and applications. *Crit. Rev. Biotechnol.* **2017,** *37* (2), 163-176.
304. Egbelowo, O.; Sarathy, J. P.; Gausi, K.; Zimmerman, M. D.; Wang, H.; Wijnant, G.-J.; Kaya, F.; Gengenbacher, M.; Van, N.; Degefu, Y., Pharmacokinetics and Target Attainment of SQ109 in Plasma and Human-Like Tuberculosis Lesions in Rabbits. *Antimicrobial agents and chemotherapy* **2021,** *65* (9), e00024-21.
305. Rohs, P. D.; Buss, J.; Sim, S. I.; Squyres, G. R.; Srisuknimit, V.; Smith, M.; Cho, H.; Sjodt, M.; Kruse, A. C.; Garner, E. C., A central role for PBP2 in the activation of peptidoglycan polymerization by the bacterial cell elongation machinery. *PLoS genetics* **2018,** *14* (10), e1007726.
306. Henriksen, P. A., The potential of neutrophil elastase inhibitors as anti-inflammatory therapies. *Current opinion in hematology* **2014,** *21* (1), 23-28.
307. DeClerck, Y.; Imren, S., Protease inhibitors: role and potential therapeutic use in human cancer. *European Journal of Cancer* **1994,** *30* (14), 2170-2180.

308. Bhakuni, B. S.; Balkrishna, S. J.; Kumar, A.; Kumar, S., An efficient copper mediated synthetic methodology for benzo[d]isothiazol-3(2H)-ones and related sulfur–nitrogen heterocycles. *Tetrahedron Lett.* **2012,** *53* (11), 1354-1357.
309. Elkaeed, E. B.; An, J.; Beauchemin, A. M., Synthesis of Indazolones via Friedel–Crafts Cyclization of Blocked (Masked) N-Isocyanates. *J. Org. Chem.* **2017,** *82* (18), 9890-9897.
310. Han, Z.-Z.; Dong, T.; Ming, X.-X.; Kuang, F.; Zhang, C.-P., Synthesis and Biological Evaluation of CF3Se-Substituted α-Amino Acid Derivatives. *ChemMedChem* **2021,** *16* (20), 3177-3180.
311. Lassen, K. M.; Lee, J.; Joullié, M. M., An efficient synthesis of the tamandarin B macrocycle. *Tetrahedron Lett.* **2010,** *51* (13), 1635-1638.
312. Novak, A.; Štefanič, M.; Grošelj, U.; Hrast, M.; Kasunič, M.; Gobec, S.; Stanovnik, B.; Svete, J., A Simple Synthesis of Polyfunctionalized 4-Aminopyrazolidin-3-ones as 'Aza-deoxa' Analogs of D-Cycloserine. *Helv. Chim. Acta* **2014,** *97* (2), 245-267.
313. Page, Z. A.; Bou Zerdan, R.; Gutekunst, W. R.; Anastasaki, A.; Seo, S.; McGrath, A. J.; Lunn, D. J.; Clark, P. G.; Hawker, C. J., A di-tert-butyl acrylate monomer for controlled radical photopolymerization. *J. Polym. Sci. Part A: Polym. Chem.* **2017,** *55* (5), 801-807.
314. Jana, R.; Tunge, J. A., A Homogeneous, Recyclable Polymer Support for Rh(I)-Catalyzed C–C Bond Formation. *J. Org. Chem.* **2011,** *76* (20), 8376-8385.
315. Mehta, S.; Brahmchari, D., Phosphazene Superbase-Mediated Regio- and Stereoselective Iodoaminocyclization of 2-(1-Alkynyl)benzamides for the Synthesis of Isoindolin-1-ones. *J. Org. Chem.* **2019,** *84* (9), 5492-5503.
316. Hellal, M.; Cuny, G. D., Microwave assisted copper-free Sonogashira coupling/5-exo-dig cycloisomerization domino reaction: access to 3-(phenylmethylene)isoindolin-1-ones and related heterocycles. *Tetrahedron Lett.* **2011,** *52* (42), 5508-5511.
317. Kumar, J. S.; Reddy, G. S.; Medishetti, R.; Ray, A.; Bele, S. D.; Hossain, K. A.; Thirupataiah, B.; Edwin, R. K.; Behera, P.; Joseph, A.; Shenoy, G. G.; Rao, C. M.; Pal, M., Sonochemical synthesis of rosuvastatin based novel 3-methyleneisoindolin-1-one derivatives as potential anticancer agents. *J. Mol. Struct.* **2021,** *1240*, https://doi.org/10.1016/j.molstruc.2021.130574130574.
318. Stockwell, B. R.; Zask, A.; Kaplan, A. Neuroprotective pdi modulating small molecules and methods of use thereof. WO2020113222A1, 2020.
319. Liu, S.; Abboud, M. I.; John, T.; Mikhailov, V.; Hvinden, I.; Walsby-Tickle, J.; Liu, X.; Pettinati, I.; Cadoux-Hudson, T.; McCullagh, J. S., Roles of metal ions in the selective inhibition of oncogenic variants of isocitrate dehydrogenase 1. *Commun. Biol.* **2021,** *4* (1), 1-16.

Chapter 9 Appendix

9.1 IC_{50} curves for compounds 319 against M^{pro}

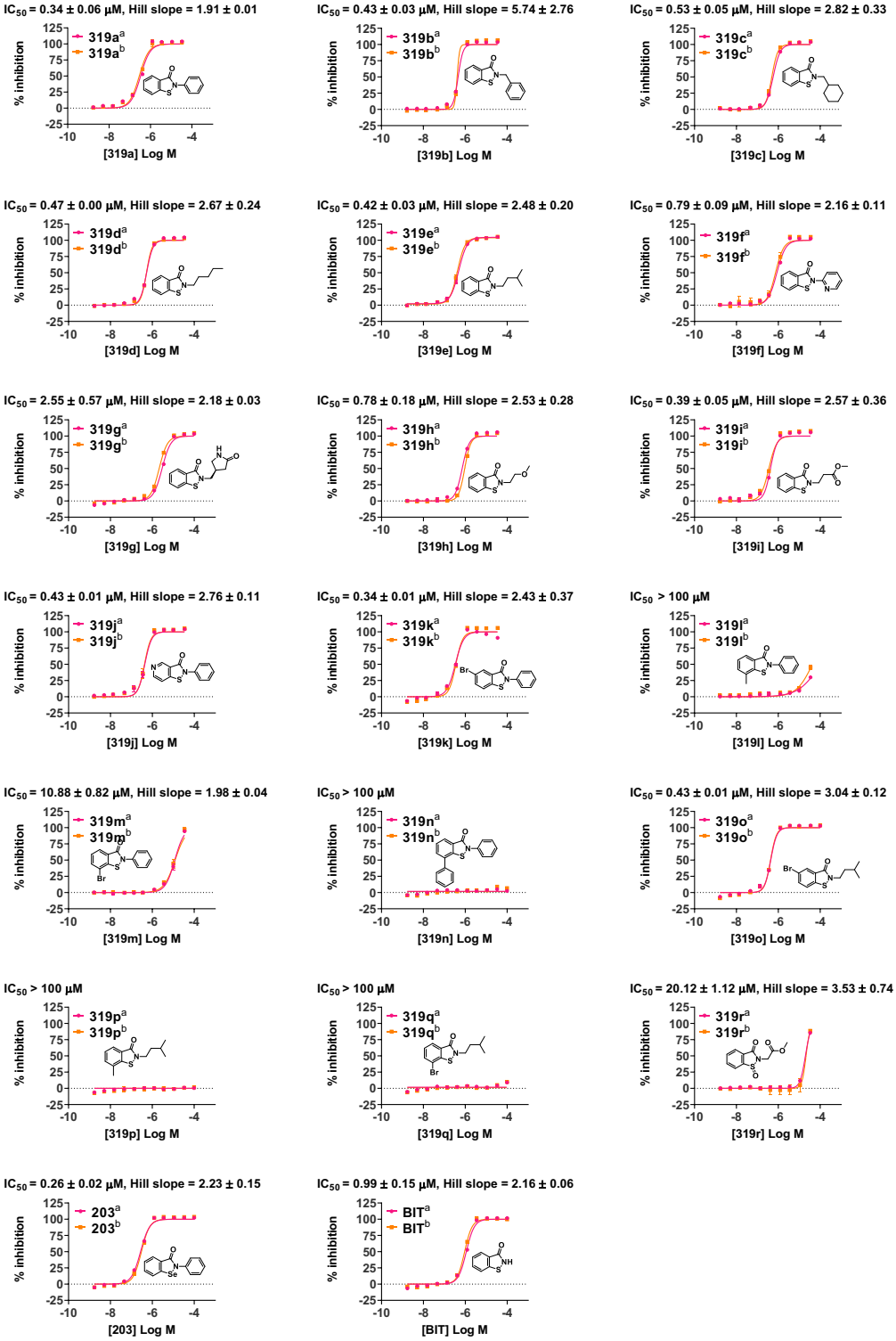

Figure 9-1 | SPE-MS IC_{50} curves for ebsulfur compounds against M^{pro}.

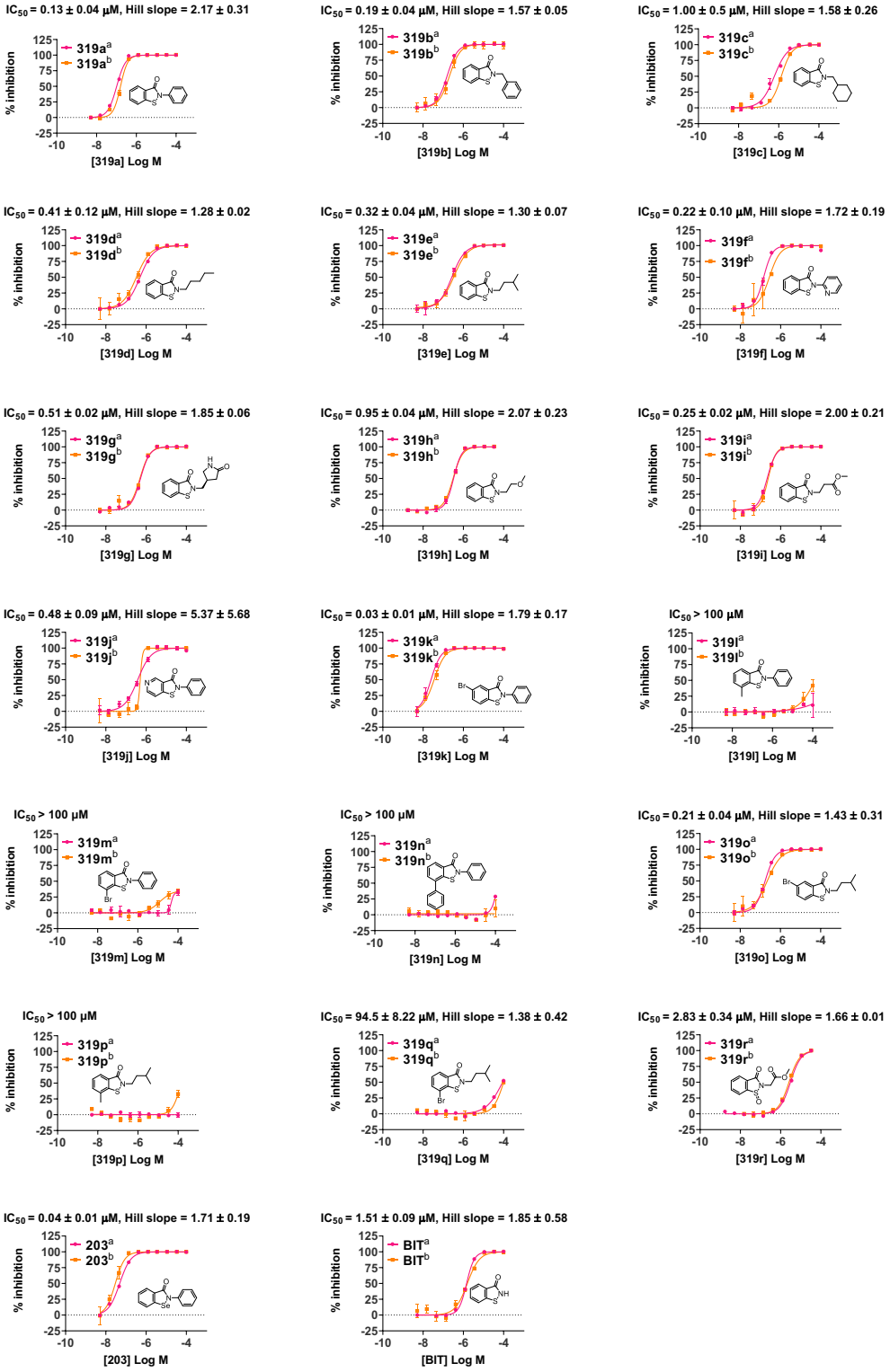

Figure 9-2 | FRET IC_{50} curves for ebsulfur compounds against M^{pro}.